Interactions Between Systemic Inflammation, Frailty And Neuroinflammation In Ageing And Neurodegeneration

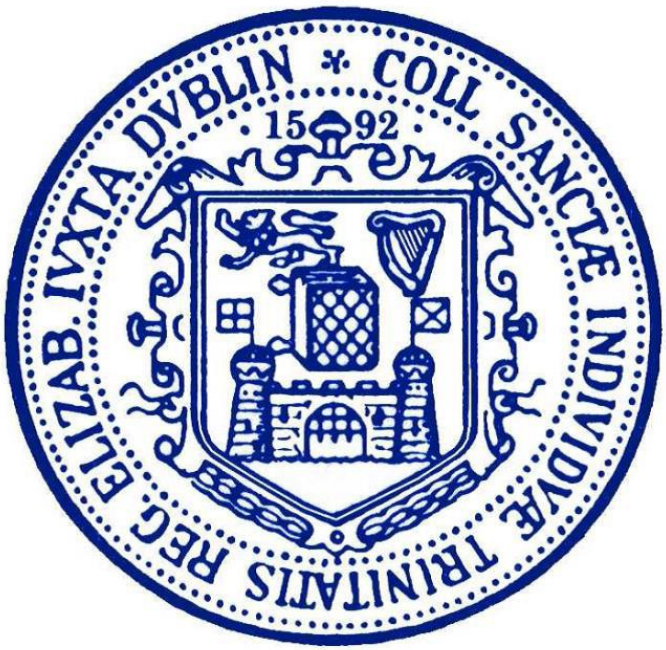

By

Dáire Healy

Thesis submitted for the degree of Doctor of Philosophy

at the University of Dublin, Trinity College

Submitted February 2022

School of Biochemistry & Immunology and Trinity College Institute of Neuroscience, Trinity College Dublin, Dublin 2

Declaration

I declare that this thesis has not been submitted as an exercise for a degree at this or any other university and it is entirely my own work except elements of figures 4.2-4.3, 4.6-4.9 where labelling was performed by students under my tutelage and supervision and Figure 3.8 which was the product of behavioural research by Dr. Carol Murray pertinent to the tissue I worked with, and that it has not been previously submitted as an exercise for a degree at this or any other University.

I agree to deposit this thesis in the University's open access institutional repository or allow the Library to do so on my behalf, subject to Irish Copyright Legislation and Trinity College Library conditions of use and acknowledgement.

I consent to the examiner retaining a copy of the thesis beyond the examining period, should they so wish (EU GDPR May 2018).

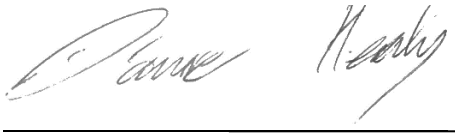

Dáire Healy

Acknowledgements

First and foremost. thank you to my supervisor Colm Cunningham for giving me this great opportunity, for his guidance, candour and for always pushing me to better myself as a scientist.

To all the members of the Cunningham lab, past and present who have helped teach and support me. Ana-Belen Lopez-Rodriguez, Lucas Tortorelli, John Kealy, Arshed Nazmi and Carol Murray, thank you all for your help in getting me this far and I look forward to working alongside and hopefully collaborating with you all in the future.

To all the undergraduate and postgraduate students who have worked alongside me and contributed to this work; Ruth Power, Joanna Laskowska, Jessica Lambe-Beth, Eoin Lawlor, Ciara McAdams and Ethan Murphy thank you for your work and I wish you all the best in your own future careers in science and beyond.

On a personal note, I would like to thank all of my friends and family who have been an invaluable network of support and encouragement throughout this process. To my parents, Trish and Andy, thank you for always motivating me without once ever making me feel pressured but always loved. To Ciara, there are no words to express how much you've helped me, but I know that you know exactly how I feel. I can't wait for our next chapter together.

Finally, I would also like to thank my grandmother, Nana Kay. While I miss your sincerity and guidance every day, without you I may never have found my voice and purpose and I hope you would have been proud of what I've done with those lessons you had time to give me. This is for you.

Abbreviations

Abbreviation	Full Name
7-AAD	7-aminoactinomycin D
Aβ	Amyloid Beta
ABC	Avidin Biotin Complex
AD	Alzheimer's Disease
AF	Aged Cognitively Frail
AP-1	Activating protein -1
Alum	Ammonium sulphate
ANOVA	Analysis of variance
ANXA1	Annexin-A1
APP	Amyloid precursor protein
APP.PS1	B6.Cg-Tg(APPswe,PSEN1dE9)85Dbo/Mmjax mouse strain
AR	Aged Cognitively Resilient
ARC	Arcuate Nucleus
ARDs	Age-related diseases
ATG5	Autophagy-related gene 5
ATM	Ataxia telangiectasia mutated
ATP	Adenosine 5-triphosphate
β-glucan	β-1,3 glucans
BBB	Blood-Brain Barrier
BCSFB	Blood-Cerebrospinal Fluid Barrier
BCL10	B cell lymphoma 10
BDNF	Brain-Derived Neurotrophic Factor
C1qα	Complement Component 1q
C3	Complement Component 3
C57BL/6	C57 Black 6
CA1	Cornu Ammonis 1
CA2	Cornu Ammonis 2
CA3	Cornu Ammonis 3

CARD9	Caspase recruitment domain family member 9
CC	Corpus Callosum
CCL2 (MCP-1)	C-C motif Chemokine Ligand 2
CCL3	C-C motif Chemokine Ligand 3
CCL4	C-C motif Chemokine Ligand 4
CD11b	Cyclin-dependent kinase 11B
CD11c (Itgax)	Integrin Subunit Alpha X
CD36	Cluster of Differentiation 36
CD45	Cluster of Differentiation 45
CD68	Cluster of Differentiation 68
cDNA	complimentary deoxyribonucleic acid
CFC	Contextual Fear Conditioning
ChAT	Choline acetyltransferase
Clec7a	C-type lectin domain family 7 member A
COX2	Cyclooxygenase 2
CNS	Central nervous system
CRP	C-reactive protein
CSF	Cerebrospinal fluid
CSF1R	Colony Stimulating Factor 1 Receptor
Cst7	Cystatin 7
Ctss	Cathepsin S
Ctx	Cortex
CXCL10	C-X-C Motif Chemokine 10 (IP-10)
CXCL13	C-X-C Motif Chemokine 13
DAB	3,3' Diaminobenzidine
DAMP	Damage Associated Molecular Pattern
DAVID	Database for Annotation, Visualisation and Integrated Discovery
DC	Dendritic cell
DG	Dentate Gyrus
dH2O	Distilled water
DHA	Dorsal hypothalamic area
DMN	Dorsomedial nuclei

DN	Dentate Nucleus
DNA	Deoxyribonucleic acid
dNTP	Deoxyribonucleotide triphosphate
E-coli	Escherichia coliform
EAE	Experimental autoimmune encephalomyelitis
ELISA	Enzyme linked immosorbant assay
EOAD	Early Onset Alzheimer's Disease
FACs	Fluorescence Activated Cell Sorting
FAO	Fatty acid oxidation
FFPE	Formalin fixed paraffin embedded
FI	Frailty Index
FN	Fastigial Nucleus
FSC-A	Forward scatter area
FSC-W	Forward scatter width
GAPDH	Glyceraldehyde-3-Phosphate Dehydrogenase
Gbp2	Guanylate Binding Protein 2
GF	Germ free
GFAP	Glial fibrillary acidic protein
GH	Growth hormone
GSs	Geriatric Syndromes
Hes5	Hes Family BHLH Transcription Factor 5
HFD	High fat diet
HRP	Horse radish peroxidase
IBA-1	Ionized calcium-binding adapter molecule 1
i.c.	Intracerebral
i.c.v.	Intracerebroventricular
IFN	Interferon
IGF-1	Insulin-like growth factor 1
IHC	Intrahippocampal
IL-10	Interleukin 10
IL-12	Interleukin 12
IL-1α	Interleukin 1α

IL-1β	Interleukin 1β
IL-1R	Interleukin 1 Receptor
IL-23	Interleukin 23
IL-4	Interleukin 4
IL-6	Interleukin 6
IN	Interposed Nucleus
i.p.	Intraperitoneal
IRF7	Interferon Regulatory Factor 7
KO	Knockout
Lgals9	Galectin 9
LHA	Lateral hypothalamic area
LMN	Lateral mammillary nuclei
LPS	Lipopolysaccharide
LPL	Lipoprotein lipase
MALT1	Mucosa-associated lymphoid tissue lymphoma translocation protein 1
MCP-1	Macrophage chemoattractant protein one
ME7	ME7 Prion Disease
MHC	Major histocompatibility complex
MS	Multiple Sclerosis
MWM	Morris Water Maze
NF-κb	Nuclear factor kappa b
NFAT	Nuclear factor of activated T cells
NFT	Neurofibrillary tangle
Nlrp3	Nucleotide-binding oligomerization domain-like receptor protein 3
NO	Nitric Oxide
NTS	Nucleus tractus solitarius
OAS1a	2'-5'-oligoadenylate synthase 1A
OPC	Oligodendrocyte progenitor cell
Osm	Oncostatin M
OsmR	Oncostatin M Receptor
p16	p16INK4a

p19	p19ARF
p21	p21WAF1/CIP1
p53	Tumor protein p53
p62	Sequestome 1 (SQSTM1)
PAI-1	Plasminogen activator inhibitor-1
PAMPs	Pathogen Associated Molecular Patterns
Pax7	Paired box protein 7
PBS	Phosphate Buffered Saline
PCA	Principle Component Analysis
PCR	Reverse transcriptase
PD	Parkinson's Disease
PFC	Prefrontal Cortex
PHA	Posterior hypothalamic area
PNs	Pyramidal Neurons
Poly I:C	Polyinosinic:polycytidylic acid
PRRs	Pattern Recognition Receptors
Ptx3	Pentraxin 3
qPCR	Quantitative polymerase chain reaction
PVN	Paraventricular nucleus
RNA	Ribonucleic acid
RER	Respiratory exchange ratio
ROS	Reactive Oxygen Species
Rt-PCR	Real time polymerase chain reaction
SAMP8	Senescence Accelerated Mouse-Prone 8
SASP	Senescence associated secretory phenotype
SCN	Suprachiasmatic nucleus
SEM	Standard error of the mean
SMA	Spinal Muscular Atrophy
SMN	Supramammillary nuclei
SPARC	Secreted Protein Acidic And Cysteine Rich
SSC-A	Side scatter area
SSC-W	Side scatter width

Stat3	Signal Transducer And Activator Of Transcription 3
STT	Spinal trigeminal tract
SUM	Subiculum
Sy38	Synaptophysin
Syk	Spleen tyrosine kinase
TAMRA	Tetramethylrhodamine
TBI	Traumatic Brain Injury
TEM	Transendothelial migration
Tfeb	Transcription factor EB
TFL	Trinity Frailty Index
TGF-β	Transforming growth factor beta
TG	Transgenic
Tgm1	Transglutaminase 1
TLRs	Toll Like Receptors
TMB	3,3',5,5'-Tetramethylbenzidine
TMN	Tuberomammillary nuclei
TNFα	Tumour necrosis factor alpha
TNFR	Tumour necrosis factor receptor
TREM2	Triggering Receptor Expressed On Myeloid Cells 2
TYROBP	TYRO Protein Tryrosine Kinase Binding Protein
VCN	Ventral cochlear nucleus
VIM	Vimentin
VMH	Ventromedial Hypothalamus
VMN	Ventromedial Nuclei
VTA	Ventral Tegmental Area
WT	Wild type
Y	Young
ZO	Zonula Occludens

List of Figures & Tables

Table of Contents

Abstract

Compelling evidence continues to define the pivotal role which inflammation plays in the progression of neurodegenerative diseases and ageing. It has emerged that inflammation outside the brain significantly contributes to inflammatory and degenerative changes inside the brain at least partly via alteration of the properties of microglial cells, the key brain immune cell population. Age-associated low-grade inflammation may contribute to brain aging but varies significantly among individuals, consistent with the idea that chronological ageing has limited predictive power for brain ageing. The main hypothesis pursued in this thesis is that frailty, a state of increased vulnerability due to the accumulation of multiple deficits in physiological systems, may contribute to the development of neuroinflammation.

We have demonstrated robust regional differences in innate immune transcriptional signature across the ageing brain as well as evidence for ubiquitous microglial across all assessed regions. Novel physiological and cognitive frailty indices were designed to capture different aspects of the pathology of ageing, including metabolism, physiological condition and cognitive status. The research herein assessed the degree with which they, as individual components, contribute to the frailty of an individual as well as how this cumulative frailty status informs on the brain's vulnerability to, and recovery from, an acute stressor and found frailty and metabolism to be inextricably linked. The data showed that frailty status in ageing mice at the physiological, cognitive and molecular levels is strongly correlated with inflammatory and metabolic indicators in the blood and in discrete brain regions and structures. Following this characterisation of relationships between frailty and brain inflammation/integrity I have demonstrated the ability of repeated episodic systemic inflammation to exacerbate neuroinflammation and cognitive function. Using fluorescence activated cell sorting I isolated and assessed molecular indices of inflammation and glial activation and demonstrated evidence of microglial and astrocytic priming in response to amyloid pathology and repeated episodic systemic inflammation. A generally increased susceptibility of females in APP/PS1 pathology to cognitive and physiological impairment was observed here.

These data suggest that across the lifespan age more strongly predicts microgliosis, but that within tighter age brackets, frailty adds to the neuroinflammatory status. The extent to which this increases an individual's vulnerability and susceptibility to secondary inflammatory insults has implications for our understanding of the interrelationship of frailty and dementia and remains the subject of further study.

Chapter 1:

Introduction

1.1 Introduction

An important role for inflammation in the progression of neurodegenerative diseases and ageing has begun to emerge over the last 2 decades. It is now relatively clear that peripheral inflammation contributes significantly to inflammatory and degenerative changes inside the brain and microglia, the brain's primary resident macrophage population, forms an integral part of our inflammatory response to systemic and central insults. Under chronic activation, such as that imposed in neurodegenerative conditions, it has been shown that they adopt a "primed" phenotype characterised by an exaggerated inflammatory response to secondary insults. A chronic, low-grade inflammation has also been shown to occur with age, but this varies significantly among individuals, consistent with the idea that chronological ageing has limited predictive power for brain ageing. Frailty may better define the risk for brain inflammation with age.

The work within this thesis pursues the hypothesis that the phenotypic state of microglia and their consequent degree of vulnerability to secondary insults increases with age in a way that is contingent on the frailty of the individual, i.e. it is proposed that the number of deficits, accumulated with ageing, will contribute to the impairment of the animal's general health and will result in increased vulnerability to stressor events within the CNS. Due to the regional heterogeneity in immune responses across the ageing brain it was also predicted this will occur in a regionally variable manner.

1.2 The Immune System & Inflammation

1.2.1 Inflammation & the CNS

The Central Nervous System (CNS) consists of the spinal cord and brain, which are surrounded by cerebrospinal fluid to cushion and protect it from trauma and to facilitate transport into, and clearance from, the extracellular space. Mounting evidence continues to emphasise and define the pivotal role which inflammation plays in the progression of neurodegenerative diseases and ageing. Indeed, chronic immune activation has been found to be a key common factor associated with many neurodegenerative processes and ageing (Amor et al. 2014; Nachun 2019). Inflammation can be broadly described as the process whereby the body responds to injury, infectious agents, autoimmune responses, and tissue ischaemia. It is now widely regarded as having a significant contributory role in CNS disease processes. For instance, chronic expression of Interleukin 1 (IL-1) in a mouse model of Parkinson's disease has been shown to exacerbate neurodegeneration and microgliosis in the substantia nigra (Godoy et al. 2008). Nonsteroidal anti-inflammatory drugs have been shown to have protective effects with long term use, highlighting the significant impact which

peripheral inflammation can have upon the brain and the potential therapeutic importance of regulating and resolving inflammation in the vulnerable brain (Stewart et al. 1997). Systemic circulating levels of TNFα have been linked with the progression of Alzheimer's disease (Holmes et al. 2003) and elevated levels have been shown to be present in the brain and cerebrospinal fluid (CSF) of Parkinson's patients (Mogi et al. 1994). In recent years genome wide association studies have also revealed a large number of common gene variants associated with small but significantly increased risk of the development of AD, many of which are involved in innate immunity including CLU, CR1, PICALM, BIN1 (Jun et al. 2010; Harold et al. 2009; Lambert et al. 2009). Of these, one of the most significant risk factor loci identified thus far is TREM2, a macrophage gene involved in phagocytosis and associated with the activated phenotype of the brains resident immune cell population, microglia (Neumann et al. 2013; Karch et al. 2015).

1.2.2 The Immune System

The immune system plays a crucial role in the maintenance of homeostasis and in the process of tissue regeneration following injury. It consists of a complex network of cells, tissues, and organs which all work in unison to achieve this goal. It can be divided into two subbranches, innate immunity and Adaptive immunity. The innate immune response is relatively non-specific and will come into play within minutes to hours of pathogen detection. It is composed primarily of physical barriers such as the skin and membranes, and chemical barriers such as sweat, saliva and mucus in addition to a panoply of cell types capable of recognizing infiltrating pathogens and driving antimicrobial innate immune responses as well as initiating adaptive immune response (Iwasaki et al. 2004). The adaptive immune response is then capable of mounting highly specific immune responses to specific pathogens, offering long term protection in addition to targeted destruction of invading pathogens and toxic molecules they might produce (Bonilla et al. 2010). Since the work presented herein deals primarily with the innate immune system, only a brief introduction to the adaptive immune system will be discussed here while the innate immune system will be focussed upon in more detail.

Adaptive immune response - B cells & T cells

While the innate immune response is considered the body's first line of defence, the more complex adaptive immune system employs antigen-specific responses, usually taking days to come into effect relying, as it does, upon signals from the innate immune system to provide information about the origin and nature of the antigen in question (Janeway et al. 2002). It consists primarily of 2 types of lymphocytes: B cells and T cells. B cells originate and mature in the bone marrow, differentiating into plasma cells and circulating throughout the circulatory and lymphatic system. Their principle

function is to produce antibodies which will bind specifically to foreign antigens (Borghesi et al. 2006). In contrast, T cells mature in the thymus, where they will multiply and differentiate into the sub-types of T cells: T-helper cells, T-regulatory cells, cytotoxic T-killer cells, T-memory cells and suppressor T cells. They then migrate to peripheral tissues or circulate in the blood or lymph. T-helper cells are capable of recognising foreign antigens and stimulating B cells to produce antibodies through their secretion of cytokines. T-regulatory cells control immune reactions while the cytotoxic T cells can bind to and kill infected/cancerous cells. T-memory cells are unique among the T cells in that once exposed to a pathogen during an infection they will persist long after an infection has passed and will recall the optimal strategy used to clear the pathogen, allowing for a quicker resolution of subsequent infection. Finally, suppressor T cells are capable of inactivating the B cells and killer T cells in order to aid in the return of the immune system to homeostasis (Janeway et al. 2002).

Innate immune response

The innate immune system is the body's first line of defence, utilising physical barriers, such as tight junctions in the skin, epithelial and mucous membrane surfaces (Gallo et al. 2011), and a non-specific defence to pathogens using white blood cells, known as leukocytes, developed from the hematopoietic stem cells in the bone marrow. They can be sub divided further into neutrophils, basophils, eosinophils, natural killer cells and antigen presenting cells, including macrophages and dendritic cells (Iwasaki et al. 2004). These immune leukocytes become activated during the inflammatory response: a natural, protective response of the body to foreign pathogens, cellular damage and injury. This involves complex interactions between immune cells, mediators and the tissue itself, in order to eliminate the stimulus which instigated the process. The function is ultimately to eliminate the cause, clear necrotic cells and initiate tissue repair (Ferrero-Miliani et al. 2007). This is achieved through the recognition of the evolutionarily conserved structures on pathogens, known as pathogen-associated molecular patterns (PAMPs) (Mogensen 2009). Activation of Pattern Recognition Receptors (PRRs) on immune cells by PAMPs results in the activation of the complement cascade, opsonisation, phagocytosis, induction of apoptosis (Janeway et al. 2002) and activation of inflammatory processes, stimulating the release of pro-inflammatory cytokines and chemokines and sometimes neurotoxic mediators (Glass et al. 2010).

Cytokines

Cytokines are a body of small proteins secreted from cells and used in intercellular signalling, most notably during inflammation (Feghali et al. 1997). They are key modulators of inflammation participating in acute and chronic inflammation via a complex network of interactions involving pro and anti-inflammatory molecules and signalling (Turner et al. 2014). Cytokines have been shown to

be released from a broad range of cell types including endothelial cells, smooth muscle cells, myeloid, T cells and glial cells (Barna et al. 1994; Cushing et al. 1990). Studies have implicated important pro-inflammatory cytokines such as IL-1β, tumour necrotic factor alpha (TNFα) and IL-6 as key mediators of systemic inflammation and signal transduction in the CNS (Dinarello 2005; Konsman et al. 2002). They are often subdivided based off the source of their production and the nature of the immune response, i.e. adaptive immunity, pro-inflammatory signalling or anti-inflammatory signalling (Turner et al. 2014). In addition to being pivotal mediators of the immune response it has been shown that elevated basal expression of pro-inflammatory cytokines is a pathological marker of several chronic conditions ranging from Alzheimer's disease to ageing and frailty (Franceschi et al. 2018; Mitnitski et al. 2015; Ng et al. 2015)

Chemokines

Chemokines are a family of small, secreted chemotactic cytokines with pivotal roles in the chemotaxis and regulation of leukocyte migration between blood and tissue via the establishment of chemotactic concentration gradients. Chemokines bind to G protein-coupled receptors resulting in receptor activation and triggering of an intracellular signalling cascade to regulate cell migration, adhesion, phagocytosis, cytokine secretion, proliferation and apoptosis (Bachelerie et al. 2014). Chemokines have been shown to be induced in response to the presence of inflammatory cytokines. Normal animals challenged intraperitoneally with IL-1β and TNFα showed increased expression of C-C motif chemokine ligand 2 (CCL2/MCP1) and C-X-C Motif chemokine ligand 1 (CXCL1) (Skelly et al. 2013). CCL2, also known as monocyte chemoattractant 1 (MCP1) is one of the best studied for its ability to promote extravasation of effector cells from the blood stream across the endothelium when induced by inflammatory stimuli (Deshmane et al. 2009; Ajuebor et al. 1998). Its ability to drive chemotaxis of monocytes (Huang et al. 2007; Qian et al. 2011) as well as lymphoid cells (Sallusto et al. 2008) to the tumour microenvironment in cancer models is well documented. However, chronically elevated CCL2 has been implicated in the pathogenesis of several chronic age-associated conditions including rheumatoid arthritis (Stankovic et al. 2009), atherosclerosis (Harrington 2000), multiple sclerosis (Mahad et al. 2003) and diabetes (Panee 2012) through sustained recruitment of immune cells and their resulting inflammation. For several years now research into identifying biomarkers associated with inflammatory conditions have investigated circulating chemokines as potential early biomarkers. C-X-C Motif chemokine ligand 13 (CXCL13/BCA-1) has been shown to be involved in the pathogenesis of several autoimmune and inflammatory conditions including multiple sclerosis and myasthenia gravis and has been proposed as a biomarker for them (Kramer et al. 2013). Consistent with the theory of inflammaging (see section 1.3.3), expression of chemokines including CCL2, CXCL10 and CXCL13 have been shown to be positively correlated with age (Antonelli et al. 2006; Lisignoli et al. 2003) and in a longitudinal

study to assess circulating biomarkers of frailty, CCL2 and CXCL13 were identified to have a strong positive association with frailty prevalence (Lu et al. 2016).

Complement System

The complement system is a critical part of the innate immune system playing a crucial role in host defence and inflammation. It is comprised of 30 proteins which typically circulate as inactive precursors until triggered by the detection of an immune stimulus. This will result in a proteolysis-based sequential activation cascade causing an escalation in local immune responses and formation of a membrane attack complex. Complement opsonizes pathogens and facilitates their subsequent removal by phagocytosis and cell lysis. Additionally, in recent years evidence has come to light indicating that triggering of the complement cascade also plays an important role in adaptive immunity involving T and B cells to aid in the elimination of pathogens and in maintaining the immunological memory to prevent a subsequent resurgence of the pathogen (Dunkelberger et al. 2010; Molina et al. 1996). Furthermore complement has been implicated in tissue regeneration, tumour growth and several human pathological conditions including age-related macular degeneration (Wagner et al. 2010).

Recent studies have begun to appreciate that there is significant crosstalk between the complement system and other systems. One such study by Lian et al. revealed a complement-dependent intracellular cross talk in which neuronal overproduction of Aβ resulted in the activation of astrocytic NF-κB, instigating an extracellular release of C3. This in turn encourages a pathogenic cycle whereby C3 in turn will interact with neuronal and microglial C3a receptor to impair the phagocytosis of Aβ and alter cognitive function (Lian et al. 2016). Normal aging has been shown to have a region-specific vulnerability of synapses to loss and dysfunction (Morrison et al. 2012) and C1q and C3 have both been shown to differentially affect this age-dependent synaptic vulnerability (Shi et al. 2015; Stephan et al. 2013). Indeed, cortical atrophy is one of the primary pathological markers in ageing-associated neurodegenerative diseases such as Alzheimer's disease and recent evidence has suggested that aberrant activation of the complement system mediates synaptic loss which can be mediated by targeted inhibition of the system (Hong et al. 2016; Shi et al. 2017; Dejanovic et al. 2018). Similar findings have been demonstrated in mouse models of Multiple Sclerosis (MS), Spinal Muscular Atrophy (SMA) and traumatic brain injury (TBI) with complement 3 (C3) mediated synaptic loss being ameliorated by genetic loss or inhibition of C3 in the murine brain (Hammond et al. 2020; Werneburg et al. 2020; Alawieh et al. 2021; Vukojicic et al. 2019; Lui et al. 2016).

Macrophages and Monocytes

Monocytes are the largest type of white blood cells and express a wide range of receptors which monitor and sense environmental changes. As such, they have been shown to play a crucial role in the immune response, as they are capable of killing pathogens via phagocytosis, production of ROS and inflammatory cytokines (Serbina et al. 2008). Originating in the bone marrow, monocytes will circulate throughout the bloodstream but are extremely infiltrative and will migrate into tissues, whereupon they can differentiate into dendritic cells or macrophages in response to inflammation (Liu et al. 2009; Nahrendorf et al. 2007). Homeostatic control of monocyte/macrophage development is regulated primarily by production of CSF-1 from stromal cells within the blood and tissue (Hamilton 2008; Lin et al. 2008; Hume et al. 2012).

Like monocytes, macrophages are tissue mononuclear cells capable of phagocytosis which are distributed throughout the mammalian body with a variety of morphologies dependent on the tissue, region, and state of activation. During development, erythromyeloid progenitors from yolk sac and foetal liver give rise to tissue-resident macrophages which persist during adult life as long-lived cells of widely varying morphology that turn over locally, notably within the liver, skin, spleen, gut and lungs (Gordon et al. 2017; Epelman et al. 2014). After birth however tissue resident macrophage populations who suffer high cellular turnover, such as the gut, rely on bone marrow-derived monocytes to replenish their numbers. Traditionally it had been believed that their primary origin was from the systemic reservoir of monocytes (Liu et al. 2009); however in recent years it has also been demonstrated that they can also develop directly from the bone marrow under certain conditions (Ajami et al. 2007). Therefore, depending on the particular tissue location and requirements, the tissue macrophages will consist of a mixed population of resident macrophages of embryonic origin and recruited marrow-derived blood monocytes. As with monocytes, they play a significant role in host response to metabolic, atherogenic and neoplastic stimuli contributing to wound repair (Wynn et al. 2016) and an immune defensive role in cellular immunity through their ability to phagocytose and kill ingested microbes. Furthermore, secreted cytokines from macrophages will initiate the local tissue activation as well as the activation of the adaptive immune response lymphocytes, B and T cells (De Groot et al. 1992).

The macrophage populations of the CNS include perivascular macrophages, meningeal macrophages, macrophages of the circumventricular organs and choroid plexus and of course, the most abundant and widely studied primary resident immune cells of the CNS, the microglia (De Groot et al. 1992). Microglia account for 5-12% of the total number of glial cells within the adult mouse brain (Lawson et al. 1990). Unlike peripheral macrophages, microglia originate not from progenitor monocytes or the bone marrow but are exclusively derived from yolk sac progenitors

(Ginhoux et al. 2010; Kierdorf et al. 2013) and acquire their unique regional density in specific CNS structures shortly after birth and a wave of microglial proliferation during the early postnatal stages (Nikodemova et al. 2015). Traditionally the microglial population was believed to be long lived and maintained by self-renewal (Lawson et al. 1992), in human studies the approximate rate of turnover has been shown to be 0.08% a day with the average lifespan of a microglial cell being 4.2 years (Réu et al. 2017). However recent evidence has shown that the population of microglia can be rapidly reconstituted by the proliferation of resident cells after a genetic or pharmacological elimination of microglia (Bruttger et al. 2015; Elmore et al. 2014). This high rate of proliferation in the adult mouse and human brain has been shown to be temporally and spatially coupled to intrinsic apoptosis, resulting in the upkeep of a comparatively steady number of microglia from the neonatal through to the aged individual (Askew et al. 2017). These data suggest that the microglia are a dynamic and heterogenous population capable of variable responses to stimuli.

Like their peripheral cousins however microglia are typically found in their homeostatic, surveillant state (Nimmerjahn et al. 2005) but upon activation microglia adopt a more condensed morphology and are capable of producing ROS, pro-inflammatory cytokines such as IL-1β (a central regulator of pro-inflammatory responses) and TNF-α as well as chemokines to attract other immune cells to the locus of stimulation (Dudvarski Stankovic et al. 2016). While microglia are the primary immune cells of the CNS they have been shown to work alongside several other cells with inflammatory roles including astrocytes, endothelial cells and perivascular macrophages under central and peripheral inflammatory conditions (Liu et al. 2020; Cai et al. 2020; Liddelow et al. 2017).

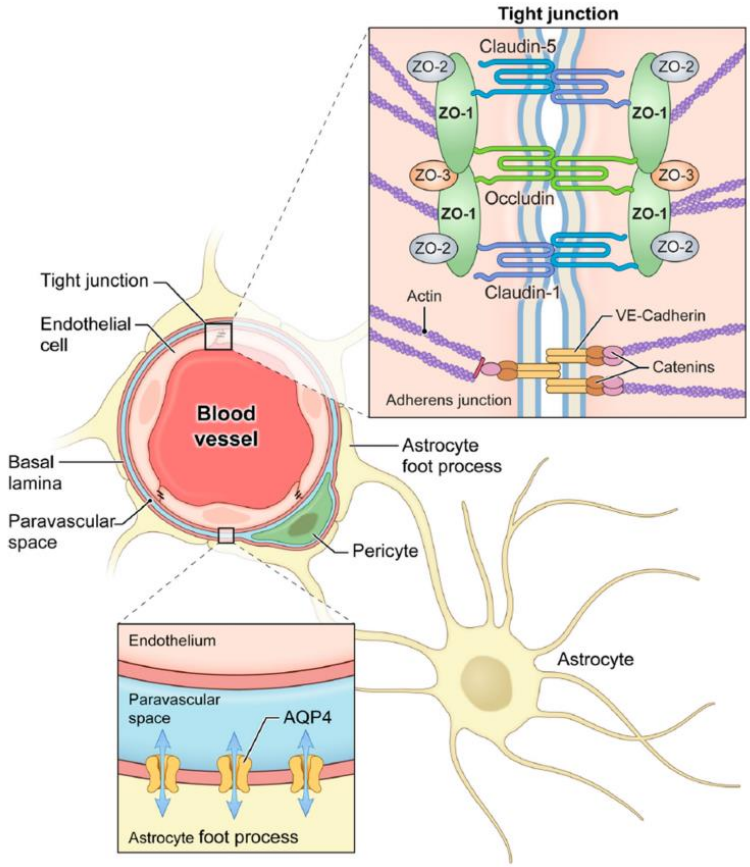

Figure 1.1: Blood-brain barrier tight junctions and aquaporin-4 channels. Tight junctions between endothelial cells of the microvasculature comprise the blood-brain barrier. Claudin-5, claudin-1, and occludin are key tight junction proteins in this barrier. All three contain four transmembrane spanning regions with cytosolic amino and carboxy termini. Zonula occludens (ZO) proteins ZO-1, ZO-2, and ZO-3 anchor these tight junction proteins to the endothelial cell actin cytoskeleton. Adherens junctions also contribute to the blood-brain barrier. Vascular endothelial cadherin (VE-cadherin) is the primary component of adherens junctions and is anchored to the actin cytoskeleton by catenins. Finally, foot processes of astrocytes envelop the microvasculature also contributing to the integrity of the blood-brain barrier. Aquaporin-4 channels are located on theses foot processes facing the vessel. These channels allow for bidirectional water flow between the astrocyte and the perivascular space (Murayi et al. 2016).

Endothelial cells are one of the two main cell types which form the blood brain barrier (BBB). Endothelial cells make up the walls of the blood vessels in the brain but do so, forming tighter gap junctions than the same cells in other tissue types. The second cell type, pericytes, are contractile cells which in turn surround the endothelial cells of blood vessels and control blood flow and permeability of these vessels through their contraction **(Figure 1.1).** Thus, entry and exit of cells, including peripheral immune cells, to the CNS is highly regulated by the blood brain barrier (BBB).

1.2.3 The Impact Of Systemic Inflammation's Upon The Brain

Immune privilege of the brain:

Traditionally the brain has been thought of as an immune-privileged organ due to its failure to mount adaptive immune responses to intracerebral infectious insults and slower, limited innate immune responses compared to those of the periphery. This was widely believed to be a result of the perceived isolation of the CNS (as a result of structures such as the BBB), the lack of draining lymphatics and the limited immunocompetence of the resident CNS macrophages, microglia. However, this concept has evolved significantly, and it is now clear that, while tightly regulated, the brain can initiate adaptive and innate immune responses. The former are dependent on the escape of soluble antigens from the brain via perivascular spaces and dural and nasal lymphatics (Galea et al. 2007; Engelhardt et al. 2017) while the latter are initiated by the brain's microglial population. There has been an explosion in our knowledge about this cell population in the last decade and this is clearly a competent resident tissue macrophage. The CNS is not only immune competent but actively interacts with the peripheral immune system (Steinman et al. 2004) and it is now well established that systemic inflammation can significantly impact on the brain's inflammatory, or neuroinflammatory, state. Much of the evidence we have for the interaction and influence between the immune and nervous systems arose from early studies examining the sickness behaviour response in rodents. These demonstrated that a peripheral challenge of the inflammatory cytokine IL-1β (Kent et al. 1992) or Poly I:C, a synthetic dsRNA viral mimetic (Fortier et al. 2004), were sufficient to elicit a fever response in rodents.

Typically, systemic inflammation occurs in response to infection, surgery or physical trauma, resulting in the induction of innate immune responses. Immune cells then respond to the challenge, migrating to the site of infection/injury and release inflammatory cytokines and mediators in an effort to resolve the event (Serhan et al. 2008). The BBB is a selectively permeable membrane which separates circulating blood from the brain's extracellular fluid. It is composed of endothelial cells linked together by tight junction proteins, such as claudins and occludins **(Figure 1.a)** (Haseloff et al. 2015). Under the right conditions peripheral immune cells and immunomodulatory agents such as TNFα can permeate, though saturable influx transport, retrograde axonal transport systems and at circumventricular organs where the BBB is incomplete and cytokines may cross by simple diffusion (D'Mello et al. 2014; Johanson 2018; Ghosh et al. 2018). In a mouse model of inflammatory liver injury it was shown that peripheral TNFα signalling was required to stimulate microglia to produce CCL2 and induce infiltration of monocytes into the subfornical region (D'Mello et al. 2009). Transendothelial migration (TEM) of peripheral immune cells into the CNS is a complex and dynamic process involving a meticulous series of adhesion and signalling events between leukocyte and endothelial cells. First chemokines, such as CCL2 induce increases in E-selectin on the endothelium

of blood vessels (Gerszten et al. 1999), this in turn induces rolling of neutrophils and macrophages (Sumagin et al. 2010). Rolling cells are then able to recognise chemokines expressed on the endothelium which induces upregulation of LFA-1 (αLβ2 Integrin) and Mac-1 (αMβ2 Integrin) required for the adhesion of neutrophils and macrophages respectively to the endothelium and subsequent TEM. Under inflammatory conditions, integrins allow the inflammatory cells to move to regions of vessels with high expression of cellular adhesion molecules such as VCAM and ICAM which will be upregulated under inflammation and will modulate TEM (Gorina et al. 2014); these regions are also areas with lower expression of basement membrane proteins (Wang et al. 2006). TEM occurs through two distinct mechanisms paracellular (between the endothelial cell-cell contacts) and transcellular (through the EC body). Under inflammatory conditions, VE-Cadherin junctions are disrupted and facilitates paracellular leukocyte diapedesis (TEM) (Gavard 2014).

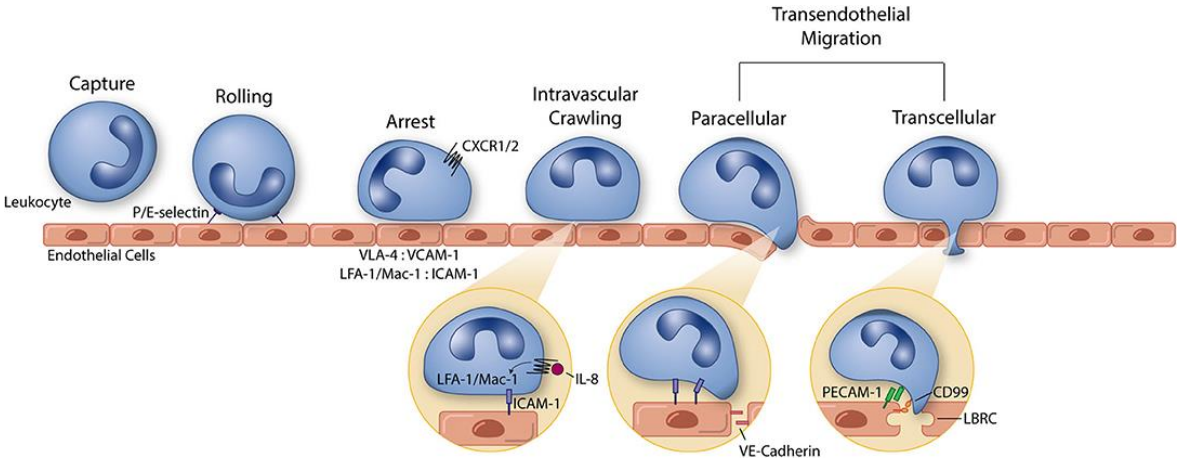

Figure 1.2: Transendothelial cell migration process (Salminen et al. 2020).: P and E selectin bind leukocytes to aid in the capture and rolling phases of extravasation. LFA-1/Mac-1: ICAM-1 and VLA-4: VCAM-1 form high affinity/avidity integrin/ligand interactions to halt leukocytes on the apical endothelial cell surface during arrest. Integrin activation is aided by chemokine signaling (neutrophil chemokine IL-8 and its receptors CXCR1/2 pictured here). In addition to leukocyte arrest and intravascular crawling, LFA-1/Mac-1: ICAM-1 interactions function to signal VE-cadherin junctional turnover and opening of the endothelial cell-cell junctions.

However under systemic inflammatory conditions, it is possible for the blood-CSF barrier to become compromised allowing leakage of blood into the CNS via the CSF (Johanson 2018). Indeed, TNFα transport across the BBB has been shown to be upregulated in response to LPS inflammation (Osburg et al. 2002), pathological aging mouse models (Banks et al. 2001) and spinal cord injury (Pan et al. 2003). Radioactive labelling of TNFα has shown its movement from the peripheral blood supply into the brain and CSF is facilitated by receptor-mediated endocytosis (Pan et al. 1997; Gutierrez et al. 1993). Studies investigating knockout mice lacking the TNFR1 and TNFR2 have shown that they are both involved in the saturable transport of TNFα across the BBB as their absence completely abolishes this transport (Pan et al. 2002).

Furthermore, cytokines themselves may also damage the BBB and increase its permeability through activation and destruction of tight junctions of microvascular endothelial cells (Dermietzel et al. 2007). In the middle cerebral artery occlusion model of ischaemic stroke it has been shown that following reperfusion microglial produced TNFα induces necroptosis in endothelial cells increasing the BBB permeability (Chen et al. 2019). Neutralisation of TNFα using a neutralizing monocolonal anti-TNFα antibody has been shown to attenuate CNS inflammation and BBB disruption when administered intraventricularly immediately after reperfusion in an ischaemic stroke model (Nawashiro et al. 1997; Yang et al. 1999; Chen et al. 2019) as well as following intraperitoneal injection in the experimental autoimmune encephalomyelitis (EAE) model of MS (Valentin-Torres et al. 2016). *In vitro* cultures of endothelial models of BBB's has shown that TNFα (500U/ml) also altered permeability through selective reorganization of F-actin filaments (Deli et al. 1995). In the same *in vitro* model Aslam et al. demonstrated that TNFα (10ng/ml) achieves this alteration of BBB structure through the reduction of the Claudin-5 promoter activity and downregulation of its mRNA expression (Aslam et al. 2012) courtesy of its induction of NFκB signalling and consistent with this BBB has been shown to be ameliorated by disruption of NFκB (Aslam et al. 2012; Trickler et al. 2005; Chen et al. 2019). Intracerebral injection of IL-1β (100U/µl) into juvenile rats has also been shown to be capable of altering the BBB permeability through the loss occludin, tight junctional proteins and zonula occludens-1 as well as a redistribution of Vinculin, a cell-cell junction adherens protein (Bolton et al. 1998). Intraperitoneal injection of the bacterial endotoxin LPS at high doses (3mg/kg) has been shown to result in significant disruption of the BBB as evidenced by the decrease in ^{14}C-sucrose, radioactive albumin in serum, indicating increased leakage of peripheral capillary beds (Banks et al. 2015). Recently Zhao and colleagues have demonstrated the presence of bacterial LPS in brain lysates derived from the hippocampus and superior temporal lobe of the neocortex of brains from Alzheimer's disease (AD) patient and have suggested it may originate in the gut and be able to cross physiological barriers to reach the hippocampus to induce these cognitive disruptions (Zhao et al., 2017). However, radioactive labelled LPS showed minimal penetration across the BBB when administered peripherally via intravenous injection, with most detectable LPS associated with the BBB, reversibly bound to endothelial cells and only a small volume crossing (0.025%) (Banks et al. 2010). This minimal penetration is unlikely to be capable of eliciting the neuroinflammation caused by peripheral LPS challenge and so it is propose that this is mediated by secondary inflammatory molecules, such as nitric oxide (NO) and interleukin 1 (IL-1) released by endothelial cells in response to the LPS (Singh et al. 2004). Additionally, it has been shown that under inflammatory conditions such as those induced by lipopolysaccharide (LPS) and IL-1, the enzyme cyclooxygenase-2 (COX2) is induced and will in turn synthesise the prostaglandin H2 (PGH2) from arachidonic acid (DuBois et al. 1998). PGH2 is the common substrate for a series of specific isomerase and synthase enzymes which will produce PGE_2, PGI_2, PGD_2, PGF_{2a}, and TXA_2 (Smyth et

al. 2009). These prostaglandins as small lipophilic molecules can diffuse from endothelial cells into the brain parenchyma resulting in the activation of glial cells in the BBB , which can in turn be conveyed to glial cells within the CNS, initiating a cascade of neural communication events and affecting the fever response (Louveau et al. 2015; Steinman 2004; Lima et al. 2017).

While inflammation's role in driving the progression of dementia is now largely accepted, the exact pathways which underlie this remain elusive. Villeda and colleagues demonstrated using heterochronic parabiosis that blood-borne factors, CCL2/CCL11, present in the systemic milieu of ageing individuals were responsible for regulating neurogenesis and cognitive function with young animals exposed to an old systemic environment showing decreased synaptic plasticity and impaired contextual fear conditioning and spatial learning and memory (Villeda et al. 2011). Peripheral challenge of Lipopolysaccharide (LPS), a bacterial endotoxin protein which has been widely used as a bacterial mimetic (Kelley et al. 2003; Palin et al. 2009) in order to induce an acute innate immune response similar to the initial stages of a bacterial infection and to allow the study of effects of this systemic inflammation on the CNS. Toll Like Receptors (TLRs) are the primary family of Pattern Recognition Receptors (PRRs) that recognise Pathogen Associated Molecular Pattern (PAMPs) and, of these, TLR4 is responsible for signal transduction in response to LPS binding. This is facilitated by the binding of LPS by LPS-binding protein and docking at a receptor complex comprising TLR4, CD14 and MD2). Within the CNS the microglia, the brain's resident immune cell population, also express TLR4 and have been shown to produce pro-inflammatory cytokines such as IL-1β and TNF-α upon activation (Lee et al. 1993). Studies of the systemic effects of LPS have shown that TNF-α is initially produced, which in turn induces IL-1β, which subsequently induces IL-6 (Dantzer et al. 1998).

These cytokines can cause significant perturbation of behaviour, largely coordinated by activation of the hypothalamus (Kelley et al. 2003). This behaviour, known as "Sickness Behaviour" describes a broad range of evolutionarily conserved adaptive alterations in body temperature and energy utilisation and changes in mood (anhedonia), motivation, spontaneous and social activity, fatigue, lack of appetite and sleep (Kelley et al. 2003). It is proposed that these changes are implemented by the host in an attempt to reprioritise activities in order to optimise the host response to the infection, by providing the optimal physiological environment (body temperature and energy substrate utilisation) to mount a response to infection (Kluger et al. 1979). An important driver of this is the mounting of a systemic pro-inflammatory response and corresponding CNS inflammatory changes that appear to contribute to this plethora of behavioural and bioenergetic changes. It is now thought that inducing a negative energy balance through caloric restriction, and the redirection of appropriate energy substrates to immune cells, can optimise bacterial or viral

clearance for the modest price of suppressed activity and short term weight loss (Maes et al. 2012; Aviello et al. 2021).

In a healthy individual the inflammatory mediators produced in the brain in response to the systemic inflammation typically do not cause tissue damage or neurodegeneration (although this is dose-dependent) but rather, acts upon the brain regions responsible for this sickness behaviour co-ordinating the immune response. However, as discussed above, animals suffering chronic inflammation, due to neurodegeneration, obesity or advanced age are vulnerable to exaggerated inflammatory and sickness behaviour responses. This exacerbated sickness behaviour in vulnerable animals in response to peripheral challenge has been shown previously in the neurodegenerative ME7 model of murine prion disease where animals at the preclinical stage of disease (19 weeks post-inoculation) who were challenged with a 100μg/ml bolus of LPS exhibited an exaggerated sickness behaviour response, reduced locomotor activity and hypothermia compared to control animals (Combrinck *et al.* 2002). An exaggerated sickness behavioural response to peripheral immune activation has also been demonstrated in aged mice with reductions in social behaviour and activity persisting significantly longer than that of adult control mice treated with LPS as well as greater reductions in food intake and body mass than controls. Furthermore, these aged mice exhibited exaggerated and prolonged induction of inflammatory cytokines and oxidative stress within the aged brain compared to LPS challenged adult controls (Godbout et al. 2005). This exaggerated sickness behaviour in response to existing prior pathology might be seen as a maladaptive response by the organism, divergent from the normal adaptive nature of sickness behaviour in resilient, healthy individuals (Cunningham et al. 2013). This maladaptive response has the potential for adverse consequences in vulnerable individuals, suffering from an existing condition. Elderly patients with dementia or AD frequently demonstrate episodes of delirium following peripheral infection which is likely a manifestation of this exaggerated sickness behaviour (George et al. 1997; Elie et al. 1998; Koivisto et al. 1995), with negative long term consequences for the individual. In animal studies examining chronic inflammation, due to neurodegeneration, obesity or advanced age, it has been shown that vulnerable animals may suffer increased BBB permeability (Farrall et al. 2009; Salameh et al. 2019) and regulation of the infiltration of immune cells, molecular transport of cytokines to the brain might be altered; resulting ultimately in an altered central inflammatory and sickness behaviour response (D'Mello et al. 2014).

1.2.4 Microglia – the brain's resident immune population

Unlike all other cells in the brain which are derived from neuroectodermal cells, microglia are derived from progenitors in the embryonic yolk sac, which migrate into the developing brain early on and form the basis of the microglial population (Ginhoux et al. 2010). They are broadly distributed throughout the brain and spinal cord (Lawson et al. 1990) and account for between 15-

20% of the total cell population within the brain parenchyma (Carson et al. 2007; Melchior et al. 2006). Microglia are heavily responsible for maintaining immune homeostasis within the CNS and constantly survey and monitor their environment, determining actions in response to the signals that they receive (Davalos et al. 2005; Nimmerjahn et al. 2005). They can be activated by a variety of stimuli including PAMPS (such as LPS), chemokines, cytokines and protein aggregates like Aβ (Boche et al. 2013).

Microglia can be found in a variety of morphological states dependent on their functional status at any given time. Typically, microglia are found in their homeostatic, surveillant state which is characterised by heavily ramified branches in constant motion, extending and contracting to test the environment (Nimmerjahn et al. 2005). Transcriptome analysis of microglia have shown that microglia in this surveillant state show higher expression of fractalkine, *Cx3cr1,* osteonectin, and *Sparc* (Holtman et al. 2015) and of the transcription factor Sall1 (Buttgereit et al. 2016) which is typically associated with repair, down regulation and protection from inflammation. As such it is broadly considered to be in an anti-inflammatory state (Cherry et al. 2014). Upon detection of disruption within the CNS environment microglia are capable of mounting a swift response through a host of different mechanisms. Activated microglia typically contract their branches to adopt a more condensed morphology. In this activated state they are capable of producing pro-inflammatory cytokines such as IL-1β (a central regulator of pro-inflammatory responses) and TNF-α as well as chemokines to attract other immune cells to the locus of stimulation (Dudvarski Stankovic et al. 2016). Additionally, they can emit a cytotoxic burst of H_2O_2 or NO to kill foreign micro-organisms or dying cells. Furthermore, microglia are capable of adopting an amoeboid morphology reflecting and facilitating their capability to phagocytose and degrade foreign objects, micro-organisms and dying cells. As part of their phagocytic capabilities microglia can also act as antigen presenting cells (APCs) in order to activate cells of the adaptive immune system when they have been activated to upregulate their levels of MHC II (Wlodarczyk et al. 2014) although evidence that they can present antigens to naïve T cells is still lacking.

The diversity displayed by microglia allows them to carry out their many homeostatic functions. However, their phenotypic diversity may also account for their susceptibility to dysregulation in age-related neurodegenerative diseases. As microglia age, their environmental sampling capabilities are compromised. This is characterised by a decrease in the expression of genes involved in matrix interaction and genes such as *Trem2* (and it's signalling partner *Tyrobp*) and *P2ry12*, which sample the extracellular environment for foreign microbes, cell debris and released purines (Hickman et al. 2013). Healthy microglia typically return the brain to homeostasis in order to minimise damage to the CNS. Under normal conditions neuronal ligands such as CD200 and fractalkine can induce an anti-inflammatory state in the microglia to assist in the resolution of a

pro-inflammatory response and return to homeostasis. However, as neurons degenerate these signals might be lost and with it their anti-inflammatory effect, potentially resulting in poor resolution of homeostasis and prolonged periods of inflammation.

Microglial priming

Microglia can produce pro-inflammatory mediators in response to intrinsic and extrinsic stimuli under tightly regulated conditions. However, under chronic activation, such as that imposed under neurodegenerative conditions and ageing, microglia display an exaggerated IL-1β response to a secondary, acute, inflammatory insult. When microglia assume this "preconditioned" activated state it is known as "priming". Macrophage priming was first described using IFNγ to sensitise macrophages to sub-threshold doses of LPS, resulting in exacerbated pro-inflammatory effects (Williams et al. 1992; Pace et al. 1983). Microglial priming was subsequently demonstrated in the ME7 prion model of chronic neurodegeneration and was defined as an exaggerated production of IL-1β and iNOS in response to a secondary inflammatory stimulus of LPS (Cunningham et al. 2005). Since then it has been corroborated in mouse models of ageing (Godbout et al. 2005), Parkinson's (Godoy et al. 2008), Wallerian degeneration (Palin et al. 2008) and AD (Lopez-Rodriguez et al. 2021; Holtman et al. 2015). The diseased brain has been shown to have increased expression of chemokines from primed astrocytes resulting in elevated cellular infiltration of immune cells (Hennessy et al. 2015, Lopez-Rodriguez 2021). This exaggerated production of pro-inflammatory cytokines by primed glial cells can have significant long-term negative consequences on neuronal function however. In the ME7 model of prion disease IL-1β has been shown to contribute to brain injury in mice initially challenged with LPS (Skelly et al. 2019). Furthermore, it was demonstrated that the progression of the neurodegenerative disease was accelerated by the acute challenge of the secondary stimulus, LPS (Cunningham et al. 2009).

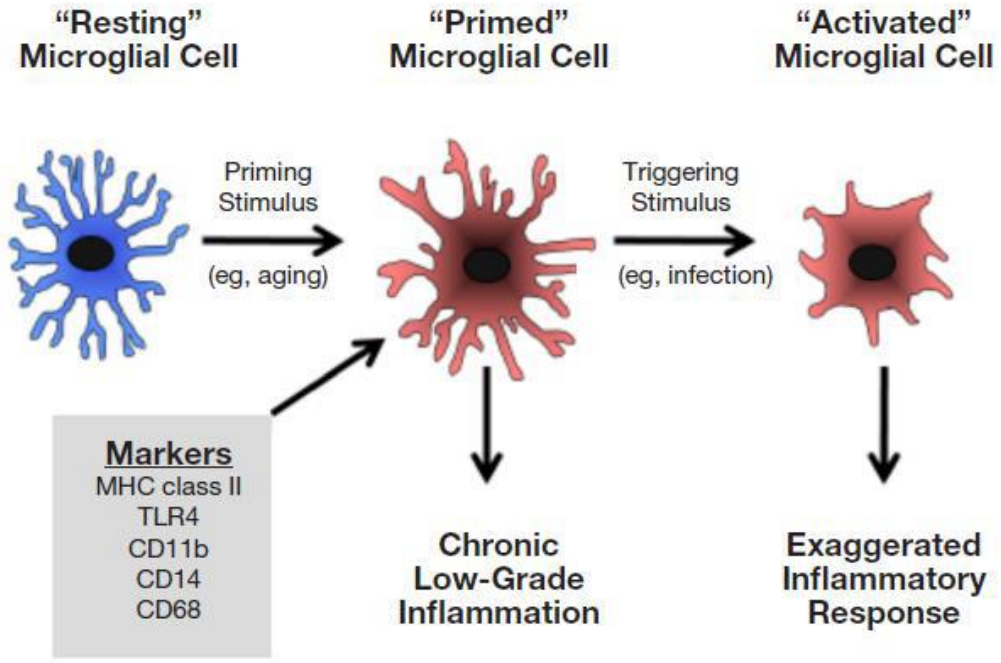

Figure 1.3: Microglial priming: priming of microglia (with ageing) and the subsequent inflammatory response (Dantzer et al. 2008; Perry et al. 2007)

The chronic stressor, or sensitizing signal which induces this primed phenotype in glial cells **(Figure 1.3)** may be unique to the disease state in question. In the Tg-2576 model of Alzheimer's Disease excessive IL-1β was produced in the cortex and hippocampus of Tg+ animals compared to Tg- when subject to a secondary LPS challenge i.v. (Sly et al. 2001). The inevitable and irreversible chronic ageing process has also shown to result in primed glial cells as shown by their exaggerated IL-1β expression when subsequently challenged with LPS (Henry et al. 2009). In ageing the phenomenon known as "Inflammaging" where by a chronic low grade state of inflammation manifests and persists has been hypothesised to be a driving force in this glial priming (Fransceschi et al. 2006). Although the majority of studies done to date have utilised LPS as an acute trigger 'stressor' event, the appearance of LPS in the CNS is an extremely infrequent pathological event. Conversely, sterile inflammation such as that resulting from traumatic brain injury or stroke is more common in patients. Trauma and stroke frequently occur in the elderly population and can result in a significant decline in physiological reserves of the patient. It has been demonstrated that microglial cells primed by ME7 prion disease, also produce exaggerated levels of IL-1β and chemokines in response to local challenge with IL-1β or TNF-α (Hennessy et al. 2015) and this has been partly replicated in the APP/PS1 model of AD (Lopez-Rodriguez et al. 2021).

Under healthy homeostatic conditions microglia express a signature set of hub genes including *Mertk, Tmem119, P2ry12, P2ry13, Sparc* and *Cx3cr1*. However, the expression of these genes is

decreased upon activation or the adoption of the primed phenotype (Butovsky et al. 2014). A recent study isolating microglia and analysing their RNA expression profile demonstrated that microglial activation and priming induces a rather conserved transcriptional signature albeit with ageing and disease-specific aspects. The core hub signature of primed microglia **(Figure 1.4)** shows upregulation in expression of *Axl, Clec7a, Lgals3* and *Cd11c (Itgax)* (Holtman et al. 2015). Of particular interest in this core hug signature of primed microglia is *Clec7a.*

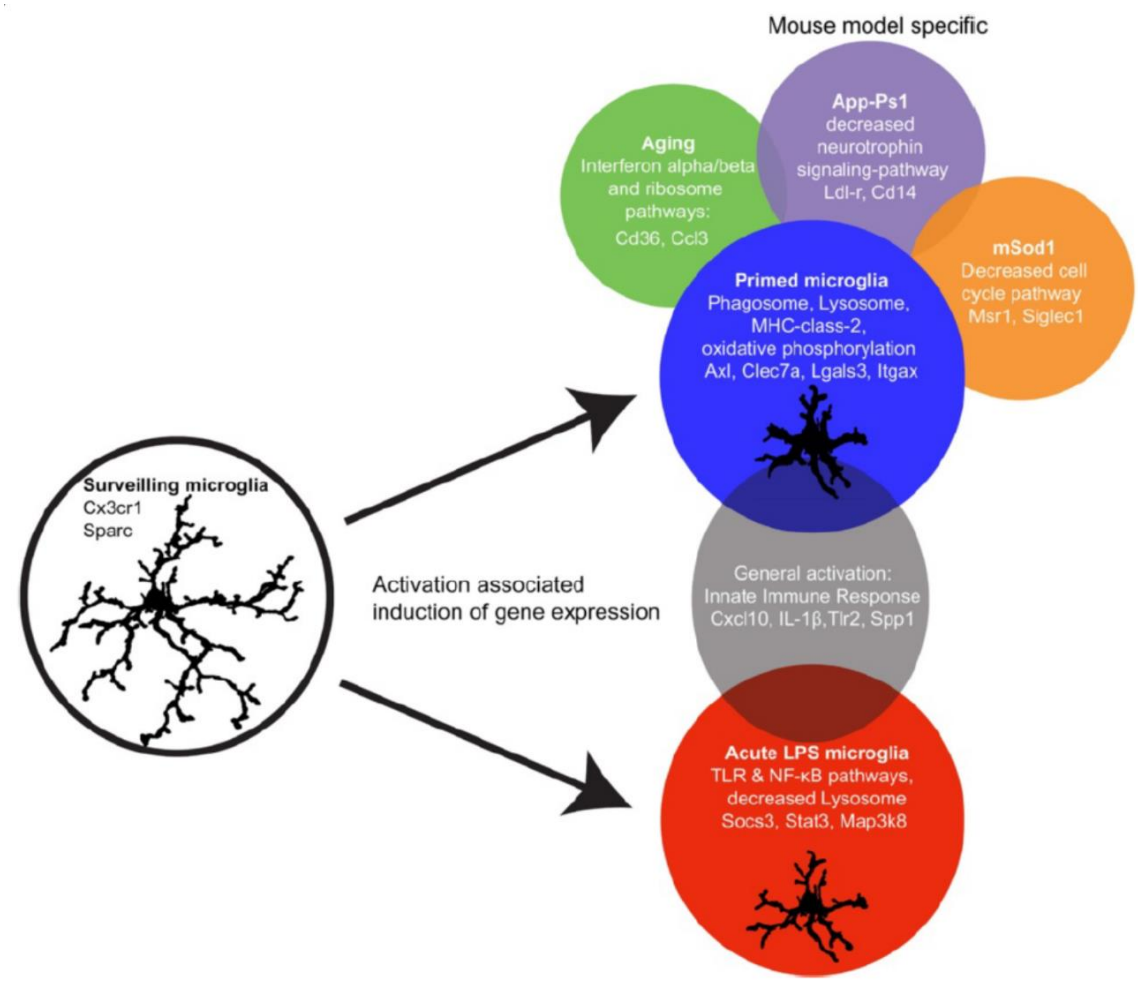

Figure 1.4: Transcriptional signature of microglial states: summary figure describing core microglial signatures under different conditions and pathologies (Holtman et al. 2015)

C-type lectin-like receptors (CTLRs) are expressed mostly by myeloid cells and have been gaining growing attention for their role in both innate and adaptive immunity. Of increasing interest in CNS immunity is the C-type lectin domain containing 7a (*Clec7a*), which encodes the transmembrane protein Dectin-1, and as discussed above is one of the core hub signature genes of primed microglia (Holtman et al. 2015). Since then it has been shown that β-Glucan activation of Dectin-1 on microglia *in vitro* primes microglia (Heng et al. 2021; Van der Meer et al. 2015). This pattern recognition receptor has also been shown to be detrimentally pathogenic in animals models of spinal cord injury (Gensel et al. 2015) stroke (Ye et al. 2020), EAU (Stoppelkamp et al. 2015) and in

an intracerebral haemorrhage model its deletion was shown to alleviate neurological dysfunction and promote an anti-inflammatory phenotype, encouraging hematoma clearance (Fu et al. 2021).

Dectin-1 is known to recognise and bind a variety of fungal molecules including β-1,3-glucan (Dennehy et al. 2007) and zymosan (Yoo et al. 2021) and is known to be important in orchestrating innate immune responses (Deerhake et al. 2019). Dectin-1 ligand binding has been most widely studied for fungal molecules such as β-glucan and zymosan to date, however these are considered unlikely to be endogenous ligands within the CNS but cannot be ruled out as recent data has suggested bacterial LPS in brain lysates derived from the hippocampus and superior temporal lobe of the neocortex of brains from Alzheimer's disease (AD) patient may originate in the gut and be able to cross physiological barriers to reach the hippocampus to induce these cognitive disruptions (Zhao et al., 2017). However, as discussed earlier radioactive labelled LPS showed minimal penetration across the BBB %) (Banks et al. 2010) and as such increasing study has been done into identifying potential ligands within the CNS. Of note among these have been vimentin (Thiagarajan et al. 2013), galectin-9 (Lgals9) (Daley et al. 2017; Itoh et al. 2017) and annexins (Bode et al. 2019). Dectin-1 binding is capable of inducing signalling via two divergent pathways; a neuroinflammatory response via the CARD9-dependent pathway (LeibundGut-Landmann et al. 2007) or a more beneficial neuroprotective pathway independent of CARD9 (Deerhake et al. 2021).

Of the two, the Syk-CARD9-dependent coupling is the best studied in the CNS with microglia challenged with β-Glucan showing increased ROS production and phagocytosis (Shah et al. 2008; Shah et al. 2009). Pathway analyses have revealed that Card9-dependent genes showed enrichment in pathways for pro-inflammatory factors, such as TLR signalling, MyD88 signalling, IL-1 signalling and were enriched for NFκB-family TF-binding sites **(Figure 1.5)** (Deerhake et al. 2021). The CARD9-independent pathway is less well documented but in the EAE model of MS, Deerhake and colleagues demonstrated that it is mediated by the nuclear factor of activated T cells (NFAT) and is associated with a more neuroprotective response (Deerhake et al. 2021). Recently, Deerhake and colleagues demonstrated that Dectin-1 activation by astrocytic Lgals9, is capable of promoting a beneficial myeloid-cell-astrocyte cross talk in the EAE model through the upregulation of the neuroprotective cytokine Oncostatin M (Osm) production from myeloid cells **(Figure 1.5)** (Deerhake et al. 2021).

Taken together these data highlight the important potentially pathogenic role of Dectin-1 in ageing and disease pathology but also the substantial impact which the ligand itself, as well as the timing and frequency of ligation, will have upon the subsequent immune tolerising or priming effect on the CNS innate immune response.

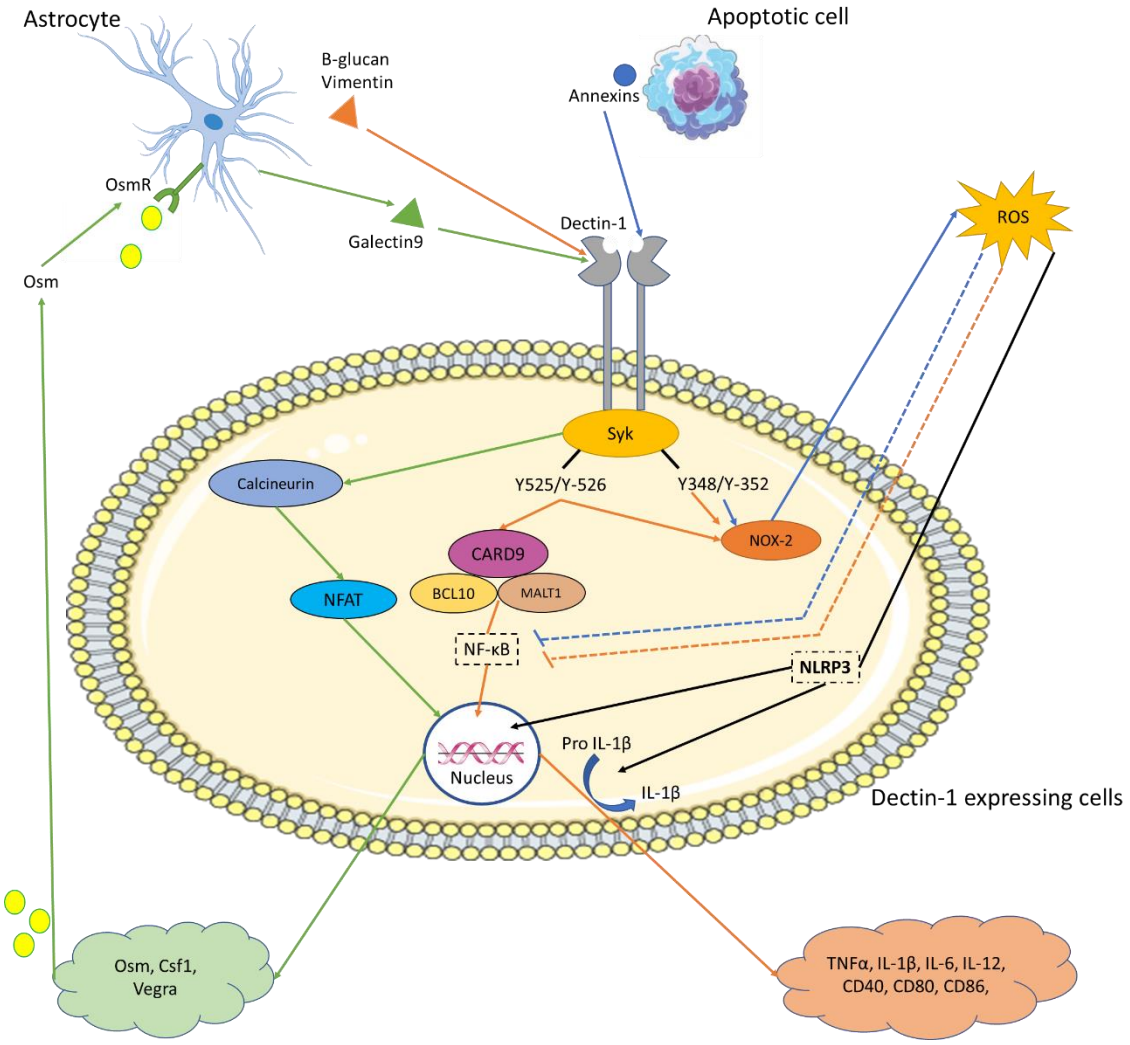

Figure 1.5: Graphical representation of Dectin-1 signalling pathways in Dectin-1 expressing dendritic and microglial cells of the CNS adapted from (Deerhake et al. 2021; Bode et al. 2019; Thiagarajan et al. 2013; Tang et al. 2018; Kalia et al. 2021).

1.2.5 Heterogeneity of microglia in the young and aged brain

As stated previously in this text, ageing is associated with changes in the neuroinflammatory environment and inevitably impacts upon the microglial population. Microglia are present in large numbers throughout the brain, but they are not uniformly distributed. The hippocampus, substantia nigra, basal ganglia and olfactory telencephalon have been shown to be the most densely populated areas of the CNS. In contrast, the cerebellum, brain stem and fibre tracts are markedly more sparsely populated (Lawson et al. 1990). Furthermore, it has been shown that the human brain has a higher density of microglia within the white matter compared to the grey matter (Mittelbronn et al. 2001). The inverse is true for the mouse brain which shows greater density within the grey matter (Farthing 1995). Recent studies have demonstrated that microglial responses to injury, disease and inflammatory challenge also vary dependent on their neuroaxis location. For instance, lesion-induced inflammatory responses in the brain and spinal cord demonstrated that the acute inflammatory response was significantly stronger in the spinal cord

than in the cerebral cortex. Similarly, the area of BBB breakdown was substantially larger and the numbers of recruited macrophages and neutrophils was greater in the spinal cord compared to the brain (Schnell 1999). Furthermore, LPS treatment in young and aged mice revealed that white matter regions such as the fimbria, corpus callosum and cerebellar white matter were vulnerable to increased expression of FcγR1 following systemic challenge compared to grey matter areas such as the dentate gyrus (Hart et al. 2012). The ageing brain adds a further layer of heterogeneity to the microglial population with aged mice displaying increased expression of CD11b, CD11c, CD68, F4/80 and FcγRI in the white matter compared to the grey matter and this upregulation was most pronounced in the caudal areas compared to the rostral areas of the aged brain (Hart et al. 2012). The marked alterations in expression of CD11c in the white matter of the cerebellum of aged mice is of particular interest. CD11c is a known cellular marker of dendritic cells, of which the brain has very few, and it has been demonstrated in an experimental autoimmune encephalomyelitis model that $CD11c^{+}$ microglia are formidable antigen presenting cells for a T cell proliferative response, thereby enhancing the inflammatory response (Wlodarczyk et al. 2014). Similarly, animals subjected to high fat diets have been shown to display morphological changes of microglial with elevated expression of phagocytic markers such as *Clec7a* (Yin et al. 2018). Conversely, animals on a low-fat diet showed reduced levels of these markers. Interestingly, *Clec7a* and *Cd11c* have both been identified as core genes known to be upregulated in activated primed microglia under neuroinflammatory conditions (Holtman et al. 2015).

These findings suggest that the ageing of microglia occurs non-uniformly in a region-dependent manner. This has been further highlighted in a recent study by Grabert et al., it was shown that in the young adult brain (4 months old) the transcriptional signature of microglia was most distinct within the cerebellum when assessed by principle-component analysis (PCA) compared to the cortical and striatal microglia whose PCA plots of their expression profile converged heavily. The hippocampus exhibited an intermediate profile, between that of the cerebellum and the cortical/striatal areas. Analysis of Gene Ontology biological processes using the Database for Annotation, Visualisation and Integrated Discovery (DAVID) revealed that these differences were a result of genes related to immune function and energy metabolism being heavily differentially regulated across the four regions. The immune vigilant cerebellum and hippocampus were shown to have higher expression of MHC I and II alongside other antigen and self-recognising genes. However, with increasing age it was shown that these patterns changed, with the cerebellar microglia increasing in distinctiveness while the hippocampal microglia became less distinctive (Grabert et al. 2016). Despite this alteration to their transcriptional pattern, the core microglial signature differentiating them from macrophages was retained.

It was shown that the cerebellar and hippocampal microglial exist in a more immune vigilant state compared to cortical microglia as assessed by their immune alertness transcriptional profiles as well as using a bacterial phagocytosis and replication assay, with cortical microglia failing to control net replication of internalized bacteria compared to the cerebellum (Grabert et al. 2016). The authors have posited that these regions, where microglia demonstrate stronger immune functioning capabilities, may coincide with regions of the brain where an evolutionary drive for greater protection exists (Grabert et al. 2016). Mounting data suggests that the hypothalamus is also significantly vulnerable to age-associated deficits and immune activation (Suda et al., 2021). While these heightened immune capabilities serve a neuroprotective role under normal conditions, they come with the potential of being highly damaging and neurotoxic should the microglial neuroinflammatory processes become dysregulated which can have substantial widespread impact upon cognitive function across the brain courtesy of its intricate connectivity.

The hippocampus is widely studied for its notable roles in learning and memory and has been shown to have substantial neuronal projections between each of these regions of interest; and disruption has been shown to have significant implications for cognitive and metabolic function **(Figure 1.6)**. Long-term excitation of inputs from the ventral hippocampus (vHIP) to the medial prefrontal cortex (mPFC) in wild-type mice has been shown to impair social memory, whereas their long-term inhibition in Mecp2 knockout mouse model of the autism spectrum disorder Rett syndrome mice rescued social memory deficits (Phillips et al., 2019). The primary motor cortex also runs extensive projections through the corpus callosum (Muñoz-Castañeda et al., 2021), one of the primary white matter tracts of the hippocampus whose function is to integrate and transfer information from both cerebral hemispheres to process sensory, motor, and high-level cognitive signals (Tzourio-Mazoyer, 2016). The cerebellum is also classically associated with motor control, but a mounting body of evidence suggests its functions may extend to cognitive processes including navigation (Babayan et al., 2017; Petrosini et al., 1998; Stoodley et al., 2017). This has been proposed to be a product of inputs to the hippocampal regions including the dentate gyrus and subiculum (SUM), directly from the cerebellar vermal lobule VI routed through caudal fastigial nucleus (FN), and from Crus I, routed through the dentate nucleus (DN) (Watson et al. 2018; Iglói et al. 2015; Yu et al. 2015) and relayed projections through the thalamus nuclei which are connected to the same cerebellar nuclei (Bohne et al. 2019). Furthermore, there is growing reports of the role of the cerebellum's modulation of immune function, visceral and behavioural responses through its projections between the IN, DN and FN to the lateral hypothalamic area (LHA), posterior (PHA), and dorsal (DHA) hypothalamic areas; the supramammillary (SMN), tuberomammillary (TMN) and lateral mammillary (LMN) nuclei; the dorsomedial (DMN) and ventromedial (VMN) nuclei; and in the periventricular nuclei (PVN) (Cao et al., 2013; Jing-Ning et al., 2006).

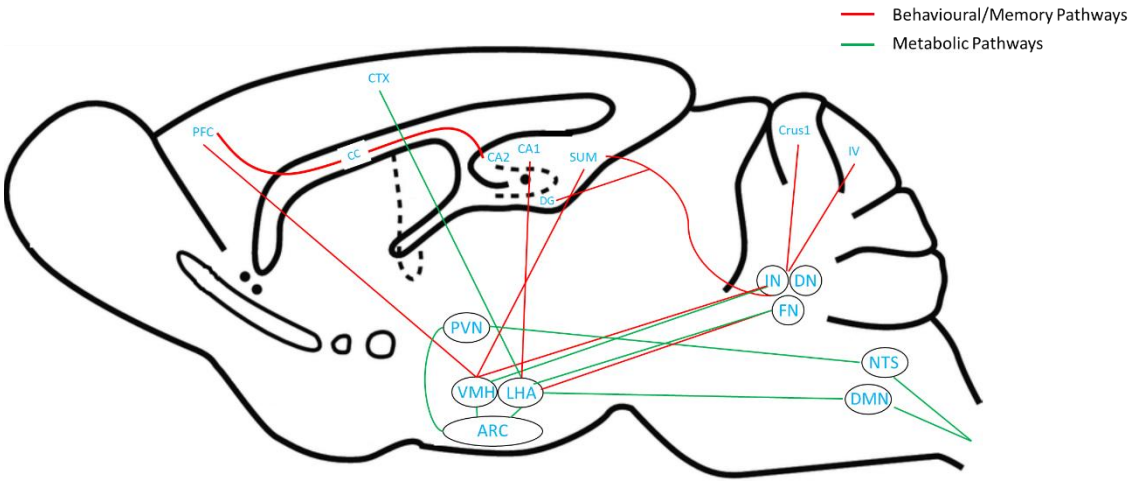

Figure 1.6: Neuronal projections of the hippocampus and hypothalamus to the cortex and cerebellum involved in metabolism and behaviour

The hypothalamus is best known for its role as the central hub for the regulation of food intake and metabolism, as it integrates homeostatic and hedonic circuits courtesy of activating projections originating in cortical regions, such as the agranular insula, ventrolateral orbitofrontal and secondary motor cortex with the LHA as has been demonstrated in ALS patients and models where disruption of thiese projections induces hypermetabolic states (Bayer et al., 2021). The ventromedial hypothlamaus (VMH) mainly receives neuronal projections from the hypothalamic arcuate nucleus (ARC) and projects their axons to the ARC, dorsomedial nucleus (DMN), LH and brain stem regions such as the (NTS) for the regulation of satiety and glucose homeostasis (Bouret et al., 2004). Ablation of this region has been shown to result in hyperphagia, obesity and hyperglycaemia (Shimzu et al., 1987). Indeed, the hypothalamic PVN and suprachiasmatic nucleus (SCN), are responsible for regulating changes in metabolic settings, temperature and glucose availability (la Fleur et al.; 2000; Kalsbeeket al., 2012; Bohlandet al., 2014; Guzm´an-Ruizet al., 2015). The SCN is known to be a key regulator of maintaining an animal's natural circadian rhythm can also set day–night differences in the intensity of the temperature and cytokine response to help leucocytes fight infection while also inhibiting the growth of certain microorganisms (Elmquist et al., 1997). Ablation has been shown to result in disturbed circadian rhythmicity and exacerbated inflammatory responses (Castanon-Cervantes et al., 2010; Guerrero-Vargas et al., 2014; Guerrero-Vargas et al., 2015). This is consistent with extensive reports in the literature of the importance of maintaining healthy circadian rhythms in healthy biological ageing and longevity with disrupted night/day routines and poor diet and exercise substantially worsening these longterm outcomes (Acosta-Rodriguez et al. 2021). Indeed, the hypothalamus is a hub for the control of these autonomic and endocrine functions as well as the emotional and behavioural state courtesy of its abundant white matter connections with both brainstem and the cerebrum. Depression has been shown to result in antibody-mediated immune activation, with depressed patients usually showing

elevated pro-inflammatory cytokines, suggesting an enhanced inflammatory response (Postal et al., 2015). Projections between the hippocampal ventral CA1 population and the LHA have been shown to be activated by anxiogenic stimuli (Jimenez et al., 2018). The hippocampal SUM and PFC also has substantial inputs to the ventromedial hypothalamus (VMH) which have been shown to modulate social behaviour in mice (Lo et al., 2019). The hypothalamic supramammillary nucleus (SMN) sends long-range projections to hippocampal area CA2 pyramidal neurons (PNs), this connection is critical for social memory (Cui et al., 2013; Robert et al. 2021), novelty (Ito et al., 2009) and conditioned fear responses (Beck et al., 1995).

All of these data emphasise the high degree of interconnectivity and overlapping functionality between distinct brain regions and the crucial role that microglia hold in maintaining homeostasis, function and integrity within them. However, while their primary objective might be shared across the brain, their distribution and function is highly region-dependent and significant differences are evident in microglial responsiveness to injury and infection in white matter regions compared to grey matter. Furthermore, their dysregulation carries with it potentially severe consequences and it has been shown that the expression profile of microglia is sensitive to age-related damage and loss of function in a region-dependent manner. However, it is important to stress that ageing itself is not a uniform process. To fully understand the extent to which age impacts on microglial activation and function it is important to interrogate the disparity between chronological age and biological age that is evident within the ageing population. In the following sections I will discuss ageing per se and also consider the phenotype of frailty.

1.2.6 Astrocytes

Named by Pío del Río-Hortega for their distinct star shaped morphology, astrocytes are the most abundant of the cells in the CNS. These ubiquitous cells are pivotal in maintaining homeostasis within the CNS providing metabolic support to neurons, regulating the synaptic levels of glutamate and extracellular ion concentrations as well as synthesising and releasing glutathione and gliotransmitters such as calcium, ATP and BDNF, maintain water homeostasis, defence against oxidative stress, neurogenesis and synapse modulation (Parpura et al. 2010; Kim et al. 2019; Chun et al. 2018). Furthermore, astrocytes are capable of expressing cytokines and chemokines such as TGF-β, IL-10, Il-1β, TNFα, CXCL-1 and CCL2 (Fuller et al. 2009; Eroglu 2009; Zamanian et al. 2012). In addition to their intricate relationship with neuronal synapses at the tri-partite junction, astrocytes are responsible for modulating the status of microglial activation (Von Bernhardi et al. 2004; Eyüpoglu et al. 2003). Reactive astrocytes, as has been discussed, secrete factors such as adenosine triphosphate (ATP), the chemokine fractalkine (CX3CL1), and complement factor 3 (C3), each of

which can bind to the corresponding microglial receptor, enhancing or modulating microglial activation and the subsequent release of microglia -derived pro-inflammatory agents (Chun et al. 2018). This astro-microglial crosstalk under chronic conditions has been referred to as the astrogliosis-microgliosis axis and is implicated in driving progression of conditions such as AD by exacerbating Aβ plaque formation and neuronal death **(FIgure 1.7)** (Carter et al. 2012; Furman et al. 2012; Chun et al. 2018).

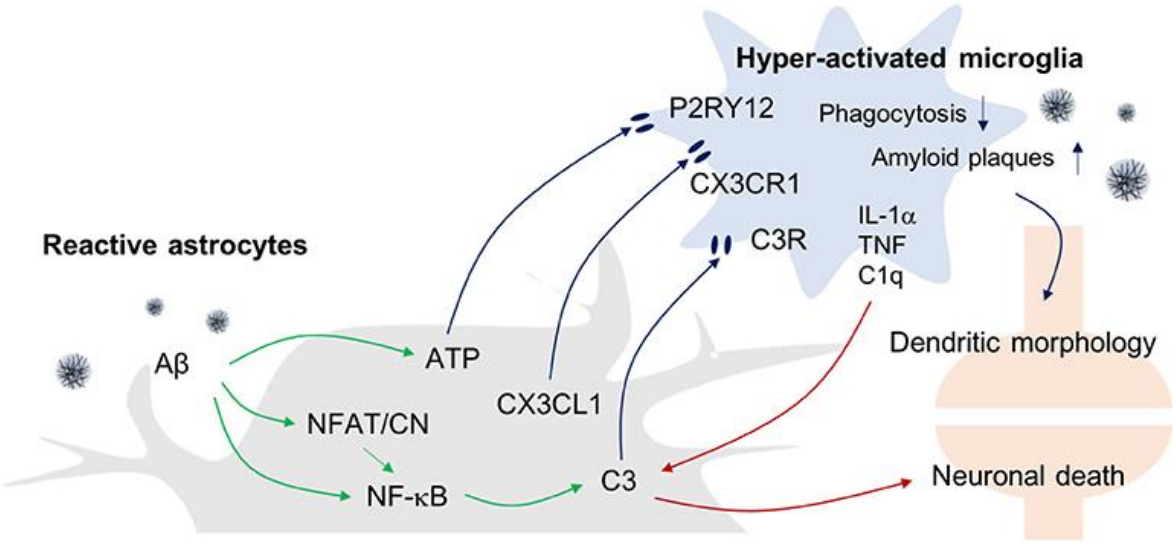

Figure 16. Astrogliosis-Microgliosis Axis (AMA) in AD. Schematic showing the crosstalk between reactive astrocytes and hyper-activated microglia in AD. It has been reported that reactive astrocytes release ATP, CX3CL1, and C3 to activate microglia, whereas the activated microglia release inflammatory molecules such as IL-1α, TNF-α, and C1q to increase C3 expression in astrocytes, which consequently causes an increase in AD pathology indices such as Aβ plaques and neuronal death (Chun et al. 2018).

Astrocytes exposed to proinflammatory cytokines IL-1β and TNFα *in vitro* have been shown to demonstrate markedly decreased glycogen levels, altered glutamate-stimulated glucose utilisation and lactate release, decreased cellular glutathione content with a corresponding increase in glutathione concentration in the extracellular space as well as stimulating ROS production. It was found that these modifications to the astrocytic metabolism by pro-inflammatory cytokines also modulated neuronal susceptibility to an excitotoxic insult in co-cultures (Gavillet et al. 2008; Bélanger et al. 2011). Conversely, it was demonstrated that exposure to the anti-inflammatory IL-10 was found to partially ameliorate these pro-inflammatory cytokines effects on astrocytes' metabolic profiles (Bélanger et al. 2011). Taken together these findings demonstrate that astrocytes' metabolic profile are differentially affected by the inflammatory environment with functional consequences for surrounding neurons.

Recent studies have attempted to categorise and describe reactive astrocytes into two distinct phenotypes, A1 and A2, in the brain. The putative A1 reactive phenotype is characterized as being induced under systemic inflammatory conditions with a corresponding pro-inflammatory phenotype that is neurotoxic. In contrast A2 reactive astrocytes are elicited under conditions such as stroke and reportedly act in a more neuroprotective fashion (Liddelow et al. 2017). A1 reactive astrocytes are induced following a release of pro-inflammatory mediators such as TNFα and IL-1α from microglia and are defined as showing elevated C3 and increased transcript expression of markers such as *Gpb2* and *Serping1*. While A2 reactive astrocytes have elevated transcript expression of *Tgm1* and *Ptx3* among others (Liddelow et al. 2017). That astrocytes can be so simply categorised has been contested in a number of more recent articles (Escartin et al. 2021; Cunningham et al. 2019). It has been shown in mouse models of AD that transgenic models display substantial reactive gliosis, in both microglia and astrocytes, resulting in amplified neuroinflammatory responses and robust neuronal dysfunction (Bornemann et al. 2001; Benzing et al. 1999) However these astrocyte profiles do not readily conform to the A1/A2 categories (Haim et al. 2015). Nonetheless, there is a significant interest in targeting astrocyte-microglial interactions for therapeutic benefit.

1.3 Ageing

1.3.1 The Ageing Phenotype

Ageing can be defined as the intrinsic, cumulative, progressive and deleterious loss of function as a result of the life-long accumulation of molecular and cellular defects (Kirkwood 2005; Chesky 2007). With remarkable improvements in healthcare and life expectancy the number of people aged 65 and over is estimated to grow to 1.5 billion by 2050 (World Health Organization; 2011). This phenomenal increase will in turn see the rise in prevalence of neurodegenerative and ageing-associated disorders and impose greater burdens upon already strained health and social care systems. It is estimated that approximately 50 million people are living with Alzheimer's disease (AD) or some form of dementia today, by 2050 this number is predicted to triple to a staggering 152 million (World Health Organization; 2020). Thus, to improve our healthcare and management of geriatric syndromes to combat this rise it is imperative to understand the primary mechanisms which underlie the pathology of the ageing process.

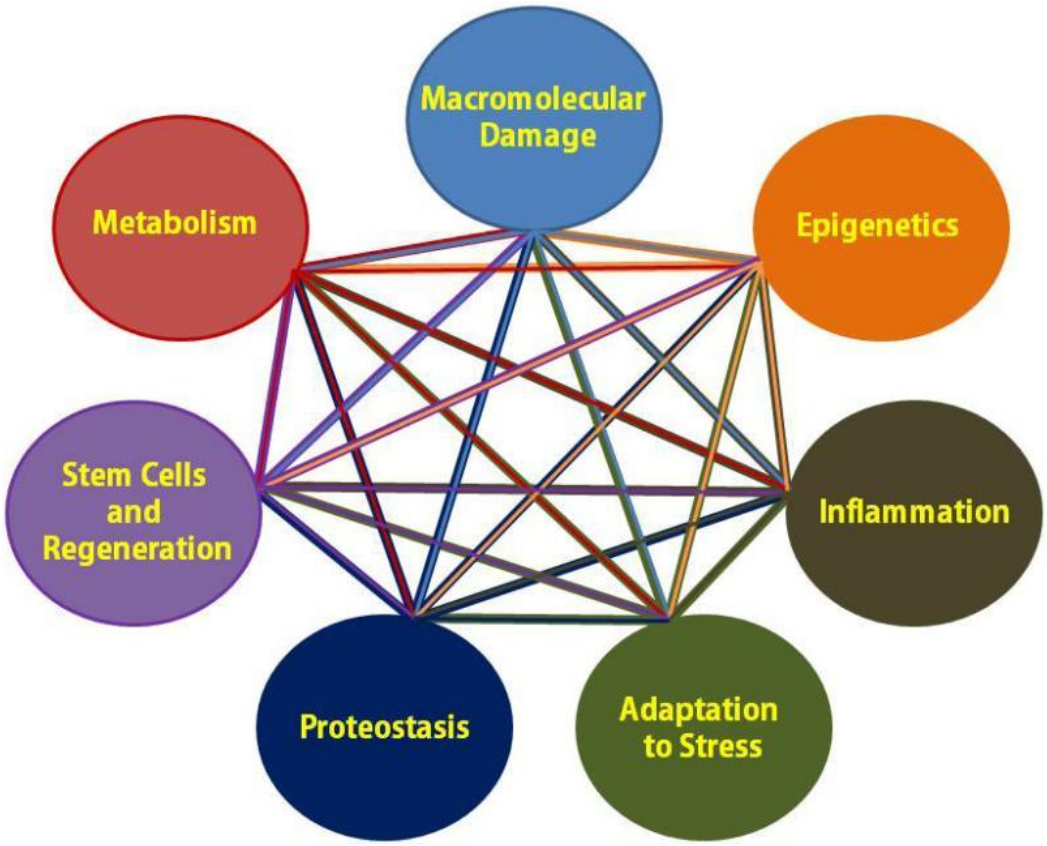

FIgure 1.8: The seven pillars of ageing (Kennedy et al. 2014)

The perpetual and pernicious process of ageing is characterized by declining functional capacity and a resulting increasing vulnerability to disease, disability and ultimately death. Kennedy et al. proposed the seven pillars of ageing, with each contributing to the ageing process to a different degree dependent on the individual in question. These pillars include 1) adaptation to stress, 2) epigenetics, 3) macromolecular damage, 4) metabolism, 5) proteostasis, 6) stem cells and regeneration and 7) inflammation (Kennedy et al. 2014).

The physiological deterioration resulting from the "weathering" of these pillars can be seen to manifest across the whole body, including the brain which will undergo a reduction in size, composition, vasculature and plasticity (Esiri 2007; Dekaban et al. 1978). One of the most obvious age-related changes to human CNS function is the deterioration in motor performance and cognitive function. In the absence of distinct pathology a minor but significant decline in cognitive performance occurs in 38% of 60-78 year olds (Koivisto et al. 1995); specifically within episodic memory processing, working memory, spatial memory, processing speed and implicit memory function (Hedden et al. 2004). Motor function is also notably sensitive to the normal ageing process with all adults displaying a gradual slowing of motor movements and a loss of fine motor control over time (Mattay et al. 2002). These changes are most likely explained by one of two possible

neural mechanisms, age-related neuronal loss or age-related reduction in synaptic efficacy.

1.3.2 Cellular ageing & senescence

While the majority of medical professionals' work to treat ageing at the physiological level, the ageing phenomenon can be attributed in no small part to cellular ageing; to which, cellular senescence is considered to be a substantial contributor. Cellular senescence is the permanent entry of individual cells into a viable, but non-dividing state (Yeoman et al. 2012). Usually this is a by-product of repeated cell division resulting in telomere shortening. In 1961 Hayflick and Moorhead first introduced the term "replicative senescence", the shortening of telomere lengths with extensive cellular divisions, and proposed a role for it in ageing (Hayflick et al. 1961). It is theorised, in early life, to offer a protective mechanism whereby tumour growth is prevented, aiding survival (Coppé et al. 2010). In addition to telomere erosion, several other tumour-associated stresses have been linked to the induction of senescent growth arrest *in vitro*, including certain DNA lesions and reactive oxygen species (ROS) (Von Zglinicki 2002; Sedelnikova et al. 2004). Both of these stresses, like telomere shortening, will result in the activation of the DNA damage response, a signalling pathway in which ataxia telangiectasia mutated (ATM) and RAD3-related (ATR) kinases block cell-cycle progression through stabilization of p53 and transcriptional activation of the cyclin-dependent kinase inhibitor $p21^{CIP1}$ **(FIgure 1.11)**.

Recently, it has been demonstrated that in later life, the onset of cellular senescence results in a reduction of cellular turnover, loss of tissue repair capacity and is typically associated with a shift to a pro-inflammatory phenotype: the senescence-associated secretory phenotype (SASP), as a result of their production of pro-inflammatory and matrix-degrading molecules (Coppé et al. 2010). The SASP is typically induced in response to DNA damage and is characterised by its secretion of a myriad of biologically active molecules, including TGF-β, IL-1β and TNF-α, associated with inflammation and tumorigenesis and the altered function of the p53 tumour suppression protein. As such it has been hypothesised to promote the development of age-related cancer (Coppé et al. 2008). Not only will these SASP products, such as TGF-β and CCL2, serve to instigate or exacerbate inflammatory events but they have also been shown to function in a paracrine fashion, inducing cellular senescence in adjacent, healthy cells through regulation of $p15^{INK4b}$ and $p21^{CIP1}$ (Gonzalez-Meljem et al. 2018; Acosta et al. 2013).

Senescent cells have been shown to accumulate in ageing tissue based on the detection of their high SA-β-GAL activity and increased expression of the senescence master regulator $p16^{Ink4a}$, a potent inhibitor of the G1/S-phase transition of the cell cycle (Lauer 2009; Burd et al. 2013). Why senescent cells accumulate in tissues and organs with age is still being investigated. One theory

suggests that combined cellular stresses accumulate over time and drive the rate to increase over time (Baker et al. 2004). Alternatively, the processes responsible for the elimination of senescent cells may decrease in efficiency with age; it has been demonstrated that senescent cells can be killed and disposed of by immune cells in a mouse model of hepatocellular carcinogenesis and liver fibrosis (Krizhanovsky et al. 2008). Given that the process of ageing is well documented to induce a complex series of changes to the innate and adaptive immune responses, culminating in age-associated immunodeficiency this is a likely contributor (Nikolich-Žugich 2008).

In a mouse model of ageing, mutant BubR1^{-} mice have low levels of the spindle assembly checkpoint protein BubR1 which is responsible for the accurate separation of duplicated chromosomes, as a result these BubR1^{-} mice will develop progressive aneuploidy in addition to multiple other progeroid features including cachectic dwarfism, short lifespan, lordokyphosis, cataracts, impaired wound healing, loss of subcutaneous fat and infertility (Baker et al. 2004). Senescent cells were selectively targeted for deletion in this model *in vivo* using a novel transgene INK-ATTAC, in which both GFP and a fusion protein of FK506-binding protein and caspase 8 (FKBP–CASP8) are expressed under the control of a minimal *Ink4a* promoter. Administration of AP20187, a synthetic drug which induces dimerization of a membrane-bound myristoylated FKBP–CASP8 on senescent cells which express the senescent cell marker p16^{Ink4a}. In these mice the onset of age-related pathologies including cataracts and sarcopenia were delayed following deletion of senescent cells (Baker et al. 2011).

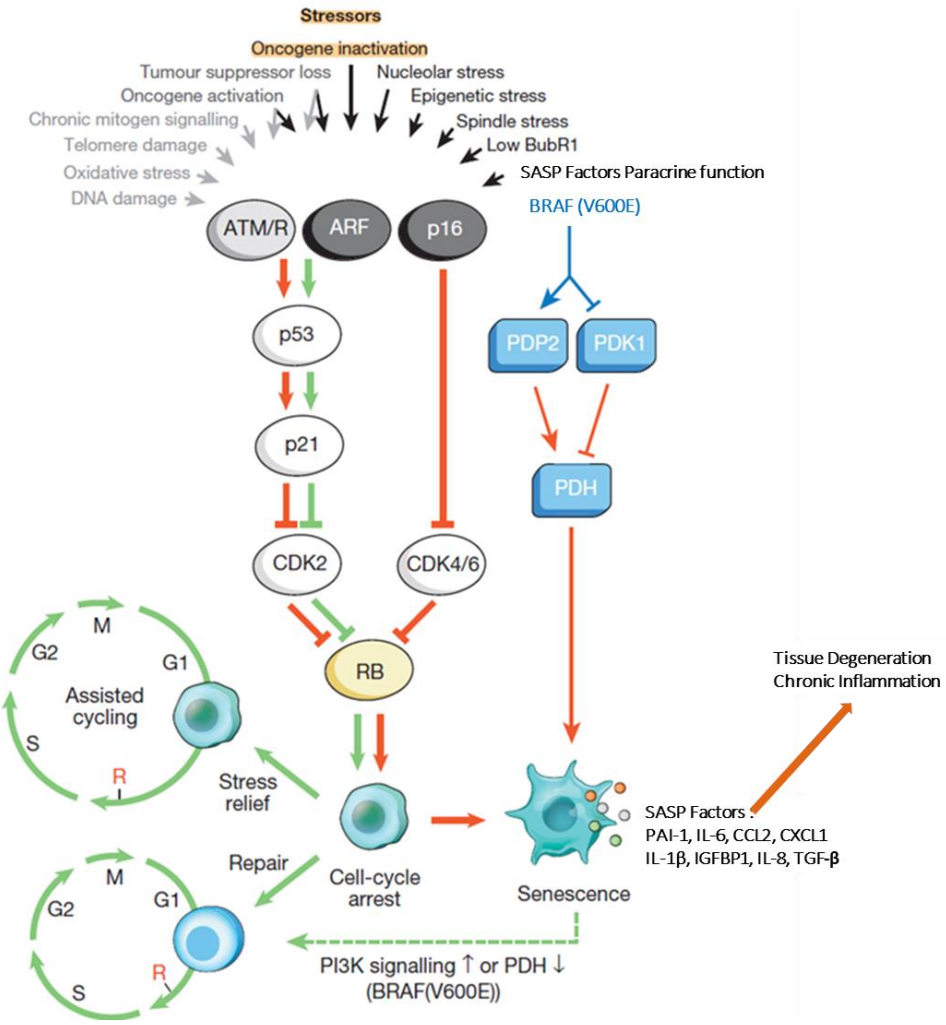

FIgure 1.9 Figure 1 | Senescence-inducing stimuli and main effector pathways. A variety of cell-intrinsic and -extrinsic stresses can activate the cellular senescence program. These stressors engage various cellular signalling cascades but ultimately activate p53, p16Ink4a, or both. Stress types that activate p53 through DDR signalling are indicated with grey text and arrows (ROS elicit the DDR by perturbing gene transcription and DNA replication, as well as by shortening telomeres). Activated p53 induces p21, which induces a temporal cell-cycle arrest by inhibiting cyclin E–Cdk2. p16Ink4a also inhibits cell-cycle progression but does so by targeting cyclin D–Cdk4 and cyclin D–Cdk6 complexes. Both p21 and p16Ink4a act by preventing the inactivation of Rb, thus resulting in continued repression of E2F target genes required for S-phase onset. Upon severe stress (red arrows), temporally arrested cells transition into a senescent growth arrest through a mechanism that is currently incompletely understood. Cells exposed to mild damage that can be successfully repaired may resume normal cell-cycle progression. On the other hand, cells exposed to moderate stress that is chronic in nature or that leaves permanent damage may resume proliferation through reliance on stress support pathways (green arrows). This phenomenon (termed assisted cycling) is enabled by p53-mediated activation of p21. Thus, the p53–p21 pathway can either antagonize or synergize with p16Ink4a in senescence depending on the type and level of stress. BRAF(V600E) is unusual in that it establishes senescence through a metabolic effector pathway. BRAF(V600E) activates PDH by inducing PDP2 and inhibiting PDK1 expression, promoting a shift from glycolysis to oxidative phosphorylation that creates senescence-inducing redox stress. Cells undergoing senescence induce an inflammatory transcriptome regardless of the senescence inducing stress (coloured dots represent various SASP factors). Red and green connectors indicate 'senescence-promoting' and 'senescence-preventing' activities, respectively, and their thickness represents their relative importance. The dashed green connector denotes a 'senescence-reversing' mechanism (Van Deursen 2014).

Another study using SAMP8 mice, a model of accelerated senescence, demonstrated that advanced cellular senescence resulted in a significant deficit in long term potentiation (LTP) at the CA1 medial prefrontal synapse across successive eye blink conditioning sessions and presented with functional deficits in novel object recognition compared to controls suggesting deficits in hippocampal and prefrontal cortical circuits (López-Ramos et al. 2012). Recently the MAPT^{P301S}PS19 model of tau-dependent neurodegenerative disease has been shown to exhibit significant gliosis, localised neurodegeneration and cognitive impairment in response to the hyperphosphorylation and deposition of tau as neurofibrillary tangles ((NFT) (Bussian et al. 2018). Notably microglia and astrocytes, but not neurons, were shown to exhibit significant increased p16^{Ink4a} expression of in the hippocampus at 4 months and in the neo cortex at 6 months, preceding tau deposition. Elimination of p16^{Ink4a} expressing cells using the INK-ATTAC system mitigated this pathology (Bussian et al. 2018).

Given these data it is evident that accumulated cellular damage from DNA lesions, exposure to ROS and telomere shortening results in a distinct cellular phenotype, SASP, which accumulates with age and has the capacity to further drive the ageing progression.

1.3.3 Inflammaging

Ageing is known to be associated with the development of a low-level, systemic, chronic inflammation (Mooradian et al. 1991). It is now widely recognised that these impaired mechanisms regulating inflammation might contribute to the susceptibility of elderly individuals to infection and age associated chronic diseases (Pawelec et al. 2014). “Inflammaging” is the term given to this condition of chronic, low-grade inflammation that characterizes ageing and is present even in the absence of overt infection. The concept and term was first coined in 2000 to underpin the intimate relationship between the process of ageing and life-long activation of the inflammatory response (Franceschi et al. 2006). It has been suggested that this inappropriate and persistent inflammation results in tissue damage which in turn results in further inflammation and more tissue damage, leading to the “cycle of inflammaging” and predisposing the individual to age-related diseases (Baylis et al. 2013). Indeed it has been shown that inflammaging is a significant risk factor for morbidity and mortality in aged individuals (Franceschi et al. 2000).

This hypothesis predates the more recent proposal by Kennedy et al. of the “Seven Pillars of Ageing” but is recognised as one of these seven pillars which contributes to the onset and severity of the ageing process (Kennedy et al. 2014). Intriguingly, the wealth of literature on age-related diseases and geriatric syndromes suggests that alteration of any one of these seven pillars will result in a convergence upon chronic inflammation, i.e. inflammaging is the most common output from

disruption of any of these systems. As a result of this it has been proposed by Franceschi et al. that age-related diseases and geriatric syndromes are manifestations of accelerated aging which result from different combinations of alterations to the same basic set of mechanisms, including, inflammaging (Franceschi et al. 2014).

Extensive study of centenarians has revealed that inflammaging appears to be the evolutionary consequence of the degeneration of the body's damage sensors; as such the body's capability to distinguish between self and non-self and to mount an appropriate inflammatory response becomes increasingly blurred over time (Franceschi, et al. 2018). During ageing it has been shown that a degeneracy in immune response receptors such as TLR2 and TLR4 will respond to the presence of saturated fatty acids to activate an innate immune response and the release of pro-inflammatory mediators (Lee et al. 2004; Huang et al. 2012). With advancing age there is an endless progression and perturbation of energy homeostasis, oxidative stress, DNA lesions and damaged proteins which inevitably results in increased cell death and atrophy (Burtner et al. 2010; Joaquin et al. 2001; Pollack et al. 2001). The resulting cell debris from these, acting as DAMPs, have in turn been shown to induce an inflammatory response (Pasparakis et al. 2015). As a result of these findings, Franceschi et al. has conceptualized that overall inflammaging is largely an autoimmune/autoinflammatory process which may be associated with the presence of auto-antibodies or increased phagocytic responses to aid in the clearance of molecular and cellular detritus, DAMPs, which has accumulated with age (Franceschi et al. 2017). Interestingly, centenarians are also characterized by high levels of non-organ specific autoantibodies, supporting the concept of "protective autoantibodies" whose function may extend to binding senescent cell antigens and facilitate their lysis and removal (Weksler et al. 2009). The immune system of aged individuals is progressively filled and dominated by the presence of T and B cell clones. This likely represents an adaptation of the immune system to the chronic attrition of constant antigen exposure from the age-related dysregulation of the production of "molecular garbage" resulting from cell death, metabolism and gut microbiota function (Franceschi, Garagnani, et al. 2018). In a young individual this is balanced by the production of anti-inflammatory molecules to down-regulate inflammatory responses, but this process becomes impaired with age and the balance between DAMP generation and disposal becomes skewed (Franceschi et al. 2017; Rea et al. 2018). A recent parabiosis study demonstrated that exposing young mice to an aged systemic environment resulted in decreased synaptic plasticity, impaired contextual fear conditioning and spatial learning and memory (Villeda et al. 2011). Specifically, blood-borne factors such as the circulating chemokine CCL11 were implicated in this reduced neurogenesis. Moreover, exposing older animals to young parabionts, in the reversed experiment, improved function on most of these parameters. Conversely, it has been shown that aged mice suffering experimentally-induced demyelination

demonstrated a beneficial, enhanced recovery from exposure to a young systemic environment (Ruckh et al. 2012). Similarly the age-associated decline in pancreatic β-cell proliferation in aged animals has been shown to be reversed thanks to pairing with young parabionts (Salpeter et al. 2013). An intriguing aspect of the inflammaging theory proposed by Franceschi et al. purports that the ageing processes' dysregulation of inflammatory processes leads to an overpowering convergence of cells upon pro-inflammatory phenotypes, resulting in decreased cell heterogeneity, encouraging further clonal expansion and the propagation of the inflammatory wave (Franceschi, Zaikin, et al. 2018). As age-related disorders and geriatric syndromes may be thought of as manifestations of accelerated aging, it is imperative to identify markers to distinguish between biological and chronological age to identify patients at higher risk. The trajectory of decline which an individual will follow is ultimately a result of their genetics and lifestyle's impact upon their physiologic reserve and how vulnerable this leaves them in coping with stressors. Some of these vulnerabilities and accumulations of multiple impacts are captured in the concept of frailty.

1.4 Frailty

1.4.1 Frailty

Typically, ageing is thought of as an inevitable decline which marches to meet us at an inexorable and relentless pace. In truth, ageing is a process defined by declining functional capacity and increased vulnerability to morbidity and mortality but this physiological decline is not uniform. Age-associated decline is a result of the gradual accumulation of molecular and cellular defects over time (Kirkwood 2005) but individuals of a given chronological age will vary greatly in how far these processes have advanced, dependent largely on lifestyle and genetic factors. Some individuals will show reliance in their biological age despite advancing chronological age while others of the same age will age poorly, biologically speaking, and fall into a state of increased risk. This is known as frailty (Clegg et al. 2013). Frailty can be defined as a state of increased vulnerability to poor resolution of homeostasis after a stressor event, which in turn will cause an increased risk of adverse outcomes, such as falls, delirium and disability (Fried et al. 2001; Eeles et al. 2012). The opposite of frailty is termed resilience, and is characterised by the conservation of functional capacity after the occurrence of a clinical stressor (Schorr et al. 2018; Kirkland et al. 2016). However, frailty is also thought to accelerate the gradual decline in physiological reserves associated with ageing. The accumulation of these multiple deficits decreases an individual's resilience to future insults resulting in an ever-widening spiral of decline of their physiological reserves and growing frailty **(FIgure 1.8).**

Frailty is a dynamic process which, if managed properly, can improve over time but more often than not will worsen. The majority of individuals will progress to greater levels of frailty with time (Clegg et al. 2013). The importance of frailty as a clinical syndrome was highlighted in a ten year prospective cohort study which identified frailty as the leading cause of death in community dwelling older people (Gill et al. 2010). This study (n=754) found frailty to be a greater cause of mortality (27.9%) in comparison to organ failure (21.4%), cancer (19.3%), dementia (13.8%) and other causes (14.9%) among the participants. It is estimated that between 25-50% of individuals over the age of 85 can be classified as frail putting them at a substantially higher risk of debilitating illness or disability resulting in expensive long-term care and potentially death (Fried et al. 2001). Conversely, this means that between 50-75% of individuals over 85 years of age are not frail.

It has been shown consistently across several longitudinal studies that high frailty is associated with increased risk of mortality (Mitnitski et al. 2005; Eeles et al. 2012; Joosten et al. 2014; Vasconcellos Romanini et al. 2020). Furthermore, the frail individual will be at increased risk of developing further morbidity including disability, delirium, and dementia which can render them dependent upon long-term healthcare **(FIgure 1.11)** (Clegg et al. 2013; Searle et al. 2015; Kojima et al. 2016; Mahanna-Gabrielli et al. 2020; Mitnitski et al. 2005).

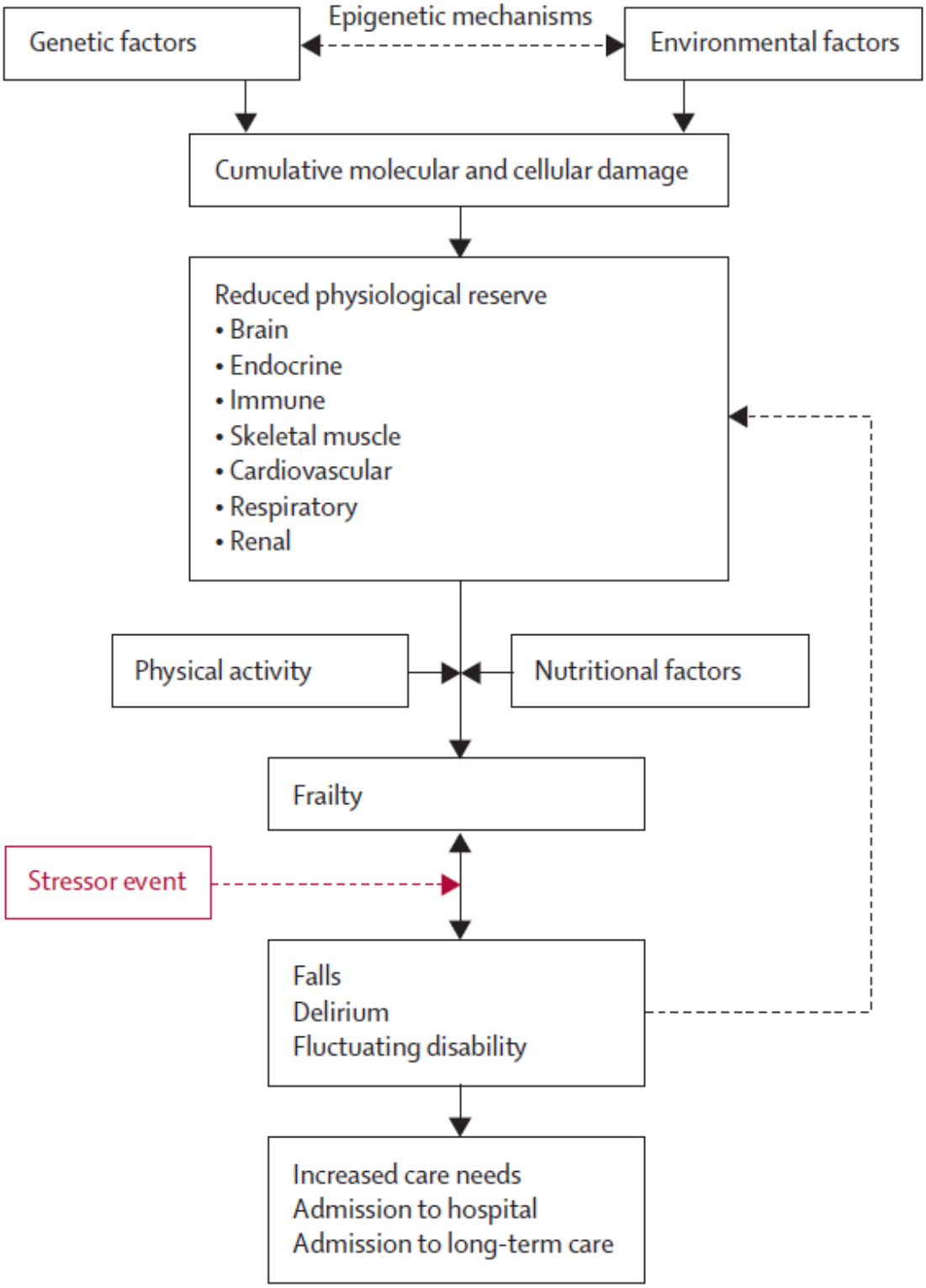

FIgure 1.10: The pathophysiology of Frailty: schematic representation of the pathophysiology of frailty (Clegg et al. 2013)

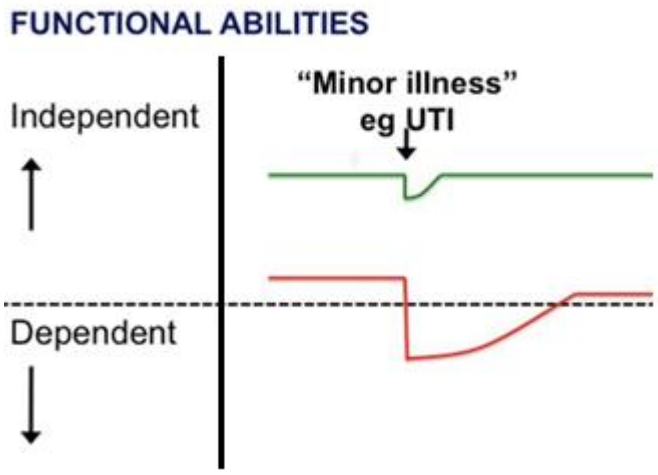

FIgure 1.11: Increased vulnerability with frailty: Illustration of the increased vulnerability of a frail individual (red) compared to a healthy individual (green) in coping with an acute stressor (Clegg et al. 2013)

Despite this it is currently unknown how exactly frailty develops, whether it is a complex common pathway to all frail individuals or the result of independent development of several comorbid conditions converging into the frailty phenotype remains to be elucidated. With the quality of healthcare in today's modern world leading to an ever-increasing life span it is imperative that we understand the underlying pathology that leads to this state of frailty and in turn, how to efficiently treat it at the "pre-frail" stage so as to prevent the individual's condition worsening and offer them the greatest quality of life for as long as possible.

1.4.2 Quantifying Frailty – Frailty Indices

As an emerging syndrome with significant prevalence in geriatric medicines there is high demand for accurate and readily testable measures of frailty. Currently two main models of frailty are employed in the clinical setting:

Integrated Phenotype Model

Pioneered by Linda P. Fried and her colleagues (Fried et al. 2001), a frailty phenotype can be established for a patient from five variables (**Table 1.1)**, (i) unintentional weight loss, (ii) self-reported exhaustion, (iii) low energy expenditure (iv) slow gait speed and (v) weak grip strength. Individuals who displayed three or more of the factors were deemed frail, those with one or two were "pre-frail" and those with none were classified as not frail, or resilient, elderly people. Diagnosed in this manner the study population of 5,210 men and women, aged 65-years and above, were categorised as 7% frail, 47% pre-frail and 46% resilient. Follow up assessments were taken at 3 and 5 years, and it was found that individuals classified as frail were reported to have more adverse outcomes than those classified as resilient or pre-frail. The reported mortality at 7 years post initial assessment was 12%, 23% and 43% for those classified as resilient, pre-frail and frail

respectively. While these data suggest a reasonably predictive and readily assessable measure of frailty in a clinical setting it fails to take account of important factors such as cognitive impairment, existing morbidities and disability, all of which are highly prevalent conditions with functional decline (Rothman et al. 2008).

1	**Weight Loss** Self-reported weight loss of more than 4.5kg *or* recorded weight loss >5% per annum
2	**Self-reported exhaustion** Self-reported exhaustion on US Centre for Epidemiological Studies depression scale (Radloff 1977) 3-4 days per week or most of the time
3	**Low energy expenditure** Energy expenditure <383kcal/week (men) <270kcal /week (women)
4	**Slow gait speed** Standardised cut off times to walk 4.57m, stratified by sex and height
5	**Weak grip strength** Grip strength, stratified by sex and body-mass index

Table 1.1: Integrated Phenotype Model Measures: The five phenotype model indicators of frailty and their associated measures (Fried et al. 2001)

Deficit Accumulation Model

The cumulative deficit model was originally developed as part of the Canadian Study of Health and Ageing (CSHA) and draws on a greater range of physiological systems. It takes into account 92 baseline variables of symptoms, signs, disease states, disabilities and abnormal laboratory values, to generate a comprehensive frailty score from the cumulative effect of the individual deficits (Rockwood et al. 2005). While each individual deficit need not carry an imminent threat to mortality, taken together this model describes a system with a built-in redundancy whose homeostatic reserve can be reduced by the cumulative contribution of multiple deficits, leading in turn to a state of increased vulnerability. More recently it has been shown that this formidable list of 92 variables can be narrowed down to a more clinically manageable 30 criteria without the loss of predictive validity (Song et al. 2010). Mortality has been shown to be significantly related to the value of the individual's cumulative frailty score across multiple large scale longitudinal studies (Mitnitski et al. 2005; Eeles et al. 2012; Joosten et al. 2014).

1.4.3 Frailty in humans

Serological biomarkers of frailty

Several studies in recent years have attempted to identify markers associated with the frailty phenotype in patients. These studies have highlighted an association between inflammation and cellular immunity with frailty. To date, the focus has been on serological and immune markers of frailty and inflammation has been identified as one of the key contributing factors to frailty. So far however, few studies have looked at neurological markers of frailty, despite the fact that inflammation has also been shown contribute to the pathogenesis of neurodegenerative diseases, dementia and delirium (Clegg et al. 2013).

The Newcastle 85+ study was the first comprehensive study of frailty biomarkers of inflammation, immune senescence and cellular ageing (Collerton et al. 2012). This population-based study collected comprehensive data from measures of health across several biological, clinical and psychosocial domains. Serological biomarkers were identified and analysed using blood samples from the participants who were over 85 years of age (n=845). The findings presented in that report showed that biological markers of frailty differ between distinct aged cohorts. The biomarkers identified in the very old (85+ years) were different to those previously identified in the younger old (65+ years). This highlights the heterogeneity in the manifestation of frailty and emphasises the progressive nature of this geriatric syndrome. These findings in older patients were consistent with previous studies that had illustrated the importance of inflammatory biomarkers such as IL-6, TNF-α, CRP and neutrophils (previously been shown to be elevated in the younger old population (65+ years) (Collerton et al. 2012)). Additionally, it was found that these markers have an inverse association with albumin. Albumin is the most abundant plasma promoter acting as a transporter for substances such as calcium and maintaining oncotic pressure, i.e. pushing water and small molecules out of the blood into the interstitial spaces within the arterial end of capillaries and interstitial colloidal osmotic pressure (Levick et al. 2010). Its plasma level peaks at approximately 20 years of age and decreases with age thereafter and is an important marker for many systems whereby its presence in low levels is associated with inflammation, malnutrition, skeletal integrity and disease status (Weaving et al. 2016). Furthermore, an increase in neutrophil count and the presence of elevated levels of inflammatory cytokines have a positive association with frailty. Several cellular markers of ageing such as oxidative stress, peripheral blood mononuclear cell telomere length or DNA damage and repair were shown to have no correlation with frailty as assessed by this cumulative deficit model (Collerton et al. 2012). Within the very old (85+ years) individuals there was a significant association of aberrant DNA methylation with frailty (Collerton et al. 2014). Several further studies have since reported significant correlations of DNA

methylation and relative telomere length with frailty as assessed using the Fried phenotype instead (Haapanen et al. 2018; Bellizzi et al. 2012; Gale et al. 2018).

A longitudinal study carried out in Singapore identified 8 serological markers of frailty from individuals over 55 years. These markers included CCL2 (MCP-1), CXCL13 and IL-6R, which suggest that chronic systemic inflammation is associated with frailty (Ng et al. 2015). This study also identified the importance of immune cells in the process of frailty. It was found that there was an increase in the number of exhausted B-cells (i.e. B-cells with a decreased capacity to proliferate in response to de-novo stimuli and by an increased expression of multiple inhibitory receptors, identified by the surface markers CD19+IgD-CD27-, CD38+ B cells and CD14+CD16+ cells in frail individuals. Ng et al. also determined that frailty is associated with an inverted CD4:CD8 ratio and a high prevalence of CD8+CD28- T cells. One of the key cytokines which induces the CD28- phenotype is TNF-α (Ng et al. 2015). Therefore, CD8+CD28- T cells are generated in a pro-inflammatory environment associated with ageing and frailty.

Several studies have corroborated these longitudinal studies of frailty biomarkers, such as CRP, IL-6 and albumin, as well as identifying several new ones including metabolic markers such as 25-hydroxyvitamin D, leptin, immune mediators such as CXCL10, CX3CL1, PTX3, C3/C1q and calreticulin, and hormonal growth factors such as BDNF, IGF-1, TGF-β, testosterone and estrogen (Mailliez et al. 2020; Cardoso et al. 2018; Carcaillon et al. 2012; Morley et al. 2013; Morley et al. 1997).

These studies highlight the positive association between frailty, ageing and inflammation in patients. Recently, the importance and prevalence in the use of frailty in predicting surgery success and recovery outcomes has been growing. Traditionally, perioperative surgery risk scores predicting mortality were mainly based on clinical and angiographic factors with limitations in their application to elderly populations as the data is primarily derived from a middle-aged population and fails to account for frailty and the impact the procedure may have on quality of life. As such, incorporation of frailty measures into existing risk scoring systems is growing. The English National Health Service general practice contract for 2017/2018 lists frailty identification as a requirement prior to all surgeries in elderly patients (Record et al. 2017). More clinically-focussed applications include chemotherapy toxicity dosage in lung cancer patients (Ruiz et al. 2019) and risk stratification for all liver transplant patients using the Short Physical Performance Battery (SPPB) as well as more focussed assessment using the Liver Frailty Index (Lai et al. 2019). In cardiology the use of the frailty indices, generated from the Cardiovascular Health Status (CHS) and Study of Osteoporotic Fractures (SOF) in cardiovascular surgery patients, has been shown to accurately predict vulnerability to

adverse outcomes including prolonged ventilation, pneumonia, long-term ICU stays and readmissions (Henry et al. 2019).

1.4.4 Frailty and sex

Epidemiological studies have revealed that frailty and cognitive impairment are influenced by sex in the geriatric population. Women show higher prevalence and severity of frailty as well as a greater susceptibility to late onset dementia than men of similar age, despite having a lower risk of mortality than males (Ott et al. 1998; Mitnitski et al. 2005; Song et al. 2010). While frailty in men has been shown to be strongly predicted by lower testosterone levels (Mailliez et al. 2020; Travison et al. 2011) it has been proposed that the higher risk of frailty in women is a result of changes in estrogen levels in women due to menopause and the associated increased risk of age-associated diseases this brings (Carcaillon et al. 2012). Menopausal women are more susceptible than men to several age-associated diseases with chronic inflammatory components including obesity, diabetes, depression, atherosclerosis and osteoporosis (Lane et al. 2006; Laws et al. 2016). Similarly, women who have undergone a hysterectomy show substantially elevated prevalence of frailty (Verschoor et al. 2019). Consistent with this is the observation that menopausal women may experience increased inflammatory cytokines due to decreased ovarian function, most notably including CRP, IL-6 and TNF-α (Vrachnis et al. 2014; Perry et al. 2008; Chagas et al. 2017), all of which are significant serological predictors of frailty (Mailliez et al. 2020; Mitnitski et al. 2015). In one longitudinal study of 2,146 people aged 60-90 years old high CRP levels were found to be a stronger predictor of the incidence of frailty in women than in men (Gale et al. 2013). Hormonal replacement therapy in post-menopausal women have been shown to improve bone mineral density and muscle mass in combination with physical training in frail elderly women (Villareal et al. 2001; Sipilä et al. 2003). Regardless of biological mechanism, the prevalence of frailty increases substantially with age, with 5.2% of men over the age of 65 years presenting with frailty and 9.6% in women (Collard et al. 2012).

1.4.5 Frailty prevention and building resilience

One of the primary and most widely used practices for managing frailty is hormone replacement therapy which is widely prescribed to menopausal women to combat the negative conditions associated with the loss of estrogen. As discussed in the previous section, hormonal replacement therapy in post-menopausal women for estrogen loss have been shown to improve bone mineral density and muscle mass in combination with physical training in frail elderly women (Villareal et al. 2001; Sipilä et al. 2003). Likewise, growth hormone secretion rates decline exponentially from a peak of approximately 150μg/kg/day during puberty to about 25μg/kg/day by the age of 55

(Melmed *et al.* 2021). As this decline occurs elderly patients show a commensurate increase in body fat, reduced aerobic capacity, reduced muscle mass and weakness and can present with cognitive impairment (Cummings et al. 1999; Cummings et al. 2003). These deficits have been shown to ameliorated by growth hormone replacement therapy or stimulation of GH secretion using secretagogues such as GH releasing hormone have been shown to be ameliorate many of the hallmark traits of frailty, reducing adiposity, increasing lean muscle mass and overall improved activity levels (Rudman et al. 1990; Holloway et al. 1994; Papadakis et al. 1996; Johannsson et al. 1997; Lange et al. 2002; Franco et al. 2005).

While unexpected weight loss is one of the five criteria of the Fried frailty phenotype, studies have found that frail older adults have a higher adiposity and greater average waist circumference than non-frail patients (Crow et al. 2019) and that obese geriatric women were twice as susceptible to frailty compared to non-obese women of the same age (Monteil et al. 2020). This increased obesity is frequently shown to be concomitant with a loss of muscle tone. This sarcopenic obesity, a loss of muscle mass and strength with a concomitant increase in adiposity has been shown to be a driver of frailty (Crow et al. 2019) with further, longitudinal studies of ageing, demonstrating that, in elderly men, low muscle mass and high adiposity have a doubled risk for frailty over a 5 year period (Hirani et al. 2017). Therefore, diet and exercise are the most robust methods of prophylaxis and combatting established frailty available today. In longitudinal human studies it has been shown that low fat diets with high fruit, vegetable and omega-3-fatty acid intakes, such as the Mediterranean Diets is associated with substantial reductions in risk of frailty development in aged individuals (García-Esquinas et al. 2016; Feldman 2018; León-Muñoz et al. 2015) and has even been shown to be effective in combatting established frailty (Voelker 2018; Frison et al. 2017; Hutchins-Wiese et al. 2013; Lopez-Garcia et al. 2018).

While low fat diets rich in omega-3—fatty acids are associated with attenuation and improvement of frailty status, protein intake is extremely important also as proteostasis is significantly impaired in aged individuals. Aged muscles require greater and greater amounts of amino acids to stimulate muscle anabolism due to a reduced muscle protein synthesis response as a result of hyperaminoacidemia, anabolic resistance which develops with age (Volpi et al. 2000; Katsanos et al. 2005; Katsanos et al. 2006; Wall et al. 2015). Thus, between 1.0–1.5 grams of protein per kg of body weight may be required in older adults to stimulate muscle protein synthesis, significantly more than the recommended dietary allowance of 0.8g/kg BW/day for adults (Moore et al. 2015)**.** As such protein supplementation has also been shown to improve muscle mass and physical performance in pre-frail and frail subjects, particularly when combined with exercise therapy (Park et al. 2018; Liao et al. 2019). Aerobic exercise and resistance training have been demonstrated to yield substantial improvements in grip, limb strength, agility, gait, fat and muscle mass, postural

stability and mortality as well as improvements in cognition, IGF-1 signalling, gut microbiome diversity and reduced inflammation (Talar et al. 2021; Aguirre et al. 2015; Angulo et al. 2020; Arrieta et al. 2019; Cadore et al. 2013; Giné-Garriga et al. 2014; De Labra et al. 2015).

Unfortunately, these studies often face serious issues in low participation, high attrition rates, failure to retest frailty post-intervention and issues with randomisation and blinding of study personnel (Dent et al. 2019). As a result, there is insufficient evidence from resiliently designed and executed studies to gauge the effect of these interventions in improving long-term functional ability. With this growing use of frailty indexes in modern medicine, it is increasingly necessary to identify new and accurate FI component measures in order to develop suitable animal models of frailty which can provide further information on how frailty, ageing, sex and inflammation are linked. Additionally, they will help to answer the question as to why only certain individuals of the same chronological age will exhibit significantly different biological age, i.e. frailty, offering insights into potential prophylactic and therapeutic targets for intervention. As neurodegeneration is prevalent in the ageing and frail population, modelling brain inflammation may provide suitable insights into this relationship.

1.4.6 Animal Models of Frailty

Animal models have been developed in order to help elucidate the physiological and molecular mechanisms underpinning frailty. Animal modelling has the advantage of allowing us to euthanise animals at various time points to examine and manipulate changes in various biological systems, to measure responses to acute stressors and also provides an opportunity to test interventions and to collect data which would not be readily attainable in patient research (Seldeen et al. 2015). Due to their relatively short lifespan mouse models are an attractive model organism for longitudinal studies of frailty and ageing. Depending on the strain, the average murine lifespan ranges from 1-3 years. Furthermore, mice express several characteristic and visible signs of ageing common to humans, including a decline in physical performance, increased adiposity, loss of lean muscle, loss of sensory acuity and age related cellular changes (Ballak et al. 2014; Barreto et al. 2010; Fujita et al. 2015; Brown et al. 2021).

Cumulative Deficit Frailty Index

The murine cumulative deficit frailty index was based upon the deficit accumulation model used in the CSHA study discussed above. Designed by Parks et al. it uses 31 non-invasive parameters to score normal mice for frailty by taking the average of a z-score, generated as a function of the individual's standard deviation away from the mean value of a group of young healthy control animals for all 31 measures. These measures ranged from behavioural testing of activity, strength and speed, metabolic, body composition to hemodynamic measures (Parks et al. 2012). This broad

and comprehensive list mirrors the age-related cross-sectional frailty index scores observed in humans and as such has strong translational potential. Variations in this index in both mice and humans have utilised as few as eight select measures focussing on activity and body weight to calculate individual frailty scores which have been shown to correlate consistently with those generated by the 31 item index (Whitehead et al. 2014).

This model has the advantage that unlike other animal models of frailty it does not rely upon aggressive genetic models or procedures, like high-sucrose/high-fat diets, to induce traits associated with the frailty phenotype universally in every animal. Rather, it allows a more natural, diverse, range of the ageing phenotype that will naturally occur, presenting a diverse array of frailty characteristics and a continuum of frailty scores within a population instead of the binary, frail/resilient, that is typically found in other models.

Recent work has shown that machine learning analysis of this 31 item cumulative deficit model conducted longitudinally until time of death was able to generate predictive clocks of the animal's age and survival time remaining (Schultz et al. 2020). As such this suggests that while frailty, a result of multiple co-morbidities in the ageing animal diminishing their physiological reserve and thus increasing vulnerability, may benefit from a broad range of measures including metabolic, physiological, and cognitive in the frailty index used to capture their frailty; it is also advantageous to be selective and discerning in choosing which measures to include in such an index. This is important not only in ensuring accurate capture of frailty but also to create an index with strong translational potential.

Interleukin 10 knockout mouse

One of the best studied mouse models of frailty to date is that of the Interleukin 10 knockout mouse (IL-$10^{-/-}$). These mice display several key characteristics of the frail phenotype including accelerated sarcopenia, reduced longevity and chronic low grade inflammation over the course of their life (Walston et al. 2008). Due to the knockout of the key anti-inflammatory cytokine IL-10 from early in development these mice produce increased expression of NFκB-induced mediators (Rennick et al. 1995), resulting in higher concentrations of several pro-inflammatory cytokines including IL-1β, TNF-α and IL-6 compared to control groups (Ko et al. 2012). IL-6 and TNF-α have both been shown to induce IGF-1 resistance in neurons and muscle cells (Kelley 2004) which likely relates to the observed accelerated muscle loss in this model. As discussed already, muscle loss is one of the most common measures of frailty used in geriatric medicine today and combined with the chronic low-grade inflammation which mimics the phenomenon of inflammaging in humans this offers support for the validity of this as a model of frailty. Additionally, IL-$10^{-/-}$ mice have been shown to be vulnerable to cognitive dysfunction after an acute challenge with LPS (Richwine et al. 2009).

Furthermore, as one would expect from individuals with advanced frailty it was shown that these knockouts displayed a significantly higher mortality rate ratio of 1:2.64 C57BL/6J controls compared to IL-10 KO animals (Ko et al. 2012).

One caveat with this model however is that as a result of the knockout of IL-10 from birth these animals will have inflammation arising for the manipulation of this single factor, rather than arising naturally with age as is the case in humans. Furthermore, this higher inflammation is present from birth, unlike that developing with age in humans, and as such will likely have a significant impact on the mouse's health during development. Therein lies a significant limitation of the model as a means to understand mechanisms of frailty (Mohler et al. 2014).

Interleukin 6-inducible mouse

Interleukin-6 is a highly pleiotropic cytokine capable of diverse responses during acute and chronic responses through the IL-6 cytokine itself as well as its soluble receptor sIL-6Rα. During the acute response it is the chief stimulator of most acute phase proteins (Gauldie et al. 1987) but also has the capability to govern anti-inflammatory responses by stimulating the production of IL-1 receptor antagonist (Gabay et al. 1997). The expression of IL-6 is primarily modulated by NF-κB (Li et al. 2002) and, during chronic immune responses, IL-6 together with its soluble receptor, sIL-6Rα, forms a complex to activate endothelial cells to secrete IL-8 and CCL2, ultimately regulating leucocyte infiltration (Romano et al. 1997). IL-6 has been shown to be significantly elevated in a range of chronic conditions including arthritis, cancer, autoimmune diseases and ageing (Gabay 2006; Ishihara et al. 2002; Ershler et al. 2000) and is one of the most consistent serological biomarkers of frailty found in ageing studies alongside CCl2 and TNFα (Ng et al. 2015; Mitnitski et al. 2015; Ershler et al. 2000; Leng et al. 2004). Consistent with this higher serological expression as an indicator of greater frailty, it has been demonstrated that infusing animals' muscles with IL-6 resulted in significant skeletal muscle atrophy and has since been replicated more recently in an inducible IL-6 model using doxycycline to induce IL-6 to levels equivalent to those observed in frail mice. This resulted in a corresponding increase in the animals' frailty scores, with notably reduced grip strength and disrupted muscle mitochondrial homeostasis (Jergović et al. 2021). Recent work in the IL-10$^{-/-}$ model of frailty and chronic inflammation (Walston et al. 2008) revealed that in double knockout animals targeting IL-10 and IL-6 for deletion, animals demonstrated an improvement in short-term performance on functional and metabolic assays associated with the frail, ageing phenotype, however, this transient improvement ultimately resulted in higher mortality, highlighting the pleiotropic nature of IL-6, while reduced levels might have short term benefits, its complete removal has substantial negative effects on longevity (Ma et al. 2021). Taken together these recent findings suggest that elevated IL-6 serum levels may drive age-related frailty, possibly

through disruption of mitochondrial metabolic mechanisms and present a new inducible and highly controllable model in which to examine frailty.

Growth hormone knockout mice

Growth hormone (GH) is a protein secreted by the anterior pituitary which circulates throughout the body, mediating growth and metabolic processes through interaction with the Growth hormone receptor (Moffat et al. 1999). One of its best described roles is in stimulating the secretion of IGF-1 which mediates many of the same actions as GH (Holzenberger 2004). GH levels have been shown to consistently decline with advancing age and resulting in many of the characteristics of frailty, including increased body fat, reduced aerobic capacity, decreased muscle mass and weakness and can present with cognitive impairment in humans (Cummings et al. 1999; Cummings et al. 2003); all of which have been shown to be ameliorated by treatment with growth hormone replacement therapy in elderly patients (Rudman et al. 1990; Holloway et al. 1994; Papadakis et al. 1996; Johannsson et al. 1997; Lange et al. 2002; Franco et al. 2005).

As such growth hormone-deficient mice, which show significant growth retardation, reduced IGF-1 serum levels and pituitary hypoplasia (Alba et al. 2004), are of interest as mouse models of frailty. This targeted disruption of the GH would appear to display many qualities of an ideal frail animal including decreased fertility, reduced muscle mass, increased adiposity, smaller body size, glucose intolerance and an enhanced insulin sensitivity. However, despite these numerous negative traits $GH^{-/-}$ mice actually consistently outlive wild type littermates and show reduced cellular senescence, delayed cognitive decline, delayed neuromusculoskeletal frailty, delayed sexual maturation and a robustly extended lifespan (List et al. 2021). For this reason, despite the numerous frailty-like qualities that $GH^{-/-}$ mice show they are not frequently used as mouse models of frailty. However, the role of Growth Hormone and IGF-1, which when disrupted results in similar pathology to that of $GH^{-/-}$ mice (Yakar et al. 2002), in frailty pathology and prevention is an area of continuing interest.

SAMP8

The senescence-accelerated prone (SAMP) 8 mouse strain is widely used as a model of age-related cognitive loss and neurodegeneration. The SAMP8 mouse was produced through selective breeding of the AKR/J mouse strain to produce offspring who showed a phenotype of early senility. This produced several strains of SAMP mice ideal for studying different aspects of age-associated pathologies (Butterfield et al. 2005). The SAMP8 mouse specifically demonstrates age-related learning and memory deficits, an impaired immune system and age-dependent deposition of Aβ. In addition to this they display several other key traits of the frailty phenotype including reduced longevity, activity and deteriorating body condition (Miyamoto et al. 1986; Takeda et al. 1981). Unlike the $IL\text{-}10^{-/-}$ model the mice are born healthy but will manifest the phenotype early on.

Furthermore, unlike the other models discussed so far these mice have a robust cognitive impairment. These mice display accelerated ageing, increased hair loss, brain atrophy, kyphosis, periophthalamic disorders, reduced activity and life span, higher incidences of emotional disorders, abnormal circadian rhythms and hearing impairments (Takeda et al. 1997). The broad range of deficits which can potentially manifest to different degrees of severity within this model make it a powerful model of frailty. However, the age at which these deficits manifest can vary widely between animals depending on the deficit in question. SAMP8 mice have been shown to manifest degeneration in the brain stem as young as 1 month and peaks anywhere between 4-8 months of age (Akiguchi et al. 2017), elevated ROS and oxidative stress damage in SAMP8 mice occurs as early as 4 and increasing thereafter to 12 months of age and possibly beyond (Farr et al. 2003), learning and memory deficits develop between 8-10 months of age (Flood et al. 1995), Aβ expression begins at 6-8 months while amyloid pathology occurs well after this from 16-18 months (Morley et al. 2000). Given the short lifespan of these mice, these 2-3-month windows during which pathology may manifest and develop, coupled with the substantial difference in age at which different pathologies will emerge emphasizes that there is significant variability in biological ageing within this model of frailty. This would necessitate that frailty should be assessed individually in these animals but this has not typically been done in experiments to date, with SAMP8 mice being regarded as a uniformly frail group. This model has the potential to offer a highly variable frail population, which could be stratified using a frailty index such as the Cumulative deficit model to investigate, in detail, the severity of frailty across the lifespan.

High fat diet-induced obesity

One of the biggest limiting factors in these animal models is the lack of variation amongst these inbred populations, raised in pathogen-free environments on uniform diets; unlike human populations where poor diet, lack of exercise and environmental stressors are among the leading drivers of frailty. High fat diets have been shown to increase plasma levels of IL-6 significantly (Lundman et al. 2007) as well as accelerating the ageing process (Yu 1996). High fat diets have been shown to affect multiple markers of ageing and frailty negatively including memory impairment, cholinergic dysfunction, elevated oxidative stress, neurodegeneration, increased inflammation and accelerated ageing (Iqbal et al. 2019; Pistell et al. 2010; Morrison et al. 2010). Therefore, there has been growing interest in using existing high fat diet-induced obesity mouse models to investigate frailty in a more directly translatable fashion than genetic models. One such study, assessing the impact of a dietary stressor on frailty directly, has demonstrated enhanced frailty and reduced lifespan in male animals but higher frailty scores overall in females (Antoch et al. 2017), consistent with data from longitudinal human ageing studies (Mitnitski et al. 2002; Song et al. 2011). In contrast dietary restriction has demonstrated reduced hypothalamic inflammatory gene expression

and frailty with a concurrent increase in lifespan in male mice (Henderson et al. 2021; Richardson et al. 2021).

Caveats of current animal models of frailty

While mouse models offer many advantages in the effort to characterise frailty, they are not without drawbacks and there is a growing push for more directly translatable murine models of ageing. For instance, some strains of mice are predisposed to health challenges. The commonly used C57BL/6J strain for instance is well documented to be susceptible to osteoarthritis and cancer of the lymphatic and hematopoietic systems (Brayton et al. 2012; Hubbard-Turner et al. 2015; K. Yamamoto et al. 2005). At this early stage in unravelling the pathophysiology of frailty we cannot delineate yet whether it is possible that the mechanisms driving this cancer are also driving frailty, possibly by different pathways to those which underlie the progression of frailty in humans. Similarly, many of the animal models utilised rely on aggressive mutant knock out animals with severe and ubiquitous pathology in every animal, failing to capture the natural diversity of ageing and the resulting continuum of frailty that we observe with the normal ageing process.

While there has been a rise in the use of cumulative deficit frailty models to capture frailty in the naturally ageing population and provide a more translatable model to humans, these animal frailty studies conducted to date have not fully explored the relationship between specific frailty measures and their compound score with predicted outcomes such as functional capacity. That is, there is a strong motivation to see frailty as a construct comprised of innumerable factors, relying on the sheer number of measures to capture a snapshot of frailty. This approach discourages deconstruction of established frailty constructs for the purpose of examining the degree of contributions of some of the frailty index features compared to others, and risks real high impact measures being diluted by dozens of less relevant components. For instance, in the cumulative index proposed by Parks et al., equal weighting is given to loss of hair colour as is for tumours; despite development of tumours likely being a stronger predictor of adverse outcome or increased frailty than greying hair.

If we are to unravel the mechanism by which frailty manifests and progresses it is imperative that we choose carefully what measures are included in a cumulative deficit frailty index for the purposes of the generating a frailty score; choosing measures who contribute to and correlate strongly with the ageing phenotype. In turn, clear understandings of how these measures relate to pathology, survival and functional capacity individually, as well as collectively will be imperative in generating translatable models of frailty to human populations for the purposes of managing and improving outcomes for frail patients in the clinical setting.

1.5 Dementia

Dementia is an umbrella term used to describe a range of conditions associated with changes or damage to the brain. At its core however it is defined as a loss of cognitive functioning and behavioural abilities which may include an impairment of the individual's ability to acquire and recall new information, impaired reasoning and handling of complex tasks, decreased visuospatial ability, reduced language ability and altered personality and behaviours (McKhann et al. 2011). The prevalence and severity of these symptoms, as well as their underlying cause of which, can range widely between individuals. Alzheimer's disease is by far the most prevalent of the various forms of dementia, accounting for 50% of all diagnosed demented patients. As a result, Alzheimer's disease is commonly used as a synonym for dementia; however, it is a condition contributed to by a wide spectrum of pathologies and as such accounts for more than those specifically associated with Alzheimer's disease.

1.5.1 Alzheimer's Disease

According to the Alzheimer Society of Ireland there are currently over 64,000 people currently living with dementia in Ireland with 1 in 20 people over the age of 65 affected by dementia (Pierse et al. 2019). The current economic impact of this in Ireland is estimated at €1.69 billion per annum, 48% of which can be attributed to costs of informal care and 43% a result of long-stay residential care costs (Connolly et al. 2014). With current projections estimating the number of people suffering this condition expected to double over the next 25 years (Alzheimer Europe 2019) the increased economic and social challenges this presents is a growing concern that affects all of the globe as improvements in healthcare and life expectancy predict the number of people aged 65 and over is estimated to grow to 1.5 billion by 2050 (World Health Organization; 2011).

As such, there has been a focus on identifying risk factors and potential predictors associated with the development of dementia. To this end meta-analysis studies of longitudinal ageing studies have revealed that frailty analysis by way of 'the Fried Phenotype model' confirmed that frail older adults were at higher risk of cognitive disorders compared to non-frail elders over 7 year longitudinal studies (Borges et al. 2019). Similarly, meta-analysis studies have shown that the prevalence of frailty within the Alzheimer's disease community ranged between 11-50% of the total population across five studies (Kojima et al. 2017). Frailty has been shown to be more prevalent in women, with 9.6% of women and 5.2% of men over the age of 65 presenting with frailty (Collard et al. 2012) and this in turn correlates with recent figures showing 2 thirds of diagnosed AD cases in the US in 2019 were women (Alzheimer'sAssociation 2015). Furthermore, studies which have shown that the loss of estradiol observed in women post-menopause is associated with higher expression of Aβ

(Marongiu 2019). Brain atrophy rates and patterns of neuronal and synaptic loss have been found to be significantly faster in women than men (Ferretti et al. 2018)

Genome-wide association studies (GWAS) have also revealed a large number of common variants associated with small but significantly increased risk of the development of AD. Many of these genes are involved in innate immunity including CLU, CR1, PICALM, BIN1 (Jun et al. 2010; Harold et al. 2009; Lambert et al. 2009). One of the most significant risk factor loci identified thus far is TREM2, a macrophage gene involved in phagocytosis and associated with the activated phenotype of the brain's resident immune cell population, microglia (Neumann et al. 2013; Karch et al. 2015).

Disruption of homeostatic metabolic processes have been strongly implicated in the development of AD. Recent meta-analysis studies of diabetes mellitus and AD revealed a 70% increased risk in the development of dementia of all types and a 60% increased likelihood of developing AD specifically (Gudala et al. 2013).

Insulin is responsible for promoting glucose and neurotransmitter reuptake as well as regulating food intake and reproduction through the hypothalamus and endocrine system and upregulation of glucose transporters such as Glut4 (Plum et al. 2005). Insulin resistance, a state of hypo-responsiveness towards insulin, can occur as a result of defective insulin receptor signalling (typically as a result of genetic defects) or as a result of overstimulation of the insulin receptor (Brown et al. 2008) and while best described in the periphery in metabolic disorders such as diabetes it has recently been shown to occur in the brain (Kullmann et al. 2016). Recent studies have demonstrated that impaired insulin signalling in the hippocampus as a result of insulin resistance causes significant impairment of memory and cognitive function (Ferreira et al. 2018; Rorbach-Dolata et al. 2019; Ormazabal et al. 2018; Duarte et al. 2012). This phenomenon has recently come to be described by the term type 3 diabetes and, while widely debated, the link between altered brain glucose metabolism and cognitive impairment in mouse models is an area of increasing interest as impaired insulin signalling in the brain in turn will lead to impaired glucose utilisation and transport inside the neurons as the number of their cells membrane GLUTs are decreased as a result of the insulin signalling deficiency (Li et al. 2007; Nguyen et al. 2020). This altered glucose metabolism is a significant risk factor to neuronal cells as both glucose deprivation or excess levels have been shown to be toxic to cells (Semra et al. 2004; Suh et al. 2003). In the APP/PS1 mouse model of AD brain glucose levels have been shown to be significantly elevated, putatively as a result of the development of amyloid pathology causing a reduction in glucose utilization and decreased energy and NT metabolism (Q. Zhou et al. 2018). Furthermore, a high-sucrose diet has been shown to aggravate Aβ pathology, increase neuroinflammation and exacerbate insulin resistance (Yeh et al. 2020). Conversely, S14G-humanin alleviates insulin

resistance and oxygen deprivation in APP/PS1 mice through reactivation of Jak2/Stat3 signalling and PI3K/AKT pathway increasing autophagy of neurons and improving learning ability and memory (Gao et al. 2017; Han et al. 2018). APOE4, a cholesterol carrying protein, is one of the strongest known genetic risk factors for AD. Defects in cholesterol metabolism have been shown to lead to structural and functional CNS diseases such as AD, PD and HD (Block et al. 2010; Di Paolo et al. 2011; Wang et al. 2011). APP/PS1 mice subjected to intense treadmill exercise demonstrated reduced hippocampal soluble Aβ and greater lipid metabolism (Zeng et al. 2020). Taken together these data suggest that insulin resistance and the resulting impairment of glucose metabolism is a potent contributor to Alzheimer's disease pathology in humans and animal models of disease and may offer a range of prophylactic and therapeutic strategies to target metabolic dysfunction for high-risk patients in the coming years.

Early diagnosis is imperative to management of the condition as currently there are no disease-modifying therapies and treatment options are only address symptoms over a relatively short period. Currently diagnosis of Alzheimer's is assessed by general practitioners through presentation of a gradual onset of impaired cognitive functioning, a history of worsening cognition and amnestic, visuospatial, language presentation or executive dysfunction. Alzheimer's pathology is characterised primarily by cortical atrophy, synaptic and neuronal loss, and accumulation of Aβ plaques and neurofibrillary tau tangles (Kinney et al. 2018; Vehmas et al. 2003). The physiological function of APP is not fully understood still and for many years these misfolded protein deposits were believed to be the key causative factor in the development of AD, this became known as the Amyloid-β cascade hypothesis (Glenner et al. 1984). However, since then the ineffectiveness of Aβ therapies (Selkoe et al. 2016) coupled with mounting data implicating metabolic (Gudala et al. 2013) and blood brain barrier disruption and the role of inflammation (Kinney et al. 2018) in AD pathogenesis have brought other dimensions to this Aβ-centric paradigm. Furthermore, recent epidemiological and PET studies have shown that in younger-age onset AD appears to be primarily driven by tau and amyloid pathology (Koychev et al. 2018) while, with advancing age, the prevalence of tau and amyloid pathology increases in non-demented individuals making Amyloid and Tau pathology poorer predictors of dementia. Cortical atrophy however remains a significant indicator of dementia regardless of advancing age (Wharton et al. 2011) and loss of pre-synaptic terminals remains the best predictor of cognitive impairment in AD (Terry et al. 1991). This presents a dual issue to our current approach to translational research on AD. Firstly, the transgenic animal models popularly used focus primarily on their expression of altered APP or tau and the resulting presentation of extensive neuritic plaques and neurofibrillary tangles but show only minimal neuronal and synaptic loss. Secondly, these animal models rely on colony inbreeding to provide pure transgenic lines with minimal genetic variation and as such fail to account for inter animal

differences in frailty or resilience that manifest with increasing age at different rates in different individuals which we know to be a correlated with the prevalence of AD (Borges et al. 2019).

1.5.2 Animal models of Alzheimer's Disease

1.5.2.1 Transgenic models expressing human APP and Psen1 mutations

The majority of animal models currently in use in AD translational research are transgenic models which focus on the expression of mutated forms of APP and tau, inducing protein aggregate pathology rather than cortical atrophy/neuronal death. The Tg2576 model of AD overexpresses a human mutant form of APP (Swedish mutation KM670/671NL), resulting in elevated levels of Aβ and consequent amyloid plaques and impaired cognition (Hsiao et al. 1996). Mice exhibit elevated levels of insoluble Aβ at approximately 6 months of age which in turn aggregates into Aβ plaques around 7-8 months of age (Kawarabayashi et al. 2001). Many studies have reported commensurate cognitive deficits, in the TG2576 model performance in spatial memory tasks such as the MWM and Radial arm maze, manifesting as early as 6-8 months of age (Hsiao et al. 1996; Westerman et al. 2002; Chauhan et al. 2007; Golub et al. 2008). Recent analysis assessing the impact of sex on pathology and cognition revealed that female mice consistently showed worse reference memory than males at 12, 14 and 16 months of age as well as demonstrating that the degree of cognitive impairment correlated with amyloid pathology (Schmid et al. 2019). However it should be noted that the B6;SJL/Tg2576 strain carries a recessive rd1 mutation leading to early retinal degeneration, with homozygous rd1 carriers lose almost all rod photoreceptor cells within the first 7 weeks after birth and developing significant visual deficits (Carter-Dawson et al. 1978) which has been shown to impact on performance in visual cued, spatial orientation tasks (Brown et al. 2007; Chang et al. 2002; Yassine et al. 2013).

The most aggressive APP/PS1 mouse model currently in use is the 5xFAD model; these mice express the Swedish ($APP^{K670N/M671L}$), London (APP^{V717I}) and Florida (APP^{I716V}) APP mutations and the $PS1^{M146L}$ and $PS1^{L286V}$ mutations. The expression of these five FAD mutations results in intraneuronal Aβ accumulation as early as 6 weeks with plaque formation as early as 2 months (Oakley et al. 2006). This aggressive pathology has been shown to cause significant gliosis and cognitive impairment in the Y-maze alternation task (Heuer et al. 2012). Recent frailty analysis in the 5xFAD model has demonstrated a substantial increase in frailty with advancing age but also revealed a substantial sexual dimorphism with female mice being less frail than male littermates (Todorovic et al. 2020).

The APP/PS1 double transgenic mouse model is one of the most widely used mouse models of Alzheimer's Disease favoured for its expression of a chimeric mouse/human amyloid precursor

protein (Mo/HuAPP695swe) alongside a mutant human presenilin 1 (PS1-dE9) both of which are directed at CNS neurons, mimicking familial AD (although no AD patients carry both of these mutations). In these mice the expression of human APP is 3-fold higher than the endogenous murine APP and Aβ40/Aβ42 both increase with age, with Aβ42 being preferentially generated. Amyloid plaque deposition in the hippocampus begins as early as 3 months around the dentate gyrus and the CA1 at 4-5 months. As the animals age these plaques progress from small congophilic dense core plaques to large plaques with a dense core surrounded by a well-defined corona of diffuse amyloid (Radde et al. 2006).

While all of these models have been shown to have robust plaque pathology none showed any significant correlation between plaque pathology and the degree of cognitive impairment as assessed by the Morris water maze task (Foley et al. 2015). Similarly, they exhibit only very minor neurodegeneration and only in very specific brain regions in older animals. Furthermore, while some of these models showed localised hyperphosphorylated tau in neurites proximal to plaques, none of these developed full neurofibrillary tangles that are a classical neuropathological marker of AD (Oakley et al. 2006; Tomiyama et al. 2010; Sturchler-Pierrat et al. 1997).

When challenged with 2.5mg/kg of LPS 16-month-old aged Tg2576 animals demonstrated elevated cortical and hippocampal IL-1β protein which was absent in young (6 month) TG2576 and age matched non-transgenic littermates. Aβ1-40 levels were shown to be increased in both young and aged Tg2576 animals treated with LPS, however, Aβ1-42 levels were raised only in aged transgenics with LPS (Sly et al. 2001). While the literature largely agrees the robust plaque pathology associated with this transgenic model there is in turn associated with astrocytosis and microgliosis and glial priming like expression of IL-1β there is extensive debate over the impact of this on cognition. Some studies have reported reductions in normal learning and memory in spatial reference and alternation tasks as young as 3 months of age (Hsiao et al. 1996) while others using the Morris water maze spatial reference task have shown no correlation with plaque pathology and cognitive performance (Foley et al. 2015). Recent work by our group has demonstrated astrocytic and microglial priming phenotypes in glial isolates from the plaque-rich hippocampus of aged APP/PS1 animals (Lopez-Rodriguez et al. 2021).

1.5.2.2 Sexual dimorphism in APP/PS1 mice

As discussed previously, sex has been shown to have a significant impact upon the prevalence of AD with females being significantly more susceptible (Alzheimer'sAssociation 2015; Hebert et al. 2001). Estradiol replacement therapy in mice subjected to ovariectomy, as a model for the hormonal shift associated with menopause, was shown to attenuate the increase in Aβ levels caused by the hormone loss (Marongiu 2019). Growing evidence continues to highlight the

substantial impact that sex has on disease progression of AD and indeed in the TG2576, 5XFAD and APP/PS1 animal models we use to study the condition (Todorovic et al. 2020; Schmid et al. 2019; Jiao et al. 2016; Richetin et al. 2017; C. Zhou et al. 2018; Dubal et al. 2012)

Recent studies have shown that APP/PS1 female animals display accelerated manifestation of disease pathology as evidenced by earlier accumulation of amyloid plaque as well as consistently expressing higher levels of circulating Aβ40 and Aβ42 and severe amyloid plaque deposits compared to male littermate controls from as young as 4 to 17 months of age (Wang et al. 2003). In turn this more aggressive plaque pathology has been associated with increased risk of subsequent microhaemorrhage, greater gliosis, higher levels of pro-inflammatory cytokines and synaptic, increased cognitive impairments, reduced hippocampal neurogenesis (Jiao et al. 2016; Richetin et al. 2017) and reduced white matter integrity (C. Zhou et al. 2018) at 12 and 10 months of age respectively compared to male littermate controls. Furthermore, female APP transgenic mice have been shown to exhibit greater cytokine response, downregulation of anti-inflammatory mediators and altered metabolism in the hippocampus of animals challenged with intravenous LPS compared to APP/PS1 males (Agostini et al. 2020). Unpublished work by our group has recently shown that APP/PS1 females show more robust sickness behaviour responses to a systemic challenge of LPS than male littermates and WT control animals.

The impact of amyloid pathology on cognition and neuronal degeneration have been hotly debated across multiple AD transgenic models with many papers reporting mild cognitive deficits and neuronal and synaptic loss in select regions associated with plaque pathology (Zhu et al. 2017; Bruce-Keller et al. 2011) and other studies reporting no significant deficits (Foley et al. 2015). These recent sexual dimorphism studies have highlighted the importance of assessing deficits as a function of sex with clear deficits in cognitive performance in the MWM spatial learning task being reported in females but not males (Mifflin et al. 2021; Li et al. 2016; Gallagher et al. 2012). Indeed, estradiol replacement therapy has been shown to protect hippocampal neural stem cells and improve cognition in ovariectomized female APP/PS1 mice (Qin et al. 2020). Progesterone treatment has been shown to suppresses the cholesterol esterification which occurs in APP/PS1 female mice, AD is associated with a dysfunction of cholesterol metabolism (Shi et al. 2021).

Taken together this growing pool of data suggests that sex is a significant contributor to the pathogenesis of the AD condition which must be accounted and controlled for in all studies. As such these data highlight the pressing need for a more comprehensive understanding of the molecular mechanisms underlying the sex dimorphism which has been shown to occur in animal models and the AD patient population, in order for better early diagnostic markers to be identified and more targeted therapies to be developed.

1.5.3 Delirium

Delirium can be defined as a profound and rapid onset of fluctuating confusion and impaired awareness, sometimes referred to as acute confusion. Diverse etiology and a wide spectrum in the severity and manifestation of symptoms complicates precise definition and identification and diagnosis of the syndrome. It is a serious, but usually transient, complication. That is, patients typically recover from a delirious episode once the precipitating factor has been identified, treated and resolved, but episodes of delirium are associated with long-term sequelae. Research has highlighted the increased risk of loss of independence and cognitive decline in vulnerable patients recovered from bouts of delirium (Rockwood et al. 1999). It is highly prevalent in elderly patients: approximately 30% of elderly patients admitted to hospital will develop delirium (Clegg et al. 2013). Moreover, those admitted to hospital with delirium are at much greater risk of increased moribundity and mortality compared to patients of similar age admitted without delirium (MacLullich et al. 2009; Ely et al. 2004). Elderly patients with dementia or AD frequently demonstrate episodes of delirium following surgery or infection, with deleterious consequences for subsequent cognitive function (Davis et al. 2015; Fong et al. 2015) and negative impacts on independence and survival. Acute systemic inflammation (and/or delirium) significantly increase the risk of long-term cognitive decline and dementia (MacLullich et al. 2009; Davis et al. 2012) and have been shown to worsen the severity of existing dementia (Holmes et al. 2009; Fong et al. 2009). However, milder systemic inflammation not resulting in delirium can also induce cognitive decline (Holmes et al. 2009). Unsurprisingly it has been shown in many recent studies that there is a significant correlation between a patients frailty status severity and their risk factor for experiencing delirium following surgery, injury or infection (Eeles et al. 2012; Joosten et al. 2014; Persico et al. 2018; Sanchez et al. 2020; Choutko-Joaquim et al. 2019; Li et al. 2021; Mahanna-Gabrielli et al. 2020). As such it has been proposed that delirium is a manifestation of the frail individual's cognitive vulnerability following an acute stressor such as a fractured hip or illness.

Taken together these findings suggest that multi system co-morbidities may exacerbate and/or accelerate the progression of AD. These co-morbidities may range from metabolic dysfunction to genetic risk factors, with associated innate immune responses precipitating and exacerbating cognitive dysfunction. Those with higher baseline cognitive dysfunction and/or greater underlying frailty may be predicted to show greater susceptibility and sex may be an additional factor in this risk for decline.

1.6 Aims and objectives

The phenomenon of chronic, low-grade inflammation which has been shown to occur with age varies significantly among individuals, consistent with the idea that chronological ageing has limited predictive power for brain ageing. I propose that the severity of an individuals' "Frailty" may define the risk for brain inflammation with age. Furthermore, the ageing process is not uniform within the CNS, it suggests that different regions of the brain are more immune vigilant and perhaps more sensitive to immune challenge than others. I hypothesise that microglial priming will increase with age in a regionally variable manner which will correlate with the consequent vulnerability to secondary insults in a way that is contingent on the frailty of the individual (i.e. the accumulation of deficits that affect the general health of the animal).

To this end I will attempt to reconcile molecular and histochemical indices of inflammatory cell populations and mediators across the ageing brain to better characterise the regional heterogeneity under acute inflammatory and basal conditions and how this relates to cognitive vulnerability. I will use behavioural and physiological assays on mouse models of ageing and to determine the extent to which frailty status correlates with molecular changes in inflammatory cell populations and mediators across the ageing brain and predicts vulnerability to and recovery from cognitive and behavioural deficits to acute inflammatory stressors. I will utilise mouse models of Alzheimer's disease to determine how AD pathology affects vulnerability to metabolic and cognitive deficits following repeated inflammatory challenges to mimic a chronic inflammatory condition and attempt to reconcile this with histochemical and molecular indices of inflammatory cell populations in FACS isolated glial cells.

Chapter 2:

Materials and Methods

2.1 Materials:

2.1.1 Animals and *in vivo* Products:

Alpha-Trak Glucometer	Veterinary Surgeons Supply Co.
Alpha-Trak Glucose Strips	Veterinary Surgeons Supply Co.
Animal Recovery Chamber HE010	Vet Tech, UK
Animal restraint tube (10cm long, 2cm diameter)	Custom designed in TCD
Animal Treadmill Exer 3/6	Columbus Instruments
ANY-maze video tracking software	ANY-maze
APP/PS1 mice	Jackson Laboratories, USA
Burrowing tubes	
CalR Version 1.2 app for calorimetry analysis	CalR
C57BL/6 mice	Jackson Laboratories, USA
Contextual Fear Conditioning Chamber	Ugo Basille
DAS-7009 thermal transponders reader	BMDS
EasyFLOW ventilated cage control unit	Tecniplast
GM500 Sealsafe Plus ventilated cage system	Tecniplast
Heating pad	Physitemp
Horizontal bar	Custom designed in TCD
Implantable electronic ID transponders	BMDS
Infrared vari-focal 2.7-13.5mm CCTV camera lens	Fujifilm
Inverted Screen	Custom designed in TCD
Laboratory mouse diet	Red Mills, UK
MM-1 Load Cell	Sable Systems
Morris Water Maze Tank	Ugo Basille
Mouse weights	Custom designed in TCD
Nestlets mouse bedding	Lab Supply USA
Non-toxic water-based paint	Crayola
Open Field Box	Custom designed in TCD
Precision X-tra Blood Glucose Test Strips	Abbott Technologies
Precision X-tra Blood β-Ketone Test Strips	Abbott Technologies
Promethion cages	Sable Systems
Promethion metabolic cage system	Sable Systems
Thermocouple rectal probe	Physitemp
T-Maze	Custom designed in TCD
Tunnel (6cm high X 9cm wide X 40cm long)	Custom designed in TCD

Vari-focal camera 2.7-13.5mm 60516 digital USB	Basler
Vaseline	Vaseline

2.1.2 Animal Surgery & Sacrifice Products

1 ml syringes	Terumo
2,2,2 Tribromoethanol	Sigma Aldrich, UK
23, 25, 26-gauge needles	Braun, Ireland
25-gauge butterfly needles	Terumo
Active Scavenging Unit Mk II - 240V AN005	Vet Tech, UK
Aesculap Isis small animal electric razor	Kerbl
Anaesthetic Isoflurane Vapouriser Std Fill 5% CM	Vet Pharma
Buprecare 0.3mg/ml	Animalcare Ltd., UK
Carbon Steel Burrs 0.7mm diameter	Fine Science Tools (F.S.T)
Calibrated microcapillaries	Drummond
Cot Tip Appl. Sticks	Mason Technology
EMLA lidocaine 2.5% prilocaine 2.5%	Aster Zenaca
Euthatal (Sodium pentobarbitol)	Alfasan
Germinator 500	Electon Microscopy Services,
High speed stereotaxic micro drill	David Kopf Instruments, USA
Hydrex chlorhexidine 4% w/v	ECOLAB
Isolfurin 1000mg/g	Vet Pharma
Mini Thermacage with diffuser	Datesand
OT-ELITE 5 oxygen concentrator	Vet Tech, UK
Sterotaxic frame, ear bars and nose piece	David Kopf Instruments, USA
Surgical Instruments	Fine Science Tools (F.S.T)
Scalpel blade 10	Swan-morton
Surgibond Tissue Adhesive	Vet Pharma
Tertiaryamyl alcohol (2-methyl-2-butanol)	Merck
Trusilk sutures 6/0 gauge, 0.7 metric, 45 cm long black unbraided	Sutures India
Videne Povidone Iodine Solution 10% 500ml	ECOLAB
Visdisk 0.2% w/w eye gel	Bausch & Lomb
WB-1 Small Animal Warming Blanket	Physitemp

2.1.3 Treatments:

0.9% Sodium Chloride (Sterile)	Sigma Aldrich, UK
Salmonella equine abortus Lipopolysaccharide (LPS)	Sigma Aldrich, UK

Mouse recombinant Tumour necrotic factor α (TNF-α)	Peprotech, UK
Polyinosinic-polycytidylic acid (Poly I:C)	Sigma Aldrich, UK

2.1.4 Immunohistochemistry Reagents & Products:

3,3' Diaminobenzidine	Sigma Aldrich, UK
Acrylic nail varnish - OPI RapiDry Top Coat 15ml	Boots
Ammonium nickel chloride	Sigma Aldrich, UK
Boric acid	Sigma Aldrich, UK
Cell A imaging software	Phi
Citric Acid	Sigma Aldrich, UK
Coplin staining jars clear soda lime glass 100X100X100	VWR
Coplin jar metal 25 rack	VWR
Cresyl Violet	Sigma Aldrich, UK
DPX Mountant	Sigma Aldrich, UK
Formalin solution, neutral buffered, 10%	Sigma Aldrich, UK
Glacial Acetic Acid	Sigma Aldrich, UK
Harris haemotoxylin	VWR
Histoclear II	National Diagnostics, USA
Hoescht	Thermo Fisher
Humidity staining tray black plastic	Pyramid Innovation
Kartell Schifferdecker Staining Jar	Fisher Scientific
Immersion oil	Raymond Lamb
ImageJ Software	NIH, Bethesda, Maryland
Leica confocal SP80 microscope	Leica Germany
Leica DM100 double header microscope	Leica Germany
Leica DM3000 Imaging microscope	Leica Germany
Leica RM2235 Microtome	Leica Germany
Leica EG1150C Tissue Embedder Cold Plate	Leica Germany
Leica EG1150H Tissue Embedder	Leica Germany
Leica TP1020 Tissue Processor	Leica Germany
Lens cleaning tissue paper	Whatman
Luxol Fast Blue	Clinisciences
Microslide Superfrost Plus White Slides	VWR
Menzel Microscope Coverslips	Thermo Fisher
Normal chicken serum	Vector Laboratories, UK
Normal donkey serum	Vector Laboratories, UK

Normal goat serum	Vector Laboratories, UK
Normal horse serum	Vector Laboratories, UK
Normal rabbit serum	Vector Laboratories, UK
Olympus DP25 lens	Olympus, EU
Super Pap Pen Liquid Blocker	Ted Pella Inc.
Paraffin wax	Leica Germany
Paraformaldehyde	Sigma Aldrich, UK
MINIPULS3 Peristaltic pump and tubing	Gilson
Plastic cassettes	Labonord, France
Plastic wax containers for cassettes	Labonord, France
Prolong gold antifade mounting medium	Thermo Fisher
Staining trough black plastic BRAND™	Fisher Scientific
Straight razor blades	Boots
SuperFrost Plus microscope slides	Menzel-Glaser Germany
Vectastain ABC kit	Vector Laboratories, UK

2.1.5 Antibodies

6E10 mouse polyclonal anti-human	Biolegend
Biotinylated Anti-Goat IgG made in Rabbit	Vector
Biotinylated Anti-Mouse IgG made in Horse	Vector
Biotinylated Anti-Rabbit IgG made in Goat	Vector
C-C motif chemokine 2 polyclonal goat anti-mouse	R&D Biosystems
Chicken anti-Rabbit IgG (H+L) Cross-Adsorbed Secondary Antibody, Alexa Fluor 488	Thermo Fisher
Choline O-acetyltransferase goat anti-human	Cell Signalling Technology
C-X-C motif chemokine 10 polyclonal goat anti-mouse	Peprotech
Donkey anti-Goat IgG (H+L) Cross-Adsorbed Secondary Antibody, Alexa Fluor 633	Thermo Fisher
Glial Fibrillary Acidic Protein (GFAP) polyclonal rabbit anti-mouse	DAKO
Ionised calcium binding adpator molecule 1 (IBA-1) polyclonal goat anti-rat	Abcam
Ionised calcium binding adpator molecule 1 (IBA-1) polyclonal rabbit anti-mouse	WAKO
Purine -rich box 1 (Pu.1) polyclonal rabbit anti-human	Cell Signalling Technology
Synaptophysin (Sy38) monoclonal mouse anti-mouse	Merck-Millipore

2.1.6 Molecular Reagents & Products:

0.2ml qPCR sterile tubes	Fisher Scientific
Acrylamide 30%	BioRad
Ammonium persulfate	Sigma Aldrich, UK
Biometra Trio RT-PCR thermocycler	Analytick Jena
Chemidoc MP gel imager	BioRad
Consor EV261 power supply	Medical Supply Company
FastStart SYBR green PCR master mix	Roche, UK
FastStart universal ROX probe PCR master mix	Roche, UK
Gel loading pipette tips	Cruinn
GelRed™ nucleic acid stain	Scientific laboratory supplies
Gel tank AE6450 ATTO	Medical Supply Company
High Capacity cDNA Reverse Transcriptase Kit	Applied Biosystems, UK
iScript cDNA synthesis kit	BioRad
MicroAmp 384-well Reaction Plate	Applied Biosystems, UK
MicroAmp 96-well Reaction Plate	Applied Biosystems, UK
Molecular grade absolute ethanol	Sigma Aldrich, UK
Molecular grade chloroform	Sigma Aldrich, UK
Molecular grade glycogen	Thermo Fisher
Molecular grade isopropanol	Honeywell
Molecular grade water	Sigma Aldrich, UK
Nanodrop ND1000 Spectrophotometer	Thermo Fisher
Optical adhesive covers	Applied Biosystems, UK
pGEM® DNA Markers	Promega
Primers custom designed oligonucleotides	Sigma Aldrich, UK
Qiashredder columns	Qiagen, UK
QuantStudio 384 well qPCR machine	Thermo Fisher
Ribolock Rnase Inhibitor	Thermo Fisher
RNase-free DNase I enzyme	Qiagen, UK
RNeasy Plus micro kits	Qiagen, UK
RNeasy Plus mini kits	Qiagen, UK
StepOne 96 well qPCR machine	Thermo Fisher
TEMED	Sigma Aldrich, UK
TRIzol™ Reagent	Invitrogen

2.1.7 Protein Reagents & Products

ELISA MAX™ Standard Set Mouse IL-6	Biolegend Way, USA
Greiner Plate sealer transparent	Greiner, USA
Mouse CCL2 DuoSet ELISA	RnD Biosystems, USA
Mouse CXCL13/BLC/BCA-1 DuoSet ELISA	RnD Biosystems, USA
Mouse TNFα DuoSet ELISA	RnD Biosystems, USA
Mouse Ultra-Sensitive Insulin ELISA	Crystal Chem, USA
Nunc™ MaxiSorp™ ELISA Plates, Uncoated	Biolegend Way, USA
Spectra max Plus 384 plate reader	Molecular devices LLC
Streptavidin poly-HRP - Sanquin	Sanquin, USA
Substrate Reagent Pack	RnD Biosystems, USA
TMB Liquid Substrate for ELISA	Applied Biosystems

2.1.8 FACS Reagents & Products:

70µM cell strainers	Sigma Aldrich, UK
7AAD conjugated antibody	Miltenyi
BD FACS Aria II Cell Sorter	BioSciences, USA
CD11b FITC conjugated antibody	Miltenyi
Purified Rat Anti-Mouse CD16/CD32 (Mouse BD Fc Block™)	BioSciences, USA
CD45 APC conjugated antibody	Miltenyi
Collagenase	Roche
Dnase I	Thermo Fisher, USA
FBS	BioSciences, USA
GLAST ACSA-1-PE conjugated antibody	Miltenyi
HBSS	BioSciences, USA
HEPES	Merck
Lobind 1.5ml Eppendorfs	Fisher Scientific
LS positive selection columns	Miltenyi
MACS anti myelin beads	Miltenyi
MACS Buffer	Miltenyi
MACS sorting rig	Miltenyi
TRIzol™ LS Reagent	Invitrogen

2.19 General Laboratory Chemicals:

β-Mercaptoethanol	Sigma Aldrich, UK
Bovine Serum Albumin >98%	Sigma Aldrich, UK
Disodium hydrogen phosphate heptahydrate	VWR, USA
EDTA	Sigma Aldrich, UK
Ethylene Glycol	Capitol Scientific
Formic Acid	Sigma Aldrich, UK
Glycerol	Sigma Aldrich, UK
Guanidine Hydrochloride	Sigma Aldrich, UK
Heparin (bovine)	Leo Laboratories, UK
Hydrochloric acid	VWR, USA
Hydrogen peroxide (H_2O_2)	Sigma Aldrich, UK
Lithium Carbonate	Sigma Aldrich, UK
Magnesium sulphate	Acros
Methanol	Sigma Aldrich, UK
Monosodium dihydrogen phosphate	VWR, USA
Paraformaldehyde	Sigma Aldrich, UK
Pepsin from porcine gastric mucosa	Sigma Aldrich, UK
Phosphate-buffered saline (PBS)	Sigma Aldrich, UK
Potassium Bicarbonate	Sigma Aldrich, UK
Sodium Bicarbonate	Sigma Aldrich, UK
Sodium Carbonate	Sigma Aldrich, UK
Sodium Chloride (NaCl)	Sigma Aldrich, UK
Sodium Hydroxide	Sigma Aldrich, UK
Sodium phosphate dibasic heptahydrate	Sigma Aldrich, UK
Sodium phosphate monobasic dihydrate	Sigma Aldrich, UK
Sucrose	Sigma Aldrich, UK
Sulphuric acid (H_2SO_4)	VWR, USA
Tris-base	Sigma Aldrich, UK
Tris-HCl	Sigma Aldrich, UK
Triton X-100	Sigma Aldrich, UK
Tween 20	Sigma Aldrich, UK
Urea	Sigma Aldrich, UK
Xylene	VWR, USA

2.1.9 General Laboratory Products:

Autoclave tape	Sigma Aldrich, UK
Eppendorfs 0.5ml	Lennox
Eppendorfs 1.5ml	Lennox
Eppendorfs 2ml	Lennox
Nitrile gloves	Polyclo Heatlhline
Non-sterile Pipette tips	Greiner, Germany
Nuclease-free PCR tube	Applied Biosystems
Parafilm laboratory roll	Pechiney Plastic Packaging, USA
Pasteur pipette 3ml	Sigma Aldrich, UK
Standard grade No. 1 filter paper	GE Healthcare, UK
Sterile 7ml Bijou tubes	Sterilin, UK
Sterile automatic pipette tip	Lennox
Sterile Falcon 15ml & 50ml tubes	Sarstedt, Ireland
Sterile Pipette tips (RNAse free) 10, 20, 200, 1000µl	Starlab, Germany
Syringes (sterile 1ml)	Braun, Ireland
Tubes 200µl, 500µl, 1ml	Greiner, Germany

2.1.10 General Equipment

800W compact microwave	SANY
AutoRep E automatic pipette	Ranin
Cryogenic liquid nitrogen TR7 Dewar 7 litre	Air Liquide
Driblock DB-2A tube heating block	Techne
Easy-Read® thermometer	Sigma Aldrich, UK
Economy incubator	Boekel
Edge pH Probe	Hanna
FB15012 TopMix vortex	Fisher Scientific
Finn pipettes	Cruinn
Gilson pipettes	Gilson
JB Aqua Pluss Water Bath	Grant
Kimble Motorised Pestle	Kontes
Mag stirrer heat stir CB162	Stuart
ME1002 weighing Scale	Mettler Toledo
Micro CL21R desktop centrifuge	Thermo Fisher
Milliq water dispenser	MilliQ
Paraffin stretching GFL 1052 Water Bath	Medical Supply Company

PC-10 capillary puller	Narishige International
PS-M3D orbital shaker	Grant Bio
PYREX™glassware beakers 100, 250, 500, 2000ml	Fisher Scientific
PYREX™media bottles 100, 250, 500, 1000ml	Fisher Scientific
S810R eppendorf centrifuge	Merck
Sarstedt Cardboard Microtube Sample 10X10	Sarstedt
See saw rocker SSM4	Stuart
Stainless steel liquid nitrogen Dewar 2 litres	Dilvac
Technico mini picofuge	Analytix
Ultra Low Temperature Freezer -86℃ DW-86L828J	Haier Biomedical

2.2 Methods:

2.2.1 – Animals

Male & female C57BL/6J and APP/PS1 mice (Harlan, Bicester, United Kingdom) were bred and housed in groups of five where possible at 21°C with a standard 12:12 hour light dark cycle with access to food and water *ad libitum*. Mixed sex populations were used for all studies to provide the most balanced and complete representation of the population. All animal experimentation was performed under a licence granted by Health Products Regulatory Authority (HPRA), Ireland, with approval from the local TCD Animal Research Ethics Committee and in compliance with the Cruelty to Animals Act, 1867 and the European Community Directive, 86/609/EEC, with every effort made to minimize stress to the animals.

2.2.2. – Administration of inflammatory stimuli

2.2.2.1 Intraperitoneal Lipopolysaccharide

For behavioural and molecular studies, experimental groups were scruffed and injected intraperitoneally (i.p.) with 100µg/kg or 250µg/kg of the bacterial endotoxin LPS (equine arbortus, Sigma, L5886, Poole, UK) prepared in non-pyrogenic 0.9% sterile saline (Sigma, Poole, UK). This dose mimics a mild to moderate infection rather than severe sepsis, eliciting small changes (<1°C) in core body temperature and acute working memory deficits. Control animals were injected with sterile saline (Sigma, Poole, UK) 200µl per 20g body weight.

2.2.2.2 Intraperitoneal Polyinosinic-polycytidylic acid (Poly I:C)

For behavioural and molecular studies, experimental groups were scruffed and injected with 12mg/kg of the viral mimetic Poly I:C (Amersham) prepared in non-pyrogenic 0.9% sterile saline (Sigma, Poole, UK) in the peritoneum. This dose mimics a mild to moderate viral infection, eliciting small changes (<1°C) in core body temperature and acute working memory deficits. Control animals were injected with sterile saline (Sigma, Poole, UK) 200µl per 20g body weight.

2.2.2.3 Intraperitoneal Tumour necrosis factor alpha (TNFα)

For behavioural and molecular studies, experimental groups were scruffed and injected i.p. with 250µg/kg of mouse recombinant TNFα (Peprotech) prepared in non-pyrogenic 0.9% sterile saline (Sigma, Poole, UK). Control animals were injected with sterile saline, 200µl per 20g body weight.

2.2.2.4 Intrahippocampal surgery and injection of Tumour necrosis factor alpha (TNFα)

Intrahippocampal TNFα (Peprotech) was prepared in non-pyrogenic 0.9% sterile saline (Sigma, Poole, UK) to a dose of 300ng/µl. The animal was anaesthetized by i.p. administration of Avertin (2,2,2-tribromoethanol; ≈20 ml/kg body weight)) and once anaesthetised had its scalp shaved and swabbed with 70% Ethanol (EtOH). A localised analgesic EMLA (lidocaine 2.5% prilocaine 2.5%; Astra-Zeneca) was applied, to the position of the ear bars upon the skull, before being placed in the stereotaxic frame (David Kopf Instruments, Tunjunga, CA, USA) upon a heating pad (Physitemp) with a rectal probe inserted (Physitemp) to maintain and monitor body temperature under anaesthesia. Visdisk 0.2% w/w eye gel (Bausch & Lomb) was applied to the animal's eyes, to prevent drying and irritation, and the scalp was swabbed with iodine before making an incision down the centre of the scalp. A hole was drilled in the cranium and 1µl (300ng) of TNFα in sterile saline was administered using a microcapillary at the following coordinates from bregma; anteroposterior -2.0mm, lateral -1.6mm, depth -1.6mm. The capillary left in place for one minute to allow diffusion of the injected material and to minimise reflux along the injection tract. Control animals were injected with 1µl of sterile saline in the same fashion. The animal's scalp was sutured closed with Trusilk sutures 6/0-gauge, 0.7 metric and sealed with VetBond Tissue Adhesive and placed in a recovery chamber at approximately 25°C until fully conscious and mobile. At this point animals were placed back into their home cage with 'Nestlets' bedding material and a 5% sucrose solution in place of normal drinking water (for 24 hours). Recovery and incision site healing was monitored until fully healed or the animal was sacrificed or resutured as appropriate.

2.2.3 – Behavioural and Physiological Tests

For all behavioural experiments, mice were brought from the housing room and left in the test room for 15 minutes prior to beginning testing to ensure each animal was in an optimal state of arousal.

2.2.3.1 – Open Field Activity

The open field consisted of a plastic base (58cm x 33cm) surrounded by walls 19cm in height. The floor of the box was divided into a grid of equal sized squares.

2.2.3.1.1 Manual measurement

Open Field activity was assessed in mice over 2 minutes based on the distance travelled (in grid squares crossed) and the total number of rears (the frequency with which a mouse stood on their hind legs).

2.2.3.1.2 ANY-Maze measurement

In some animals open Field activity was filmed over a ten-minute period using a ceiling-mounted Vari-focal camera 2.7-13.5mm 60516 digital USB (Basler) fitted with an infrared vari-focal 2.7-13.5mm lens (Fujifilm) and analysed using ANY-maze video-based software to score, distance travelled, time mobile, meander and average speed (Stoelting, Europe). Additionally, speed during the ten-minute testing period was assessed at 200sec intervals. Rearing and grooming were recorded manually.

2.2.3.2 – Visuospatial reference memory Y-maze task

To investigate hippocampal-dependent reference memory, a "paddling" Y-maze visuospatial task was used, as described in (Deacon et al. 2002; Reisel et al. 2002). A clear Perspex Y-maze consisting of three arms with dimensions 30 x 8 x 13 cm was mounted on a white plastic base. The distal end of each arm contained a hole, 4 cm in diameter and 2 cm above the floor. The maze was placed in the centre of a small room with prominent distal extra-maze cues. During any given trial the exits from two arms were blocked by insertion of a closed black plastic tube thus preventing mice from exiting, while the third exit had an open black tube where mice could exit the maze and enter a black burrowing tube to be returned to their home cage. This designated "escape arm" was defined according to its given spatial location relative to the room cues. Each of the three plastic tubes had a burrowing tube over them on the outside of the maze so that from the centre of the maze all arms looked identical. The maze was filled with 2 cm of water at 20 to 22°C, sufficient to motivate mice to leave the maze by paddling to an exit tube at the distal end of one arm, 2 cm above the floor. Mice exit to the burrowing tube, inside which they are returned to their home cage. Mice were placed in one of two possible start arms in a pseudorandomised sequence for 12 trials and the groups were counter-balanced with respect to the location of the exit and start arm. For any individual mouse, the exit arm was fixed. An arm entry was defined as entry of the whole body (all 4 paws), excluding the tail. A correct trial was defined as entry to the exit arm without entering other arms. The number of trials completed, across all 5 days of training, before making 8 consecutive correct choices was determined and used to score their baseline cognitive status and included in the generation of their frailty index. Retention of the memory of their exit location on this cognitive task, during systemic inflammation induced by LPS (250µg/kg) was assessed over ten trials. Thereafter, their ability to locate and choose a new exit arm, requiring an abandoning of their prior exit location and adopting a new exit strategy was assessed by moving the exit arm to a new. This attending to a novel exit was assessed over 12 trials. During this 'reversal testing' mice were placed into either of the two possible start arms in a pseudorandomised sequence, as before, with the exception that they could not start in their original escape arm on the first trial.

2.2.3.3 – Morris Water Maze (MWM)

The Morris water maze (MWM) consisted of a stainless-steel tank 150cm in diameter, 60 cm in depth filled with water to a depth of 31 cm. The water temperature was maintained at 21-22°C (Room Temperature) and water opacity was achieved using non-toxic white tempura paint powder (Crafty Devils, UK). The water maze was theoretically divided into four quadrants), designated north, south, east, and west, and a raised transparent platform (30cm in height,) submerged 1cm below the surface of the water, was placed in one of these quadrants. Activity was recorded using a ceiling-mounted video camera directly above the apparatus and analysed using ANY-maze software to track distance and path travelled. For each trial the animal was placed, facing the wall of the tank, into the water at a position. The start position was changed from trial to trial, and the time and distance travelled to reach the platform was measured. Animals each underwent four trials per day and trials were spaced approximately 1-1.5 hours apart. After each trial the animals were dried and placed in a recovery chamber at 37°C for approx. 3mins before being returned to their home cage. On the first day of training if the animals had not found the platform after 1min they were guided to it using a Perspex rod. This was not necessary after the first day of training. After the fourth trial each day animals were returned to their home cage and then to their holding room. After training a probe test was performed. The probe test involved removing the raised platform, placing the animals in the water directly opposite where the platform should be and measuring the time spent and distance travelled in the quadrant where the platform had previously been over 1min. Following this a flag trial was performed with the platform flagged by a yellow marker flag to indicate its location and confirm any visual impairment in the animals tested.

2.2.3.4 – Contextual and auditory fear conditioning

Fear conditioning was assessed as an index of associative fear learning and memory using a box (40cm x 16cm x 16cm) with transparent walls and with a floor containing metal rods which were wired to a shock generator (UGO Basile, Italy) controlled via an ANY-maze interface and video capturing software (Shoji et al. 2014). Black and white chequered cards were fitted to three of the four walls, the fourth containing the door into the cage was left un-patterned. The mice were placed into the box and allowed to explore for 100secs. A tone at 20dB, 5kHz was presented for 20 seconds, followed by a 20 second pause before presentation of a shock of 0.4 mA for 2 seconds. A 100 second interval followed before presentation of the tone, pause and shock once again. After a further 30 seconds of exploration mice were removed to a holding cage. After a minimum of 30 seconds in the holding cage, or completion of all animals' testing from the same home cage, mice were returned to the home cage. 10% EtOH was used to clean down the shock cage between each animal.

	Description	Time (s)
Day 1	Exploration	100
	Auditory Cue	20
	Break before shock	20
	Shock	2
	Intertrial Interval	100
	Auditory Cue	20
	Break before shock	20
	Shock	2
	Wait	30
	Return To Home Cage	
Day 2		
Day 3	Contextual fear conditioning assessment	300
	Auditory-cued fear conditioning assessment	300

Table 2.1 Fear conditioning protocol breakdown CFC

48 hours after fear conditioning training mice were placed back into the shock cage with the same patterned background for 300 seconds. During this time no tones or foot shocks were administered, but white noise was played constantly. ANY-maze video analysis software was used to assess freezing behaviour, which is defined as complete immobility with the exception of breathing. Freezing threshold for a freezing event was set at 1500ms and mice were scored on their total time spent frozen, total freezing events, latency to first freezing event and freezing score, a function of freezing duration and number of episodes.

Upon completion of contextual fear testing, auditory-cued fear testing was assessed by changing the chequered pattern of the shock cage walls to a uniform grey and placing the animal inside the shock cage for 300seconds. After 100secs the same auditory cue was presented as in their training, 20dB, 5kHz for 20 seconds and the time spent freezing after the cue was assessed using ANY-maze video analysis software as was done for contextual fear testing. A second tone was presented at 240 seconds.

2.2.3.5 –T-maze alternation task

Hippocampal-dependent working memory was assessed in mice using alternation behaviour in a novel water T-maze task designed to assess working memory performance, free from confounds introduced by reduced or slowed locomotor activity (frequently observed in animals experiencing sickness behaviour). T-maze alternation was performed by Dr. Carol Murray in order to provide behavioural data on the cohort of animals subsequently used to quantify age-associated neuropathology. The T-maze was constructed of black Perspex with the following dimensions (cm): long axis 67, short axis 38, depth 20 and arm width 7. Single 4cm diameter holes were at the end of each choice arm, 2 cm above floor level and black exit tubes could be placed into them or blocked entirely as needed. During the first arm entry a "guillotine" door was inserted to prevent access to one or other choice arm. Prior to introducing the mouse, the maze was filled with water to a depth of 2cm at 20°C in order to motivate mice to leave the maze by "paddling" or walking "tip-toe" to an exit tube. Animals were taken with their cage mates to a holding cage. Each mouse was then individually placed in the start arm of the maze for their first trial with one arm blocked, selected in a pseudorandom sequence (equal number of left and right turns with no more than 2 consecutive runs to the same arm). Upon making this turn the mouse could then escape from the water into a small escape tube into a second transit tube in which they were transported to another holding cage. The mouse was held here for a 30 second intra-trial interval during which time the guillotine door was removed, and the exit tube switched to the alternate arm. The mouse was then replaced in the starting arm for its "choice trial" and could choose either arm. However, in order to successfully escape the mouse must alternate from its original turn to escape. Upon choosing correctly mice escape to the transit tube as before and are returned to their home cage. Should an incorrect choice be made then the mouse was allowed to self-correct. Animals were trained targeting a performance of correct alternation greater than 80%. No animals were experimentally challenged unless they performed at 70% or above for consecutive days before challenging. Furthermore, no animals that performed at lower than 80% in the last block of 5 trials or displayed evidence of a side preference on the day prior to experimental challenges were included. During training some animals developed a side preference which could be broken using a correction strategy. Instead of allowing an animal to self-correct the entrance to the correct arm was closed off once the incorrect arm was chosen, thus forcing the animal back to the start arm and to commence the trial again with the correct arm open once more. This was repeated until the animal finally chose the correct body turn when starting from the start arm. This correction strategy was only employed for animals employing a complete side preference, was discontinued once broken and was never employed within 2 days of administration of substances to examine effects on working memory.

5-9-month-old animals were classified as “Young” while 23–24-month-old animals were classified as “Aged”. These classifications were then used to assess markers of microglial activation as a function of cognitive status. Individual animal’s performance under the acute effect of saline, LPS (100µg/kg) and Poly I.C. (12mg/kg) was used to stratify animals by their cognitive vulnerability into cognitively frail and cognitively resilient groups. “Cognitively frail” refers to animals who scored less than or equal to 60% alternation, in 3 or more of the 6 blocks of 5 trials following their acute inflammatory challenges. “Cognitively Resilient” animals scored greater than 60% correct alternation over a minimum of 4 blocks following the same challenges.

		% correct alternation in a block of 5 trials						
		LPS (100µg/kg)			Poly I:C (2mg/kg)			Cognitive Vulnerability
		Block 1	Block 2	Block 3	Block 4	Block 5	Block 6	
Young	5-7 Months	80	80	80	100	80	80	Resilient
	5-7 Months	100	100	80	100	80	100	Resilient
	5-7 Months	80	80	80	60	60	60	Frail
Aged	24 Months	80	80	80	80	100	100	Resilient
	24 Months	100	80	80	100	60	80	Resilient
	24 Months	60	60	100	60	60	80	Frail
	24 Months	80	80	80	60	60	60	Frail

Table 2.2: Exemplar cognitive vulnerability classification by percentage correct alternation over blocks of 5 trials, “Cognitively frail” refers to animals who scored ⩽60% alternation, in 3 or more of the 6 blocks of 5 trials following their acute inflammatory challenges. “Cognitively Resilient” animals scored >60% correct alternation over a minimum of 4 blocks following the same challenges.

2.2.3.6 –T-maze spontaneous alternation task

Spontaneous Alternation was measured in the same black Perspex T-maze. Each animal was initially placed at the bottom of the T facing the junction of the arms. During the first half of each trial a divider is placed in the centre of the two arms so that the animal cannot see into either arm when initially choosing which arm to explore first **(Fig 2.1. A).** Once an arm is chosen the exit is blocked off **(Fig 2.1. B)** and the animal contained within and allowed to explore for 30 seconds. After 30 seconds (30s) the animal is removed to a holding cage. The divider and the wall blocking the chosen arm are removed and on the second half of each trial the animal can freely choose which arm to explore. The animal typically chooses to explore the opposite arm to the first one chosen (i.e. spontaneously alternates). Alternation over five trials was measured.

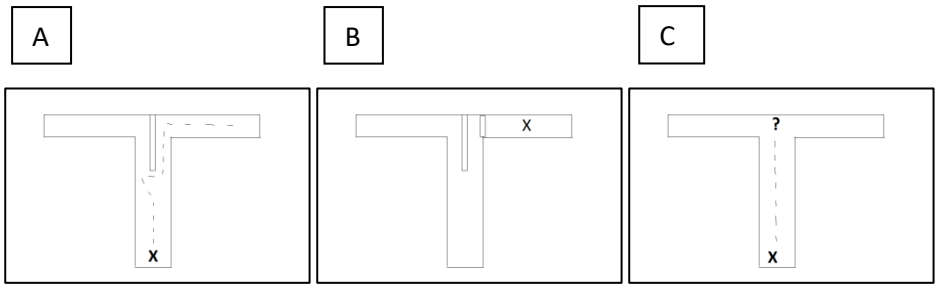

Figure 2.1: Spontaneous alternation apparatus set-up

2.2.3.7 –Horizontal Bar

The horizontal bar was designed to assess forelimb muscular strength and co-ordination. A 26cm long metal bar 2mm in diameter was supported by a 19.5cm high wooden support pillar at each end. Each mouse was gripped firmly at the base of the tail and lifted above the bar to allow it to grip the centre point of the bar with only its forepaws. The tail was then quickly released, and the mice scored based on the time they held on before falling off the bar onto a sponge padded mat below the bar. The test was continued for up to a maximum of 60 seconds. Reaching the support platform atop the support pillars was scored as the maximum 60 seconds, as was simply hanging on for 60 seconds. For those animals falling off the bar, they were scored according to the time at which they fell off.

2.2.3.8 – Inverted Screen

The inverted screen (Cunningham et al. 2009) was used to assess the muscular strength of all four limbs. The screen consisted of a wooden frame, 43cm squared, covered in a wire mesh of 12mm squares of 1mm diameter wire. The mouse was placed in the centremost section of the screen and raised to a height of approximately 80cm above padding to cushion the fall. The screen was then slowly inverted over 2 seconds such that the animal's head descended first. Mice were assessed on their time to fall up to a maximum of 2-15mins dependent upon the Frailty Index in use.

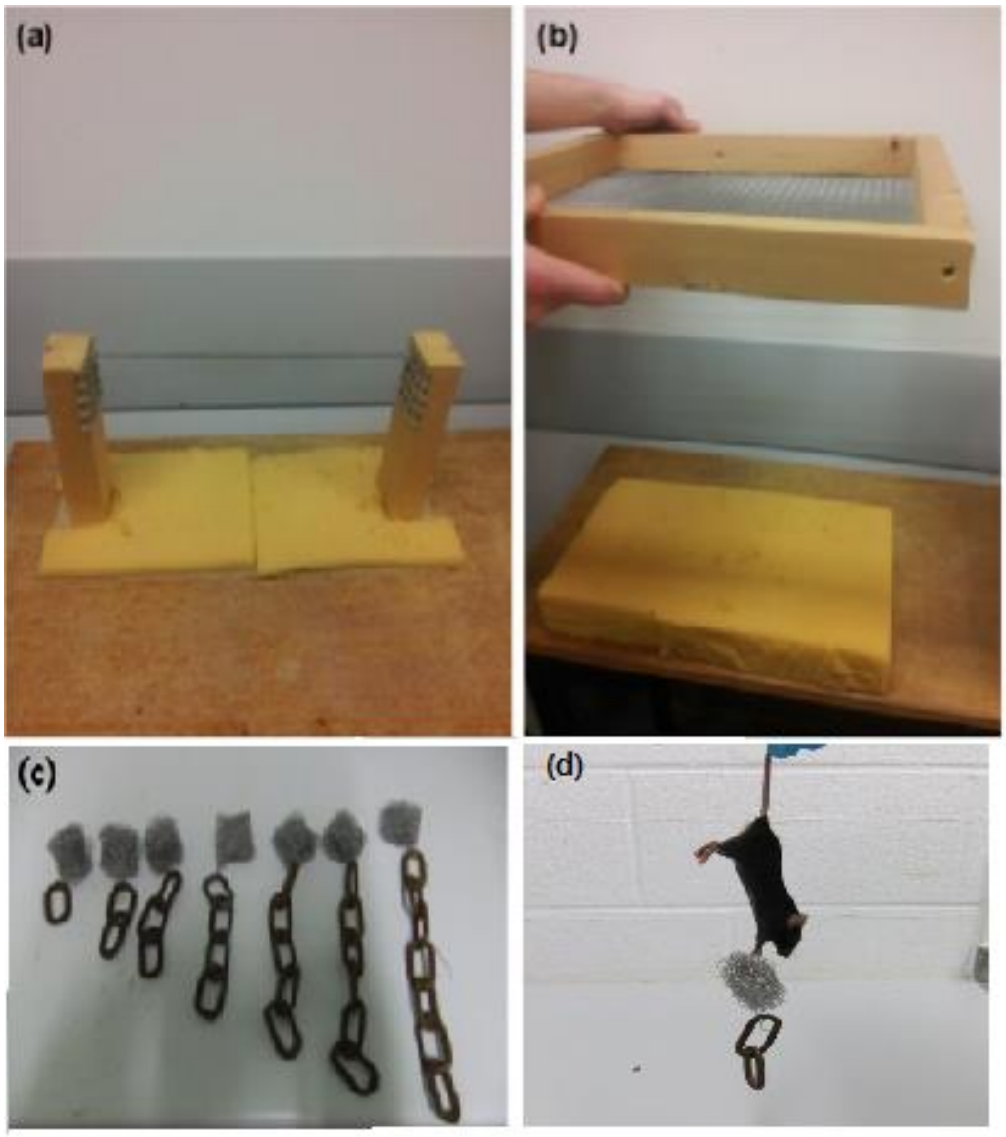

Figure 2.2: Strength & motor coordination testings: ***A photographic representation of motor co-ordination and strength tests.*** **(a) Horizontal bar task for forelimb muscular strength and co-ordination. (b) Inverted screen task to assess the muscular strength of all four limbs. (c) (d) Weightlifting task to assess forelimb muscular strength**

2.2.3.9 – Weightlifting

Each weight consisted of a series of chain links connected to a ball of tangled fine gauge stainless steel wire ("scale collector" used to prevent lime scale formation in domestic kettles). The weight (g) of each of these weights is listed in **Table 2.2**. The mouse was gripped by the middle/base of the tail, lowered to the first weight and allowed to grip it. Once the mouse has grasped the wire scale collector with only its forepaws the timer was started, and the mouse raised until the last chain link was clear of the bench top. A hold of three seconds was the criterion for successful completion of the trial and progression to the next higher weight. If a mouse dropped the weight before 3 seconds, then the time the weight was held was noted and the mouse allowed to rest for a minimum of 10 seconds before repeating the trial. If failed three times the trial was terminated, and the mouse was assigned the maximum time for which the weight was held. A final total score was calculated according to the below formula:

- **heaviest weight held for 3 seconds:** weight score X 3
- **heaviest weight held for <3 seconds:** + weight score X (seconds held for)

= Total Weight Lifting Score

Older mice, or those more accustomed to being handled would sometimes be unmotivated to grip the apparatus. To minimise this, the length of time the mouse was gripped and held aloft before being brought within gripping distance could be extended.

Weight (g)	20	33	44	60	72	85	101
Score	1	2	3	4	5	6	7

Table 2.3: Weightlifting Test: Weightlifting task, apparatus weights and the scores assigned to them.

2.2.3.10 – Fatigue Testing

On day 1 of training mice were placed on separate lanes of the Animal Treadmill Exer 3/6 (Columbus Instruments) and allowed to explore the lane for 3 minutes. Speed was set at 3m/min and slowly increased to the starting speed at which point the timer was started and followed the outline in **(Table 2.3 (A)**. The speed was increased by 2m/min if the mouse successfully ran clear of the exhaustion zone (the last 10cm of the treadmill lane) for the appropriate duration of time. Should a mouse lag into the exhaustion zone they were motivated by mechanical prodding to speed up and clear the zone. This was repeated across days 2-3 **(Table 2.3 (B)** and on Day 4 Fatigue Testing was undertaken as outlined in **(Table 2.3 (C).** Mice continued running on the treadmill, steadily increasing speed, until the mouse lagged into the exhaustion zone and was unable to run further.

Fatigue was defined by spending 10+ seconds in the exhaustion zone, unable to run further despite mechanical prodding as described by (Bi et al. 2016; Yue et al. 2016). At this point the distance covered and the maximum speed achieved before becoming exhausted was calculated and recorded. 10% EtOH was used to clean down the treadmill belt and walls between animals.

(A) Training Day 1

Speed (m/min)	Duration (mins)	
3-8	5	
9	2	
10	3	
	10	Total

(B) Training Day 2-3

Speed (m/min)	Duration (mins)	
3-10	5	
11	5	
12	5	
	15	Total

(C) Testing Day

Speed (m/min)	Duration (mins)
12	0.5
14	1
16	2
18	5
20	5
22	5
24	5
26	5
28	5

Table 2.4: Treadmill training and fatigue testing parameters

2.2.3.11 – Body Temperature

2.2.3.11.1 Rectal Probe

Core body temperature was measured using a thermocouple rectal probe (Thermalert TH5, Physitemp; Clifton, NJ, USA). In order to minimise stress effects, the probe was coated with a thin layer of Vaseline and mice were acclimatised to insertion and measurement of the rectal probe for 2 days prior to experimentation. Thereafter baseline temperature was taken at time of challenge and at set time points afterward.

2.2.3.11.2 Subcutaneous Transponders

Mice were anesthetized to a mild degree of sedation for transponder implantation by placing them in an anaesthetic chamber filled with general isoflurane/oxygen anaesthesia (Isoflo® from Zoetis), mean minimum alveolar concentration for isoflurane was established as 1.85% (±0.15%) and administered at a flow rate of 5. One experimenter scruffed the animal while a second injected the transponder (BMDS) on the right flank subcutaneously. Following the injection, animals were

placed into a recovery chamber at 37°C until recovered from anaesthesia and active once more. Temperature was taken thereafter by scanning the DAS-7009 thermal transponders reader above the mouse, roughly above the area of implantation, for a period of approximately 3 seconds until a reading was registered.

2.2.3.12 – Blood Glucose Levels

2.2.3.12.1 Tail Vein Lancing

Animals were restrained in a plastic restrainer made from a 3cm diameter Perspex tube, dilation of the tail vein was achieved by immersing the tail in warm water. The tail was then dried off and a thin coating of Vaseline applied to aid with droplet formation. The tail vein was lanced using a 30G needle and the resulting droplet's glucose content was measured using a veterinary glucometer giving blood glucose levels in mmol/L (AlphaTRAK 2, Zoetis, USA).

2.2.3.12.2 Atrial Terminal Measurement

Animals were terminally anaesthetised with sodium pentobarbital (40mg per mouse i.p. Euthatal, Merial Animal Health, Essex, UK). The thoracic cavity was opened, and blood sampled directly from the right atrium of the heart using a glucometer (Alphatrak, Zoetis USA), giving blood glucose levels in mmol/L.

2.2.3.13 –Sensory Testing

2.2.3.13.1 Vision Test

The Menace or Poke Test is a simple test used to determine if an animal can see in a binary fashion by approaching each eye with a cotton bud. If the animal can discern the incoming object it will blink before contact is made with the cornea. Care must be taken to avoid touching the animal's whiskers upon approach. This simple binary measure was applied to each eye and a scored according to **Table 2.5** below:

Degree of sight	**Blind**	**Sight in one eye**	**Sight in both eyes**
Score	0	1	2

Table 2.5: Scoring of visual sight in frail animals.

2.2.3.13.2 Auditory Test

Mice were placed in the Open Field Maze and exposed to 4 different tones at various frequencies and decibels (**Table 2.5**). Each tone was repeated 3 times, randomly, 25 seconds apart. Upon sounding of the tone animals who orientated to the sound or visibly froze in response to it were scored as having heard the tone. Should an animal react to any one of the three repeats of a tone they were scored as being able to discern that intensity and frequency. A score of one was given

for a positive reaction to a tone. As such, a completely deaf animal would score 0 and an animal with intact hearing 4.

	Tone 1	**Tone 2**	**Tone 3**	**Tone 4**
Decibel (dB)	70	70	85	85
Frequency (Hz)	8,000	15,000	8,000	15,000

Table 2.6: Acoustic startle response tones decibel and frequency levels.

2.2.3.14 –Gait Analysis

Mouse gait was analysed by scruffing the mouse and painting their paws with a non-toxic water-based paint (Crayola). Mice were then placed at one end of a tunnel (6cm high, 9cm wide, 40cm long) with a bright light source at one end and a dark burrow tube at the opposite end. Mice were motivated by the aversive light and/or mechanical prodding by the experimenter to traverse the length of the tunnel to the enclosed space of the burrowing tube. Only clear footprints while in motion were assessed with a minimum of 3 footprints from left and 3 from the right taken to average for each measurement of their gait.

2.2.3.14.1 Stride Length

Stride length, i.e. the average distance of forward movement between alternate steps, was calculated by measuring the distance travelled divided by the number of steps used to traverse that distance for a minimum of three step on the left and an equivalent number of steps on the right. **(Figure 2.3 A).**

2.2.3.14.2 Gait Width

Gait width, i.e. the average lateral distance between opposite left and right steps, was determined by measuring the perpendicular distance of a given step (at the heel) to a line connecting its opposite preceding and succeeding steps for an minimum of three step on the left and an equivalent number of steps on the right **(Figure 2.3 B).**

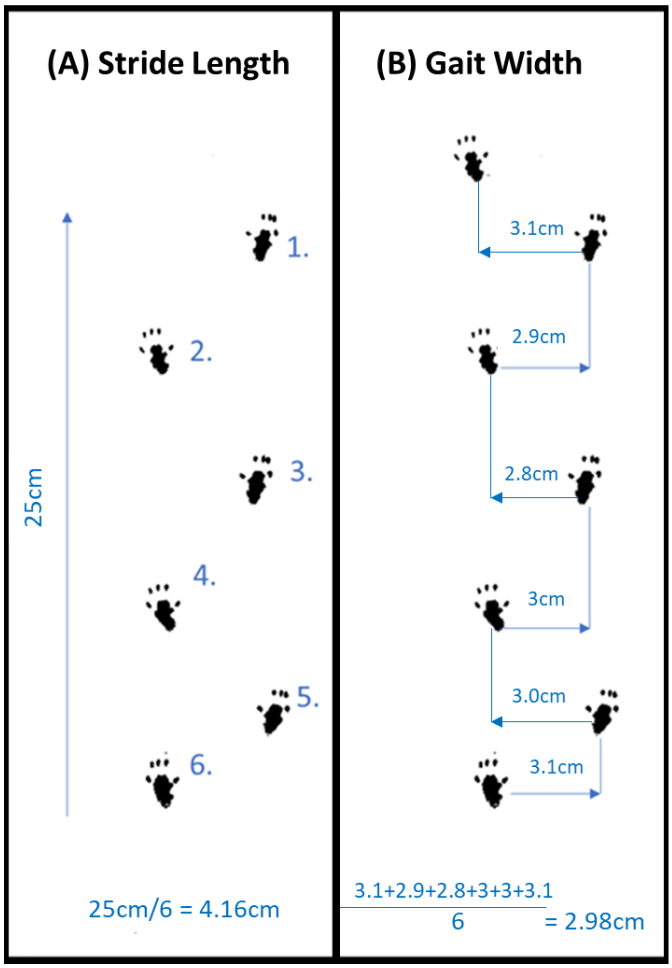

Figure 2.3 **Gait Analysis measures : (A) stride length and (B) gait width**

2.2.3.15 –Burrowing

Burrowing behaviour is a species-typical and apparently rewarding behaviour for mice which has been shown to be significantly decreased by acute illness and by neurodegeneration (Deacon 2006; Cunningham et al. 2009). A plastic PVC tube 320mm in length, 100mm in diameter with two 80-mm blots placed 25mm from the open end and spaced 75mm apart to raise the open end up 60mm above the cage floor was used. The burrowing tube was placed into the mouse home cage overnight in advance of testing to habituate the mouse to the apparatus. On the day of testing mice were singly housed from at 4pm, three hours before commencement of the dark cycle into a testing cage along with a burrowing tube filled with 200g of food pellets. At 6pm the amount of material displaced from the burrow was weighed to determine the mass burrowed over a two-hour period. The animal and burrow, with its remaining material in it, to the cage overnight and at 9am the mass of food pellets left in the tube were weighed to determine the mass burrowed overnight. Animals were then returned to their grouped, home cages.

2.2.4. – Trinity Frailty Index components and scoring

2.2.4.1 Assigning Z-scores for each measure of frailty

Mean reference, or normal, values for each parameter used in the calculation of frailty were obtained from four male and four female adult mice and used to construct the frailty index (FI). All parameters were weighted equally in the calculation of frailty. Each individual mouse had their score from each frailty measure scored against these mean reference values from our adult reference animals' according to the following formula to generate a Z-score (i.e. an expression of Standard Deviations away from the reference group mean):

$$\frac{\text{(Individual's Score)} \quad - \quad \text{(Adult Mean Reference Values)}}{\text{Adult Reference Standard Deviations}} = \text{SD Apart}$$

SD Apart	Z-Score
-4	1
-3	0.75
-2	0.5
-1	0.25
0	0
1	0.25
2	0.5
3	0.75
4	1

Table 2.7: Frailty Scoring system for Z-scores

2.2.4.2 Assigning frailty scores from z-scores

A graded scale was used to determine frailty (**Table 2.6**). Values that were 1 standard deviation *(SD)* above or below the mean reference value were given a frailty value of 0.25. Values that differed by 2 *SD* were scored as 0.5, values that differed by 3 *SD* were given a value of 0.75, and values that were more than 3 *SD* above or below the mean received the maximal frailty value of 1. Parameters that differed from adult reference values by less than 1 *SD* received a score of 0.

For the Trinity Frailty Index certain parameters were only scored if they fell below the adult reference value, see **Table 2.8**. This is because, in certain instances, significantly deviating from the adult reference value, in either direction, is indicative of impaired functionality, for instance being obese or significantly underweight are both detrimental to an individual's health. For these measures, frailty would be scored above and below the mean reference value. In contrast, for some

measures scoring above the adult reference value would not be a negative impact on the animal's health, for instance scoring better in a strength measure test compared to the adult reference value is not indicative of the reduced physiological reserve which frailty represents and as such would a frailty score would not be assigned for it.

2.2.4.3 Assigning exhaustion z-scores from change in speed over time (proxy for exhaustion):

In some experiments the change in speed across the open field activity measurement was used as a proxy for exhaustion, reasoning that the speed of a given animal's ongoing movement likely indicates increasing tiredness rather than motivation (since movement continues in any case). Animals were scored on their average speed (cm/s) in three 200-second blocks in the Open Field maze as well as the change in their speed as a percentage (%) from Block 1 to 2 and from Block 1 to 3. A z-score was calculated as described above in section 2.2.4.2 for speed in each block as well as for the percentage decline in speed from blocks 1 to 2 and 1 to 3. An average of these 5 z-scores (speed (cm/s) in 3 blocks, 2 % change in speed between blocks) was taken to generate an Exhaustion score. Scoring as faster than control animals or demonstrating an increase in speed from block 1 to block 2 or 3 was not counted as a deficit and scored as 0. Exemplar shown in **Table 2.8.**

	Speed cm/s			Percecntage Change (%) from Block 1	
	Block 1 Speed	Block 2 Speed	Block3 Speed		
	0 - 200 secs.	200 - 400 secs.	400 - 600 secs.	Block 2	Block 3
Aged Animal 1	3.42	5.25	4.44	+53.44	+29.74
Aged Animal 2	5.96	3.47	3.63	-41.88	-39.22
Young Animal	5.72	4.75	7.08	-16.90	+23.85

	Adult Reference Group Mean Scores		
	Avg. Speed	Percentage change (%) in speed	
		Block 1-2	Block 1-3
Mean	5.41	-10.34	-24.79
SD	0.7814	15.0966	21.3395

	Standard Deviations Away From Young Control Mean Group				
	Block 1 Speed	Block 2 Speed	Block3 Speed	Percecntage Change (%) from Block 1	
	0 - 200 secs.	200 - 400 secs.	400 - 600 secs.		
Aged Animal 1	-2.54	-0.21	-1.24	4.23	2.56
Aged Animal 2	0.72	-2.48	-2.28	-2.09	-0.68
Young Animal	0.40	-0.84	2.14	-0.43	2.28

	Z-score based off standard deviations away From Young Control Mean Group					
	Block 1 Speed	Block 2 Speed	Block3 Speed	Percecntage Change (%) from Block 1		Z-Score avg. for frailty score
	0 - 200 secs.	200 - 400 secs.	400 - 600 secs.			
Aged Animal 1	0.50	0.00	0.25	0.00	0.00	**0.15**
Aged Animal 2	0.00	0.50	0.50	0.50	0.00	**0.30**
Young Animal	0.00	0.00	0.00	0.00	0.00	**0.00**

Table 2.8: Exemplar z-score generation for exhaustion z- scores from change in speed over time (proxy for exhaustion):

2.2.4.3 Assigning Total Frailty Score per individual

These individual z-score values for each measurement of frailty were summed and the resulting number divided by the total number of parameters measured to yield a Frailty Index Score (FI) for each animal; such that an animal with no deficits in any assessed category would have a score of 0 and an animal with all possible maximal deficits would have a score of 1. In practice however any animal scoring close to this maximum would likely be in a state of advanced moribundity and past their humane endpoint and would not be included in analyses. As such the maximum finalised frailty score typically found from our assays would be circa. 0.6.

Trinity Modified Integrated Phenotype Frailty Index

Version 1

Measure		Score Z-score +	Score Z-score -
1	Glycaemic Status	✓	✓
2	Temperature	✓	✓
3	Weight	✓	✓
4	Sight		✓
5	Audio		✓
6	Screen		✓
7	Weight Lifting		✓
8	Distance	✓	✓
9	Average Speed		✓
10	Rears	✓	✓
11	Meander	✓	✓
12	Decline in speed		✓
13	*Spont. Altern. Cognition*		✓

Version 2

Measure		Score Z-score +	Score Z-score -
1	Glycaemic Status	✓	✓
2	Temperature	✓	✓
3	Weight	✓	✓
4	Weight Loss	✓	
5	Gait Width	✓	
6	Stride Length		✓
7	Sight		✓
8	Screen		✓
9	Weight Lifting		✓
10	Decline in speed		✓
11	Distance To Fatigue		✓
12	Distance	✓	✓
13	Max Speed		✓
14	Average Speed		✓
15	Rears	✓	✓
16	Meander	✓	✓
17	Angular Velocity	✓	✓
18	Y-maze Cognition	✓	

Table 2.9: Frailty measures of Trinity Frailty Index Versions 1 & 2 and scoring criteria: Measures with a ✓ *were* scored for frailty, blacked out boxes indicate measures which were not scored for frailty if they fell above the adult reference value as they did not represent a reduction in physiologic reserve, i.e. increased frailty.

2.2.5. – Dalhousie Cumulative Deficit Model Frailty Scoring

Brain tissue for this study were supplied by the Howlett lab in Dalhousie University, Halifax, Canada. Mice of different ages ranging from 3-25 months of age were scored using a cumulative deficit model frailty index **(Table 2.10).** Behavioural analyses and dissections were conducted by the Howlett research lab. Frailty scores were generated in the same manner as described in Sections 2.2.4.1-3 using an average of each individual measure of frailty's z-score. Animals were anesthetised by injecting 0.1mL sodium heparin (100 units/mL) and sodium pentobarbital (65mg/mL). Brains were removed, cut in half longitudinally, transferred to cryo tubes and flash frozen using liquid nitrogen. These samples were then sent to Ireland on dry ice and stored at -80^{o}C. Molecular analyses were conducted upon mRNA from cerebellum and cerebrum homogenates. Due to limitations in how the tissue was dissected and stored I was unable to take a more region-specific approach when isolating RNA.

	Cumulative Frailty Measures		
1	Body Weight	18	Vestibular disturbance
2	Avg Temp	19	Hearing loss
3	Temp Score	20	Cataracts
4	Body Weight Score	21	Eye discharge/swelling
5	Alopecia	22	Microphthalmia
6	Loss of fur colour	23	Corneal opacity
7	Dermatitis	24	Vision loss
8	Loss of whiskers	25	Menace reflex
9	Coat condition	26	Nasal discharge
10	Tumours	27	Malocclusions
11	Distended abdomen	28	Rectal prolapse
12	Kyphosis	29	Vaginal/uterine/penile prolapse
13	Tail stiffening	30	Diarrhoea
14	Gait disorders	31	Breathing rate/depth
15	Tremor	32	Mouse grimace scale
16	Forelimb grip strength	33	Piloerection
17	Body condition score		

Table 2.10: Dalhousie Cumulative Deficit Frailty Measures: Individual measures assessed to generate a Cumulative Deficit Model Frailty Score

2.2.6 – Real-time Polymerase Chain Reaction (PCR)

2.2.6.1 – Tissue for quantitative PCR

Animals were terminally anaesthetised using approximately 200µl Sodium Pentobarbital (Euthatal, Merial Animal Health, Essex, UK) administered intraperitoneally and transcardially perfused with heparinised saline using a peristaltic pump (Anachem, Luton, UK). Brains were removed and left and right cerebellum, left and right hippocampus, prefrontal cortex and hypothalamus were dissected out. The tissue was placed in sterile Eppendorfs and snap frozen in a liquid nitrogen containing stainless steel liquid nitrogen dewar (Dilvac) being stored at -80°C.

2.2.6.2 – RNA isolation

Prior to commencing work, the RNA area and all equipment was thoroughly cleaned and sterilised using 70% ethanol. The tissue was removed from the -80°C freezer and stored on dry ice. All samples were weighed to ensure they were within the required weight restrictions of the RNeasy Plus Mini Kit (Qiagen, Crawley, UK) or to determine the correct volume of Trizol (TRI Reagent® Solution, Ambion) to be used for the Double Extraction.

2.2.6.2.1 RNeasy Plus Mini Kit

Manufacturer's recommended protocol was followed with minor alterations for optimisation. Lysis Buffer was prepared using 10µl in 1ml of Buffer RLT Plus. 600µl of Lysis Buffer was added to tissues weighing above 20mg and 350µl to all tissues below 20mg. A sterile pestle and mechanical homogeniser were used to disrupt the tissue. Once a homogenous solution was achieved it was transferred to Qia shredder tubes and centrifuged in the IEC MicroCL 21R Centrifuge (Thermo Electron Corporation) for 3 minutes at 14,800rpm. The supernatant was transferred to a Genomic DNA Eliminator (Qiagen, Crawley, UK) and spun for 30 seconds at 14,800rpm. 550µl of 70% ethanol was added to the flow through and transferred to RNeasy Spin Columns and spun for 15 seconds at 14,800rpm to allow the RNA to bind to the column. The flow through was discarded and the RNeasy columns washed with 350µl of RW1 buffer spun for 15 seconds at 14,800rpm. The flow through was discarded once more. To ensure complete removal of all DNA 80µl of a DNase (prepared as described for bulk mRNA in **Table 2.11)** was added to each column for 15 mins. The columns were washed once more with 350µl of RW1 buffer and spun for 15 seconds at 14,800rpm. The flow through was discarded. 500µl of Buffer RPE was added to each column and spun for 15 seconds at 14,800rpm. The flow through was discarded and an additional 500µl of Buffer RPE was added to each column and spun for 2 minutes at 14,800rpm. The flow through was discarded. The column was then transferred to a fresh sterile tube and spun for 1 minute at 14,800rpm to ensure complete removal of Buffer RPE and drying of the column. The column was then placed in a fresh sterile

collection tube and 30µl of RNase free water was added and spun for 1 minute. The water in this step serves to elute the RNA from the columns' membrane. The samples were then placed on ice and quantified by Nanodrop ND1000 Spectrophotometer (Thermo Fisher Scientific) before storing all samples at -80°C until cDNA synthesis. All RNA isolations pertaining to Chapter 3 were performed using the RNeasy Plus Mini Kit as described here.

2.2.6.2.2 Trizol Double Extraction

Manufacturer's recommended protocol was followed with minor alterations for optimisation. 1ml of Trizol was added per 50-100mg of tissue. The sample volume could not exceed 10% of the volume of Trizol used. A sterile pestle and mechanical homogeniser were used to disrupt the tissue. Upon complete homogenisation in Trizol, a 5-minute incubation at room temperature followed. 200µl of chloroform was added per 1ml of Trizol used. Samples were vigorously shaken to ensure complete mixing and incubated at room temperature for 3 minutes. Centrifugation at 12, 000g for 15 minutes at 4°C yielded a three-phase separation of RNA (upper colourless phase), DNA (opaque interphase) and protein (lower red phase). The upper aqueous phase of RNA and lower protein phase were separated into new LoBind Eppendorf tubes (Fisher Scientific) for individual isolation, the protein phase was incubated overnight at 4°C and isolation completed the following day. 500µl of 100% isopropanol with 10µl of glycogen was added to precipitate the RNA and incubated overnight at -20°C. The following day a 10-minute centrifugation at 12,000g at 4°C was conducted and resulting supernatant removed. The RNA pellet was washed with 1ml of 75% EtOH and centrifuged at 7,500g for 10mins at 4°C and the supernatant discarded. The resulting pellet RNA pellet underwent a DNase digest to ensure removal of all DNase. DNase digest was prepared as appropriate for bulk tissue or FACs isolated cells per **Table 2.11** and was added to each sample for 15 mins.

	DNase digest	
	Volume Per Sample (µl)	
Component	Bulk tissue	FACs isolates
DNase	10	2.5
RDD Buffer	70	10
RNase free water	0	87.5

Table 2.11: DNase digest makeup solution

A 75% EtOH wash was used to wash off the DNAse and incubated at 4°C for 5 minutes before a final 15-minute centrifugation at 7,500g at 4°C. The supernatant was discarded and the RNA pellet air dried for 5-10mins. Samples were then resuspended in 30µl of RNase free water containing an RNase inhibitor (1:10000), placed on ice and RNA concentration determined using the Nanodrop ND1000 Spectrophotometer (Thermo Fisher Scientific). All samples were then stored at -80°C until

cDNA synthesis. All RNA isolations pertaining to Chapters 4-5 were performed using the RNeasy Plus Mini Kit as described here.

2.2.6.3 – RNA quantification

The total concentration and purity of the RNA in each sample was quantified using the Nanodrop ND1000 Spectrophotometer (Thermo Fisher Scientific). 1µl of RNase free water was pipetted onto the fibre optic pedestal and the machine blanked against it. 1µl of sample was then pipetted on and absorbance measured at wavelengths of 260nm and 280nm. This gives the concentration of RNA as ng/µl using Beers Law and the formula $A=\varepsilon Cl$ where A is the absorbance at 260nm, ε is the RNA extinction coefficient (25µl/µg/cm), C is RNA concentration and l is the pathlength of the spectrophotometer (0.05mm – 0.1mm). The ratio of 260:280 determines the purity of the RNA isolate, an ideal ratio of pure RNA should be between 1.8 and 2.1. The RNA isolate was subsequently stored at -80°C until required for cDNA synthesis.

2.2.6.4 –Reverse transcription cDNA synthesis

2.2.6.4.1 High-Capacity cDNA Reverse Transcriptase Kit (Thermo Fisher)

A High-Capacity cDNA Reverse Transcriptase Kit (Thermo Fisher, USA) was used for cDNA synthesis on all bulk tissue isolated mRNA. All calculations were based on a reaction using 20ng of RNA per 1µl of final volume with volumes of cDNA between 10µl and 30µl being made up as required. RNA yield was quantified using a nanodrop and allowed calculation of the sample volume for a concentration of 20ng/1µl. This was then brought up to a total volume of 10µl using RNase free water. The other 10µl of the reaction was composed of the Master Mix. Master Mix was made up using the following: 2µl 10X RT Buffer, 0.8µl 25X dNTP mix, 2µl 10X RT random primers, 1µl Multiscribe Reverse Transcriptase, 4.2µl RNase free water to a total volume of 10µl. This Master Mix would typically be made in bulk. Two negative controls were prepared with the first lacking RNA and the second lacking Reverse Transcriptase, with their respective volumes being replaced with RNase free water. The 10µl of Master Mix and 10µl of sample were placed in a sterile PCR mini tube. The samples were then vortexed and picofuged to ensure a homogenous mixture, at the bottom of the PCR tube and to completely remove bubbles before being placed in the thermocycler (Peltier Thermal Cycler PTC-200) at 25°C for 10 minutes, 37°C for 120 minutes, 85°C for 5 minutes and finally maintained at 4°C until collection. Samples were then centrifuged and stored at 4°C and used within 4 weeks or stored at -20°C for long term storage.

2.2.6.4.2 iScript cDNA Synthesis Kit (BioRad, USA)

The iScript cDNA synthesis kit (Thermo Fisher, USA) was used for cDNA synthesis on all FACs isolated glial cells isolated mRNA. All calculations were based on a reaction using 3ng RNA per 1µl with total

volumes of cDNA being 20µl. RNA yield was quantified using a nanodrop and allowed calculation of the sample volume for a concentration of 3ng/1µl. This was then brought up to a total volume of 15µl using RNase free water. The other 5µl of the reaction was composed of the Master Mix which was prepared using the following: 4µl of 5X iScript Reaction Mix and 1µl iScript Reverse Transcriptase. Two negative controls were prepared with the first lacking RNA and the second lacking Reverse Transcriptase with these volumes being replaced with RNase free water. The 5µl of Master Mix and 15µl of sample were placed in a sterile PCR mini tube. The samples were then vortexed and picofuged to ensure a homogenous mixture, at the bottom of the PCR tube and to completely remove bubbles before being placed in the thermocycler (Peltier Thermal Cycler PTC-200) at 25°C for 5 minutes, 46°C for 20 minutes, 95°C for 1 minutes and finally maintained at 4°C until collection. Samples were then centrifuged and stored at 4°C and used within 4 weeks or stored at -20°C for long term storage.

2.2.6.5 – Quantitative PCR assay

The StepOne™ Real-Time polymerase chain reaction (PCR) system was supplied by Applied Biosystems (Warrington, UK) and used in 96-well with a 25µl reaction volume per well and 384-well formats with a 15µl reaction volume per well. All primers and probes used are shown in table 2.12 and were obtained from publications or designed and produced by Sigma-Aldrich. Primers and probes were designed to cross introns to increase their specificity to cDNA. When no probe was available SYBR green, a fluorescent DNA binding probe, was used. All primer-pairs' specificity was tested following standard RT-PCR using gel electrophoresis to produce a discrete band corresponding to the expected amplicon length.

PCR Master Mix was made up according to the volumes required for the respective 96-well, 384-well format per **Table 2.12:**

(A)	96-well Format	
	Volume Per Sample (µl)	
Component	**TaqMan MasterMix**	**SYBR-Green**
2X Master Mix	12.5	12.5
Rnase Free Water	9	9.5
10µM Probe	0.5	0
10µM Forward	0.5	0.5
10µM Reverse	0.5	0.5

(B)	384-well Format	
	Volume Per Sample (µl)	
Component	**TaqMan MasterMix**	**SYBR-Green**
2X Master Mix	7.5	7.5
Rnase Free Water	4	4.5
6.25µM Probe	0.5	0
6.25µM Forward	0.5	0.5
6.25µM Reverse	0.5	0.5

Table 2.12 qPCR MasterMix formula for 96-well and 384-well formats

Once synthesised, cDNA was diluted 1:2 with RNase free H_2O and 2µl of the sample's cDNA was then pipetted into each well and mixed thoroughly. The plate was then sealed using the ABI Prism Optical Adhesive Cover and centrifuged to there are no bubbles in the mix.

The plate was placed in the Applied Biosystems 7300 Real Time PCR machine for the 96-well format and the Quantstudio 5 for the 384-well format and ran through its cycles. The PCR cycles consist of 4 stages; the first stage lasts 2 minutes at 50°C, the second 10 minutes at 95°C, the third and fourth stages are then repeated a minimum of 40 times at 95°C for 15 seconds and 60°C for 1 minute. During the 60°C stage quantification occurred at the end of every cycle. The fluorescent emission from each well is generated by the 5`to 3`activity of the Taq Polymerase on the probe. The probe, which binds specifically to the gene's sequence of interest, is labelled with the reporter dye FAM and the quencher TAMRA. While the probe is intact, TAMRA will quench the fluorescence of FAM by way of Fluorescence Resonance Energy Transfer (FRET). However, during the PCR process Taq Polymerase is activated and will proteolytically cleave probe during the polymerisation of a new DNA strand, thereby separating FAM and TAMRA. Thus, allowing FAM, now in solution, to fluoresce freely, the degree of which will be directly related to the quantity of the gene of interest present. Premade primers and GAPDH used VIC reporters with the quencher TAMRA. Alternatively, SYBR Green was used on compatible primer sets and by binding to the minor groove of double-stranded DNA molecules and by intercalating between the DNA bases loses its mobility resulting in the release of its energy as fluorescence when excited with blue light at 480nm. The intensity of this fluorescent emission is therefore directly associated with the concentration of the double stranded DNA target sequence.

All PCR data were normalised to the expression of the housekeeping gene 18s ribosomal RNA because of its invariant expression across tissues, cells, experimental treatments and acute stressors such as viruses (Kuchipudi et al. 2012). Assays were quantified using a relative standard curve. This was constructed from total RNA isolated from mouse brain tissue for the respective region being analysed, from 25-month-old male mice challenged with a 250µg/kg bolus of LPS and sacrificed 4 hours challenge. These treatments and the use of a higher concentration of RNA in the reverse transcriptase reaction than that in the samples for analysis ensured that low expression genes such as those of the chemokines and cytokines transcription of all experimental animal groups would fall within the range of the standard curve. 1 in 4 serial dilutions of the cDNA synthesized from the brain tissue were made and a curve plotted of the Ct value (cycle threshold – the cycle number at which the fluorescence of the product of transcribed gene crosses the threshold of detection) versus the log of the concentration (an arbitrary value given that the absolute concentration of cytokine transcripts is unknown). For all bulk tissue mRNA preps a six-point standard curve was used, while glial isolates utilised a seven-point standard curve.

Target	Accession Number	Oligonucleotide	Sequence	Amplicon Size (bp)
18S	NR_003278.3	Forward Reverse	5'-CGCCGCTAGAGGTGAAATTCT-3' 5'-CATTCTTGGCAAATGTCTTTCG-3'	67
Anx1	NM_010730.2	Forward Reverse	5'-ATGTTGCTGCCTTGCACAAA-3' 5'-CCAAGGGCTTTCCATTCTCCT-3'	138
Atg5	NM_053069.6	Forward Reverse	5'-CTTGCATCAAGTTCAGCTCTTCC-3' 5'-AAGTGAGCCTCAACCGCATCCT-3'	107
Bdnf	NM_007540.4	Forward Reverse	5'-GCGGCAGATAAAAAGACTGC-3' 5'-GCAGCCTTCCTTGGTGTAAC-3'	141
C1qα	NM_007572.2	Forward Reverse	5'-GCCGAGCACCCAACGGGAAGG-3' 5'-GGCCGGGGCTGGTCCCTGATA-3'	268
C3	NM_009778.2	Forward Reverse	5'-AAAGCCCAACACCAGCTACA-3' 5'-GAATGCCCCAAGTTCTTCGC-3'	115
Ccl2 (MCP-1)	NM_011333	Forward Reverse Probe	5'-GTTGGCTCAGCCAGATGCA-3' 5'-AGCCTACTCATTGGGATCATCTTG-3' 5'-TTAACGCCCCACTCACCTGCTGCTACT-3'	81
Ccl3 (MIP1a)	NM_011337.2	Forward Reverse	5’-CCCAGCCAGGTGTCATTTTCC-3’ 5’-GCATTCAGTTCCAGGTCAGTG -3’	103
Ccl4 (MIP1b)	NM_013652.2	Forward Reverse	5’-CTCAGCCCTGATGCTTCTCAC-3’ 5’-AGAGGGGCAGGAAATCTGAAC-3’	65
Cd11b	NM_001082960.1	Forward Reverse	5’-TCATTCGCTACGTAATTGGG-3’ 5’-GATGGTGTCGAGCTCTCTGC-3’	71
Cd36	NM_016741.1	Forward Reverse	5'-TGCGCTCGGCGTTGT-3' 5'-GGGTCTATGCGGACATTCTTG-3'	78
Cd68	NM_009853	Forward Reverse Probe	5’-CAAGGTCCAGGGAGGTTGTG-3’ 5’-CCAAAGGTAAGCTGTCCATAAGGA-3’ 5’-CGGTACCCATCCCCACCTGTCTCTCTC-3’	75
Cd11c (Itgax)	NC_000073.6	Forward Reverse	5'-CTGGATAGCCTTTCTTCTGCTG-3' 5'-GCACACTGTGTCCGAACTC-3'	115
Clec7a	NM_020008.3	Forward Reverse	5'-CCCAACTCGTTTCAAGTCAG-3' 5'-AGACCTCTGATCCATGAATCC-3'	82
Csf1r	NM_001037859.2	Forward Reverse	5'-GCAGTACCACCATCCACTTGTA-3' 5'-GTGAGACACTGTCCTTCAGTGC-3'	140
Cst7	NM_009977.3	Applied Biosystems premade primer Cat No. 4331182 ID No. Mm00438351_m1		
Ctss	NM021281	Forward Reverse	5'-GCCACTAAAGGGCCTGTCTCT-3' 5'-TCGTCATAGACACCGCTTTTGT-3'	80

Cxcl10 (IP-10)	M33266.1|	Forward Reverse Probe	5'-GCCGTCATTTTCTGCCTCAT -3' 5'-GCTTCCCTATGGCCCTCATT-3' 5'-TCTCGCAAGGACGGTCCGCTG-3'	127
Cxcl13 (BCA-1)	NM_018866.2	Forward Reverse	5'-CTCTCTCCAGGCCACGGTATT-3' 5'-TTTGGCACGAGGATTCACAC-3'	198
Gapdh	NM_008084.2	Forward Reverse Probe	5'-GACGGCCGCATCTTCTTGT-3' 5'-CACACCGACCTTCACCATTTT-3' 5' - CAGTGCCAGCCTCGTCCCGTAGA - 3'	65
Gbp2	NM_010260.1	Forward Reverse	5'CAGCTGCACTATGTGACGGA3' 5'AGCCCACAAAGTTAGCGGAA3'	94
Gfap	K01347.1	Forward Reverse	5'-CTCCAACCTCCAGATCCGAG-3' 5'-TCCACAGTCTTTACCAGATGT-3'	90
Hprt	NM_013556.2	Forward Reverse	5' - TCATGGACTGATTATGGACAGG - 3' 5' - AATCCAGCAGGTCAGCAAAG - 3'	128
Hes5	NM_010419.4	Forward Reverse	5' - GGTGGAGAAGATGCGTCGG - 3' 5' - GCGAAGGCTTTGCTGTGTTT - 3'	159
Igf1	BC_012409	Forward Reverse	5'-CTGGACCAGAGACCCTTTGC-3' 5'-AGAGCGGGCTGCTTTTGTAG-3'	218
Il10	M37897.1	Forward Reverse	5'-GGTTGCCAAGCCTTATCGGA-3' 5'-ACCTGCTCCACTGCCTTGCT-3'	191
Il1a	NM_010554	Forward Reverse	5'-TGTTGCTGAAGGAGTTGCCAG-3' 5'-CCCGACTTTGTTCTTTGGTGG-3'	150
Il1β	M15131	Forward Reverse	5'-GCACACCCACCCTGCA-3' 5'-ACCGCTTTTCCATCTTCTTCTT-3'	69
Il1r1	NM_001123382.1	Forward Reverse Probe	5'-GCAATATCCGGTCACACGAGTA-3' 5'-ATCATTGATCCTGGGTCAGCTT-3' 5'-TCCTGAGCCCTCGGAATGAGACGATC-3'	117
Il6	NM_031168	Forward Reverse Probe	5'-TCCAGAAACCGCTATGAAGTTC-3' 5'-CACCAGCATCAGTCCCAAGA-3' 5'-CTCTGCAAGAGACTTCCATCCAGTTGCC-3'	72
Irf7	NM_016850	Forward Reverse	5'-CGAGGAACCCTATGCAGCAT-3' 5'-TACATGATGGTCACATCCAGGAA-3'	108
Lgals9	NM_010708.2	Forward Reverse	5' - TCAAGGTGATGGTGAACAAGAAA - 3' 5'- GATGGTGTCCACGAGGTGGTA - 3'	74
Nlrp3	NM_145827.3	Forward Reverse	5'-GAGCCTACAGTTGGGTGAAATGT-3' 5'-CCACGCCTACCAGGAAATCTC-3'	115
Oas1a	NM_145211	Forward Reverse	5'-CTTTGATGTCCTGGGTCATGT -3' 5'-GCTCCGTGAAGCAGGTAGAG-3'	123

Osm	NM_001013365.2	Forward Reverse	5' - AACTCTTCCTCTCAGCTCCT - 3' 5' - TGTGTTCAGGTTTTGGAGGC -3'	105
OsmR	NM_011019.3	Forward Reverse	5' - CGTTCCCCTGTGAGGCCGAG -3' 5' - TCCTCCAAGACTTCGCTTCGGG - 3'	149
P16 (Cdkn2a)	NM_009877.2	Forward Reverse	5' - GTCGCAGGTTCTTGGTCACT - 3' 5' - CATGTTCACGAAAGCCAGAGC - 3'	131
P21 (Cdkn1a)	NM_007669.5	Forward Reverse	5' - TCCAGACATTCAGAGCCACAG - 3' 5' - CAAAGTTCCACCGTTCTCGG - 3'	177
P53	NM_011640	Forward Reverse Probe	5'-CCACAGCGTGGTGGTACCT-3' 5'-TGTACTTGTAGTGGATGGTGGTATACTCA-3' 5'-AGCCACCCGAGGCCGGCT-3'	71
p62 (Sqstm1)	NM_011018.3	Forward Reverse	5' - GCTGAAGGAAGCTGCCCTAT - 3' 5' - TTGGTCTGTAGGAGCCTGGT - 3'	132
Pai-1	NM_33960	Forward Reverse Probe	5'-GGGACACCCTCAGCATGTTC-3' 5'-TGTTGGTGAGGGCGGAGA-3' 5'-TCGCTGCACCCTTTGAGAAAGATGT-3'	79
Ptx3	X83601	Forward Reverse Probe	5'-ACAACGAAATAGACAATGGACTTCAT-3' 5'-CTGGCGGCAGTCGCA-3' 5'-CCACCGAGGACCCCACGCC-3'	62
Sparc	NC_000071.6	Forward Reverse	5'-CCACACGTTTCTTTGAGACC-3' 5'-GATGTCCTGCTCCTTGATGC-3'	95
Stat3	NM_213659.2	Forward Reverse	5'-CCCACTCCTTGCCAGTTGTG-3' 5'-CGCTTGGTGGTGGACGAGAA-3'	186
Tfeb	NM_011549.3	Forward Reverse	5' - AAGGTTCGGGAGTATCTGTCTG - 3' 5' - GGGTTGGAGCTGATATGTAGCA - 3'	188
Tgf-β	AJ009862	Forward Reverse Probe	5'-CGTGGAAATCAACGGGATCA-3' 5'-GGCCATGAGGAGCAGGAA-3' 5'-ACCTGGGCACCATCCATGACATGA-3'	84
Tgm1	NM_001161714.1	Applied Biosystems premade primer Cat No. 4331182 ID No. Mm00498375_m1		
Tlr4	NM_021297.2	Forward Reverse Probe	5'-GGCTCCTGGCTAGGACTCTGA-3' 5'-TCTGATCCATGCATTGGTAGGT-3' 5'-CATGGCACTGTTCTTCTCCTGCCTGA-3'	114
Tnf-α	M11731	Forward Reverse Probe	5'-CTCCAGGCGGTGCCTATG-3' 5'-GGGCCATAGAACTGATGAGAGG-3' 5'-TCAGCCTCTTCTCATTCCTGCTTGTGG-3'	149
Tnfr	X57796.1	Forward Reverse	5'-GCTGACCCTCTGCTCTACGAA-3' 5'-GCCATCCACCACAGCATACA-3'	132

Trem2	NM_031254	Forward Reverse Probe	5'-TGTGGTCAGAGGGCTGGACT-3' 5'-CTCCGGGTCCAGTGAGGA-3' 5'-CCAAGATGCTGGGCACCAACTTCAG-3'	68
Tyrobp	NM_011662.2	Forward Reverse	5'-CGTACAGGCCCAGAGTGAC-3' 5'-CACCAAGTCACCCAGAACAA-3'	91
Vimentin	NM_011701.4	Forward Reverse	5'-GCTGCAGGCCCAGATTCA-3' 5'-TTCATACTGCTGGCGCACAT-3'	100

Table 2.13: qPCR primer & probe sequences

2.2.7 – Metabolic Status- Promethion Cages

A sixteen-channel Promethion system (Sable Systems International) was used to measure and record indirect calorimetry and activity data in live mice. Individual cages (interior dimensions of 31.5 × 15.5 (floor), up to 34.5 × 19.0 (ceiling) × 13.0 cm tall) include a ceiling-mounted food hopper, water spigot and small "hut" into which mice can climb. Use of a MM-1 Load cell (Sable Systems International) with the ceiling mounted hut, water or food hoppers permitted measurement of body mass or water/food consumption respectively. The BXYZ Beambreak Activity Monitor photoelectric beam motion detectors are positioned around the cage and allowed for movement tracking in the X- and Y-axis (horizontal plane). Air flow through the chamber was negative (2,000 mL/min) and gas analyses were recorded once per minute. Cages are mounted inside of thermally controlled cabinets that are maintained at 21°C. Mice were housed individually under a 12-hour light-dark cycle with ad libitum access to food and water. Mice were acclimated for a minimum of 12 hours in the metabolic chamber cage before recording of any calorimetric or activity variables. Mice were returned to their home cage after a maximum of 72 hours in the metabolic cages. All data were compiled using CalR version 1.2 online web application for indirect calorimetry analysis and exported as raw data to excel for final statistical analysis and graphing.

2.2.8 - Enzyme linked immunosorbent assay (ELISA)

2.2.8.1 - Plasma ELISA

Animals were terminally anaesthetised with sodium pentobarbital (40mg per mouse I.P., Euthatal, Merial Animal Health, Essex, UK). The thoracic cavity was opened, and blood collected in heparinised tubes directly from the right atrium of the heart. This blood was spun at 1.5g for 15 minutes to remove cells; the supernatant plasma was aliquoted and stored at -20°C.

2.2.8.1.1 – TNF-α and CCL2

Plasma TNF-α and CCL2 concentrations were quantified by sandwich-type ELISA using the R&D system duo set kits (R&D systems, Minneapolis, MN, USA) in accordance with the manufacturer's recommended protocol. A polymerized form of horseradish peroxidase (HRP) conjugated to strepavidin (Sanquin) was used on all Frailty samples to improve the signal and aid with pro-inflammatory mediators with low-abundance in Frailty animals without a systemic inflammatory challenge. Poly-HRP contains a HRP polymer core which will supply a greater enzymatic activity per binding event of its conjugated strepavidin to the biotin conjugated detection antibody bound to the protein of interest, and a dramatic signal amplification when RnD Substrate Solution (RnD Biosystems) was applied. HRP-TMB reaction was stopped by addition of 2N H_2SO_4 solution to the

well and plates were read at wavelengths according to the manufacturer's recommended protocol on the Spectra max Plus 384 plate reader within 30 minutes.

2.2.8.1.2 – IL-6

Plasma IL-6 concentration were quantified by sandwich-type ELISA using Biolegend assay kits (Biolegend Way, San Diego, CA, USA) in accordance with the manufacturer's recommended protocol. A polymerized form of horseradish peroxidase (HRP) conjugated to strepavidin (Sanquin) was used on all Frailty samples to improve the signal and aid with pro-inflammatory mediators with low-abundance in Frailty animals without a systemic inflammatory challenge. Poly-HRP contains a HRP polymer core which will supply a greater enzymatic activity per binding event of its conjugated strepavidin to the biotin conjugated detection antibody bound to the protein of interest, and a dramatic signal amplification when 3,3',5,5'-Tetramethylbenzidine (TMB) (Applied Biosystems) was applied. HRP-TMB reaction was stopped by addition of 2N H_2SO_4 solution to the well and plates were read at wavelengths according to the manufacturer's recommended protocol on the Spectra max Plus 384 plate reader within 30 minutes.

2.2.8.1.3 - Insulin

Plasma Insulin concentrations were quantified by sandwich-type ELISA using the Crystal Chem system duo set kits (Crystal Chem Inc., Illinois, IL, USA) in accordance with the manufacturer's recommended protocol. Plates were read at wavelengths according to the manufacturer's recommended protocol on the Spectra max Plus 384 plate reader.

2.2.9 – Immunohistochemistry on formalin-fixed brain tissue

2.2.9.1 – Tissue Preparation

Animals were terminally anaesthetised using approximately 200µl Sodium Pentobarbital (Euthatal, Merial Animal Health, Essex, UK) administered intraperitoneally and transcardially perfused with heparinised saline, followed by 10% formalin (Sigma, Poole, UK) for approximately 10 minutes using a peristaltic pump (Anachem, Luton, UK). Brains were then removed and post fixed in bijou tubes immersed in 10% formalin for 2 days before being placed in PBS until embedding.

2.2.9.2 – Paraffin wax embedding & sectioning

Brains for embedding were placed in plastic cassettes (Thermo Fisher Scientific, Dublin, Ireland) and placed in a 70% EtOH solution for a minimum of 20 minutes to begin the dehydration process. The cassettes were then automatically processed through a series of dehydration and paraffin fixing steps as in **Table 2.14**.

Embedding moulds were filled with paraffin wax and placed upon a cooling stage and brain embedded vertically with the anterior face on the base. Cassettes were placed atop the mould and more wax poured atop. The wax was allowed to solidify on the cooling stage overnight. 10µM coronal sections were subsequently cut on a Leica RM2235 Rotary Microtome (Leica Microsystems, Wetzlar, Germany) and floated on water 37°C in a paraffin stretching GFL 1052 Water Bath (MSC) to allow the sections to spread. Sections were then floated onto electrostatically charged slides (Menzel-Glaser, Braunschweig, Germany) and placed on the water baths rim to initially dry before being dried at 37°C overnight in an incubator (Boekel).

Step	***Duration***
70% EtOH	60mins
80% EtOH	60mins
95% EtOH	60mins
100% EtOH	60mins
100% EtOH	60mins
100% EtOH	60mins
50/50% EtOH/Xylene	60mins
100% Xylene	60mins
100% Xylene	60mins
Paraffin	60mins
Paraffin under vacuum	120mins

Table 2.14: Dehydration and fixing conditions

2.2.9.3 – General Immunohistochemistry Protocol

Sections were dewaxed in xylene and rehydrated through alcohols of decreasing concentration immediately before beginning a staining protocol. Immunohistochemistry was performed for the microglial markers Pu.1 and IBA-1, chemokines CCL2 and CXCL10, amyloid plaque marker 6e10 and neuronal markers ChAT and synaptophysin. Dehydrated sections were dewaxed in xylene for 15 minutes and through two 10-minute baths in Histoclear II to ensure complete removal of wax from the tissue. The sections were subsequently rehydrated through successively decreasing concentrations of ethanol, 100% EtOH II, 100% EtOH I, 95% EtOH, 80% EtOH, 70% EtOH. Upon completion of the rehydration process, non-specific endogenous peroxidase activity was quenched through a 15-minute incubation in 1% hydrogen peroxide in methanol. For some immunohistochemical targets, antigen retrieval was required as described in the next section and summarised in **Table 2.15.**

Following antigen retrieval sections were washed three times in PBS for 3 minutes before being circled with a ring of wax using a PAP pen (Sigma, Poole, UK). 40µl of the appropriate concentration and species of blocking serum and primary antibodies were applied and incubated at 4°C overnight. Subsequently sections were washed three times again in PBS before application of 40µl of the appropriate secondary antibody (Biotinylated secondary antibodies from Vector Laboratories, Peterborough, UK) and incubated at room temperature for 45 minutes. Three 5-minute washes with PBS followed and sections were incubated in ABC solution (1 drop reagent A and 1 drop reagent B added to 5 ml PBS as per the manufacturers instruction; Vector Laboratories, Peterborough, UK) for 45 minutes followed by three washes in PBS, and finally developed in 3,3' Diaminobenzidine (DAB) solution (250 ml 0.1 M phosphate buffer, 5ml DAB (250µg/ml), 125µl hydrogen peroxide). In some instances, a 0.004% Ammonium Nickel Chloride DAB reaction was used to enhance contrast.

In some cases, Harris haemotoxylin (VWR) was used as a nuclear counterstain. Slides were first immersed in Harris haemotoxylin for 30 seconds allowing the mordant ammonium sulphate (alum) to strengthen the positive ionic charge of the hematin encouraging its binding to the anionic nuclear chromatin. The alum causes the stained nuclei to be red in colour and slides were then immersed in an acid alcohol solution (1% concentrated hydrochloric acid in 70% EtOH) for 5 seconds to allow the this red Harris haemotoxylin stain to differentiate, followed by a brief immersion in dH_2O to wash off excess stain. Slides were then immersed in the basic blueing solution, Scott's Blue Tap water (0.2% potassium bicarbonate, 3% magnesium sulphate) to alter the pH and turn the red hematoxylin stained nuclei blue. Slides were let sit until nuclei were a suitable intensity of blued staining was achieved.

Sections were dehydrated through a series of ethanols of increasing concentration for 3 minutes each (70 %, 80 %, 95 %, 100 % I, 100 % II), followed by two changes of xylene for 15 minutes. Slides were finally mounted in DPX (Sigma, Poole, UK) and coverslips applied.

Target	Fixative	Marker	Antigen Retrieval Pretreatments	Block	Incubation	Secondary	Nickel DAB	Counter Stained
6E10	FFPE	Amyloid plaques	none	10% Horse	1/1000 90 mins @ RT	Horse anti-mouse	x	✓
CCL2	FFPE	Chemokines	Citrate Pepsin (20mins)	10% Rabbit	1/100 Overnight @ 4°C	Rabbit anti-goat	x	✓
CXCL10	FFPE	Chemokines	Citrate Pepsin (20mins)	10% Goat	1/10,000 Overnight @ 4°C	Goat anti-rabbit	x	✓
ChAT	FFPE	Cholinergic neurons	Citrate	10% Rabbit	1/500 Overnight @ 4°C	Rabbit anti-goat	x	x
GFAP	FFPE	Astrocyte Cytoskeleton	none	10% Goat	1/2,000 Overnight @ 4°C	Goat anti-rabbit	x	✓
IBA-1	FFPE	Microglia Cytoplasm	Citrate Pepsin (20mins)	10% Rabbit	1/2,000 Overnight @ 4°C	Rabbit anti-goat	x	✓
Pu.1	FFPE	Microglia	Citrate, 1% Triton (20mins)	10% Goat	1/400 Overnight @ 4°C	Goat anti-rabbit	✓	x
SY38	FFPE	Synaptophysin	0.2M Boric Acid, pH 9, 65°C (30mins)	10% Horse	1/2,000 Overnight @ RT	Horse anti-mouse	✓	x

Table 2.15: Immunohistochemical antigen retrieval, blocking and antibody conditions used

2.2.9.4 – Antigen Retrieval

2.2.9.4.1 Citrate Buffer

For some immunohistochemical reactions a heat-based antigen retrieval was performed using citrate buffer (0.01M citric acid, pH6). Slides were incubated in citrate buffer in black plastic BRAND™ staining troughs (Fisher Scientific) and microwaved (800W SANY) for 5 minutes to a roiling boil and then let sit at room temperature for 5 minutes, falling below 100°C. This procedure was then repeated such that the samples experienced a 20-minute total incubation of two 5 minute periods of active heating to a boil and two 5 minute cooling periods. Slides were then cooled to room temperature by slow addition of cold tap water. Slides were then washed three times in PBS for 3 minutes per wash.

2.2.9.4.2 0.04% Pepsin 0.1M HCl

For some immunohistochemical reactions an acidic enzyme-based antigen retrieval was performed using 0.04% porcine pepsin diluted in a 0.01M HCl solution pH'd to 1. Sections were first circled with a PAP pen before application of 40-50µl of pepsin, sufficient to completely cover the section, and incubated at room temperature for exactly 20 minutes. Slides were then washed three times in PBS for 3 minutes per wash.

2.2.9.4.3 1% Triton

For some immunohistochemical reactions a detergent-based antigen retrieval was used to permeabilise membranes and allow antibodies access to nuclear based antigens. Slides were immersed in a 1% Triton solution for 20 minutes. Slides were then washed three times in PBS for 3 minutes per wash.

2.2.9.4.4 Boric Acid

For synaptophysin (Sy38) staining a boric acid wash was used as antigen retrieval. Slides were treated by immersion in a glass coplin jar containing 0.2 M boric acid, pH 9 which was pre heated to 65°C in a JB Aqua PlusS water bath (Grant), for 30 mins. The water bath heating element was switched off and the water allowed to cool passively to room temperature (19-20°C approx.) over approximately 90mins. Slides were then washed three times in PBS for a duration of 3 minutes per wash.

2.2.9.5 – Quantitative Analysis using ImageJ

2.2.9.5.1 ChAT

ChAT positive cells were identified and counted using Image J software (NIH, Bethesda, Maryland 20810, USA). Photomicrographs were taken at 20X under constant illumination, converted to 8-bit and inverted. Background was subtracted using the "Subtract background" function and

thresholded using the “Auto local threshold” to correct for the variability in background staining between images. Particles under a certain size (<200) were eliminated theoretically leaving only ChAT positive puncta to analyse and obtain a quantification of cholinergic terminal numbers and %percentage area of the image covered by them using the “Measure” function.

2.2.9.5.2 IBA-1

In the case of the microglial cell surface marker IBA-1, both morphology and quantity of the microglia were analysed. Photomicrographs were taken at 20X under constant illumination. To eliminate background cell and objects, images were converted to 8-bit in Image J software (NIH, Bethesda, Maryland 20810, USA). and thresholds established to eliminate non-labelled background and preserve positively stained cells presence and morphology. A mask was drawn around the region of interest, excluding irrelevant regions or damaged areas of the section. Particles under a certain size (250 pixels) were eliminated theoretically leaving only the microglia to analyse and obtain a count of and the total area of the mask which they occupied. All counts were then normalised to a uniform area so as to be comparable between sections.

2.2.9.5.3 Pu.1

A similar approach was taken for analysis of the microglia specific marker Pu.1 as was conducted for IBA-1 above with the exception that particles under 50 pixels in size were eliminated due to the fact this nuclear stain is a far smaller area of staining than IBA-1.

2.2.9.5.4 Synaptophysin (SY38)

Presynaptic terminal density was assessed using immunolabelling of the presynaptic marker synaptophysin using the monoclonal antibody SY38 as described above. Photomicrographs were taken at 10X centred on the hippocampus under constant illumination. Images were converted to 16-bit grayscale in Image J software (NIH, Bethesda, Maryland 20810, USA). and transmittance was quantified using the measure function. I then subtracted transmittance in the areas of interest from those for the corpus callosum and divided by transmittance in the overlying cortex to standardise for differences in density of labelling from section to section. I thus quantified the density of labelling according to the calculation:

$$\frac{\text{Transmittance (Corpus Callosum)} - \text{Transmittance (ROI)}}{\text{Transmittance (Corpus Callosum)} - \text{Transmittance (Cortex)}}$$

2.2.9.5.5 Luxol fast blue

White matter integrity was assessed using histological staining using the copper phthalocyanine dye Luxol Fast Blue (LFB), which binds myelin lipoproteins. Slides were immersed overnight in LFB solution (Michrome Labs, UK) at 37 °C overnight in an incubator (Boekel). Sections were then immersed in 95% ethanol to remove the excess stain and rinsed with deionized water.

Differentiation was initiated with immersion in 0.05% aqueous lithium carbonate for 10 s followed by 70% ethanol until the white matter was distinguished. Sections were counterstained using a 0.1% cresyl violet solution (TAAB Laboratories, UK) at 37 °C in a JB Aqua PlusS water bath (Grant) for 5 minutes. Finally, sections were dehydrated and cover slipped. Photomicrographs were taken at 10X centred on the hippocampus under constant illumination. Images were converted to 16-bit grayscale in Image J software (NIH, Bethesda, Maryland 20810, USA). and transmittance was quantified using the measure function and subtracted its value from that of pure white (255) to give a metric whereby high density (minimal light transmittance) gave a greater value than a region of low density (high light transmittance). I thus quantified the density of labelling according to the calculation: 255 – (Transmittance of ROI).

2.2.10 – Immunofluorescence on formalin-fixed brain tissue

Sections were dewaxed and rehydrated as described above in section 2.2.9.3. Antigen retrieval pre-treatments were performed as described in the previous section and summarised in **Table 2.16**. Following antigen retrieval sections were washed three times in PBS for 3 minutes before being circled with a ring of wax using a PAP pen (Sigma, Poole, UK). 40µl of the appropriate concentration of primary antibodies for the first target in 10% BSA were applied and incubated at 4°C overnight. Subsequently slides were washed three times again in PBS before application of 40µl of the appropriate fluorescent secondary antibody and incubated at room temperature for 45 minutes. Three 5-minute washes with PBS followed and the process was repeated for the secondary fluorescent target.

Hoescht stain 488nm (Thermo Fisher) was applied at 40µl per section (1:1000 in PBS) for 10 minutes and coverslipped with Prolong Antifade Gold medium (Thermo Fisher) and sealed with an acrylic nail varnish, stored at 4°C in darkness until imaging.

Target		Fixative	Antigen Retrieval Pretreatments	Block	Incubation	Secondary
IBA1 & GFAP	IBA1	FFPE	Citrate Heat, Pepsin 0.04% in 0.01M HCl 20mins	10% BSA	1 in 500 goat polyclonal anti mouse (Abcam)	1 in 800 Donkey anti goat (633nm)
	GFAP				1 in 500 rabbit polyclonal anti-mouse (DAKO)	1 in 800 Chicken anti rabbit (488nm)
IBA1 & CCL2	IBA1	FFPE	Citrate Heat, Pepsin 0.04% in 0.01M HCl 20mins	10% BSA	1 in 500 rabbit polyclonal anti mouse (WAKO)	1 in 800 Chicken anti rabbit (488nm)
	CCL2				1 in 100 goat polyclonal anti-mouse (R&D)	1 in 800 Donkey anti goat (633nm)
GFAP & CCL2	GFAP	FFPE	Citrate Heat, Pepsin 0.04% in 0.01M HCl 20mins	10% BSA	1 in 500 rabbit polyclonal anti mouse (DAKO)	1 in 800 Chicken anti rabbit (488nm)
	CCL2				1 in 100 goat polyclonal anti-mouse (R&D)	1 in 800 Donkey anti goat (633nm)

Table 2.16: Immunofluorescent antigen retrieval, blocking and antibody conditions used

2.2.11 – Fluorescence-activated Cell Sorting

2.2.11.1 – Tissue Preparation

Dissected brain tissue (hippocampus and overlying cortex) was finely chopped with a sterile scalpel blade and digested in 2mls of 5% FBS, 10µM HEPES in HBSS with collagenase @ 2mg/ml & DNAse solution for 45minutes at 37 °C in a JB Aqua PlusS water bath (Grant), triturating with a pipette every 15 minutes. The resulting homogenate was passed through a 70µn cell strainer and centrifuged at 1400rpm for 5 minutes. The resulting supernatant was discarded and the homogenate pellet resuspended in anti-myelin magnetic-activated cell sorting beads (MACS) (Miltenyi) diluted in MACS buffer (Miltenyi) and incubated on ice for 20 minutes. 4mls of MACS buffer was added and centrifuged at 1400rpm for 5 minutes. The resulting supernatant was discarded and the homogenate pellet resuspended in 1ml of MACs buffer. Myelin was depleted from the tissue homogenate by passing it through LS columns (Miltenyi) and centrifuged at 1400rpm for 5 minutes. The resulting supernatant was discarded and the subsequent myelin-depleted homogenate's FC receptors were blocked using CD16/CD32 (BD Pharmigen) before labelling with antibodies against targets for FACS sorting: CD11b, CD45, GLAST and 7-Aminoactinomycin D (7-AAD) (BD Pharmigen). 2mls of MACS buffer was added and centrifuged at 1400rpm for 10 minutes. The resulting supernatant was discarded and the homogenate pellet resuspended in 200µl of MACs buffer. BD FACS Aria cell sorter was used to separate and sort astrocytic and microglial cells directly into Trizol for RNA isolation as described in section 2.2.6.2.1. All antibody dilutions, fluorochromes and excitations are listed in **Table 2.17.**

Target	Dilution Factor	Fluorochrome	Excites @	Supplier
Myelin	1/10	N/A	N/A	Miltenyi
CD16/CD32	1/100	N/A	N/A	BD Pharmigen
CD11b	1/100	FITC	488	Biolegend
CD45	1/100	APC/Cyanine7	633	Biolegend
GLAST	1/100	ACSA-1-PE	565	Biolegend
7AAD	1/40	PE	650	BD Pharmigen

Table 2.17: MACS & FACS antibody flurochromes and dilution factors

2.2.11.2 – Fluorescence activated cell sorting of glia

Fluorescent antibody labelled hippocampal homogenate was then gated down to single cells, excluding debris or cell doublets. To this end cells were gated sequentially according to their relative size as indicated by their forward scatter area/width of light, and according to their relative

granularity (complexity) as indicated by their side scatter area/width of light. The first stage of gating was to remove debris and so were gated according to their side scatter area (SSC-A) against their forward scatter area (FSC-A) **(Figure 2.4 A)** refraction of light. Next single cells were distinguished from doublets by two sequential gating strategies, first by their FSC-A against forward scatter width (FSC-W) **(Figure 2.4 B)** and then by SSC-A against side scatter width (SSC-W) **(Figure 2.4 C).** Any cells which fell in the upper range of these plots due to their size and/or their granularity (complexity) were likely debris or doublets and thus excluded. Following this sequential gating strategy a population of single cells was now identified and available to be separated into living and dead cells based on 7-aminoactinomycin D (7AAD) positive labelling of lysed cells' DNA and plotted against FSC-A **(Figure 2.4 D)**. Microglia were identified and separated from this population of living cells based on high CD11b-FITC^{+} and intermediate CD45-APC^{+} expression to distinguish them from macrophage populations **(Figure 2.4 E)**; astrocytes were identified and isolated based on of high GFAP-PE^{+} staining against FSC-A **(Figure 2.4 F)**. Cells were sorted in Sheath Fluid (BD FACS™) and collected in an RNase free 1.5ml Eppendorf tubes containing 800µl of Trizol LS (Invitrogen). RNA isolation was completed as described in section 2.2.6.2.2

To determine the purity and efficiency of FACS isolation of glial cell isolates qPCR analysis was performed to assess expression of microglial and astrocytic specific markers, CD11b and GFAP.

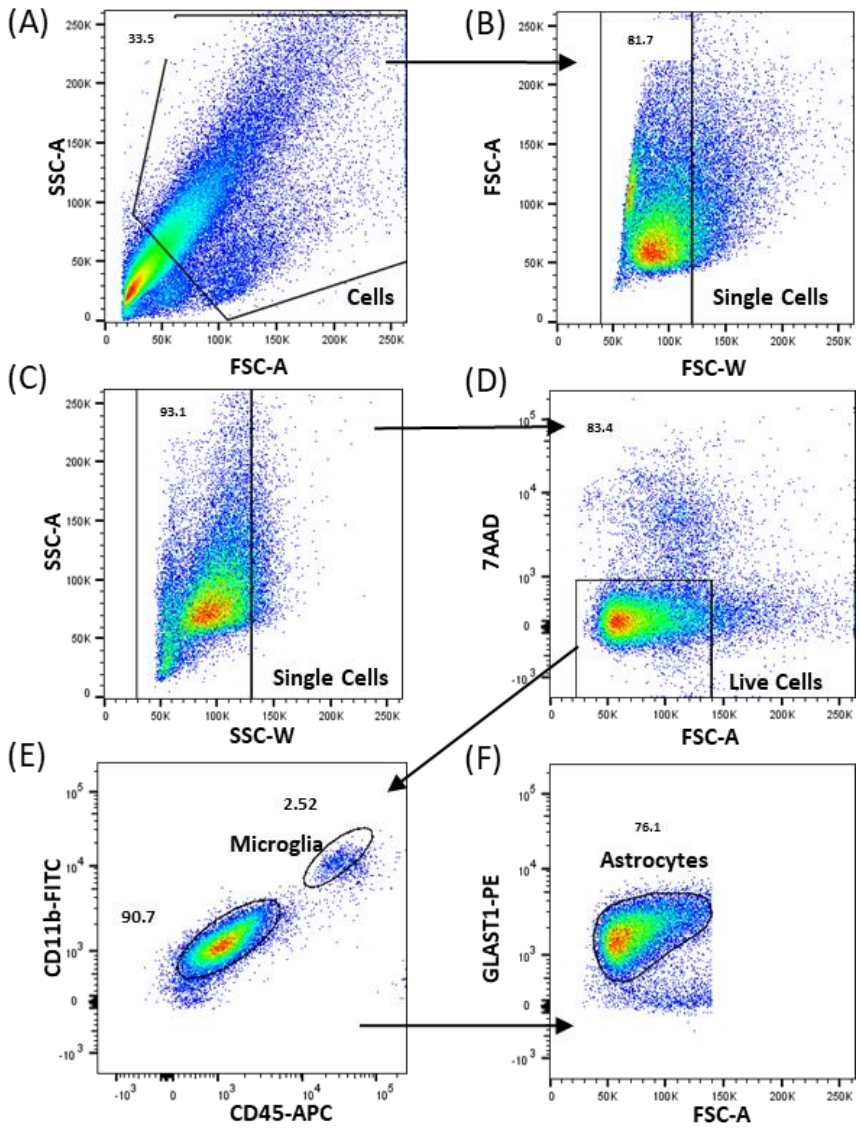

Figure 2.4 FACS isolation of glial cells – Fluorescent activated cell sorting (FACS) of astrocytes and microglia (A – B) gating cells to single cells, (D) separating live from dead cells using the DNA marker 7AAD staining of lysed cells, (E) identifying and separating microglia based off high CD11b-FITC$^+$ and intermediate CD45-APC$^+$ staining and (F) identifying astrocytes according to high GLAST1-PE$^+$ staining.

2.2.12 – Statistics & graphing

Statistical analyses were performed using IBM SPSS statistics version 24 for Windows or Graphpad Prism Version 8. GraphPad Prism Version 8 was used to graphically represent all data.

2.2.12.1 Chapter 3

Data were systematically assessed for homoscedasticity by Shapiro-wilk normality test and in all cases where appropriate parametric data were represented as mean ± SEM. For all behavioural, ELISA and qPCR data pertaining to sections 3.2.1-3, two-way ANOVA analyses were performed, age

state (young vs aged) and treatment (saline vs LPS 100µg/kg) were the factors examined. Bonferroni post-hoc tests were performed following a significant ANOVA. Pearson linear regression analysis was performed to determine whether Clec7a gene expression correlated with Il1b expression and significant p-values and r^2 values were reported. Longitudinal assessment of cognitive vulnerability to dysfunction over 48 hours pre and post i.p. challenge with saline, LPS (100µg/kg) and Poly I:C (12mg/kg) was analysed by two-way repeated measures ANOVA with age (5-7 months, 16-19 months, 24 moths) as the between subjects factor and time (hours pre/post challenge) as the within subjects factor. Bonferroni post-hoc tests were performed following a significant ANOVA. Immunohistochemical cell counting and positively stained area were analysed by Student's t test for parametric data or Mann Whitney U test for non-parametric data. Factors used were age (young vs aged) and cognitive vulnerability (cognitively resilient vs cognitively frail). Pearson linear regression analysis was performed to determine whether myelin density or ChAT terminal density (light transmitted) correlated with $IBA1^+$ area or cognitive dysfunction, assessed as number of errors under acute challenge, and significant p-values and r^2 values were reported.

2.2.12.2 Chapter 4

Data were systematically assessed for homoscedasticity by Shapiro-wilk normality test and in all cases where appropriate parametric data were represented as mean ± SEM. Pearson linear regression analysis was performed to determine whether qPCR gene expression correlated with age (months) or frailty score and significant p-values and r^2 values were reported. Where linear relationships were inappropriate qPCR gene expression was fitted to a Gaussian curve and assessed for degree of fit by the r^2 value. Pearson linear regression analysis was performed to determine whether ELISA protein concentrations, frailty index component measures values or cognitive function correlated with age (months) or frailty score and significant p-values and r^2 values were reported. Longitudinal assessment ability to learn and retain the hippocampal-dependent y-maze task pre and post i.p. challenge with LPS (250µg/kg) was analysed by two-way repeated measures ANOVA with age (3-9 months, 14-19 months, 20-24 moths) or frailty status (high frailty 0.35<, mid frailty 0.25<x<0.35, robust <0.25) as the between subjects factor and number of trials (presented as blocks of 12 trials training, 10 trials retention, 6 trials reversal) as the within subjects factor. Area under the curve analysis of ability to learn and retain the hippocampal-dependent y-maze task pre challenge with LPS (250µg/kg) assessed over five days, each a block of 12 trials, between groups by age (3-9 months, 14-19 months, 20-24 moths) or frailty status (high frailty 0.35<, mid frailty 0.25<x<0.35, robust <0.25) assessed and presented as area ± SEM. Bonferroni post-hoc tests were performed following a significant ANOVA. Longitudinal assessment of vulnerability to and recovery from deficits in frailty index component measures and frailty score itself over 168 hours pre and post i.p. challenge with LPS (250µg/kg) was analysed by two-way repeated measures ANOVA with

age (3-9 months, 14-19 months, 20-24 moths) or frailty status (high frailty 0.35<, mid frailty 0.25<x<0.35, robust <0.25) as the between subjects factor and time (hours pre/post challenge) as the within subjects factor. Bonferroni post-hoc tests were performed following a significant ANOVA.

2.2.12.3 Chapter 5

Data were systematically assessed for homoscedasticity by Shapiro-wilk normality test and in all cases where appropriate parametric data were represented as mean ± SEM. Longitudinal assessment of animals' ability to learn and retain the hippocampal-dependent y-maze task was analysed by two-way repeated measures ANOVA with genotype (C57 WT vs APP/PS1) as the between subjects factor and time (blocks of 4 trials) as the within subjects factor. Bonferroni post-hoc tests were performed following a significant ANOVA. Frailty index component measures, frailty score and fat deposits were analysed by Student's t test for parametric data or Mann Whitney U test for non-parametric data. Factors used were genotype (C57 WT vs APP/PS1). Longitudinal assessment of animals' Promethion cage measurements of metabolism, food and water intake and activity were analysed by two-way repeated measures ANOVA with genotype (C57 WT vs APP/PS1) or treatment (saline vs TNFα) as the between subjects factor and time (hours) as the within subjects factor. Bonferroni post-hoc tests were performed following a significant ANOVA. Longitudinal assessment of animals' weight loss and recovery and ability to learn the visuospatial MWM task were analysed by two-way repeated measures ANOVA with genotype/treatment (C57 WT saline/TNFα vs APP/PS1 saline/TNFα) as the between subjects factor, combined and also split by sex (male vs female), and time (days) as the within subjects factor. Bonferroni post-hoc tests were performed following a significant ANOVA. For all frailty index component measures, CFC, MWM flag and probe trials, and qPCR data two-way ANOVA analyses were performed, genotype (C57 WT vs APP/PS1) and treatment (saline vs TNFα 250µg/kg) were the factors examined. Bonferroni post-hoc tests were performed following a significant ANOVA.

Immunohistochemical cell counting and positively stained area were analysed by Student's t test for parametric data or Mann Whitney U test for non-parametric data. Factors used were genotype (C57 WT vs APP/PS1). Pearson linear regression analysis was performed to determine whether Immunohistochemical cell counting and positively stained area correlated between markers of glial activation and amyloid pathology; significant p-values and r^2 values were reported. Immunohistochemical positively stained area for $IBA1^+$, $GFAP^+$ and $6E10^+$ staining analysis, two-way ANOVA analyses were performed on data, genotype (C57 WT vs APP/PS1) and treatment (saline vs TNFα 250µg/kg) were the factors examined. Bonferroni post-hoc tests were performed following a significant ANOVA.

Chapter 3:

The ageing brain and regional heterogeneity in innate immune response to systemic inflammation

3.1 Introduction

The continuous and pernicious onslaught of age can be characterized by declining functional capacity, resulting in an ever-increasing vulnerability to morbidity and ultimately mortality. The physiological deterioration which accompanies the progression of age can range from the seemingly banal greying of hair, to debilitating kyphosis and cachexia. The brain is not exempt from this and will undergo significant reduction in size, composition, vasculature and plasticity (Esiri 2007; Dekaban et al. 1978). In addition to the physiological impairments, a significant decline in cognitive performance occurs in 38% of 60-78 year olds with no distinct pathology (Koivisto et al. 1995); specifically within episodic memory processing, working memory, spatial memory, processing speed and implicit memory function (Hedden et al. 2004). Furthermore, with the progression of age, a low-grade inflammation known as Inflammaging has been shown to emerge. Inflammation is now recognised as a driver of dementia and as such this chronic activation of the inflammatory response has significant consequences for the CNS immune cell populations and perhaps for brain integrity.

Microglia are the brain's resident immune cell population and are responsible for maintaining the homeostasis of the CNS environment. However, under chronic activation such as the conditions imposed in ageing and neurodegenerative conditions these cells become primed. Microglial priming is characterised by changes in the activation state of the microglial cell in response to chronic activation which renders it highly responsive to further challenge. Cunningham and colleagues were the first to demonstrate there was an altered response in the ME7 prion model in C57BL/6J mice to peripheral challenge with the bacterial mimetic LPS. Chronic neurodegeneration in the hippocampus was shown to prime the microglia of that region to produce a greater inflammatory response to an acute LPS challenge (Cunningham et al. 2005). This has since been corroborated in a number of mouse models of PD (Godoy et al. 2008), Wallerian degeneration (Palin et al. 2008), AD (Sy et al. 2011) and ageing (Godbout et al. 2005). This exaggerated production of pro-inflammatory cytokines can potentially be harmful (Perry et al. 2010). In the ME7 model of prion disease it was demonstrated that the progression of the neurodegenerative disease was accelerated by the acute challenge of the secondary stimulus, LPS (Cunningham et al. 2009) and that new neuronal death occurring during systemic LPS challenge was partially dependent on IL-1b (Skelly et al., 2019), the key output of these microglia upon LPS challenge.

In the ageing animal a bacterial or viral infection can serve as this triggering, secondary, stimulus to the primed immune cells and results in heightened sickness behaviour. ME7 animals challenged with the bacterial mimetic LPS have been shown to display significantly reduced locomotor activity and hypothermia were observed compared to control animals (Combrinck et al. 2002; Godbout et

al. 2005; Cunningham et al. 2009). This exaggerated sickness behaviour response to an acute LPS stimulus has also been demonstrated in aged mice, and these animals also showed greater reductions in food intake and body mass than younger LPS-treated animals (Godbout et al. 2005). The significant impact that systemic inflammation has upon the CNS is well documented (Dantzer et al. 1998) and is theorised to be a driver of dementia with evidence suggesting that bacterial and viral infections may trigger its development (Sochocka et al. 2017; Perry et al. 2007) and worsen existing pathology including exacerbated Aβ and phosphorylated tau protein (p-tau) deposits (Gasparotto et al. 2018).

However, there is increasing evidence from recent studies that there is distinct heterogeneity in the responsiveness of the microglia within the ageing brain. Principal component analysis (PCA) of RNA microarray data from microglia that were isolated from young and aged microglia revealed significant differences in the principle component genes of the cerebellum, hippocampus, cortex and striatum (Grabert et al. 2016). Of these, the cerebellum's principal components were the most distinct from the other assessed regions in the young animal. In contrast the cortex and striatum shared very similar component genes while the hippocampus displayed an intermediate signature between that of the cerebellum and cortex/striatum. Further analysis of the genes which make up this PCA signature revealed that their primary genes are linked to the immune response, indicating that the cerebellum and hippocampus exist in a more immune vigilant state than the striatum and cortex. However, as age advanced it was shown that cerebellum became increasingly distinct, adopting an ever more immune vigilant signature, while the hippocampus began to lose its distinct signature, becoming more like the cortex and striatum with time. From this it was concluded that the microglia are sensitive to age-related damage and loss of function, in a region-dependent manner (Grabert et al. 2016).

Thus, I hypothesised that markers of microglial activation, priming and neuroinflammation would change with age in a region dependent manner and, in particular, that microglia of the cerebellum might show particularly exaggerated innate immune responses to systemic challenge with LPS. To this end, 8 and 25-month-old mice were challenged with a 100μg/kg bolus of LPS by intraperitoneal (i.p.) injection and open field analysis of their behaviour conducted 3 hours post challenge. The animals were then euthanised and perfused and the cerebellum, hypothalamus, hippocampus and frontal cortex dissected at 4 hours post challenge for molecular analysis. qPCR analysis was conducted across these regions for markers of microglial activation, proliferation and priming in addition to inflammatory cytokines, chemokines and IFN-induced genes.

The propensity of existing microglial priming to facilitate exaggerated CNS responses to systemic inflammation leads to the hypothesis that advancing age would render animals increasingly

vulnerable to cognitive dysfunction under systemic inflammatory conditions and that the degree to which they were susceptible to cognitive impairment would correlate with the extent of their microgliosis. Using the animals' hippocampal-dependent working memory (alternation in an escape from water T-maze task) animals were stratified into cognitively frail and resilient groups based on their T-maze performance when challenged with the bacterial mimetic LPS and the viral mimetic Poly I:C as described in section 2.2.3.5. Histochemical analysis was conducted to assess the degree of microglial activation, pre-synaptic terminal density and myelin integrity in the hippocampus and cerebellum of this cognitive frailty cohort and analysed as a function of their assigned frailty status in order to study correlates of age-associated neuroinflammation and of cognitive frailty.

3.2 Results

3.2.1 Age confers exaggerated sickness behaviour

Open field analysis of 25 and 8-month-old animals treated with saline or LPS revealed significant differences in sickness behaviour, at 3 hours post challenge, as a function of age. The number of rears and squares crossed following treatments, as a percentage of their base line performance, revealed age conferred significant vulnerability to LPS-induced sickness behaviour **(Figure 3.1 A, B)**. In both the number of rears (***$p<0.001$) and distance covered (**$p<0.01$) aged animals treated with LPS scored significantly lower than age matched controls treated with saline and adult animals treated with LPS (+++$p<0.01$). Core body temperature was also measured 4 hours post challenge with aged animals showing a significant reduction from baseline (**$p<0.01$) when treated with LPS compared to aged saline treated controls that was not observed in 8-month-old adult animals regardless of treatment (++$p<0.01$) **(Figure 3.1 C)**. In both open field analysis and assessment of core body temperature it was found that treatment with LPS alone was insufficient to elicit a statistically significant reduction in activity or body temperature in 8-month-old adult animals when compared to saline treated controls.

However, while clear sickness behaviour was only evident in the aged population treated with LPS and not in younger animals, analysis of systemic proinflammatory cytokines and chemokines levels, IL-1β and CXCXL1, in blood plasma by ELISA revealed that age had no statistically significant impact upon systemic levels of the pro-inflammatory mediators following LPS exposure **(Figure 3.1 F & G).**

Since a relationship between blood glucose and sickness behaviour has recently been shown (Kealy et al. 2020)blood glucose levels were also taken 4 hours post challenge by glucometer, at time of death, directly from the heart's right atrium, in this instance treatment again had a significant effect but this was not affected by age, with an equivalent reduction in systemic glucose levels found

between adult and aged LPS-treated animals. **(Figure 3.1 D).** A corresponding inverse trend was observed by ELISA for blood insulin levels **(Figure 3.1 E)** with LPS-treated animals exhibiting higher systemic insulin expression compared to saline treated control animals.

These results suggest that the chronic condition of the ageing process has left the aged animal more vulnerable to greater CNS responses to acute inflammation that would be explained by differences in circulating inflammatory mediators. Therefore, an assessment of whether this was regionally preserved or whether there were regional differences in microglial and inflammatory mediator responses to LPS, in the aging brain.

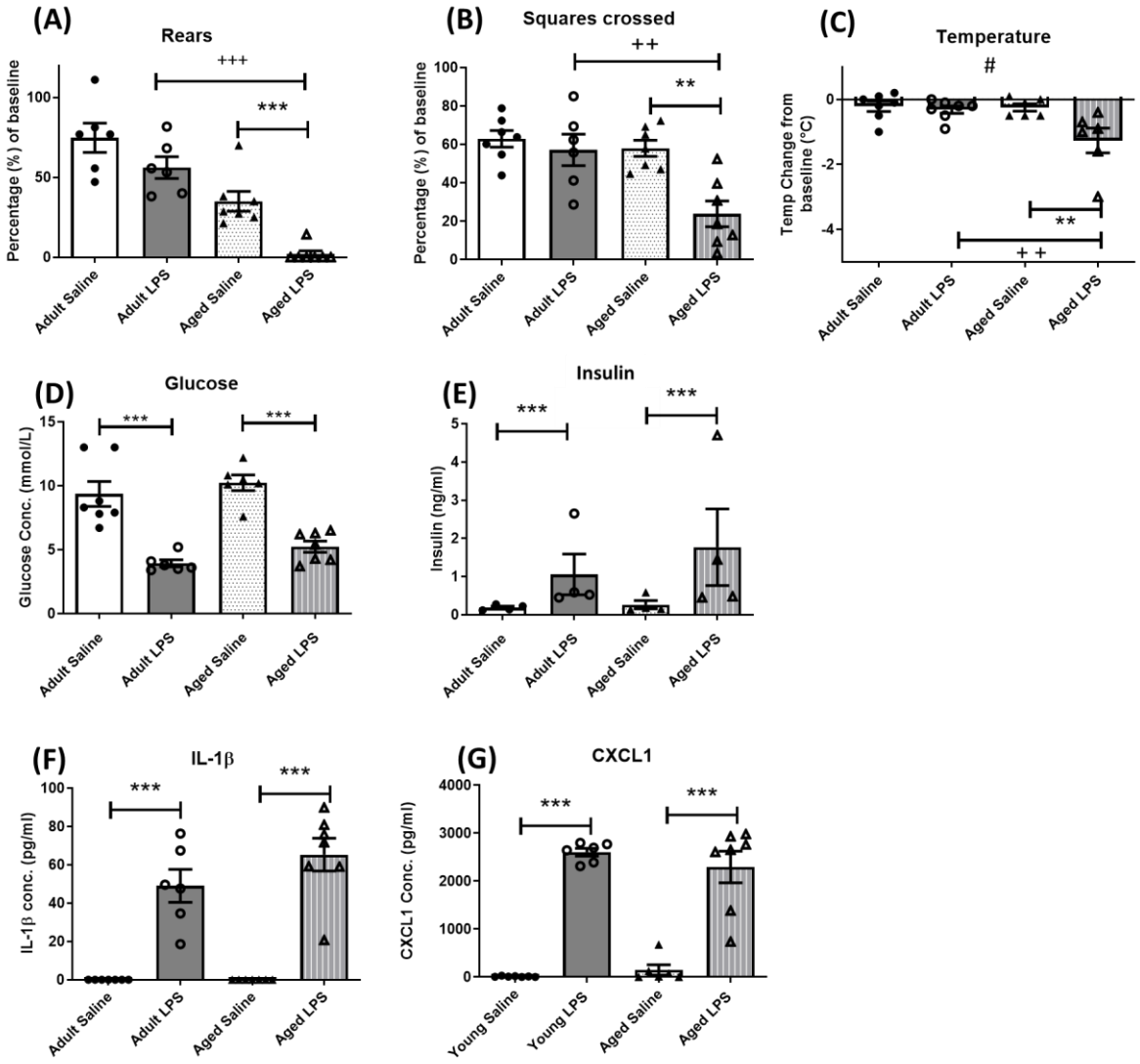

Figure 3.1: Exaggerated sickness behaviour assessed 3 hours post i.p. LPS (100µg/kg), metabolic and systemic inflammatory cytokines measured post mortem 4 hours post challenge, all data are represented as the mean ± SEM. All main effects analysed by two-way ANOVA followed by a Bonferroni multiple comparison Post Hoc Test (n = 6-7), * denotes a statistical significant effect of treatment in aged animals (P<0.05),(p<0.01), ***(p<0.001). # denotes a statistically significant interaction between age and treatment; # (p<0.05), ## (p<0.01), ### (p<0.001). + denotes significant effect of age on response to LPS treamted animals, ++(p<0.01), +++(p<0.001).: (A) (B) Main effect of age and treatment on sickness behaviour as measured by open field activity (A) number of rears and (B) distance covered expressed as a percentage of baseline in adult and aged cohorts under acute systemic challenge by LPS (100µg/kg) i.p. treatment. (C) Main effect of LPS (100µg/kg) treatment on body temperature (°C). LPS treatment causes (D) a significant reduction in plasma blood glucose levels (mmol/L) with a (E) corresponding trend to increased blood insulin levels (ng/ml) (n=4). The impact of LPS (100µg/kg) treatment on (F) IL-1β and CXCL1 levels.**

3.2.2 Regional differences in innate immune response

Based on previous work by Grabert et al. which asserted that the cerebellum exists in a more immune vigilant state than other regions (Grabert et al. 2016), analysis of cytokine, chemokine and type I interferon responsive transcripts revealed a similar pattern of expression across the hippocampus, cortex, hypothalamus and cerebellum in response to the acute challenge, LPS.

Basal expression of the pro-inflammatory cytokines, *Il1α, Il1b* and *Tnfα* was found to be significantly higher in both the cerebellum and hypothalamus **(Table 3.1 (A), Figure 3.2 A-F)** of aged-saline treated animals compared to adult saline controls (**Figure 3.2)**. On the other hand, the hippocampus and cortex demonstrate only modest and non-significant age-dependent alteration to their baseline cytokine expression **(Figure 3.2 G-L)**, with the exception of *IL1b* expression being elevated in the cortex **(Figure 3.2 I)**.

A similar pattern of basal expression was observed for the type I IFN-induced genes, *Irf7* and *Oas1a* as well as the chemoattractant *Cxcl10*. In both cerebellum and the hypothalamus, increased basal expression was observed in aged saline animals compared to adult controls **(Figure 3.3 A-F)** but no such increase was seen in the hippocampus and cortex **(Figure 3.3 G-L)**.

However, across all brain regions examined, systemic challenge with LPS was shown to result in increased expression of all assessed proinflammatory mediators' transcripts with a significant interaction between age and treatment seeing a significantly greater, exaggerated proinflammatory response in aged LPS-treated animals compared to adults treated similarly for all proinflammatory cytokines and chemokines. Although some trends were observed, this exaggerated response was not observed for type 1 interferon-dependent genes **(Table 3.1 (B) & (C), Figure 3.2 and 3.3)**.

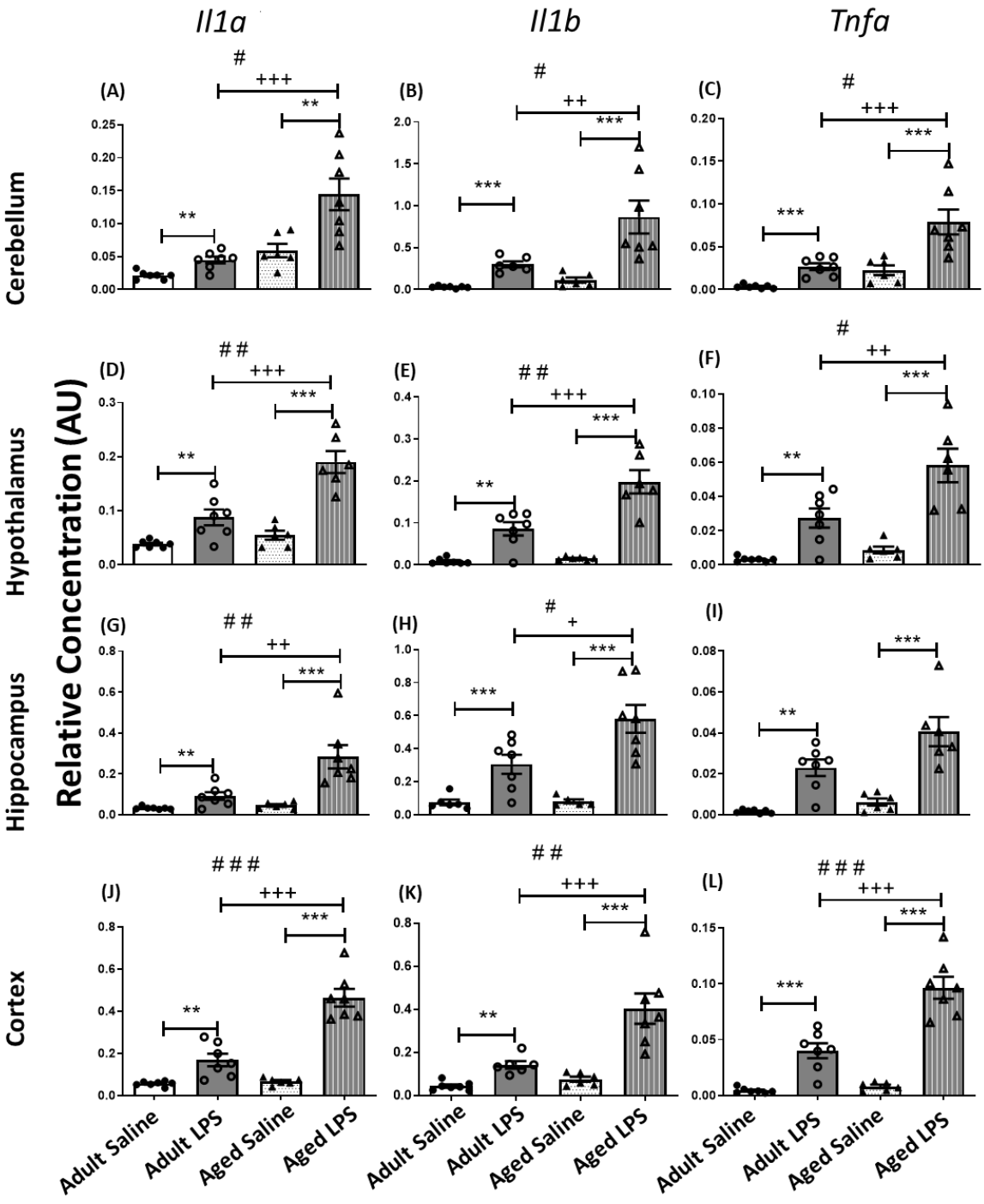

Figure 3.2: Pro-inflammatory cytokines expression across the aged brain: Effect of age on pro-inflammatory cytokine gene transcript expression in cerebellum, hypothalamus, hippocampus and prefrontal cortex 4 hours post LPS (100 µg/kg) i.p. challenge, assessed by qPCR and transcripts normalised to the housekeeping gene 18s. All data represented by mean ± SEM (n=6,7) and analysed by two-way ANOVA followed by a Bonferroni post-hoc test; * denotes a statistically significant effect of LPS treatment, * (p<0.05), ** (p<0.01), * (p<0.001). # denotes a statistically significant interaction between age and treatment; # (p<0.05), ## (p<0.01), ### (p<0.001). + denotes a statistically significant effect of age on response to LPS treatment; + (p<0.05), ++ (p<0.01), +++ (p<0.001).**

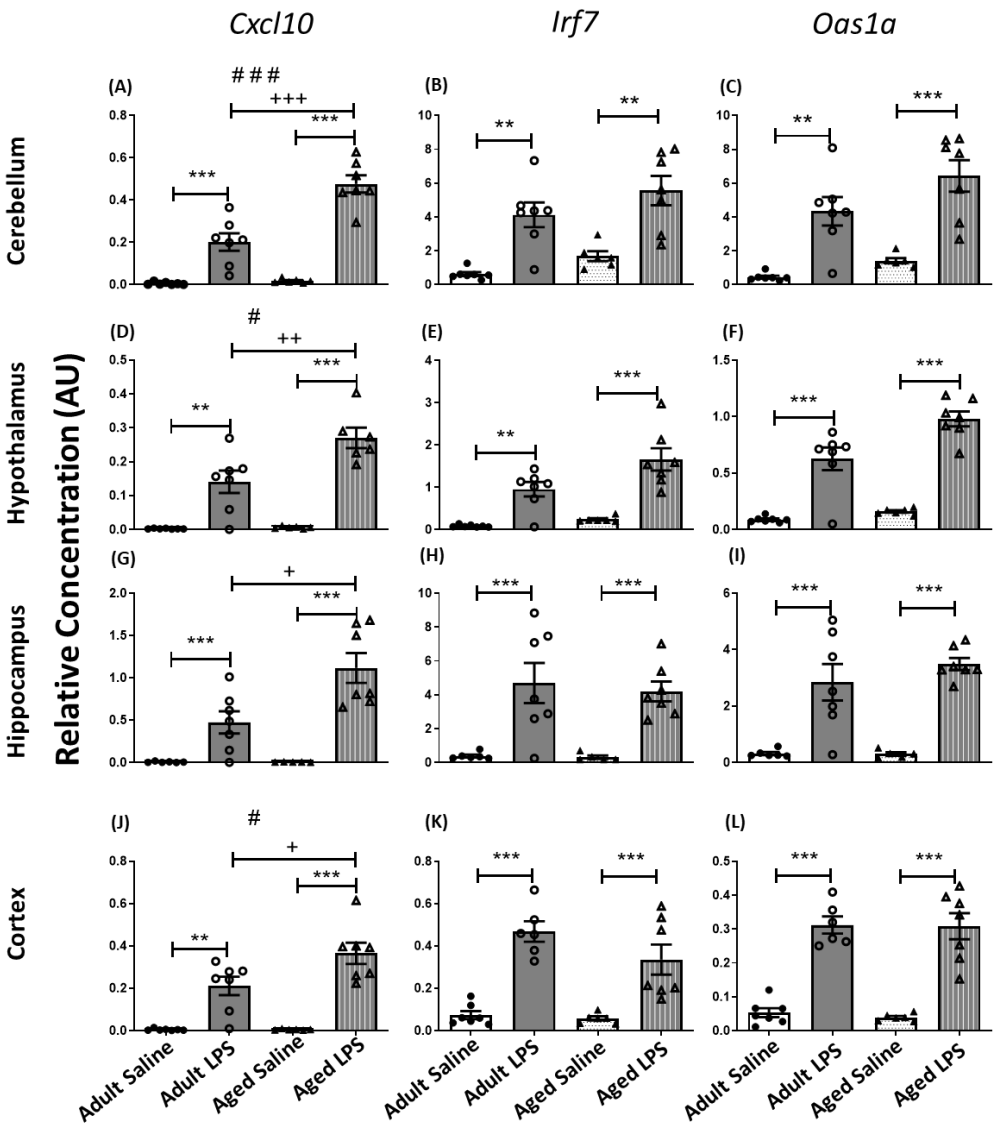

Figure 3.3: Type1 IFN induced expression across the aged brain: Effect of age interferon-induced gene transcript expression in cerebellum, hypothalamus, hippocampus and prefrontal cortex 4 hours post LPS (100 µg/kg) i.p. challenge, assessed by qPCR and transcripts normalised to the housekeeping gene 18s. All data represented by mean ± SEM (n=6,7) and analysed by two-way ANOVA followed by a Bonferroni post-hoc test; * denotes a statistically significant effect of LPS treatment, * (p<0.05), ** (p<0.01), * (p<0.001). # denotes a statistically significant interaction between age and treatment; # (p<0.05), ## (p<0.01), ### (p<0.001). + denotes a statistically significant effect of age on response to LPS treatment; + (p<0.05), ++ (p<0.01), +++ (p<0.001).**

(A)

		Basal Expression of proinflammatory mediators					
		Il1 α	*Il1 b*	*Tnf α*	*Cxcl10*	*Irf7*	*Oas1a*
Cerebellum	**Significance**	**	*	**	*	**	***
	P-Value	p<0.01	p<0.05	p<0.01	p<0.05	p<0.01	p<0.001
Hypothalamus	**Significance**	*	**	*	*	***	***
	P-Value	p<0.05	p<0.01	p<0.05	p<0.05	p<0.001	p<0.001
Hippocampus	**Significance**	Non Sig.	Non Sig.	Non Sig.	Non Sig.	Non Sig.	Non Sig.
	P-Value	0.0747	0.7884	0.0906	0.8436	0.5695	0.8692
Cortex	**Significance**	Non Sig.	*	Non Sig.	Non Sig.	Non Sig.	Non Sig.
	P-Value	0.1951	p<0.05	0.0553	0.8753	0.4937	0.3791

(B)

		Proinflammatory Cytokines, Chemokines and IFN associated genes								
		Il1 α			*Il1 b*			*Tnf α*		
		Age	**Treatment**	**Interaction**	**Age**	**Treatment**	**Interaction**	**Age**	**Treatment**	**Interaction**
Cerebellum	**Significance**	***	***	*	**	***	*	***	***	*
	P-Value	0.0001	0.0006	0.0334	0.0073	0.0001	0.0382	0.0001	0.0001	0.0493
	F-Value	25.2	15.75	5.123	8.725	21.92	4.86	18.56	23.34	4.036
Hypothalamus	**Significance**	***	***	**	***	***	**	**	***	*
	P-Value	0.0001	0.0001	0.003	0.0001	0.0001	0.025	0.0033	0.0001	0.0312
	F-Value	21.2	51.17	11.09	14.85	70.99	11.68	10.85	44.76	5.295
Hippocampus	**Significance**	**	***	**	*	***	*	*	***	Non Sig.
	P-Value	0.0035	0.0001	0.0093	0.0438	0.0001	0.438	0.0409	0.0001	0.1164
	F-Value	10.57	22.24	8.054	4.6	35.72	4.186	4.695	17.25	2.2662
Cortex	**Significance**	***	***	***	**	***	**	***	***	***
	P-Value	0.0001	0.0001	0.0001	0.0013	0.0001	0.0088	0.0001	0.0001	0.0001
	F-Value	31.84	88.18	27.63	13.6	28.83	8.269	23.04	98.29	17.77

(C)

		Proinflammatory Chemokines and IFN associated genes								
		Cxcl10			*Irf7*			*Oas1a*		
		Age	**Treatment**	**Interaction**	**Age**	**Treatment**	**Interaction**	**Age**	**Treatment**	**Interaction**
Cerebellum	**Significance**	***	***	***	*	***	Non Sig.	*	***	Non Sig.
	P-Value	0.0001	0.0001	0.0001	0.0498	0.0001	0.762	0.0296	0.0001	0.4023
	F-Value	22.27	115.6	18.67	4.18	36.78	0.9389	5.378	45.75	0.7282
Hypothalamus	**Significance**	**	***	*	*	***	Non Sig.	***	***	Non Sig.
	P-Value	0.0077	0.0001	0.0114	0.0149	0.0001	0.1063	0.0001	0.0001	0.0708
	F-Value	8.594	78.53	7.627	6.925	48.95	2.826	16.71	325.4	3.328
Hippocampus	**Significance**	*	***	*	Non Sig.	***	Non Sig.	Non Sig.	***	Non Sig.
	P-Value	0.0322	0.0001	0.0319	0.7094	0.0001	0.7835	0.427	0.0001	0.4077
	F-Value	5.299	46.02	5.323	0.1427	29.22	0.07742	0.6563	53.47	0.7138
Cortex	**Significance**	*	***	*	Non Sig.	***	Non Sig.	Non Sig.	***	Non Sig.
	P-Value	0.0358	0.0001	0.0366	0.1204	0.0001	0.216	0.7334	0.0001	0.8397
	F-Value	4.975	66.87	4.928	2.611	54.03	1.623	0.119	109.3	0.04187

Table 3.1 - Statisical summary for inflammatory mediator expression in young and aged ± LPS: (A) summary of statistical differences between saline treated 8 and 25-month-old animals in basal expression of proinflammatory cytokines, chemokines and type one interferon associated genes, assessed by qPCR and transcripts normalised to the housekeeping gene 18s, from Figure 3.2-3, across the cerebellum, hypothalamus, hippocampus and cortex. Data analysed by unpaired student t-test or Mann Whitney u-test, * denotes a significant difference in transcript expression between adult and aged animals, *p<0.05, **p<0.01, ***p<0.001 (n=6,7). (B) (C) summary of statistical differences between saline and LPS treated 8 and 25 month old animals expression of proinflammatory cytokines, chemokines and type one interferon associated genes by qPCR across the cerebellum, hypothalamus, hippocampus and cortex. Data analysed by two-way ANOVA with Bonferroni post hoc test , * denotes a significant difference in transcript expression, *p<0.05, **p<0.01, ***p<0.001 (n=6,7).

Microglial-related transcripts were then assessed in the same four distinct brain regions with the specific hypothesis that while each region would exhibit the primed microglial phenotype, exemplified by the priming hub gene Clec7a (Holtman et al. 2015), that the cerebellum would be particularly affected by age. Consistent with this the ageing brain showed a ubiquitous microglial priming signature across all regions assessed (**Figure 3.4 A, F, K, P).**

For both the cerebellum and hypothalamus a clear induction of *Trem2* **(Figure 3.4 B, G)**, *Tyrobp* **(Figure 3.4 C, H)** and *Cd68* **(Figure 3.4 E, J)** was observed with age in aged saline treated animals compared to adult saline controls. The level of expression was found to be statistically equivalent in saline and LPS-treated aged animals, indicating that acute treatment has no effect upon the induction of this activated microglial phenotype. Rather, age alone has been a sufficient stimulus to induce this state of microgliosis. Interestingly in the cerebellum alone no statistically significant upregulation of *Csf1r* **(Figure 3.4 D)** was observed, which is critical for the survival, maintenance and proliferation of microglia (Han et al. 2019; Han et al. 2017). No such statistically significant alteration in *Csf1r* expression level was observed across the other three regions.

In contrast the hippocampus displayed more reserved microglial activation with age. While there was a trend toward an age dependent increase in the gene expression of *Tyrobp,* and *Cd68* this was non-significant. However, LPS-treated aged animals showed robust increases in expression of *Trem2* **(Figure 3.4 L),** *Tyrobp* **(Figure 3.4 M)**, and *Cd68* **(Figure 3.4 O)**, which was absent in adult LPS-treated animals.

Finally, the cortex shows the most reserved innate immune response activation of the four regions. Indeed, *Trem2* **(Figure 3.4 Q)** and *Csf1r* **(Figure 3.4 S)** show no significant alteration in expression with age or treatment. However, *Tyrobp* **(Figure 3.4 R)** and *Cd68* **(Figure 3.4 T)** both show upregulated expression in aged animals treated with LPS, indicating that while age alone was not sufficient to induce changes, it did leave the animals susceptible to altered expression when challenged with a secondary stimulus.

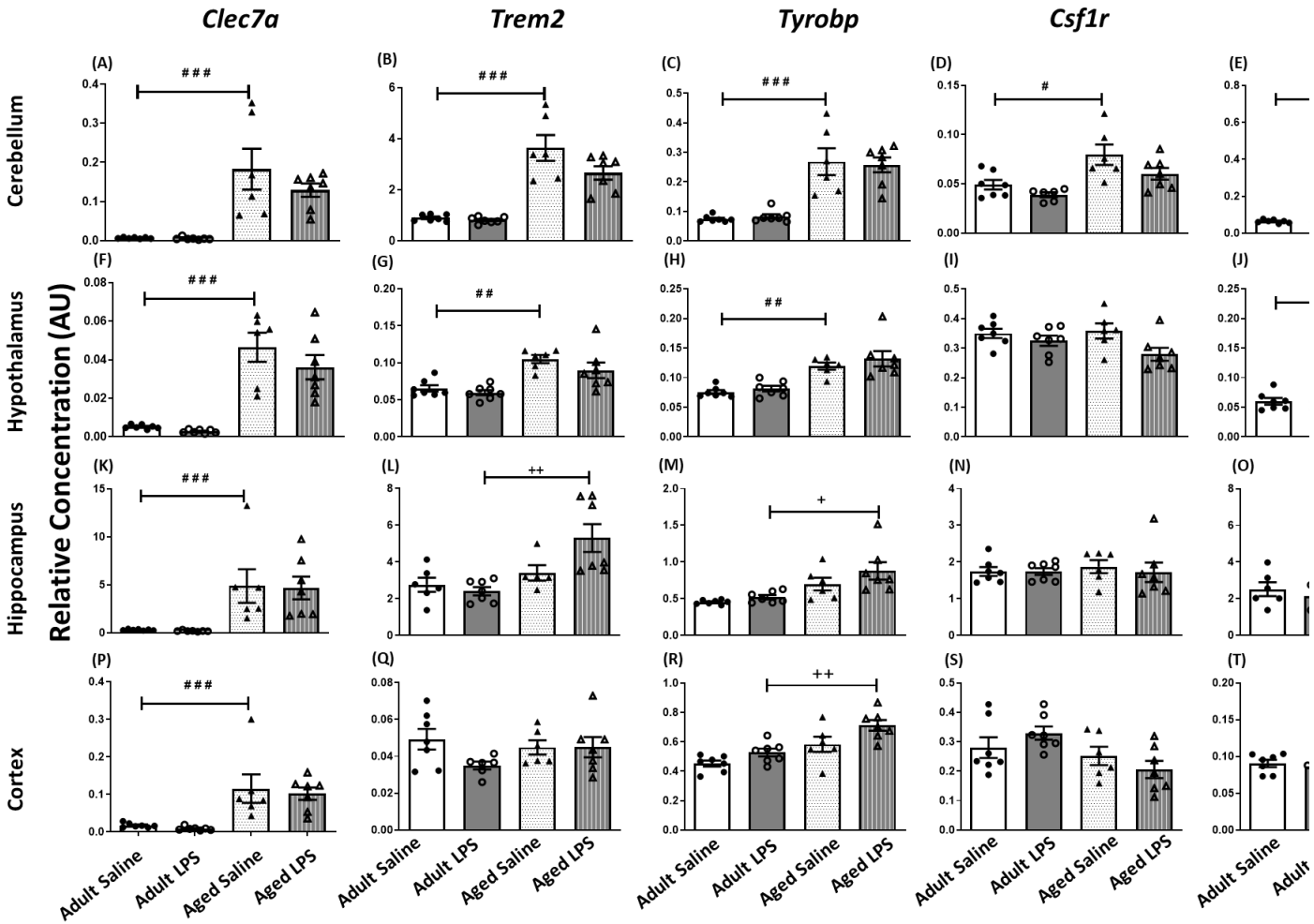

Figure 3.4: Microglial associated markers expression across the aged brain: Effect of age microglial transcript expression in cerebellum, hypothalamus, hippocampus and prefrontal cortex under acute systemic challenge with LPS (100 µg/kg) i.p. treatment, assessed by qPCR and transcripts normalised to the housekeeping gene 18s. All data represented by mean ± SEM (n=6,7) and analysed by two-way ANOVA followed by a Bonferroni post-hoc test, # denotes a statistically significant effect of age on transcript expression; # ($p<0.05$), ## ($p<0.01$), ### ($p<0.001$). + denotes a statistically significant effect of age on response to LPS treatment; + ($p<0.05$), ++ ($p<0.01$), +++ ($p<0.001$).

		Microglial associated genes														
		Clec7a			Trem2			Tyrobp			Csf1r			CD68		
		Age	Treatment	Interaction	Age	Treatment	Interaction	Age	Treatment	Interaction	Age	Treatment	Interaction	Age	Treatment	Interaction
Cerebellum	Significance	***	Non Sig.	Non Sig.	***	Non Sig.	Non Sig.	***	Non Sig.	Non Sig.	***	*	Non Sig.	***	Non Sig.	Non Sig.
	P-Value	0.0001	0.2797	0.3	0.0001	0.0558	0.1062	0.0001	0.9609	0.6979	0.0001	0.0318	0.4875	0.0001	0.4235	0.3338
	F-Value	36.8	1.226	1.124	74.99	4.057	2.827	57.22	0.0025	0.1545	16.04	5.254	0.4986	58.05	0.664	0.9744
Hypothalamus	Significance	***	Non Sig.	Non Sig.	***	Non Sig.	Non Sig.	***	Non Sig.	Non Sig.	Non Sig.	*	Non Sig.	***	Non Sig.	Non Sig.
	P-Value	0.0001	0.185	0.4011	0.0001	0.1272	0.4817	0.0001	0.2559	0.6802	0.3625	0.0175	0.1954	0.0001	0.9363	0.7879
	F-Value	63.66	1.867	0.7318	27.75	2.505	0.5115	36.54	1.358	0.1743	0.8633	6.557	1.778	53.88	0.0065	0.0741
Hippocampus	Significance	***	Non Sig.	Non Sig.	**	Non Sig.	*	***	Non Sig.	Non Sig.	Non Sig.	Non Sig.	Non Sig.	**	Non Sig.	*
	P-Value	0.0001	0.8726	0.9664	0.0205	0.1272	0.04	0.0001	0.11	0.4502	0.7597	0.6647	0.6749	0.0022	0.1272	0.0402
	F-Value	20.96	0.02631	0.0018	11.81	2.263	4.795	16.62	2.763	0.5901	0.0958	0.1927	0.1804	12.2	1.995	4.786
Cortex	Significance	***	Non Sig.	Non Sig.	Non Sig.	Non Sig.	Non Sig.	***	**	Non Sig.	*	Non Sig.	Non Sig.	*	Non Sig.	Non Sig.
	P-Value	0.0001	0.5596	0.8976	0.5651	0.1466	0.1419	0.0001	0.0067	0.557	0.0188	0.6647	0.557	0.0125	0.659	0.338
	F-Value	25.54	0.3506	0.0169	0.3412	2.264	2.321	28.09	8.861	0.3545	6.394	0.0026	0.1233	7.392	0.2002	0.9595

Table 3.2 - Summary table of statistical differences between saline and LPS-treated 8 and 25-month-old animals expression of microglial associated genes from Figure 3.4 across the cerebellum, hypothalamus, hippocampus and cortex, assessed by qPCR and transcripts normalised to the housekeeping gene 18s. Data analysed by two-way ANOVA with Bonferroni post hoc test , * denotes a significant difference in transcript expression, *p<0.05, **p<0.01, ***p<0.001 (n=6,7).

Looking further into the regional differences in innate immune response, key transcripts of the complement system were analysed; *C1qα*, *C3* and *Cd11b* **(Table 3.3)**. Once again, the cerebellum and hypothalamus demonstrated elevated expression in the aged saline-treated animals for *C1qα* **(Figure 3.5 A, D)** and C3 **(Figure 3.5 B, E)** alike which was not present in the hippocampus or frontal cortex. However, the hippocampus demonstrated that ageing left it susceptible to a secondary insult and, when challenged with LPS, a heightened expression of *C1qα* and *C3* compared to adult LPS treated controls was observed **(Figure 3.5 G, H)**. No such age dependent effect on *C1qα* and *C3* transcript expression was observed in the frontal cortex **(Figure 3.5 J, K)**.

CD11b expression deviated from the other two components pattern of expression slightly. The cerebellum displayed a significant heightened basal expression with age but not within the hypothalamus as had been observed for *C1qα* and *C3* in the hypothalamus **(Figure 3.5 C, F, I)**. Rather a modest increase in expression of *Cd11b* was observed in the hippocampus in LPS-treated aged animals. Thus, the hippocampus showed little change with age per se, but older age facilitated selective *C1qα*, *C3* and *Cd11b* responses to acute LPS challenge.

The frontal cortex was once again the least susceptible to age related innate immune system changes with no significant alteration to the complement system genes *C1qα, C3* and *Cd11b* **(Figure 3.5 J, K, L)** with age or LPS.

		Complement System associated genes								
		C1qα			C3			CD11b		
		Age	Treatment	Interaction	Age	Treatment	Interaction	Age	Treatment	Interaction
Cerebellum	Significance	***	Non Sig.	Non Sig.	***	Non Sig.	Non Sig.	***	Non Sig.	Non Sig.
	P-Value	0.0001	0.5524	0.1696	0.0001	0.6068	0.1572	0.0001	0.6068	0.1572
	F-Value	52.39	0.3637	2.011	42.14	0.2723	2.138	24.66	1.477	2.216
Hypothalamus	Significance	***	Non Sig.	Non Sig.	Non Sig.	*	*	**	Non Sig.	Non Sig.
	P-Value	0.0001	0.341	0.4504	0.216	0.02	0.0174	0.0015	0.3154	0.4734
	F-Value	18.39	0.9456	0.5897	1.628	6.339	6.66	12.98	1.053	0.5312
Hippocampus	Significance	***	**	**	Non Sig.	Non Sig.	Non Sig.	*	*	Non Sig.
	P-Value	0.0001	0.0031	0.0061	>0.9999	0.2724	>0.9999	0.01	0.0356	0.097
	F-Value	12.15	11.16	9.314	0.0006	1.262	0.0002	8.005	5.004	3.019
Cortex	Significance	*	**	Non Sig.	Non Sig.	*	Non Sig.	*	Non Sig.	Non Sig.
	P-Value	0.0472	0.0085	0.1932	0.7596	0.0492	0.911	0.013	0.0972	0.7254
	F-Value	3.893	8.292	1.797	0.0961	4.312	0.0128	7.365	3.014	0.1268

Table 3.3 - Summary table of statistical differences between saline and LPS-treated 8 and 25 month old animals expression of complement system associated genes from Figure 3.5, sacross the cerebellum, hypothalamus, hippocampus and cortex, assessed by qPCR and transcripts normalised to the housekeeping gene 18s. Data analysed by two-way ANOVA with Bonferroni post hoc test , * denotes a significant difference in transcript expression, *p<0.05, **p<0.01, ***p<0.001 (n=6,7).

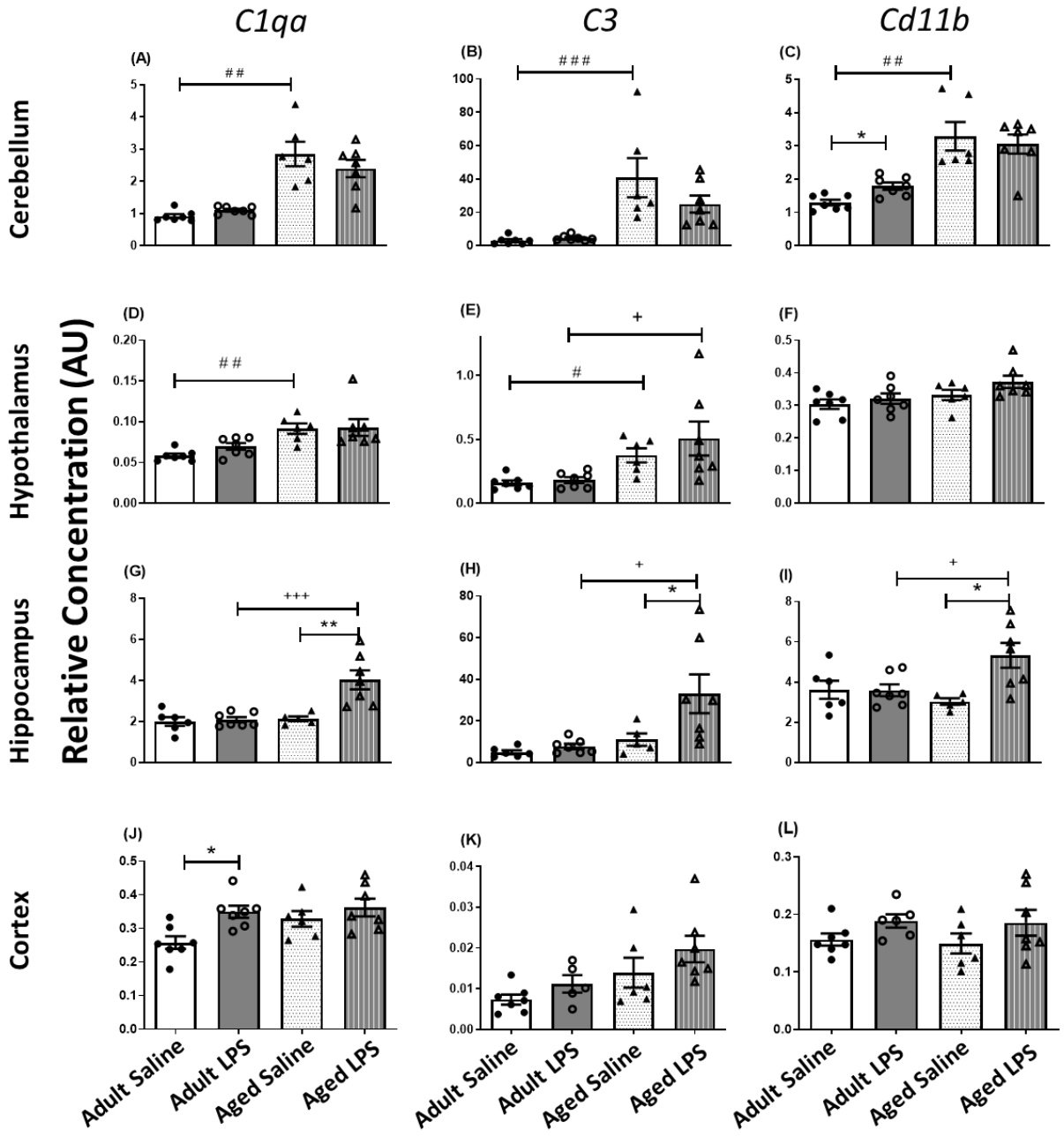

Figure 3.5: Complement system expression across the aged brain: Effect of age on complement system transcript expression in cerebellum, hypothalamus, hippocampus and prefrontal cortex 4 hours post LPS (100 µg/kg) i.p. challenge, assessed by qPCR and transcripts normalised to the housekeeping gene 18s. All data represented by mean ± SEM (n=6,7) and analysed by two-way ANOVA followed by a Bonferroni post-hoc test; * denotes a statistically significant effect of LPS treatment, * (p<0.05), ** (p<0.01), * (p<0.001). # denotes a statistically significant interaction between age and treatment; # (p<0.05), ## (p<0.01), ### (p<0.001). + denotes a statistically significant effect of age on response to LPS treatment; + (p<0.05), ++ (p<0.01), +++ (p<0.001).**

3.2.3 Common microglial priming signature across the aged brain

Despite these different regional dependent aged responses, the one consistent change observed across the ageing brain was its ubiquitous expression of the microglial priming signature across all regions (**Figure 3.6).** As discussed in the previous section, this is evident from the age induced expression of *Clec7a* which is observed in all aged animals completely, regardless of the treatment received, across all the regions **(Figure 3.6 A, D, G, J)**. *Clec7a* as discussed previously, is one of the key core genes of the primed microglial transcriptional signature (Holtman et al. 2015).

As discussed previously in this text, microglial priming was originally definition in the ME7 model by the exaggerated production of IL-1β and iNOS in response to a secondary inflammatory stimulus of LPS (Cunningham et al. 2005). As demonstrated in the previous section and consistent with this characterisation I showed this expected robust primed microglial response in the aged animal's exaggerated expression of pro-inflammatory mediator *Il-1β* when compared to adult LPS-treated controls across all brain regions. **(Figure 3.6 B, E, H, K).** Furthermore, it was found that *Clec7a* expression was tightly correlated with *Il-1β* expression across all brain regions in LPS-treated animals **(Figure 3.6 C, F, I, L).** Of these, a marginally weaker association was found in the hippocampus compared to the other three regions.

As discussed in the previous section, all pro-inflammatory cytokine and chemokine transcripts showed severely excessive responses following a secondary challenge of LPS in aged animals **(Figure 3.2 and 3.3)**, with the exception of the hippocampal transcript expression of *Tnfa* which was not statistically significantly different from LPS-treated adult animals. However, it was observed that the type I IFN induced genes *Irf7* and *Oas1a* both exhibited no age dependent exaggerated response to LPS across all regions, albeit with a good degree of variability in the individual's degree of response **(Figure 3.5).** This was conspicuously at odds with the pattern of expression observed in these proinflammatory cytokines and chemokines and at odds with the predicted pattern of expression for the priming phenotype. Thus, to further assess regional variation of inflammatory mediator transcript expression, aged animals' LPS-induced expression was assessed as fold change compared to the adult LPS-treated animal's group mean. No statistically significant difference in LPS induced fold change expression, compared to adult saline animals, of pro-inflammatory cytokines or chemokine with age was found for any of the regions assessed. However, when type one interferon associated transcript expression was assessed in this manner the cerebellum and hypothalamus both exhibited statistically greater fold change in expression which was absent in the cortex and hippocampus **(Figure 3.7 E & F).** This demonstrates that the more immune-reactive regions, the cerebellum and hypothalamus, show evidence of the microglial primed phenotype pattern of gene expression for type-one interferon associated genes while the less immune-reactive hippocampus and cortex do not.

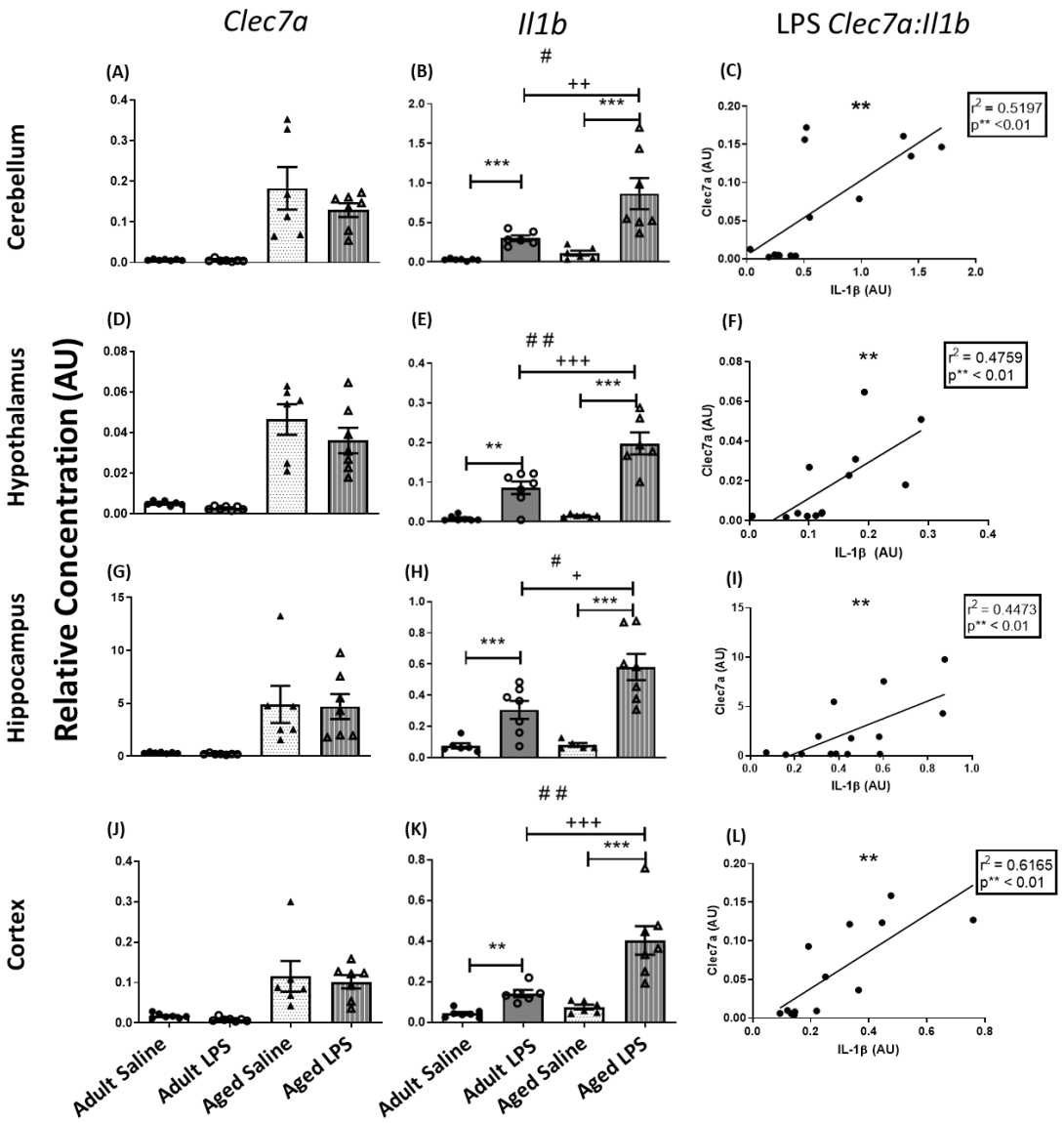

Figure 3.6: Clec7a expression in regions of the ageing brain predicts Il1b expression: Effect of age on IL-1β and Clec7a transcript expression in (A) (B) cerebellum, (D) (E) hypothalamus, (G) (H) hippocampus and (J) (K) prefrontal cortex 4 hours post LPS (100 µg/kg) i.p. challenge, assessed by qPCR and transcripts normalised to the housekeeping gene 18s. All data represented by mean ± SEM (n=6,7) and analysed by two-way ANOVA followed by a Bonferroni post-hoc test; * denotes a statistically significant effect of LPS treatment, * (p<0.05), ** (p<0.01), * (p<0.001). # denotes a statistically significant interaction between age and treatment; # (p<0.05), ## (p<0.01), ### (p<0.001). + denotes a statistically significant effect of age on response to LPS treatment; + (p<0.05), ++ (p<0.01), +++ (p<0.001). Correlation analysis performed by Pearson's linear regression analysis of IL-1β against Clec7a transcript expression in (C) cerebellum, (F) hypothalamus, (I) hippocampus and (L) prefrontal cortex 4 hours post LPS (100 µg/kg) i.p. challenge**

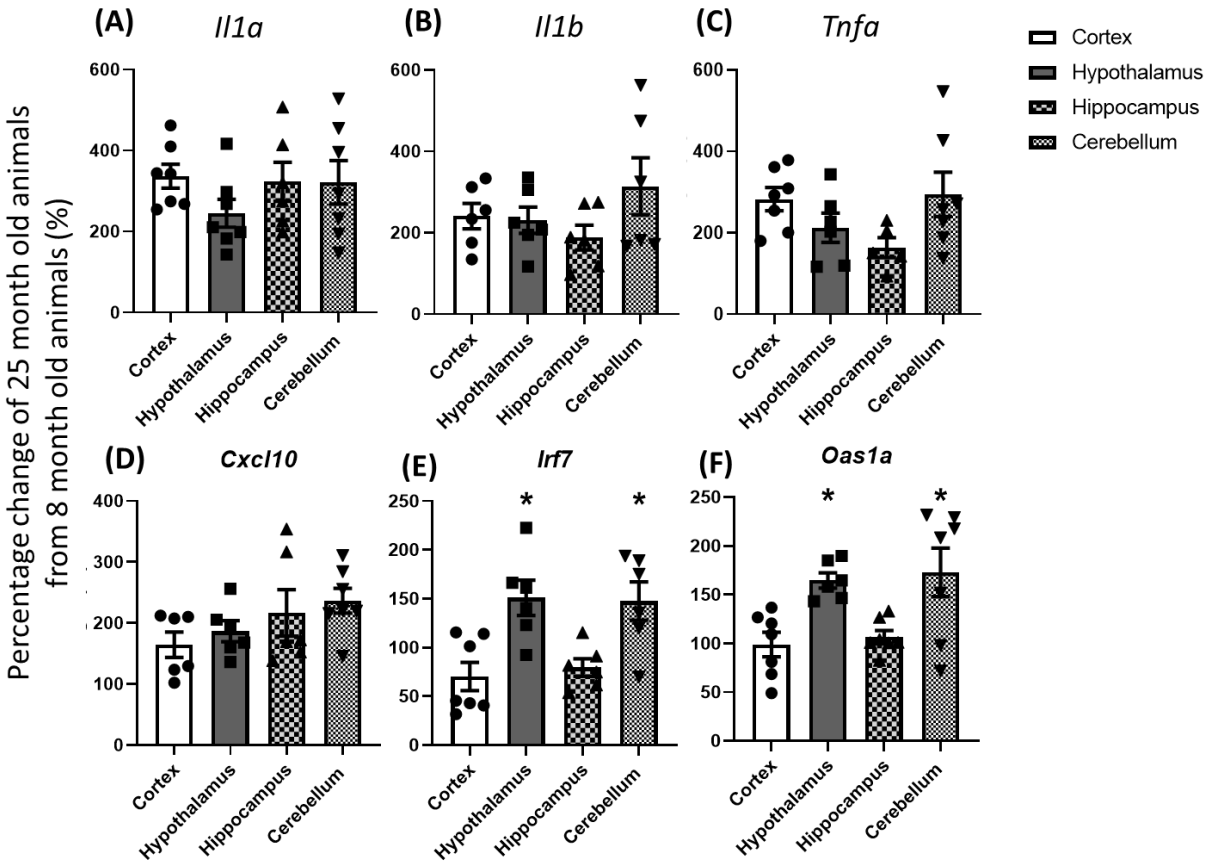

Figure 3.7: Fold change comparison of LPS-induced inflammatory mediator transcript expression, assessed by qPCR and transcripts normalised to the housekeeping gene 18s, in different regions. A-F) Expression of LPS-induced proinflammatory (A-C) and interferon-dependent (D-F) genes were expressed as % increase from the mean expression in young LPS-treated animals. All data are represented by mean ± SEM (n=6,7) and analysed by one way ANOVA; * denotes a statistically significant difference in fold change expression compared to other regoins, * ($p<0.05$)

3.2.4 Cognitive vulnerability arises with increasing age

At any given time in the mammalian body there are endogenous levels of cytokines and chemokines expressed at low levels by our immune cells. However, as stated already under chronic activation, such as that imposed in ND conditions the microglia may adopt a primed phenotype, characterised by an exaggerated inflammatory response to an acute secondary challenge. Having shown evidence that microglial priming and evidence for exaggerated acute cytokine responses to acute systemic LPS, it was hypothesised that advancing age would lead to a corresponding progressive vulnerability to acute cognitive impairment following an acute challenge. To this end, mice aged 5-7 months, 16-19 months and 24 months were trained on a hippocampal-dependent working memory task, the shallow water T-maze (Murray et al. 2012). Each animal was trained for 10 trials on several consecutive days until reaching criterion performance for inclusion, i.e., scoring 80%< correct on 3 consecutive blocks of 3 trials in the days leading up to challenge. Once this cognitive baseline was established, each animal was challenged with saline followed by a 72-hour washout period before then being challenged with a bolus of LPS (100µg/kg) and after a final 48-hour washout period challenged one final time with the viral mimetic Poly I:C (12mg/kg) as represented graphically in **Figure 3.8 A**. After each challenge their cognitive integrity was assessed by their performance in the shallow water T-maze and scored at several time points over a 24-hour period following the challenge **Figure 3.8 B-D**.

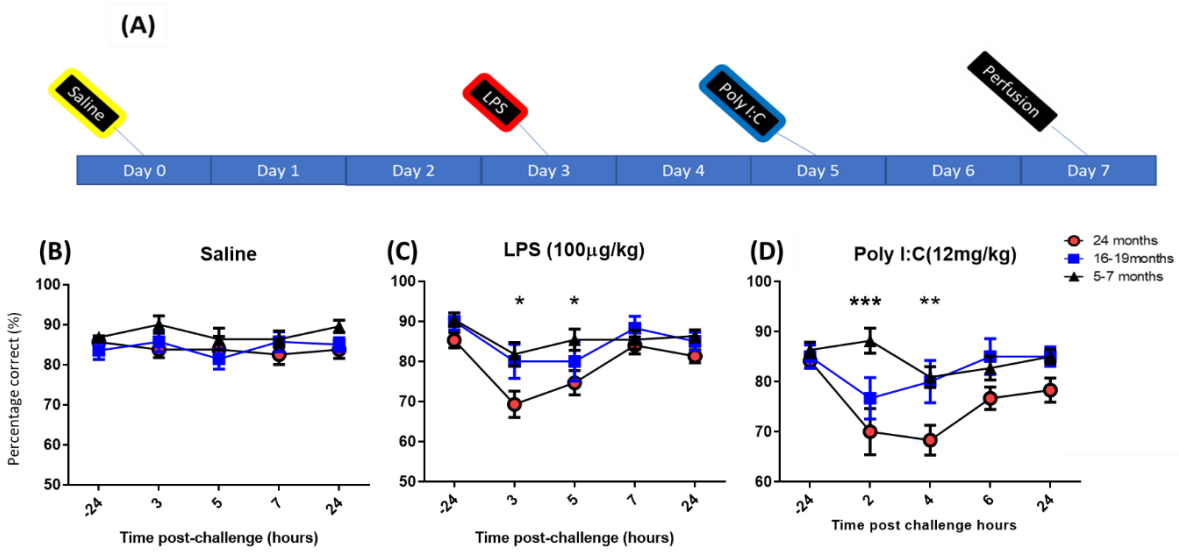

Figure 3.8: **Age-dependent cognitive vulnerability to acute systemic inflammation-induced impairment (A) Timeline of challenges and perfusion. Impact of Saline (B), LPS (100µg/kg i.p.) (C) or Poly I:C (12mg/kg i.p.) (D) on working memory assessed by T-Maze (cognitive experiment performed by Dr. Carol Murray). All data are represented graphically by mean ± SEM (24 months n=12, 16-19 months n=12, 5-7 months n=22), analysed by repeated measures two-way ANOVA with multiple comparisons by Bonferroni post-hoc test, * denotes treatment is significantly different between 24-month and 5-7-month cohorts *(P<0.05), ***(p<0.001)**

Initial challenge with saline caused no significant impairment in performance in the maze **(Figure 3.8 B)**. However, it was shown that when treated with the bacterial mimetic LPS, this elicited significantly impaired cognition in the 24-month-old cohorts compared to their younger 16-19 and 5–7-month counterparts at 3 and 5 hours (*p<0.05) post challenge **(Figure 3.8 C)**. A more robust effect was seen with the viral mimetic poly I:C at 2 (***p<0.001) and 4 hours (*p<0.05) post challenge for the same age groups **(Figure 3.8 D)**. However, by 4 hours post challenge the 16–19-month group had recovered to an equal performance level as the youngest group, while the 24-month aged group was still significantly lower. As animals age they showed progressively more robust acute cognitive dysfunction in response to the acute challenge. This is clearest in the animals' response to poly I:C, where a significant difference in the severity of the acute cognitive impairment between the 16-19 month and 24-month-old group is evident. These data indicate advancing age imposes increasing cognitive vulnerability to systemic challenge.

These data facilitated the generation of a cognitive frailty score for these animals, comprising their response to all three challenges. Their cognitive performance data was thus used to stratify the cohort into 1) cognitively healthy "Resilient" (n=9) and 2) cognitively vulnerable "Frail" (n=10) animals for molecular and immunohistological and chemical analysis here **(Table 3.4)**. Cognitively frail refers to animals who scored below ≤60% correct alternation, in 3 or more of the 6 blocks of 5 trials that immediately followed their acute inflammatory challenges (i.e. 3,5 and 7 hours post-LPS and post-poly I:C). Resilient animals are defined by their scoring above that 60% correct alternation threshold a minimum of 4 blocks following the same challenges. 5–9-month-old animals were classified as "Young" (n=9) while 23–24-month-old animals were classified as "Aged" (n=10). These classifications of old/young and frail/resilient were then used to assess markers of microglial activation as a function of cognitive status.

	Young	Aged	Total
Resilient	7	3	10
Frail	2	7	9
Total	9	10	

Table 3.4: Cognitive Frailty Cohort breakdown: C57BL/6 mice 5-9 months classified as "Young" (n=9), 23-24 months old classified as "Aged" (n=10). <60% correct alternation in T-maze = Cognitively Frail (n=9), 60%< correct alternation – Resilient (n=10).

3.2.5 Microgliosis progressively increases with age.

As discussed previously, microglia undergo significant morphological changes as a feature of their activation. To examine these microglial changes in the context of ageing and frail brains, microglia from several regions along the Anterior-Posterior (AP) axis were labelled with the microglial marker IBA-1. The microglial morphology and number of cells in each region were qualitatively and quantitatively analysed to assess whether microgliosis is associated more strongly with age or with cognitive frailty.

As would be predicted in the ageing brain there is an age-dependent increase in microgliosis **(Figure 3.9)**. A significant increase in cell number was visible in the aged animals in each hippocampal and cerebellar structure in comparison to the younger animals. In the healthy young brain, the microglia are evenly dispersed with a ramified morphology, small cell soma and fine processes **(Figure 3.9).** Within the young brain the hippocampal grey matter **(Figure 3.9 A)** appears to have a lower number of resting microglia than the white matter. In contrast microgliosis is clearly evident, throughout the aged brain from the slight condensation in processes and altered branch morphology. Microglia in the aged white matter regions, the fimbriae and late corpus callosum (CC), appear to display particularly short, thick processes with large cell bodies, indicative of activation.

Age is the major determinant of frailty. Therefore, though one would expect that frailty may offer a more nuanced stratification within any one age group, in this study, of ages 5-9 months up to 24 months, age is a very strong determinant of microgliosis. Any association between microglial status and cognitive frailty was difficult to assess at the qualitative level since age was such a strong determinant of microglial activation. Moreover, the number of aged resilient (n=3) and young frail (n=2) animals was relatively small. Consequently, in order to ascertain whether quantitative analysis would corroborate these qualitative observations, and potentially elucidate any association between cognitive frailty and microgliosis, statistical analysis for the number of Pu.1 and IBA-1 positive cells and the percentage of $IBA1^{+}$ area they cover was calculated across the ageing brain **(Figure 3.9)**. A significant association between age and microglial cell number was

demonstrated for all regions when quantified by the number of cells stained positively for the microglial cell surface marker IBA-1 and the microglial nuclear marker Pu.1 **(Figure 3.10-12)**.

Cognitively frail animals displayed elevated cell counts and % area compared to "Resilient" animals within the hippocampus **(Figure 3.10-11)**. This held true for the Cornu Ammonis 1 (CA1), Cornu Ammonis 3 (CA3), dentate gyrus (DG), fimbriae and the early and late corpus callosum (CC) when number was assessed by the microglial cell surface marker IBA-1 for count and % area **(Figure 3.10-11 E & J) and** was corroborated by the microglial specific nuclear marker Pu.1 **(Figure 3.10-11 O)**. This difference between cognitively resilient and frail animals was strongest in the fimbriae (***p<0.001) **(Figure 3.10 A – C)** however, age was an equally powerful predictor in this regard. A large contributor to this region achieving such a strong significance was a result of microgliosis being consistently greater within the white matter regions along the anterior posterior (AP) axis, notably within the fimbria, corpus callosum and within the cerebellar middle cerebellar peduncle **(Figure 3.10-12)**. The early corpus callosum (CC) demonstrated a significant increase in microgliosis with age (*p<0.05) as well as with cognitive frailty and continued to be the case through to the late CC**.**

Assessment of the cerebellum revealed a similar pattern of microglial activation with age showing a robust increase in cell number in regions such as the dentate nucleus (DN) and the ventral cochlear nucleus (VCN) **(Figure 3.12).** Within the cerebellum he VCN showed robust increases of microglial activation with age (**p<0.01) and to a lesser degree with cognitive frailty (*p<0.05) **(Figure 3.12)**. The VCN is largely made up of grey matter and is responsible for encoding the intensity and timing of auditory input (Michael-Titus et al. 2010). In contrast the white matter heavy region, the DN, showed the clearest increases in microglial activation and proliferation with age and cognitive frailty. Indeed, it showed a stronger increase in the IBA-1+ % area **(Figure 3.12 D & E)** and number of Pu.1 positive cells **(Figure 3.12 K & L)** with cognitive frailty (***p<0.001) than was observed with age (**p<0.01). This correlates well with the known role of the DN which contains afferent white matter projection fibres connecting the cerebellum to the pons and as such is involved in the coordination and planning of motor tasks (Morales et al. 2015).

Increasing age is clearly associated with increased microgliosis across the ageing brain, particularly in white matter regions, and while overall cognitive frailty might not better predict the degree of this microgliosis, it may be that within a given age range, cognitive frailty may better predict differential microgliosis. To assess whether this was true, aged frail animals were compared to aged resilient **(Figure 3.13).**

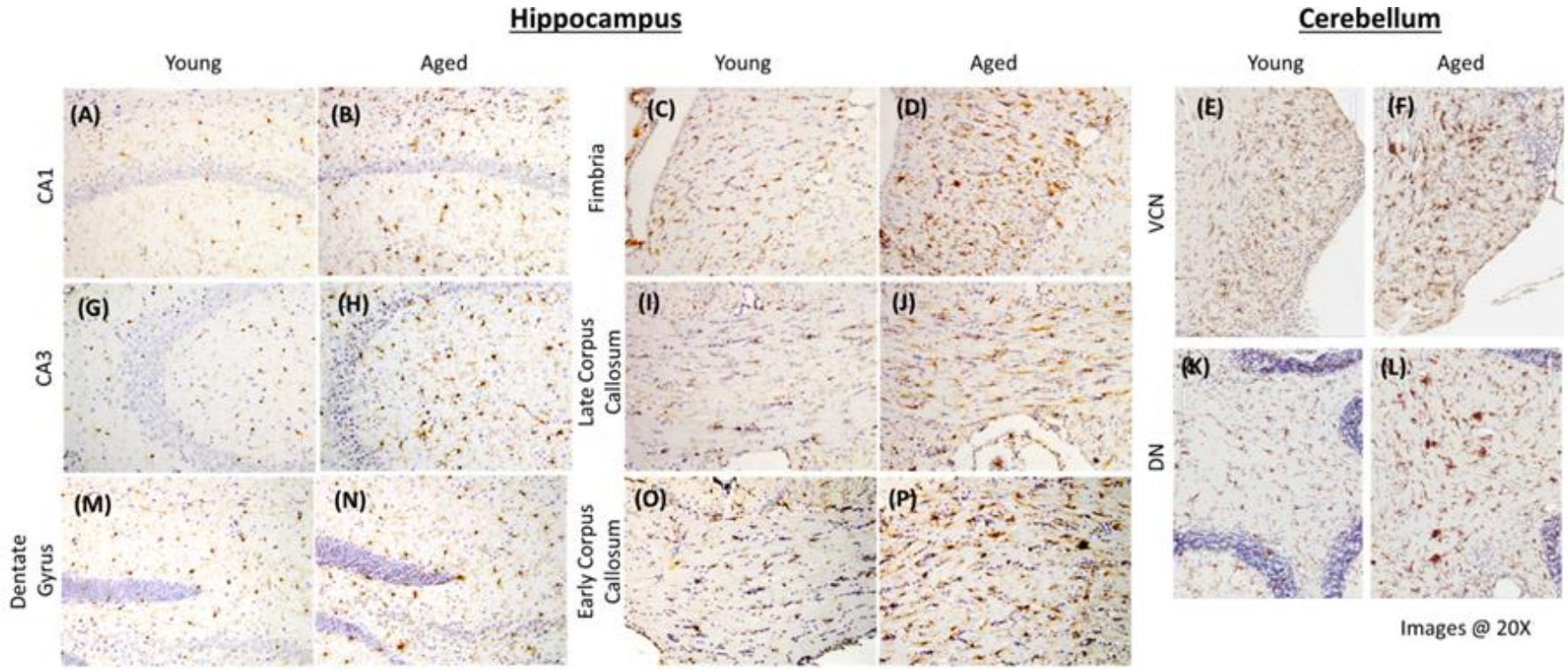

Figure 3.9 **Microglial activation across the young and aged brain: Histochemical analysis of microglial activation and morphology in young and aged mice. Microglia labelled with IBA-1 in the hippocampal and cerebellar regions Cornu Ammonis 1 (CA1) (A-B), fimbriae (C-D), Cornu Ammonis 3 (CA3) (G-H), dentate gyrus (M-N), early corpus callosum (O-P), late corpus callosum (I-J), ventral cochlear nucleus (E-F) and dentate nucleus (DN) (K-L). Analyses grouped by age; young (5,7 months; n=9), old (23-26 months; n=10). Images taken at 20x using Cell^A software.**

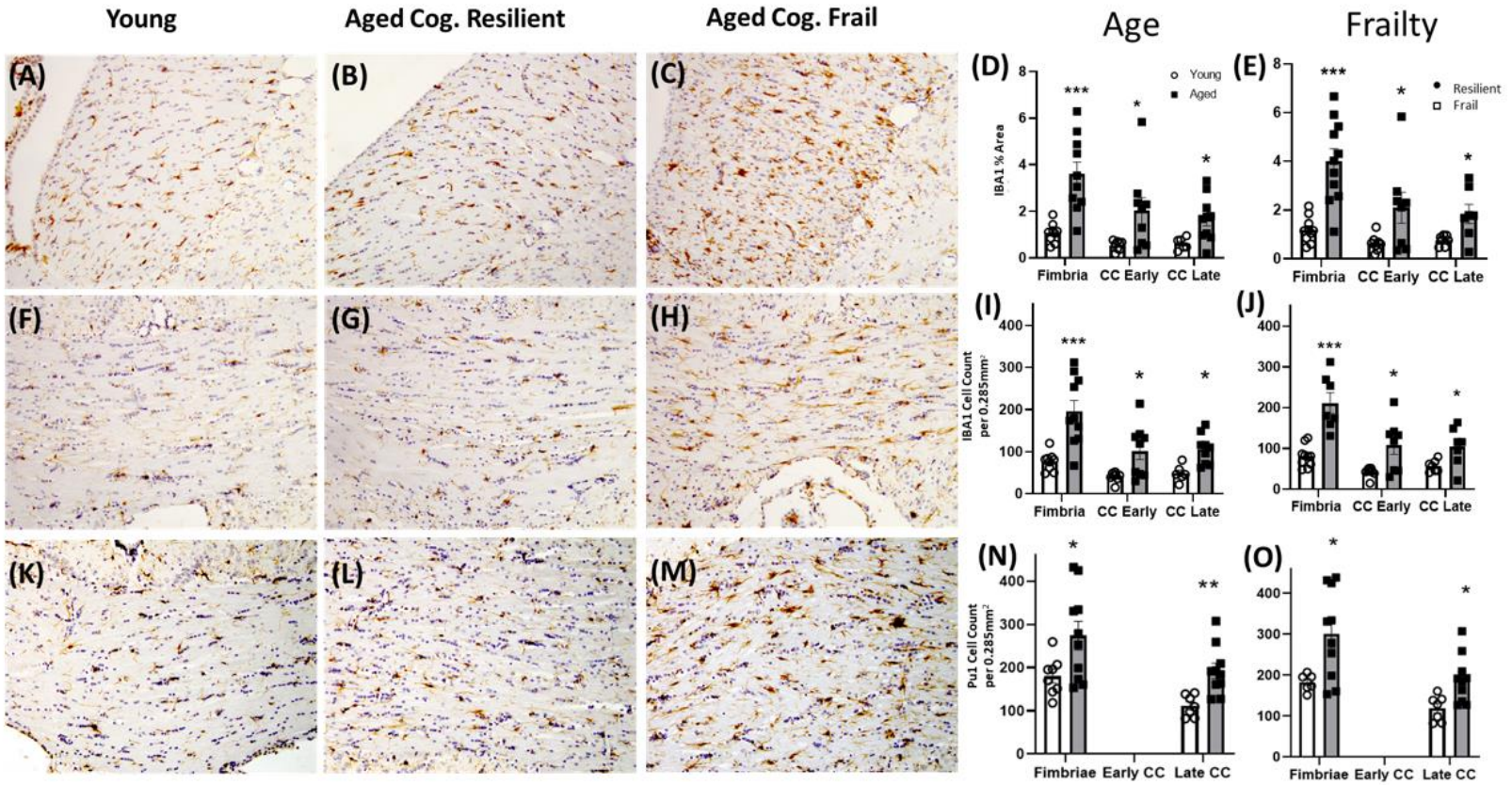

Figure 3.10: **Histochemical and quantitative analysis of microglial activation across the young and aged hippocampus and with cognitive frailty: Histochemical analysis of microglial activation and morphology. Microglia stained with IBA-1 in the fimbria (A)-(C), early corpus callosum (CC) (F-H) and late corpus callosum (K-M). Microglia stained with IBA-1 and Pu.1 were quantified using Image J (NIH) at 20x. Panels (E), (J) and (O) categorise data by cognitive frailty, (D), (I) and (N) by age. All data represented by mean ± SEM and analysed by student's t- test or Mann-Whitney u-test for non-parametric data to detect effect age (n=9,10) or cognitive frailty (n=9, 10) on microglial morphology, activation and polutlation, statistical significance is denoted by ***p<0.001 and *p<0.05.**

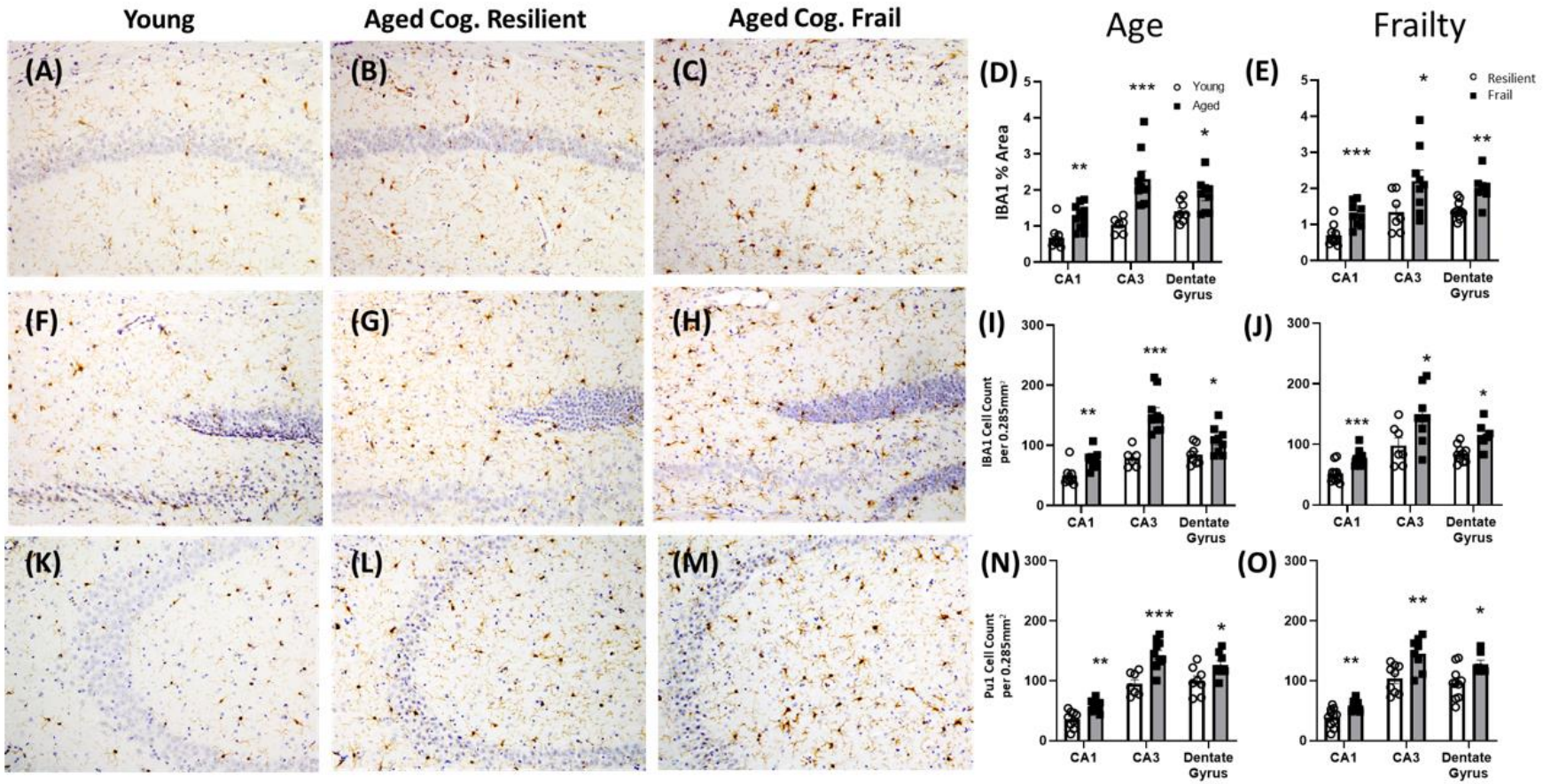

Figure 3.11: **Histochemical and quantitative analysis of microglial activation across the young and aged hippocampus and with cognitive frailty: Histochemical analysis of microglial activation and morphology. Microglia stained with IBA-1 in the Cornu Ammonis 1 (CA1) (A-C), dentate gyrus (DG) (F-H) and Cornu Ammonis 3 (CA3) (K-M). Microglia stained with IBA-1 and Pu.1 were quantified using Image J (NIH) at 20x. Panels (E), (J) and (O) categorise data by cognitive frailty, (D), (I) and (N) by age. All data represented by mean ± SEM and analysed by student's t- test or Mann-Whitney u-test for non-parametric data to detect effect age (n=9,10) or cognitive frailty (n=9, 10) on microglial morphology, activation and polutlation, statistical significance is denoted by *p<0.05, **p<0.01 and ***p<0.001.**

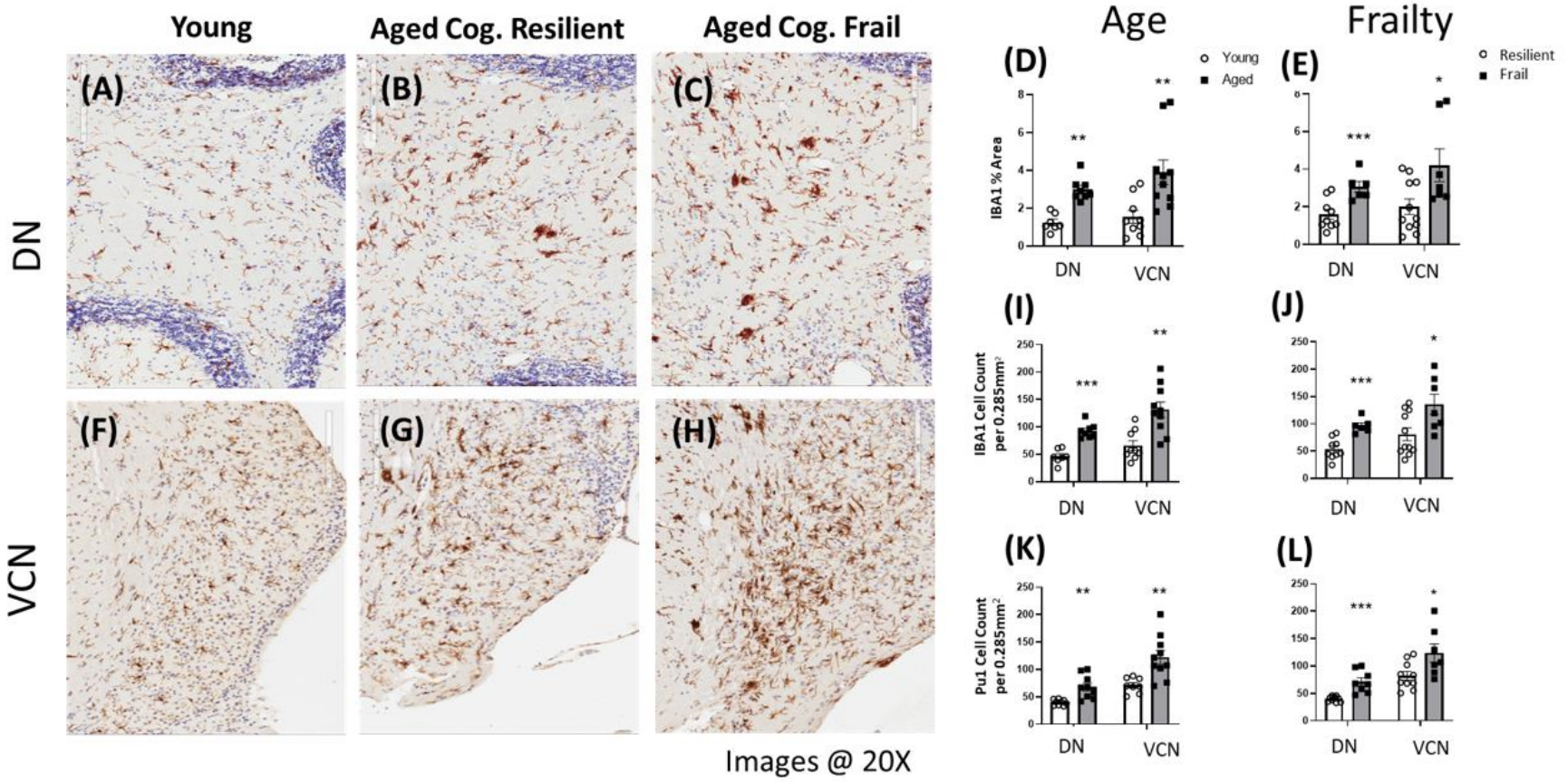

Figure 3.12: **Histochemical and quantitative analysis of microglial activation across the young and aged cerebellum with cognitive frailty: Histochemical analysis of microglial activation and morphology. Microglia stained with IBA-1 in the dentate nucleus (DN) (A)-(D) and ventral cochlear nucleus of the cerebellum fimbriae (E)-(H). Microglia stained with IBA-1 ((I) - (L)) and Pu.1 ((M) - (N)) quantified using Image J (NIH) at 20x. Panels (J), (L) and (N) categorise data by cognitive frailty, (I), (K) and (M) by age. All data represented by mean ± SEM and analysed by student's t-test or Mann-Whitney u-test for non-parametric data to detect effect age (n=9,10) or cognitive frailty (n=9,10) on microglial morphology, activation and population, statistical significance is denoted by *p<0.05, **p<0.01 and ***p<0.001.**

Aged cognitively frail animals showed a significantly more advanced state of microgliosis than old resilient animals. It is clear, that old resilient animals have clear microglia activation, as assessed by the increase in cell number with shorter thicker processes. However, with the development of cognitive frailty in an already old animal, a further increase in cell number and change in microglial morphology is evident as illustrated by more frequent large cell soma and condensed processes. However, this significantly greater microgliosis was observed only in the white matter regions such as the fimbriae and at multiple levels on the anterior posterior (AP) axis of the corpus callosum and within the DN of the cerebellum **(Figure 3.13)** and not within grey matter regions such as the CA1, CA3, dentate gyrus or VCN. Indeed, microglial activation in the old cognitively frail animal is especially striking in the fimbriae of the hippocampus and the DN of the cerebellum **(Figure 3.13 G, H, M, N)** where the microglial morphology indicates they may have adopted a fully activated state as suggested by the marked contraction of their processes.

This phenomenon of increased microglial activation between aged cognitively frail and cognitively resilient animals is represented quantitatively in **(Figure 3.13 A – F)**. There is a significant increase in IBA-1 positively stained cell number between the two groups in the regions of white matter analysed: fimbriae (*$p<0.05$), early CC (**$p<0.01$), late CC (*$p<0.05$) and cerebellum (*$p<0.05$). Additionally, a trend toward an increase in cell number and area was observed in the CA1, CA3, DG and VCN. This increase in cell number was corroborated by staining for the microglial specific nuclear marker Pu.1 in the fimbriae (*$p<0.05$), late CC (*$p<0.05$) and DN (*$p<0.05$) **(Figure 3.13 E & F)**. This trend is mirrored in % area of the IBA-1 positive microglia, with each hippocampal white matter region showing a small significant increase in % area for the aged cognitively frail animals compared to aged cognitively resilient animals (*$p<0.05$) **(Figure 3.13 A)**. In contrast, analysis of the cerebellum revealed a resilient increase in the number of IBA-1 and Pu.1 positive microglial cells (*$p<0.05$) in the white matter region of the DN but not the grey matter heavy ventral cochlear nucleus in aged cognitively frail versus aged cognitively resilient animals, IBA1 positive % area showed no change within the cerebellum **(Figure 3.13 B, D, F)**.

In contrast to the observed relationship between cognitive frailty and microgliosis in older animals, there are no clear qualitative differences in microglial activation states between young cognitively resilient and cognitively frail animals in the hippocampus or cerebellum. While there was clear activation of microglia in young frail animals, these are rare in the study population and there were insufficient young frail animals (n=2) to prove this statistically.

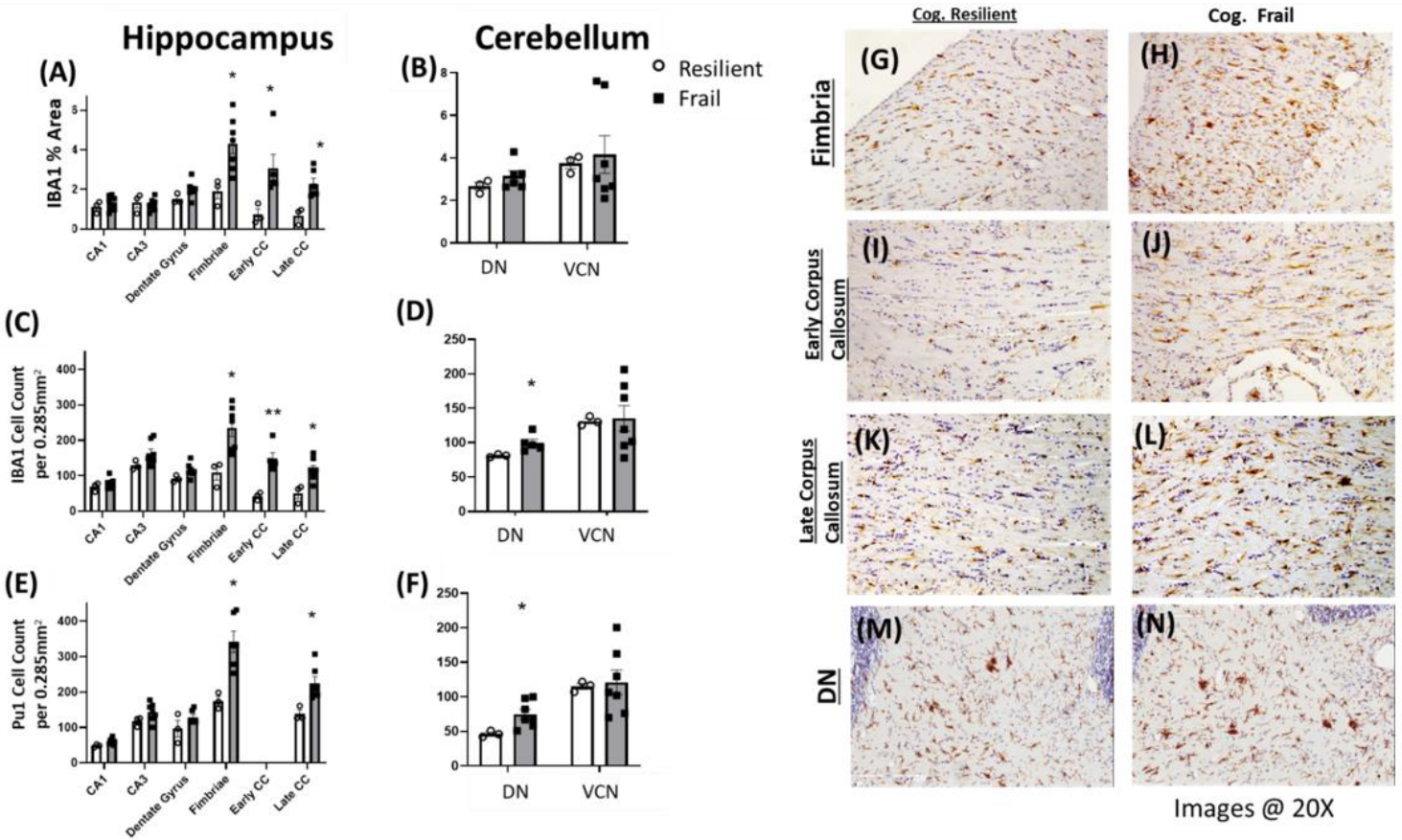

Figure 3.13: **Histochemical and quantitative analysis of microglial activation between aged frail and resilient brains: Histochemical analysis of microglial activation and morphology. Microglia stained with IBA-1 in the fimbriae (G-H), early corpus callosum (I-J), late corpus callosum (K-L) and the dentate nucleus (DN) of the cerebellum (M)-(N) Microglia stained with IBA-1 (A - D) and Pu.1 (E - F) quantified using Image J (NIH) at 20x. All data represented by mean ± SEM and analysed by student's t- test or Mann-Whitney u-test for non-parametric data to detect effect cognitive frailty status in aged animals (n=3, 7) on microglial population, activation and morphology, statistical significance is denoted *p<0.05 and **p<0.01.**

It can be concluded from these findings that age is a very significant factor in predicting microgliosis. Cognitive frailty shows a relatively similar influence on microgliosis overall, but it is evident that within the aged cohort, those with cognitive frailty show further escalation of microgliosis. These data suggest that across the lifespan, age strongly predicts microgliosis, but that among an already aged cohort, cognitive frailty is associated with more severe activation, particularly within white matter regions.

3.2.7 Impact of age and cognitive frailty on white matter integrity

To further investigate the relationship of age and cognitive frailty-associated microgliosis in white matter, brain sections were histologically stained with Luxol Fast Blue for myelin quantification in the hippocampus **(Figure 3.14 I)** and cerebellum **(Figure 3.15 I)**. Myelin density was assessed by the degree of light transmittance through the stained section as described in section 2.2.9.5.5.

In the hippocampal formation it was found that the white matter integrity of the corpus callosum and fimbria both showed a significant reduction in aged animals compared to young adult control animals **(Figure 3.14 J, S)**. Similarly, cognitively frail animals also demonstrated reduced white matter integrity compared to cognitively resilient animals **(Figure 3.14 K, T)**. Stratification of the aged population by cognitive frailty revealed that cognitively resilient aged animals showed modest reduction in myelin density but were not significantly different from young animals whereas cognitively frail aged animals showed significantly reduced white matter compared to young animals (**p<0.01) **(Figure 3.14 L, U)**. Despite this, cognitively frail and cognitively resilient older animals did not show a significant difference on this parameter.

However, these frail/resilient groups are categorical rather continuous but linear regression analysis did demonstrate a negative correlation between increasing cognitive dysfunction, assessed as the number of errors under acute systemic challenge, and white matter integrity for both the corpus callosum (*p<0.05, r^2 = 0.2749) and fimbria (**p<0.01, r^2 = 0.4453) **(Figure 3.14 H, W).** To determine to what degree this compromised white matter integrity is associated with microgliosis, Luxol Fast Blue staining was plotted against IBA-1^+ percentage area in each region. The corpus callosum showed a significant correlation between heightened microglial reactivity and reduced white matter integrity (*p<0.05, r^2 = 0.3712) which was not present in the fimbria (p = 0.7725, r^2 = 0.0053) **(Figure 3.14 G, V).**

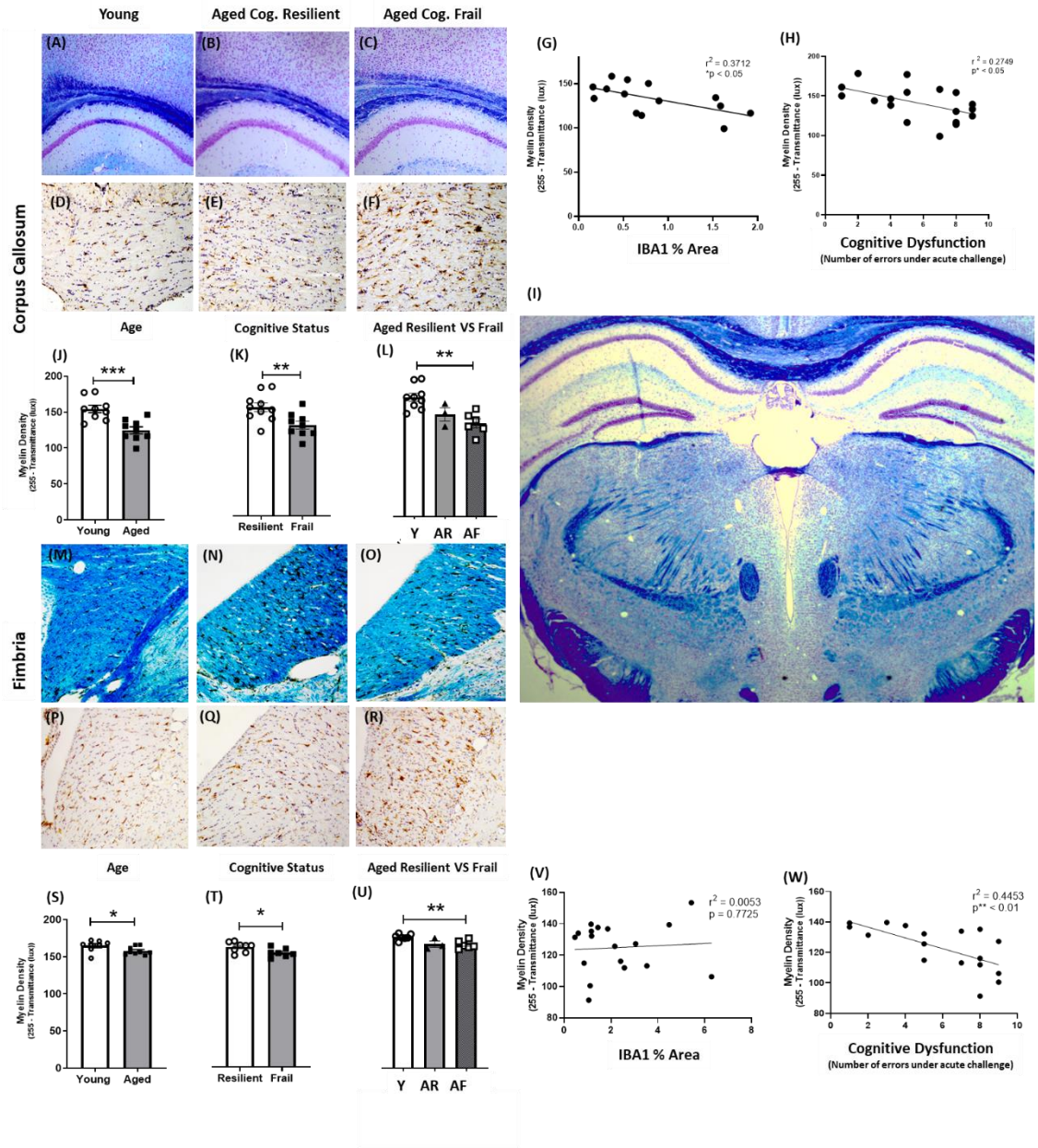

Figure 3.14: **Correlating microglial immunoreactivity in white matter tracts of the hippocampus – high power photomicrographs of Luxol fast blue staining in the hippocampus (L) at 2.5x, corpus callosum (CC) and fimbria with myelin density. Histochemical and quantitative analysis of myelin density by LFB staining of LFB staining of the CC (A-C, J-L) and fimbria (M-O, S-U) (n=9,10). All data represented by mean ± SEM and analysed by student's t-test test or Mann-Whitney u-test or Kruskal wallis for non-parametric data to detect effect cognitive frailty status in aged animals. IBA-1$^+$ immunostained CC (D-F) and fimbria (P-R). Correlations assessed by Pearson's linear regression analysis (n = 18) of myelin density vs. % of IBA-1$^+$ area in the CC and fimbria (G, V); myelin density vs. cognitive dysfucntion (H, W). All images quantified using Image J (NIH) at 20x, statistical significance indicated by *p<0.05, **p<0.01, ***p<0.001.**

In the cerebellum, age showed a significant and consistent reduction in the white matter integrity in the DN of aged animals, regardless of frailty status (*p<0.05) **(Figure 3.15 I –K). T**he white matter integrity (myelin density) in the cerebellar DN region showed no significant correlation with cognitive dysfunction in the hippocampal-dependent working memory task **(Figure 3.14 H)** but was correlated with microglial reactivity, (*p<0.05, r^2 = 0.2204) **(Figure 3.14 G).**

The spinal trigeminal tract (STT) is one of the most substantial white matter tracts within the cerebellum at this AP position, located beneath and adjacent to the DN and VCP respectively. The STT showed no statistically significant changes in microgliosis when stratified by age or frailty. But Luxol fast blue staining revealed a significant reduction in myelin density with age (***p<0.001) **(Figure 3.14 S)** and a strong correlation with increasing microgliosis (**p<0.01, r^2 = 0.4816) **(Figure 3.14 V).** When stratified by cognitive frailty it was shown that aged cognitively frail animals exhibited very modestly reduced myelin density compared to cognitively resilient animals (*p<0.05) **Figure 3.14 T-U).** Although increasing cognitive dysfunction was correlated with reduced myelin density (*p<0.05, r^2 = 0.2228) this correlation was weak and the slope was minimal (**Figure 3.14 W)** indicating that cognitive dysfunction is a very poor predictor of myelin density in the SST.

It can be concluded from these findings that, across the lifespan age is a better predictor of myelin density compared to categorised cognitive resilience/frailty, but that within aged animal groups cognitive frailty still has additional predictive value with respect to myelin density.

Furthermore, reduced myelin density is strongly correlated with increased microgliosis in cerebellar white matter and in the corpus callosum. As was found to be the case with microgliosis, though age per se is a strong predictor, within the aged population cognitive frailty does bring additional predictive power: cognitively frailty predicted more extensive reduction in myelin density and, within hippocampal white matter tracts, this reduced myelin density correlated strongly with cognitive dysfunction under acute systemic challenge in the hippocampal-dependent working memory T maze task.

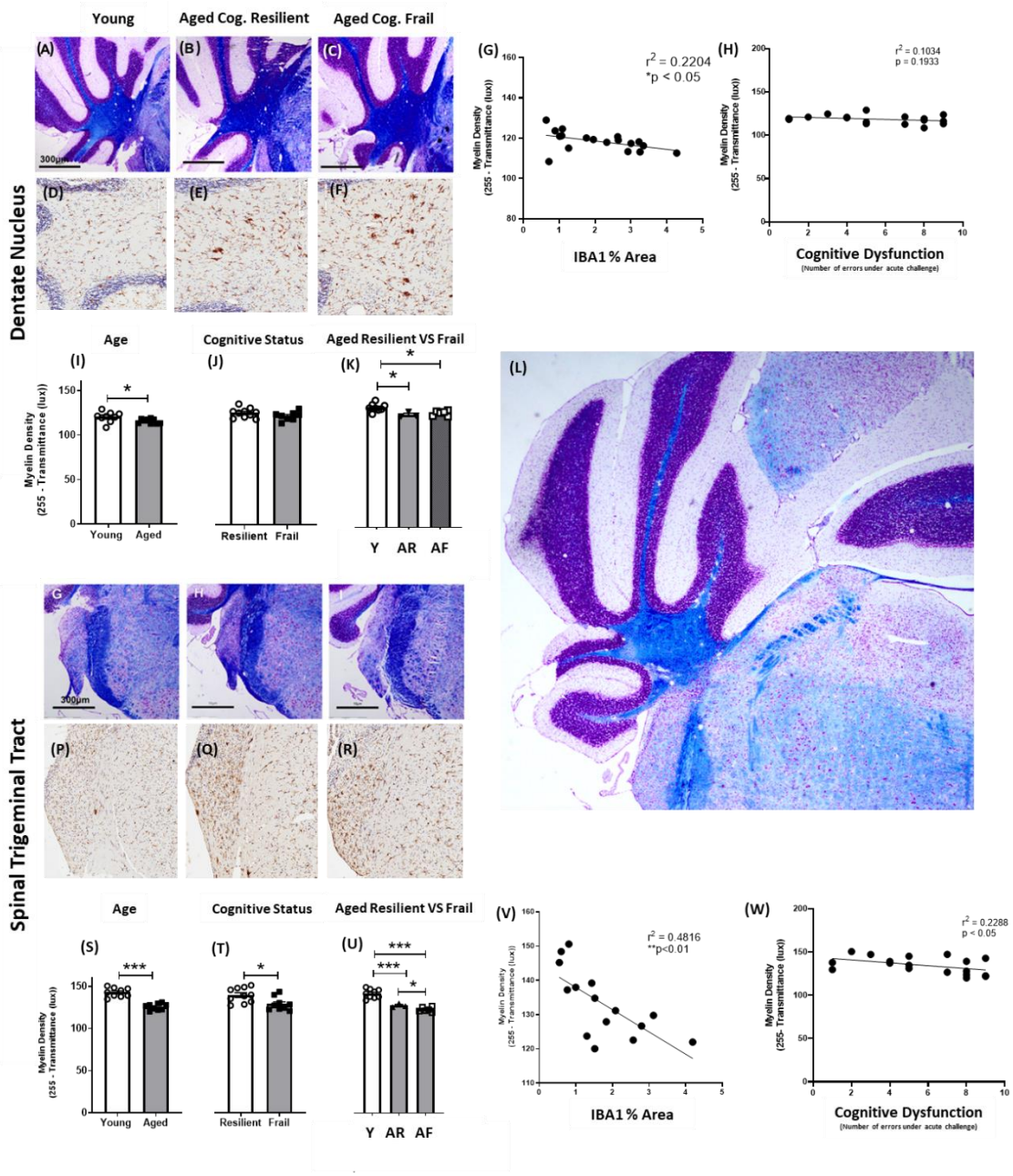

Figure 3.15: **Correlating microglial immunoreactivity in white matter tracts of the cerebellum – high power photomicrographs of Luxol fast blue staining in the cerebellum (L) at 2.5x, dentate nucleus (DN) and spinal trigeminal tract (STT) with myelin density. Histochemical and quantitative analysis of myelin density by LFB staining of LFB staining of the DN (A-C, J-L) and STT (M-O, S-U) (n=9,10). All data represented by mean ± SEM and analysed by student's t- test or Mann-Whitney u-test or Kruskal wallis for non-parametric data to detect effect cognitive frailty status in aged animals. IBA-1+ immunostained DN (D-F) and STT (P-R). Correlations assessed by Pearson's linear regression analysis (n = 18) of myelin density vs. % of IBA-1+ area in the DN and STT (G, V); myelin density vs. cognitive dysfucntion (H, W). All images quantified using Image J (NIH) at 20x, statistical significance indicated by *p<0.05, **p<0.01, ***p<0.001.**

3.2.8 Cognitive frailty better predicts presynaptic terminal density with age

Cognitive frailty, classified as frail or resilient based on errors in the hippocampal-dependent working memory T-maze task during acute systemic inflammation, was associated with disrupted myelin density in white matter regions of the hippocampal formation. Therefore, it was important to examine whether there were additional differences in neuronal/synaptic integrity in this region of aged and frail brains. To this end the intensity of immunohistochemical labelling for the pre-synaptic terminal marker synaptophysin was quantified in the hippocampus. Section to section differences in intensity of labelling was corrected for using subtraction from the high transmittance white matter (corpus callosum) and density change, selective to the hippocampus was calculated by presenting the hippocampus as a ratio to the overlying cortex (described in greater detail in section 2.2.9.5.4).

Synaptic density was quite variable and stratification of animals by age failed to demonstrate any statistically significant reduction in synaptophysin density with age in this cohort **(Figure 3.16 A)**. This was true for all of the neuronal layers analysed in the hippocampus. However, the aged group was characterised by greater variability in synaptic density compared to young animals, consistent with the idea that chronological age may not be a strong determinant in this regard. Stratifying, instead, by cognitive frailty revealed significantly reduced (*$p<0.05$) **(Figure 3.16 B)** synaptic densities in the stratum oriens, radiatum and molecular layers of the hippocampus in cognitively frail animals compared to cognitively resilient. Moreover, when assessing the aged cohort only, but stratifying these into cognitively frail and cognitively resilient **(Figure 3.16 C)**, the latter showed higher synaptic density than aged cognitively frail animals in the stratum oriens, radiatum and molecular layer (*$p<0.05$).

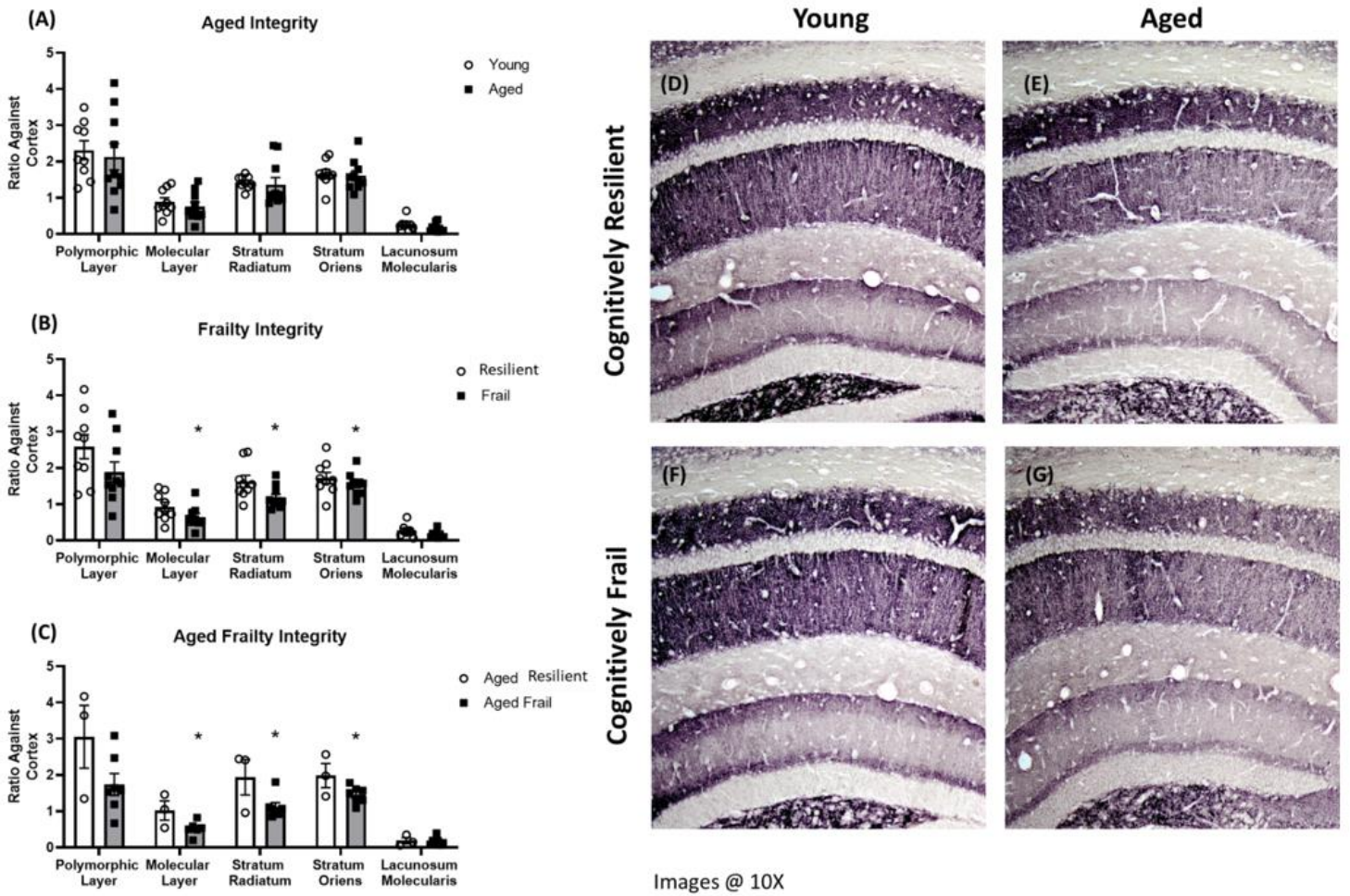

Figure 3.16: **Quantitative and histochemical analysis of presynaptic neuronal integrity in the young and aged brain and with cognitive frailty: Presynaptic neuronal terminals density in the hippocampal layers stained with SY38 (D-G) and quantified using Image J (NIH) (A-C) at 10x. All data represented by mean ± SEM and analysed by student's t-test or Mann-Whitney u-test for non-parametric data to detect effects of age (n=9,10), cognitive frailty (n=9,10) or aged cognitive frailty status (n=3-7) on pre-synaptic terminal density, statistical significance is denoted by *p<0.05.**

3.2.9 Hippocampal cholinergic density of the CA3 declines significantly with age and increasing cognitively frailty

To further investigate the relationship of age and cognitive frailty on neuronal integrity and function, immunolabelling for choline acetyltransferase, the biosynthetic enzyme responsible for the final step in the synthesis of the neurotransmitter, acetylcholine, was conducted in the hippocampus of the young and aged brains and analysed in light of their age and cognitive frailty.

Theoretically a depletion of ChAT positive neurons would be expected in aged and supposedly also in cognitively frail brains. Consistent with this, a weak significant correlation (*$p<0.05$, $r^2 = 0.2856$) was demonstrated between cholinergic density and cognitive dysfunction, measured as the number of errors made under acute challenge, in the CA3 region **(Figure 3.17 H)**. This reduction in cholinergic density in the CA3 region of the hippocampus had a similar weak but non-significant trend ($p=0.0991$, $r^2 = 0.1822$) toward decreased ChAT density in the dentate gyrus (DG) **(Figure 3.17 J)**. Stratification by age and cognitive frailty once again revealed significantly reduced (*$p<0.05$) cholinergic density in the CA3 region of the hippocampus **(Figure 3.17 L, M)** and separation of aged animals by cognitive resilience and frailty showed that aged cognitively resilient animals showed equivalent cholinergic density to young animals, while aged cognitively frail animals were significantly lower (*$p<0.05$) **(Figure 3.17 N)**. A similar trend was observed in the the central area of the dentate gyrus of aged cognitively frail brains compared to aged cognitvely resilient but was highly variable and was found to be non-statistically significant **(Figure 3.17 Q)**.

Furthermore, the degree of gliosis in the CA3 region, assessed by percentage of area positive for IBA1, was found to have a weak significant negative correlation with cholinergic density (*$p<0.05$, $r^2 =0.2586$) **(Figure 3.17 I)** but was not the case in the dentate gyrus (DG) **(Figure 3.17 K).** This suggests that as cholinergic density becomes impaired with cognitive frailty there is a commensurate increase in microgliosis.

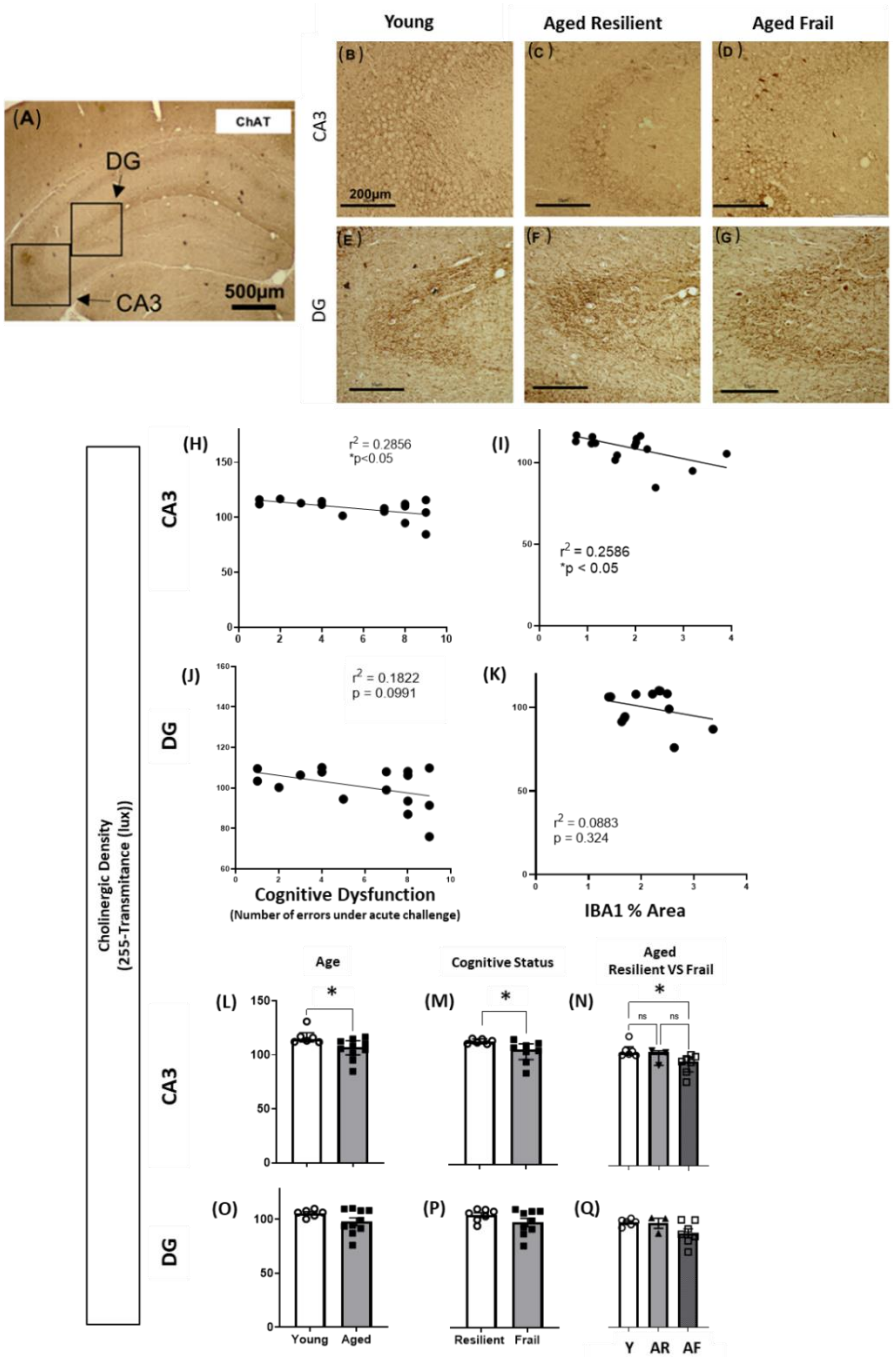

Figure 3.17: ChAT-positive terminal immunolabelling in the hippocampus. (A) Gross view of a hippocampus stained for ChAT at approximately bregma -2.255 mm (AP) in a young cognitively resilient animal, scale bar: 500µm;. (B-D) High power representative micrographs of the boxed areas used for quantification of ChAT immunostaining in the CA3 field and (E-G) region immediately lateral to the Lateral Outer Shell of the Dentate Gyrus (DG); scale bar: B-G, 200µm. Correlation analysis performed by Pearson linear regression analyses of cognitive dysfunctino with cholinergic density in the (H) CA3 and (J) DG, n = 16. Correlation analysis performed by Pearson linear regression analyses of IBA1$^+$ % area with cholinergic density in the (I) CA3 and (K) DG, n = 16,. Categorisation of cholinergic density in the CA3 by (L) age, (M) by cognitive status and (N) by age and cognitive status, comparing young (Y) with aged resilient (AR) and aged frail (AF) cohorts. Categorisation of cholinergic density in the DG by (O) age, (P) by cognitive status and (Q) by age and cognitive status, comparing young (Y) with aged resilient (AR) and aged frail (AF) cohorts. Data analysed by Mann-whitney u-test or Kruskal Wallis and represented by median ± I.Q

3.3 Discussion

In summary the results shown here demonstrate that the ageing brain is primed to show exaggerated sickness behaviour and brain cytokine responses to acute systemic inflammation. There are regional differences in the innate immune transcriptional signatures with the cerebellum and hypothalamus displaying the most immune reactive state, the frontal cortex being the least reactive of the four and the hippocampus intermediate between these states **(Table 3.3)**. However, across all four regions there is clear evidence of microglial priming, as evidence by elevated expression of *Clec7a*, associated with the strong upregulation of *Il1b* in response to systemic LPS. These exaggerated CNS responses in aged animals occur despite equivalent systemic cytokine responses to LPS in young and aged mice. Furthermore, within an ageing population there is significant vulnerability to cognitive dysfunction in response to an acute systemic challenge. Within these aged animals, I have assigned scores to reflect their cognitive frailty or resilience to cognitive dysfunction under acute stressors and demonstrated that within an aged population cognitive frailty corresponded with a greater degree of microgliosis, particularly in white matter regions. This in turn corresponded with significantly reduced myelin density, cholinergic and pre-synaptic terminal density compared to age-matched cognitively resilient animals.

3.3.1 Regional variation in innate immune response in the ageing brain

As discussed previously, a microarray study by Grabert et al. demonstrated that the brain's primary immune cell population, the microglia, exhibit distinct regional profiles within the brain. They demonstrated that the microglia of the cerebellum and hippocampus exhibit a transcriptional profile which favours immune function and energy metabolism, setting them distinctly apart from the cortex and striatum. However, with advancing age they showed that the hippocampus was sensitive to the loss of this distinct transcriptional signature (Grabert et al. 2016). Here I have also shown that the cerebellum exhibits a more immune vigilant profile at baseline with advancing age as evidenced by distinct age-dependent increases in basal expression of markers of microglial activation, *Trem2, Tyrobp, Csf1r* and *CD68*, as well as pro-inflammatory cytokines*, IL1b, IL1a* and *Tnfa* and type 1 IFN-induced genes *Cxcl10*, *Irf7* and *Oas1a* **(Table 3.1).** Here it is also demonstrated that the hypothalamus exhibits a similar state of heightened immune reactivity as that seen in the cerebellum.

In contrast to this the hippocampus and cortex have shown a more intermediate profile of immune reactivity. In saline-treated animals there is no significant difference between adult and aged animals for the majority of microglial markers, pro-inflammatory cytokines or chemokines and type-1 IFN-induced genes. However, upon stimulation with LPS these genes did all show a significantly exaggerated expression compared to adult controls. This suggests that though the aged

hippocampus shows lower basal microglial activation compared to the cerebellum, it remains in a primed state, capable of exaggerated response to secondary stimulation. Therefore, these regions' immune reactivity is still sufficient to result in an exaggerated production of proinflammatory mediators and a higher induction of microglial markers of activation such as *Trem2, Tyrobp* and *CD68* for the hippocampus and *Tyrobp* and *CD68* in the cortex.

Despite this clear region dependent heterogeneity in immune responsiveness across the ageing brain a ubiquitous microglial priming signature was demonstrated here. While microglial priming in the ageing brain has been previously established (Godbout 2005), I demonstrate for the first time the presence of the microglial priming signature *Clec7a* across multiple distinct brain regions in addition to the expected associated exaggerated pro-inflammatory response to an acute stimulus as shown here by *Il1b, Il1a* and *Tnfa*. All regions assessed showed equivalent exaggerated expression of inflammatory mediator expression in aged animals in response to LPS compared to adult LPS-treated controls. In particular it was striking that *Il1b* expression was positively correlated with *Clec7a* expression in all 4 regions.

Clec7a is the gene for Dectin-1, a pattern recognition receptor (PRR) that has high specificity for β-1,3 glucans and carbohydrates found on yeast cell walls (Brown 2006). Its stimulation initiates signalling events which are capable of producing inflammatory cytokines such as IL-1β, IL-6 and IL-23 from human dendritic cells (DCs). This PRR is involved in antifungal immunity (Elder et al. 2017). There is also evidence that β-glucan (via Dectin-1/Clec7a) expression on macrophages can exhibit a prolonged enhanced functional state after adequate priming known as "trained innate immunity" (Van der Meer et al. 2015; Heng et al. 2021) or "immune tolerising" depending upon the timing and frequency of stimulation (Lajqi et al. 2019). Upregulation of *Clec7a* could therefore play a protective role, with respect to responsiveness to infection, in the ageing brain but such 'trained' response may also produce deleterious effects (Neher et al. 2019). These beneficial/detrimental effects are likely dependent on the nature, timing and dose of both primary (priming) stimulus and the secondary stimulus (Neher et al. 2019). While increased *Clec7a* expression might be indicative of a neuroprotective response to resolve a fungal infection, this obviously an exogenous substance that would not be present in the current experiments. However there is some emerging evidence for endogenous Dectin-1 ligands such as vimentin (Thiagarajan et al. 2013), Galectin-9 (Daley et al. 2017) or annexins (Bode et al. 2019) and all of these can arise in the CNS.

Regardless, the exaggerated cytokine production in response to an acute stimulus associated with the priming state, of which Clec7a is core hub defining gene, is unlikely to be beneficial. The characteristic higher baseline expression of inflammatory mediators and lower activation threshold

of primed microglia cells (Lull et al. 2010) means that a systemic insult, which may not affect a healthy young individual in any significant fashion, may not only have an exaggerated pro-inflammatory response with poor resolution, but might also be capable of eliciting severe behavioural deficits, such as exacerbated sickness behaviour and cognitive impairment, and exacerbated pathology in an aged or diseased individual as I have demonstrated here and as previously described in the literature (Godbout et al. 2008; Godbout et al. 2005). The recent COVID-19 global pandemic has highlighted this further in the clinical setting, with a recent case study reporting that 71.1% of patients aged over 75 years admitted with confirmed COVID-19 presented with comorbid delirium and 75% with fever (Vrillon et al. 2020). In aged animal models it has been shown that this prolonged and exacerbated sickness behaviour in response to an acute challenge is associated with exaggerated production of pro-inflammatory cytokines (Godbout et al. 2005; Godbout et al. 2008). In the clinical setting it is believed that the underlying chronic morbidity, be it ageing, or neurodegeneration primes the microglia and upon exposure to a new trauma the resulting exaggerated, flooding release of pro-inflammatory cytokines and other microglial neurotoxic substances elicited under acute inflammatory conditions such as nitric oxide, oxygen radicals and proteolytic enzymes, will cause further damage to the vulnerable brain (Dilger et al. 2008; Mangano et al. 2009; Block et al. 2007; Blaylock et al. 2011). While cytokines are not directly neurotoxic themselves they, along with other acute microglial neurotoxic products, as nitric oxide, oxygen radicals and proteolytic enzymes, have been shown to significantly exacerbate neuronal damage and the loss of neurons in the vulnerable brains in multiple rodent models of neurodegenerative disorders such as MS, TBI, AD, and white matter injury (Paul Stroemer et al. 1998; Perry et al. 2010; Beck et al. 1988; Zindler et al. 2010; Hickman et al. 2013; Barnett et al. 2018; Norden et al. 2015) contributing to cognitive decline (Holmes et al. 2009; Widmann et al. 2014; Pandharipande et al. 2013). In the ME7 model of prion disease it was demonstrated that the progression of the neurodegenerative disease and neuronal death was accelerated by the acute challenge of the secondary stimulus, LPS (Cunningham et al. 2005). These findings suggest that while the innate immune response might vary from region to region in the ageing brain, each region may be equally at risk of harm from the exaggerated production of pro-inflammatory cytokines by the ubiquitously primed microglia.

3.3.2 Exaggerated sickness behaviour

In addition to the presence of the primed microglial signature in the CNS I observed the distinct, exaggerated sickness behaviour in response to acute LPS treatment. Intraperitoneal or intravenous injection of high doses of endotoxin lipopolysaccharide (LPS) into animals have been shown to induce the systemic production of inflammatory cytokines, including TNF-α and IL-1β, dysregulation of core body temperature and in high enough doses, lethality (Fink, 2014; Poli-de-Figueiredo et al.,

2008; Remick et al., 2005). For this reason, LPS has been used as an experimental model of septic shock for nearly 100 years. Under normal conditions in healthy ambulatory patients the mean endotoxin level has been reported to be 5.1 ± 7.3(SD) pg/mL. In contrast, septic patients were reported to have endotoxin levels with a mean (± SD) value was 581 ± 49 pg/mL (Opal et al., 1999). One minor limitation of the direct translatability of this work arises as a result of these levels reported in human septic populations being substantially lower than the dose of LPS utilised in our own murine experiments. LPS-induced endotoxemia differs from human sepsis with respect to high plasma inflammatory cytokine concentrations, which peak earlier and at greater values and demonstrate faster resolution (Chen et al., 2014; Remick et al., 2005). Furthermore, mice have been shown to have a substantially higher LD50 for LPS (median lethal dose) compared to humans (Fink, 2014) and varying expression of protective proteins such as hemopexin (Chen et al., 2014; Fink, 2014; Poli-de-Figueiredo et al., 2008). Furthermore, it has also been shown that injection of low (sublethal) doses of LPS into animals can induce a state of "LPS tolerance" that alters subsequent responses to treatment with LPS or other inflammatory stimuli or shifts macrophage activation profiles to more M2 like states (Rahtes et al., 2020; Seeley et al., 2017). Factoring in these conditions it is not uncommon for a higher bolus of endotoxin LPS to be required for use in mice than the levels which would be traditionally found in septic patients. However, this resilience to LPS-induced mortality has been shown to be diminished in aged mice which have been reported to be approximately 6.5-fold more sensitive to the lethal toxicity of LPS in micrograms per mouse compared to young mice (Tateda et al., 1996). As such, this dose was selected through careful assessment of various LPS doses' severity of impact upon sickness behaviour and subsequent validation of expression of molecular markers of inflammation in an early pilot study conducted by Dr. Carol Murray in our lab.

Despite displaying clear exaggerated sickness behaviour and a primed inflammatory response in the CNS however it was found that analysis of the systemic inflammatory state for IL-1β by ELISA revealed no exaggerated expression in aged animals treated with LPS compared to adult controls. This exaggerated sickness behaviour has been shown previously in the ME7 model of murine prion disease when challenged with LPS (Cunningham et al. 2009) and with age (Godbout et al. 2005). This exaggerated sickness behaviour in response to existing prior pathology is believed to be a maladaptive response by the organism, divergent from the normal adaptive nature of sickness behaviour in resilient, healthy individuals (Cunningham et al. 2013) with the potential for adverse long-term consequences in vulnerable individuals, suffering from an existing condition, including falls, delirium and loss of independence. Numerous studies in recent years have reported close relationships between peripheral inflammation and cognitive dysfunction in cases of mild cognitive impairment (MCI) and AD (Bermejo et al., 2008; Van Himbergen et al., 2012). Meta analyses have

also reported the elevated expression of peripheral cytokines and markers of immune activation in patients with AD (Swardfager et al., 2010). Previous work by Holmes et al. identified an association between circulating levels of TNFα and the progression of cognitive decline in AD patients. Indeed it was found that patients with high baseline levels TNFα experienced a 4 fold greater rate of decline compared to those with low TNFα, who also showed no significant cognitive decline (Holmes et al. 2009). Furthermore, following a systemic inflammatory event AD patients suffered a significant rise in circulating TNFα levels which resulted in an increase in their rate of cognitive decline (Holmes et al. 2009). Indeed it has been shown in a large scale hospital study that there is an association beween severe infections requiring hospital treatment with long-term increased risk of dementia (Pandharipande et al., 2013; Sipilä et al. 2021). Substantial changes in not only cognitive status but also EEG readings as well as hippocampal atrophy have been reported in sepsis survivors (Semmler et al., 2013). As discussed earlier in this text delirium can be defined as a profound and rapid onset of fluctuating confusion and impaired awareness, sometimes referred to as acute confusion. Delirium frequently occurs during acute illness has been shown to correlate with baseline and predict long-term outcomes of Mini-Mental status examinations (Davis et al., 2015), within AD populations it is known to accelerate cognitive decline (Fong et al., 2009) and within the general, undemented population, it increases the risk of developing dementia eight-fold Davis et al. 2017). Recent studies that shown that a patients frailty status severity significantly predicts their risk factor for experiencing delirium following surgery, injury or infection (Eeles et al. 2012; Joosten et al. 2014; Persico et al. 2018; Sanchez et al. 2020; Choutko-Joaquim et al. 2019; Li et al. 2021; Mahanna-Gabrielli et al. 2020). Consistent with these findings I have demonstrated that while ageing conferred an increased vulnerability to acute cognitive dysfunction in the hippocampal-dependent T-maze task following systemic challenge this was not uniform and several animals displayed cognitive resilience to the acute stressor despite their advanced age. Acute systemic inflammation coupled with delirium have been shown to significantly increase the risk of long-term cognitive decline and dementia (MacLullich et al. 2009; Davis et al. 2012), to worsen the severity of existing dementia (Holmes et al. 2009; Fong et al. 2009) and also confers a greater risk of increased moribundity and mortality compared to patients of similar age admitted without delirium (MacLullich et al. 2009; Ely et al. 2004).

A significant contributor to this arises from the fact that systemic inflammation has been shown to be one of the primary causes of blood-brain barrier damage and disruption, allowing entry of peripheral immune cells into the brain (Galea et al., 2007; Hennessy et al., 2017; Man et al., 2007; S. Takeda et al., 2013). Furthermore, chronic inflammation induced by high-fat diets have been reported to result in increased blood-brain barrier permeability and a commensurate microglial activation with significant hippocampal-dependent learning deficits (Davidson et al., 2012; Freeman

& Granholm, 2012; Tucsek et al., 2014). This robust impact upon the hippocampal function is consistent with previous reports have shown that early degeneration correlates with increased BBB permeability within the hippocampus (Bell et al., 2010; Montagne et al., 2015). This ventricle rich region is known to be significantly affected by decreased pericyte numbers, and reduction of their coverage, and BBB breakdown on post-mortem tissue analysis in AD (Sengillo et al., 2013) rendering it particularly vulnerable to the effects of chronic systemic inflammation associated with ageing and frailty driving factors such as obesity and recurrent infections. With the estimated populations of aged individuals 65yrs< and AD patients set to reach 1.5 billion and 152 million respectively by the year 2050 (World Health Organization; 2011; World Health Organization; 2020) it is imperative we understand the primary mechanisms which underlie the pathology of the ageing process and its associated vulnerability to cognitive dysfunction. As such a better understanding of the underlying pathophysiology in individuals who display cognitive resilience and frailty which may allow us to better manage and prevent delirium with a more targeted approach to precision medicine treatment options.

3.3.3 Microgliosis and neuronal pathology in the ageing and frail brain

As discussed previously in this text characteristic features of microglial activation in the ageing brain include an increase in the number of activated microglia and alteration of morphology (Hart et al. 2012). Consistent with this I have demonstrated here a significant increase in cell numbers and their percentage area was associated with age for all regions of the brain examined. Under pathological conditions such as those imposed with age and chronic neurodegenerative conditions, microglia are capable of rapidly altering their morphology and adopting an activated state in order to react to the stimuli (Spittau 2017). Activated microglia will typically condense and retract their processes, altering their cell surface markers in the process. While young microglia exhibited a resting state with a more ramified morphology, thin processes and a smaller cell soma this activated phenotype was evident in the aged microglia in all regions assessed. Several studies have reported that a change in microglia morphology toward that of being dystrophic, is indicative of them becoming senescent. Indeed, it has been reported in ageing rodent models that microglia are subject to replicative senescence with advancing age and show this phenotype (Streit 2006). Senescent microglia will typically display retracted thick processes, large cell bodies, perinuclear cytoplasmic hypertrophy and fragmentation of their cell bodies (Spittau 2017). This in turn will result in decreased functionality of their neurotrophic and synaptic maintenance activities. However, the microglial morphology observed here was not consistent with that of senescence, as no fragmentation was observed, and cells maintained a modest degree of ramification in aged cognitively frail and resilient animals alike. Microgliosis was most strongly correlated to an increase in age, rather than an increase in cognitive frailty. This is unsurprising since the cohort ranges from

only 5 months old to 24 months and substantial microgliosis arises across this range. However, within the older animals, microgliosis was more robust in those who showed higher cognitive frailty, or vulnerability, to acute dysfunction upon secondary stimulation with LPS.

As stated previously in this text it is believed that frailty is capable of accelerating the gradual decline in physiological reserve caused by the process of ageing, and will result in a state of increased vulnerability compared to robust individuals of the same age (Clegg et al. 2013). This was captured in the cognitive analysis of young and aged animals treated with acute inflammatory stimuli where I not only demonstrated that increased age confers increasing vulnerability to cognitive deficit following a stressor, but within each of these age groups I identified animals with differing degrees of cognitive vulnerability. As discussed previously, due to the dramatic differences in an aged frail and young frail animal, cognitive frailty alone shows a similar degree of variability as with age contrary to our hopes to better describe biological ageing with cognitive frailty over chronological ageing. However, when these animals were grouped as cognitively frail and resilient, quantitative analysis of microglial cell number and their percentage area revealed an increase in the aged frail compared to aged resilient animals within the white matter regions of the ageing brain but not the grey matter. This was not observed in the young frail compared to young resilient and as such suggests that frailty has had an additive effect upon the existing age-induced vulnerability of the animal.

It should be noted that the repeated exposure of animals to acute systemic stressors may have had an impact upon the immune profile of central and peripheral immune cells. The six days wash out period between exposure to 100µg/kg of the endotoxin LPS and a secondary challenge with 2mg/kg of the viral mimetic ds RNA Poly I:C may not have been sufficient for all effects of the LPS exposure to have worn off. The effect of LPS systemic challenge on the animals' immune profile over the first 24 hours is well characterised in the literature and most pro-inflammatory effects are typically reported to be resolved to non-significant differences from baseline by 48 hours post challenge (Custódio et al., 2013; Nordgreen et al., 2018). Depending upon the magnitude of initial LPS challenge and the timing between secondary challenge (and whether tested *in vivo* or *in vitro*) an "immune training" or "immune tolerising" effect has been previously reported to be exhibited in immune cells a week after initial acute stressor; with significant implications for pathology and behavioural outcomes (Heng et al., 2021; Ifrim et al., 2014; Jeljeli et al., 2019; Neher et al., 2019). Given the profile of heightened immune activation in ageing vulnerable animals I have exhibited by immunohistochemical staining of microglia here, an immune tolerising effect is unlikely, but an immune training sensitising effect to the subsequent viral Poly I:C challenge as a result of initial exposure to LPS cannot be ruled out at this time. Future work could seek to confirm whether there was an immune training effect present as a result of the recurrent systemic stressors and indeed,

whether the magnitude of this immune training effect might correlate with the cognitive resilience/frailty of that animal.

White matter integrity has been shown previously to decline with age and, more recently, this has been demonstrated to be associated with a decline in cognitive function as well as an increase in microgliosis in white matter rich tissues with ageing and many neurodegenerative disorders including AD and PD (Bendlin et al. 2010; Raj et al. 2017; Safaiyan et al. 2021; Klosinski et al. 2015; Ruckh et al. 2012). Furthermore, neuroimaging studies have shown that white matter disease and/or cortical atrophy have been shown to be substantial risk factors for delirium (Wijdicks 2015; Nitchingham et al. 2018). Here, Luxol fast blue staining of myelin in white matter tissue showed a robust inverse correlation between myelin density and microgliosis in the corpus callosum and cerebellar white matter tracts. Thus, this enhanced state of microgliosis and reduced myelin density in the aged frail animals indicates a potentially increased vulnerability to cognitive dysfunction. Indeed, reduced myelin density in the white matter regions surrounding the hippocampus correlated strongly with increased vulnerability to cognitive dysfunction under acute systemic stress in the hippocampal-dependent T-maze task. The potential contribution of white matter gliosis to cognitive dysfunction is an area of increasing interest with several gene expression studies highlighting the immune-vigilant phenotype of microglia in the white matter of the ageing brain (Safaiyan et al. 2021; Bachiller et al. 2018). Furthermore, microglia of the white matter have been previously shown to exist in a less quiescent state and exhibit an enhanced microglia response following activation compared to grey matter (Hart et al. 2012). More recent work by Safaiyan and colleagues has demonstrated that white matter microglia exist in a heightened activation state in the ageing brain, showing elevated gene expression of the core hub genes of primed microglia, *Clec7a, Axl* and *Cd11c,* as well as activated nodules engaged in phagocytosing and clearing degenerated myelin. (Safaiyan et al. 2021; Sloane et al. 1999). Further evidence from a recent small-scale human study examining age-associated changes in cortical white matter microglial density reported relatively lower white matter activated microglia in the corpus callosum of “Super Agers” (individuals 80yrs< who exhibited equivalent or better memory test scores than 50-65yr old cognitively normal aged adults) compared to equivalently aged individuals with poorer test scores (Gefen et al. 2019). This is consistent with our own findings of lower microgliosis and greater myelin density in the corpus callosum of aged cognitively resilient animals. Recent use of remyelinating drugs such as Fingolimod and Minocycline with N-acetylcysteine in ageing, MS and TBI models has demonstrated a concurrent improvement in cognition alongside remyelination (Haber et al. 2018; Bergold et al. 2011; Zhang et al. 2020; Preziosa et al. 2020). However, at this time it is impossible to tell whether this increased microglial activation and reduced myelin density observed in cognitively frail individuals is a result of degenerating white matter activating microglia, or that chronic

activation of microglia is inducing the age-related myelin disruption. Microglia have been shown to be pivotal in the process of myelogenesis through their secretion of growth factors like IGF-1 (Wlodarczyk et al. 2017) as well as for their phagocytic role in clearing myelin debris (Sosa et al. 2013; Rawji et al. 2018) which has been shown to negatively affect oligodendrocyte progenitors cells (OPC) (Syed et al. 2008; Plemel et al. 2013) impairing remyelination (Kotter et al. 2006). However, while acute microglial production of pro-inflammatory mediators such as IL-1β and TNFα have been shown to be important in promoting OPC activation and proliferation to mediate remyelination (Mason et al. 2001; Voß et al. 2012) under chronic conditions such as those imposed in ageing and neurodegeneration the expression of mediators such as NF-κB take on a role in autoimmune demyelination (Baker et al. 1994; Goldmann et al. 2013; Steeland et al. 2017; Lévesque et al. 2016; Paré et al. 2018). Going forward it will be advantageous to disrupt microglial activation and function using antibodies or anti-sense oligonucleotides targeting microglial receptors, such as TREM2, in ageing mouse models and subsequently assess myelin integrity to determine whether this microgliosis is a cause of the reduced myelin pathology in ageing or a result of it.

Whichever outcome proves to be the case, this microgliosis is not without risk to the neuronal integrity of the ageing brain. As discussed earlier in this text activated microglia in a proinflammatory state are capable of producing proinflammatory cytokines and chemokines as well as several potentially neurotoxic substances elicited under acute inflammatory conditions such as nitric oxide, oxygen free radicals and proteolytic enzymes, which can significantly exacerbate neuronal damage and loss in vulnerable brains as has been shown in multiple rodent models of neurodegenerative disorders (Paul Stroemer et al. 1998; Perry et al. 2010; Beck et al. 1988; Zindler et al. 2010). To this, end animals were assessed for changes in their pre-synaptic terminal density with advancing age through immunohistochemical staining for $Sy38^{+}$, a pre-synaptic terminal marker. The density of functional synapses is a crucial parameter in determining the efficacy of synaptic transmission and a reduced density has been shown to confer an increased vulnerability to neuronal impairment in several neurodegenerative disorders including AD and PD (Seo et al. 2021; Scheff et al. 2011; Sri et al. 2019; Perez-Cruz et al. 2011). Interestingly it was recently demonstrated in a small-scale human study that individuals presenting with AD pathology but who were deemed cognitively resilient (i.e. asymptomatic for clinical dementia) exhibited greater dendritic spine density than those with dementia (Boros et al. 2017). As such I hypothesised that cognitively frail animals would show a reduced pre-synaptic terminal density. Consistent with our previous observations of increased microglial activation and reduced myelin integrity in aged cognitively frail animals, a significantly reduced $Sy38^{+}$ pre-synaptic terminal density was found in the stratum radiatum, oriens and molecular layer of the hippocampus of aged animals scored as

cognitively frail in the hippocampal-dependent T-maze task compared to cognitively resilient age-matched animals. These results are consistent with previous findings that normal aging results in a region-specific vulnerability of synapses to loss and dysfunction (Morrison et al. 2012) as well as an imbalance between excitatory and inhibitory synapses, (Canas et al. 2009). The reasons for this synaptic loss with age and neurodegeneration is a subject of widespread debate. Mounting evidence suggests that aberrant synaptic pruning by the complement system is responsible, specifically C1q and C3 have both been shown to differentially affect this age-dependent synaptic vulnerability (Shi et al. 2015; Stephan et al. 2013). Consistent with this theory of complement mediated synaptic loss, it has been shown that *Trem2*$^{-/-}$ mice exhibit cognitive resilience, reduced age-associated hippocampal synaptic loss and enhanced hippocampal LTP compared to age matched wild-type animals (Qu et al. 2020). Recent work by Olesen and colleagues has demonstrated that impaired synaptic mitochondrial function plays a role in ageing mice and is associated with impaired novel object recognition and spatial memory and could be rescued by preservation of mitochondrial function using MitoQ or Curcumin (Olesen et al. 2020).

In addition to the reduced Sy38^{+} pre-synaptic terminal density observed in the hippocampus I also assessed the density of cholinergic terminals in the hippocampus and demonstrated a significant reduction in ChAT^{+} terminal density in the Cornu Ammonis 3 (CA3) region as well as a broad trend in the dentate gyrus (DG) with increasing cognitive dysfunction. The CA3 and DG regions both receive cholinergic input from the medial septum and vertical limb of the diagonal band of Broca, which pass through the fimbria (Teles-Grilo Ruivo et al. 2013), which as discussed earlier in this section is a hippocampal white matter region which showed robust microgliosis and reduced myelin density with cognitive dysfunction. Human studies of aging and AD have attributed the loss of basal forebrain cholinergic neurons a significant role in the cognitive decline associated with age and disease (Baxter et al. 1999; Paul et al. 2015), indeed the CA3 regions cholinergic modulation has been shown to be crucial for information encoding (Nolan et al. 2011). Work by our lab in mouse models has demonstrated that cholinergic neurodegeneration in the basal forebrain system, which provides input to hippocampal regions including the CA and DG, is associated with heightened vulnerability to inflammation-induced cognitive dysfunction (Field et al. 2012) as well as a decrease in ChAT^{+} terminals in the CA1 region of the hippocampus (Nazmi et al. 2021). Furthermore, administration of the anticholinergic drug, scopolamine to the CA3 region of the hippocampus has been shown to precipitate deficits in contextual fear conditioning spatial memory tasks (Rogers et al. 2004). Additionally, reduced cholinergic tone as a result of basal forebrain lesions with the immunotoxin p75-saporin has been shown to not only reduce the cholinergic tone but will result in the priming of microglia to elicit exaggerated responses to a systemic LPS challenge (Nazmi et al. 2021). Consistent with this I demonstrated that cholinergic tone correlated with microglial

activation, assessed by $IBA1^{+}$ percentage area, in the same region. As with the reduction in presynaptic terminal density, this loss of cholinergic tone observed in the CA3 of aged cognitively frail animals could be a result of aberrant synaptic pruning, as suggested by the correlating increase in microgliosis in animals with low cholinergic tone or the microglial activation may simply be symptomatic of the pathology rather than causative.

Taken together these data suggest that while ageing is a pernicious and unrelenting process conferring a substantial increase in vulnerability to immune activation and cognitive dysfunction there is substantial variability within not only the regional immune response of the ageing brain, but significant variation between individual animal's vulnerability to acute cognitive dysfunction following a systemic stressor. At this time it is impossible to say whether the cognitive resilience or frailty observed in our population is a result of the correlated reduced myelin and synaptic terminal density and the heightened microgliosis a compensatory response to this, or whether the opposite is true and the exaggerated microgliosis observed in the ageing brain is causing this neuronal dysfunction and in turn cognitive dysfunction.

Chapter 4:
The frail brain - ageing and vulnerability

4.1 Introduction

In 1825 Benjamin Gompertz first published the Gompertz-Makeham law which outlined that across the adult lifespan the risk of mortality will increase exponentially with age (Kirkwood 2015). This illustrated that while a single-system illness is usually the primary cause of death in early life, the acceleration in mortality risk which manifests in later years reflects the fact that multiple interacting factors are typically responsible for death. Additionally, this implies that individuals with multiple co-morbidities will likely be at an increased risk of death compared to their fitter age peers. This state of increased risk due to accelerated deficit accumulation is known as frailty (Kirkwood 2005), while the inverse is referred to as resilience (Kirkland et al. 2016). It is hypothesised that as ones' resilience is reduced, their frailty will increase commensurately. In a clinical setting frailty is typically quantified using a frailty index. The Fried Integrated Phenotype model establishes a frailty phenotype based off five variables, (i) unintentional weight loss, (ii) self-reported exhaustion, (iii) low energy expenditure (iv) slow gait speed and (v) weak grip strength (Fried et al. 2001). The main alternative model, the Cumulative Deficit model takes into account 92 baseline variables of symptoms, signs, disease states, disabilities and abnormal laboratory values, to generate a comprehensive frailty score from the cumulative effect of the individual deficits (Rockwood et al. 2005), but multiple variations are now in use in the clinical setting to predict patient vulnerability and plan recovery and treatment plans.

As such I hypothesised that as frailty severity increases an individual would display increasingly elevated markers of neuroinflammation and immune activation in the ageing brain proportionately. Furthermore, I hypothesised that frail individuals would be more vulnerable to cognitive and physiological dysfunction in response to a systemic challenge. To this end I set out to assess animals using established and novel frailty indices to generate individualised numerical frailty scores to capture their "biological" age and assess markers of neuroinflammation and immune cell activation against this score.

Therefore, our first frailty index used was comprised of a 33-point physiological cumulative deficit index, provided by Professor Susan Howlett in Dalhousie University. Frailty testing was carried out in Dalhousie University and frozen brain cerebrum and cerebellum from those animals was provided to our laboratory and analysed by quantitative PCR for a number of neuroinflammatory transcripts. This frailty cohort however failed to account for cognition at all, an important feature in frailty as discussed in the previous chapter. Therefore, a second and third cohort were established in order to design, define and refine novel frailty indices that incorporated cognitive components. These indices were modified versions of the integrated phenotype index and

combined multiple physiological, behavioural and cognitive analyses to generate an individualised frailty score as described in more detail in section 2.2.4.

Complimentary DNA (cDNA) was synthesised from RNA isolates of the cerebrum and cerebellum from the Dalhousie's "cumulative deficit frailty" cohort and the hippocampus, hypothalamus and cerebellum from the first modified integrated phenotype cohort, "Trinity Frailty Index I (TFL I)". qPCR analysis was conducted to assess markers of microglial activation *Trem2* (Rivest 2015; Cantoni et al. 2015), microglial population *Tyrobp* (Audrain et al. 2021) and microglial priming *Clec7α* and *Cd11c* (Holtman et al. 2015); growth factors such as *Igf1, Bdnf* and *Tgfb* as well as inflammatory mediators, including cytokines such as *IL-1β* and *TNFα* and chemokines like CCL2, *CXCL10* and *CXCL13*. To assess the extent to which frailty scores predicted the brain expression of neuroinflammatory markers, I performed linear regressions of correlation between age, frailty and inflammatory transcripts. To determine whether age or frailty might better predict an individual's vulnerability to an acute stressor, animals' frailty status was assessed using our second modified integrated phenotype cohort, Trinity Frailty Index II (TFL II), challenged with LPS and their vulnerability to sickness behaviour and recovery assessed over a week-long recovery.

4.2 Results

4.2.1 Cumulative deficit frailty index & the innate immune response

In collaboration with the Howlett lab in Dalhousie University Canada we received brain tissue for molecular analysis from normal mice scored for frailty using a 33-point cumulative deficit frailty index across a range of ages, from 5 up to 25 months old. The assigning of these frailty scores are explained in **Section 2.2.4** and **2.2.5**. This score ranges from 0-1. An animal with no deficits receives a Frailty index (FI) of 0 and an animal with maximal deficits would receive a value of 1. Typically, however, the highest FI are between 0.5-0.6 as any animal scoring greater than this would be severely unwell, indicative of moribundity and possibly close to the humane end points. In contrast to the previous cognitive frailty assay (chapter 3) which was a purely cognitive evaluation of frailty, this frailty score was generated from measures of the physical condition of the animal **(Table 2.10)**. The question posed was whether this measure of frailty would be a strong predictor of neuroinflammation in the ageing brain using molecular indices of brain inflammation or whether age was a better predictor. To this end, molecular analyses were conducted on the right hemispheres' cerebellum and cerebrum samples provided by Dalhousie University.

	Cumulative Frailty Measures		
1	Body Weight	18	Vestibular disturbance
2	Avg Temp	19	Hearing loss
3	Temp Score	20	Cataracts
4	Body Weight Score	21	Eye discharge/swelling
5	Alopecia	22	Microphthalmia
6	Loss of fur colour	23	Corneal opacity
7	Dermatitis	24	Vision loss
8	Loss of whiskers	25	Menace reflex
9	Coat condition	26	Nasal discharge
10	Tumours	27	Malocclusions
11	Distended abdomen	28	Rectal prolapse
12	Kyphosis	29	Vaginal/uterine/penile prolapse
13	Tail stiffening	30	Diarrhoea
14	Gait disorders	31	Breathing rate/depth
15	Tremor	32	Mouse grimace scale
16	Forelimb grip strength	33	Piloerection
17	Body condition score		

Table 2.9: Dalhousie Cumulative Deficit Frailty Measures: Individual measures assessed to generate a Cumulative Deficit Model Frailty Score for each mouse individually

4.2.1.1. Cumulative Deficit Frailty score is not a strong predictor of microgliosis

Analysing first the microglial priming's core transcriptomic signature, genes *Clec7a* and *Cd11c*, it was found that across both regions, the two genes correlated strongly with age **(Figure 4.1 E-H)** (***p<0.001). Additionally, within the cerebrum frailty also had a tight significant correlation with priming **(Figure 4.1 A-B)** (**p<0.01). In contrast, while the same genes correlated with age in the cerebellum (***p<0.001) no significant correlation was achieved for frailty, though a weak trend was observed for each **(Figure 4.1 C-D)**. These data indicate that microglial priming tracks significantly with age across the whole brain, while frailty only significantly correlates with the incidence of microglial priming within the cerebrum and not, the cerebellum.

Next, I assessed the microglial markers *Trem2* and *Tyrobp*. *Trem2* demonstrated no statistically significant change with age in either the cerebrum or cerebellum **(Figure 4.1 M – P).** While *Trem2* expression showed no statistically significant relationship with frailty in the cerebellum it showed a trend toward a negative linear relationship **(Figure 4.1 K),** but a strong non-linear relationship was evident in the cerebrum **(Figure 4.1 I)**. A similar, non-linear relationship was evident in the expression of the microglial specific marker *Tyrobp* against frailty in the cerebrum with peak expression occurring in the mid frailty range of 0.2-0.4 and diminishing thereafter **(Figure 4.1 J)**; a weaker non-linear relationship was also present in the cerebellum **(Figure 4.1 L)**. Like *Trem2*, Tyrobp failed to achieve significance when correlated against age but did demonstrate a weak trend towards a positive expression **(Figure 4.1 N & P).** Due to its specificity to microglia, Tyrobp is

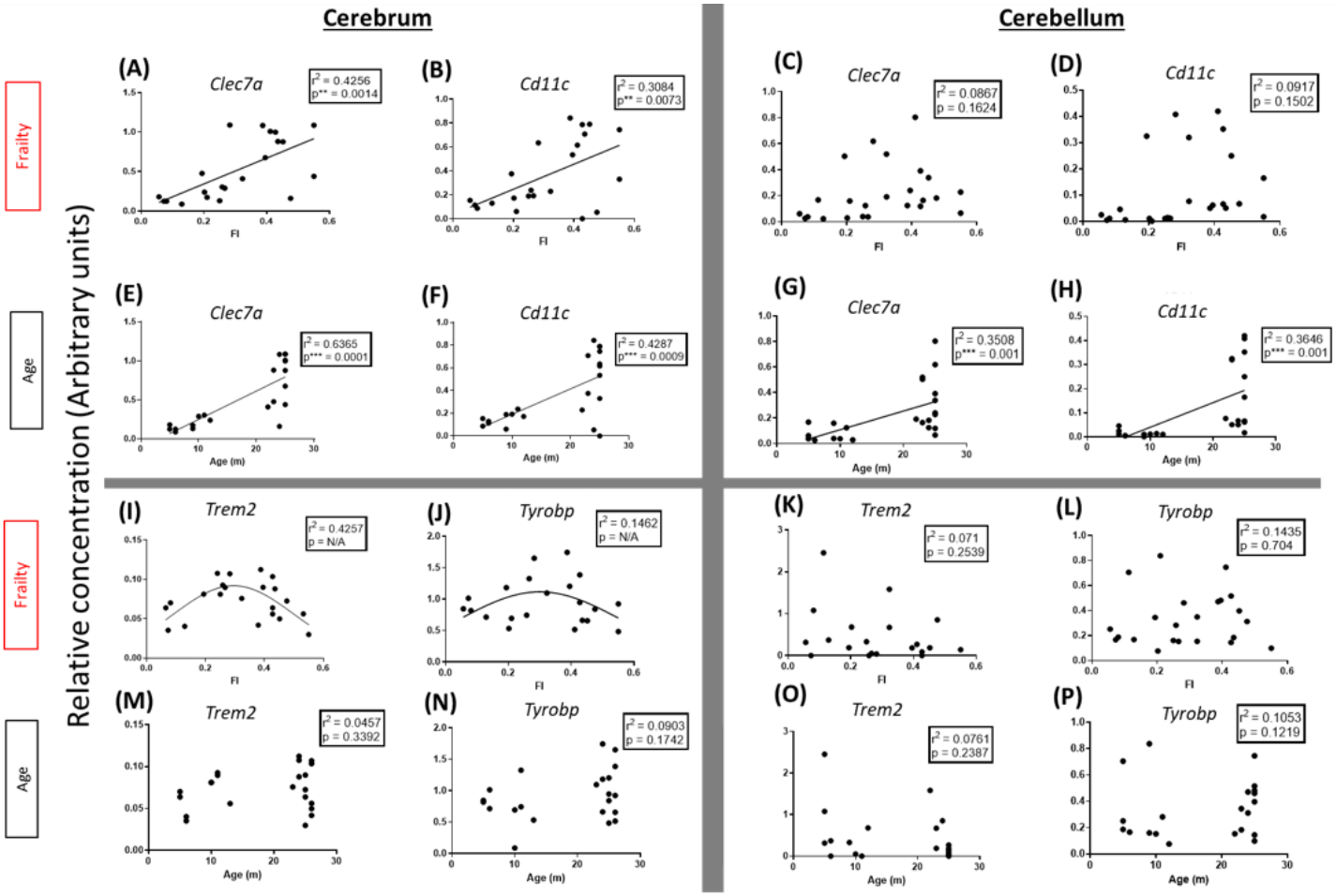

Figure 4.1: **Correlation of brain microglial associated markers genes' expression with age or frailty: Correlation by Pearson linear regression analysis and non-linear gaussian regression correlation of microglial priming core transcriptomic signatures, Clec7a and CD11c, and microglial markers Trem2 and Tyrobp, gene expression assessed by qPCR and transcripts normalised to the housekeeping gene 18s, in the cerebellum and cerebrum against Age (months) and Frailty Index score (FI) (n=25), significance denoted by *p<0.05, **p<0.01, ***p<0.001.**

commonly used as a proxy for microglial number, these data suggest that as frailty increases so too will the immune cell population up to a certain point of frailty, after which it declines with further development of frailty.

Analysis of the growth factor genes Brain-derived neurotropic factor (*Bdnf*) and Insulin-like growth factor (*Igf1*) revealed a statistically significant negative correlation (*p<0.05) with expression for both age and frailty in the cerebrum **(Figure 4.2 A-B, E-F).** Within the cerebellum the same response was observed for *Bdnf* (p<0.05) **(Figure 4.2 G)** but not for *Igf-1* despite a weak correlation with age and frailty **(Figure 4.2 F, H).** These data indicate that as frailty increases the transcriptional expression of genes involved in maintaining neuronal integrity become compromised, reinforcing the theory that with increased frailty individuals may become progressively vulnerable to cognitive dysfunction or decline.

In order to assess the impact of ageing and frailty on complement system function across the ageing brain *C3* expression was assessed. Here I demonstrated a robust correlation between frailty and *C3* expression in both cerebrum (*p<0.05) and cerebellum (**p<0.01) (**Figure 4.3 A-B).** Additionally, *C3* transcription was significantly correlated with age in the cerebellum (p<0.001) but not in the cerebrum (p=0.3834) (**Figure 4.2 C-D).**

The expression of pro-inflammatory cytokines *Il1b* and *Tnfa* as well as the chemokine *Cxcl10* and the Type I IFN-induced gene *Irf7* were also assessed. Both cerebrum and cerebellum showed poor correlation between expression of these pro-inflammatory cytokines with age. Only in the cerebellum did *Il1b* achieve significance (*p<0.05) with age, however, *Tnfa* showed a weak non-significant correlation in the cerebrum and the cerebellum with age **(Figure 4.4 E-H).** *Il1b* failed to demonstrate any correlation with frailty in either the cerebrum or the cerebellum, while *Tnfa* achieved a significant linear correlation with frailty in the cerebrum (*p<0.05) and interestingly *Tnfa* expression exhibited evidence of a strong non-linear correlation (r^2 = 0.354) with frailty within the cerebellum (**Figure 4.4 A-D)** similar to that seen in the expression of the microglial markers *Trem2* and *Tyrobp*. No such gaussian relationship was found with age but this was primarily a result of the lack of intermediate ages, 12-22-months-old, available within the population. This

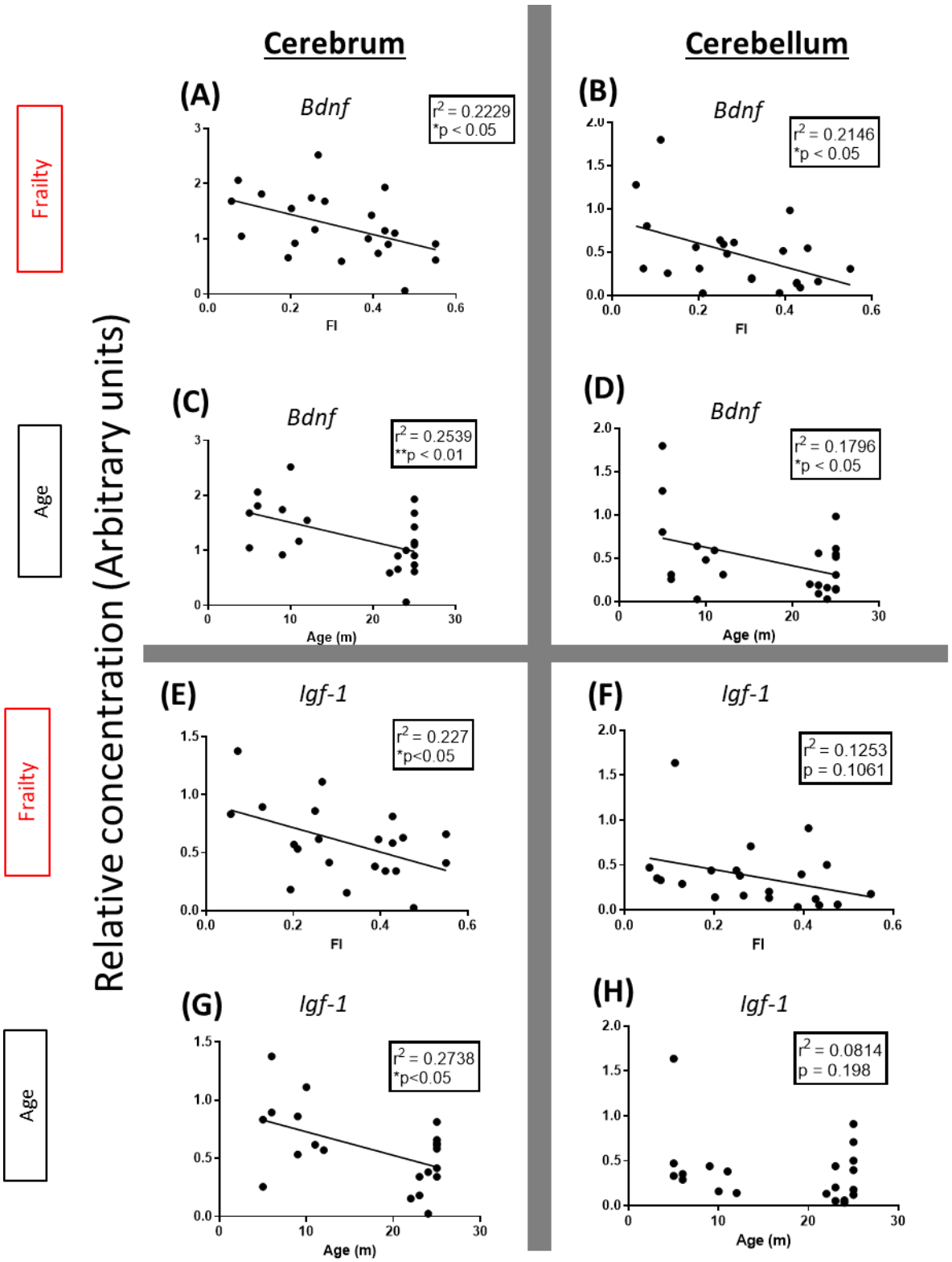

Figure 4.2: Correlation of brain microglial associated growth factor genes' expression with age or frailty: Correlation by Pearson linear regressoin analysis of microglial associated growth factor genes (n=25), (A-D) BDNF & (E-H) IGF1, gene expression assessed by qPCR and transcripts normalised to the housekeeping gene 18s, in the cerebrum and cerebellum against Age (months) and Frailty Index score (FI), significance denoted by *p<0.05, **p<0.01, ***p<0.001.

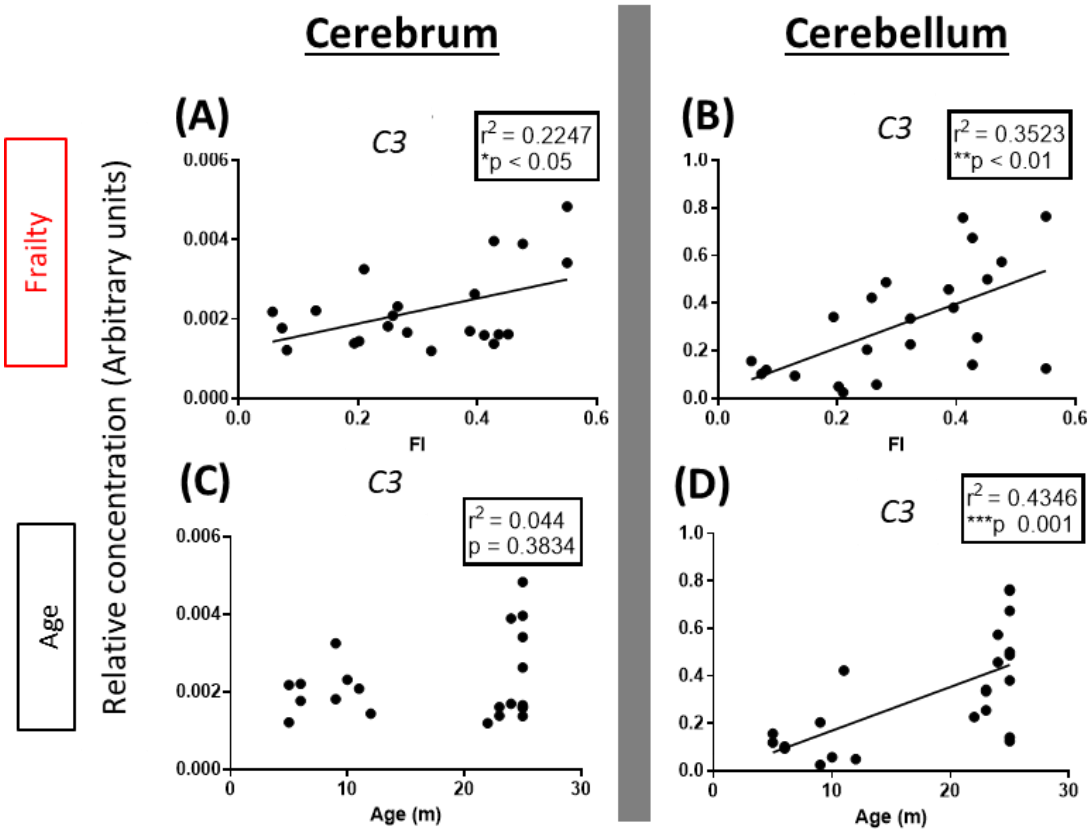

Figure 4.3: Correlation of brain complement system component genes' expression with age or frailty: Correlation by Pearson linear regressoin analysis of complement system component genes (n=25), C3, gene expression assessed by qPCR and transcripts normalised to the housekeeping gene 18s, in the cerebrum and cerebellum against Age (months) and Frailty Index score (FI), significance denoted by *p<0.05, **p<0.01, ***p<0.001.

Further analysis of the inflammatory status of each animal revealed a similarly varied pattern of expression for the chemokine *Cxcl10* and the Type 1 interferon induced gene *Irf7*. *Irf7* achieved significance with age in the cerebellum ($p<0.05$) but not the cerebrum **(Figure 4.4 N, P)**. When plotted against frailty however *Cxcl10* exhibited a significant relationship within the cerebellum (*$p<0.05$) but not the cerebrum **(Figure 4.4 , I, K)**. *Irf7* expression showed a significant correlation with frailty in either region **(Figure 4.4 J, L)**. Conversely *Cxcl10* demonstrated a significant linear correlation with age in the cerebrum (*$p<0.05$) and a strong trend within the cerebellum **(Figure 4.4 M, O)**.

Overall, it was found that frailty was a weaker predictor by linear regression of microglial activation and inflammatory status compared with age. However, the results here emphasised the importance of having a wide range of ages for assessment within the population as there was a lack of any intermediate aged animals 12-22-months-old, making it difficult to accurately assess the impact of age on linear and non-linear relationships on gene expression. Furthermore, evidence here emphasises the importance of taking a regional specific approach to assessing these criteria in the ageing brain and reinforced the observation that while frailty may not be the primary driving factor in microgliosis it is almost certainly a significant contributor to the extent of activation.

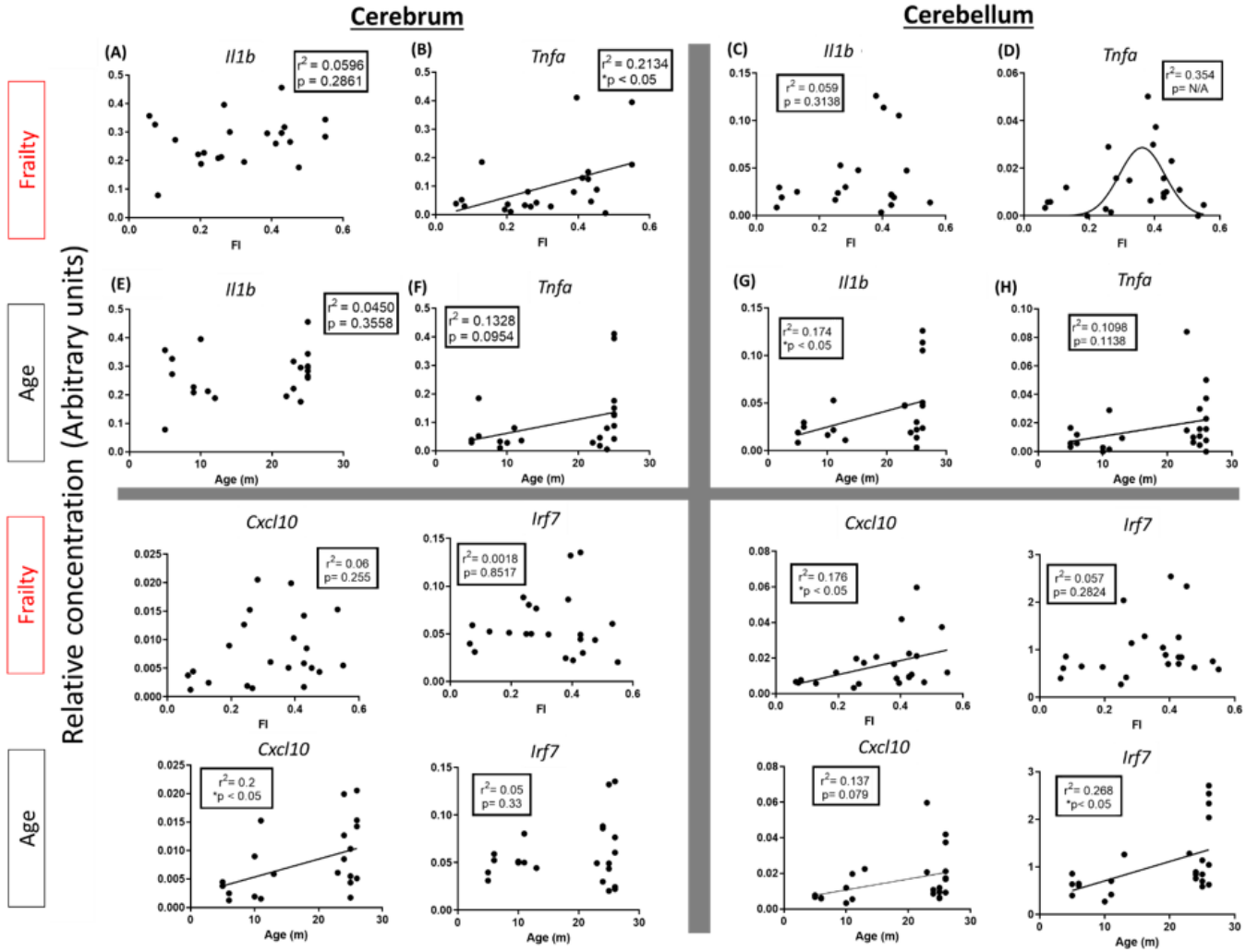

Figure 4.4: **Correlation of brain pro-inflammatory transcripts genes' expression with age or fraity: Correlation by Pearson linear regression analysis and non-linear regression correlation of pro-inflammatory cytokine transcripts, *Il1b* and *Tnfα*, and chemokine *Cxcl10* and Type I IFN induced gene *Irf7*, gene expression assessed by qPCR and transcripts normalised to the housekeeping gene 18s, in the cerebellum and cerebrum against Age (months) and Frailty Index score (FI) (n=25), significance denoted by *p<0.05, **p<0.01, ***p<0.001.**

Dalhousie Cumulative Deficit Model				
Gene	Cerebrum		Cerebellum	
	Frailty	Age	Frailty	Age
Clec7a	0.4256	0.6365	0.0867	0.3508
Cd11c	0.3084	0.4287	0.0917	0.3646
Trem2	0.4257	0.1462	0.071	0.0761
Tyrobp	0.1462	0.0903	0.1435	0.1053
C3	0.2247	0.044	0.3523	0.4346
Bdnf	0.2229	0.2539	0.2146	0.1796
Igf-1	0.227	0.2738	0.1253	0.0814
Il1β	0.0596	0.045	0.059	0.174
Tnfα	0.2134	0.1328	0.354	0.1098
Cxcl10	0.06	0.2001	0.178	0.137
Irf7	0.0018	0.05	0.057	0.21

No significant linear correlation				
Significant linear correlation with	Frailty	***p<0.001	**p<0.01	*p<0.05
Significant linear correlation with	Age	***p<0.001	**p<0.01	*p<0.05
Strong fit to non-linear correlation	Gaussian			

Table 4.1: Dalhousie cumulative deficit model summary table of linear correlations: summary of Figures 4.1-4, fit to the line, r^2 values, and their significance colour coded, by age or frailty with qPCR gene transcript expressions normalised to 18s, of Dalhousie cumulative deficit frailty model young and aged animals cerebrum and cerebellum tissue isolated RNA.

4.2.2 Modified Integrated Phenotype Frailty Scale – Trinity Frailty Indices

In the Dalhousie cumulative deficit model, above, I was restricted by the fact that it measured physiological but not cognitive features **(Table 2.10)**. There was a further limitation in that the brain tissue was supplied in a manner that prevented dissection of specific brain regions and there was a lack of intermediate aged animals. Therefore, the design and use of a novel frailty index, selecting measures that better capture the ageing of systems including the brain, was undertaken. A frailty index using relatively non-invasive measures was modelled after the Fried Integrated Phenotype Frailty Scale analysing body mass, exhaustion, low activity, slow speed and weak grip strength **(Table 4.2)**. In addition to these typical Fried Scale measures, I incorporated several other measures including metabolic measures of temperature and blood glucose levels and a working memory assay of cognitive function. This index was therefore constructed to capture key components of ageing and frailty, cognition, physiological capacity and metabolism, to a more comprehensive degree than that applied in the cumulative frailty index from which the prior brain tissue arose. Furthermore, our prior ageing study (chapter 3) indicated the importance of taking a region-specific approach to characterising neuroinflammation/microglial activity. This index allowed the collection of brain tissue from a larger population of animals with a wide range of ages, according to regions of interest without the constraints imposed by the brain tissue collection methods exploited by the Howlett Lab.

4.2.2.1 Frailty Index; Measures & Scoring

In order to identify what behavioural and physiological components were sensitive and discerning enough to the effect of ageing all animals were first assessed on a range of tasks and stratified by age to assess how age affected changes and variability within the population. See section 2.2.4. of Materials & Methods for further information on the design of these frailty assays and their scoring. No statistical analysis was done on these age groups as ageing associated trend changes and variability were more important and informative in order to identify viable frailty index component measures to generate a frailty score to describe an individual's biological age as opposed to their chronological age. Finalised frailty index behavioural, physiological and metabolic measures included for frailty assessment summarised in **Figure 4.8 D.**

Open Field Activity

Open field analysis was conducted in order to assay locomotor and rearing activity of the mice **(Figure 4.5)**. Rearing activity was manually scored over a 10-minute window, while ANY-maze tracking software was employed to calculate, for each mouse, (i) speed, (ii) distance travelled and (iii) meander (absolute turn angle divided by distance covered, a descriptor of the animal's path) within the box and (iv) number of rears. These measures allowed us to capture a representation of

the animal's activity and speed of movement as proxies for energy expenditure and slowness of movement, criteria 3 & 4 of the Fried Integrated Phenotype Frailty model **(Table 4.2).** Furthermore, analysis of the animals' speed of movement was assessed across the 10minute period in 200sec time bins to assess the change in their speed of movement across the 10min testing period **(Figure 4.5 E)** in order to capture a representation of the animal's exhaustion, (criteria 2 of the Fried model).

1.	**Weight Loss**
2.	**Self-reported exhaustion**
3.	**Low energy expenditure**
4.	**Slow gait speed**
5.	**Weak grip strength**

Table 4.2 Criterion for Fried frailty phenotype

Distance

The total distance travelled by the animal around the open field maze over the 10min testing period was calculated and revealed that animals in the 5-7-month and 27–29-month groups showed that aged animals covered a significantly smaller distance with the least variation **(Figure 4.5 A)**. The greatest distances covered, as well as variability, was found in the 9-18-month range while this decreased substantially thereafter for 20-month and 27-29-month-old animals. The oldest aged animals, 27-29 months, showed the smallest scores of all age groups assessed.

Speed

The animal's speed was calculated as a function of the distance covered (cm) divided by the total time (seconds) the animal was mobile, i.e., in motion, within the open field maze during the 10min testing period. Speed revealed a similar pattern to that of the total distance moved with the highest speeds and greatest variation within groups being in the 9-18-month groups **(Figure 4.5 B)**. As with distance the speed began to decline in animals older than these with the 27–29-month aged group again being the slowest of all assessed animals.

Meander

The animal's meander was calculated by dividing its absolute turn angle by the total distance covered over the 10min testing period. An animal with a larger absolute turn angle would have a greater meander score than animal who covered an equivalent distance with a smaller absolute turn angle. This indicates the animals' path shape within the maze. This is a useful measure as meandering is a description of the efficiency of exploration to cover, or scan, an area for an animal in a novel environment. While meander was found to be similar to angular velocity in its relative consistency across the ages, there was a greater degree of variability within age groups, the greatest

of which was seen within the 15-18-month age group **(Figure 4.5 C)**, consistent with observations across numerous measures and the existing literatures' data that identifies 17 months as the average age which frailty is found to manifest in mice (Kwak et al. 2020) and so was included in the final frailty index measures.

Angular velocity

Angular velocity was calculated as a function of the animals' absolute turn angle divided by their total time mobile over the 10min testing period. This was calculated to provide a numerical representation of the speed with which the animal was correcting their course, as an additional measure of the Fried phenotype criteria of slow speed, i.e. a frail animal might have a low angular velocity score as they might be impaired in their ability to adjust speed quickly. However, it was found that angular velocity was relatively consistent across the ages **(Figure 4.5 D)** and particularly within age groups and so it was deemed not to be a sufficiently discerning criteria which might be used to generate a frailty index to stratify animals by biological status more accurately than chronological age.

Rears

Rearing may be defined as when the mouse stands on their hind legs, with the fore paws not touching the floor and with their core engaged and head raised so as to survey their environment in the open field maze and is a measure of exploratory activity. There was significant variation in the number of rears by animals within each age group but as age progresses, I can see a trend toward a decrease in the number of rears between 5-20 months of age **(Figure 4.5 E)**. The 27–29-month aged group clearly shows a starkly reduced number of rearing events overall.

Decline in speed (proxy for exhaustion):

To assess exhaustion in animals I examined the decline in their speed across the 10 minutes of open field activity, reasoning that the speed of a given animal's ongoing movement likely indicates increasing tiredness rather than motivation (since movement continues in any case). As a proxy measurement of their exhaustion animals were scored on their average speed (cm/s) in each of the assessed three 200-second blocks in the Open Field maze as well as the change in their speed as a percentage (%) from Block 1 to 2 and from Block 1 to 3. A z-score for each of these measurements was calculated as described above in section 2.2.4.1-3 (exemplar below in **Table 2.8** for speed in each block as well as for the percentage decline in speed from blocks 1 to 2 and 1 to 3. An average of these 5 z-scores (speed (cm/s) in three blocks, two percentage decline in speed between blocks) was taken to generate an Exhaustion score. Scoring as faster than control animals or demonstrating an increase in speed from block 1 to block 2 or 3 was not counted as a deficit and scored as 0.

Exhaustion z-scores revealed that animals in the 5-9-month age groups scored consistently lowest (0-0.2), with higher and more variable scores manifesting in the 15-18-month age group (consist with the literatures reports that frailty is typically reported to manifest around 16 months old in mice (Kwak et al. 2020)) and continued to grow in variability and severity as age advanced with the 29-month-old animals reporting the highest and most varied exhaustion scores (0.1-0.9) **(Figure 4.5 F).**

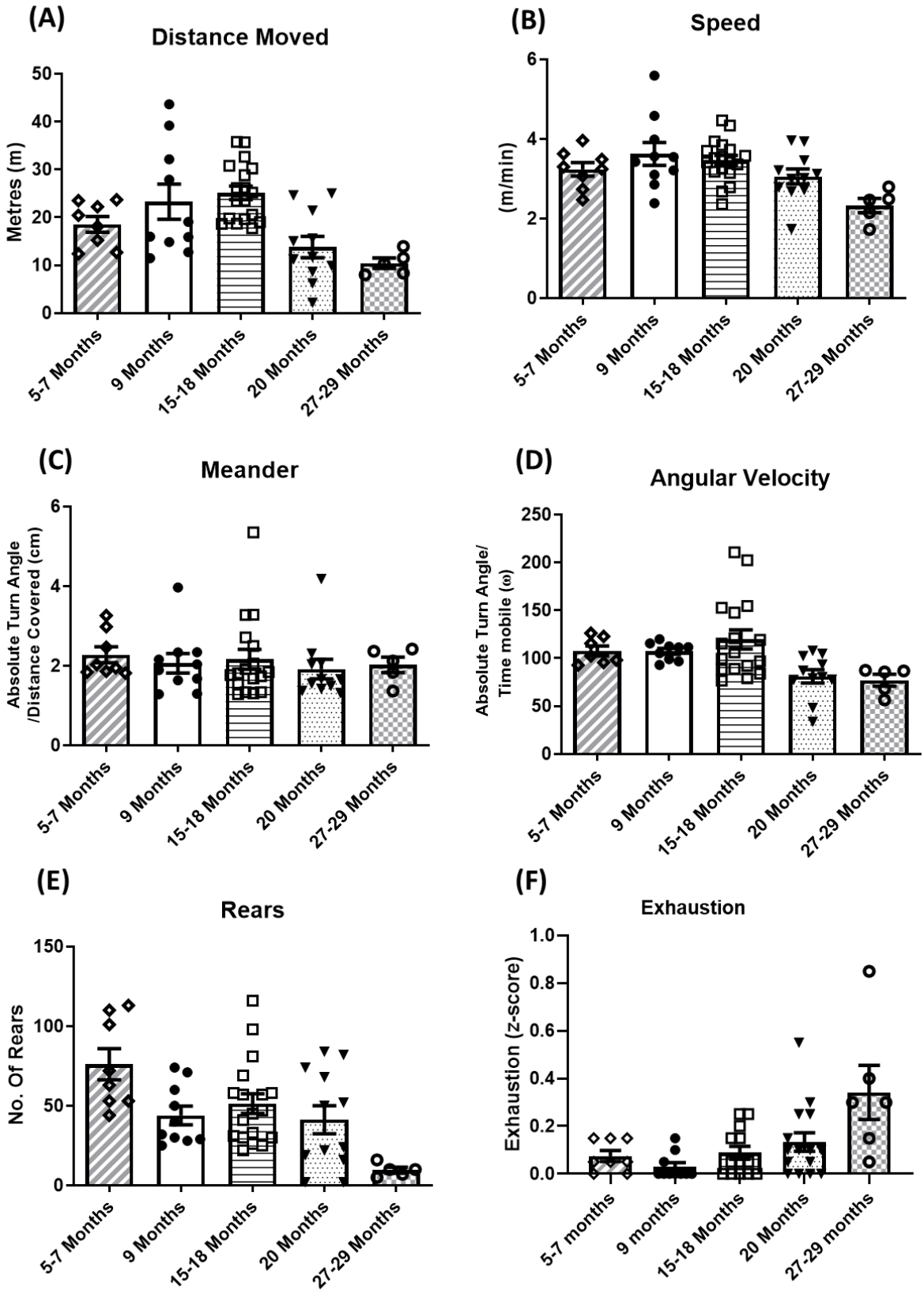

Figure 4.5: Trinity Frailty Index I Open Field analysis measures measures of Activity over 10mins; (A) Distance Moved (m) (B) Speed (distance/time mobile (C) Meander (absolute turn angle/distance) (D) Angular velocity (absolute turn angle/time mobile) and (E) Number of Rears. Exhaustion measure, z-score of speed and % decline in speed over 200sec blocks of the 10min testing period (F). All data represented by mean ± SEM, (n=8, 10, 13, 15, 6).

Strength Testing

In order to capture best the animal's grip strength, criteria 5 of the Fried model, animals were tested on three different measures of grip strength. The first of which was Kondziela's Inverted Screen (Cunningham et al. 2009). Animals' ability to remain on an upturned metal wire grid (1X1cm squares), 1.5m above the ground, was timed up to a maximum period of 120 seconds. Therefore, the animals were scored as the number of seconds for which they remained on the grip up to a maximum of 120 **(Figure 4.6 A)**. Within the youngest animals, 5-9-months old the majority of animals were able to last the full 120sec testing time. However, from 15-months up to 29-months old the animals displayed significant variability in their performance, with some animals meeting criterion for successful completion while others fell as quickly as 20 seconds into testing in each age group.

Secondly, forelimb grip strength alone was calculated using the Deacon weightlifting task (Deacon 2013). Animals were assigned a score based on the maximum weight lifted and the time they held it for **(Figure 4.6 B).** Within each age group assessed there was significant variability, with the exception of the 17–29-month age group who showed a greater variability and trended toward an overall lower forelimb grip strength score in the oldest animals.

In addition to these two strength assays, mice were tested on the Horizontal Bar **(Figure 4.6 C)**. However, as virtually all mice, except for the significantly obese, were able to successfully complete the task, this measure of strength/coordination was not included in our final frailty score as it was not sufficiently discerning in its ability to sensitively assess animals and failed to stratify the mice into a spectrum of physiological conditions as a frailty measure should.

Glucose

To assess changes in glycaemic status across the ageing population blood glucose levels were taken by glucometer, at time of euthanisation, directly from the heart's right atrium. It was found that with advancing age a trend towards decreasing serological glucose concentration was evident with 5-7-month animals showing the highest consistent levels as a group, while 27-29-month-old animals showed consistently lower levels. While an overall decreasing trend with advancing age was the prevailing pattern there was notably high variability in the 15-20-month age groups, with several animals showing hyperglycaemia. Once again, this variability is consistent with the literatures reports that frailty begins to manifest and increase in prevalence and severity from approximately 16 months on in ageing mice (Kwak, Baumann and Thompson, 2019).

Body weight

Similarly, body weight at time of euthanisation was found to be substantially higher and more variable in the 15-20-month aged groups compared to 5-9-month-old animals. This is consistent with this age group's pattern of reduced activity observed in the Open Field task, greater variability and reductions in muscle strength as assessed by Kondziela's screen and Deacon's weight-lifting task as well as the literature on reduced lipid turnover (Held et al. 2021) and resulting in weight gain in ageing animals. Interestingly, the oldest animals, and theoretically those with the highest likelihood of frailty, showed body weights equivalent to young, 5-9-month-old animals. This is consistent with the Fried phenotype's model of frailty which states unexpected weight loss as a significant contributor to frailty pathology and is likely at least partly a result of age associated sarcopenia. Sarcopenia is essentially a loss of muscle tone and density (impaired proteostasis) as a result of reduced food intake (anorexia of ageing) and a resulting protein deficiency (Morley et al. 1988). This sarcopenic obesity, i.e. loss of muscle mass and strength with concomitant increase in adiposity has been shown to be linked to frailty (Crow et al. 2019).

Core body temperature

As with our other metrics of metabolism, body weight and glycaemic status, core body temperature at time of euthanisation as assessed by rectal thermal probe showed the highest variability in 15-20-month-old animals compared to the youngest aged groups, 5-9-months of age. Similarly, the oldest age group, 27–29-month-old animals exhibited notably different recordings and were consistently 1-2 degrees Celsius colder compared to younger groups. This is consistent with established findings in geriatric populations that body temperature decreases and has higher variability with advancing age as elderly individuals are unable to regulate their body temperatures to the same degree as young adults (Howell 1948; Salvosa et al. 1971; Roghmann et al. 2001).

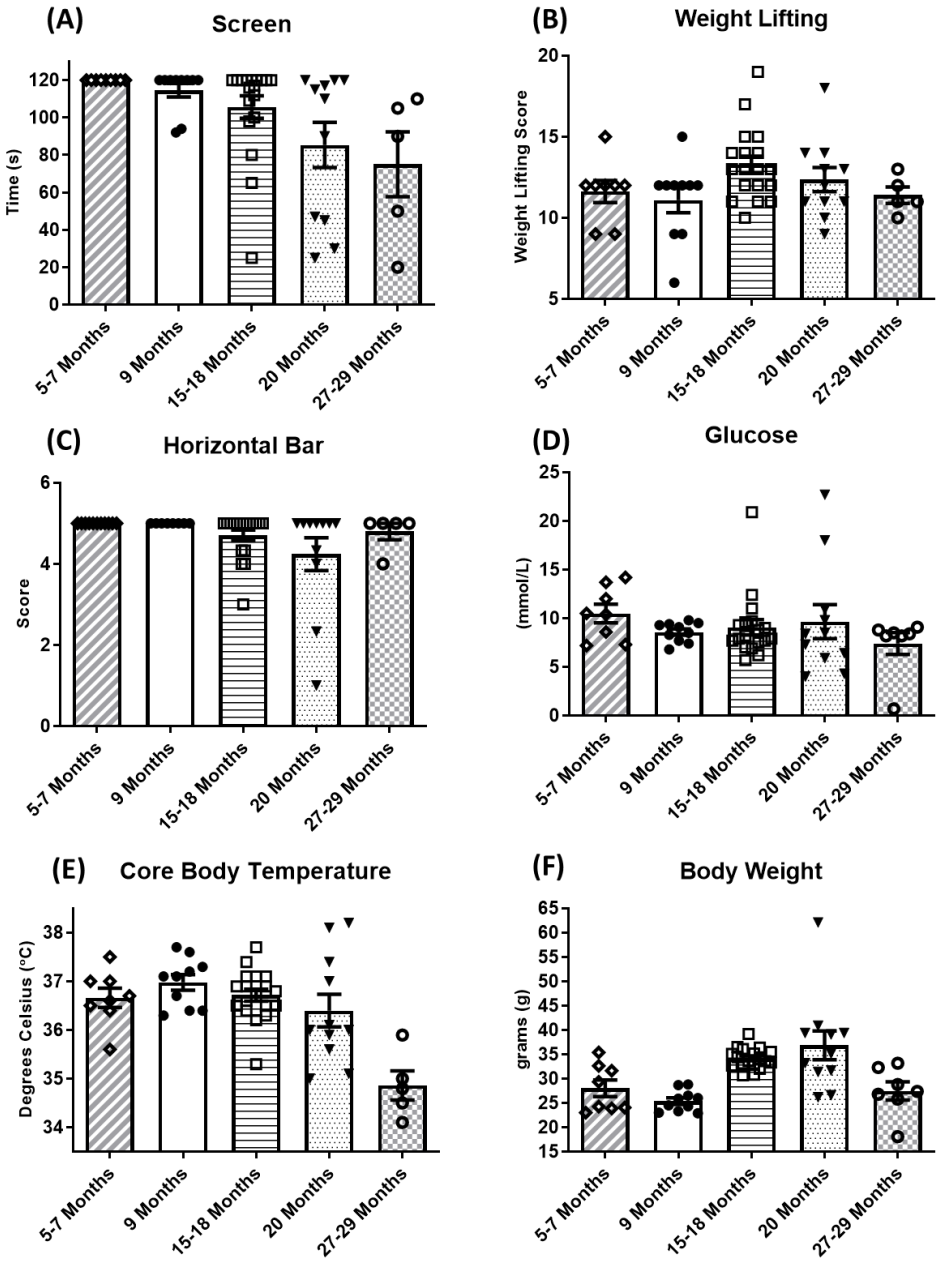

Figure 4.6: Trinity Frailty Index I strength testing & physiological measures; Inverted Screen (A) Horizontal Bar (B) and Weightlifting (C). Physiological and metabolic measures; Blood glucose conc. (D) Core body temperature (E) Body Mass (F). All data represented by mean ± SEM, (n=8, 10, 13, 15, 6).

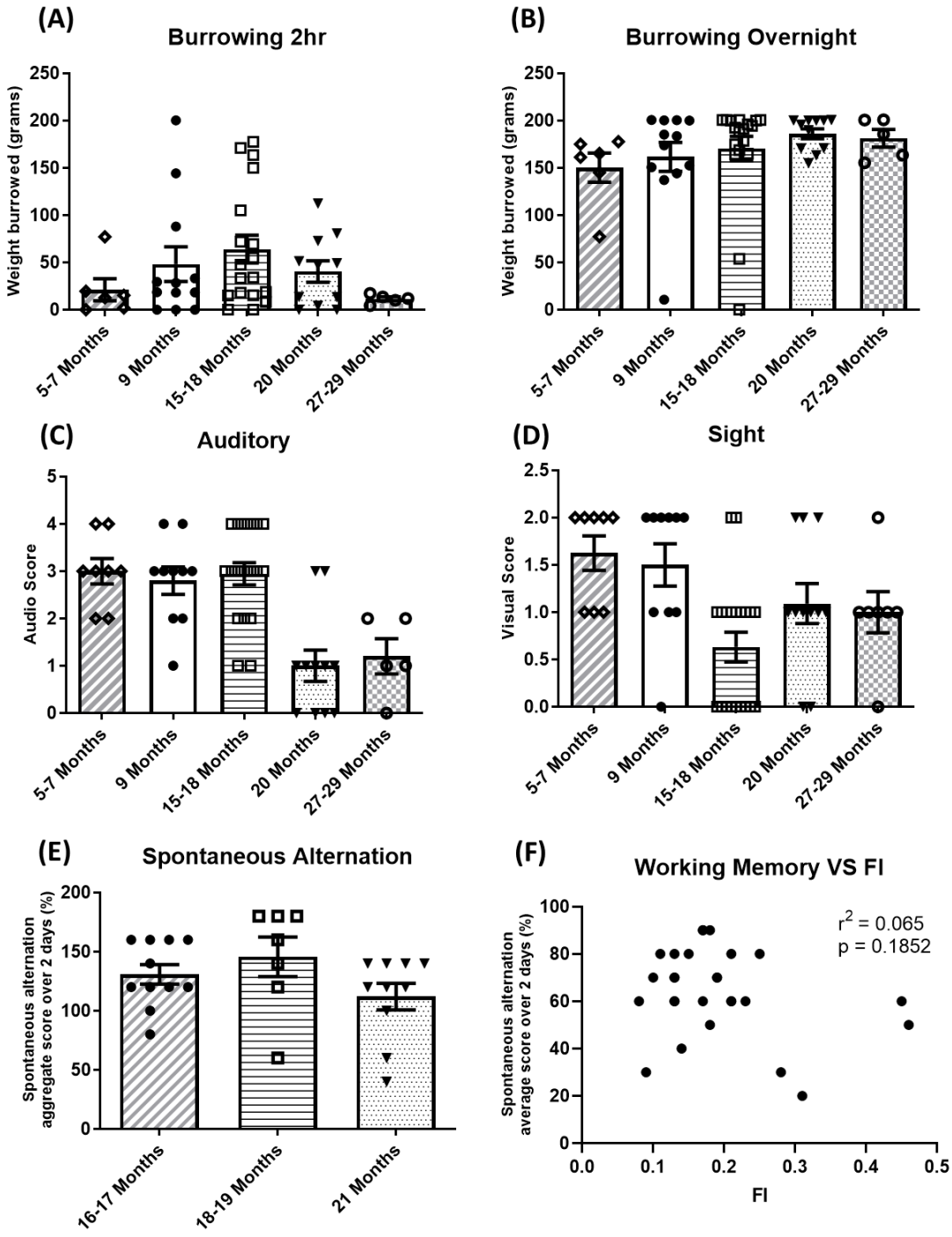

Figure 4.7: **Trinity Frailty Index I burrowing, sensory acuity and cognition: Trinity Frailty Index I measures Burrowing 2hr (A) and Overnight (B), Auditory Acuity (C) and Menace Reflex Vision testing (D) and Reference Memory in a spontaneous alternation T maze assessment (E). All data represented by mean ± SEM, (n=8, 10, 13, 15, 6).**

Burrowing

Burrowing behaviour is a species-typical and apparently rewarding behaviour for mice which has been shown to be significantly decreased by acute illness and by neurodegeneration (Deacon 2006; Cunningham et al. 2009). As such, it was assessed in these animals for potential inclusion in this modified frailty index. After 2 hours of burrowing a rather low weight of food pellets was typically displaced but the overnight weight reveals that virtually all animals are motivated and capable to burrow the majority of the tube's contents **(Figure 4.7 A-B).** As the 2-hour scores were very low and the overnight scores failed to stratify the population to any significant degree, this task offered little value to the frailty index and was not included in the finalised frailty index.

Sensory Acuity Testing

Deterioration in hearing and sight are common age dependent deficits and as such a relevant measure of frailty. Firstly, the animals' sight was tested using the Menace (Poke) Test to determine whether the animal was blind in each eye or not **(Figure 4.7 D)**. Auditory acuity was tested by exposing the animals to a combination of tone intensities and frequencies **(Table 2.6)** and measuring their startle (freezing) response to the tone **(Figure 4.7 C)**.

Due to the limited number of potential scores for animals to achieve (0= both eyes impaired, 1=impaired in one eye, 2=vision fully intact) these data was highly variable across all ages but did show a broad trend toward decreasing auditory and visual acuity with age.

Spontaneous Alternation

Currently frailty indices utilising physiological measures alongside measures of cognition in a clinical setting are rarely used; despite the crucial aspect cognition plays in the clinical frailty syndrome. As such, for this novel frailty index one of the main queries was whether the frailty score assessed might correlate with cognition. To this end working memory was assessed in a dry T-maze as a measure of working memory in a sub-group of the whole cohort. Due to time constraints at the time of testing it was not feasible to conduct this assay on all animals and so it was decided to assay only animals older than 16 months of age as this is window in which frailty has been reported to begin to manifest (Kwak et al. 2020). It was found that there was a great degree of variability in the working memory scores of each age group **(Figure 4.7 E)**. When plotted against frailty no significant correlation was found by linear regression analysis however **(Figure 4.7 F).**

Frailty score calculation

Once the behavioural, physiological and metabolic component measures of the frailty index were finalised each animal was scored on each measure and a z-score of their performance compared to a mean control group of adult animals calculated as described in detail in section 2.2.4.1-3. Each animal could score a maximum of 1 for each measures z-score if they were greater than four standard deviations (SD) from the control groups score, 0.75 if three SD, 0.5 if two SD, 0.25 if one SD, 0 if <1 SD. They then received an overall frailty score from the average of all of these z-scores for each frailty measure as described in section 2.2.4.3 and shown in **Figure 4.8 A.** Prevalence of frailty was shown to increase significantly with age **(Figure 4.8 C)** and correlated strongly with age **(Figure 4.8 D)**. An animal with no deficits receives a Frailty index (FI) of 0 and an animal with maximal deficits would receive a value of 1. Typically, however, the highest FI possible are between 0.4-0.6 as any animal scoring greater than this would be severely unwell, indicative of moribundity and possibly close to the humane end point.

(A)

Animal ID	Age (m)	Temperature	Weight (g)	Glucose	Distance (cm)	Meander	Average Speed (m/s)	No. Of Rears	Audio	Sight	Screen	Grip	Exhausation	Frailty Score
158	29	0.75	0.00	0.00	0.25	0.00	0.00	0.50	0.25	0.25	1.00	0.00	0.15	0.26
160	29	0.25	0.00	0.00	0.50	0.00	0.25	0.50	0.50	0.75	0.25	0.00	0.30	0.28
166	28	0.50	0.00	0.00	0.25	0.25	0.25	0.50	0.75	0.75	0.25	0.00	0.30	0.32
167	28	0.75	0.00	0.00	0.50	0.00	0.50	0.50	0.25	0.75	0.75	0.00	0.40	0.37
168	28	1.00	0.25	0.00	0.00	0.00	0.00	0.50	0.50	0.75	0.50	0.00	0.05	0.30
1	22	0.50	0.00	0.50	0.75	0.00	1.00	0.50	0.75	0.25	0.00	0.00	0.85	0.43
2	22	0.25	0.00	0.50	0.00	0.00	0.00	0.00	0.50	0.00	0.25	0.00	0.00	0.13
3	22	0.25	0.25	0.00	0.25	0.00	0.00	0.00	0.75	0.25	0.50	0.00	0.00	0.19
4	22	0.25	0.50	0.25	0.25	0.25	0.00	0.25	0.75	0.00	0.00	0.00	0.05	0.21
5	22	0.25	0.50	0.25	0.50	0.00	0.00	0.50	0.50	0.25	0.75	0.00	0.25	0.31
6	22	0.25	1.00	1.00	0.50	0.25	0.00	0.50	0.75	0.00	1.00	0.00	0.10	0.45
188	22	0.25	0.50	0.00	0.25	0.00	0.00	0.00	0.50	0.25	0.25	0.50	0.10	0.22
189	22	0.00	0.50	0.25	0.25	0.00	0.50	0.25	0.00	0.75	0.25	0.50	0.55	0.32
191	21	0.50	0.00	0.00	0.00	0.00	0.00	0.00	0.50	0.25	1.00	0.50	0.05	0.23
192	21	0.50	0.00	0.50	0.25	0.25	0.00	0.00	0.50	0.25	0.00	0.50	0.25	0.25
193	20	0.50	0.25	0.00	0.00	0.00	0.25	0.00	0.00	0.75	0.75	0.00	0.15	0.22
197	19	0.00	0.25	0.00	0.00	0.00	0.00	0.00	0.00	0.75	0.00	0.50	0.00	0.13
198	19	0.00	0.25	0.25	0.00	0.00	0.00	0.00	0.25	0.25	0.00	0.50	0.10	0.13
199	19	0.00	0.00	0.25	0.50	0.25	0.00	0.25	0.00	0.75	0.00	0.50	0.10	0.22
203	19	0.00	0.25	0.25	0.00	0.00	0.00	0.00	0.50	0.75	0.25	0.00	0.00	0.17
209	19	0.00	0.25	0.00	0.00	0.00	0.25	0.25	0.00	0.25	0.50	0.50	0.30	0.19
211	18	0.00	0.00	0.00	0.50	0.00	0.00	0.00	0.00	0.75	0.00	0.00	0.05	0.11
214	18	0.00	0.25	0.00	0.75	0.00	0.00	0.00	0.00	0.25	0.00	0.00	0.00	0.10
219	18	0.00	0.25	0.25	0.25	0.25	0.00	0.25	0.00	0.00	0.25	0.50	0.00	0.17
220	18	0.00	0.25	0.25	0.00	0.00	0.00	0.00	0.00	0.75	0.25	0.50	0.15	0.18
221	18	0.50	0.25	0.00	0.50	0.00	0.00	0.00	0.00	0.25	1.00	0.50	0.00	0.25
223	18	0.00	0.00	0.25	0.00	1.00	0.25	0.25	0.00	0.75	0.25	0.50	0.20	0.29
224	18	0.00	0.50	0.00	0.25	0.00	0.00	0.25	0.00	0.25	0.25	0.50	0.05	0.17
225	18	0.00	0.25	0.25	0.25	0.00	0.00	0.25	0.00	0.25	0.50	0.50	0.05	0.19
226	18	0.00	0.25	0.75	0.25	0.00	0.00	0.25	0.00	0.75	0.00	0.50	0.25	0.25
227	17	0.00	0.00	0.00	0.75	0.25	0.00	0.25	0.25	0.00	0.00	0.50	0.00	0.17
228	17	0.00	0.25	0.00	0.00	0.00	0.00	0.25	0.25	0.75	0.00	0.00	0.00	0.13
229	17	0.25	0.25	0.00	0.25	0.00	0.00	0.25	0.50	0.25	0.00	0.00	0.25	0.17
230	17	0.25	0.25	0.00	0.75	0.00	0.00	0.25	0.00	0.25	0.25	0.00	0.15	0.18
1	10	0.25	0.25	0.25	1.00	0.25	0.00	0.00	0.00	0.00	0.00	0.00	0.00	0.17
2	10	0.00	0.00	0.00	0.25	0.00	0.00	0.25	0.25	0.25	0.00	0.00	0.10	0.09
3	10	0.25	0.00	0.00	0.00	0.50	0.00	0.00	0.25	0.00	0.00	0.25	0.00	0.10
4	10	0.25	0.00	0.25	0.00	0.00	0.25	0.00	0.00	0.00	0.25	0.00	0.15	0.10
5	10	0.00	0.00	0.00	1.00	0.25	0.00	0.25	0.00	0.00	0.25	0.00	0.00	0.15
6	10	0.00	0.00	0.25	0.50	0.00	0.00	0.25	0.00	0.25	0.00	0.00	0.00	0.10
7	10	0.00	0.25	0.00	0.25	0.00	0.00	0.25	0.00	0.00	0.00	0.00	0.05	0.07
8	10	0.00	0.00	0.00	0.00	0.00	0.00	0.25	0.00	0.25	0.00	0.00	0.00	0.04
9	10	0.00	0.00	0.00	0.00	0.00	0.00	0.25	0.00	0.00	0.00	0.00	0.00	0.02
10	10	0.00	0.00	0.00	0.50	0.00	0.00	0.00	0.00	0.75	0.00	0.00	0.00	0.10
267	8	0.00	0.00	0.00	0.25	0.00	0.00	0.25	0.25	0.00	0.00	0.00	0.00	0.06
268	7	0.25	0.00	0.25	0.00	0.00	0.00	0.00	0.00	0.00	0.00	0.00	0.05	0.05
270	6	0.00	0.25	0.00	0.25	0.00	0.00	0.25	0.25	0.00	0.00	0.00	0.05	0.09
271	6	0.00	0.00	0.00	0.25	0.00	0.25	0.00	0.00	0.25	0.00	0.00	0.15	0.08
272	6	0.00	0.00	0.25	0.00	0.00	0.00	0.00	0.00	0.00	0.00	0.00	0.05	0.03
273	6	0.25	0.00	0.00	0.25	0.25	0.25	0.00	0.00	0.00	0.00	0.00	0.15	0.10
274	6	0.00	0.00	0.25	0.00	0.00	0.00	0.25	0.00	0.25	0.00	0.00	0.00	0.06
275	6	0.00	0.25	0.25	0.00	0.00	0.00	0.00	0.00	0.25	0.00	0.00	0.15	0.08

Frailty Score	
0 - 0.09	
0.1-0.19	
0.2-0.29	
0.3-0.5	

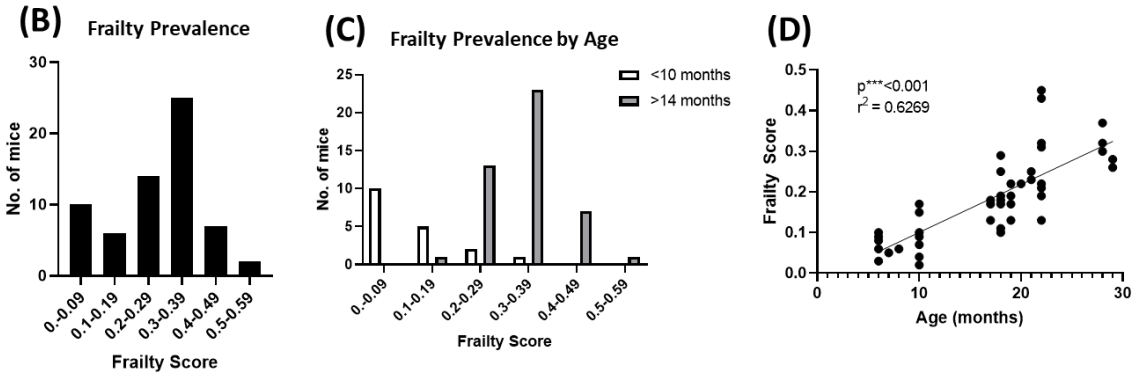

Figure 4.8: **Individual frailty scores and prevalency of frailty: (A) summary table of each animal's individual frailty measures z-score and overall cumulative frailty score (n=53) (B) Prevalency of frailty scores in the total population and (C) broken down into young (<10 months, n=19) and aged (>16 months, n=34). (D) Linear assessed by Pearson linear regression analysis of correlation of age in months against individualised frailty scores.**

4.2.2.2 Systemic inflammation and metabolism better predicted by frailty

Having developed this novel frailty index and applied it to the current cohort of 53 animals, it was then possible to assess blood and brain markers relevant to frailty and examine their relationship with the frailty scores as measured here.

Relationship between systemic inflammation, metabolites and age or frailty

As discussed previously, in this text the phenomenon of inflammaging predicts that with increasing age there is an increased state of basal inflammation in the ageing animal. Furthermore several pro-inflammatory cytokines have been proposed as serological markers of frailty in humans, including TNFα, IL-6 (Collerton et al. 2012) and CCL2 (MCP-1) (Ng et al. 2015). As such levels of these proteins were assessed in blood plasma collected from animals in this cohort at time of euthanisation and assessed against their age and frailty score in order to further validate our frailty scale and determine whether age or frailty might better predict the extent of basal inflammation with age. Frailty proved a stronger predictor of CCL2 protein levels in the blood than did age **(Figure 4.9 C, F, I).** Surprisingly, despite the observed CCL2 relationship, TNFα levels appeared inversely correlated with increasing age and frailty **(Figure 4.9 B, E, H)**. Although this correlation was contrary to previous findings in human frailty studies (Ng et al. 2015; Mitnitski et al. 2015) it must be added that only a small number of samples showed detectable TNF-α so the significance of this negative correlation is debatable. Although showing a positive correlation with age, IL-6 was also undetected in the majority of samples **(Figure 4.9 A, D, G)**. Rodent ageing studies have previously reported negligible elevation with age for IL-6 and TNFα also (Xin et al. 2011).

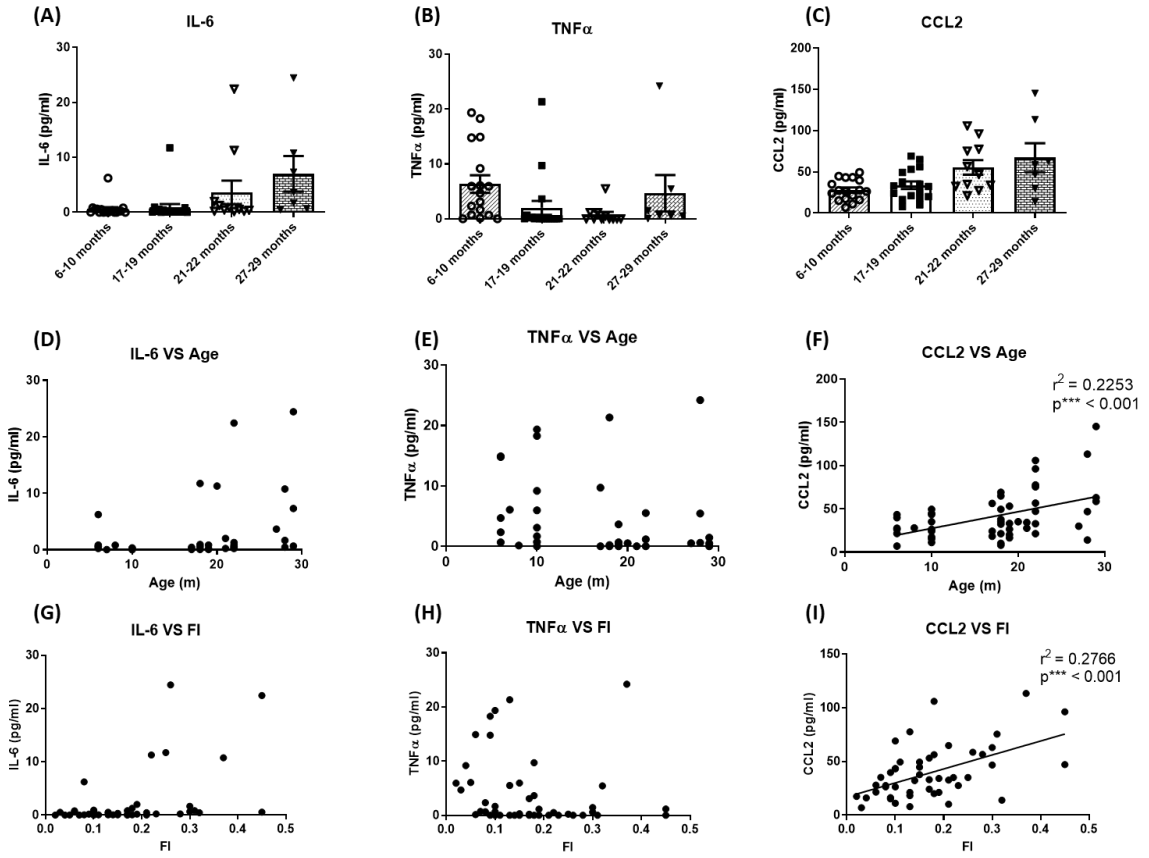

Figure 4.9 Predicting basal systemic inflammatory status by age or frailty: Frailty better predicts serological basal expression of inflammatory cytokines and chemokines in young and aged animals. Serological expressoin of IL-6 (A) (D) (G) and TNFα (B) (E) (H) and CCL2 (C) (F) (I) was assessed by ELISA against age and frailty score. Correlation by Pearson linear regression analysis, (n = 53), significance denoted by *p<0.05, **p<0.01, ***p<0.001.

Metabolic measures are better predicted by frailty than age

Assessment of all frailty index components and behavioural measures revealed that all measures associated with metabolic status (i.e. body weight, body core temperature and glucose levels) were better predicted by frailty than age when assessed by linear regression analysis. In each case, the frailty score was adjusted so as not to include the component being assessed.

Glycaemic status was assessed by testing atrial blood directly from the heart at time of euthanisation using a glucometer and was found to be weakly correlated with age (*$p<0.05$; $r^2 = 0.09$) **(Figure 4.10 C).** As with the majority of measures assessed, substantial variability was observed in the 15-21-month-old animals while 29-month-old animals were surprisingly consistent and displayed slightly lower levels than 5-7-month young animals. When stratified by frailty, glycaemic status found to be far more strongly predicted by frailty than by age (***$p<0.001$; $r^2 = 0.1500$) **(Figure 4.10 D).** The inverse was shown when serological levels of insulin were tested by ELISA with age failing to show any significant correlation with insulin concentration ($p=0.321$; $r^2 = 0.0185$) with substantial variability in 15-21-month-old animals while 29-month-old animals were comparatively and consistently hypoinsulinaemic **(Figure 4.10 A)**. In contrast, as was shown with glycaemic status, serological insulin levels exhibited a significant positive correlation with frailty (**$p<0.01$; $r^2 = 0.1806$) **(Figure 4.10 B).** As frailty increases animals tended to become hypoglycaemic and commensurately exhibited hyperinsulinemia and as such a weak positive correlation was found between insulin and glucose levels (**$p<0.01$; $r^2 = 0.1505$).

Blood insulin levels showed a trend toward elevated expression with age but were highly variable, notably in the 15–21-month age range but failed to achieve significance when age associated expression was assessed by simple linear regression analysis due to the oldest animals 27-29 exhibiting hypoinsulinemia. However, when stratified by frailty rather than age a strong positive correlation was found (**$p<0.01$; $r^2 = 0.1806$) **(Figure 4.10 A,B)**. An inverse relationship was found to be evident for glucose levels with a significant decreasing expression with age (*$p<0.05$; $r^2 = 0.09$) but a more robust fit to the line was found when stratified by frailty (**$p<0.1500$; $r^2 = 0.09$) **(Figure 4.10 C,D).**

Assessment of body weight revealed a very weak significant positive correlation with age (*p<0.05; r^2 = 0.097) but the population was better described by a non-linear gaussian regression (r^2 = 0.2829) with the highest body weights found in the 15–21-month age range, while animals aged further tended to decrease in body weight with the 27-28-month-old tending to be equivalent or lighter in weight than 5–9-month adult animals **(Figure 4.10 E).** However, when grouped by frailty this positive linear correlation was a significantly better fit to the line (***p<0.001; r^2 = 0.1688) **(Figure 4.10 F).**

Core body temperature assessed by rectal thermal probe as discussed in the previous section showed an overall trend towards reduction with age and substantial variability was evident in 15-20-month-old animals, while 27-29-month animals were evidently hypothermic **(Figure 4.96 E)**. Consistent with these observations, a Pearson linear regression analysis revealed a strong statistically significant negative correlation with age (***p<0.001; r^2 = 0.2257). Assessment of animals by their individualised frailty scores as opposed to age revealed a marginally stronger fit to the line with frailty (***p<0.001; r^2 = 0.2447) **(Figure 4.10 G, H).**

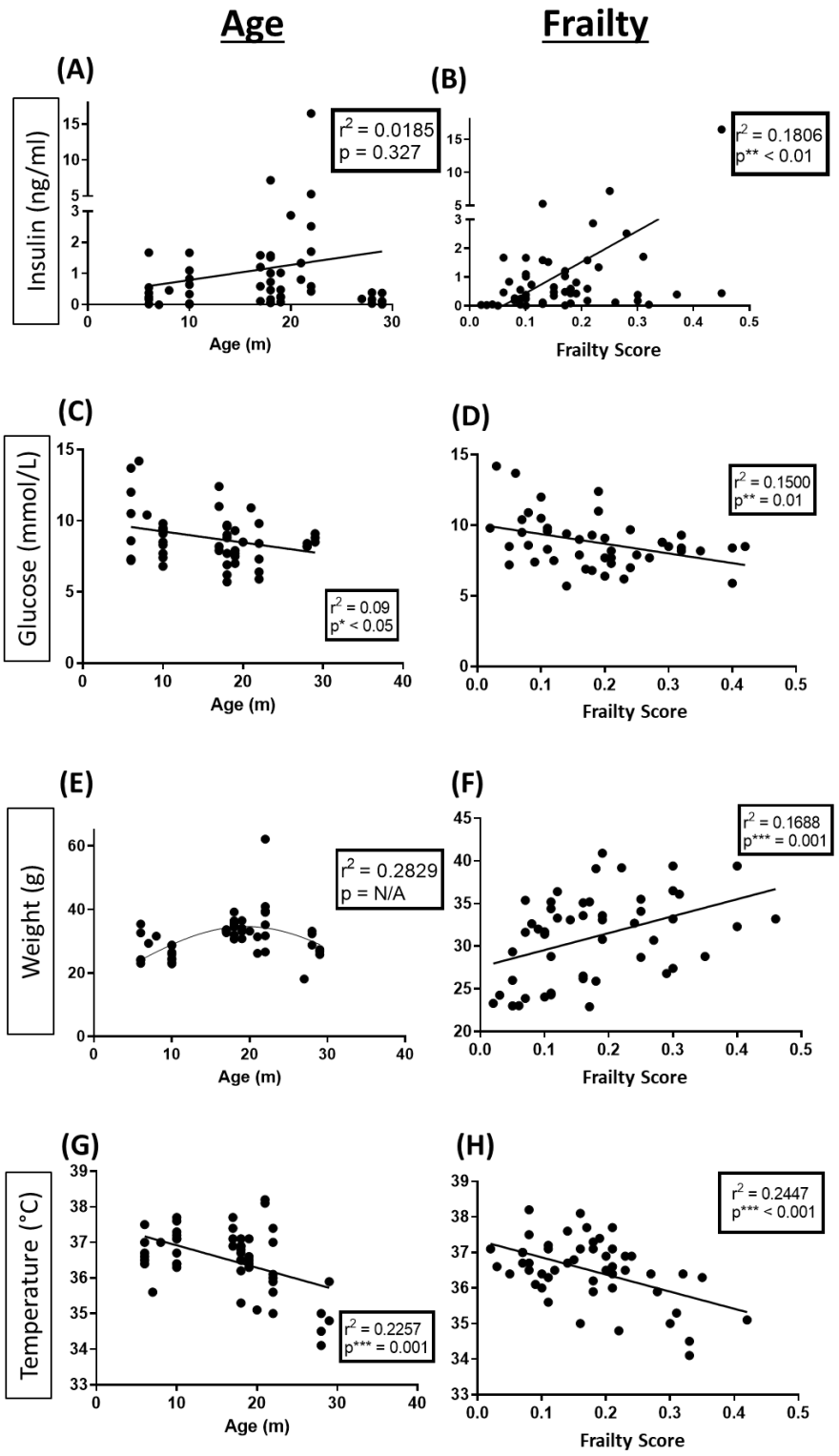

Figure 4.10 **Metabolic measures in aged animals across the frailty range: Insulin expression levels (A-B) in plasma were assessed by ELISA, glycaemic status (C-D) of atrial blood by glucometer, body weight (E-F) and core temperature (G-H) by rectal probe were plotted against age and frailty score (minus the respective component). Correlation by Pearson linear regressoin analysis, (n = 53), significance denoted by *p<0.05, **p<0.01, ***p<0.001.**

4.2.2.3 Regional heterogeneity in microgliosis with frailty

Given the heterogeneity in microglial markers observed with age (Chapter 3) and differences between the cerebrum and cerebellum (Chapter 4.2) the regional heterogeneity in neuroinflammatory responses with frailty (as calculated in the modified integrated phenotype model, "Trinity Frailty Index I" (TFL I)) were next interrogated. Quantitative PCR was performed upon cDNA isolated and synthesised from homogenates of dissected hippocampal, hypothalamic and cerebellar tissue.

The signature genes for microglial priming, *Clec7a* and *Cd11c* were assessed, and as expected from our previous findings, linear regression analyses showed that these two genes correlated strongly with age in all cases, with the exception of *Cd11c* in the hypothalamus **(Figure 4.11 D-F, J-L)** ($p<0.05$-0.001). Additionally, expression significantly correlated with frailty in all three regions **(Figure 4.11 A-C, G-I)**, albeit to a lesser degree than age (i.e. slightly weaker significance ($p<0.05$-0.01) and a poorer fit to the line of best fit (i.e. r^2)). The one exception once again was the hypothalamic expression of *Cd11c* which failed to achieve significance for either age ($p=0.7329$) or frailty ($p=0.3671$). These data indicate that microglial priming tracks with the frailty status of each animal as assessed and scored by our Trinity Frailty Index I. However, age is a stronger predictor of microglial priming than frailty.

Analysis of the microglial markers *Trem2* and *Tyrobp* revealed an interesting pattern of expression with age and frailty. In the hippocampus, *Tyrobp*, a marker of microglial population and a proxy for microglial numbers was significantly positively correlated with frailty (**$p<0.01$, $r^2=0.1688$) and even more strongly with age (***$p<0.001$, $r^2=0.2743$) **(Figure 4.12 A, D)** and that was true to a lesser degree in the cerebellum **(Figure 4.12 C, F)**. Conversely, there was a weak negative correlation between *Tyrobp* and age in the hypothalamus (*$p<0.05$, $r^2=0.08.99$) and a weak non-significant trend with frailty **(Figure 4.12 B, E).**

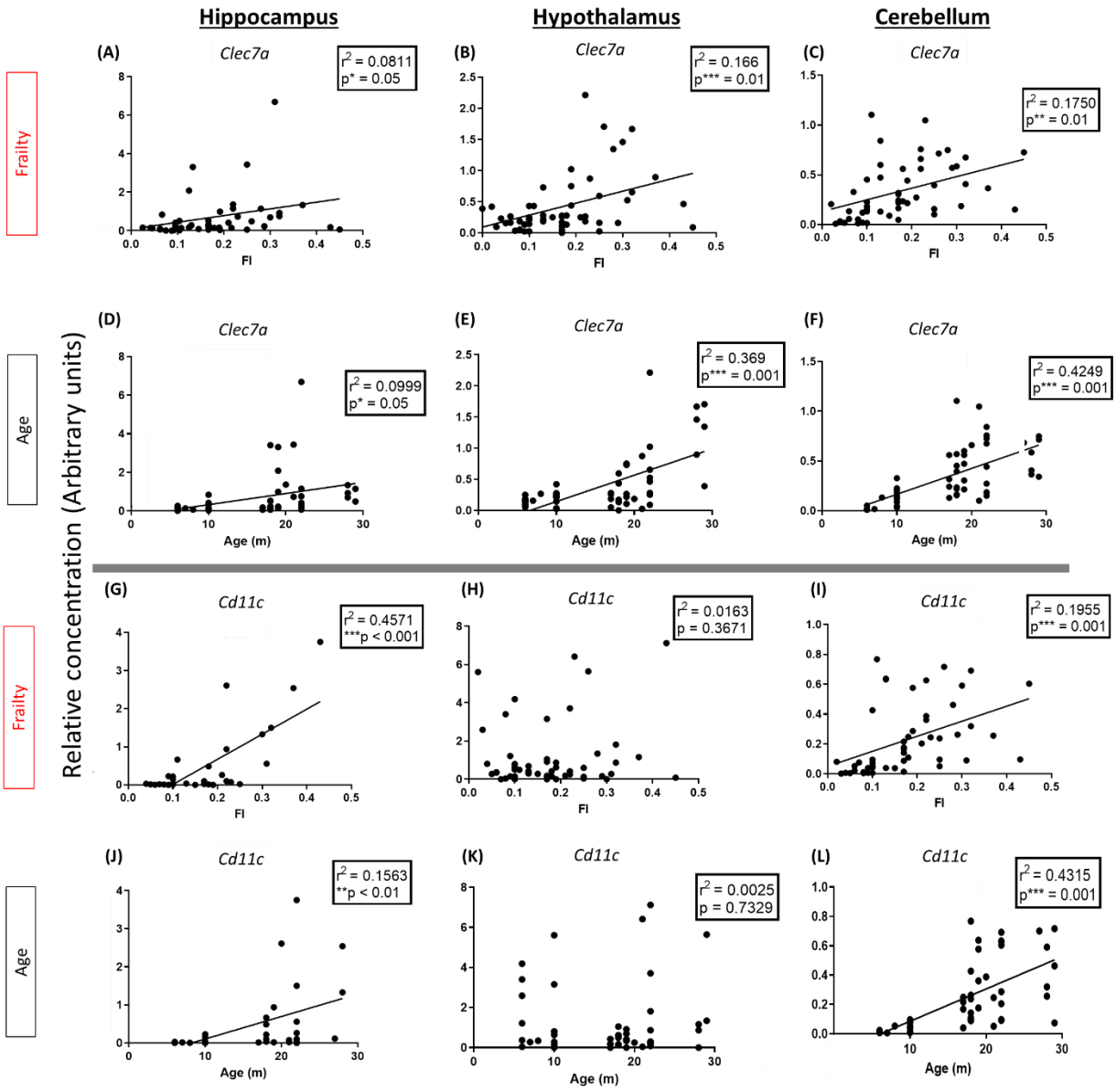

Figure 4.11: Correlation of brain microglial associated priming markers transcripts' expression with age and frailty: Correlation by Pearson linear regression analysis of microglial priming core transcriptomic signatures, (A-F) *Clec7a* and (G-L) *Cd11c*, gene expression assessed by qPCR and transcripts normalised to the housekeeping gene 18s, in the hippocampus, hypothalamus and cerebellum against Age (months) and Frailty Index score (FI), (n=53) *p<0.05, **p<0.01, ***p<0.001 signifies significant difference.

Hippocampal *Trem2*, was neither significantly correlated with frailty nor age (p=0.3965; 0.2222 respectively) **(Figure 4.12 G, J)** and cerebellar *Trem2* was weakly correlated with age (**p<0.01, r^2=0.1183) but not frailty **(Figure 4.12 I, L).** Like *Tyrobp*, but unlike all other significant correlations found with age thus far the hypothalamic expression of *Trem2* was negatively correlated with both frailty (*p<0.05, r^2=0.086) and age (**p<0.01 r^2 =0.1604) **(Figure 4.12 H, K)**.

Investigation into the expression of the complement system with age and frailty revealed that *C3* mirrored the pattern of expression observed for the microglial markers *Trem2* and its signalling partner *Tyrobp* in the hypothalamus with a significant negative correlation (*p<0.05) with age and a broad trend toward decline observed when plotted against increasing frailty **(Figure 4.13 B, E)**. In contrast, the cerebellum demonstrated a strong significant positive correlation with increased expression in response to advancing age (***p<0.001, r^2 = 0.3722) and similarly a more scattered expression pattern but strong significant correlation with increasing frailty (**p<0.01, r^2 = 0.1686) **(Figure 4.13 C, F)**. The hippocampus did not show a significant correlation with age or frailty **(Figure 4.13 A, D)**. C1qα was also assessed in some regions and showed a slight tendency towards negative correlation in the hippocampus but was highly variable.

Taken together these data indicates increasing microglial activation with both advancing age and frailty in the hippocampus and cerebellum corroborating and elucidating observations made previously in the cumulative deficit frailty model regarding the incidence of linear and non-linear correlations with frailty. In contrast an unexpected negative correlation with advancing age and frailty was shown in the hypothalamus.

This is in sharp contrast to the strong correlation of the hypothalamus with expression of the microglial priming signature gene *Clec7a* which displayed strong significant increases in expression with age alongside those of the hippocampus and cerebellum. Notably though *CD11c,* the second of the microglial priming signature genes did not show any significant correlation with age or frailty in the hypothalamus (**Figure 4.11 H, K).**

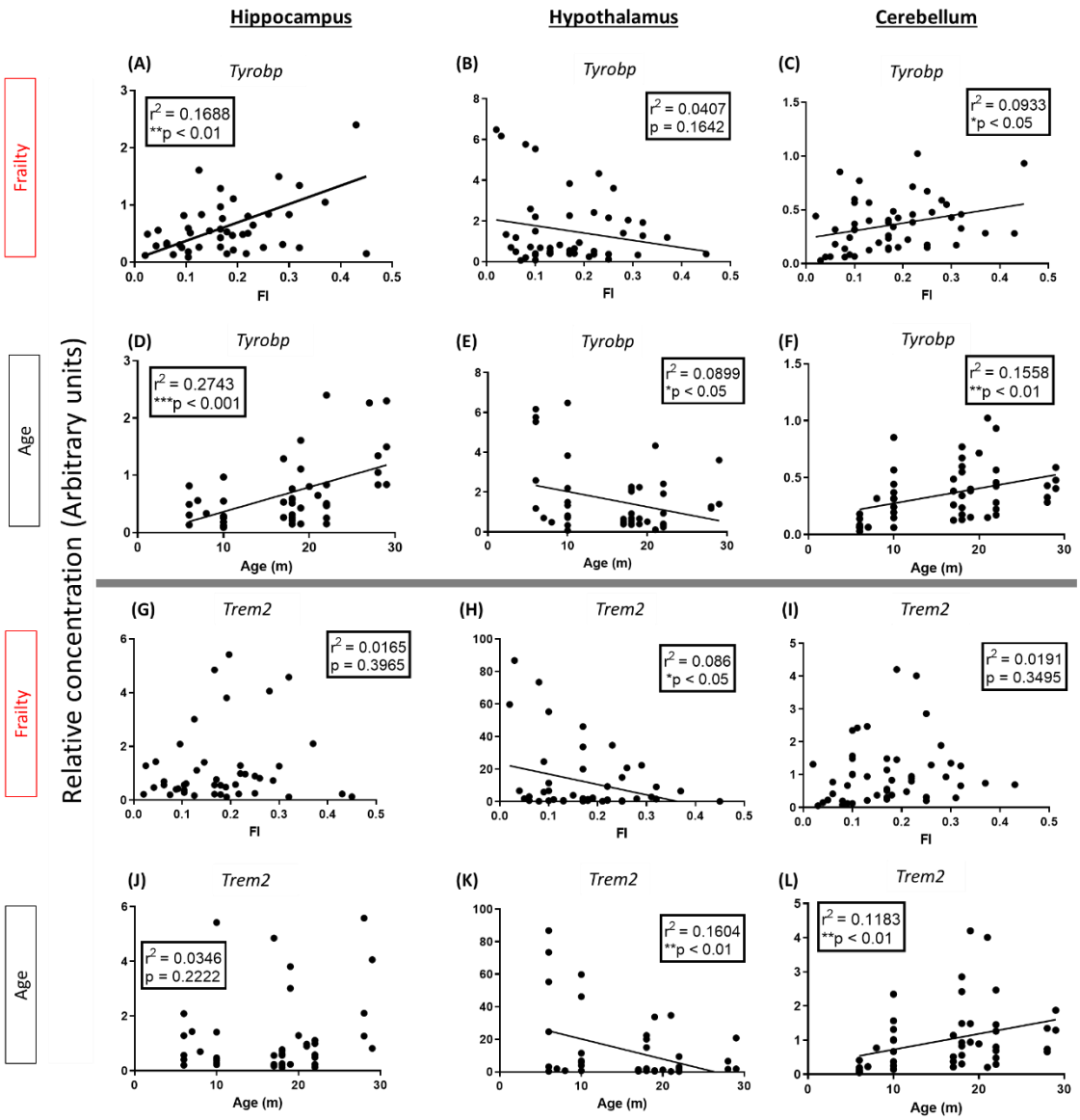

Figure 4.12: Correlation of brain microglial associated markers transcripts' expression with age and frailty: Correlation by Pearson linear regression analysis of microglial microglial activation and population markers (A-F) *Tyrobp* and (G-L) *Trem2*, gene expression assessed by qPCR and transcripts normalised to the housekeeping gene 18s, in the hippocampus, hypothalamus and cerebellum against Age (months) and Frailty Index score (FI), (n = 53) *p<0.05, **p<0.01, ***p<0.001 signifies significant difference.

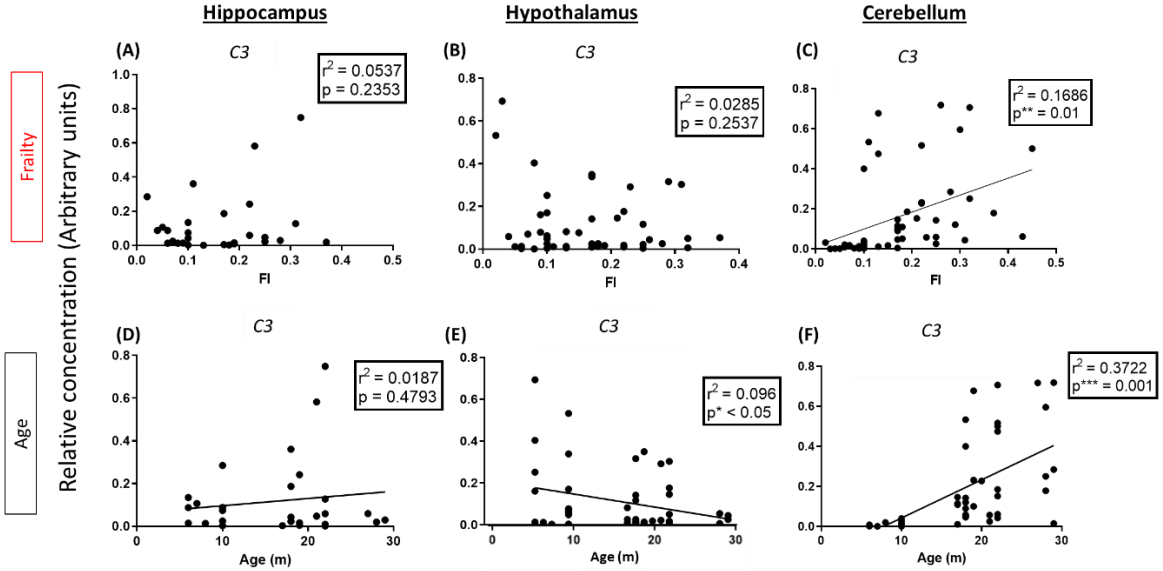

Figure 4.13: Correlation of brain complement system associated markers transcripts' expression with age and frailty: Correlation by Pearson linear regression analysis of microglial microglial activation and population markers (A-F) *C3*, gene expression assessed by qPCR and transcripts normalised to the housekeeping gene 18s, in the hippocampus, hypothalamus and cerebellum against Age (months) and Frailty Index score (FI), (n = 53) *p<0.05, **p<0.01, ***p<0.001 signifies significant difference.

Assessment of the growth factor genes *Bdnf* and *Igf1* and Transforming Growth Factor Beta 1 (*Tgfb*) revealed further region-dependent negative correlations. *Igf-1* in the hippocampus was not correlated with age or frailty **(Figure 4.14 A, D)**, whereas there was a significant negative association between hypothalamic *Igf1* and frailty (*p<0.05, r^2 = 0.132), and a stronger correlation with age (**p<0.01, r^2 = 0.2175) **(Figure 4.14 B, E).** Interestingly while age showed no significant correlation on *Igf1* expression in the cerebellum, assessment by frailty revealed a clear negative correlation (*p<0.05, r^2 = 0.079) **(Figure 4.14 C, F)**.

The expression of *Bdnf* showed negative correlations with both age and frailty in all three regions **(Figure 4.14 G-L)**. Although none of these correlations were particularly strong, they reveal that BDNF is decreasing with age and frailty across multiple brain regions. This was most obvious in the hypothalamus **(Figure 4.14 H, K).** In the case of the hippocampus and hypothalamus age was a stronger predictor than frailty but interestingly, as was observed for *Igf-1* in the cerebellum age failed to demonstrate any significant correlation with *Bdnf* expression whereas frailty classification did (*p<0.05, r^2 = 0.079) **(Figure 4.14 I, L).**

Transforming Growth Factor Beta (*Tgfb*), a pleiotropic growth factor gene known to have a role in cell differentiation, proliferation and apoptosis is also an established marker of cellular senescence and a serological marker in elderly frail individuals (Mitnitski et al. 2015). *Tgfb* was assessed against age and frailty and showed clear negative correlations with both age and frailty in both the hippocampus and in the cerebellum **(Figure 4.14 M, P, O, R)**. Within the hippocampus age was the stronger predictor (***p<0.001, r^2 = 0.2489) compared to frailty (**p<0.01, r^2 = 0.1676) **(Figure 4.14 M, P)**, while the cerebellum correlations were not substantially different for age or frailty **(Figure 4.14 O, R)**. Conversely, the hypothalamus showed positive correlations with both frailty and age **(Figure 4.14 N, Q)** and this was most prominent with frailty (***p<0.001; r^2 = 0.2009). Due to the pleiotropic nature of *Tgfb* this can be interpreted in several ways (see discussion).

These results taken alongside our previous findings on the microglial activation suggest that the cerebellum is the most reactive and vulnerable of the regions assessed with the highest microglial population and activation alongside reduced expression of microglial maintenance genes. Furthermore, the hypothalamus appears to be particularly susceptible to the effects of age and frailty with strong evidence of a downregulation of growth factor genes associated with neuronal maintenance as well as a reduction in microglial number and activation. This further corresponds with the robust increase in expression of *Tgfb* which is known to have a role in senescence.

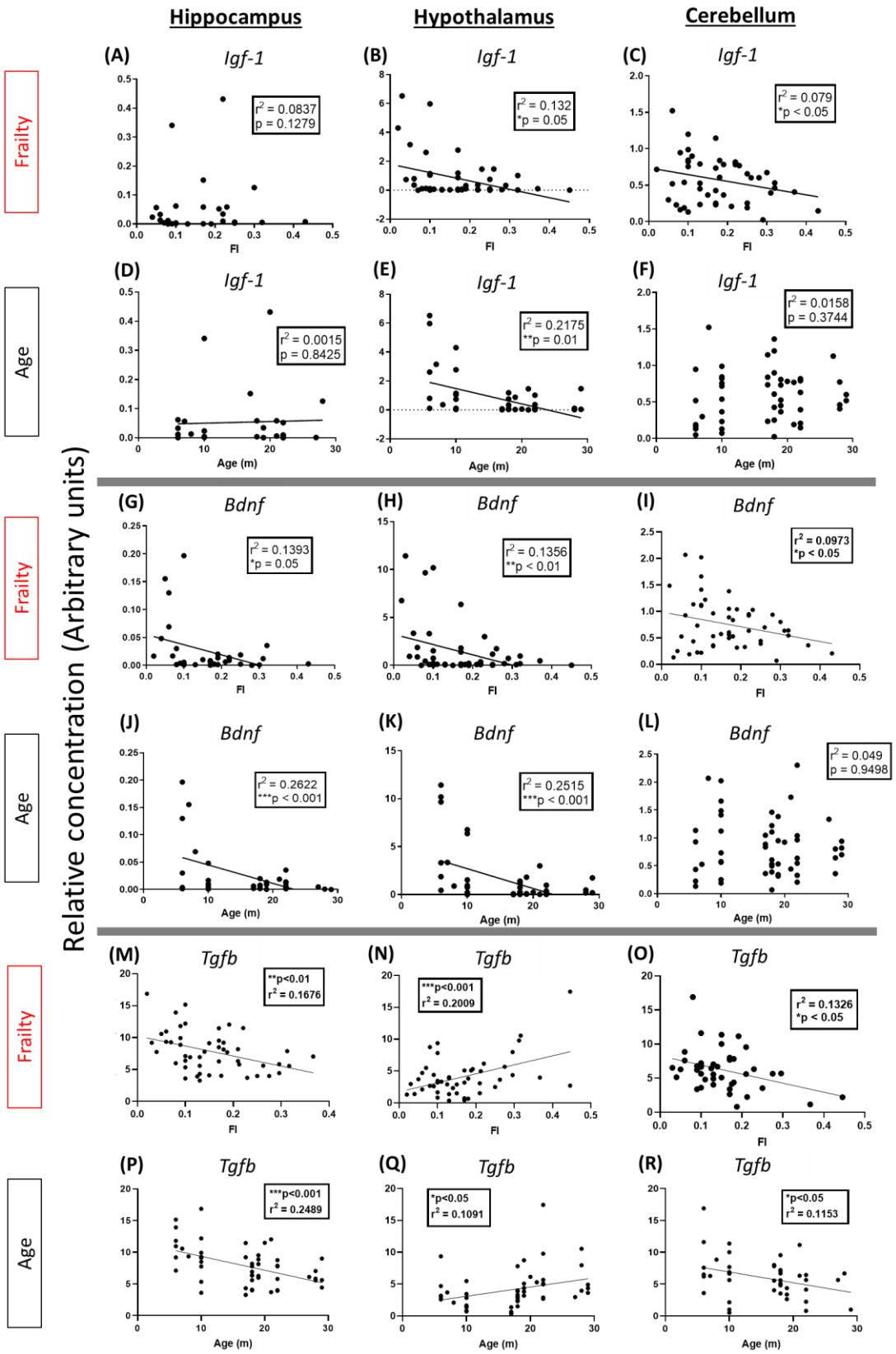

Figure 4.14: Correlation of brain microglial associated neuronal maintenance growth factor transcripts' expression with age and frailty: Correlation by Pearson linear regression analysis of microglial associated growth factor genes, *Igf1*, *Bdnf* and *Tgfb*, gene expression assessed by qPCR and transcripts normalised to the housekeeping gene 18s, in the hypothalamus and cerebellum against Age (months) and Frailty Index score (FI) , (n = 54) *p<0.05, **p<0.01, ***p<0.001 signifies significant difference.

Investigation into changes in transcription of inflammatory cytokines with frailty and age revealed poor correlation with age and frailty alike for the pro-inflammatory cytokines *Il1b* and *Tnfα*, similar to that which was observed in our previous analyses of the inflammatory state in the Dalhousie cumulative deficit frailty model. Expression of the pro-inflammatory cytokine *Il1b* revealed no significant correlation with either frailty or age in any of the three regions assessed **(Figure 4.15 A-F)**. In contrast, the hypothalamic expression of *Tnfα* was noteworthy as this region's pattern of expression with age I observed a significant negative correlation of *Tnfα* expression with age (*p<0.05, r^2=0.1063) **(Figure 4.15 K)** which corresponds with our previous observations of reduced microgliosis in this region. Once again, the cerebellum showed a robust positive correlation with age (**p<0.01, r^2=0.1506) as well as with frailty (**p<0.01, r^2 = 0.1907) **(Figure 4.15 L)**. The hippocampus showed a broad trend toward a positive relationship with age and frailty but failed to achieve statistical significance correlation **(Figure 4.15 G & J)**.

Analysis of the chemokines *Cxcl13* and *Ccl2*, known serological markers of frailty (Ng et al. 2015), revealed robust positive correlations with both age and frailty for all regions assessed. In the case of *Ccl2* age was a better predictor of *Ccl2* than was frailty (higher r^2 values with age compared to frailty indicating a tighter fit to the line of best fit estimated by the linear regression analysis) **(Figure 4.16 G-L).** *Cxcl13* expression may be slightly better predicted by frailty over age, but these metrics of age are effectively equivalent in all but the cerebellum which exhibited a better fit to the line with frailty (**p<0.01, r^2=0.2853) than age (*p<0.05, r^2 =0.1625) **(Figure 4.16 A-F).**

By contrast, analysis of the expression levels of the chemokine *Cxcl10* revealed no significant correlation within the hypothalamus **(Figure 4.17 B, E)** or hippocampus **(Figure 4.17 A, D)** with age and frailty. Once more, the cerebellum exhibited the strongest expression of the pro-inflammatory chemokine with age as well as with frailty (**p<0.01, r^2 =0.1989) with a slightly stronger correlation with age over frailty (*p<0.05, r^2 = 0.1412) **(Figure 4.17 C & F)**.

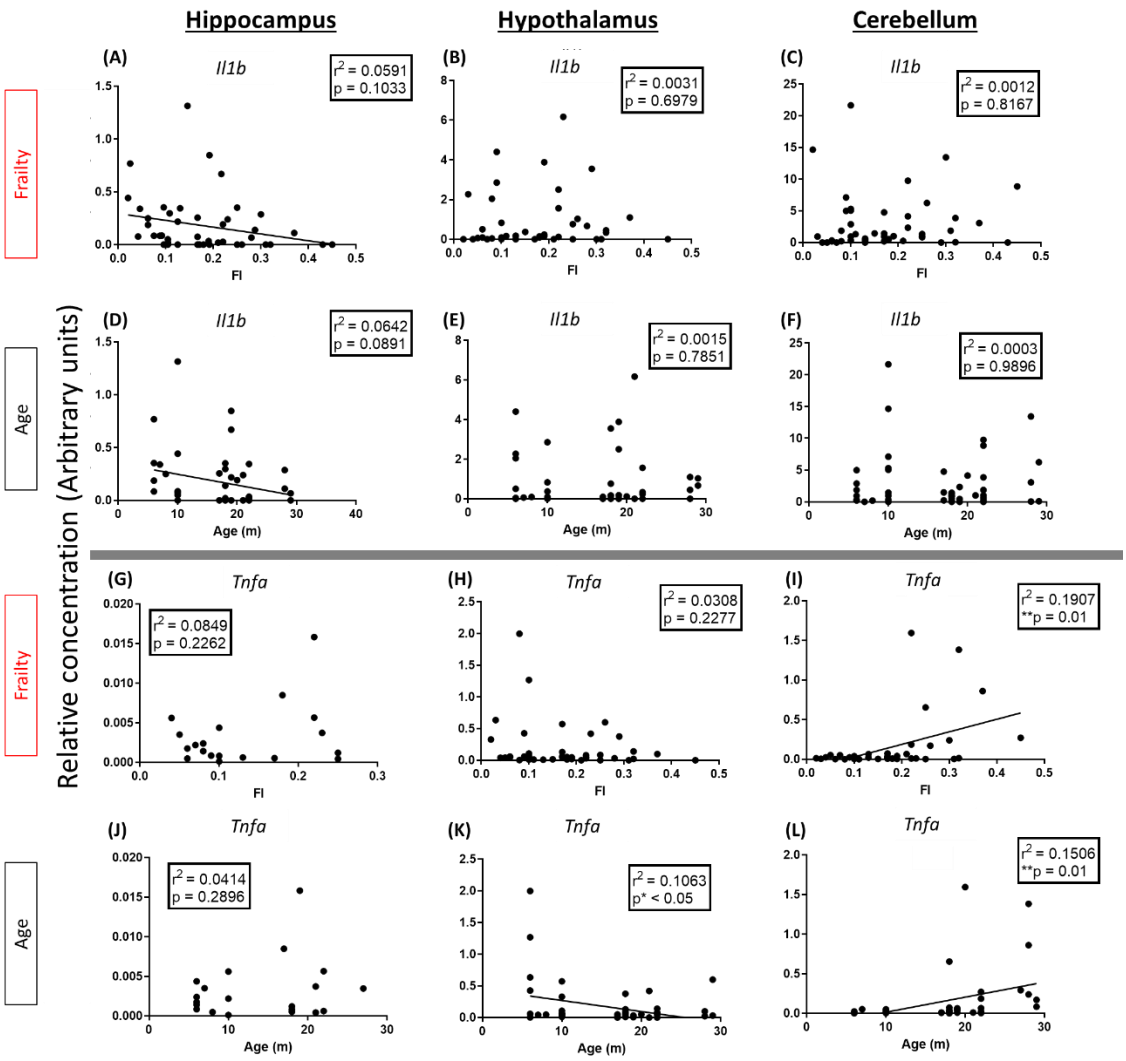

Figure 4.15: Correlation of brain pro-inflammatory cytokines transcripts' expression with age and frailty: Correlation by Pearson linear regression analysis of the pro-inflammatory cytokines, (A-F) *Il1b* and (G-L) *Tnfα*, gene expression assessed by qPCR and transcripts normalised to the housekeeping gene *18s*, in the hippocampus and hypothalamus against Age (months) and Frailty score (FI), (n = 53) *p<0.05, **p<0.01, ***p<0.001 signifies significant difference.

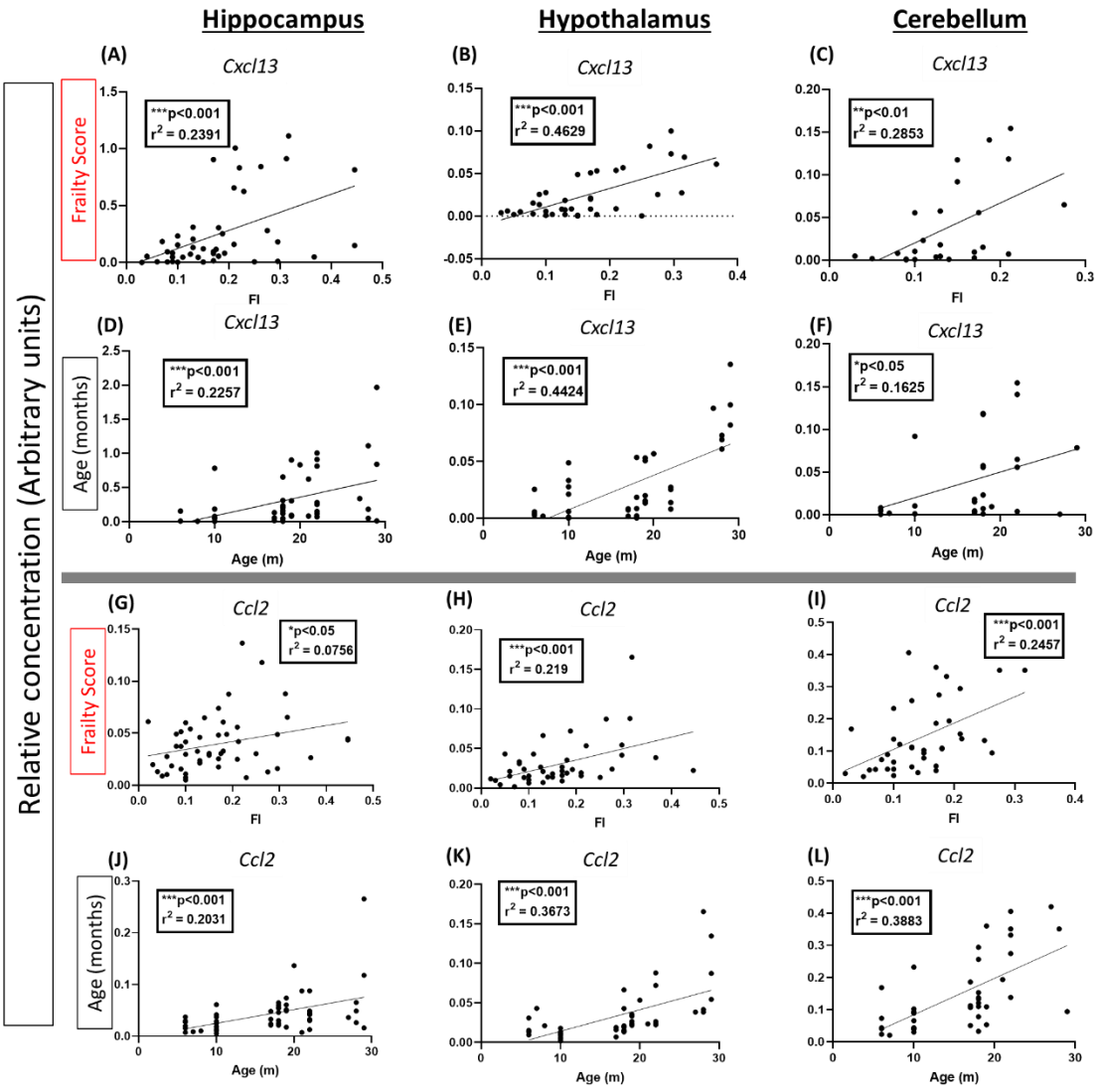

Figure 4.16: Correlation of brain pro-inflammatory chemokines transcription with age and frailty: Correlation by Pearson linear regression analysis of the chemokines (A-F) *Cxcl13* and (G-L) *Ccl2*, gene expression assessed by qPCR and transcripts normalised to the housekeeping gene *18s*, in the hippocampus and hypothalamus against Age (months) and Frailty score (FI) , (n = 53) *p<0.05, **p<0.01, ***p<0.001 signifies significant difference.

As discussed previously in this text, the interferon system is a vital part of the inflammatory response and *Irf7* is a strong marker of its activation in the diseased animal. Analysis of its transcriptomic expression revealed no significant effect of advancing age (p=0.1601) or frailty (p=0.3682) on its levels in the hippocampus **(Figure 4.17 G, J)** but did reveal a positive correlation in expression for both frailty and age (*p<0.05) in the cerebellum **(Figure 4.17 H, P)**. This is in keeping with our previous findings on microglial heterogeneity across the ageing brain with the microglial reactivity increasing as we move along the dorsal to ventral axis with the hippocampus showing little to no significant increase in pro-inflammatory cytokines, chemokines or interferon associated genes until challenged with an acute systemic insult. In contrast, the cerebellum shows a consistent increasing, robust inflammatory status with advancing age.

As discussed previously, *Il-10* is an anti-inflammatory cytokine implicated strongly in frailty and utilised in KO animal models of frailty. Unfortunately, however analysis of IL-10 expression in the hippocampus, hypothalamus and cerebellum failed to reveal any significant correlation with age or frailty in this cohort. IL-6 is another pleiotropic cytokine known to be involved in both pro and anti-inflammatory events depending on the situation but systemic expression has been shown to increase with advancing age in rodents (Xin et al. 2011), furthermore alongside its receptor IL-6R it is a known serological marker of frailty in humans (Song et al. 2010; Ng et al. 2015). Analysis of its expression across the ageing and frail brain revealed a weak positive correlation favouring frailty over age but significant for both in the hippocampus and hypothalamus but showed no significant relationship in the cerebellum.

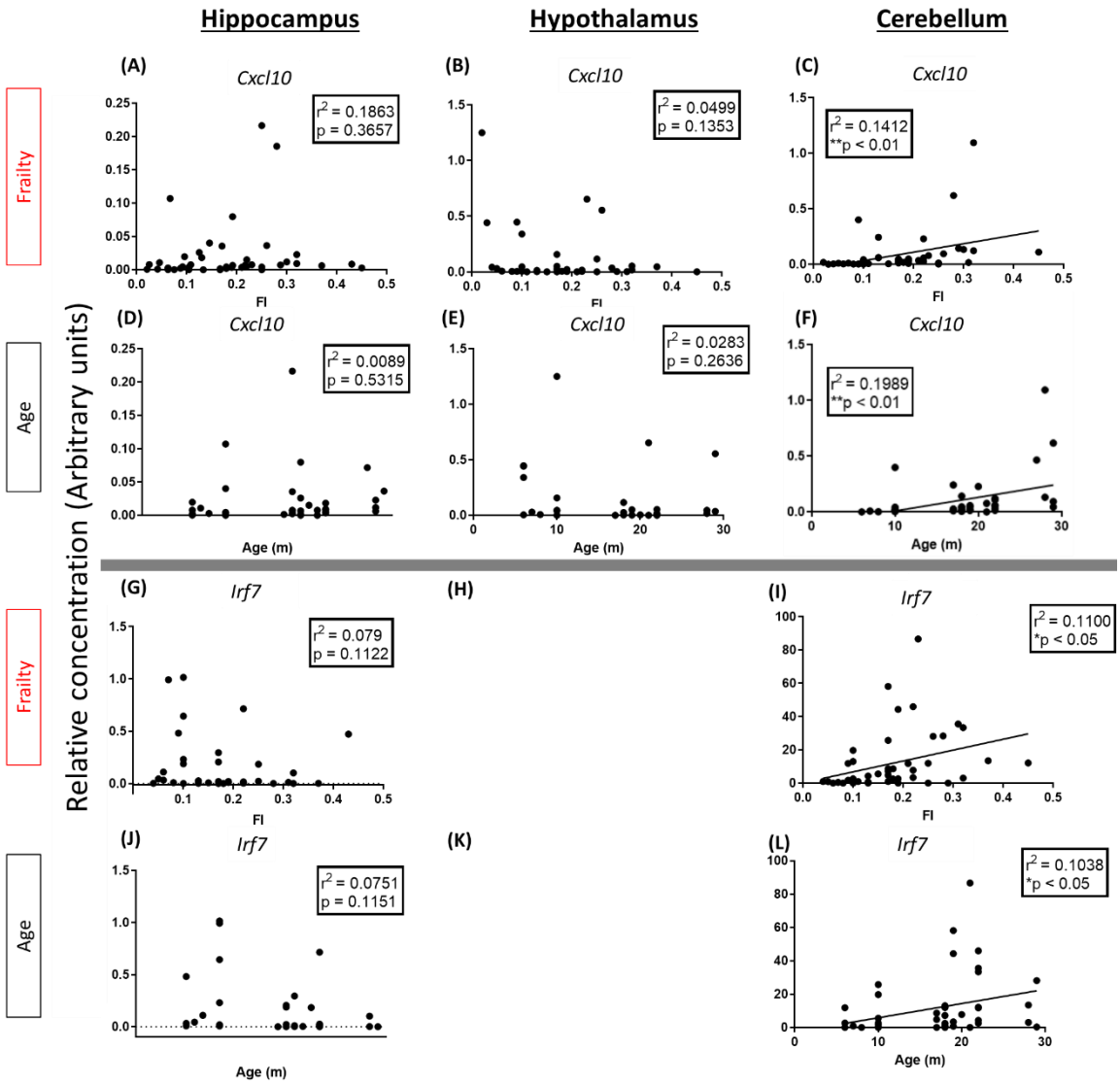

Figure 4.17: Correlation of brain pro-inflammatory chemokine *Cxcl10* and type one interferon associated gene *Irf7* expression against age and frailty: Correlation by Pearson linear regression analysis of the chemokine (A-F) *Cxcl10* and (G-L) interferon associated gene *Irf7*, gene expression assessed by qPCR and transcripts normalised to the housekeeping gene *18s*, in the hippocampus, hypothalamus and cerebellum against Age (months) and Frailty score (FI) , (n = 53) *p<0.05, **p<0.01, ***p<0.001 signifies significant difference by simple linear regression.

4.2.2.4 Hypothalamic changes in senescence, autophagy and Dectin-1 associated signalling pathways

Given how often the hypothalamic transcripts expression differed from that in other brain regions, an additional panel was run focussing solely on the hypothalamus to probe the expression of genes indicative of altered autophagy or senescence and genes associated with Dectin-1 signalling in ageing and in frailty.

As has been discussed previously in this text, Dectin-1, the receptor protein encoded by the gene *Clec7a*; is one of the core hub genes of the microglial priming signature and has been shown in the current work, to be robustly associated with age and to a lesser degree with frailty across several frailty indices and multiple brain regions. Therefore, Dectin-1 signalling is an area of potential pathogenic importance. Although fungal β-glucan is the primary exogenous pathogenic molecular pattern recognised by Dectin-1, several endogenous molecules are under investigation for their role as ligands in the CNS for these pathways. These include annexins expressed on the surface of apoptotic cells (Bode et al. 2019), the astrocytic structural protein vimentin (Thiagarajan et al. 2013)and galectin 9 released by injured or stressed cells (Daley et al. 2017; Deerhake et al. 2021; Itoh et al. 2017). As described in section 1.2.4. of this text signalling can occur through two distinct pathways, a CARD9-dependent inflammatory and CARD9-independent neuroprotective pathway **(Figure 4.18)**. Furthermore, depending upon the timing, frequency and severity of challenge could result in immune tolerising (Lajqi et al. 2019) or training effects (Heng et al. 2021; Van der Meer et al. 2015). As such I set out to assess which Dectin-1 signalling pathway may be in effect in ageing and frail animals by assessing downstream products transcriptional signatures of each.

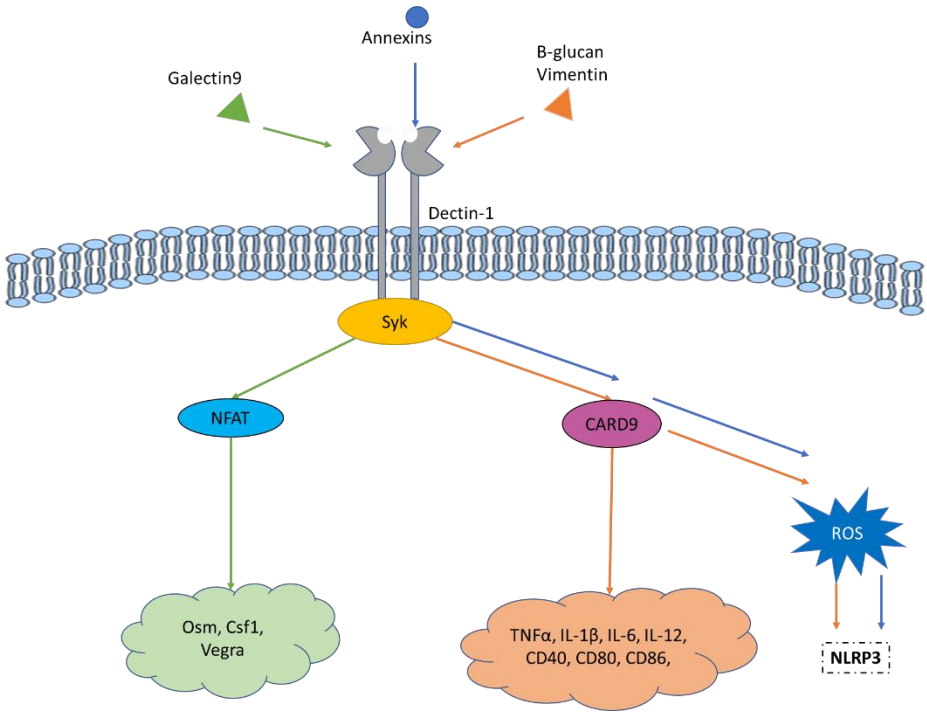

Figure 4.18 Simplified graphical representation of Dectin-1 signalling pathways in Dectin-1 expressing microglial and dendritic cells of the CNS adapted from (Deerhake et al. 2021; Bode et al. 2019; Thiagarajan et al. 2013; Tang et al. 2018)

While *Clec7a* transcript expression showed a robust increase with age **(Figure 4.19 D)**, and to a lesser degree frailty **(Figure 4.19 A)**, assessment of the CARD9 dependent downstream pro-inflammatory markers *Nlrp3, Il1b,* and *Tnfa* showed no commensurate increase. Rather *Nlrp3* signalling was found to be highly variable when plotted with age **(Figure 4.21 H)**, while plotting against frailty showed a significant negative linear correlation (*$p<0.05$, $r^2 = 0.079$) **(Figure 4.19 E)** indicating a suppression of pro-inflammatory pathways in the hypothalamus of frail animals. This was consistent with earlier qPCR analysis of the pro-inflammatory cytokines *Il1b* and *Tnfa* as discussed earlier in this section; with *Il1b* transcript expression showing no change with age or frailty **(Figure 4.19 F, I)** while *Tnfa* showed a significant age-associated reduction (* $p<0.05$, $r^2 = 0.1063$) and a broad negative trend with frailty **(Figure 4.19 G, J).** Taken together these data suggest that despite an increase in *Clec7a* gene transcript expression, there is no evidence of increased Dectin-1 signalling through its CARD9 dependent pathway at the transcriptional level, rather there is some evidence of a suppression of this pathway.

Recent work by Bode and colleagues has demonstrated that annexins upon apoptotic cells are capable of binding to Dectin-1 in dendritic cells and signalling through the PI3k-SYK pathway causing an increase in reactive oxidative species but no change in pro-inflammatory cytokine expression (Bode et al. 2019). Given the overall trend in reduced pro-inflammatory transcript levels demonstrated, I assessed Annexin A1 (*Anxa1)* transcript levels by qPCR to determine whether an upregulation in Annexins might be indicative of increased apoptosis which in turn might correlate with our observed increased *Clec7a* expression. Annexin A1 mRNA levels have been shown to increase leading to increased ANXA1 protein levels upon apoptotic cells in cancer and viral infection animal models, however, *Anxa1* showed no significant changes with either age or frailty **(Figure 4.19 B, D).** This suggests there is no significant increase in apoptosis at the transcriptional level.

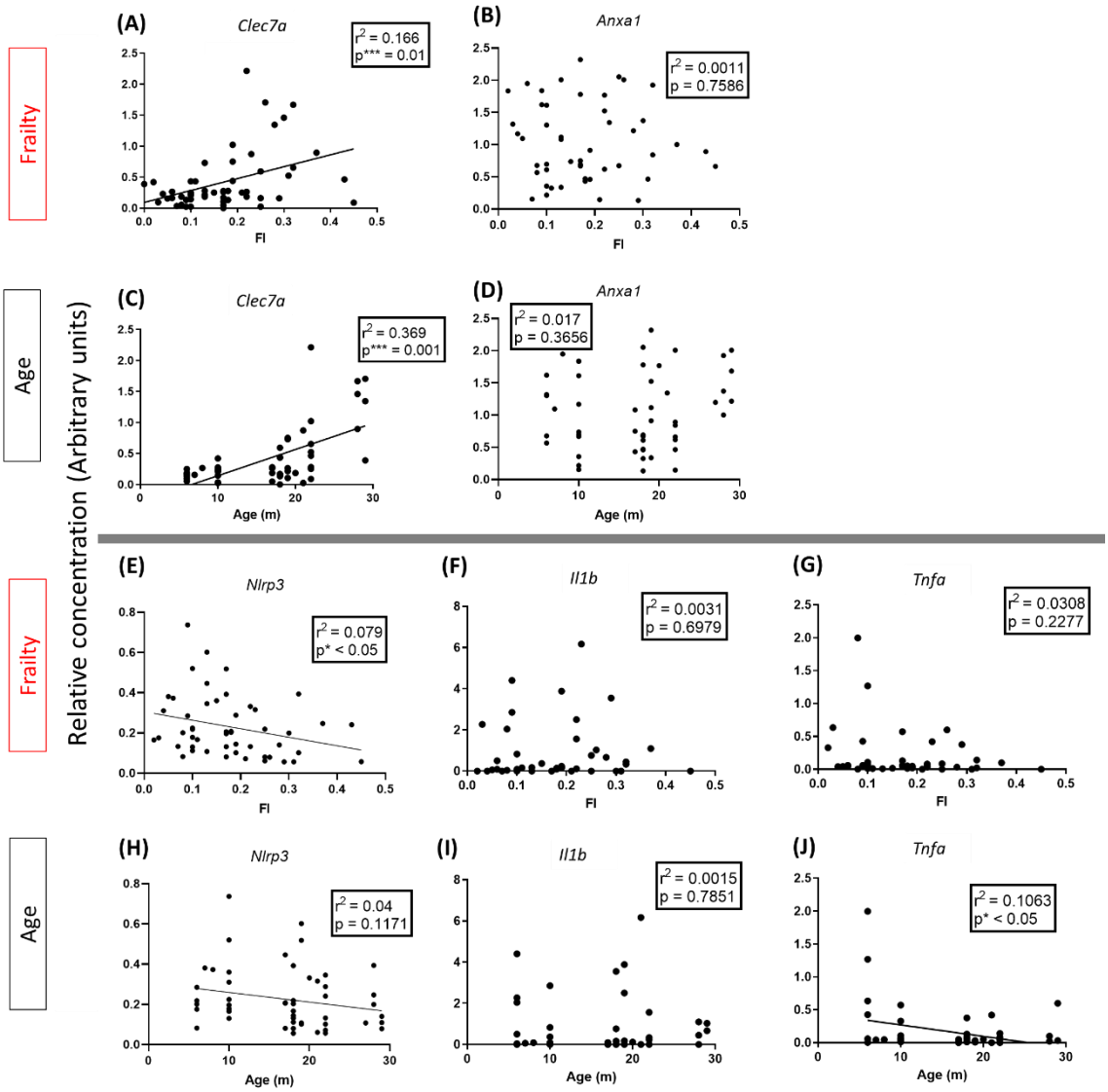

Figure 4.19: Correlation of brain hypothalamic CARD-9 independent Dectin-1 signalling pathway genes' expression with age and frailty in mice: Correlation by Pearson linear regression analysis of (A) (C) *Clec7a*, (B) (D) *Anxa1,* (E) (H) *Nlrp3*, (F) (I) *Il1b,* and (G) (J) *Tnfa*, gene expression assessed by qPCR and transcripts normalised to the housekeeping gene *18s*, in the hypothalamus against Age (months) and Frailty score (FI) , (n = 53) *p<0.05, **p<0.01, ***p<0.001 signifies significant difference by simple linear regression.

Given this lack of CARD9 dependent downstream markers **(Figure 4.19)** there is little evidence of the induction of this pro-inflammatory Dectin-1 response pathway. As such, in order to assess whether the upregulated gene transcript expression of *Clec7a* associated with age and frailty **(Figure 4.20 A, C)** in the hypothalamus is associated instead with the neuroprotective (CARD9-independent) Dectin-1 pathway response reported by Deerhake and colleagues (Deerhake et al. 2021) qPCR analysis of the reported CNS astrocytic produced, endogenous ligand, *Lgals9* was conducted alongside that for the resulting downstream microglial product *Osm* and its astrocytic receptor *OsmR*.

Lgals9 expression failed to show any statistically significant correlation with age or frailty **(Figure 4.20 B, D)** suggesting that while it has been reported to be an endogenous ligand of *Clec7a's* protein Dectin-1 (Daley et al. 2017; Deerhake et al. 2021) it is unlikely to be responsible for the robust increase in the neuroprotective cytokine expression of microglial *Osm* that is observed with both age (***$p<0.001$, $r^2=0.3098$) and frailty (**$p<0.01$, $r^2=0.1635$) **(Figure 4.20 E, G)**. The expression of *OsmR* does show a weak positive correlation with age (*$p<0.05$, $r^2=0.1113$) but shows no such correlation with frailty **(Figure 4.20 F, H)**. This may suggest that astrocytic produced Lgals9 is not the endogenous ligand triggering Osm expression by myeloid cells, rather perhaps alternative CNS ligands, might be responsible for this in ageing and frail animals and additional work would be required to probe this further.

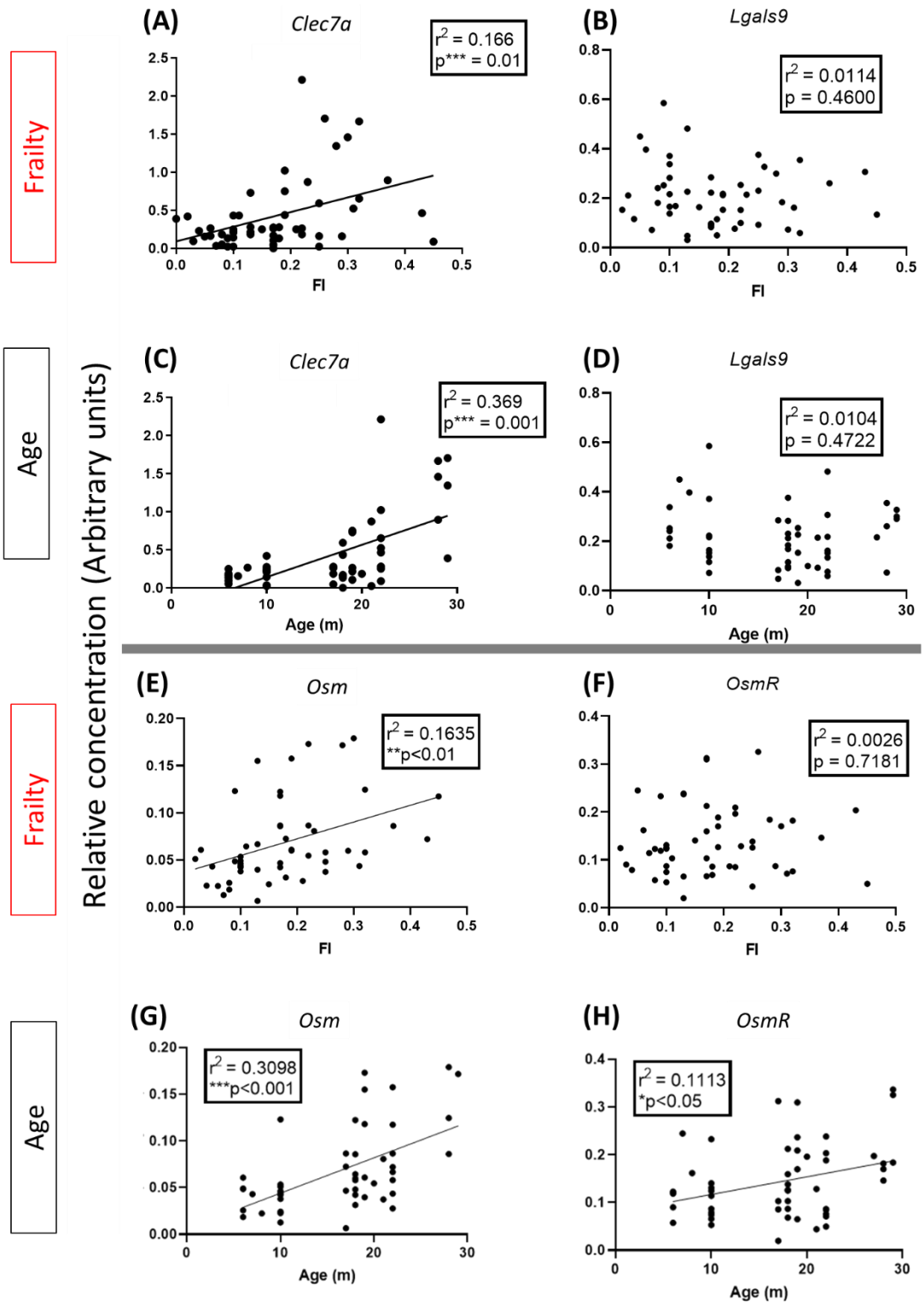

Figure 4.20: Correlation of brain hypothalamic CARD-9 independent Dectin-1 signalling pathway genes' expression with age and frailty in mice: Correlation by Pearson linear regression analysis of (A) (C) *Clec7a*, (B) (D) *Lgals9*, (E) (G) *Osm* and (F) (H) *OsmR*, gene expression assessed by qPCR and transcripts normalised to the housekeeping gene *18s*, in the hypothalamus against Age (months) and Frailty score (FI) , (n = 53) *p<0.05, **p<0.01, ***p<0.001 signifies significant difference by simple linear regression.

Furthermore, recent work by Ulland and colleagues has highlighted that autophagy is amplified in Trem2 $^{-/-}$ mice and that promoting Dectin-1 signalling can compensate for this excessive autophagy in microglia from *Trem2* $^{-/-}$ mice. In order to determine whether the robust correlation between *Clec7a* expression and advancing age and frailty **(Figure 4.20 A, C)** might be indicative of a compensatory Dectin-1 signalling for the reduced *Trem2* expression I observed in the hypothalamus as has previously been reported in Trem2 deficient mice by Ulland et al. (Ulland et al. 2017) I assessed transcriptional markers that might be indicative of autophagy: *p62* **(Figure 4.21 A, D)**, *Tfeb* **(Figure 4.21 B, E)**, and *Atg5* **(Figure 4.21 C, F)**. Pearson linear regression analysis revealed no clear relationship with either age or frailty. However, *Tfeb* and *Atg5* both showed the greatest degree of variability in mid aged and mid-frailty animals, after which expression levels declined.

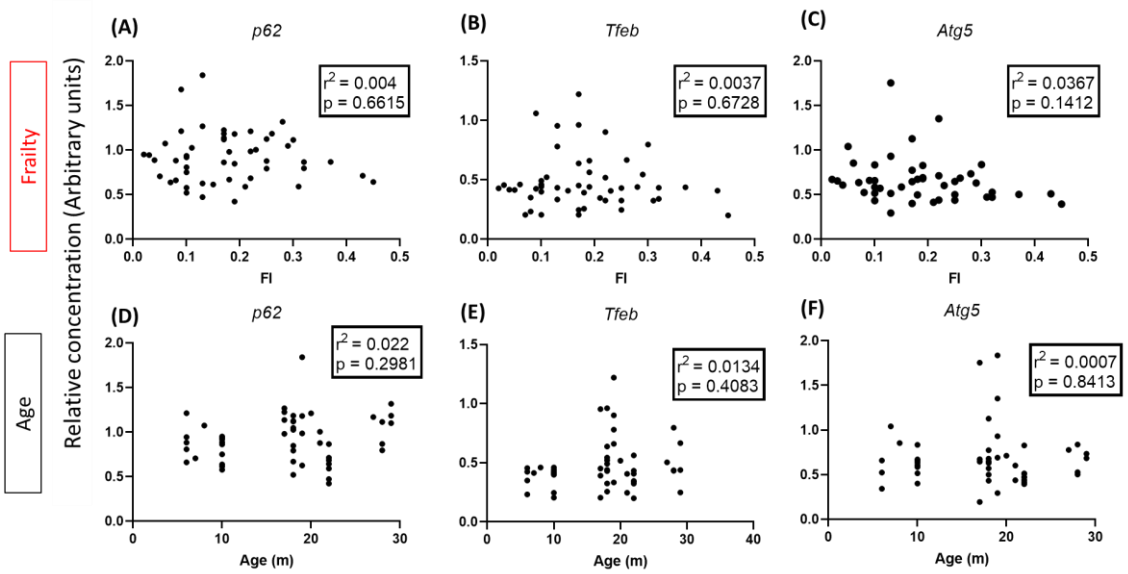

Figure 4.21: Correlation of brain hypothalamic autophagye associated genes' expression with age and frailty in mice: Correlation by Pearson linear regression analysis of (A) (D) *p62*, (B) (E) *Tfeb,* and (C) (F) Atg5, gene expression assessed by qPCR and transcripts normalised to the housekeeping gene *18s*, in the hypothalamus against Age (months) and Frailty score (FI) , (n = 53) *p<0.05, **p<0.01, ***p<0.001 signifies significant difference by simple linear regression.

Senescent cells accumulate during ageing (Adams, 2009; López-O*tín et al*, 2013), this is heavily associated with the Hayflick limit of cells (the point at which "replicative senescence" arrests cell division due to the shortening of telomere lengths with extensive cellular divisions (Hayflick 1965)) as a result of the unavoidable accumulation of cellular damage over the years. Analysis of *p16^{INK4a} (p16)* and *p21^{Cip1}(p21),* both known markers of senescence in ageing and DNA damage (Baker et al. 2011; Baker et al. 2008), revealed a significant correlation between upregulation of *p16* with advancing age (***p<0.001, r^2 =0.356) and, to a slightly lesser degree, with frailty (***p<0.001, r^2 =0.2414) **(Figure 4.22 B, D).** This is consistent with the existing literature documenting *p16^{INK4a}* as a senescence effector, driving pathology in ageing (Baker et al. 2008) and is consistent with the previous pattern of increasing expression with age and frailty observed for hypothalamic *Tgfb* a known senescence associated gene of the SASP (Katakura et al. 1999) **(Figure 4.22 A, C).** . In contrast *p21* **(Figure 4.22 E, G)** gene expression was found to have a broad non-significant trend toward increased expression with advancing age, consistent with reports of the close association between p16 and p21 expression due to the compensatory effect of p21 in preventing senescence and age-related pathologies *in vivo* alongside p53 and p19^{Arf} (Bake*r et al*, 2008; Baker, Weaver and VanDeursen, 2013). However no statistically significant linear relationship was found with *p21* gene transcript expression and frailty, indeed the highest expression levels and greatest variability occurred in mid-frailty animals and dropped to lower normal levels once more in the most severe frailty scores. While elevated TGF-β levels have been reported to drive *Pai1* expression, another member of the SASP secretome **(Figure 4.22 F, H)** it showed no statistically significant linear relationship with age or frailty in the hypothalamus. However, assessment by frailty did show a greater degree of variability in the mid frailty range (0.15-0.25) after which expression levelled off once more for p21.

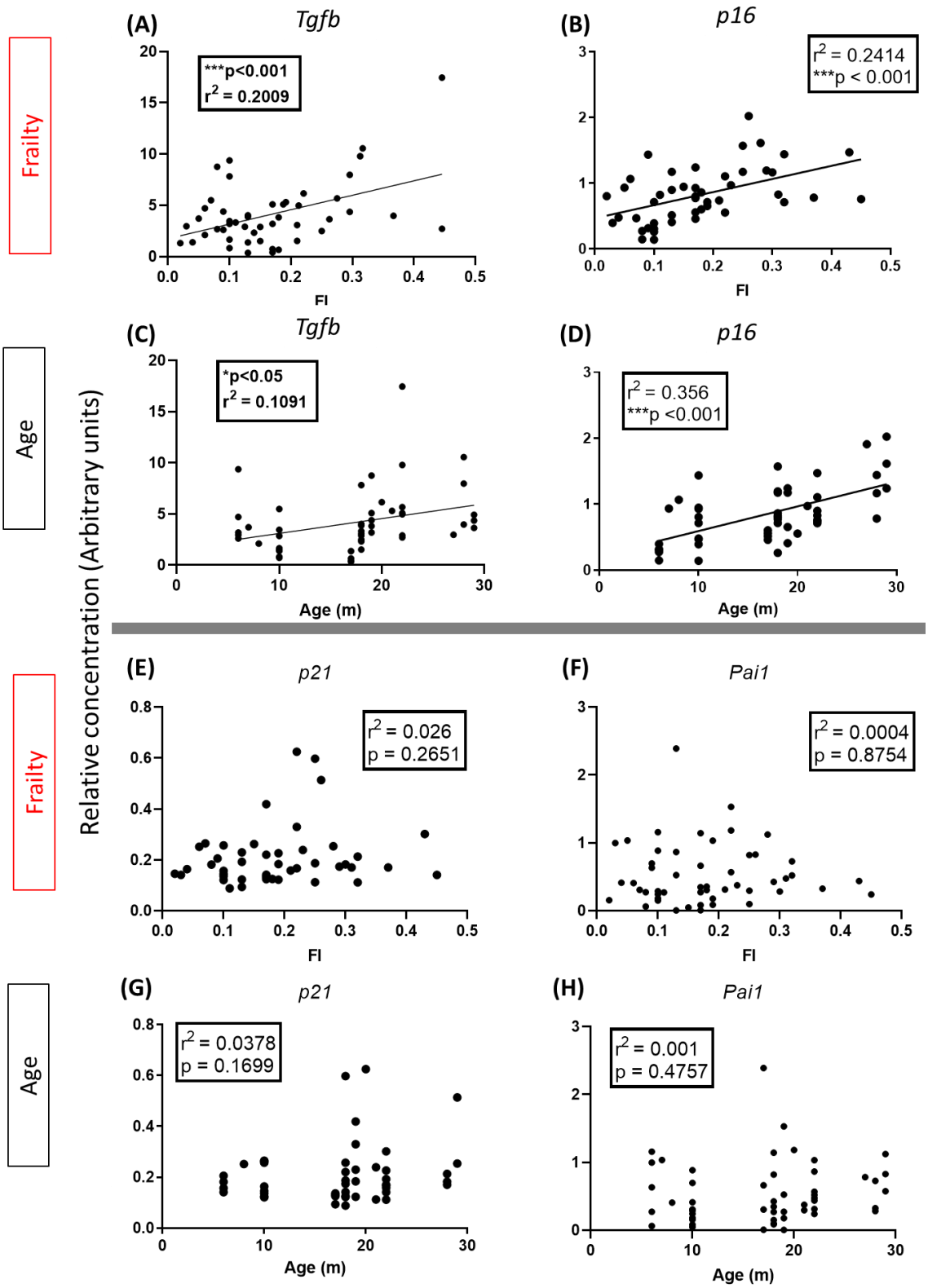

Figure 4.22: Correlation of brain hypothalamic senescence associated genes' expression with age and frailty in mice: Correlation by Pearson linear regression analysis of (A) (C) ***Tgfb***, (B) (D) ***p16,*** (E) (G) ***p21,*** (F) (H) ***Pai1***, gene expression assessed by qPCR and transcripts normalised to the housekeeping gene ***18s***, in the hypothalamus against Age (months) and Frailty score (FI) , (n = 53) *p<0.05, **p<0.01, ***p<0.001 signifies significant difference by simple linear regression.

As discussed in the previous section, our novel TFL I frailty index has been shown here to capture and describe frailty robustly in an ageing population as assessed by serological expression of known biomarkers of frailty as well as in depth assessment of animal behaviour and physiological measurements at baseline. Of these measures assessed it was found that measures of metabolism such as body weight, core body temperature and serological glucose and insulin expression were most accurately described by frailty rather than age. Furthermore, regional analysis of the ageing frail brain revealed a unique transcriptional signature in the hypothalamus, a region well documented for its intricate role in governing the body's metabolic homeostasis. Within the hypothalamus frail animals showed robust decreases in transcript expression of microglial activation, growth factors and robust increases in markers of senescence and neuroprotective cytokines such as *Osm.*

Given these novel alterations in the ageing frail brain I hypothesised that frail animals as assessed using our novel Trinity Frailty Index (TFL) would be more vulnerable to acute deficits in cognition, metabolism and physical activity in response to a systemic challenge, such as that of the bacterial mimetic LPS. Furthermore, per the definition of frailty, the more aggressive the frailty the slower and less efficient these animals would be in recovering these measures to baseline function in the time post-LPS challenge.

4.2.3 Does frailty correctly predict vulnerability to and recovery from acute bacterial endotoxin (LPS) challenge

While exact wording of the definition of frailty is debated heavily within the field of geriatric medicine the most prevalent and comprehensive definition describes it as a state of increased vulnerability to poor resolution of homeostasis after a stressor event, which in turn will leave the individual at an increased risk of adverse outcomes, such as falls, delirium and disability (Fried et al. 2001; Eeles et al. 2012) (**Figure 4.22 A)**. Building on the first modified integrated phenotype frailty index, TFL I, described in the previous section I designed a new variant incorporating a more robust measure of cognitive status into our new Trinity Frailty Index II, **(Figure 4.23 B**) to calculate an individualised frailty score for each animal based off their physiological, cognitive, and metabolic measures. See section 2.2.4. of Materials & Methods for further information on the design of these frailty assays and the generation of z-scores on each assay based of positive or negative performance in reference to a mean adult control group.

Once baseline frailty had been assessed in all animals each was then challenged with a 250µg/kg bolus of the bacterial mimetic, LPS, to assess whether this frailty score accurately predicted worse outcomes and recovery in these same measures. To this end animals were stratified into three age groups (3-9 months n=18, 14-19 months n=15, 20-24 months n=30) and frailty classifications (Robust n=16, Mid-frailty n=31, High-Frailty n=16) and were assessed for acute cognitive deficits 3 hours post challenge as well as undergoing a full assessment of frailty status acutely at six post challenge and subsequently their recovery at twenty-four hours and a week post challenge (**Figure 4.23 C).**

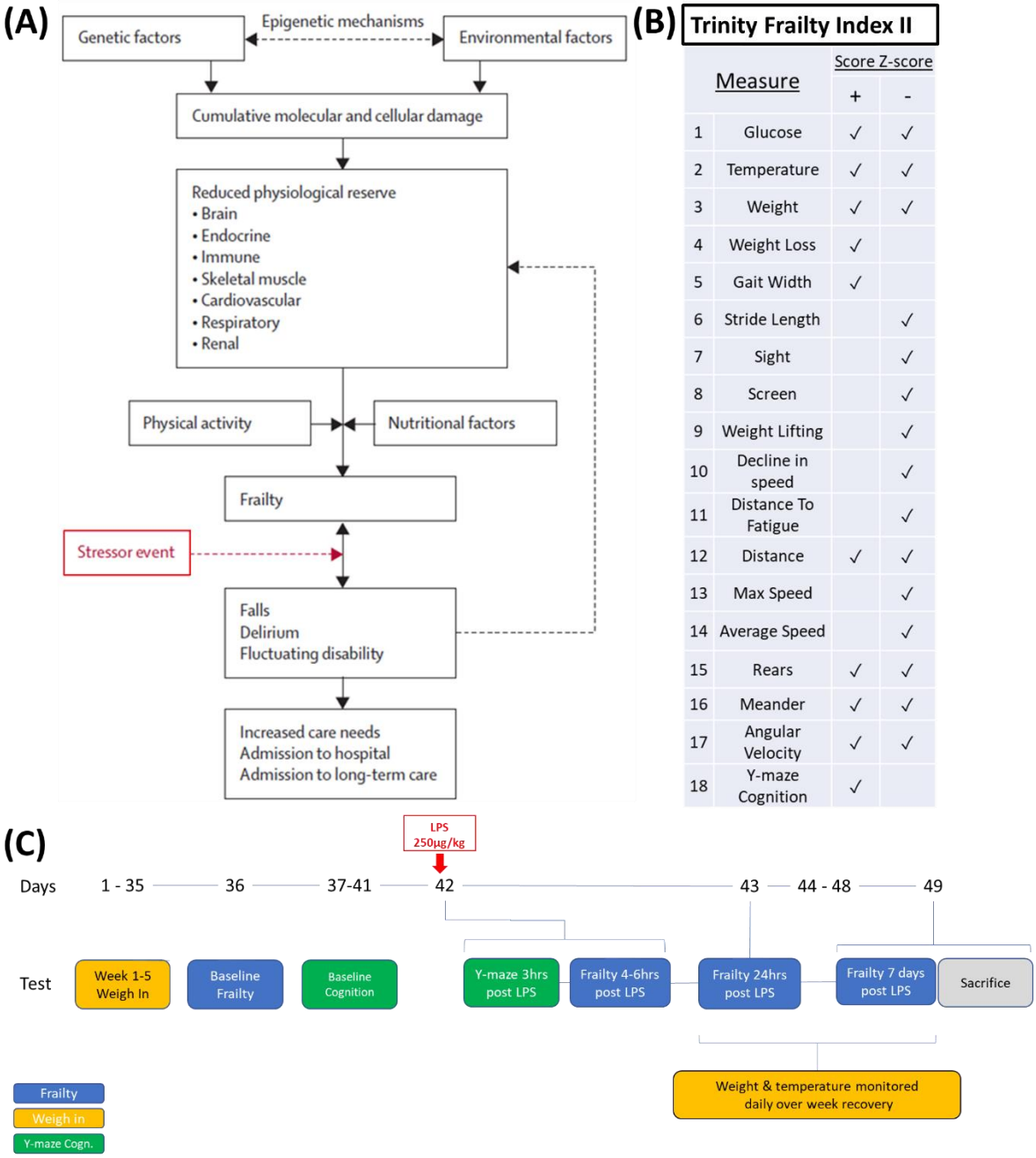

Figure 4.23: Experimental design testing vulnerability to acute systemic challenge with frailty - (A) The pathophysiology of Frailty: schematic representation of the pathophysiology of frailty (Clegg et al. 2013). (B) Modified Integrated Phenotype Frailty Index componenty measures for Trinity Frailty Index (TFL2) used to assess frailty status of animals at baseline, acutely at 6 hours post LPS and their frailty status recovery at 24 and 168 hours post challenge.(C) Timeline of frailty and cognitive testing of mice pre and post systemic challenge with 250µg/kg dose of LPS to assess severity of challenge and recovery from it over a seven-day recovery period.

4.2.3.1 Age and Frailty predict cognitive vulnerability

Learning and memory was assessed at baseline using the hippocampal-dependent shallow water visuospatial Y-maze reference memory task. Mice were trained in the maze over twelve trials a day for five days in order to test their ability to learn the task and to be scored for learning ability for inclusion in the finalised frailty index as a measure of their cognitive status. To this end each animal was assigned a cognitive score based off the number of trials it would take for them to achieve the threshold criterion of 8 out 10 trials in a row correct. The majority of animal assessed were found to be capable of learning this task and achieving the threshold criterion of 8/10 trials in a row correct within the 60 trials they underwent during the 5-day training period, the select few who failed to learn the task received a maximum score of 60 trials to criterion.

For initial assessment of frailty's impact upon cognition, a frailty score of all measures, bar this cognitive component, was first assigned and animals were stratified by this to assess the impact of frailty on cognition and whether it was a suitable metric for inclusion into the frailty index for all analyses thereafter. It was found that stratification by frailty score (minus the cognitive component) better delineated between animals' ability to learn the task than did age, when assessed as the daily percentage correct of twelve trials over the five days of training **(Figure 4.24 B).** Mid-Frailty and High-Frailty animals showed significant differences (##p<0.01) between each other on training days 2 and 3 when assessed by repeated measures two-way ANOVA. In contrast, with age all animals aged 12-24 months learnt at apparently equivalent rates from the first to fourth day of training **(Figure 4.24 A)** with a weak significant difference becoming apparent between the 20-24-month and the younger age groups on the fifth day of training (#p<0.05). Analysis of area under the curve (AUC) corroborated these observations with Mid-Frailty (1754±236.5) showing a greater AUC than High Frailty animals (1168±215.8) indicating a steeper curve to their learning performance. 20-24- and 14–19-month-old age groups effectively showed the same AUC **(Figure 4.24 C, D)**. Linear regression analysis confirmed that the frailty score generated by our index (excluding the cognitive component) more strongly predicted learning ability when plotted as the number of trials to criterion with frailty score **(Figure 4.24 F;** r^2 = 0.3136), while age also exhibited a strong correlation with the number of trials to criterion **(Figure 4.24 E;** r^2 = 0.2426) its Pearson coefficient (r^2) was weaker than that of frailty indicating a poorer fit to the line and thus a slightly weaker predictive value.

Once baseline frailty, and a good Y-maze learning basis, had been established, mice were challenged intraperitoneally with a 250µg/kg bolus of LPS to mimic a systemic inflammatory challenge and were then assessed at 3 hours post challenge on their ability to retain the task and then adapt their escape technique when the exit arm was altered. Just as baseline frailty had better differentiated between animals' abilities to learn the task, it better predicted their ability to retain the task under LPS induced inflammation during the "Retention" period of 10 trials 3 hours post systemic challenge **(Figure 4.24 A)**. Acute challenge with LPS had no impact upon the previously learned visuospatial memory when stratified by age but classification by frailty revealed small significant differences between the mid (#p<0.05) and high-frailty groups (# # p<0.01) compared to Robust animals that mirrored their slower rate in learning the task during the training period **(Figure 4.24 B)**.

In contrast, when the escape arm was reversed and the animals' ability to adapt their escape technique to these new conditions was assessed over twelve trials it was found that age better predicted their performance under acute inflammation for the second block of six trials with significant differences in performance evident between all ages **(Figure 4.24 A)**. When separated by frailty the only significant difference was between Robust and Mid Frailty animals (###p<0.001) with High Frailty animals showing a trend toward a better performance in the second block of reverse trials than the Mid Frailty group, contrary to predictions **(Figure 4.24 B)**. Indeed, assessment of the relationship between age and the inflammatory episode's impact on cognitive flexibility (the ability to learn the new exit location) by Pearson linear regression revealed a robust statistically significant positive relationship between advancing age and the number of incorrect trials performed by the animal during the 12-trial testing period(***p<0.001, $r^2 = 0.2788$) (**Figure 4.24 G).**

However, while age was the stronger descriptor the same analysis revealed a robust, if weaker, correlation with frailty (***p<0.001, $r^2 = 0.1935$) (**Figure 4.24 F)**. Further analysis of the relationship between the number failed trials during reversal against the number of incorrect trials during the training period of sixty trials revealed a weak, but significant, correlation (*p<0.05, $r^2 = 0.0651$) **(Figure 4.24 I)**. Similarly, assessment of the number failed trials during reversal against the animals' cognitive frailty component, trials to criterion, revealed a weak positive correlation (*p<0.05, $r^2 = 0.0844$) **(Figure 4.24 J).** Taken together, this suggests that frailty is also descriptive of the animals' ability to adapt their strategy to the reversed exit, albeit to a lesser extent than age.

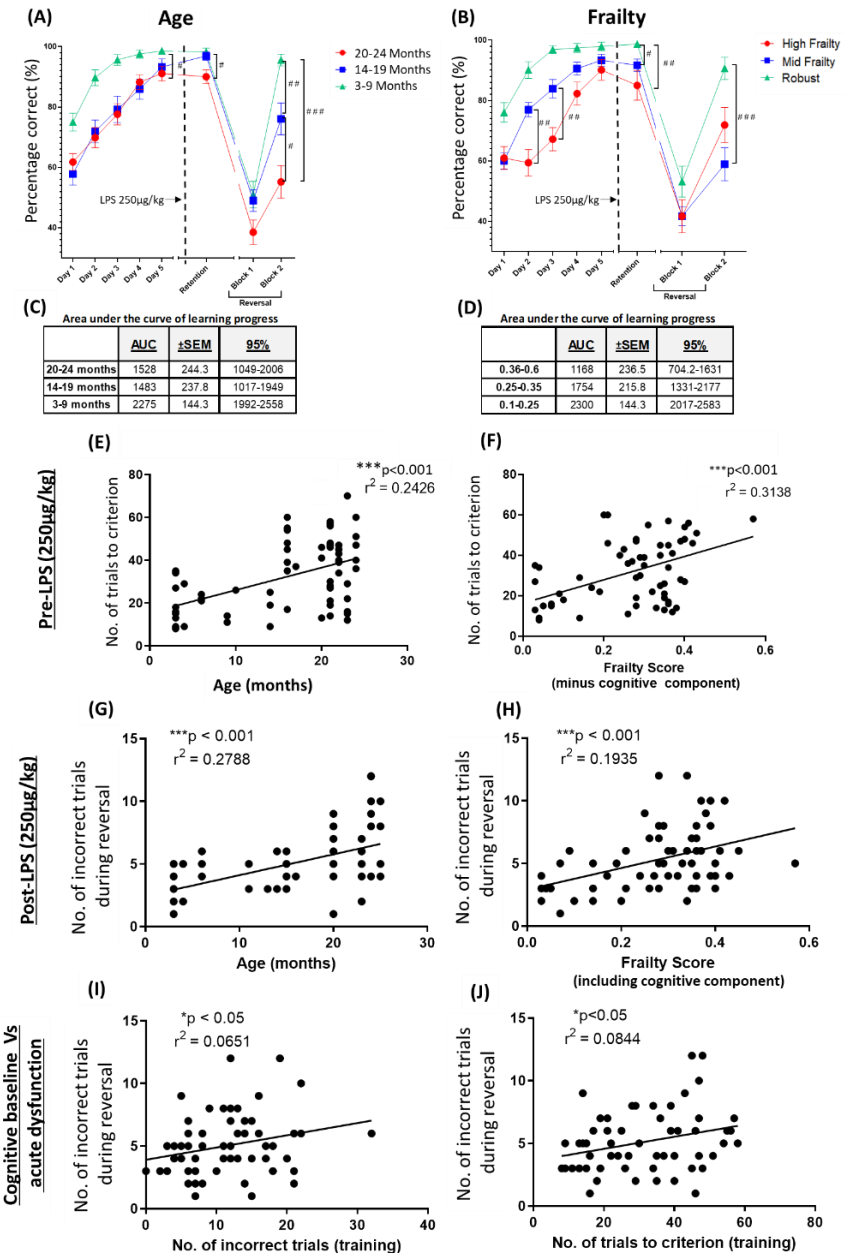

	AUC	±SEM	95%
20-24 months	1528	244.3	1049-2006
14-19 months	1483	237.8	1017-1949
3-9 months	2275	144.3	1992-2558

	AUC	±SEM	95%
0.36-0.6	1168	236.5	704.2-1631
0.25-0.35	1754	215.8	1331-2177
0.1-0.25	2300	144.3	2017-2583

Figure 4.24 – Predicting cognitive vulnerability to systemic challenge– The ability to learn the hippocampal-dependent Y-maze reference memory task was assessed and plotted with age and individualised frailty scores (minus the cognitive component) for inclusion as a metric of cognitive function in the frailty index. Frailty index (including cognitive component) used to predict animals ability at 3 hours post LPS (250µg/kg) i.p. challenge to retain and adapt when the task was reversed for both (A) age (3-9 months n=18, 14-19 months n=15, 20-24 months n=30) and frailty (Robust n=16, Mid-frailty n=31, High-Frailty n=16) (B). It was found that age better differentiated between animals' ability to retain and adapt to the tasks reversal (two blocks of six trials) using a two-way ANOVA and Bonferroni's post hoc test. Correlation by Pearson linear regression analyses predicting whether age (C) or frailty (D) better described learning to criterion during training revealed frailty to be the stronger predictor. Correlation by Pearson linear regression analysis to determine the relationship between number of incorrect reversal trials and the number of incorrect learning trials (G), "physical frailty" (F), age in months (E) and number of trials to achieve criterion of 80% correct of 10 trials (H).

Although age is indeed a powerful predictor of cognitive vulnerability to acute deficit at three hours post i.p. challenge with 250µg/kg of LPS I have shown here that frailty better describes an animal's ability to learn the hippocampal-dependent y-maze task and thereafter, their vulnerability to retaining it post LPS. In comparison age was a slightly better descriptor of an animal's cognitive flexibility to altering this task's escape strategy when reversed under acute LPS stress but this was also correlated with frailty, albeit to a lesser degree. As such the animal's ability to learn the Y-maze task was incorporated into our frailty index and used to generate the finalised individualised baseline frailty scores used hereafter to predict and assess the impact of the systemic inflammatory event on every other component of the frailty index TFL II.

4.2.3.2 Age and Frailty predict recovery from systemic challenge

Over the six weeks leading up to the assessment of baseline frailty, each animal's weight was monitored on a weekly basis **(Figure 4.25 A, C)** and their percentage weight loss from week 1-6 was scored for inclusion into the frailty index. It was found that 3–9-month animals were continually gaining weight (*p<0.05) in the weeks leading up to their baseline frailty assessment while 14-19-month animals maintained their weight and the eldest, 20-24 month, animals were gradually losing weight (*p<0.05) when assessed by repeated measures two-way ANOVA.

Following assessment of baseline frailty and challenge with 250µg/kg of LPS, body weight was monitored daily over a seven-day recovery period and stratified by age **(Figure 4.25 B)** and frailty **(Figure 4.25 D)** in order to assess which better predicted the individual animal's vulnerability to weight loss and the subsequent degree of recovery. It was found that both age and frailty showed significant reductions post challenge with significant effects and interactions with time in both cases **(Figure 4.25 E)**. However, age was shown to predict the extent of weight loss less accurately in response to the systemic challenge, following an unexpected trajectory with 14-19-month-old animals displaying greater weight loss than their older 20-24-month counterparts at 120 hours post challenge (#p<0.05). By 96 hours post challenge the youngest, 3-9-month, animals had recovered to their baseline weight while the older animals were still significantly down as a percentage of their baseline weight, 14-19-month (***p<0.001), 20-24-month (**p<0.01), at 168 hours after the challenge. At 168 hours post challenge both groups of aged animals failed to show any statistically significant recovery of weight after challenge with LPS and remained significantly different from the 3-9-month group (###p<0.001). There was no significant difference between the 14-19-month and 20–24-month animals at over this recovery period.

In contrast, when stratified by their baseline frailty scores for weight recovery there is a clearer delineation between groups' trajectories of recovery. The least frail scoring, "Robust" animals' peak weight loss occurs 24 hours post challenge and rapidly recovers to baseline by 96 hours. The higher frailty groups continue to lose weight until peaking at 48 hours post challenge and remain significantly different from baseline by 168 hours. The Mid Frailty animals show a positive trajectory for recovery, but at a much slower pace compared to the Robust group, with a significant recovery (**$p<0.01$) between their weights at 48 and 168 hours. The High Frailty animals fail to show any significant recovery in mass from their peak weight loss at 48 hours post challenge over the week recovery resulting in a significant difference between the two frail groups (#$p<0.05$) at 168 hours.

Unexpected weight loss is one of the five criteria of the classic Fried Phenotype classification of frailty (Fri*ed et al*, 2001) and our frailty index has reliably predicted the severity of acute weight loss and speed of recovery, as by definition it should, and has proved to be more discerning than age in doing so.

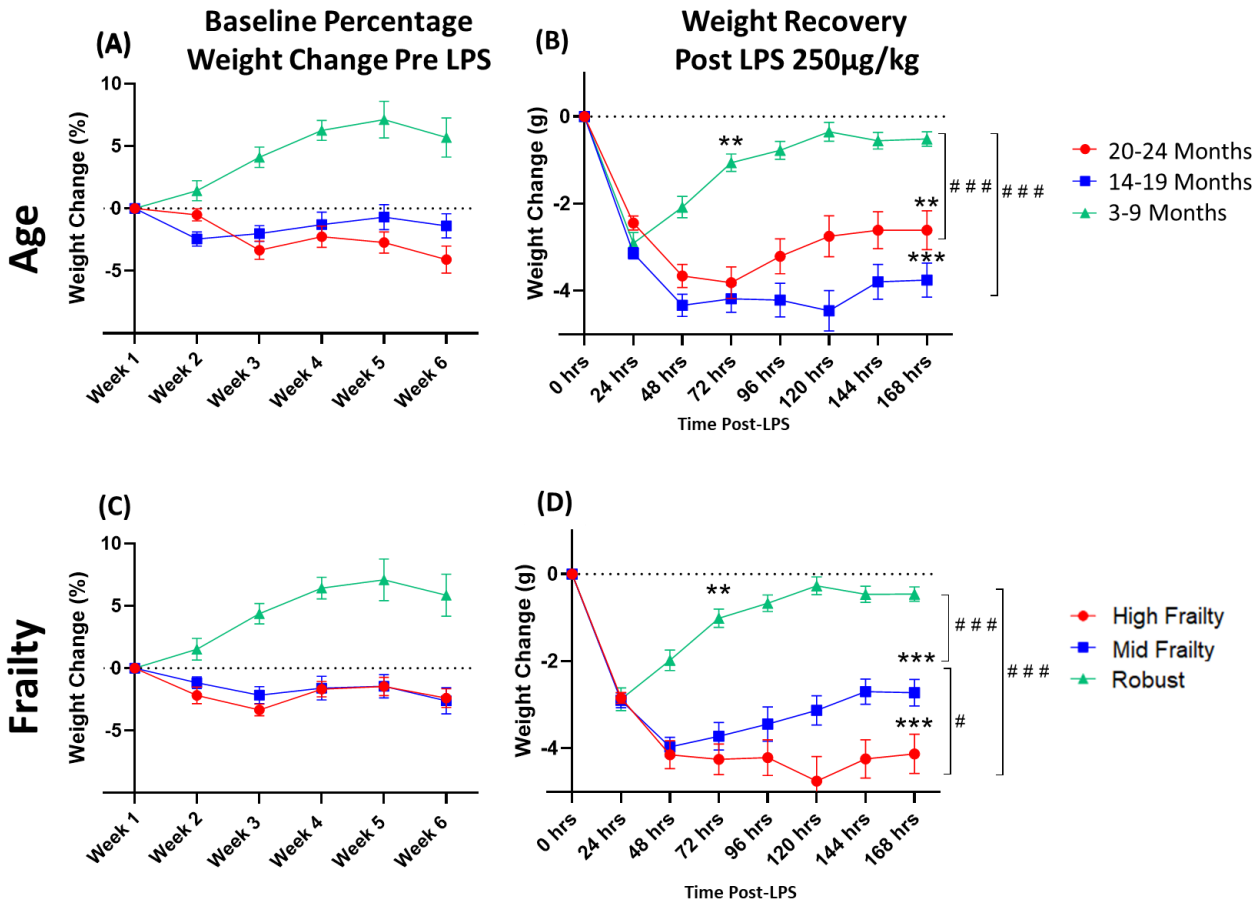

Figure 4.25 – Predicting vulnerability to weight loss following systemic challenge by age or frailty: weight gain and loss was tracked over the 6 weeks leading up to a systemic challenge of LPS (250µg/kg) and was factored into the generation of the individualised frailty score (C) for comparison with age (A) and used to predict peak weight loss following challenge with LPS (250µg/kg) and recovery trajectory over a week post challenge was compared between age (3-9 months n=18, 14-19 months n=15, 20-24 months n=30; effect of age p<0.001, F (2, 63)=19.89; effect of time p<0.001, F (2.787,140.2) = 83.55; interaction effect p<0.001, F (14, 352)=16.49), (B) and frailty (Robust n=16, Mid-frailty n=31, High-Frailty n=16, effect of frailty p<0.001, F (2, 59) = 18.70; effect of time p<0.001, F (3.128,150.1) = 75.56; interaction effect p<0.001, F (14, 336)=18.24) (D) categorisations and frailty were found to better predict the extent and speed of an animal's recovery compared to age. All data expressed as mean ± SEM and analysed by repeated measures two-way ANOVA with Bonferroni Post Hoc test for weight loss and recovery, *p<0.05, **p<0.01, ***p<0.001 signifies significant difference from starting nadir, #p<0.05, ##p<0.01, ###p<0.001 signifies significant difference between groups at the same time point.

Previous work from our group and others has revealed that LPS has a significant impact upon an animal's metabolism inducing acute hypoglycaemia (Kealy et al. 2020; Del Rey et al. 2006) and since metabolism is a key influence on frailty, these are key measures in our Frailty Index. As a result, each animal's temperature was monitored using a subcutaneous transponder over the weeklong recovery post-LPS **(Figure 4.26 B, D)** and their blood glucose level was tested at baseline before the LPS challenge, as well as at 8, 24 and 168 hours post challenge. This was done by sequential lancing of the tail vein and assessment of the venous blood by glucometer **(Figure 4.27 C, D)**.

Intraperitoneal challenge with 250µg/kg of LPS resulted in a robust hypothermic response in most animals. This reduction in core body temperature peaked at 4 hours in the oldest **(Figure 4.26 B)** and the most frail animals **(Figure 4.26 D)**, with a second more severe peak occurring at 10 hours. While this peak was most severe in the oldest animals, those with mid-level frailty were found to be more severe than High-Frailty group. One possible explanation for this is the fact that when stratified by age **(Figure 4.26 A)** and frailty **(Figure 4.26 C)** for baseline temperature there is a very high degree of variability in the baseline temperature observed within the High Frailty group. As such many of these tended to be slightly hypothermic to start with and as such did not show such drastic changes as those Robust or Mid Frailty animals who were a more typical 37°C average. This age-associated reduction in core body temperature has been well documented in the field of geronotology with many studies reporting that with increasing age baseline temperatures were generally lower in elderly patients (Roghmann *et al.* 2001) and can result in an afebrile response, i.e. the inability to mount efficient or resolve fever responses to infection in a timely fashion (Krabbe et al. 2001) is associated with poorer outcomes (Torres et al. 1998) and decreased levels of inflammatory cytokines during the acute phase (Gon et al. 1996). They SCN region of the hypothalamus is known to be important in governing circadian rhythm and time-dependent metabolic and temperature responses to an acute challenge (la Fleur et al.; 2000; Kalsbeeket al., 2012; Bohlandet al., 2014; Guzm´an-Ruizet al., 2015). As such this may be indicative of impaired signalling and function of this hypothalamic structure as has been reported in ageing studies (Acosta-Rodriguez et al., 2021). Indeed, classification by frailty showed a slower recovery to baseline in High Frailty animals between 48-168 hours post challenge (**Figure 4.26 D)**.

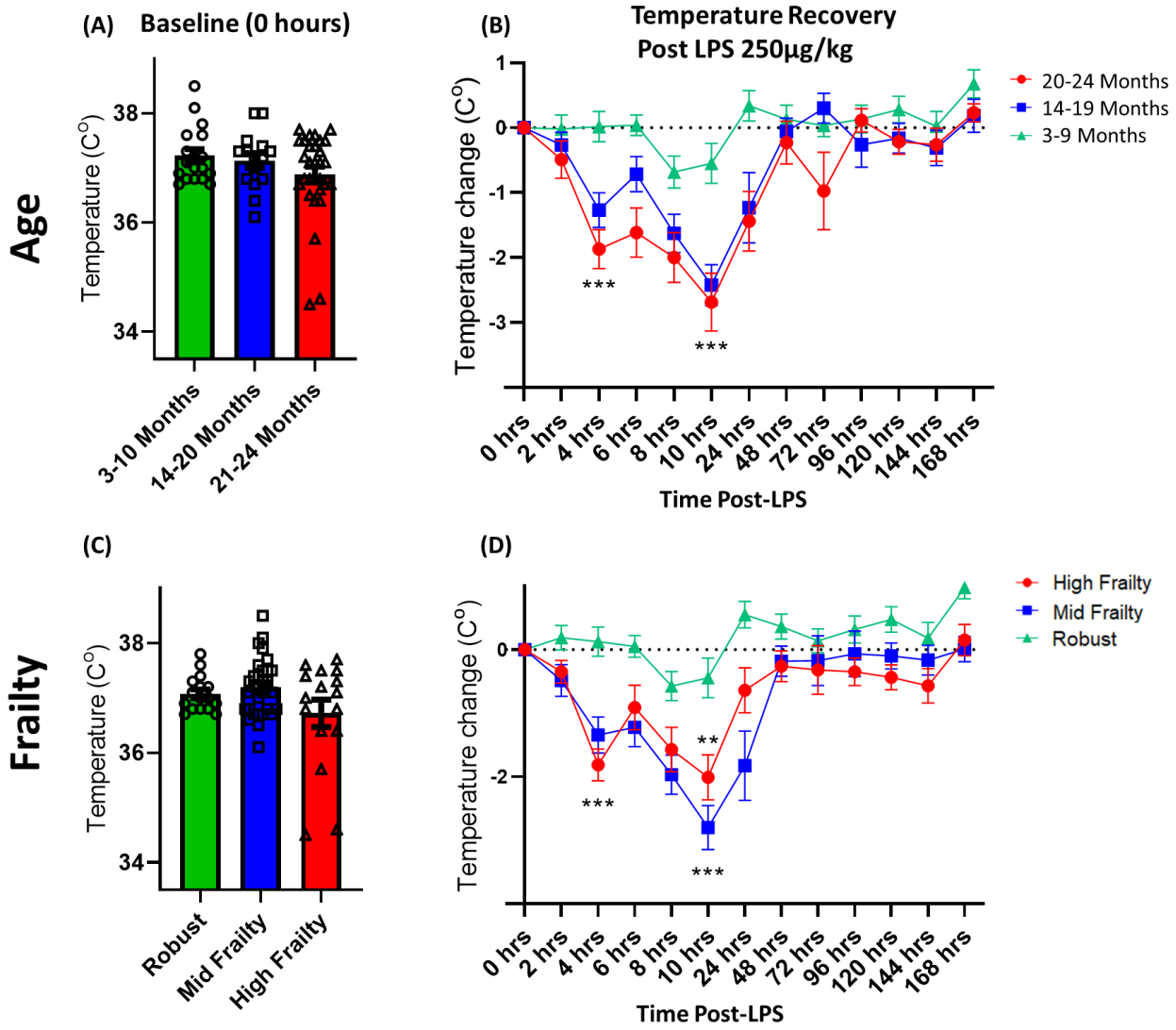

Figure 4.26 – Predicting vulnerability to systemic inflammatory induced hypothermia and recovery: Subcutaneous implanted transponders were used to assess baseline temperature (0 hours post LPS) for inclusion in the frailty index used to stratify by (C) frailty for comparison with (A) age and then subsequently used to monitor acute reduction in temperature following i.p. challenge with LPS (250µg/kg) (every 2 hours for the first ten hours post challenge) and to track daily recovery over a week post challenge when stratified by (B) age (3-9 months n=18, 14-19 months n=15, 20-24 months n=30; effect of age $p<0.001$, $F(5.127,269.6)=19.75$; effect of time $p<0.001$, $F(2,60)=7.88$, interaction effect $p<0.001$ $F(24,631)=3.042$) and (D) frailty (Robust n=16, Mid-frailty n=31, High-Frailty n=16; effect of frailty $p<001$ $F(2,59)=9.917$; effect of time $p<0.001$ $F(5.253,273.6)=17.04$; interaction effect $p<0.001$ $F(24,625)=3.396$). All data expressed as mean ± SEM and analysed by repeated measures two-way ANOVA with Bonferroni Post Hoc test, *$p<0.05$, **$p<0.01$, ***$p<0.001$ signifies a significant difference from baseline.

Glucose levels were obtained from a drop of blood from the tail vein of each animal at baseline and used in generating the individualised frailty score. Linear regression analysis revealed a significant positive correlation (*p<0.05, r^2 =0.0841) with age **(Figure 4.27 C)** and frailty (**p<0.01, r^2 =0.1029) **(Figure 4.27 D).** However, it was found that frailty showed a stronger significant correlation, coupled with the slope of the line of best fit revealing that this increase was more robust with increased frailty (slope = 4.083) than it was with age (slope = 0.683). A corresponding correlating pattern of insulin expression in blood plasma at time of euthanisation was found with frailty **(Figure 4.27 B)** showing a stronger significant correlation (***p<0.001; r^2 =0.2280) than that with age (**p<0.01; r^2 =0.1167) **(Figure 4.27 A)** as well as a more robust line of best fit with frailty (slope = 2.21) than with age (slope = 0.027).

Additionally, glucose measurements were taken in the same manner from the tail vein at 8, 24 and 168 hours after exposure to LPS and these were plotted as percentage change from baseline for age **(Figure 4.27 E)** and frailty **(Figure 4.27 F).** Intraperitoneal challenge with 250µg/kg of LPS resulted in a robust reduction in blood glucose levels at 8-hours post challenge with no significant differences between different ages or frailty status at this acute time point. All animals showed clear and progressive recovery of their glucose scores between 24-168 hours post challenge.

Analysis of animals by age using a repeated measures two-way ANOVA revealed no significant effect of age (p=0.2590) only an effect of time (***p<0.001 F(2.229,119.6)=155.5) on glucose expression levels **(Figure 4.27 E)**. However, when stratified by frailty a significant effect of frailty (**p<0.01 F(2,60)=5.263), time (***p<0.001 F(2.487,131)=205) and an interaction effect (*p<0.05 F(6,158)=2.243) between the two was found **(Figure 4.27 F)**. By 24 hours robust (***p<0.001) and mid frailty (**p<0.01) animals showed significant recovery of their glucose levels from their 8-hour time point, while high frailty animals failed to show any statistically significant increase. Both high frailty (##p<0.01) and mid-frailty (#p<0.05) animals remained lower than robust animals at 24 hours. By 168 hours robust and mid frailty animals had recovered to their baseline levels. However, high frailty animals remained significantly lower than the other groups (#p<0.05). This fits with the predicted model of frailty that high frailty results in an increased vulnerability to poor resolution of homeostasis.

Consistent with the findings from our TFL I frailty study, measures of metabolism are more accurately described by frailty status than simple chronological age. Furthermore, frailty status has been shown here to better describe an animal's vulnerability to acute disruption of metabolic systems and their recovery over a seven-day recovery period for weight-loss, core body temperature and serological concentrations of glucose and insulin.

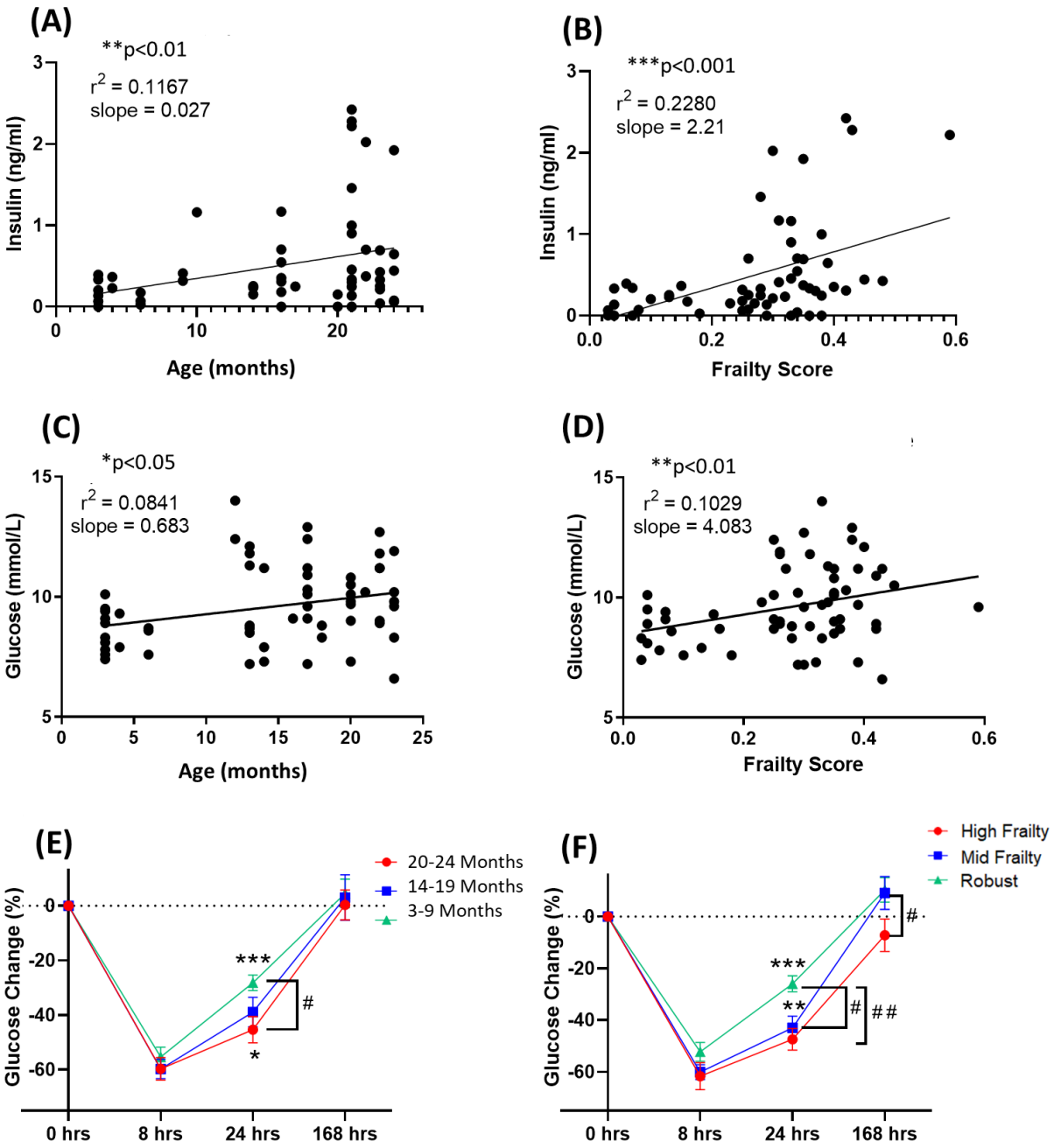

Figure 4.27 – Predicting glycaemic status and vulnerability to systemic inflammatory-induced glucose reduction and recovery: Baseline levels of glucose (C & D) and insulin (A & B) were assessed with respect to age and frailty data and analysed by simple linear regression analysis. Tail vein sampling of blood glucose levels was also assessed at baseline before LPS challenge, 8, 24 and 168 hours post LPS (250µg/kg) i.p. challenge to monitor severity of the LPS induced reduction and the recovery progress and stratified by (E) age (3-9 months n=18, 14-19 months n=15, 20-24 months n=30; ; effect of time p<0.001 F(2.229,119.6)=155.5) and (F) frailty (Robust n=16, Mid-frailty n=31, High-Frailty n=16; effect of frailty p<0.01 F(2,60)=5.263; effect of time p<0.001 F(2.487,131)=205; interaction effect *p<0.05 F(6,158)=2.243). All data expressed as mean ± SEM and analysed by repeated

measures two-way ANOVA with Bonferroni Post Hoc test, *p<0.05, **p<0.01, ***p<0.001 signifies significant difference between time points, #p<0.05, ##p<0.01, ###p<0.001 signifies significant difference between groups at the same time point.

4.2.3.3 Age and Frailty impact upon behavioural quality and speed of recovery

As part of the evaluation of vulnerability to the systemic challenge animals underwent a full assessment of the behavioural components of Trinity frailty index II **(Table 2.9)** acutely, between 5-6 hours post challenge to determine the severity of the effect of inflammatory challenge on their behaviour and physiology as well as at 24 and 168-hours post challenge to monitor their recovery towards their baseline frailty.

4.4.3.1 Vulnerability to loss of strength and recovery

Loss of strength is one of the five Fried Frailty Phenotype measures used for diagnosis of frailty in geriatrics and as such mice were assessed using the Kondziela Inverted Screen test **(Figure 4.28 A,C)** as well as the Deacon weight-lifting task proxies for their grip strength **(Figure 4.28 B,D)**.

In the case of the inverted screen, it was found that age was the stronger predictor of vulnerability to acute weakness; 3-9-month animals failed to show any significant loss in strength (i.e. time hanging upside down on the screen), while 14-19 months showing a small decrease (*p<0.05) and the oldest animals a greater reduction still (***p<0.001). When assessed on the recovery of strength over the week period it was found that whether grouped by age or frailty all animals recovered to their baseline by 168 hours. However, age was found to be the stronger predictor of recovery with the 14–19-month group showed a more rapid rate of recovery of strength between the acute 6- and 24-hour measurements compared to the 20-24-month, group which remained significantly down from baseline (***p<0.001) at 24 hours. A clear significant difference was found at 24 hours between the two aged populations (#p<0.05).

When grouped by frailty, Robust animals showed no significant acute loss in strength but both Mid and High Frailty animals showed equivalent decreases (***p<0.001). Classification by frailty failed to distinguish between Mid and High frailty groups' acutely or for their recovery at 24 and 168-hours post challenge.

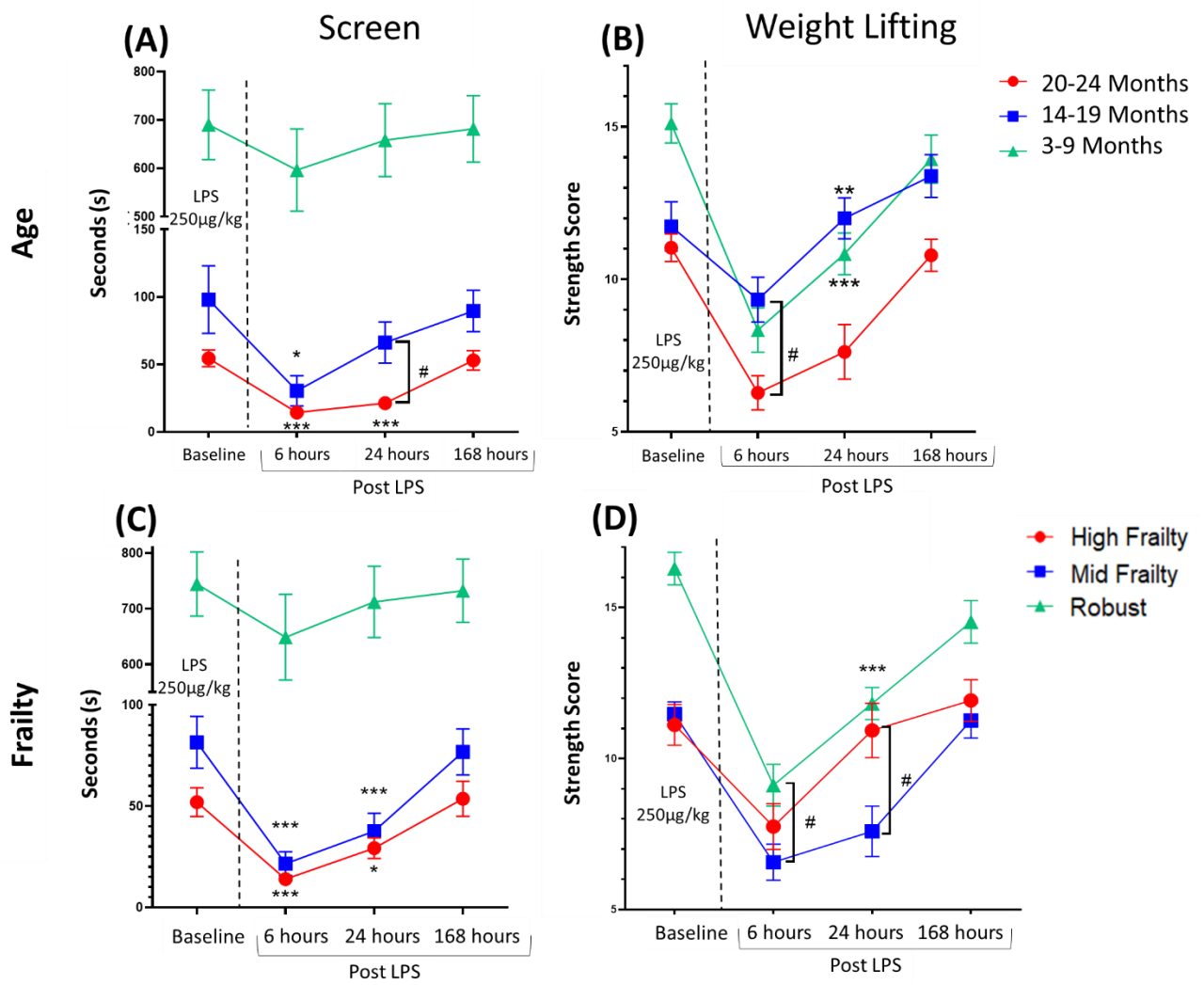

Figure 4.28 – Recovery of and vulnerability to loss of strength following systemic challenge: Assessment of overall grip strength using the Kondziela's Inverted Screen (A) age (3-9 months n=18, 14-19 months n=15, 20-24 months n=30; ; effect of time p<0.05 F(0.6228,3.28)=19.8; effect of age p<0.001 F(2,59)=88.15) and (C) frailty (n=16, 31, 16; effect of frailty p<0.01 F(2,61)=149.5; effect of time p<0.01 F(0.286,15.51)=19.77). Assessment of forelimb grip strength using the Deacon weightlifting task (A) age (n=18, 15, 30; ; effect of time p<0.001 F(2.781,148.3)=56.94; effect of age p<0.001 F(2,60)=12.05; effect of interaction p<0.001 F(6,160)=4.412) and (C) frailty (Robust n=16, Mid-frailty n=31, High-Frailty n=16; effect of frailty p<0.001 F(2,61)=14.22; effect of time p<0.001 F(2.727,148.2)=70.92; interaction effect p<0.001 F(6,163)=4.698). All data represented as mean ± SEM (3-9 months n=18, 14-19 months n=15, 20-24 months n=30; Robust n=16, Mid-frailty n=31, High-Frailty n=16) and assessed by repeated measures two-way ANOVA with Bonferroni Post Hoc test, *p<0.05, **p<0.01, ***p<0.001 signifies significant difference from baseline, #p<0.05, # #p<0.01, # # #p<0.001 signifies significant difference between groups at one timepoint

While young and robust animals showed no reduction in grip strength on the inverted screen it was found that assessment of forelimb grip strength selectively using the Deacon weightlifting task showed a significant reduction in the maximum weight the animal could lift at baseline for all ages and frailty statuses. Age appeared to be slightly more discerning in this with the oldest animals showing the greatest reduction at 6 hours post challenge and failing to show any significant recovery by 24 hours. Classification by frailty failed to predict lower scores or slower recovery for higher frailty animals. All animals recovered fully to their baseline score by 168 hours whether grouped by age or frailty.

In the inverted screen test a mouse may utilise all four paws to grip and remain on the screen and is well motivated to do so in order to prevent itself falling. In the case of the Deacon weight-lifting task, the animal may only use its fore paws to grip and lift a weight up. As such this task more selectively assesses forelimb grip strength compared to the inverted screen but, the task is reliant on the animal's natural instinct to reach out and grasp something when it is lifted up by its tail. As such motivation is a potential confounding factor on this task for anhedonic animals experiencing acute sickness behaviour. Thus, young and robust animals' apparent reduction in strength when assessed by the Deacon weightlifting task at acute timepoints that was not observed on the inverted screen, is likely not a true representation of the animal's physical strength at this time but rather an indicator of the severity of their sickness behaviour. i.e., the animal was unmotivated to engage in the task due its sickness behaviour as there were no adverse outcomes for not engaging in it.

4.4.3.2 Recovery of and vulnerability to impaired speed, ease of movement and exhaustion

Slowness and difficulty of movement is another category of the classic Fried Frailty Phenotype (Fried et al. 2001) and has since been looked at extensively as a component of frailty indices as well as an early biomarker of frailty (Noguerón García et al. 2020). As such, as part of our frailty index here I assessed the maximum speed the animal was able to travel at upon a treadmill before hitting their exhaustion criterion (as described in section 2.2.3.10 of methods) **(Figure 4.29 A,D)** as well as their gait by analysing stride length **(Figure 4.30 A, E)** and gait width **(Figure 4.30 B,F)** from analysis of footprints on paper **(Figure 4.30 C, D)** (as described in section 2.2.3.14 of methods).

To evaluate the animals' exhaustion levels, we determined the total distance the animal travelled on a treadmill, with continuous increases in speed, and the maximum speed at which they could run before fatigue became apparent (i.e. mouse lagged into the exhaustion zone and was unable to run at the current speed and they were removed from the treadmill) **(Figure 4.29 C, F)**.

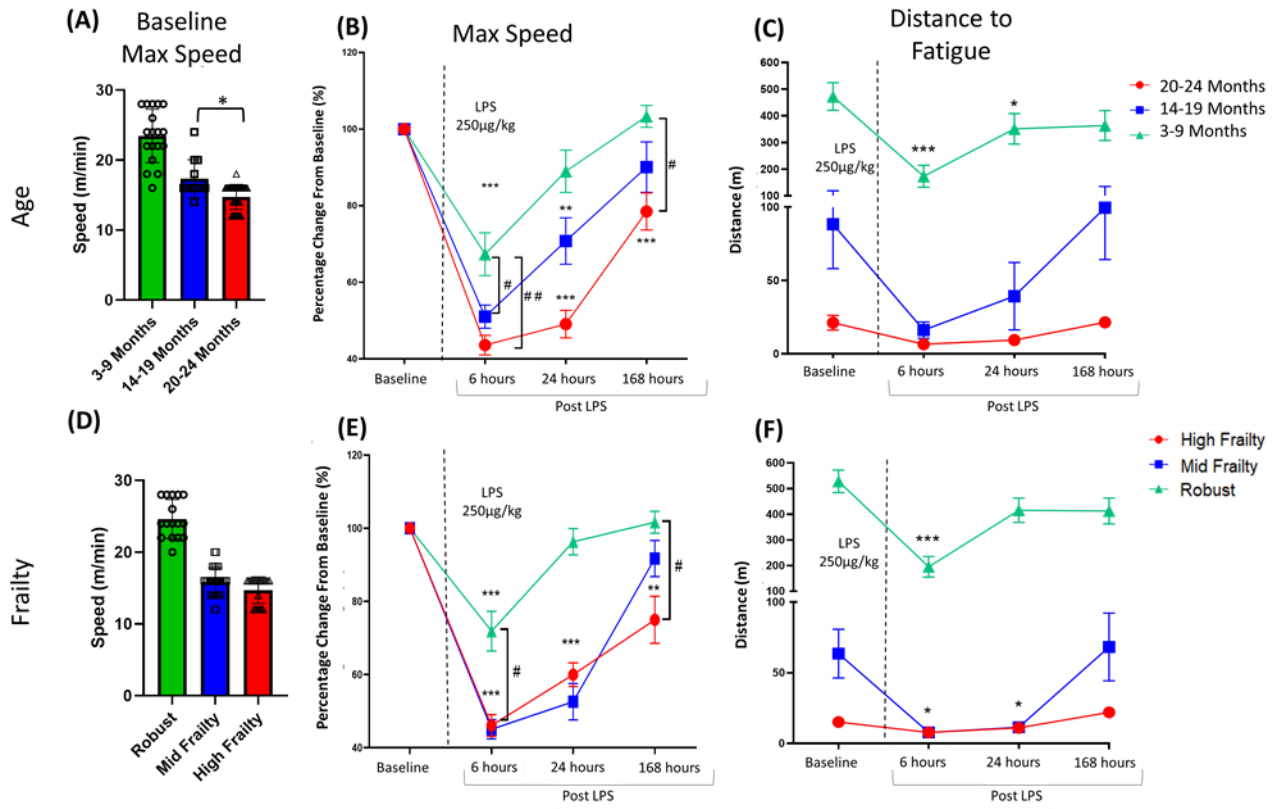

Figure 4.29 – Recovery of and vulnerability to impaired speed and exhaustion following systemic challenge: (A) (D) Baseline maximum speed assessed by treadmill fatigue test and assessed for changes as a percentage of baseline at 6, 24 and 168 hours post LPS 250µg/kg i.p. challenge for (B) age and (E) frailty. Distance travelled to fatigue on treadmill fatigue test assessed under the same conditions and presented by (C) age and (F) frailty. All data represented as mean ± SEM (3-9 months n=18, 14-19 months n=15, 20-24 months n=30; Robust n=16, Mid-frailty n=31, High-Frailty n=16) and assessed by repeated measures two-way ANOVA with Bonferroni Post Hoc test, *p<0.05, **p<0.01, ***p<0.001 signifies significant difference from baseline, #p<0.05, # #p<0.01, # # #p<0.001 signifies significant difference between groups at one timepoint

When assessing maximum speed as a proxy for slowness of movement and exhaustion it was found that classification by age was able to more strongly delineate between the animal's maximum speed at baseline with significant differences between each 14-19 and 10-24-month animals **(Figure 4.29 A)** which was absent between Mid and High frailty animals **(Figure 4.29 D).**

Intraperitoneal challenge with 250µg/kg resulted in a robust acute reduction (***p<0.001) in the maximum speed (as a percentage of their baseline performance) at which an animal could run at six hours post challenge. Of these, 3-9-month-old and Robust animals showed the smallest reduction in speed and fully recovered to their baseline by 24 hours. In contrast 14-19 (**p<0.01) and 20-24-month (***p<0.001) old animals remained significantly lower at 24-hour post challenge. By 168 hours 14-19-month animals had fully recovered but the oldest animals remained significantly lower than baseline (**p<0.01) **(Figure 4.29 B)**. Grouping by frailty showed a similar pattern of reduction and recovery highest risk factor group, High frailty animals failing to recover to baseline (**p<0.01) at 168 hours post challenge **(Figure 4.29 E)**. However, age was superior in delineating between the older, higher risk, groups reductions from baseline and trajectory of recovery with clear significant differences between groups at 6 and 24 hours while Mid and High frailty animals' reductions were equivalent at these time points.

In addition to assessing the maximum speed of movement the animal was capable of upon the treadmill I also used the distance covered during this assessment to address exhaustion **(Figure 4.29 C, F)**. The treadmill fatigue test showed all animals exhibited a significant reduction in distance to exhaustion at 6 hours, although this reduced distance was only significant in the youngest age group (***p<0.001) due to lower baseline scores and a large degree of variability in performance on this task in older groups. Grouping by frailty reduced the variability between groups considerably and revealed statistically significant reductions for Robust animals (***p<0.001) and for Mid and High Frailty animals (*p<0.05) at 6 hours post challenge. This significant reduction persevered at 24 hours for Mid and High Frailty animals and only recovered to baseline by 168 hours while Robust animals had recovered by 24 hours. All animals regardless of classification by age or frailty fully recovered to their baseline by 168 hours. In this regard frailty was no more powerful than age in discerning between animals' capability to resolve to homeostasis; however, its ability to reduce variability within groups and predict vulnerability to acute deficit was more robust than classification by age.

Evaluation of an animals' ease and efficiency of motion through measurement of their gait and stride by age proved to be a very poor predictor of impairment and recovery. At 6 hours post challenge only the oldest animals, 20-24 months, showed significant reduction (***p<0.001) in their stride length which persisted to 168 hours (*p<0.05) **(Figure 4.30 A)**. Grouping by frailty proved a better predictor reducing variability and revealing acute reductions in stride length for all animals at 6 hours **(Figure 4.30 E)**. Robust animals, who demonstrated the smallest reduction (*p<0.05) at this time, recovered fully to baseline by 24 hours while Mid and High Frailty animals remained significantly lower at this time point (p<0.05-0.001) but recovered to within their baseline by 168 hours. However, while their stride length was not statistically different from their baseline, Mid and High frailty animals exhibited a significantly different stride length compared to robust animals which had been absent at baseline (#p<0.05, ##p<0.01).

Narrow gait width is typically associated with a healthy animal capable of efficient motion, while a morbid animal will tend to have a wider, splayed gait to compensate for their impairment. Assessment of gait width by age resulted in groups with a large degree of variability and no clear statistical difference between any age group **(Figure 4.30 C)**. Classification by frailty resulted in less variation within groups and was a better predictor of the degree of endpoint recovery with High Frailty animals showing a significant increase in gait width (*p<0.05) from baseline at 168 hours post challenge, resulting in clear significant differences between them and Mid Frailty (##p<0.01) and Robust animals (#p<0.05) that were absent at baseline **(Figure 4.30 F)**.

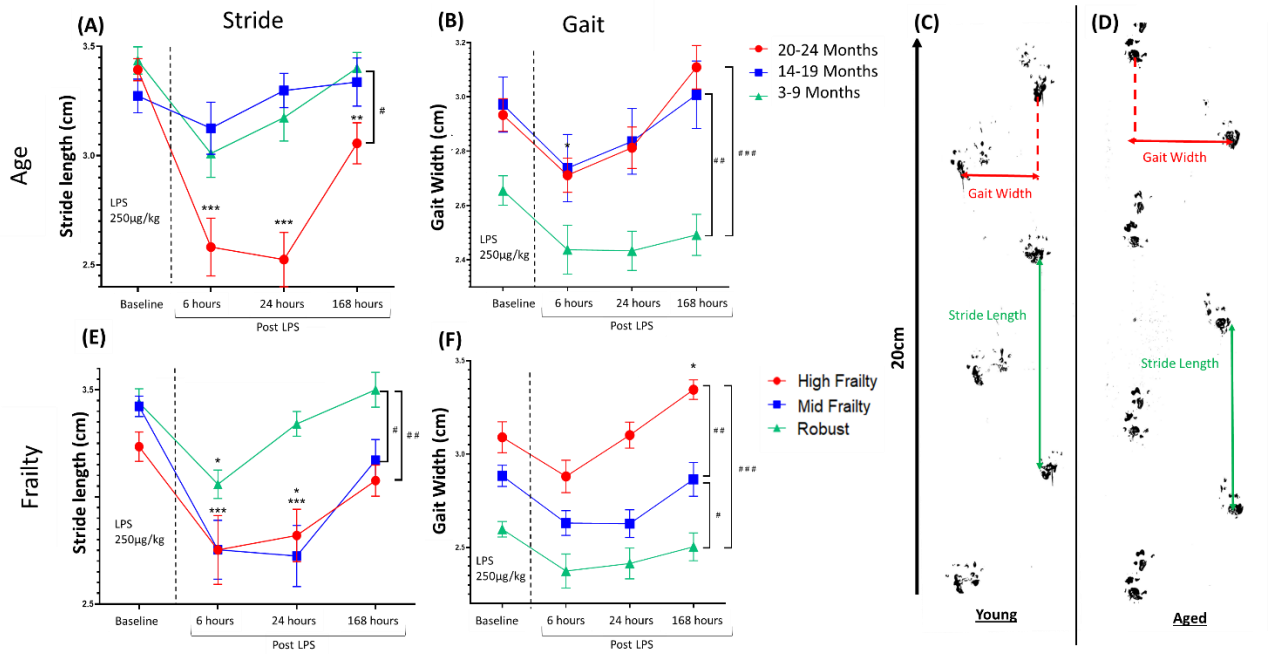

Figure 4.30 – Recovery of and vulnerability to impaired mobility to systemic inflammatory challenge: (A) (E) Stride length and (B) (F) gait width assessed at baseline, 6, 24 and 168 hours post LPS 250µg/kg i.p. challenge. All data represented as mean ± SEM (3-9 months n=18, 14-19 months n=15, 20-24 months n=30; Robust n=16, Mid-frailty n=31, High-Frailty n=16) and assessed by repeated measures two-way ANOVA with Bonferroni Post Hoc test, *p<0.05, **p<0.01, ***p<0.001 signifies significant difference from baseline, #p<0.05, # #p<0.01, # # #p<0.001 signifies significant difference between groups at one timepoint

4.4.3.3 Recovery of and vulnerability to impaired activity

The final category of Fried's Frailty phenotype are low activity levels. To address low activity in our frailty index I assessed the animal's spontaneous movement in the open field test using the number of rears **(Figure 4.31 A,C)** and the distance covered **(Figure 4.31 B,D)** during a ten-minute period of testing.

Assessment of animal's activity in the open field task showed that animals of all ages and frailties showed very marked decrease (***$p<0.001$) in rearing behaviour and open field locomotor activity following LPS challenge, with peak deficits occurring at 6 hours, very limited recovery at 24 hours and only a partial return towards baseline levels at 168 hours. The failure to return to baseline levels at 168 hours at least partly reflects habituation to the open field, which over repeated exposures loses novelty and exploration reduces accordingly.

While young animals were significantly less affected than both older groups, and robust animals were significantly less affected than both of the higher frailty groups, there were minimal differences between the 14-19 and 20-24 months and between mid and high frailty. Recovery of open field activity at 168 hours in mid-frailty was significantly different to that in high frailty (*$p<0.05$). However, most differences between the groups were explained by the difference between the groups at baseline.

In the previous sections I demonstrated frailty to be a more robust descriptor of metabolic measures deficits and recovery, as well as a predictor of cognitive vulnerability to LPS induced impairment. However, extensive assessment of physiological measures such as grip strength, distance to exhaustion, maximum speed, and activity here has revealed that age was a marginally more reliable descriptor of LPS induced impairments in and especially the extent of their recovery to baseline over a 168 hour, week-long, recovery period. However, one must bear in mind that several of these physiological measures were vulnerable to bias either by virtue of habituation effects or lack of motivation due to sickness-behaviour induced anhedonia as I have highlighted throughout.

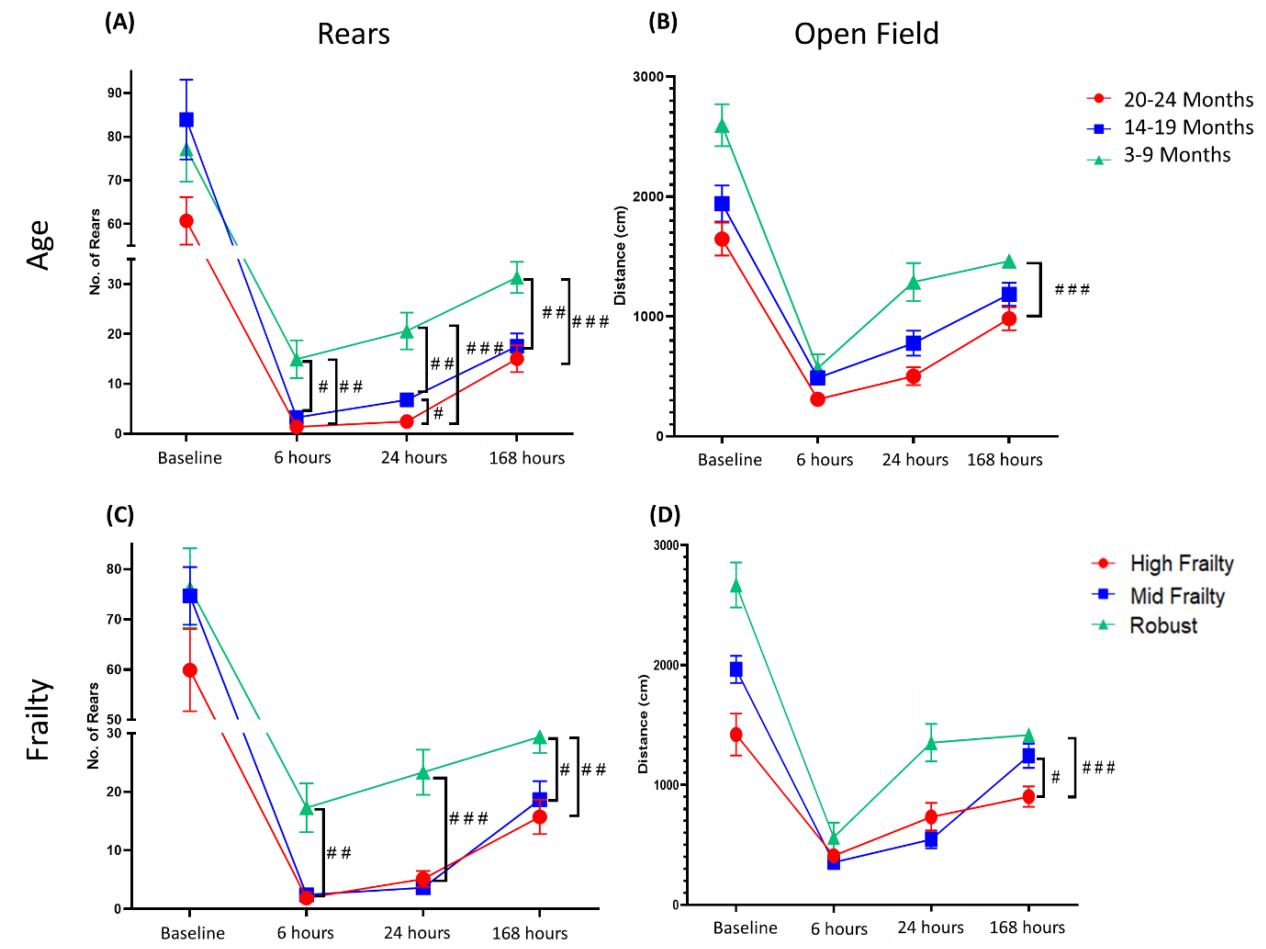

Figure 4.31 – Recovery of and vulnerability to impaired activity in the open field following systemic inflammatory challenge: Age better predicts the expected trajectory of recovery (3-9 months n=18, 14-19 months n=15, 20-24 months n=30; Robust n=16, Mid-frailty n=31, High-Frailty n=16), repeated measures two-way ANOVA with Bonferroni Post Hoc test, *p<0.05, **p<0.01, ***p<0.001 signifies significant difference from baseline, #p<0.05, # #p<0.01, # # #p<0.001 signifies significant difference between groups at one timepoint

4.4.3.4 Baseline frailty scores are exacerbated by systemic challenge with LPS and predict the degree of frailty score recovery.

As discussed previously, each animal underwent a total of four frailty assessments (the components of which I have discussed in the previous section), once at baseline and then reassessed at 6, 24 and 168-hours post exposure to the inflammogen, LPS. After each of these assessments a frailty score at that point in time was calculated for each animal. Analysis of these individualised frailty scores at each of these time points revealed that all animals experienced a significant increase in their frailty score (or a reduction in their resilience) acutely under LPS and recovered to a significantly lower point than baseline by 168 hours **(Figure 4.32 A)**. When I looked at the efficiency of recovery of the frailty score it was shown that Robust animals had significantly improved (***$p<0.001$) recovery between 6 and 24 hours and continued to improve at 168 hours post challenge. In contrast, the Mid Frailty animals failed to show any significant recovery between 6 and 24 hours but by 168 hours had shown a strong significant improvement (***$p<0.001$). Higher Frailty animals also showed no significant recovery between 6 and 24 hours and exhibited only a very weak improvement by 168 hours (*$p<0.05$). This is consistent with the idea that higher frailty renders one ever less capable of recovering to an equivalent level as their baseline before the stressor. Linear regression analysis plotting Baseline Frailty score or age against the recovery of the individual animals' frailty score at 168 hours as a percentage of their score at 6 hours post challenge, revealed that baseline frailty strongly predicted (r^2 =0.2285, slope = -0.3366) a failure to recover to prior levels of resilience, i.e. increased frailty **(Figure 4.31 B)**. While age showed a similar trend but was marginally weaker (r^2 =0.2092, slope = -0.057) **(Figure 4.32 C)**. Robust animals showed a larger improvement in resilience but did not quite return to their baseline status. While counter to what the frailty of definition might predict this is likely a result of reductions in engagement in certain components of the frailty index due to habituation as discussed earlier in this chapter.

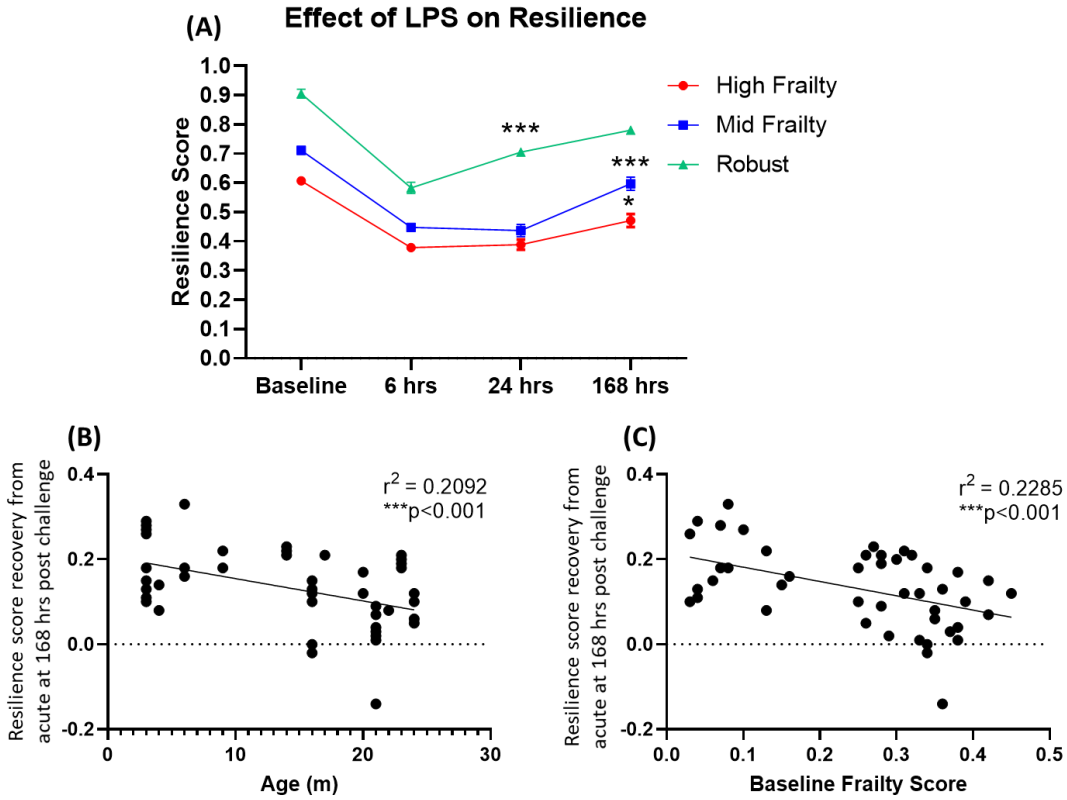

Figure 4.32 – Recovery of resilience to baseline following systemic challenge: (A) Change in resilience from baseline to assessment at 6, 24 and 168 hours post i.p. challenge LPS (250µg/kg) by frailty classification. All data represented as mean ± SEM and assessed by repeated measures two-way ANOVA with Bonferroni Post Hoc test, *p<0.05, **p<0.01, ***p<0.001 signifies significant increase from nadir. Correlation between (B) age and (C) frailty with recovery of resilience score from nadir assessed by Pearson linear regression analysis, age (3-9 months n=18, 14-19 months n=15, 20-24 months n=30; Robust n=16, Mid-frailty n=31, High-Frailty n=16).

4.2.3.4 Predicting systemic inflammatory status and mortality

Frailty better predicts systemic inflammatory status in recovered animals

Blood plasma levels were tested post-mortem one week, 168 hours, post LPS (250µg/kg) challenge from atrial blood collected at time of euthanisation for known chemokine and cytokine markers associated with age, frailty and inflammation. A Pearson linear regression analysis was performed on animals' age and their baseline frailty status against their serological chemokine/cytokine expression in order to assess whether frailty or age might better predict the degree of inflammatory resolution 7-days post LPS.

Unlike earlier analysis of plasma levels for the cytokines IL-6 and TNFα in our TFL I frailty cohort where negligible expression was found across animals at baseline, expression levels were more robust, particularly in aged animals. It was found that expression levels were more accurately predicted by baseline frailty than by age at 168 hours post LPS (250µg/kg) i.p. challenge. Furthermore, expression of the chemokine CCL2, the most robust serological marker of frailty in our TFL I cohort and within longitudinal ageing frailty studies (Ng et al. 2015) was shown to be equally correlated with age as with baseline frailty score. However, assessment of expression levels when stratified according to the animals' endpoint frailty score showed a more robust correlation than both baseline frailty score and age for these pro-inflammatory cytokines and chemokines **(Figure 4.33)**.

Despite predictions based off the fact that IL-10 -/- animals are a well-studied model of frailty, it was age that was a more accurate metric to determine systemic anti-inflammatory status as represented by serological IL-10 expression. Expression levels of the anti-inflammatory cytokine IL-10 were found to be show no significant correlation with baseline frailty but correlated quite well with age comparatively **(Figure 4.33 H, D).** While endpoint frailty score showed a weak significant correlation with IL-10 expression levels age was by far the better predictor **(Figure 4.33 L).**

Frailty status was shown to predict an animal's pro-inflammatory status more accurately after one week of recovery for all animals assessed at this time point. While baseline more accurately predicted this than age it was found the more recent the frailty assessment was conducted to the time of plasma collection the more accurately the levels of pro-inflammatory cytokines could be described **(Figure 4.33 M)**.

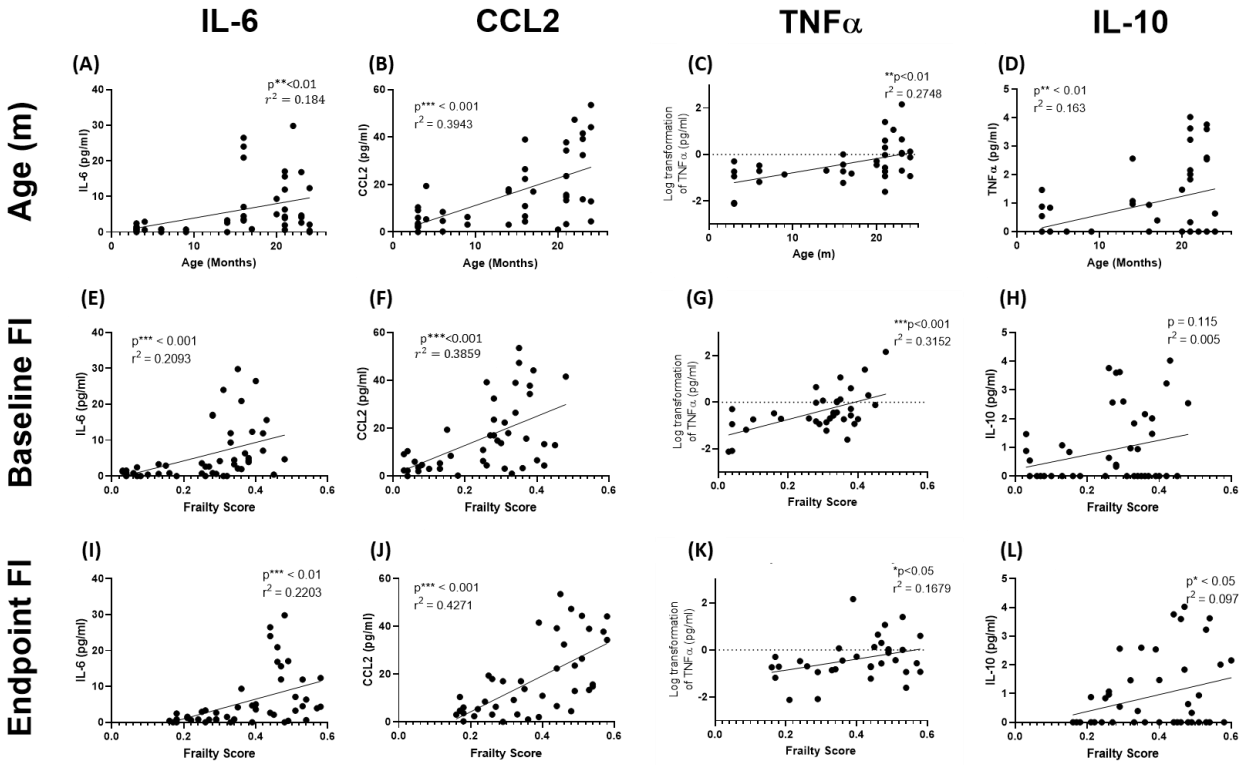

(M)

		IL-6	CCL2	TNFα	IL-10
Age (m)	p	**<0.01	***<0.001	**<0.01	**<0.01
	r^{-2}	0.184	0.3943	0.2748	0.163
Baseline FI	p	***<0.001	***<0.001	***p<0.001	0.115
	r^{-2}	0.2093	0.3859	0.3152	0.005
Endpoint FI	p	***<0.001	***<0.001	*p<0.05	*<0.05
	r^{-2}	0.2203	0.4271	0.1679	0.097

Figure 4.33 – Relationship between serological expressoin of cyotkines and chemokines 7 days post LPS (250µg/kg) challenge with age and frailty status at baseline and endpoint. IL-6 (A, E, I), CCL2 (B, F, J), TNFα (C, G, K) and IL-10 (D, H, L) was assessed against age, baseline frailty and endpoint frailty scores respectively. Simple linear regression analyses, (n = 62), significance denoted by *p<0.05, **p<0.01, ***p<0.001. (M) Summary table of pearson linear regression r^2 and p-values .

(A)

	Trinity Frailty Index Version I (TFL I)					
	Hippocampus		Hypothalamus		Cerebellum	
	Frailty	Age	Frailty	Age	Frailty	Age
Clec7a	0.0811	0.0999	0.1666	0.369	0.175	0.4249
Cd11c	0.4571	0.1563	0.0163	0.0023	0.1955	0.4315
T rem 2	0.0165	0.0346	0.086	0.1604	0.0191	0.1183
Tyrobp	0.1688	0.2743	0.0407	0.0899	0.0933	0.1558
C1q α	0.09543	0.1578			0.0227	0.0089
C3	0.0041	0.0187	0.0285	0.096	0.1686	0.3722
Bdnf	0.1393	0.2622	0.1356	0.2515	0.181	0.0054
Igf1	0.0837	0.0015	0.1322	0.2175	0.079	0.0158
Tgfb	0.1676	0.2489	0.2009	0.1091	0.1326	0.1153
Sparc	0.0201	0.0285				
Il1b	0.0592	0.0643	0.0031	0.0015	0.0012	0.0001
Tnfa	0.0849	0.0414	0.038	0.1063	0.1907	0.1506
Cxcl10	0.0186	0.0089	0.0499	0.0283	0.1412	0.1989
Cxcl13	0.2391	0.2257	0.4629	0.4424	0.2853	0.1625
Ccl2	0.0756	0.2031	0.219	0.3673	0.2457	0.3883
Irf7	0.0275	0.059			0.11	0.1038
Il6	0.0723	0.1079	0.1635	0.1404	0.0459	0.00005
Il10	0.01435	0.0087	0.0425	0.0175	0.03489	0.0187

No significant linear correlation				
Significant linear correlation with frailty	Frailty	***p<0.001	**p<0.01	*p<0.05
Significant linear correlation with frailty	Age	***p<0.001	**p<0.01	*p<0.05

(B)

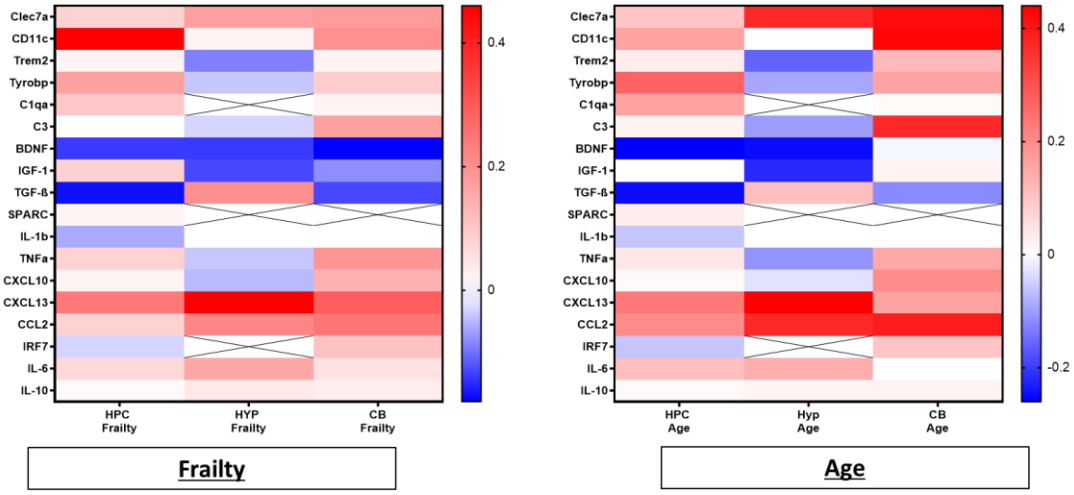

Table 4.4: Summary of significant linear correlations with frailty scores and age: (A) Summary table of all correlations between qPCR transcriptomic gene expression and frailty score/age r^2 values from Figure 4.11-17, colourcoded by p-value statistical significance, across the cerebellum, hypothalamus, hippocampus and cerebrum. All data analysed as using Pearson's linear regression * denotes a significant effect of treatment; 3-9 months n=18, 14-19 months n=15, 20-24 months n=30; Robust n=16, Mid-frailty n=31, High-Frailty n=16. (B) Heat map summary of regional significant linear correlations fit to the line, r^2 value, and slope trajectory by frailty and age.

4.3 Discussion

In summary, I have designed a novel cumulative deficit model frailty index modelled off the Fried Integrated Phenotype model of Frailty, of which I utilised two variants, capturing multiple measures of metabolism, physical activity, strength, cognition and physiology. The results shown here indicate that age is a strong determinant of microgliosis as evaluated by gene transcript using qPCR; but so too is frailty. I have demonstrated robust heterogeneity in changes to transcript expression for multiple markers associated with the microglial response across the ageing brain, depending on the region, and assessed how this correlates with frailty across two different frailty indices. Of these regions assessed the cerebellum exhibits an overall more immune reactive state with expression for microglial activity and pro-inflammatory mediators showing robust increases with advancing age and frailty and decreases in growth factor transcript expression with frailty score, but not age. In contrast the hypothalamus showed a largely inverse trend to this with microglial activity markers decreasing in expression, robust decreases of growth factors and increased expression of senescence associated genes. Notably, given the hypothalamus intricate role in regulating the body's metabolic homeostasis, it was found that consistently across both indexes their component measures associated with metabolism such as body weight, core body temperature and glycaemic status were found to be more accurately predicted by frailty than they were by age alone. This was especially true when assessing vulnerability and recovery from a systemic LPS challenge.

4.3.1 Sensitivity of Frailty Index and prevalence of frailty

In order to assess the difference between an animal's chronological and biological age I set out to design a novel cumulative deficit frailty index. This was modelled off the classic Fried Integrated Phenotype model of Frailty with measures capturing aspects of each of its five criterion of exhaustion, slowness of movement, unexpected weight loss, low activity, and weakness (Fried et al. 2001). Across the two variants of this used in different studies, TFL I and TFL II, additional assays of behaviour, metabolism and cognition were also included in an attempt to capture as accurate a snapshot of the individual's overall health and cognitive status as possible. All of these measures were scored in the fashion of a cumulative deficit index for each individual measure as z-values (standard deviations away) from the mean score of healthy young animals and averaged for all component measures. These individual z-score values for each measurement of frailty were summed and the resulting number divided by the total number of parameters measured to yield a Frailty Index Score (FI) for each animal; such that an animal with no deficits in any assessed category would have a score of 0 and an animal with all possible maximal deficits would have a score of 1.

While assessment of frailty with our TFL I and TFL II indices revealed a significant increase in frailty prevalence as age advances, as would be expected, it was found that there were relatively low

numbers of animals with significant frailty despite the relatively large populations of animals assayed. There are several factors to consider which have contributed to this.

As discussed previously in this text the first issue to consider is that in practice any animal scoring close to this maximum frailty score of 1, would likely be in such a severe state of advanced moribundity and past their humane endpoint that they would be euthanised and not be included in analyses. As such the maximum finalised frailty score typically found from our assays would be circa. 0.6. However, even with this in mind the number of animals with frailty scores between 0.4-0.6 were typically very low, even at extreme ages. This is a result of the fact that working with mouse models as we are limited by the fact that mouse colonies are inherently very homogenous populations with minimal opportunities for adverse risk and poor lifestyle choices as would be the case, for human populations. Mice colonies are inbred for the express purpose of maintaining a healthy population with as little genetic diversity as can be achieved, and where possible adverse genetic conditions are removed from the population to this end. Furthermore, these animals are raised in a deliberately homogenous environment in pathogen free cages with a uniform diet and space in which to live and be active. Recent research has highlighted the substantial impact which high fat, ketogenic and caloric restricting diets have upon CNS ageing pathology (Iqbal et al. 2019; Yin et al. 2018; Newman et al. 2017). While such uniform conditions might be advantageous in the majority of animal studies in order to have close biological replicates this is a significant disadvantage when assessing ageing conditions such as frailty which rely upon the development of chronic co-morbidities, infections and poor lifestyle choices to allow ageing populations to diverge over time and varying levels of frailty to present as would happen over the course of a normal adult lifespan. An ambitious project to address these issues and limitations in mouse models of frailty is planned to begin at the Centre de Recherches sur la Cognition Animale (CRCA) at the Université Toulouse using a population of 1576 outbred male and female SWISS mice who will be split into treatment groups with access to voluntary aerobic exercise and/or high fat high sucrose diets. They will be monitored from 6-24-months of age and have their spontaneous and voluntary physical activity continuously monitored with assessment at regular 3-6-month intervals of their behavioural cognition, body composition, immune and cardiac function, frailty, fecal, blood and urine tested and metabolic status assays using metabolic cages (Santin et al. 2021). Despite these limitations however the TFL indices did have substantial predictive ability when it came to known serological markers of frailty and performance on behavioural, physiological and cognitive assays. Notably, the chemokines CCL2 and CXCL13 which were previously identified as serological markers of frailty (Lu et al. 2016) were found to have the most robust correlations with frailty in the serum and at the transcriptomic level across the ageing brain. Previous work by Villeda and colleagues demonstrated using heterochronic parabiosis that blood-borne factors, including CCL2, present in

the serum of ageing individuals were responsible for regulating neurogenesis and cognitive function with young animals exposed to an old systemic environment showing decreased synaptic plasticity and impaired contextual fear conditioning and spatial learning and memory (Villeda et al. 2011). Consistent with this, the TFL indices also had substantial predictive ability when it came to cognitive, behavioural, and physiological assays.

Additionally, previous animal frailty studies utilising cumulative deficit or Fried phenotype models in normal wild-type mice, conducted to date have not fully explored the relationship between particular frailty measures and score with predicted outcome, i.e. survival or functional capacity. That is, there is a strong motivation to see frailty as a construct comprised of many factors, thus discouraging deconstruction of the construct for the purpose of examining differential contributions of some features compared to others. For instance, in the cumulative index utilised by Parks et al., equal weighting is given to loss of hair colour as is for tumours (Parks et al. 2012); despite development of tumours likely being a stronger predictor of adverse outcome or increased frailty than greying hair. If we are to unravel the mechanism by which frailty manifests and progresses it is imperative that we choose carefully what measures are included in the generation of the frailty score with clear understandings of how they relate to pathology, survival and functional capacity individually, as well as collectively. To this end I set out to assess the correlation between each of the frailty index component measures and the resulting frailty score, in order to determine which components are the greatest contributors to the frailty score observed and might be predictive of vulnerability to a stressor. Across both variants of the TFL index it was found that frailty score was more discerning than age in predicting animal baseline performance across all metabolic assays, including weight loss, core body temperature, insulin and glycaemic status, both at baseline and when predicting vulnerability to and recovery from a systemic challenge.

4.3.2 Frailty better predicts vulnerability to and recovery from acute metabolic deficits following systemic LPS challenge

Currently there is a lack of consensus on the quantification of Frailty in the medical field with countless iterations and variations being used and reported on throughout the field. As such it is crucial that we elucidate the underlying biological and cellular mechanisms which are driving this syndrome if we are to design frailty assays that are both accurate and translatable to the healthcare setting. The core definition of frailty is of course a state of increased vulnerability to a stressor event stemming from multiple co-morbidities and resulting in an increased risk of adverse outcomes and failure to return to baseline homeostasis. As mentioned above, across both variants of the TFL index it was found that frailty score was more discerning than age in predicting animal baseline performance across all metabolic assays, including weight loss, core body temperature, insulin and glycaemic status. This was also true when using TFL II to predict and assess an animal's vulnerability

to an acute systemic challenge with a 250µg/kg dose of the endotoxin LPS at 6 hours on the individual components of the index and their subsequent recovery at 24- and 168-hours post challenge. As with baseline analysis, it was frailty which was consistently the best descriptor of an animal's acute vulnerability, recovery trajectory and indeed, the degree to which an animal was able to recover to their baseline level over the week recovery period for the index's components associated with metabolism, such as body weight, core body temperature and glycaemic status. While frailty was superior in describing the vulnerability to and recovery of deficits associated with metabolism it was also shown to be a robust descriptor for physiological and activity measures, albeit to a lesser extent than age. This was ultimately reflected cumulatively in the change in resilience in response to LPS 250µg/kg i.p. challenge and its recovery over the week period post challenge, with robust animals showing the quickest significant improvement while higher frailty groups took progressively longer, respective to the severity of their frailty score at baseline. Furthermore, frailty was shown to better predict the expression of systemic pro-inflammatory chemokines and cytokines at time of euthanisation.

It should be noted that in our initial TFL I study glucose expression at baseline was found to be negatively correlated with age while a contrary positive correlation was observed in our TFL II study potential explanation for this discrepancy is the difference in the manner in which blood glucose levels were assessed at baseline differed between the two studies with TFL I blood glucose levels being assessed directly from atrial blood at time of euthanisation while TFL II levels were assessed by venous tail vein lancing; venous and arterial blood are known to show subtle differences in glucose concentration (Cengiz et al. 2009). However, it is more likely this discrepancy is a product of the difference between the two studies populations in terms of their range and variation in ages with TLF I having no animals aged 10-17-months old and several animals at the extreme age of 27-29-months old who showed robust hypoinsulinemia. This is noteworthy given that as older individuals lose adipose tissue it has been shown to reduce their underlying insulin resistance and commensurately their serological insulin levels (Clamp et al. 2017). Consistent with this these 27-29-month-old animals were also significantly lighter in weight than those animals at 18-22 months who had higher insulin levels.

This robust association between our frailty scores and metabolic assays is particularly interesting as ageing is of course closely associated with an age-related decline in metabolic function, characterized by changes in fat distribution, obesity and insulin resistance (Gabriely et al. 2002). Similarly, it has been shown that obesity (Villareal et al. 2005)and metabolic diseases such as type two diabetes (Eckel et al. 2011; Yokoyama et al. 2020; Munshi 2017) can exacerbate age-related decline and increase frailty and while unexpected weight loss is a classic hallmark of frailty, studies have found that frail older adults were shown to have a higher adiposity and greater average waist

circumference than non-frail patients (Crow et al. 2019). Care home studies have demonstrated that obese geriatric women were found to be twice as susceptible to frailty than non-obese women of the same age (Monteil et al. 2020). This increased obesity is frequently shown to be concomitant with a loss of muscle tone. This sarcopenic obesity, a loss of muscle mass and strength with a concomitant increase in adiposity has been shown to be linked to frailty (Crow et al. 2019) and in longitudinal studies of ageing population men with this low muscle mass and high adiposity have a doubled risk for frailty over a 5 year period (Hirani et al. 2017). Elevated endotoxin levels have been reported in animals subjected to high fat diets and contributes to the low-grade obesity associated inflammation (Kyung-Ah et al., 2012). Conversely it has been shown that low fat diets with high fruit, vegetable and omega-3-fatty acid intakes, such as the Mediterranean Diets is associated with substantial reductions in risk of frailty development in aged individuals (García-Esquinas et al. 2016; Feldman 2018; León-Muñoz et al. 2015) and has even been shown to be effective in combatting established frailty (Voelker 2018; Frison et al. 2017; Hutchins-Wiese et al. 2013; Lopez-Garcia et al. 2018). Similarly, aerobic exercise and resistance training has been shown to improve metabolism (Bittel et al. 2020; Desseille et al. 2017) and frailty characteristics including strength, agility, gait, fat and muscle mass, postural stability and mortality as well as improvements in cognition, IGF-1 signalling, gut microbiome diversity and reduced inflammation (Talar et al. 2021; Aguirre et al. 2015; Angulo et al. 2020; Arrieta et al. 2019; Cadore et al. 2013; Giné-Garriga et al. 2014; De Labra et al. 2015).

Furthermore, previous studies have demonstrated that obesity is associated with low-grade chronic inflammation, synaptic loss, hypothalamic gliosis and cognitive deficits (Bocarsly et al. 2015; Thaler et al. 2013; Kälin et al. 2015; Belkina et al. 2010). Metabolic dysfunction, obesity and its associated co-morbidities are associated with learning and memory impairment in in early old age (Singh-Manoux et al. 2012; Sabia et al. 2009) and are known to facilitate and predict neurodegenerative diseases risk (Cai *et al*., 2013; van Dijk *et al.*, 2015). Indeed recent mouse frailty studies have high-lighted that mice on a low-fat caloric restriction diet exhibited reduced microgliosis in white matter regions (Yin et al. 2018) while the opposite is true in mice on a high-fat diet demonstrating dramatic neuropathological changes, gliosis and pro-inflammatory changes in a highly regionally variable manner (Iqbal et al. 2019; Zhang et al. 2008; Guillemot-Legris et al. 2016). This well documented relationship between diet, obesity, frailty and cognition is consistent with our own frailty scores descriptions of metabolic assays at baseline and under an acute stressor, those observed on assays of cognition. Despite the now widespread acceptance of the risk factor which frailty presents for the onset and progression of dementia (Robertson et al. 2013; Buchman et al. 2014; Song et al. 2014), little frailty research has assessed how it predicts the impact of an acute systemic inflammatory stressor on cognition. Indeed, delirium a highly prevalent condition of profound,

acute confusion and awareness affecting 30% of elderly patients admitted to hospital (Clegg et al. 2013), is more prevalent again in post operative diabetic patients (Kotfis et al. 2019; Chu et al. 2021) and is predicted by frailty in diabetic patients (Lee et al. 2021). Consistent with this I have demonstrated, using the TFL II assay, that frailty status, which I have established is strongly influenced by metabolic deficits, was not only a better descriptor of cognitive ability at baseline to learn a task but also to subsequently retain it under acute inflammatory conditions, 3 hours after challenge with 250µg/kg of LPS. While at face value age better defined an animal's ability to adjust their strategy for solving the maze when the task's solution was reversed, it was shown by linear regression analysis that the number of incorrect trials during the reversal blocks correlated with the animal's frailty score and the number of incorrect trials during their learning phase which was part of their finalised frailty score. Taken together this indicates that while age is a good predictor of cognitive status in and of itself, frailty offers a more robust description over-all and is a strong contributing factor even when age appears the better descriptor.

While LPS is first and foremost a bacterial mimetic whose pro-inflammatory effects are well documented in the literature, previous work from our group and others has demonstrated that LPS treatment has a significant impact upon an animal's metabolism inducing acute hypoglycaemia (Kealy et al. 2020; Del Rey et al. 2006) which will also result in impaired cognition and delirium (Kealy et al. 2020). This is not only consistent with our observations of the strong influence metabolism has upon frailty but is consistent with the frailty literatures reports that diseases associated with glycolytic disruption such as diabetes impart increased risk of cognitive deficit in the form of dementia or delirium (Eckel et al. 2011; Yokoyama et al. 2020; Munshi 2017). Consistently here I have demonstrated a strong link between frailty status and metabolic status and dysfunction. In the clinical setting there is substantial variation amongst medical practitioners' implementation of frailty assessment with significantly different measurements and scoring employed in each instance. Taken together these data presented here emphasise the importance of including and appropriately weighting metabolic measurements scoring in assessing frailty status using the cumulative deficit frailty model in the clinical setting in order to capture an accurate representation of the individual's vulnerability to and recovery from an acute stressor. However, these data in turn also beg the question how frailty and its associated metabolic and cognitive deficits are impacting the CNS immune profile and whether regions associated with metabolism, such as the hypothalamus, are affected differently.

4.3.3 Microglial activation and function in frailty

Following on from the previous chapter's findings of regional heterogeneity in immune response across the ageing brain, with evident microglial reactivity within white matter regions, I have demonstrated further evidence of regional microglial heterogeneity in the ageing brain with frailty, as well as a clear disparity between hippocampal, and cerebellar against hypothalamic gene expression within the Trinity Frailty Index II. While not always achieving significance, the hippocampus and cerebellum typically showed a trend toward increased immune reactivity with age and frailty. This is in keeping with the existing literature previously discussed from micro array data by Grabert et al. (Grabert et al. 2016) which demonstrated the hippocampus and cerebellum were significantly more immune vigilant than the striatum and cortex. Interestingly, the hypothalamus has shown a notably divergent immune profile compared to the cerebellum and hippocampus.

Traditionally, the cerebellum has been thought of primarily as a subcortical centre for motor control, however, more recently there has been growing evidence highlighting the cerebellum's important role in cognition (Babayan et al., 2017; Petrosini et al., 1998; Stoodley et al., 2017) and immunological responses (Cao et al., 2013). Direct bidirectional connections between the cerebellar cortex and nuclei with the hypothalamic nuclei and areas have been implicated as potential pathways underlying these functions (Cao et al., 2013). The dentate nucleus as discussed earlier in this text demonstrated significant microgliosis and reductions in white matter integrity in cognitively frail animals and consistent with this large-scale human studies have reported the region to be vulnerable to reduced connectivity with advancing age (Bernard et al., 2021; Maschke et al., 2004). Consistent with this, these connections have been shown to run primarily from hypothalamic regions such as the lateral (LHA), posterior (PHA), and dorsal (DHA) hypothalamic areas; the supramammillary (SMN), tuberomammillary (TMN) and lateral mammillary (LMN) nuclei; the dorsomedial (DMN) and ventromedial (VMN) nuclei; and in the periventricular zone (PVZ), to the cerebellar cortex and nuclei including the dentate (DN), interposed (IN) and fastigial nucleus (FN) (Dietrichs et al., 1994; Haines et al., 1997). Indeed, incoming vagal sensory information arrives first at the nucleus of the solitary tract (NTS) and can be relayed to the hypothalamic PVN and suprachiasmatic nucleus (SCN), resulting in changes in metabolic settings, temperature and glucose availability (la Fleur et al.; 2000; Kalsbeeket al., 2012; Bohlandet al., 2014; Guzm´an-Ruizet al., 2015). The SCN can also set day–night differences in the intensity of the temperature and cytokine response to such an acute challenge. It has been demonstrated that during the early stages of an infection an increase in body temperature will simultaneously help leucocytes fight infection while also inhibiting the growth of certain microorganisms (Elmquist et al., 1997). However, ablation of the SCN results in disturbed circadian rhythmicity and exacerbated inflammatory responses

(Castanon-Cervantes et al., 2010; Guerrero-Vargas et al., 2014; Guerrero-Vargas et al., 2015). Furthermore, thanks to its extensive connections throughout the brain the hypothalamus is known to affect mood and memory and it has in turn been demonstrated that depression results in antibody-mediated immune activation, with depressed patients usually showing elevated pro-inflammatory cytokines, suggesting an enhanced inflammatory response (Postal et al., 2015). Finally, as discussed earlier the hypothalamic signalling via ARC-POMC neurons is integral in governing satiety and feeding responses in mice and it has been shown that caloric restriction will attenuate fever, sickness behaviour and systemic IL-6 expression. It is has been reported that differential metabolic and sickness behavioural responses to bacterial and virally-induced inflammation are adaptive and a failure to maintain these metabolic adaptations to acute inflammation is, itself, detrimental. Wang and colleagues demonstrated that glucose supplementation was detrimental to mortality outcomes following a bacterial stressor but improved them following a viral Poly I:C challenge (Wang et al. 2016). This "feed a cold, starve a fever" dichotomy has been shown to extend to cognitive dysfunction with acute LPS inflammation altering energy metabolism and impairing cognition which were mitigated or exacerbated by treatment with glucose or LPS respectively (Kealy et al. 2020; Del Rey et al. 2006). The SCN's circadian rhythm governance is also important in this as animals whose natural light-dark cycle is disrupted and results in an exacerbated response to a subsequent acute LPS challenge (Guerrero-Vargas et al., 2015). This is consistent with extensive reports in the literature of the importance of healthy circadian rhythms in healthy ageing and longevity (Acosta-Rodriguez et al. 2021). Taken together these data highlight the importance of not only the detection, integration and signalling responses to an acute systemic stressor by the hypothalamus but also the timing of them. This suggests that aged individuals who have been shown to have disrupted circadian rhythms (Acosta-Rodriguez et al. 2021) might be at an increased risk of impaired hypothalamic signalling and responses resulting in increased vulnerability to and exacerbated responses to an acute stressor and the extent of this might be dependent on the severity of their biological ageing, or frailty.

Age has been shown here to be a robust predictor of microglial activation **(Table 4.4),** however, several genes also demonstrated relatively consistent significant correlation with frailty across the ageing brain. Microglia, the brain's primary immune cell population, play a critical role in the maintenance of neuronal homeostasis but as they age, their environmental sampling capabilities become compromised due to their chronic activation with age (Hickman et al. 2013). With the retraction of their processes, they are unable to carry out this surveillant function as efficiently, which implies that activated and aged microglia have poorer sampling capabilities than younger, resting microglia. This coincides with a decrease in *Sparc* expression found in activated microglia (Holtman et al. 2015), which decreases the surveying state of these cells as well as the secretion of

the neurotrophic factors, *Igf*1 and *Bdnf* which are secreted by microglia in their M2 state and decreased upon activation (Łabuzek et al. 2015). Analysis of the growth factors *Bdnf* and *Igf1* transcripts lends support to this hypothesis with a significant negative linear correlation with frailty found for both genes in the majority of brain regions assessed, within the cerebellum it was observed that frailty was a significantly stronger predictor of expression compared to age alone. BDNF is a neurotrophic factor whose expression oscillates in a circadian manner and is secreted extracellularly, playing a pivotal role in neuronal survival and growth, functioning as a neurotransmitter molecule and participates in neuronal plasticity (Huang et al. 2001) and decreased levels have been shown to associate with neuronal loss and neurodegenerative diseases including PD (Scalzo et al. 2010), MS (Sohrabji et al. 2006), Huntington's disease (Mughal et al. 2011) and AD (Ng et al. 2019). Furthermore, systemic administration of *Bdnf* has been shown to result in an improvement in blood glucose control, resulting in decreased body weight in obese and diabetic mouse models (Smith et al. 1995). Similarly intracerebroventricular administration of *Bdnf* resulted in decreased energy intake (Ono et al. 2000) and body weight (Pelleymounter et al. 1995) in mice and has since been shown was found to be associated with a dose-dependent increase in serotonin turnover, nerve cell survival and adaptive plasticity in human longitudinal studies (Golden et al. 2010). *Igf1* has been shown to have similar downstream signalling mechanisms as *Bdnf*, via the PI3K-AKT-mTOR pathway, resulting in increased cell survival and transcription of pro-survival genes (Nakagawa et al. 2003). Taken together these data indicate that with increased frailty there is a decrease in the expression of these growth factor genes associated with neuronal maintenance and with potential detrimental impacts upon neuronal integrity and metabolism, consistent with our observations of frailty status strongly predicting cognitive and metabolic outcomes to an LPS stressor.

Trem2 is highly expressed in microglia and is an important gene for maintaining their fitness. It is a signalling receptor involved in innate immunity to clear toxic proteins by microglia (Rivest 2015; Qin et al. 2021) and as such it impacts microglia metabolism in AD models through a distinct pathway by activating the mTOR signalling pathway. This pathway supports long-term cell trophism, survival, growth and proliferation. *Trem2* deficient microglia are associated with increased autophagy and phagocytosis of accumulating apoptotic cells and debris (Ulland et al. 2017). Therefore, a deficiency of *Trem2* or lower levels of its gene expression as observed in highly frail individuals' hypothalamus in our TFL I cohort and the cerebrum of the Dalhousie cohort, may signal a loss of microglial capacity to support neuronal homeostasis adequately resulting in reduced neuronal density such as that observed in the previous chapter's aged cognitively frail animals' low presynaptic terminal (SY38+) density in the hippocampus. Furthermore, *Trem2* plays a critical role in the regulation of pro-inflammatory genes. It has been shown that *Trem2* deficient microglia cannot sustain microgliosis

and undergo apoptosis rather than becoming activated and expanding (Wang et al. 2015). Interestingly, *Trem2* and its signalling partner *Tyrobp* both displayed evidence of a non-linear regression with frailty for the cerebrum of animals who underwent assessment by the Dalhousie Cumulative Frailty Index. A mid-level frailty score saw the greatest expression of *Trem2* while a low or very high frailty score in turn saw a lower expression of *Trem2*. This may imply that mid-frailty is associated with enhanced activation of microgliosis and that expression levels fall when the animals are most frail due to apoptosis of microglia, as a result these animals will be more vulnerable to neurodegeneration or perhaps as a neuroprotective response to combat severe frailty as deficiency of TYROBP has been shown to be neuroprotective in mouse models of AD (Haure-Mirande et al. 2017). Notably though, when frailty was assessed by our own novel TFL I frailty index more variable patterns of *Trem2* expression were found, with the clearest relationship found to be a robust negative linear relationship in the hypothalamus, while the hippocampus and cerebellum were highly variable but showed the highest expression level in the mid frailty range like that of the Dalhousie cerebrum profile.

Thanks to its central role in the activation of the complement system, C3 showed a significant increase in expression with age due to the increased prevalence of inflammation in the ageing brain. It has been proposed that the complement proteins, such as C3, C1q and C4 are involved in the phagocytosis of synapses in a range of ageing-associated neurodegenerative conditions including AD, MS and SMA (Presumey et al. 2017; Vukojicic et al. 2019; Dejanovic et al. 2018; Hong et al. 2016; Lui et al. 2016; Werneburg et al. 2020). Phagocytosis is initiated by complement proteins tagging abnormal synaptic connections between neurons for removal by microglia. Therefore, the upregulation of C3 in neurodegeneration is typically associated with synaptic loss. Conversely, C3 deficiency has been shown to be negatively associated with neurodegeneration. C3-deficient C57BL/6 mice are protected against age-related and region-specific loss of hippocampal synapses and also display a degree of protection against the cognitive decline which occurs during normal ageing (Presumey et al. 2017). It was more recently shown that the complement system works in tandem with microglia, mediating synaptic loss in a wide range of neurodegenerative conditions in mouse models of AD, SMA, MS and dementia to systematically eliminate synapses in early disease pathology (Hong et al. 2016; Hammond et al. 2020; Werneburg et al. 2020; Vukojicic et al. 2019; Dejanovic et al. 2018; Lui et al. 2016; Shi et al. 2017) which was ameliorated following genetic loss or inhibition of complement system components. In this present study, *C3* was highly expressed in all regions of the brain and typically associated with an age dependent increase, with the exception of the hypothalamus which exhibited a significantly divergent age dependent decrease in expression, consistent with the decrease in transcript expression of the microglial markers *Trem2* and *Tyrobp*.

While microgliosis and complement system expression varied between regions, I have demonstrated a ubiquitous microglial priming across the ageing and frail brain. As discussed previously, microglial cells adopt an enhanced activation state known as "priming" under chronic neurodegenerative conditions (Palin et al. 2008; Sly et al. 2001) and with the normal ageing process (Godbout et al. 2005). Primed microglia are characterised by hypersensitive responses to pro-inflammatory stimuli. *Clec7a* is and *Cd11c* are microglial markers of priming and as such is upregulated in the ageing brain (Holtman et al. 2015). Since then it has been shown that β-Glucan activation of Dectin-1 on microglia primes them (Heng et al. 2021; Van der Meer et al. 2015) and is known to be important in orchestrating innate immune responses (Deerhake et al. 2019). Consistent with Parks et al.'s description of the microglial priming phenotype with age (Parks et al. 2012), here I have demonstrated a robust increase in expression levels of the microglial priming hub genes across the ageing brain with age and frailty in both Dalhouise and TFL I cumulative deficit frailty indices. Expression was found to be more strongly predicted by age than frailty in all regions analysed but achieved significance for both **(Table 4.4)**. This heightened activation due to priming could be indicative of enhanced phagocytic ability, antigen presentation and lysosomal activity, which is apparent in chronically degenerating brain tissue. The significant correlation between the expression of *Clec7a* and *Cd11c*, key hub genes of the microglial priming signature (Holtman et al. 2015), and frailty suggests that the frailty score may be either representative of the degree of this degeneration or detrimentally pathogenic itself as has been shown in animals models of spinal cord injury (Gensel et al. 2015) stroke (Ye et al. 2020), EAU (Stoppelkamp et al. 2015) and in an intracerebral haemorrhage its deletion was shown to alleviate neurological dysfunction and promote an anti-inflammatory phenotype, encouraging hematoma clearance (Fu et al. 2021).

While Dectin-1 ligand binding has been shown to induce microglial priming both *in vitro* and *in vivo* (Heng et al. 2021; Van der Meer et al. 2015), to date its ligation and signalling has been most widely studied for fungal molecules including β-1,3-glucan (Dennehy et al. 2007) and zymosan (Yoo et al. 2021). While recent work has suggested the presence of bacterial LPS in brain lysates derived from the hippocampus and superior temporal lobe of the neocortex of brains from Alzheimer's disease (AD) patient may originate in the gut and be able to cross physiological barriers to reach the hippocampus to induce cognitive disruptions (Zhao et al., 2017), these fungal molecules are unlikely to be the endogenous ligands within the CNS responsible for the detrimental pathogenicity observed with CNS disorders. As such increasing study has been done into identifying potential ligands within the CNS that may be inducing this microglial priming phenotype and driving pathology. Of note among these have been vimentin (Thiagarajan et al. 2013), galectin-9 (Lgals9) (Daley et al. 2017; Itoh et al. 2017) and annexins (Bode et al. 2019). However, Dectin-1 binding is capable of inducing signalling via two divergent pathways; a neuroinflammatory response via the

classical CARD9-dependent pathway (LeibundGut-Landmann et al. 2007) or a more beneficial neuroprotective pathway independent of CARD9 (Deerhake et al. 2021) and recent findings suggest that depending on the intensity and timing of ligation repeated stimulation of the Dectin-1 receptor can result in either an immune tolerising or training response (Lajqi et al. 2019; Heng et al. 2021; Van der Meer et al. 2015). As such going forward substantial work must be invested in probing which pathways these newly described ligands will signal along, what the products and outcomes are of this and ultimately how repeated exposures may affect these.

While age was a strong determinant of gene expression, frailty also showed a significant linear relationship with frailty; suggesting once more that the frailty scores may be correlating significantly with microgliosis, neurotrophic factors expression and potentially neuronal integrity.

4.3.4 Divergent microgliosis with age and frailty in the hypothalamus

As discussed in the previous section, the hippocampus and cerebellum typically showed a trend toward increased immune reactivity with age and frailty in keeping with previous reports by Grabert et al. (Grabert et al. 2016) which demonstrated the hippocampus and cerebellum were significantly more immune vigilant than the striatum and cortex. Intriguingly, a uniquely divergent pattern of age associated changes was observed in the hypothalamus. This was particularly notable given our observations of significant association between frailty score and metabolism and the hypothalamus' central role in integrating central and peripheral metabolic responses, regulating food intake and energy expenditure and facilitating the dynamic movement of hormones and nutrients courtesy of the unique formation of the blood-brain barrier at the ventromedial hypothalamus (Gross 1992; Haddad-Tóvolli et al. 2017). While the cerebellum had demonstrated an overall immune vigilant profile with increasing frailty, the hypothalamus demonstrated the opposite with an overall trend toward a negative linear correlation with the majority of microglial markers *(Trem2, Tyrobp),* complement system *(C3),* growth factors *(Igf1, Bdnf),* and pro-inflammatory mediators *(Nlrp3, Tnfa)* was shown in the hypothalamus. This unique profile coupled with the strength of the frailty index's predictions regarding its metabolic components led us to investigate the hypothalamus in more detail.

While the cerebellum and hippocampus alike showed a general decline with frailty in gene expression of the neurotrophic growth factors *Igf1, Bdnf* and *Tgfb,* the hypothalamus alone showed a divergent increase in *Tgfb* expression with age and frailty. The contrary trajectory of hypothalamic *Tgfb's* transcript expression compared to the other assessed growth factors, *Bdnf* and *Igf1*, is particularly interesting given its highly pleiotropic nature and reports that TGF-β has been shown to be increased in the hypothalamus under ageing and inflammatory conditions induced by HFD and positively correlated with the associated impaired glucose tolerance in obese animals (Yan et

al. 2014) as well as increased *Tgfb* gene expression and secretion observed in peripheral fatty tissue (Ricquier 1999). Thus, the expression profile of these growth factors and their robust correlation with frailty is consistent with the strong association I have demonstrated between metabolic dysfunction and its contribution to frailty status. However, TGF-β is an extremely pleiotropic cytokine capable of a wide array of functional outcomes dependent on the conditions, including inducing complete cell cycle arrest (Katakura et al. 1999), suppressing or inducing cell death (Schuster et al. 2002) and has even been previously shown to have a role in mediating the metabolic process of autophagy (Koesters et al. 2010).

Autophagy is a vital homeostatic biological process responsible for the consumption of unwanted cytoplasmic constituents by autophagosomes (Mizushima et al. 2008) and has been shown to decrease in ageing animals (Cuervo 2003; Cuervo et al. 2000) as well as many studies reporting significant deficits across multiple neurodegenerative diseases including AD (Ding et al. 2003; Nixon et al. 2000), PD (Stefanis et al. 2001) and HD (Shibata et al. 2006). Autophagy related protein 5 (Atg5) guides recruitment of light chain (LC) 3II to the membrane to allow the development of autophagosomes via lipidation of cytosolic LC3I. Several cell surface receptors, including TLR2, TIM4 and Fcγ, are constituents of the autophagy pathway and contribute to phagocytosis by stimulating recruitment of LC3 to phagosomes (Sanjuan et al. 2007; Huang et al. 2009; Martinez et al. 2011). Recently, several studies have proposed that in dendritic and macrophage cells the c-type lectin receptor, Dectin-1, is capable of triggering the synthesis and transfer of LC3II to phagosomes, which involves increased Syk, ATG5 and ROS production via NADPH oxidase (Ma et al. 2012; Tam et al. 2014; Ding et al. 2019). Additionally, Dectin-1 has also been shown to be capable of directing autophagy dependent intracellular processing and presentation of fungal antigens for the activation of the adaptive immune response in human macrophages *in vitro* (Öhman et al. 2014).

Despite the previously discussed overall reduction in microglial markers *Trem2* and *Tyrobp* transcripts, the hypothalamus did show a robust increase in expression of the microglial priming signature *Clec7a,* the gene responsible for encoding the Dectin-1 receptor, with both age and frailty. One potential explanation for this is offered by Ulland et al. who demonstrated that in *Trem2 -/-* mice there was enhanced autophagy and reduced ATP levels as a result of impaired mTOR signalling (Ulland et al. 2017) which could be ameliorated by Dectin-1 ligation with zymosan as it offered an alternative signalling route for Syk-PI3k signalling independent of TREM2. As such I theorised that the reduction in *Trem2* expression observed in our hypothalamic tissue with frailty, and the commensurate increase in *Clec7a* transcripts, might indicate increased autophagy with Dectin-1 signalling attempting to curb this and restore ATP levels as observed by Ulland et al in *Trem2 -/-* mice. However, assessment of markers associated with autophagy (*p62, Tfeb, Atg5)* by qPCR failed to show any significant changes, at the transcriptional level. On the one hand this might suggest the

observed reduction in *Trem2* is insufficient to elicit the exacerbated autophagy reported by Ulland et al. in *Trem2-/-* animals or perhaps that the upregulated *Clec7a* transcript levels correspond to increased protein receptor Dectin-1 expression and its unknown endogenous ligand were successful in abrogating this by providing an alternative Syk-PI3k signalling pathway independent of TREM2. However, given the limited information available from this qPCR data further analysis for changes in hypothalamic protein levels of autophagy markers and TREM2 and DECTIN-1 as well as manipulation of the signalling pathway using antagonists and agonists for Dectin-1 and Trem2 in the frail brain would be required to validate this.

Dectin-1 signalling

Dectin-1 signalling is an area of increasing research with recent studies highlighting the importance of the timing and nature of Dectin-1 agonism which can result in either a tolerising or priming (training) effect. It has been shown that 1µg/ml β-Glucan treatment *in vitro* primes monocytes (immune training) to elicit exaggerated responses to a secondary inflammatory stimuli (Van der Meer et al. 2015). Steelman et al. demonstrated that viral Poly IC stimulated astrocytic production of the Dectin-1 ligand, Lgals9, in turn potentiated microglial secretion of TNF and IL-6 (Steelman et al. 2014). Similar effects have been observed in microglia of mice injected peripherally by i.p. 20mg/kg of β-Glucan priming microglia to elicit an exaggerated proinflammatory response to a secondary 1mg/kg LPS challenge (Heng et al. 2021). While Steelman et al. demonstrated a potentiating effect of the Dectin-1 ligand Lgals9 on inflammatory response to Poly I:C *in vitro*, recent work by Deerhake et al. highlighted Lgals9's induction of the neuroprotective CARD9 independent pathway *in vivo*. Indeed, memory-like immune responses have been observed *in vitro* with repeated exposure of microglial cells to increasing concentrations of β-Glucan (1fg/ml-1µg/ml) over 24 hours resulting in a tolerising protection against the priming expression of inflammatory cytokines such as TNFα and IL-6 when challenged once more with 100ng/ml of LPS a week after initial tolerising challenges (Lajqi et al. 2019).

The best studied of the Dectin-1 pathways is the Syk-CARD9 dependent pathway associated with increased gene expression and production of proinflammatory cytokines in macrophage cells *in vitro* (LeibundGut-Landmann et al. 2007; Wagener et al. 2018). While numerous studies have reported on the association between obesity or age and heightened hypothalamic glial inflammatory profiles (Buckman et al. 2013; Naznin et al. 2015; Youm et al. 2013) our data shows no evidence of increased proinflammatory cytokine expression with age or frailty at the transcriptional level despite the positive association I demonstrated for age with body weight. Rather, a decrease in *Tnfa* and *Nlrp3* gene transcript expression was observed, suggesting no evidence of activation of the Syk-CARD9 dependent path. This decline in *Nlrp3* expression

suggests that this arm of Dectin-1 signalling is unlikely to be engaged despite the upregulation of *Clec7a* and in fact may be indicative of an engagement of a more neuroprotective response as previous reports by Youm et al. have reported that ablation of Nlrp3 ameliorated age-related physiological decline, decreased CNS Inflammation and extended lifespan (Youm et al. 2013). However, this lack of proinflammatory transcript expression is consistent with recent studies demonstrating that exposure of microglia to β-Glucan has been shown to stimulate ROS production and phagocytosis via Dectin-1 but no significant cytokine production was observed in microglia *in vitro* (Shah et al. 2008; Shah et al. 2009) and more recently *in vivo* when β-glucan challenged animals FACS isolated microglia were assessed by qPCR (Heng et al. 2021).

Conversely however, recent work by Deerhake and colleagues has demonstrated that Dectin-1 expressing microglia of animals challenged with the Dectin-1 specific agonist curdlan, were capable of inducing increased expression of the neuroprotective cytokine Oncostatin M (OSM*)* as assessed by FACS (albeit to a much lesser degree than monocytes, BMDMCs and neutrophils) via a CARD9 independent pathway. Furthermore, they have demonstrated by qPCR analysis of myeloid cell transcript levels that *Osm* mRNA is increased in response to Dectin-1 agonism, leading to increased protein expression and secretion from myeloid cells as assessed by FACs. Consistent with these findings I have demonstrated a significant upregulation with age and frailty of *Osm* gene transcript expression in hypothalamic bulk mRNA, which may be a microglial derived product, indicative of engagement of the neuroprotective Dectin-1 CARD9-independent signalling as a result of an endogenous ligand in the ageing brain, suggesting a potentially beneficial function of Dectin-1 signalling. Due to the unique structure of the blood brain barrier at this point we cannot rule out the presence of myeloid cells in this tissue and further analyses upon FACs isolated microglial cells from hypothalamic tissue would be required in order to determine whether this increased *Osm* expression is specifically from microglial transcripts and is indeed translated to protein.

Recent work by Bode and colleagues have demonstrated that annexins are capable of binding to Dectin-1, upon macrophages and dendritic cells, at a unique binding site, distinct from that which β-glucan is known to ligate, resulting in an increase in reactive oxidative species but no change in pro-inflammatory cytokine expression **(Figure 1.5)** (Bode et al. 2019). This is consistent with previous reports that *Clec7a* expression has been shown to be increased in naïve mouse brains injected with apoptotic neurons leading to the belief that Dectin-1 expression in the CNS is related to sensing cellular damage in the brain (Krasemann et al. 2017). To this end I assessed Annexin A1 (*Anxa1)* transcript levels to ascertain whether an upregulation in Annexins might be indicative of increased apoptosis and our observed increased *Clec7a* expression. *Anxa1* mRNA levels have been shown to increase leading to increased ANXA1 protein expression upon apoptotic cells in cancer and chronic gastritis previously (Jorge et al. 2013), however, *Anxa1*

showed no significant changes with either age or frailty in the hypothalamus suggesting there is no significant increase in apoptosis at the transcriptional level. Despite reports of Annexins as Dectin-1 ligands, these data suggests that apoptotic cells' annexin surface markers are unlikely to be the endogenous ligands associated with the increased *Clec7a* expression I observe in the hypothalamus. However, given the limited information which qPCR data affords us on actual protein expression, coupled with the positive correlation between body weight and age we have observed and reports from the literature that there is increased apoptosis in the hypothalamus in obese mice (Moraes et al. 2009), going forward further analysis by flow cytometry or western blot should be conducted to determine whether there is indeed an increase in apoptotic cells and associated ANXA1 surface and DECTIN-1 expression in the frail hypothalamus. Furthermore, *in vitro* or ideally *in vivo* analyses of annexin-Dectin-1 ligation should be assessed to determine whether microglial Dectin-1 is capable of ligating with Annexins as has been reported in macrophages and dendritic cells with the same functional outcomes.

While previous reports have identified annexins (Bode et al. 2019) and galectin-9 (Daley et al. 2017; Steelman et al. 2014; Deerhake et al. 2021) as endogenous ligands for macrophages and microglia respectively, I saw no upregulation in their transcript expression in the frail brain despite robust increases in the Dectin-1 gene *Clec7a* transcript. This may suggest there are other endogenous molecules responsible for Dectin-1 signalling in the CNS. Previous work by Thiagarajan and colleagues has also demonstrated that the cytoskeletal component, vimentin (VIM) is an endogenous ligand for Dectin-1 expressing macrophages, whose ligation will result in ROS production in atherosclerotic plaque affected tissue (Thiagarajan et al. 2013). More recently vimentin has been shown to be increased in the adipose tissue of HFD-MyD88 $^{-/-}$ obese mice alongside Dectin-1^{+} macrophages and is capable of ligating Dectin-1 resulting in an enhanced proinflammatory molecule production and the use of the Dectin-1 agonist curdlan exacerbated insulin resistance. Conversely, Dectin-1 KO mice showed a significant reduction in activated macrophages, greater anti-inflammatory molecule production in adipose tissue as well as improved glucose homeostasis and insulin sensitivity highlighting a role for Dectin-1 signalling in obesity and insulin resistance (Castoldi et al. 2017). Vimentin expression and assembly has been previously shown to be significantly increased in the ageing brain and has even been proposed to be a potential therapeutic target for ageing-related conditions as a result (Sliogeryte et al. 2019), but to date no one has demonstrated whether Dectin-1^{+} microglia are capable of ligating vimentin, an abundant component in the neuronal support cells, astrocytes, who play a substantial role in managing the CNS glycaemic status (Lee et al. 2016; Dienel 2019). Furthermore, given the role of Dectin-1-vimentin signalling in managing peripheral glucose homeostasis and the substantial correlation I have demonstrated between hypothalamic *Clec7a* expression with frailty,

a condition which in turn I have consistently shown to be most strongly influenced by the metabolic status of an animal. Additionally, previous work by Mor-Vaknin and colleagues has demonstrated that chemokines induce secretion of vimentin from activated macrophages and was potentiated or ameliorated by TNFα or IL-10 respectively (Mor-Vaknin et al. 2003). Given the robust increase in *Ccl2* and *Cxcl13* expression in the frail hypothalamus, as well as reports from the Singapore longitudinal ageing study citing them, CCL2, CXCL13 (Lu et al. 2016), and VIM (Cardoso et al. 2018) as serological biomarkers of frailty, and finally the robust increase in *Tgfb* expression in the hypothalamus which may induce increased permeability of the specialised section of the BBB around the hypothalamic arcuate nucleus as has been shown previously (McMillin et al. 2015; Heinemann et al. 2012), there is a possibility that upregulated chemokine expression and infiltration in the CNS could elicit similar effects in microglia. Taken together these data suggest that vimentin is a strong candidate to be the Dectin-1 ligand in the ageing brain responsible with potential adverse effects on the central glycaemic and inflammatory status and should be assessed for significant changes in expression in the hypothalamus and for its ability to ligate Dectin-1 in microglial cells.

To date much of our knowledge of Dectin-1's signalling mechanisms comes from analysis of peripheral cells such as macrophages, neutrophils and dendritic cells, all of which express it to varying degrees. Furthermore, much of our limited current data on microglial Dectin-1 responses comes from *in vitro* experiments and direct activation of microglial Dectin-1 have not shown the robust proinflammatory cytokine expression observed in macrophages (Shah et al. 2008; Shah et al. 2009). Previous studies assessing the translatability of *in vitro* to *in vivo* has been shown that *in vitro* culturing significantly influences microglial phenotype and responses from those found *in vivo* (Butovsky et al. 2014; Melief et al. 2016; Yamasaki 2014). As such, while microglia may well share identical signalling pathways to peripheral macrophages, there is now a concerted effort and need to identify further endogenous ligands that may be found in the CNS and assess how the intensity and frequency of their ligation of Dectin-1 may affect signalling and functional outcomes *in vivo* rather than *in vitro*.

Taken together these data highlight the important potentially pathogenic role of Dectin-1 in ageing and disease pathology but also the substantial impact which the ligand itself, as well as the timing and frequency of ligation, will have upon the subsequent immune tolerising or priming effect on the CNS innate immune response. As such, future work must make a concerted effort to identify endogenous ligands that may be found in the CNS and assess how the intensity, frequency and disruption of their ligation to Dectin-1 may affect signalling and functional outcomes *in vivo*, using flow cytometry to assess protein expression or FACS isolated cells to selectively assess microglial transcript changes.

4.3.5 Hypothalamic vulnerability to increased senescence with age and frailty

As discussed in the previous chapter microglial dystrophy is frequently associated with increasing senescence (Streit et al. 2009; Shahidehpour et al. 2021; Streit et al. 2004). This dystrophy will result in decreased functionality of their neurotrophic and synaptic maintenance activities (Spittau 2017) and in ageing rat models with increased senescence there are robust reductions in telomerase activity and telomere shortening with similar trends observed in large scale human Alzheimer's longitudinal cohorts (Flanary et al. 2007). As discussed in the previous section, in addition to its a role in mediating autophagy (Koesters et al. 2010), TGF-β is an extremely pleiotropic cytokine capable of inducing complete cell cycle arrest (Katakura et al. 1999) as well as suppressing or inducing cell death in different cell types dependent on the conditions (Schuster et al. 2002). TGF-β recruitment has been reported to have an important role in the development of adult microglia *in vitro,* with *Tgfb*$^{-/-}$ mice showing a loss of microglial cell lines (Butovsky et al. 2014) in the CNS resulting in a lethal autoinflammatory syndrome shortly after birth (Kulkarni et al. 1993; Shull et al. 1992). Interestingly, both *Trem2* and *Tyrobp* transcript expression showed gradual declines with age and frailty in the hypothalamus indicating a reduction in microglial activation and population, and consistent with this was an age-associated decrease in *C3* suggesting decreased engagement of the microglial associated complement system and phagocytosis. Furthermore, the robust decline in the growth factors *Igf1* and *Bdnf* coupled with the increase in the age-associated markers of senescence *p16*^{INK4A} and the SASP phenotype products *Il6, Ccl2* and *Tgfb* suggest an increase in senescence and decreased cellular replacement and repair. This is consistent with studies reporting that ageing induces the accumulation of senescent microglia and astrocytes in the hypothalamus (Suda et al. 2021) and that age-associated serological hyperinsulinemia, such as that observed here in highly frail animals, results in neuronal insulin resistance and cell induced senescence (Chow et al. 2019). Indeed, extensive work by Baker et al. has shown that *p16*^{INK4A} is a potent marker of age-associated senescence whose absence in *p16* $^{-/-}$ resulted in increased longevity in the BubR1 accelerated ageing mouse model (Baker et al. 2008) and consistent with this, *p16* expression was found to be robustly correlated with frailty. While TGF-β is a highly pleiotropic cytokine capable of suppressing or inducing cell death in different cell types dependent on the conditions (Schuster et al. 2002), mediating autophagy (Koesters et al. 2010), inducing complete cell cycle arrest (Katakura et al. 1999), altering BBB permeability (McMillin et al. 2015; Heinemann et al. 2012) it is also a key component of the SASP secretome along with IL-6 and CCL2 (Coppé et al. 2010). These SASP products act in a paracrine fashion, instigating or exacerbating inflammatory events and inducing cellular senescence in adjacent, healthy cells through regulation of p15^{INK4b} and p21^{CIP1} (Gonzalez-Meljem et al. 2018; Acosta et al. 2013). Here I have demonstrated that hypothalamic transcripts for *Tgfb, IL6* and *Ccl2*, all show significant upregulation with age and frailty. Plasminogen activator 1 (*Pai1)* is also considered a marker of cellular senescence and the SASP and has also previously been

shown to be increased in expression and secretion with ageing and obesity, (Rouault et al. 2021; Ota et al. 2011; Eren et al. 2014; Koji Yamamoto et al. 2005). However, despite the observed upregulation of the senescence marker *p16^{INK4A}* and the SASP products, *Tgfb, IL6* and *Ccl2*, the senescence associated marker *p21,* a p53 target gene implicated in cell-cycle arrest and senescence (Cheung et al. 2012) failed to show any significant increase in transcript expression with age or frailty despite the robust upregulation of *p16^{INK4A},* with which it is closely associated (Baker et al. 2013) reports of its induction by TGF-β in gastric cancer cells *in vitro* (Yoo et al. 1999). Likewise, previous findings have demonstrated that PAI1 can be upregulated by increased secretion of TGF-β *in vitro* (Sawdey et al. 1989) there was no commensurate increase in *Pai1* at the transcript level here. However, given that Sawdey and colleagues demonstrated the same effect was produced through treatment of cells with TNFα, which was shown to be downregulated in the hypothalamus this could suggest that the robust increase in *Tgfb* transcript expression I observe is affecting alternative pathways to senescence despite these strong correlations with *p16^{INK4A}*.

Alternatively, while the aggressive increase in *Tgfb* expression may be resulting in elevated production and secretion of SASP products exacerbating inflammation and inducing senescence in adjacent cells of the frail hypothalamus, it is also possible that *Tgfb* expression has been increased in a protective manner for its modulatory function on microglial activity. As reported earlier TGF-β is capable of suppressing or inducing cell death (Schuster et al. 2002), or complete cell cycle arrest (Katakura et al. 1999) and *in vivo* analysis of reactive astrocytes' derived TGF-β has been shown to deactivate microglial cells (Eyüpoglu et al. 2003; Norden et al. 2014). Furthermore, TGF-β and IL-6 have both been shown to be produced by gliomas *in vivo* and act in an anti-inflammatory capacity to inhibit proliferation and secretion of proinflammatory cytokines (Suzumura et al. 1993). Both of these highly pleiotropic cytokines gene transcripts were elevated in the ageing and frail hypothalamus suggesting they may be upregulated in a compensatory role to inhibit inflammation by microglia switching them from a less aggressive activated "M1 phenotype" to the anti-inflammatory "M2" as has been previously reported (Orihuela et al. 2016). Consistent with this I demonstrated a robust decrease in *Trem2, Tyrobp* and *C3* gene expression as well as a corresponding reduction in *Nlrp3* transcript expression, suggesting reduced inflammation in the hypothalamus.

Taken together these data suggest that the hypothalamus is particularly vulnerable to a substantial increase in senescent cells and the associated SASP products, with significantly reduced gliosis as predicted by their frailty status, which I have shown is itself heavily influenced by metabolic deficits. Within this TGF-β appears to play an intimate role in hypothalamic responses and may well be an important therapeutic target. However, due to the highly pleiotropic nature of TGF-β it is impossible to tell whether this apparent increase in gene expression has a neuroprotective or detrimental

outcome. Quite possibly it is both and its expression in the young brain is beneficial but with chronic inflammation as has been observed in ageing and neurodegenerative disorders this may well push TGF- β expression to detrimental levels associated with the SASP. Furthermore, the limited information available to us from our qPCR analyses it is impossible to definitively say whether this altered transcript expression is in turn associated with significant alterations in protein expression for *Tgfb* or any other transcripts. Substantial additional analyses of hypothalamic TGF-β protein levels, sources of its production and interrogation of its binding and signalling interactions using antagonists or selective gene disruption in the ageing frail brain will be required to elucidate the complex signalling mechanisms and functional outcomes at different time points in order to devise a suitable therapeutic strategy.

*

In summary age is a powerful driving, detrimental force to an organisms' overall health. As Gompertz stated in 1825 the risk of mortality increases exponentially with age, but as we now know chronological and biological age are not the same. Within aged individuals there is always a greater degree of variation in health status than is found in younger populations as the accumulation of multiple co-morbidities over a life-time chip away at an aged individual's physiological reserve. This variation can be better described and further broken down by accurate assessment of their frailty status. Frailty is a state of vulnerability to poor resolution of homeostasis after a stressor event which is strongly linked to adverse outcomes and increased morbidity and mortality. In this age of precision targeted, it is a practical and unifying theory which redirects medical practitioners from organ-specific diagnoses toward a more overarching, holistic and individualised treatment. Detection of frailty not only allows patients to make more informed choices when choosing between treatment options but also empowers medical healthcare workers to weigh up the benefits and risks when designing them. The routine use of frailty assays as part of cancer treatment regimens (Ruiz et al. 2019; Handforth et al. 2015) and as part of surgical pre and post operative treatment and recovery plans (Henry et al. 2019; Ko 2019) is growing in prevalence and reported to improve long-term prognoses. Furthermore, early detection of frailty by general practitioners can be just as important as its use in emergency care, as understanding the underlying pathology that leads to this state of frailty may also allow healthcare professionals to efficiently treat it at the "pre-frail" stage so as to prevent the individual's condition worsening and offer them the greatest quality of life and independence possible for as long as possible. Many studies to date have demonstrated that improvements in diet, exercise and lifestyle can ameliorate the severity of an individual's frailty status, improving their resilience (Cadore et al. 2013; Angulo et al. 2020; Coelho-Junior et al. 2020; Henderson et al. 2021; Feldman 2018). Currently there is a lack of consensus on the quantification of Frailty for ageing in the medical field with countless iterations and variations

being used and reported on throughout the field. As such it is crucial that we elucidate the underlying biological and cellular mechanisms which are driving this syndrome if we are to design frailty assays, with discerning and appropriately weighted measures, that are both accurate and translatable to the healthcare setting. While the Fried Frailty Phenotype is a quick and accessible measure useful for many general practitioners it is not the most accurate or discerning method, the cumulative deficit model is superior in this respect but careful selection of measures for inclusion is paramount. Here I have generated a novel frailty index incorporating for the first time physiological, behavioural, and metabolic components with a robust measure of cognition and demonstrated the substantial impact which frailty has upon vulnerability to cognitive and metabolic dysfunction, highlighting the importance of having appropriately weighted and discerning measures of metabolism in frailty indices that are to be used in the clinical setting.

While age is certainly one of the most powerful driving forces in an individual's vulnerability, our research here has shown that frailty adds a significant dimension when assessing an individual's susceptibility to a stressor at the physiological, metabolic and behavioural levels but also has a significant impact upon the CNS as has been demonstrated by frailty's ability to accurately describe baseline cognition level here. Furthermore, I have highlighted the heterogenous effect which frailty will have upon different brain regions, notably the brains CNS-periphery metabolic axis the hypothalamus, which showed significant downregulation of gene transcript expression associated with microglial activation and growth factors and an increase in markers of senescence. Taken together these data highlights the pivotal role which metabolism has upon an organisms overall physiological health and resilience, conferring substantial vulnerability to cognitive dysfunction and altered neuroinflammatory responses.

Chapter 5:

The impact of repeated systemic TNF-α challenge in the APP/PS1 model of Alzheimer's Disease.

5.1 Introduction

In recent years a number of genes conferring susceptibility to inflammatory conditions have been found to be associated with a predisposition to AD (Karch et al. 2015; Malik et al. 2015; Yokoyama et al. 2016) and in turn infection induced systemic inflammation has been proposed as a mechanistic driver of AD pathogenesis (Ashraf et al. 2019; Giridharan et al. 2019; Holmes et al. 2009). However, the exact molecular underpinnings of this remain to be elucidated. Reports from longitudinal and care home facilities have demonstrated the significant risk factor which frailty (Searle et al. 2015; Kojima et al. 2016) and metabolic dysfunction (Gudala et al. 2013; Reilly et al. 2020) confer for increased chance of developing and worsening pathological conditions such as dementia. As discussed previously in this thesis both frailty (Ng et al. 2015; Hubbard et al. 2010) and metabolic conditions such as diabetes (Miyazaki et al. 2003; Akash et al. 2018) are associated with elevated expression of TNFα. Concurrently, Holmes et al. identified an association between circulating levels of TNFα and the progression of cognitive decline in AD patients. Those patients with a high baseline level of TNFα suffered a 4 fold greater rate of decline compared to those with low TNFα, who showed no significant cognitive decline (Holmes et al. 2009). Furthermore, following a systemic inflammatory event AD patients experienced a significant rise in circulating TNFα levels and a 2 fold increase in their rate of cognitive decline (Holmes et al. 2009). Taken together these findings suggest that long term elevation in systemic TNFα levels is severely detrimental to cognitive function and that systemic inflammatory events in vulnerable patients, with prior pathology resulting in a primed immune response, can significantly alter the progression of the disease. Additionally, Holmes et al. have demonstrated that neuropsychiatric symptoms known to be associated with sickness behaviour occur more frequently in AD patients with higher circulating TNFα compared to those with low TNFα (Holmes et al. 2011).

Increased TNFα levels have also been demonstrated in centenarians and a strong association with their systemic levels of the this pro-inflammatory cytokine and moderate to severe dementia was found (Bruunsgaard 1999). In AD elevated TNFα levels in both the serum and CSF were shown to correlate with both disease severity and its progression (Paganelli et al. 2002). In a longitudinal study following the progression of patients with mild cognitive impairment who went on to develop AD it was found that TNFR1 and TNFR2 correlated BACE1 activity compared to controls as well as plasma levels of Aβ and CSF levels of tau (Buchhave et al. 2010) Unsurprisingly, when systemic TNFα levels were compared with total brain volume they were found to be inversely correlated in ageing (Jefferson et al. 2007) and AD patients; in addition to a reduction in overall total brain volume in AD patients their hippocampal volume specifically was also found to be decreased (Leung et al. 2013).

Pharmacological disruption of the TNFα signalling pathway through the subcutaneous administration of etanercept, a TNFα decoy receptor, compared to placebo treated controls has been shown to attenuate cognitive decline over a 6 month period in AD patients (Holmes et al. 2014), however, since this initial study a phase two trial in humans has proved the drug to be well tolerated but failed to show any significant difference in cognitive or functional outcome (Butchart et al. 2015). Overall, these results strongly indicate that elevated systemic TNFα levels predict an individual to be more likely to progress to mild cognitive impairment or even full-blown AD.

The straining effects of systemic inflammation upon neuronal pathology have also been demonstrated in transgenic models of AD and were found to exacerbate many features of the underlying disease. The Tg2576 model of AD overexpresses a mutant form of APP with the Swedish mutation (KM670/671NL) resulting in elevated levels of Aβ and the associated amyloid plaques and this extensive amyloid pathology is associated with cognitive deficits (Hsiao et al. 1996). When challenged with 2.5mg/kg of LPS 16-month-old aged Tg2576 animals demonstrated elevated cortical and hippocampal IL-1β protein which was absent in young (6 month) TG2576 and age matched non-transgenic littermates. Aβ1-40 levels were shown to be increased in both young and aged Tg2576 animals treated with LPS, however, Aβ1-42 levels were raised only in aged transgenics with LPS (Sly et al. 2001). In an APP transgenic model, designed to overexpress human-type APP derived from a large Swedish family with early onset AD (EOAD), a systemic challenge of 10mg/kg, a dose mimicking severe sepsis, caused significantly exaggerated sickness behaviour with a decrease in locomotor activity, social interaction and food intake compared to non-transgenic age matched littermates. In addition to these behavioural deficits, following LPS challenge, animals showed significantly elevated serological IL-6 and TNFα levels, increased BBB permeability and increased central IL-6 and TNFα protein levels compared to saline treated controls. This suggests that inflammation evoked in the periphery was propagated into the central nervous system. (Takeda et al. 2013). In the 5xFAD model of AD soluble TNFα itself has been identified as a critical mediator of the effects of neuroinflammation on early plaque pathology with targeted inhibition by dominant negative TNF inhibitors slowing the appearance of amyloid pathology and the associated cognitive deficits (McAlpine et al. 2009).

The APP/PS1 double transgenic mouse model is a widely used mouse model of Alzheimer's Disease favoured for its expression of a chimeric mouse/human amyloid precursor protein (Mo/HuAPP695swe) alongside a mutant human presenilin 1 (PS1-dE9) both of which are directed at CNS neurons, mimicking familial AD. In these mice the expression of human APP is 3-fold higher than the endogenous murine APP and Aβ40/ Aβ42 both increase with age with Aβ42 being preferentially generated. Amyloid plaque deposition in the hippocampus begins as early as 3 months around the dentate gyrus and the CA1 at 4-5 months. As the animals age these plaques

progress from small congophilic dense core plaques to large plaques with a dense core surrounded by a well-defined corona of diffuse amyloid (Radde et al. 2006).

Disruption of homeostatic metabolic processes have been strongly implicated in the development of AD. Recent meta-analysis studies of diabetes mellitus and AD revealed a 70% increased risk in the development of dementia of all types and a 60% increased likelihood of developing AD specifically in patients with T2D (Gudala et al. 2013). Insulin is responsible for glucose uptake as well as regulating food intake and reproduction through the hypothalamus and endocrine system (Plum et al. 2005). Insulin resistance, which is a prominent feature of diabetes, results in systemic hyperglycaemia, which can lead to glutamate-induced excitotoxicity in neurons (Datusalia et al. 2018). This phenomenon has been described by the term type 3 diabetes and, while widely debated, the link between altered brain glucose metabolism and cognitive impairment in mouse models is an area of increasing interest. In the APP/PS1 mouse model of AD brain glucose levels have been shown to be significantly elevated, reportedly as a result of the development of amyloid pathology causing a reduction in glucose utilization and decreases in energy and neurotransmitter metabolism (Q. Zhou et al. 2018). S14G-humanin alleviates insulin resistance and oxygen deprivation in APP/PS1 mice through reactivation of Jak2/Stat33 signalling and PI3K/AKT pathway improving learning ability and memory (Gao et al. 2017; Han et al. 2018). APOE4 a cholesterol carrying protein is one of the strongest known genetic risk factors for AD and has recently been shown to exacerbate insulin resistance through disruption of the insulin receptor signalling (Zhao et al. 2017). APP/PS1 mice subjected to intense treadmill exercise during early disease stages to improve biological ageing demonstrated upregulated Apoe4 expression with a reduction of hippocampal soluble Aβ and greater lipid metabolism suggesting a crucial role of lipid metabolism associated with Apoe4 expression in disease pathogenesis (Zeng et al. 2020). Taken together these data suggest that altered chronic inflammation, metabolism and overall physiological fitness may contribute to elevated frailty in the APP/PS1 animal, which in turn may influence the pathology of AD, lending the question as to whether repeated exposure to a chronic inflammatory challenge might exacerbate cognitive deficits or physiological status and indeed whether or not frailty status might predict cognitive outcome in APP/PS1 mice in response to this repeated systemic challenge.

Furthermore, growing evidence continues to elucidate the substantial impact which sex has upon the disease progression of the APP phenotype. Recent studies have shown that APP female animals display accelerated manifestation of disease pathology as evidenced by advanced plaque pathology, increased cognitive impairments, reduced hippocampal neurogenesis (Jiao et al. 2016; Richetin et al. 2017) and reduced white matter integrity (C. Zhou et al. 2018) at 12 and 10 months of age respectively compared to male littermate controls. Additionally, female APP transgenic mice have been shown to exhibit greater cytokine response, downregulation of anti-inflammatory

mediators and altered metabolism in the hippocampus of animals challenged with intravenous LPS compared to APP/PS1 males (Agostini et al. 2020). As such I hypothesised that APP/PS1 female animals might exhibit greater more advanced cognitive impairment at baseline and a heightened susceptibility to repeated systemic challenge with TNFα than male APP/PS1 and wild type control animals.

In order to assess the impact of repeated systemic inflammatory episodes on the APPSwe/PS1dE9 (APP) genotype and wild type (WT) littermate controls, animals were administered 250µg/kg of TNFα or sterile saline by intraperitoneal injection on four separate occasions, each five days apart as indicated in **Figure 5.1**, and their weight monitored for the duration of the experiment**.** The first cohort of animals **(Figure 5.1 A)** were sacrificed 21 days after their first challenge and microglial isolates analysed for molecular neuroinflammatory changes while cohort two **(Figure 5.1 B)** followed a more extended period of testing to assess behavioural, metabolic and cognitive changes in response to repeated systemic challenge in order to characterise the genotype prior to and after chronic systemic inflammatory episodes.

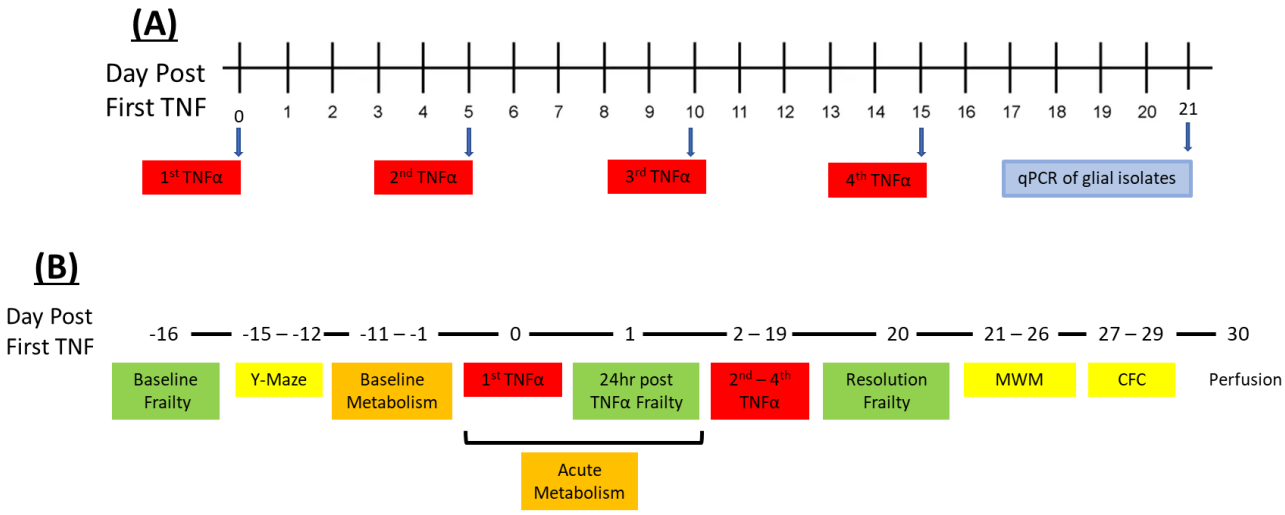

Figure 5.1 **Experimental Timeline for repeated, sequential, 250µg/kg TNFα administration. Cohort 1 and 2 received repeated systemic challenges of 250µg/kg TNFα every 5 days - (A) Cohort 1 glial isolates study timeline (B) Cohort 2 cognitive, frailty and metabolism study timeline.**

5.2 Results

5.2.1 APP/PS1 phenotype characterisation of cognition, metabolism, and frailty

Baseline cognitive status of APP/PS1 mice and wild-type (WT) litter mate controls, aged 15±2 months, was assessed using the hippocampal-dependent shallow water visuospatial Y-maze task. Although visuospatially guided, this is a relatively simple test of learning and memory, with categorical choices rather than more sensitive navigation such as that required by the Morris Water Maze. This maze was performed, in part, in order to provide groups for subsequent TNFα experiments, that were balanced for baseline cognitive performance. Animals were assessed over four days, with 12 trials per day **(Figure 5.2)**. By day three of testing both APP and WT controls had successfully learned the task, scoring >80% correct daily, with the APP mice (both sexes combined) showing no statistically significant cognitive deficit despite their age and pathology.

Assessment of baseline cognitive status in 15-month-old APP/PS1 and wild type animals' performance in the Y-maze task grouped by genotype and sex and analysed by two-way repeated measures ANOVA revealed a statistically significant interaction effect of sex with genotype (*$p<0.05$; $F(3,64) = 3.294$). Bonferroni post-hoc analysis confirmed that female APP/PS1 mice exhibited a significantly slower rate of learning than males (**$p<0.01$) on the Y-maze task over 12 trials a day for four training days compared to male APP/PS1 animals but not compared to WT animals **(Figure 5.2 C)**.

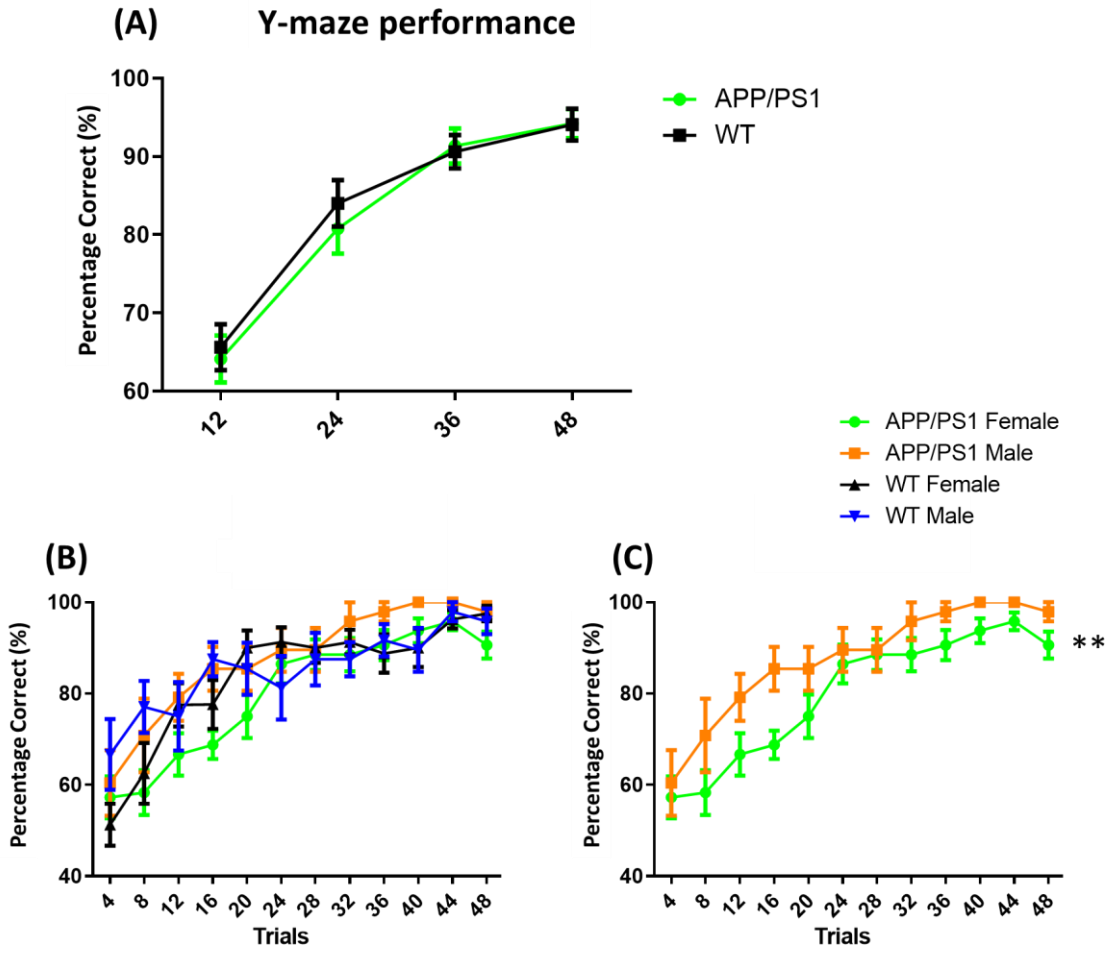

Figure 5.2 **Learning in the Y maze: Learning rate on the shallow water visuospatial Y-maze task of male and female APP/PS1 and WT mice aged 15 ±2 months old (APP Female n=7, APP Male n=12, WT Female n=11, WT male n=12). (A) Genotype comparison of APP/PS1 learning rate as a percentage of correct choices compared to age matched C57 controls. (B) for 15 ±2 months old APP/PS1 and WT controls of both sexes. (C) APP/PS1 female mice learn the Y-maze task significantly more slowly than males. Data are represented as mean ± SEM, analysed by repeated measures two-way ANOVA, with Bonferroni post hoc test.**

In order to assess the impact of the APP pathology upon the animals' overall health status, frailty was assessed at baseline using a simplified 12-point version of our TFL II cumulative deficit frailty index **(Figure 5.4 A)** to generate an individualised frailty score representative of their health status. Overall, it was found that the neurodegenerative APP/PS1 genotype resulted in transgenic animals exhibiting modestly, but significantly, higher frailty (*p<0.05) at baseline compared to WTs **(Figure 5.4 B)**. APP/PS1 mice exhibited significantly greater levels of activity in the open field task **(Figure 5.3)** when assessed by distance covered (***p<0.001), the number of rears (**p<0.01) and meander (**p<0.01) over the 10-minute testing period. Despite this apparent high level of activity APP mice had significantly lower core body temperatures (**p<0.01), as measured by thermal rectal probe, than WT animals' indicative of a potential metabolic differences.

In contrast, it was found that APP mice demonstrated a significantly higher average speed (**p<0.01) **(Figure 5.3 D)** and a stronger forelimb grip strength (**p<0.01) (**Figure 5.3 J)** compared to age matched WT controls using the Deacon weightlifting task. No significant difference in overall grip strength as assessed by the Kondziela Inverted screen task **(Figure 5.3 I)** was found as the animals were assessed for a maximum testing time of 120 seconds and this proved to be insufficient time to substantially differentiate between animals' grip strength on this task. However, a higher percentage of APP animals successfully completed the 120 second testing period compared to WT animals supporting the observation by the weight-lifting task that APP/PS1 mice have a stronger grip, contrary to their overall higher frailty status.

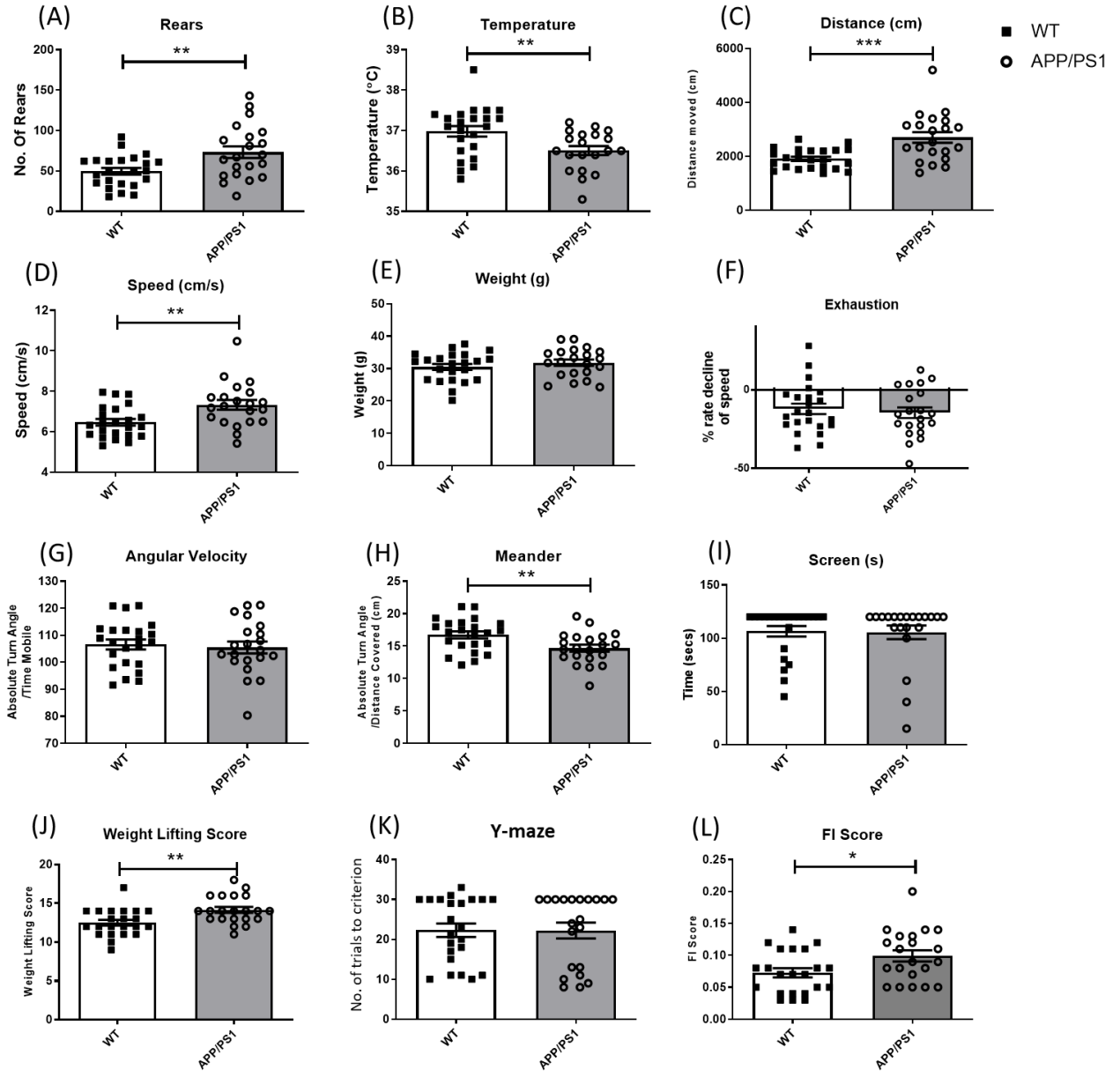

Figure 5.3 Frailty Index testing of APP/PS1 and WT mice: Behavioural and physiological measures were taken in 15 ±2 months APP/PS1 and WT animals. Data are expresed as mean ± SEM, (WT n=21, APP/PS1 n=23), analysed by unpaired t-test. All data represented by mean ± SEM and analysed by student's t- test or Mann-Whitney u-test or Kruskal wallis for non-parametric data to detect effect of genotype on frialty index component measures, statistical significance indicated by *p<0.05, **p<0.01, ***p<0.001.

(A)

	Measure	Score Z-score +	Score Z-score -
1	Temperature	✓	✓
2	Weight	✓	✓
3	Sight		✓
4	Screen		✓
5	Weight Lifting		✓
6	Distance	✓	✓
7	Speed		✓
8	Rears	✓	✓
9	Meander	✓	✓
10	Angular Velocity	✓	✓
11	Decline in speed	✓	✓
12	Y-Maze Cognition		✓

(B)

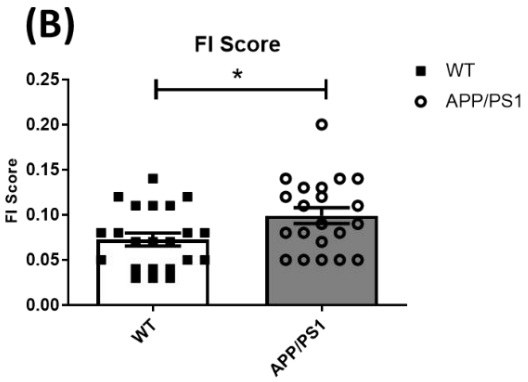

Figure 5.4 Frailty index components and prevalenge across genotypes: (A) Frailty Index and (B) finalised frailty score from index for for 15 ±2 months old APP/PS1 and WT littermate controls demonstrated a significantly higher FI score, (WT n=21, APP/PS1 n=23). All data represented by mean ± SEM and analysed by student's t- test to detect effect of genotype on frialty score, statistical significance indicated by *p<0.05, **p<0.01, ***p<0.001.

Following on from the observed mild baseline hypothermia in APP/PS1 mice, despite higher activity in the Open Field task, differences in metabolic status, between the wild-type and APP/PS1 genotypes, were then assessed. To this end animals were assessed on their basal metabolic status using the Promethion metabolic cage system, which allows non-invasive assessment of food and water intake, energy consumption, O2 consumption and CO2 production. Mice were removed from their home cages and housed individually in metabolic chambers set on top of a beam-break activity monitor under a standard 12-hour light-dark cycle with ad libitum access to food and water. Mice were acclimated to the metabolic cages for a minimum of a 12-hour habituation period before recording calorimetric and activity variables.

Contrary to their performance in the Open Field task it was found that animal activity as measured by pedestrian locomotion (m) **(Figure 5.5 A),** as well as distance moved (m) and locomotor activity (beam breaks), APP/PS1 animals showed no statistical difference compared to WT control animals but as days progressed cumulative activity (metres locomotion) appeared to be getting greater in WT animals but was non-significant. This was most evidently the case during the dark cycle and likely would have achieved significance had recording of these cumulative measures of activity continued into through another dark cycle. However, APP/PS1 transgenic animals did demonstrate a clear and significantly lower energy expenditure (**$p<0.05$; $F(1,29)=12.91$) during their nocturnal period **(Figure 5.5 B)**. Consistent with this lower energy expenditure, APP/PS1 mice also consumed significantly less food (*$p<0.05$; $F(1,29)=5.479$) **(Figure 5.5 D)** and water (**$p<0.01$; $F(1,29)=8.972$) **(Figure 5.5 C)** compared to WT littermate controls over the 48-hour testing period.

At time of euthanisation animal's fat deposits were wholly dissected out and weighed to determine each animal's adiposity. No statistically significant difference in fat mass was found to be evident in the brown fat deposits weight between genotypes **(Figure 5.5 E).** However, it was found that APP/PS1 mice exhibited significantly greater subcutaneous fat (**$p<0.01$) and gonadal fat (*$p<0.05$) deposits compared to WT littermate controls **(Figure 5.5 F, G)**.

APP/PS1 animals show an increased frailty, reduced activity, energy expenditure and food and water intake compared to WT animals. In the case of APP/PS1 female animals the genotype also confers a mild cognitive impairment to their ability to learn the shallow water visuospatial Y-maze task compared to male APP/PS1 animals. To this end I set out to assess whether this apparent higher frailty and vulnerability renders APP/PS1 animals more vulnerable to metabolic dysfunction following an acute systemic challenge of 250μg/kg of TNFα.

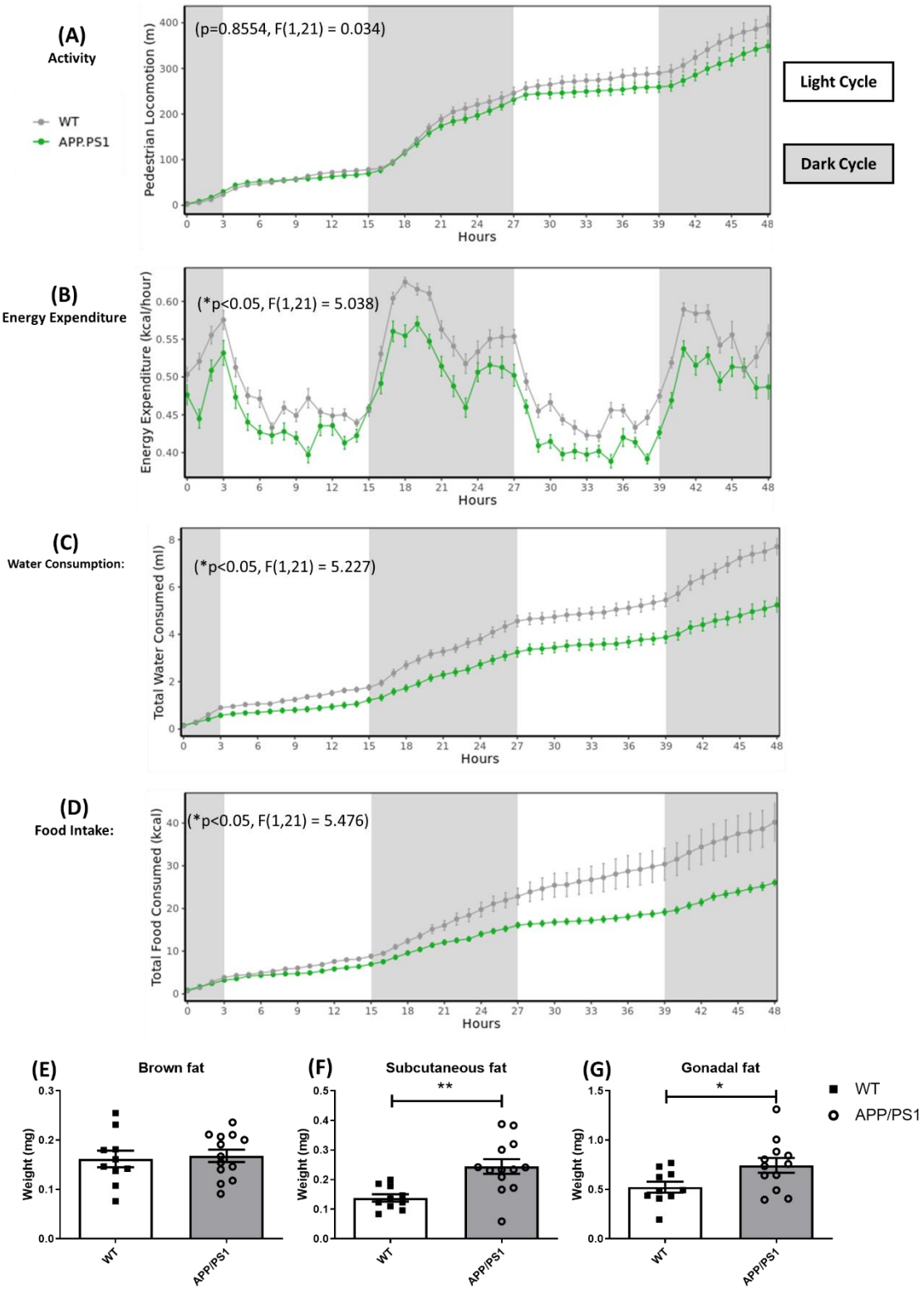

Figure 5.5 Metabolic status of 15 ±2 months old APP/PS1 and WT mice: (A) Home cage activity, (B) Energy Expenditure, (C) Water consumption and (D) Food Intake (cumulative) in APP/PS1 mice compared to littermate controls. The latter 3 paramters were all significantly lower in APP/PS1 mice. Data were analysed by repeated measures two-way ANOVA with Bonferroni post hoc test, (WT n=10, APP/PS1 n=13), significance represented by *p<0.05, **p<0.01. Brown fat deposits were equivalent while white fat deposits were found to be significantly greater in APP/PS1 animals for (F) subcutaneous and (G) gonadal fat deposits assessed by unpaired t-test, data are expressed as mean ± SEM.

5.2.2 Acute impact of TNFα on APP/PS1 metabolism

Once baseline cognitive, behavioural, and metabolic status were established, APP/PS1 and WT littermate controls were challenged intraperitoneally with four consecutive 250µg/kg doses of TNFα, five days apart, as described in **Figure 5.1**. Metabolic changes in response to TNFα were assessed using the Promethion cage system for the first 48 hours after the first or second TNFα challenge or the second or third saline challenge for all animals.

It was found that exposure to an acute systemic challenge by 250µg/kg of TNFα i.p. resulted in a significant decrease in the Respiratory Exchange Ratio (RER) (**p<0.01, F(1,21)=9.420) **(Figure 5.7 E, F)** over 24 hours for all animals, regardless of genotype. RER is the ratio between the volume of CO_2 being produced by the body **(Figure 5.7 A, B)** and the amount of O_2 being consumed **(Figure 5.6 C, D).** Under normal conditions an RER of approximately 1.0 is indicative of carbohydrates being metabolised as the body's primary fuel source while the reduction in RER following TNFα intraperitoneal injection to 0.7 is indicative of fatty acid oxidation, a stress response to the acute systemic challenge. This was most pronounced during the dark cycle when mice are most active **(Figure 5.7 G, H).**

Consistent with this, TNFα-challenged animals exhibited significantly reduced food (*p<0.05, F(1,21)=5.554) **(Figure 5.6 A, B)** and water intake (*p<0.05, F(1,21)=5.815) **(Figure 5.6 C, D)** compared to saline-treated controls over the first 24 hours. Further evidence of an acute sickness behaviour response was evident in the significantly reduced energy expenditure (*p<0.05, F(1,21)=6.604) **(Figure 5.6 G, H)** and robust reduction in activity (***p<0.001, F(1,21)=42.74) which was observed n all TNFα treated animals during their dark cycle **(Figure 5.6 E, F)**

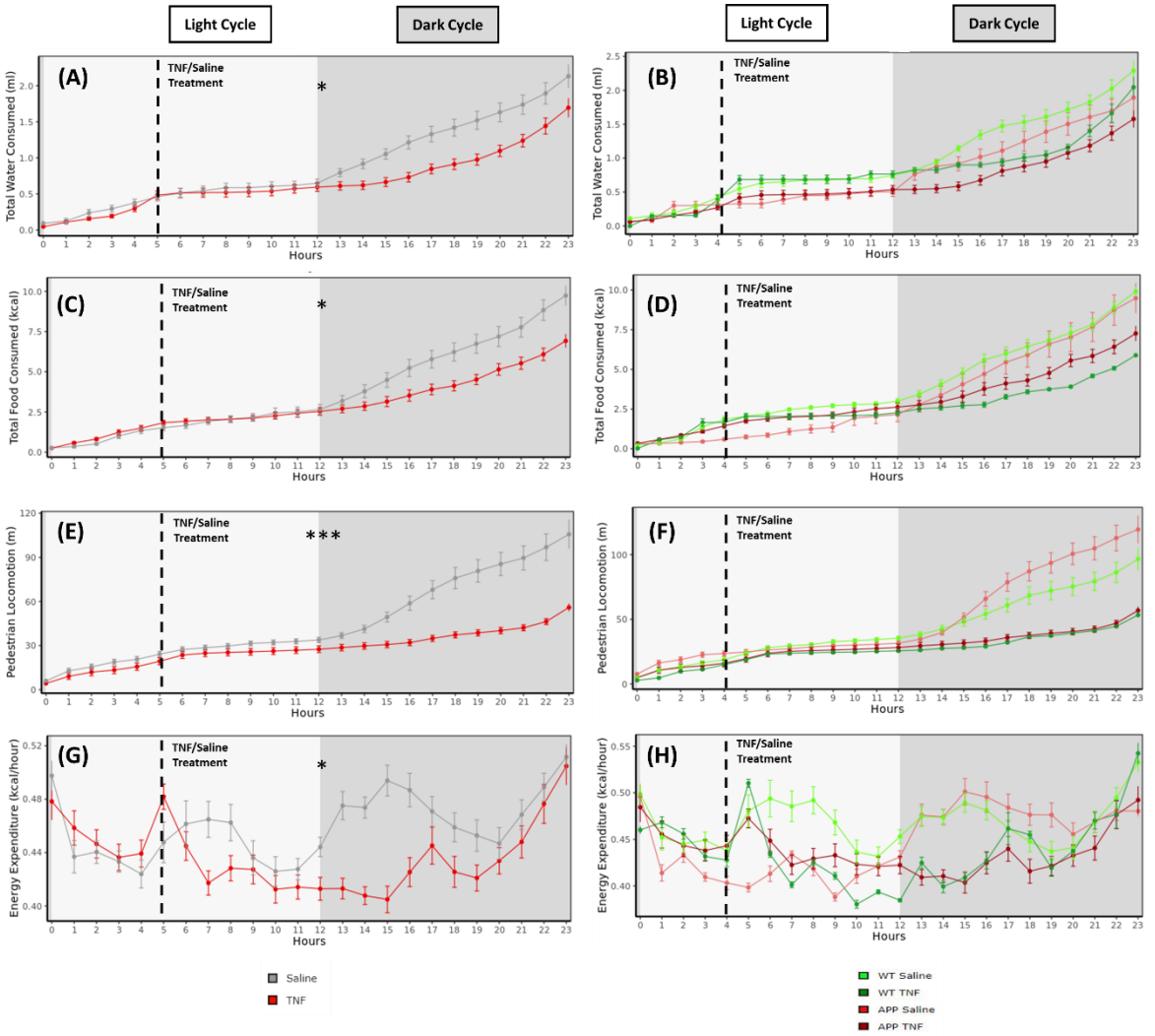

Figure 5.6 Acute changes to activity and food/energy relationship in response to intraperitoneal TNFα 250µg/kg or saline challenge in 15 ±2 old months APP/PS1 and WT animals (A-B) water consumption (ml) (C-D) food consumption (kcal) (E-F) pedestrian locomotion (m) and (G-H) energy expenditure (kcal/hr). All data represented as mean ± SEM and analysed by repeated measures two-way ANOVA, WT sal n=6, WT TNF n=4, APP sal n=5, APP TNF n=8, significance represented by *p<0.05, **p<0.01, ***p<0.001.

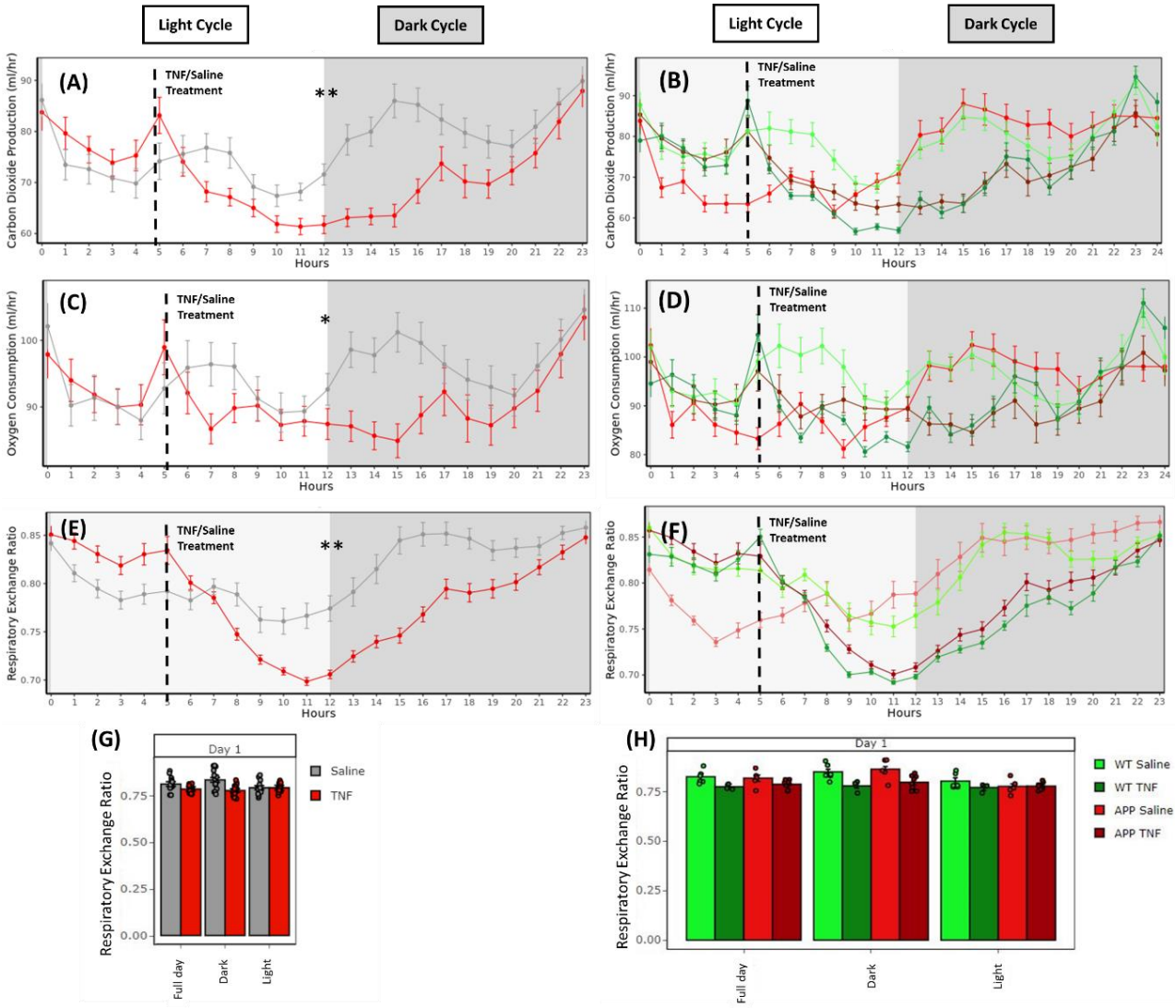

Figure 5.7 Acute metabolic response to intraperitoneal TNFα 250µg/kg or saline challenge in 15 ±2 old months APP/PS1 and WT animals. (A-B) carbon dioxide production (ml/hr) (C-D) oxygen consumption (ml/hr) and (E-F) respiratory exchange ratio (RER), (G-H) RER by time of day. All data represented as mean ± SEM and analysed by repeated measures two-way ANOVA, WT sal n=6, WT TNF n=4, APP sal n=5, APP TNF n=8, significance represented by *p<0.05, **p<0.01, ***p<0.001.

5.2.3 Cumulative impact of repeated TNFα challenge on frailty

To monitor the impact of and recovery from repeated systemic challenge with 250µg/kg of TNFα administered intraperitoneally, animals were weighed daily and their change from baseline was recorded and assessed. It was found that both APP and WT animals experienced a pronounced reduction (***p<0.001) in weight from baseline of approximately four percent at 24-hours post challenge and consistently recovered that weight over the next 4 days **(Figure 5.8 A)**. However, it was shown that APP animals recovered more efficiently than WT animals and showed progressively smaller losses after each challenge while WT animals consistently lost ≥4% from baseline at 24 hours after each 250µg/kg challenge of TNFα. Saline challenged animals failed to show any statistically significant change from baseline regardless of genotype.

Separation of animals by sex revealed that APP/PS1 female **(Figure 5.8 B)**, but not male mice **(Figure 5.8 C)** demonstrated a resistance to TNFα-induced weight loss after repeated systemic exposure that is not evident in WT mice. After the second challenge with 250µg/kg of TNFα female APP/PS1 mice failed to show any significant weight loss following the third and fourth TNFα challenges while male APP/PS1 and WTs of both sexes continued to show significant reductions from baseline weight to these challenges. That is to say, male APP/PS1 showed weight loss that was indistinguishable from WT animals challenged with TNFα, while female APP/PS1 mice selectively, appeared to develop a tolerance to TNFα-induced weight loss. Interestingly, assessment of all APP/PS1 and WT animals' weight at baseline when stratified by sex and genotype revealed a significant interaction between genotype and sex (***p<0.001, F(1,126) = 12.040). Subsequent Bonferroni post hoc analysis revealed WT control female mice are significantly heavier (*p<0.05) than APP/PS1 females **(Figure 5.8 D)**.

Following on from this, animals were assessed on their frailty status as described in **Figure 5.**4, first acutely at 24 hours after their first challenge with TNFα and secondly again 144 hours after their fourth challenge in order to ascertain whether this TNFα dosing regimen impacted on frailty in these animals. It was found that only WT animals treated with TNFα exhibited a significant increase (*p<0.05) in frailty as a percentage of their baseline frailty score between assessments at 24 after the first acute challenge and 144 hours (6 days) after the fourth **(Figure 5.9 F).** This correlated with significant reductions in activity in the open field distance covered and number of rearing events as a percentage of the animal's individual baseline scores **(Figure 5.9 A, B)**. APP/PS1 animals treated with TNFα likewise showed a significant reduction in their distance travelled between these two assessments but showed no significant increase in frailty following TNFα challenges. APP/PS1 animals, however, did show reduced exploratory behaviour in the open field at 6 days post TNFα (ii) compared to 24 hours after the first challenge as represented by their angular velocity, a measure of the rapidity of their turning within the maze, and their meander, a descriptor of the

animals' path through the maze. In both cases APP/PS1 animals showed significant reductions between the two assessed time points as a percentage of their baseline indicative of less exploratory activity (**p<0.01) **(Figure 5.9 C, D).**

TNFα treated groups exhibited significantly reduced forelimb grip strength (#p<0.05) compared to saline treated WT littermate controls as a percentage of their baseline score at 24 hours after their first TNFα challenge but subsequently recovered this significantly by 144 hours post TNFα challenge number four (*p<0.05) **(Figure 5.9 E).** All other behavioural and physiological components of the frailty index **(Figure 5.4 A)** showed no significant differences between groups or across time. No significant differences in frailty index scoring and performance were observed between male and female animals regardless of genotype.

Here I have shown that while APP/PS1 animals showed a higher prevalence of frailty compared to WT control littermates, there is evidence of a significant sexual dimorphism within the transgenic animals. I demonstrated that male APP/PS1 and WT animals show consistent and equivalent losses in body mass in response to repeated TNFα challenge, while in contrast female APP/PS1 animals show a growing tolerance to TNF-induced weight loss with repeated exposure, which WT female animals did not display. Consistent with this, while APP/PS1 animals showed highly variable frailty scores after chronic TNFα treatment, APP/PS1 animals failed to show any consistent and statistically significant increase in frailty score after repeated TNFα treatment while WT animals did. While the APP/PS1 genotype appears to confer a degree of metabolic tolerance to TNFα challenge, it was important to assess whether this repeated TNFα treatment schedule affects the cognitive integrity of these animals.

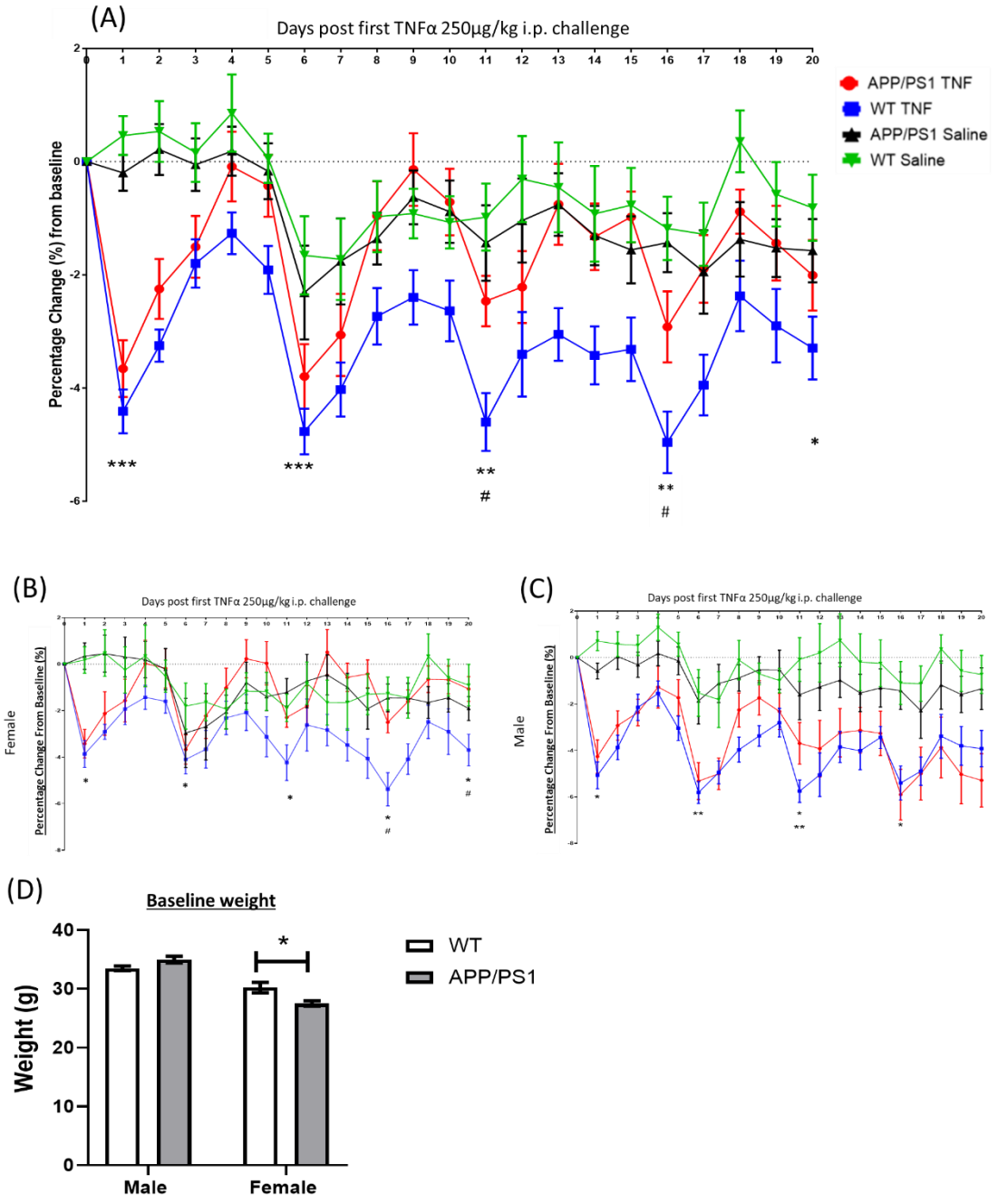

Figure 5.8 **TNFα induced changes in weight - (A) Daily weigh ins following challenge with TNFα/Saline, shown here as percentage lost from baseline weight for for 13 ±3 months old APP/PS1 and WT animals. A significant reduction in weight in TNFα treated animals but with repeated challenge WT animals fail to recover while APP/PS1 animals show progressively smaller responses in weight loss to the repeated TNFα exposure. Separation of animals by sex revealed APP/PS1 females (B) acquire resistance to TNFα induced weight loss while males (C) do not. Data expressed as mean ± SEM, (WT sal n=17, WT TNF n=20, APP sal=17, APP TNF 19), females (WT Sal n=8, WT TNF n=10, APP Sal n=7, APP TNF n=9) and (B) males (WT sal n=9, WT TNF n=10, APP sal n=10, APP TNF n=10) analysed by repeated measures two-way ANOVA with Bonferroni Post Hoc test, * represents a significant loss of weight from baseline in response to TNFα exposure, *p<0.05, **p<0.01, ***p<0.001. # represents a significant difference in weight loss between TNFα treated APP/PS1 and WT animals, #p<0.05). (D) Baseline weight of mice by sex and genotype revealed APP/PS1 females to be significantly lighter than WT female controls, Data analysed by two-way ANOVA with Bonferroni Post Hoc test, * represents a significant difference of weight at baseline in response to TNFα exposure, *p<0.05, **p<0.01, ***p<0.001.**

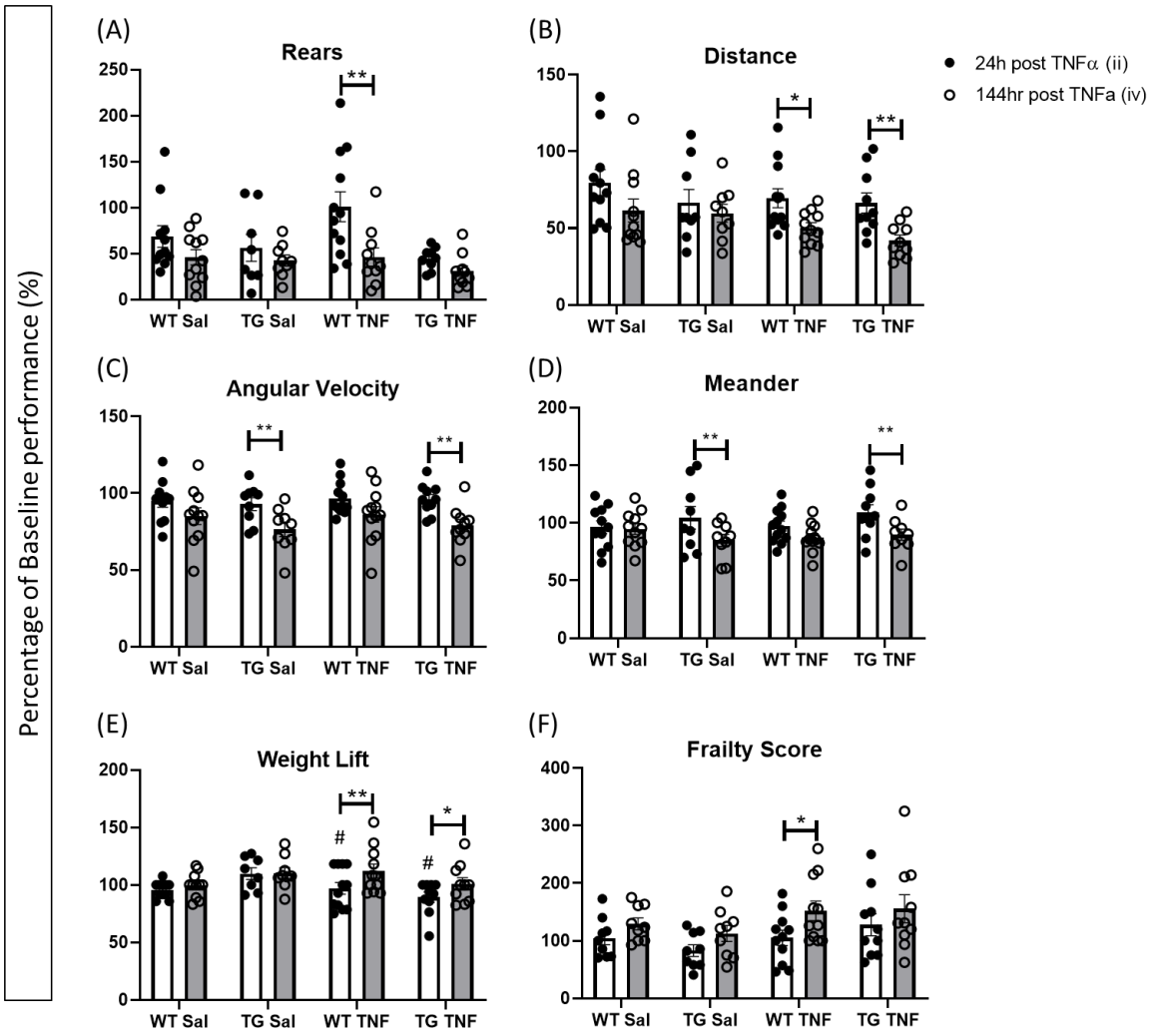

Figure 5.9 Fraily measures in APP/PS1 and WT animals post-TNF: Acute & Cumulative effect of TNFα treatment on Frailty Index measures between 14±2 month old APP/PS1 and WT animals at 24 and 144 hours (6 days) after TNFα 250µg/kg (as a percentage of baseline). (A) – (E) and frailty scoring expressed as a % of baseline frailty score (F) shows a significant effect of treatment of TNFα on frailty of WT animals but not of APP/PS1. (WT sal n=11, WT TNF n=12, APP/PS1 sal n=9, APP TNF n=10). Repeated measures two-way ANOVA with Bonferroni Post Hoc test, Data expressed as mean ± SEM

5.2.4 Cumulative impact of repeated TNFα challenge on cognitive status

In order to determine the impact of repeated systemic challenge with 250μg/kg of TNFα on the cognitive function of the APP/PS1 and WT animals, all animals underwent a five day training protocol on the Morris water maze task (Vorhees et al. 2006; Morris et al. 1982) beginning twenty one days after their first challenge, six days after their fourth challenge with TNFα as summarised in **(Figure 5.1 B).** Animals each underwent four trials per day where they were placed into different quadrants in a pseudorandom fashion and given one minute to locate a raised platform in a fixed location for each animal; during this sixty second trial their time and distance travelled were recorded and assessed by ANY-maze. Trials were spaced approximately 1-1.5 hours apart and after each, the animals were dried and placed in a recovery chamber at 37°C for approx. 3mins before being returned to their home cage. After the fourth trial each day animals were returned to their home cage and then to their holding room.

No significant difference was found between genotypes on learning rate in the Morris water maze over 5 days of testing, days 1-6 after their fourth and final challenge with TNFα, as assessed by distance travelled **(Figure 5.10 A)** and latency (time) **(Figure 5.10 D)** to locating the platform as well as the percentage of total time spent in the correct quadrant **(Figure 5.10 G).** Neither was there a significant main effect of TNFα. Stratification of animals by sex however revealed that APP/PS1 female mice challenged with TNFα exhibited worse performance in learning the task. Female APP/PS1 mice challenged with TNFα displayed worse performance on day 5 of training with significantly slower escape times from the maze (*$p<0.05$) **(Figure 5.10 C)**, longer paths taken to the platform (**$p<0.01$) **(Figure 5.10 F)** and less time spent in the correct quadrant of the maze as a percentage of their total time in the maze (***$p<0.001$) **(Figure 5.10 I)** when compared to saline-treated APP/PS1 females and WT controls. These differences were significant when assessed by two-way ANOVA and Bonferroni post hoc analysis. All male animals regardless of treatment or genotype successfully improved their performance on the task and exhibited equivalent rates of learning **(Figure 5.10 B, E, H).**

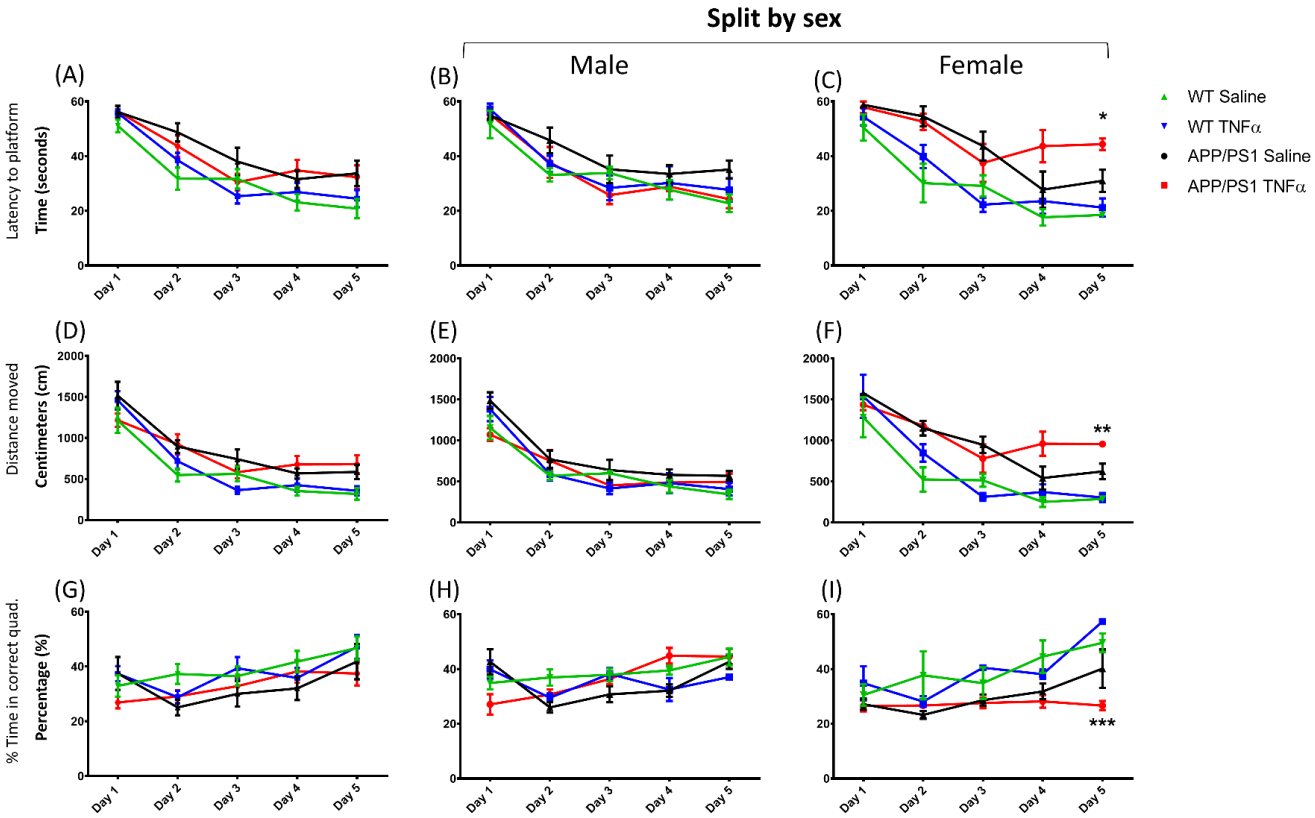

Figure 5.10 MWM analysis of hippocampal-dependent learning - Daily learning performance during morris water maze training from days 1-6 after their fourth and final challenge with TNFα 250µg/kg i.p. treatments, administered five days apart each training showed no significant difference between 15 ±2 month old APP/PS1 and WT animals regardless of treatment in their (A) latency to platform, (B) distance covered to platform and (C) their percentage of time spent in the correct quadrant. Male (WT sal n=5, WT TNF n=6, APP sal n=5, APP TNF n=6), Female (WT sal n=5, WT TNF n=6, APP sal n=3, APP TNF n=4). Repeated measures two-way ANOVA with Bonferroni Post Hoc test, Data expressed as mean ± SEM, * represents a significant difference between APP/PS1 TNFα treated animals and controls, *p<0.05, **p<0.01, ***p<0.001.

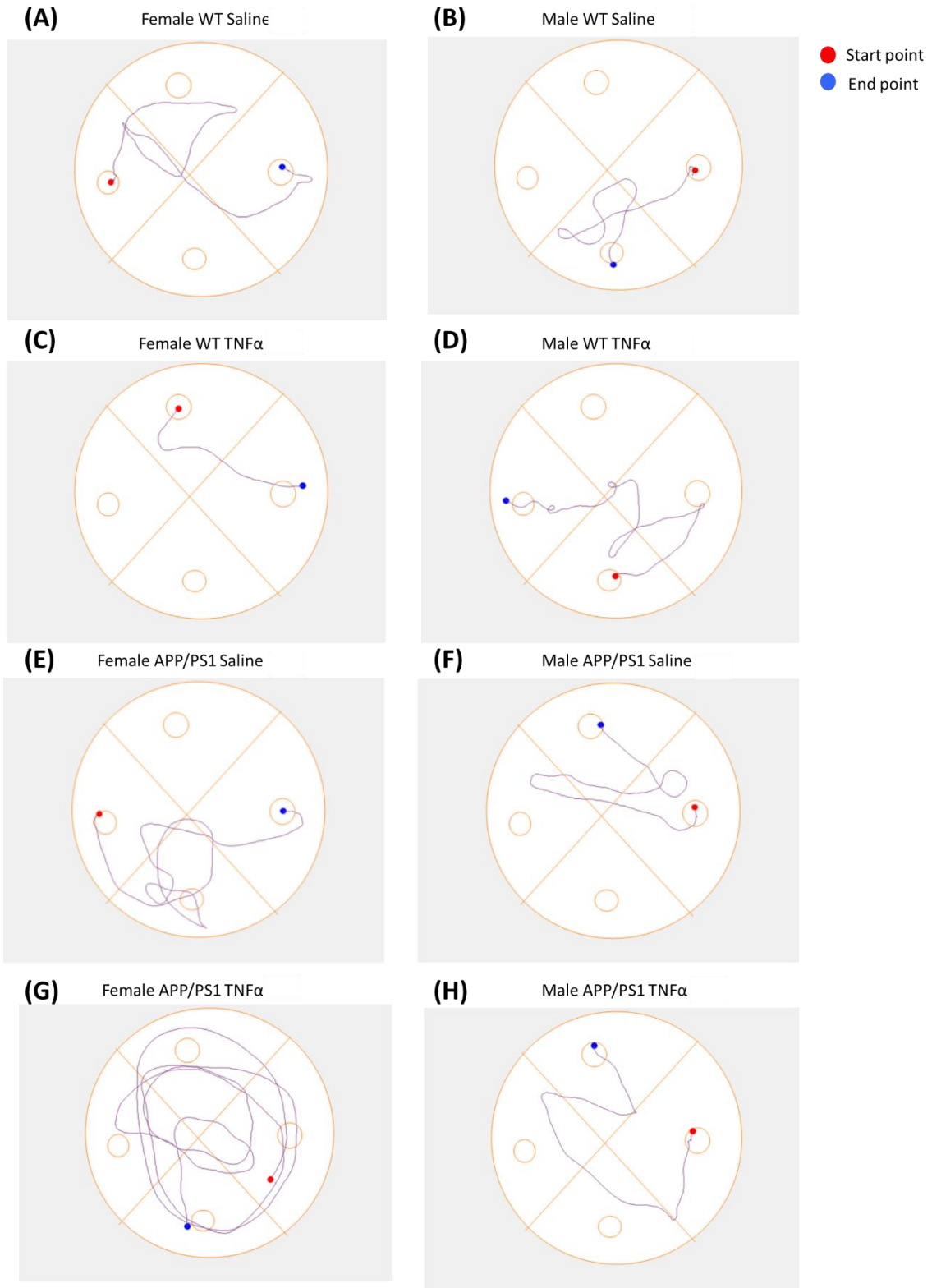

Figure 5.11 Exemplar MWM plots from day five of training, twenty five days after first saline/TNFα 250µg/kg treatment broken down by sex, genotype and treatment.

After five days of training, a probe trial was performed on day six of Morris water maze testing, six days after the fourth and final TNFα 250μg/kg or saline i.p. treatments were administered. During this sixty second trial the raised platform was removed from its fixed location, the animals placed in the water directly opposite where their platform was previously placed, and the percentage of their time spent, and the distance travelled within the quadrant, where the platform was originally located during training, were assessed over 1min. Following this a flag trial was performed with the platform replaced in the maze and flagged by a yellow marker flag to indicate its location and confirm any visual impairment in the animals tested. Animals were allotted sixty seconds to locate the flagged platform and failure to do so were removed from subsequent analyses.

No significant difference in the percentage of total time spent in the correct quadrant of the probe trial was found amongst any of the different treatment/genotype combinations **(Figure 5.12 A).** Separation by sex also demonstrated that all male animals spent equivalent percentages of time in the correct escape quadrant regardless of genotype or treatment **(Figure 5.12 B)**. However, within female animals APP/PS1 female mice spent significantly less time (*$p<0.05$, $F(1,13)=4.675$) in the correct escape quadrant compared to APP/PS1 males and WT controls**.** It was found that TNFα treatment had no bearing on APP/PS1 female performance in the probe trial **(Figure 5.12 C).**

Analysis of the flag trial data revealed APP animals had a significantly greater distance (*$p<0.05$, $F(1,36)=6.939$) (i.e. longer path) **(Figure 5.13 D)** and latency (time spent locating the platform) (*$p<0.05$, $F(1,36)=4.807$) **(Figure 5.13 G)** to the platform. Separation by sex showed this effect to be primarily a result of APP/PS1 female animals which had significantly greater distances (*$p<0.05$, $F(1,14)=5.058$) **(Figure 5.13 B)** and latency (*$p<0.05$, $F(1,14)=7.259$) **(Figure 5.13 E)** to the platforms which was absent in male animals **(Figure 5.13 C, F).**

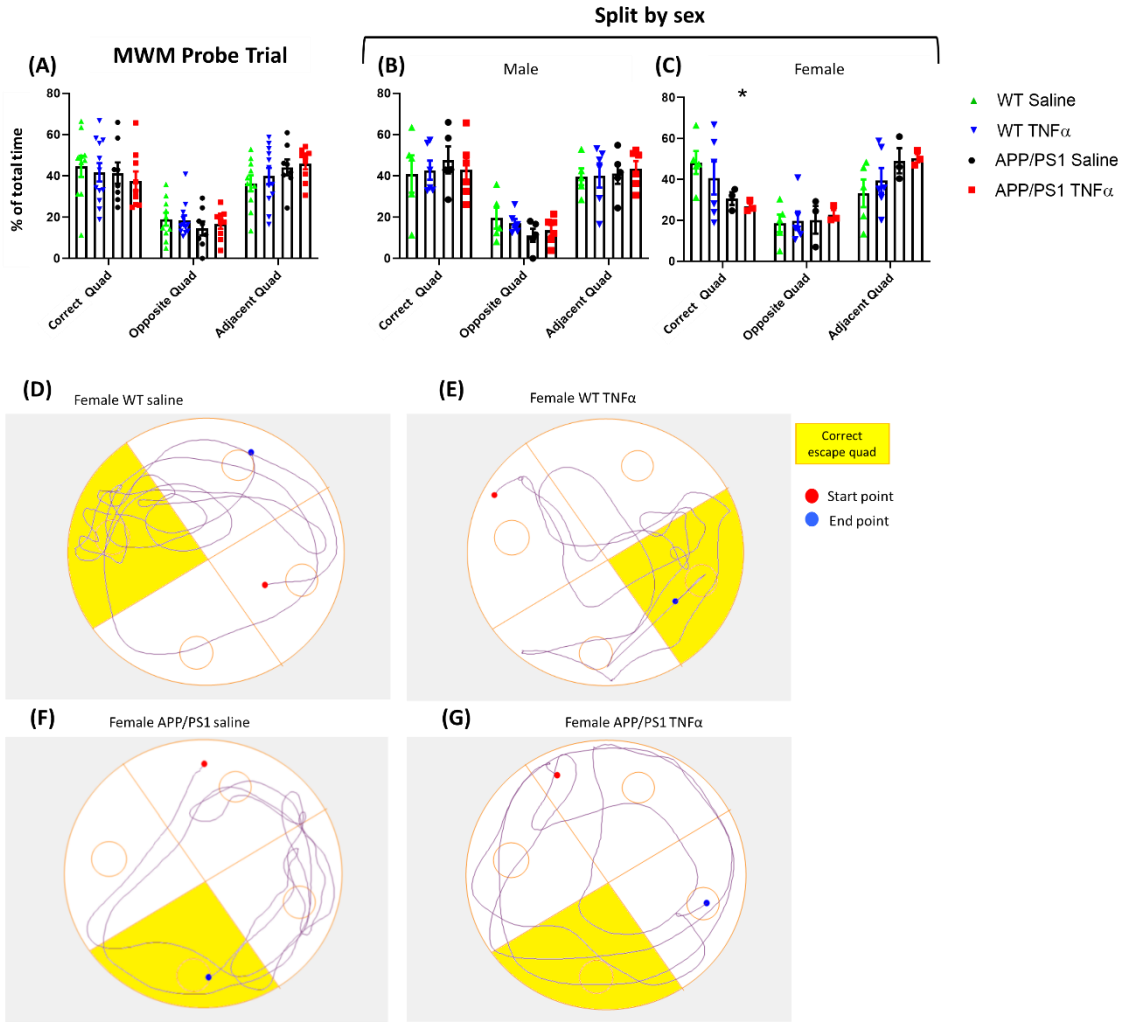

Figure 5.12 MWM Probe trial - Analysis of a 60 second probe trial in the Morris water maze six days after the fourth and final TNFα 250µg/kg or saline i.p. treatments administered 5 days apart each to 15 ±2 month old APP/PS1 and WT mice, (A) Time in correct quadrant as percentage of total time spent in the maze. Separation by sex revealed a significant reduction (*p<0.05) in percentage of total time in the correct quadrant of (C) APP/PS1 female mice that was absent in (B) male mice. (D-G) Exemplar MWM path plots of female mice *p<0.05 indicates a significant difference compared between APP/PS1 and WT controls. Male (WT sal n=5, WT TNF n=6, APP sal n=5, APP TNF n=6), Female (WT sal n=5, WT TNF n=6, APP sal n=3, APP TNF n=4). Two-way ANOVA with Bonferroni Post Hoc test, Data are expressed as mean ± SEM, * represents a significant effect of genotype, *p<0.05, **p<0.01, ***p<0.001.

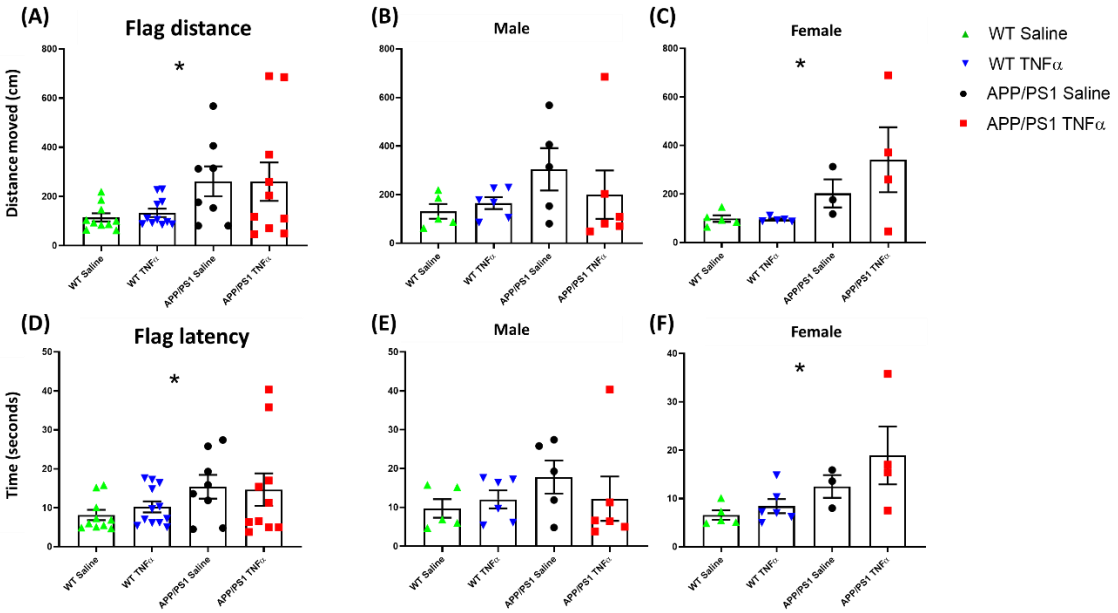

Figure 5.13 MWM Flag trial - Analysis of a 60 second flag trial in the morris water maze six days after the fourth and final TNFα 250µg/kg or saline i.p. treatments administered five days apart each to 15 ±2 month old APP/PS1 and WT mice, as percentage of total time spent in the correct escape quadrant. APP/PS1 mice took a greater (A) distance (*p<0.05) and (D) time (*p<0.05) to locate the platform during a flag trial in the MWM. This genotype effect was consistent in APP/PS1 females (C, F) but absent in APP/PS1 males (B, E). *p<0.05 indicates a significant difference compared between APP/PS1 and WT controls. Male (WT sal n=5, WT TNF n=6, APP sal n=5, APP TNF n=6), Female (WT sal n=5, WT TNF n=6, APP sal n=3, APP TNF n=4). Two-way ANOVA with Bonferroni Post Hoc test, Data expressed as mean ± SEM, * represents a significant effect of genotype, *p<0.05, **p<0.01, ***p<0.001.

To further probe the impact of repeated systemic challenge with TNFα on the cognitive status of APP/PS1 animals, animals were assessed on their ability to learn, remember and associate environmental cues with aversive experiences using a contextual and auditory cued fear conditioning (CFC) task (Shoji et al. 2014). Training in the CFC task began, one day after completion of assessment of hippocampal-dependent memory in the MWM, twenty-seven days after their first challenge with 250μg/kg of TNFα or saline, twelve days after their fourth challenge **(Figure 5.1)**, during which animals were exposed to a chequered patterned wall environment and two 20 second, 20dB auditory cues followed by a 0.4mA shock lasting 2 seconds as per the protocol described in detail in section 2.2.3.4. Testing was conducted 48 hours after training over a 300 second testing period with contextual fear conditioning responsiveness assessed first by placing the animal into the shock cage with the same patterned walls as during their training and assessing mice using ANY-maze software to assess their freezing score (average score of freezing events and duration) and latency (seconds) to their first freezing event (1sec <). No auditory cue was played for the contextual component's assessment.

Upon completion of the assessment of the contextual fear conditioning component animals were returned to their home cage for an inter-trial interval of 20 minutes and then assessed on their auditory-cued fear conditioning response. Animals were returned to the shock cage with the walls' black and white chequered patterns having been changed to a uniform grey panel to alter the environment's contextual cues. Animals were then exposed to the same two 20 second, 20dB auditory cue from their training and once again assessed over the 300 second trial for freezing score and latency to first freezing event after the auditory cue.

It was found that for both contextual and auditory fear conditioning freezing scores (a function of the number and duration of freezing episodes) showed no statistically significant differences with genotype regardless of treatment with TNFα or saline **(Figure 5.14 A, D)**. However, consistent with observations from the visuospatial shallow water y-maze and the Morris water maze tasks, separation by sex revealed that APP/PS1 female mice showed poorer freezing behaviour in response to contextual (*$p<0.05$ $F(1,14) = 4.622$) **(Figure 5.14 E)** and auditory cued (*$p<0.05$ $F(1,14) = 6.448$) **(Figure 5.14 F)** fear conditioning paradigms compared to WT controls. This was unaffected by repeated TNFα challenge. Male animals **(Figure 5.14 C, D)** showed no such genotype effect on freezing score.

Latency to first freezing event in response to contextual or auditory cued stimuli revealed a similar pattern of expression with female APP/PS1 mice showing a significantly longer latency to first freezing event in the contextual fear conditioning paradigm (*$p<0.05$ $F(1,33) = 4.414$) and a trend toward significance in auditory cued ($p=0.1031$ $F(1,33) = 2.81$) which was absent in male animals.

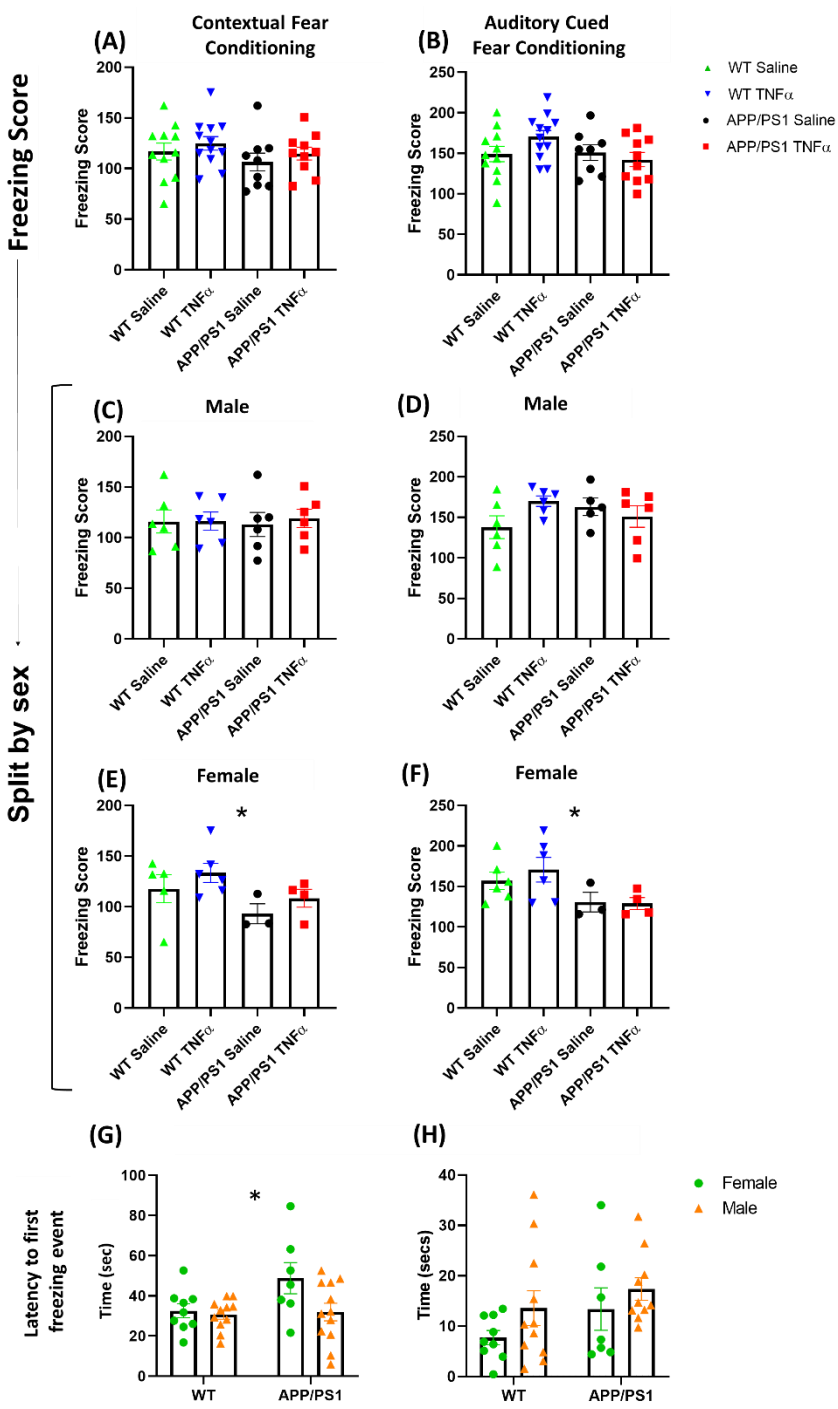

Figure 5.14 Contextual and cued fear conditioning - Contextual and auditory cued fear conditioning were assessed twenty seven days after the first of four repeated TNFα 250µg/kg or saline i.p. treatments, administered five days apart each in 15 ±2 month old APP/PS1 and WT controls. (A) Contextual and (B) auditory cued fear conditioning freezing scores separated by (C-D) male and (E-F) female revealed female APP/PS1 mice show impaired freezing compared to WT and male animals. Latency to first freezing event in (G) contextual and (H) auditory cued fear conditioning Data expressed as mean ± SEM, Male (WT sal n=5, WT TNF n=6, APP sal n=5, APP TNF n=6), Female (WT sal n=5, WT TNF n=6, APP sal n=3, APP TNF n=4). Data analysed by two-way ANOVA with Bonferroni Post Hoc test, * represents a significant effect of genotype, *p<0.05, **p<0.01, ***p<0.001.

Summarising these cognitive data, APP/PS1 female mice challenged sequentially with TNFα (250μg/kg per dose) showed a reduced ability to learn Morris water maze task compared to saline-treated APP/PS1 mice and saline or TNF-treated WT animals. This effect of TNF was not apparent on contextual fear conditioning. Moreover, across multiple hippocampal-dependent tasks female APP/PS1 mice consistently display worse cognitive deterioration than their male counterparts and appear to be largely responsible for genotype-dependent effects in this study.

5.2.5 Cumulative impact of repeated TNFα challenge on neuroinflammatory status

In order to assess the impact of repeated systemic challenge with a 250μg/kg bolus of TNFα on the microglia and astrocytes in 14±2-month-old animals. Microglia and astrocyte cells were isolated from hippocampal tissue by fluorescence activated cell sorting (FACS) 21 days after their first challenge with TNFα, 6 days after their fourth and final challenge. Quantitative PCR analysis was performed for microglial and inflammatory mediators on cDNA synthesised from RNA isolated from these isolates.

The first step in identifying and isolating glial cells from the hippocampal homogenate was to gate on single cells, excluding cell doublets etc. To this end cells were assessed on their granularity and mass and gated according to their side scatter area (SSC-A) against their forward scatter area (FSC-A) **(Figure 5.15 A)**, followed by their FSC-A against forward scatter width (FSC-W) **(Figure 5.15 B)** and finally by SSC-A against side scatter width (SSC-W) **(Figure 5.15 C),** any cells which fell in the upper range of these plots due to its size were likely doublets and thus excluded. Following this sequential gating strategy, this population of single cells could now be separated into living and dead cells based on 7-aminoactinomycin D (7AAD) positive labelling of lysed cells' DNA and plotted against FSC-A **(Figure 5.15 D)**. Microglia were identified and separated from this population of living cells based on high CD11b-FITC$^+$ and intermediate CD45-APC$^+$ expression to distinguish them from macrophage populations **(Figure 5.15 E)**; astrocytes were identified and isolated based off of high GFAP-PE$^+$ staining against FSC-A **(Figure 5.15 F)**.

To determine the purity and efficiency of the FACS isolation of glial cell isolates qPCR analysis was performed to assess expression of microglial and astrocytic specific markers, CD11b and GFAP respectively. qPCR analysis of gene expression revealed robust expression of CD11b in microglial isolates with negligible expression in astrocyte isolates **(Figure 5.16 B)**, commensurately astrocyte populations had strong expression levels of GFAP which were absent in microglial isolates **(Figure 5.16 A)**.

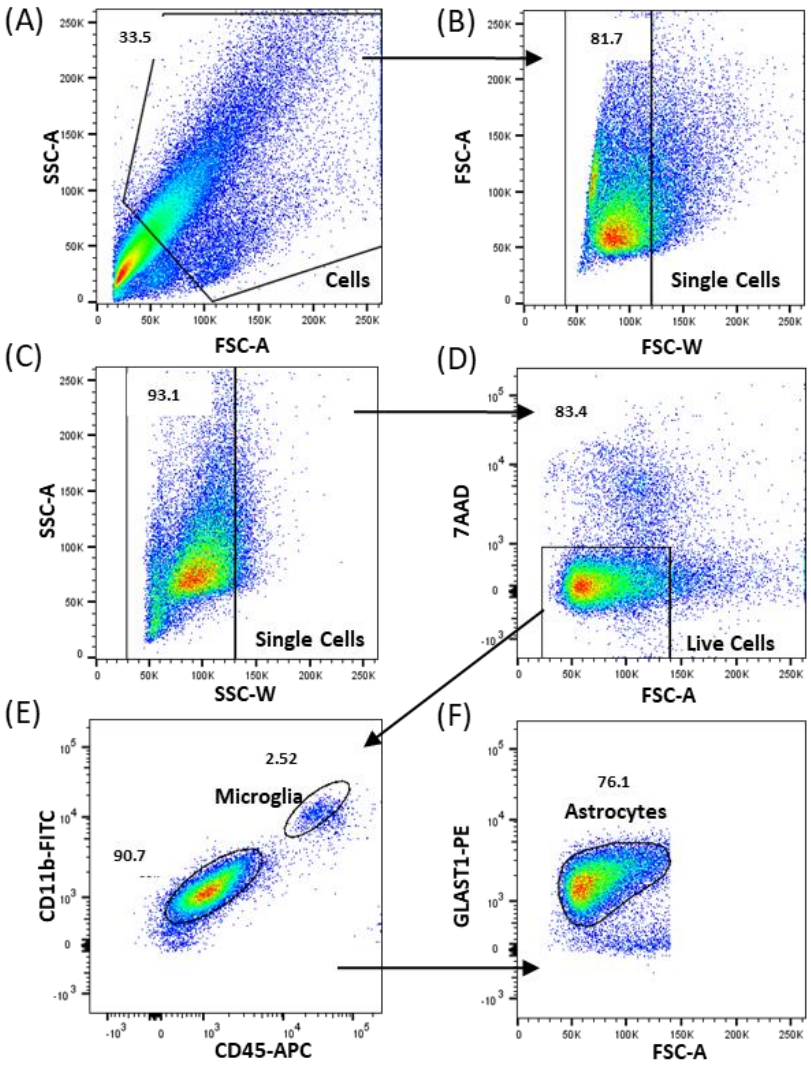

Figure 5.15 **Fluorescent activated cell sorting (FACS) of astrocytes and microglia from 14 ±2 month old APP/PS1 and WT animals 21 days after the first of four repeated TNFα 250µg/kg or saline i.p. treatments, administered five days apart (A – B) gating cells to single cells, (D) separating live from dead cells using the DNA marker 7AAD staining of lysed cells, (E) identifying and separating microglia based off high CD11b-FITC$^+$ and intermediate CD45-APC$^+$ staining and (F) identifying astrocytes according to high GLAST1-PE$^+$ staining.**

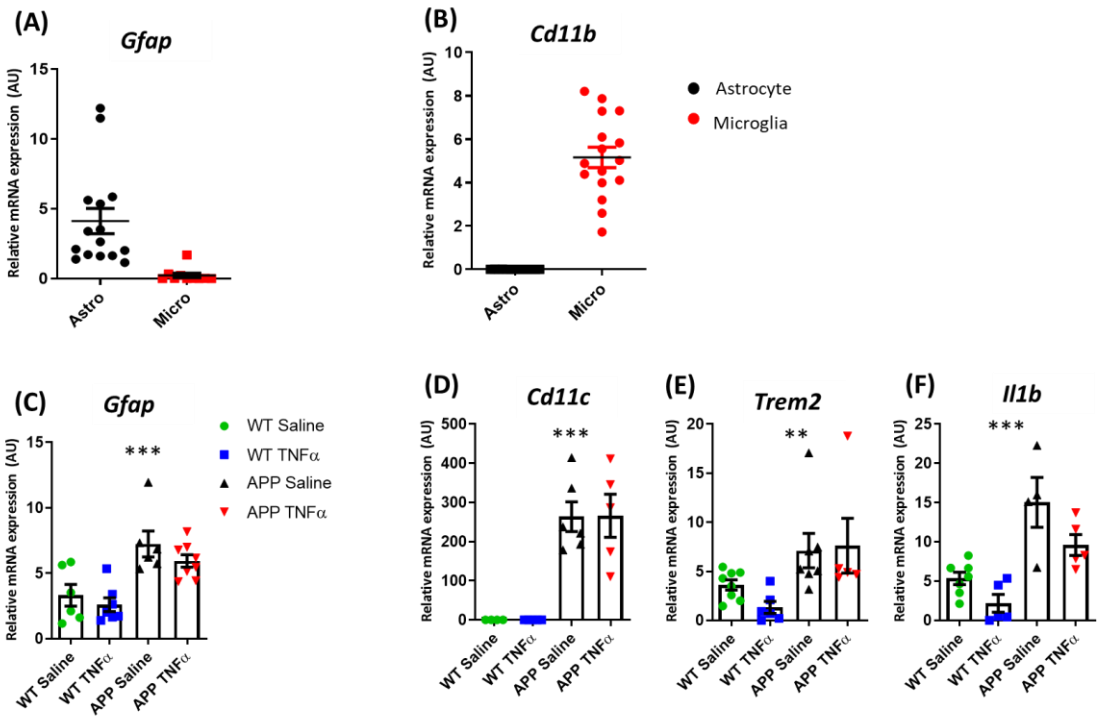

Figure 5.16 Quantitiatve PCR analysis assessing microglial and astrocytic purity markers and products : **(A) Astrocytic and (B) microglial purity in FACS isolated glial cells from 14±2 month old APP/PS1 and WT animals saline challenged animals. (C) astrocytic, *Gfap,* (D) microglial markers *Cd11c* and *Trem2* and microglial product *Il1b*, gene expression assessed by qPCR and transcripts normalised to the housekeeping gene *18s*, were assessed in 14±2 month old APP/PS1 and WT animals 6 days post the fourth consecutive challenge with TNFα (250µg/kg)/saline. All data are represented as the mean ± SEM and analysed by two-way ANOVA followed by a Bonferroni multiple comparison Post Hoc Test (n = 6, 8, 6, 5), * denotes a statistical significant effect of genotype on expression *(p<0.05),**(p<0.01), ***(p<0.001). # denotes a statistically significant interaction between genotype and treatment; # (p<0.05), ## (p<0.01).**

Cd11c as discussed previously in this text, is a key hub gene of the microglial priming genotype (Holtman et al. 2015) and as such would be expected to show elevated transcription with a genotype for a chronic condition such as the APP/PS1 plaque pathology as shown here (***p<0.001, F(1,14) = 46.61) **(Figure 5.16 D)**. Consistent with the microglial priming phenotype, analysis of the *Il1b* gene transcript revealed a significant increase in microglial expression (***p<0.001, F(1,14) = 20.61) in APP animals compared to WT controls that is unaffected by treatment with either TNFα or saline 6 days after the fourth and final challenge **(Figure 5.16 F)**.

Similarly, *Trem2* a known risk factor gene for Alzheimer's (Malik et al. 2015) as well as a strong marker for microglial activation was also elevated with genotype (**p<0.01, F(1,22) = 10.71) in microglial isolates and unaffected by treatment with TNFα in APP animals but showed a trend toward decreased expression in WT animals challenged with TNFα **(Figure 5.16 E)**. Consistent with this pattern of microglial activation, *Gfap* expression, a marker of astrocytic activation known to be elevated in the APP/PS1 transgenic animal showed significant enrichment in APP/PS1 isolated astrocytic cells that was unaffected by treatment (***p<0.001, F(1,22) = 27.19) **(Figure 5.16 C)**.

Assessment of genes which were selectively expressed at greater levels in microglia compared to astrocytes six days after the fourth and final challenge with TNFα (250µg/kg) or saline in 15-month-old animals showed that gene transcript expression of *Stat3* revealed a significant increase in the expression for both astrocytic (**p<0.01, F (1, 14) = 13.07) and microglial (**p<0.01, F (1, 19) = 14.15) isolates of APP animals compared to WT controls that was unaffected by treatment with either TNFα or saline **(Figure 5.17 B).** Toll-like receptor 4 (*Tlr4*) expression was found to show equivalent expression across all animals regardless of genotype or treatment. It is possible any effects of treatment have resolved given the time point these were assessed at, 6 days after their fourth and final intraperitoneal challenge with 250µg/kg of TNFα or saline **(Figure 5.17 A).**

Assessment of the complement system's activation in APP/PS1 animals through expression of its components *C1qa* and *C3* revealed a significant increase in expression of *C3* (*p<0.05, F (1, 17) = 5.063) within microglial isolates of APP animals **(Figure 5.17 C)**. Astrocytic expression however showed a robust induction of *C3* in response to TNFα treatment (#p<0.05, F (1, 15) = 8.028). The complement component *C1qa* showed no change in expression with either genotype or treatment for either microglial or astrocytic cells, however microglial were the most robust expressors compared to astrocytes **(Figure 5.17 D)**.

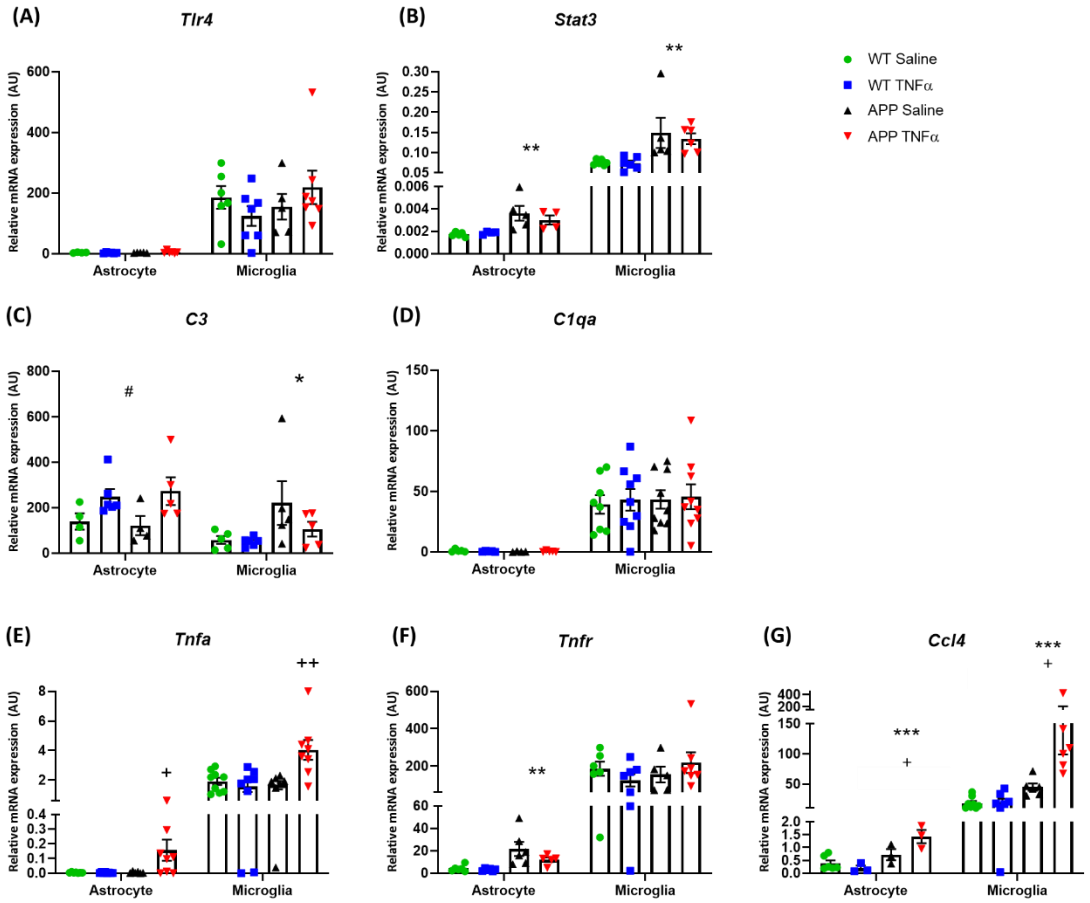

Figure 5.17 Quantitiatve PCR analysis of genes selectively expressed in microglial FACS isolates. (A) *Tlr4,* (B) *Stat3,* (C) *C3,* (D) *C1qa*, (E) *Tnfa,* (F) *Tnfr* and (G) *Ccl4* , gene expression assessed by qPCR and transcripts normalised to the housekeeping gene 18s, were assessed in 14±2 month old APP/PS1 and WT animals 6 days post the fourth consecutive challenge with TNFα (250µg/kg)/saline. All data are represented as the mean ± SEM and analysed by two-way ANOVA followed by a Bonferroni multiple comparison Post Hoc Test (n = 6, 8, 6, 5), * denotes a statistical significant effect of genotype on expression *(p<0.05),(p<0.01), ***(p<0.001), # denotes a statistically significant effect of treatment; # (p<0.05), + denotes a statistical significant interaction between treatment and genotype on expression +(p<0.05),++(p<0.01).**

In contrast assessment of the pro-inflammatory mediator *Tnfa revealed* a significant interaction between treatment and genotype with increased expression of the pro-inflammatory cytokine *Tnfα* in both astrocytes (+p<0.05, F(1,26) = 5.432) and microglia (++p<0.01, F(1,25) = 9.464) of APP/PS1 animals treated with TNFα which was absent in saline treated and WT controls **(Figure 5.17 E).** This corresponded with a robust increase in TNF-Receptor (*Tnfr)* with genotype (**p<0.01, F (1, 19) = 14.31) in the astrocytes of APP/PS1 animals which was absent in microglial isolates **(Figure 5.17 F).** However, it should be noted that *Tnfr* expression was far greater on microglia than upon astrocytic isolates. Similarly, there was a significant effect of genotype on increased expression of the pro-inflammatory chemokine *Ccl4* was observed in both microglial (***p<0.001, F (1, 23) = 10.50) and astrocytic (***p<0.001, F (1, 14) = 20.43) cells in APP/PS1 animals **(Figure 5.17 G)**. Furthermore, there was a significant interaction between genotype and treatment with APP/PS1 animals showing significantly greater production of *Ccl4* expression in response to TNFα treatment compared to WT animals for both microglia (+p<0.05, F (1, 23) = 4.709) and astrocytic (+p<0.05, F (1, 11) = 6.749) cells.

In turn I then assessed the expression of genes which were preferentially expressed in astrocytes over microglial cells and showed that *Hes-5* a transcription factor notable for its role in the regulation of neurogenesis and known to be decreased in expression under certain pro-inflammatory conditions such as acute treatment with LPS (Acaz-Fonseca et al. 2019) was shown here to be selectively expressed at greater levels in astrocytes compared to microglia. Furthermore, it was found to show decreased expression in APP/PS1 animals for both the microglial (*p<0.05, F (1, 22) = 7.390) and astrocytic cell isolates (***p<0.001, F (1, 21) = 18.37) **(Figure 5.18 A).** The type one interferon signalling associated gene *Irf7's* transcript expression was also found to be minimally expressed in microglia compared to astrocytes and was unaltered by genotype or treatment in microglial isolates **(Figure 5.18 B)** but showed a robust upregulation of expression (*p<0.05, F (1, 16) = 7.445) in the astrocytic population of APP/PS1 animals that was unaffected by treatment with TNFα**.** Similarly, Interferon-inducible guanylate-binding proteins (GBPs), such as guanylate binding protein 2 *(Gbp2),* are well-known for mediating host-defense mechanisms against cellular pathogens and were shown here to be expressed at much greater levels in astrocytic cells compared to microglia **(Figure 5.18 C)**. Furthermore, astrocytic cDNA displayed a statistically significant interaction between treatment and genotype on APP/PS1 TNFα-treated animals (++p<0.01, F (1, 17) = 11.93) expression. In contrast, expression was found to be equivalent across APP/PS1 and WT animals microglial isolates irrespective of treatment at this time point**.**

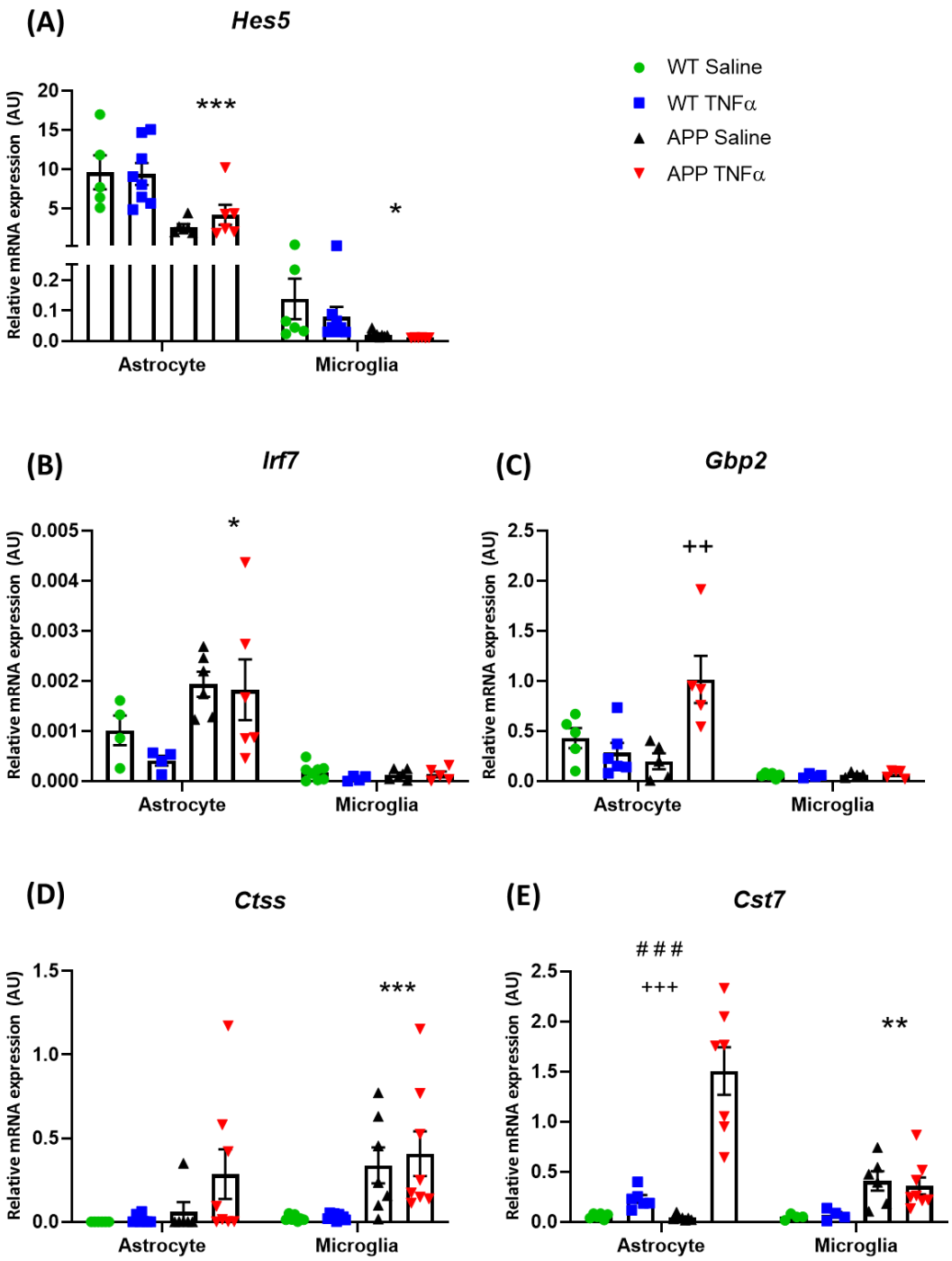

Figure 5.18 **Quantitiatve PCR analysis of genes selectively expressed in astrocytic FACS isolates. . (A) *Hes5,* (B) *Irf7,* (C) *Gbp2,* (D) *Ctss* and (E) *Cst7,* gene expression assessed by qPCR and transcripts normalised to the housekeeping gene 18s, were assessed in 14±2 month old APP/PS1 and WT animals 6 days post the fourth consecutive challenge with TNFα (250µg/kg)/saline. All data are represented as the mean ± SEM and analysed by two-way ANOVA followed by a Bonferroni multiple comparison Post Hoc Test (n = 6, 8, 6, 5), * denotes a statistical significant effect of genotype on expression *(p<0.05),**(p<0.01), ***(p<0.001). # denotes a statistically significant interaction between genotype and treatment; # (p<0.05), ## (p<0.01).

Cathepsin S (*Ctss*), a lysosomal protease known to be capable of promoting degradation via the endo-lysosomal pathway of damaged proteins (Turk et al. 2012) such as the disease-associated amyloid plaque pathology of the APP brain was shown to have significantly elevated expression in microglial isolates of APP/PS1 animals (***p<0.001, F (1, 22) = 16.61) **(Figure 5.18 D) .** Astrocytic isolates showed highly variable expression in APP/PS1 animals challenged with TNFα but failed to demonstrate a statistically significant change in expression. Cystatin-7 (*Cst7*), a protease inhibitor and well-established marker of the disease-associated microglial (DAM) subset (Hamilton et al. 2008) showed significant elevation of *Cst7* (**p<0.01, F (1, 18) = 13.81) within APP/PS1 microglial cells which was unaffected by treatment at this point of recovery after TNFα challenge **(Figure 5.18 E)**. Astrocytic *Cst7* on the other hand shows evidence also shows significant upregulation in animals challenged with TNFα (# # #p<0.001, F (1, 22) = 39.30) compared to saline controls but also a robust interaction between treatment and genotype with markedly exaggerated expression in APP/PS1 animals (+++p<0.001, F (1, 22) = 24.64) compared WT challenged with TNFα which may be indicative of a hypersensitive response of astrocytes. Both of these, have been previously reported to be key markers of astrocytosis in response to central challenges (Lopez-Rodriguez et al. 2018) however, here were preferentially expressed in microglial cells with robustly elevated expression evident in TNFα-treated APP/PS1 astrocytes.

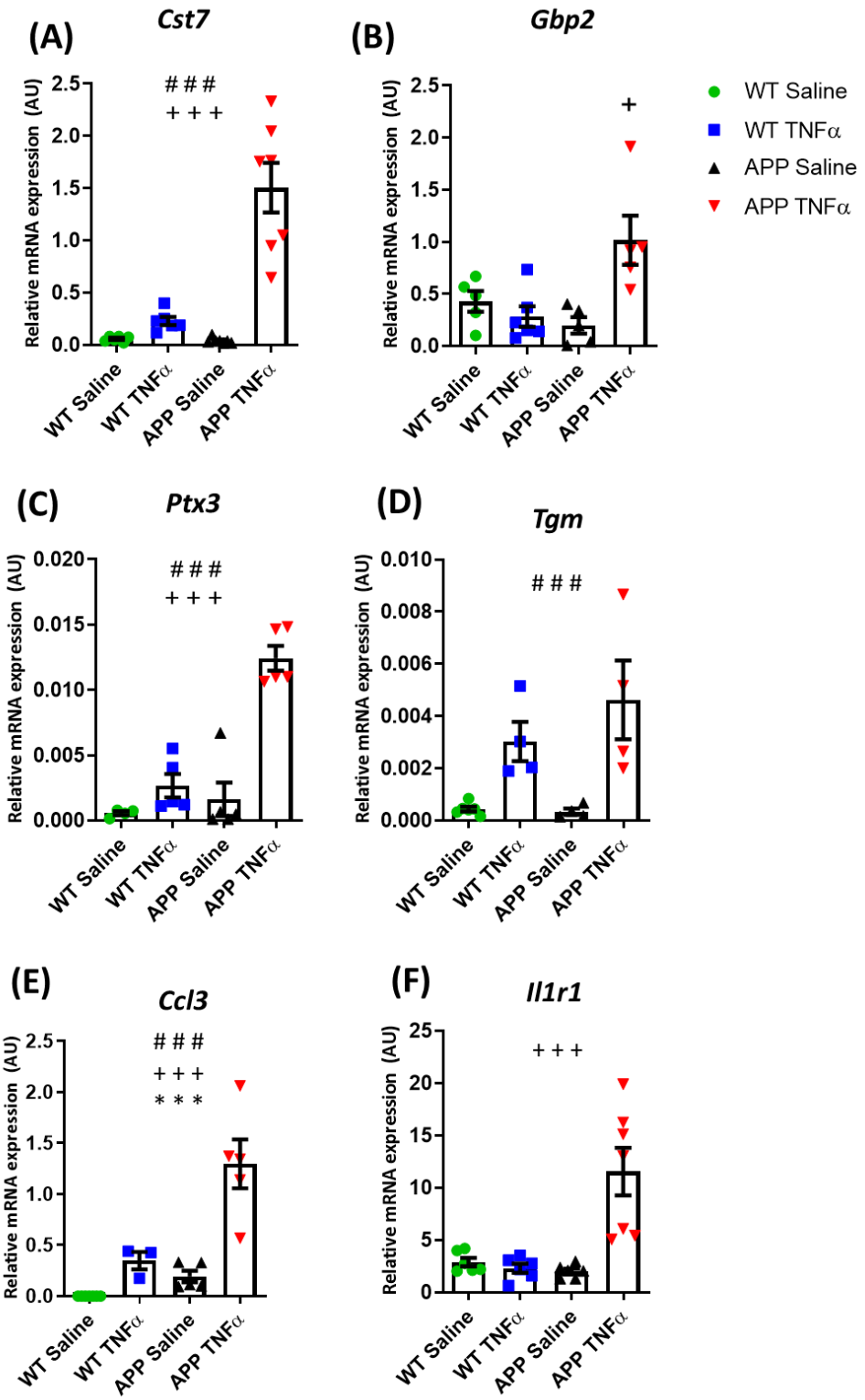

Figure 5.19 **Quantitiatve PCR analysis of astrocytic FACS isolates vulnerable to exagerrated responses to TNFα. (A) *Cst7,* (B) *Gbp2,* (C) *Ptx3,* (D) *Tgm*, (E) *Ccl3* and (F) *Il1r1* gene expression assessed by qPCR and transcripts normalised to the housekeeping gene 18s, were assessed in 14±2 month old APP/PS1 and WT animals 6 days post the fourth consecutive challenge with TNFα (250µg/kg)/saline. All data are represented as the mean ± SEM and analysed by two-way ANOVA followed by a Bonferroni multiple comparison Post Hoc Test (n = 6, 8, 6, 5), * denotes a statistical significant effect of genotype on expression *(p<0.05),**(p<0.01), ***(p<0.001). # denotes a statistically significant interaction between genotype and treatment; # (p<0.05), ## (p<0.01).**

Several genes associated with activated astrocytic cells under pathological conditions (Liddelow et al. 2017; Lopez-Rodriguez et al. 2021; Couturier et al. 2016) were shown to be enriched in astrocytic cells in response to the repeated 250µg/kg i.p. challenge of TNFα but demonstrated an exaggerated upregulation in those of APP/PS1 animals. Astrocytic *Gbp2* expression as discussed above showed a statistically significant interaction between treatment and genotype on APP/PS1 TNFα-treated animals (++p<0.01, F (1, 17) = 11.93) (**Figure 5.19 B)**. Furthermore, Pentraxin 3 (*Ptx3)* expression was shown to be enriched in animals challenged with TNFα (# # #p<0.001, F (1, 15) = 43.88) (**Figure 5.19 C)** as well as a significant interaction between the APP/PS1 genotype and treatment (+++p<0.01, F (1, 15) = 19.93) with TNFα-challenged APP/PS1 animals showing exaggerated transcript expression compared to WT controls. Astrocytic *Cst7* showed a similar pattern of expression to that observed for *Ptx3* with a significant effect of TNFα (# # #p<0.001, F (1, 22) = 39.30) as well as an interaction between treatment and genotype in APP/PS1 animals (+++p<0.001, F (1, 22) = 24.64) compared WT challenged with TNFα **(Figure 5.19 A)**. Transgluatminase 1 (*Tgm1)* also shows a similar significant effect of treatment in (# # #p<0.001, F (1, 14) = 20.78) both APP/PS1 animals and WT animals challenged with TNFα **(Figure 5.19 D)**. Interestingly, astrocytic isolates showed a robust interaction between genotype and treatment (+++p<0.001, F (1, 21) = 14.64) in gene transcript expression for Interleukin-1 receptor (*Il1r)* in APP/PS1 animals challenged with TNFα compared to WT and saline treated control animals **(Figure 5.19 F)**. Finally, astrocytic *Ccl3* showed robust effects of genotype (***p<0.001, F (1, 16) = 18.99), treatment (# # #p<0.001, F (1, 16) = 30.69) and an interaction between the two (+p<0.05, F (1, 16) = 8.272) **(Figure 5.19 E)**.

While the microglial priming phenotype which I observe here is relatively well characterised (Holtman et al. 2015; Krizanac-Bengez et al. 2006; Lopez-Rodriguez et al. 2021), astrocyte priming *in vivo* remains relatively novel . Taken together these data highlight the robust alteration of glial cell function under pathological AD conditions and the significant risk which this confers to glial dysfunction, disruption of homeostasis and vulnerability to exaggerated inflammatory responses in both astrocytes and microglia.

5.2.6 Intrahippocampal TNFα challenge

Because *Tnfr* was significantly elevated in astrocytes in APP/PS1 mice, it was hypothesised that astrocytes would show heightened sensitivity to secondary inflammatory challenge with TNFα. An additional cohort of C57 WT and APP/PS1 mice, aged 23±5-months (all male due to limited survival of female APP/PS1 mice to that age). These mice were surgically challenged with a unilateral intrahippocampal injection, via a microcapillary, of 300ng of TNFα. Animals were euthanised at 2 hours post-injection, were transcardially perfused with 10% neutral-buffered formalin and labelled with a number of antibodies in order to assess the impact of this direct CNS challenge of TNFα on markers of glial activation and inflammatory mediator synthesis. Assessment of brain pathology in 23±5-month-old male animals revealed significant amyloid-β pathology, as assessed by immunohistochemistry for 6E10, in the APP/PS1 animals while this was obviously absent in WT controls (***p<0.001) **(Figure 5.21 A – C).** Consistent with this chronic pathology APP/PS1 animals show heightened glial activation for both astrocytes, as assessed by immunohistochemical labelling of the cytoskeletal astrocytic marker GFAP (***p<0.001) **(Figure 5.21 D – F),** and for microglia, as assessed by immunohistochemical labelling of the microglial cell marker $IBA1^+$ (**p<0.01) **(Figure 5.21 G – I).** Glial cell activation was shown to be positively correlated with the extent of amyloid burden for both microglia (**p<0.01, r^2 = 0.3793) (**Figure 5.21 J)** and astrocytes (**p<0.01, r^2 = 0.3848) **(Figure 5.21 K**). Glial activation itself was positively correlated between the two cell types also (*p<0.05, r^2 = 0.2617) **(Figure 5.21 L).** Immunofluorescent double labelling was used to show the close juxtaposition of $IBA1^+$ microglia (633nm red) with $GFAP^+$ astrocytes (488nm green) in the parenchyma of a 25-month-old male mouse (**Figure 5.22 C-F)**. In general, the astrocytes show large-rounded nuclei while the microglia show smaller, slightly oblong nuclei, which may be used to make preliminary assessment of cell identities in immunohistochemical labelling.

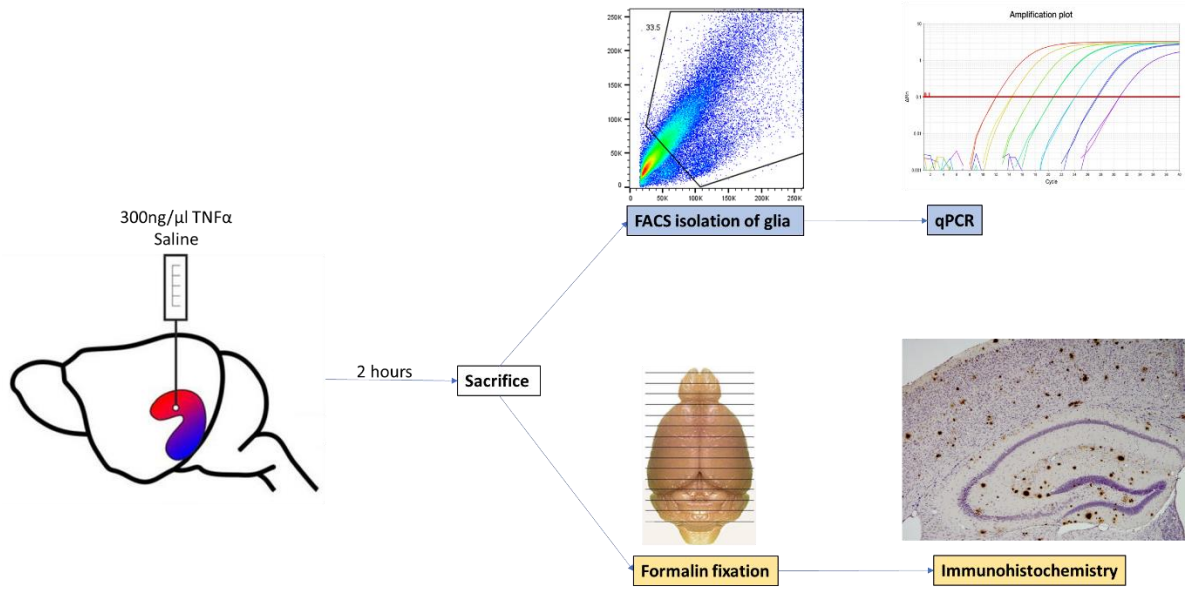

Figure 5.20 **Experimental Timeline of intrahippocampal TNFα (300ng/µl) challenge in animals aged 23 ±3-month-old APP/PS1 and WT males. Animals were sacrificed two hours post intrahippocampal challenge and tissue taken for glial isolation by FACS and qPCR molecular analysis or for formalin fixation and paraffin embedding for immunohistochemical analysis of pathology.**

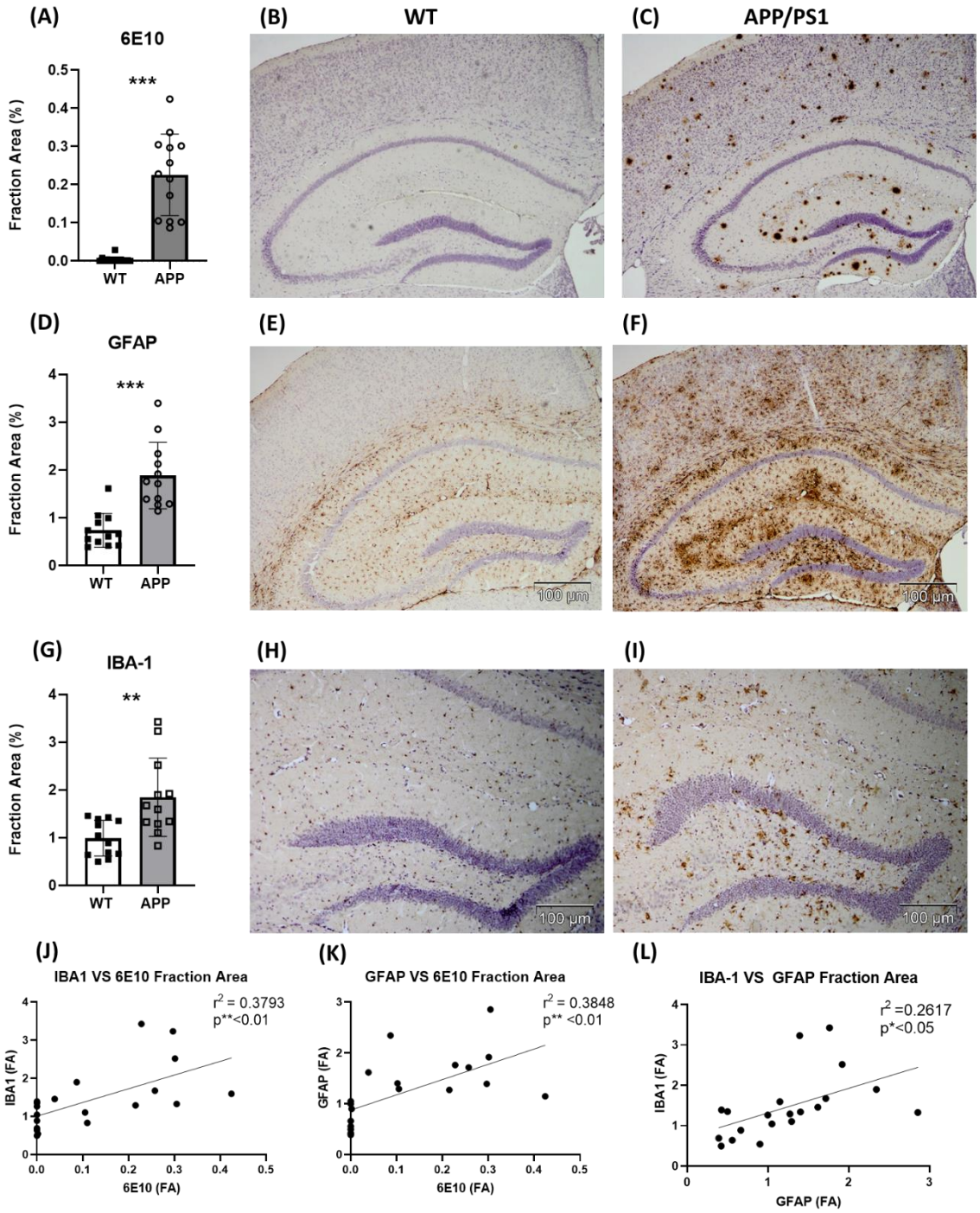

Figure 5.21 Genotype characterisation of amyloid pathology and gliosis in APP/PS1 animals - (A-C) amyloid plaque pathology, 6E10+ staining, and glial pathology for astrocytes, GFAP+ (D-F), and microglia IBA1+ (G-I) in 23 ±3-month-old APP/PS1 and WT males. Data expressed as mean ± SEM and assessed by student t-test (WT sal n=7, WT TNF n=7, APP sal n=6, APP TNF n=6). Correlation by Pearson inear regression analysis performed for microglia area against plaque pathology (J), for astrocyte area against plaque pathology (K) and microglia area against astrocyte area (L).

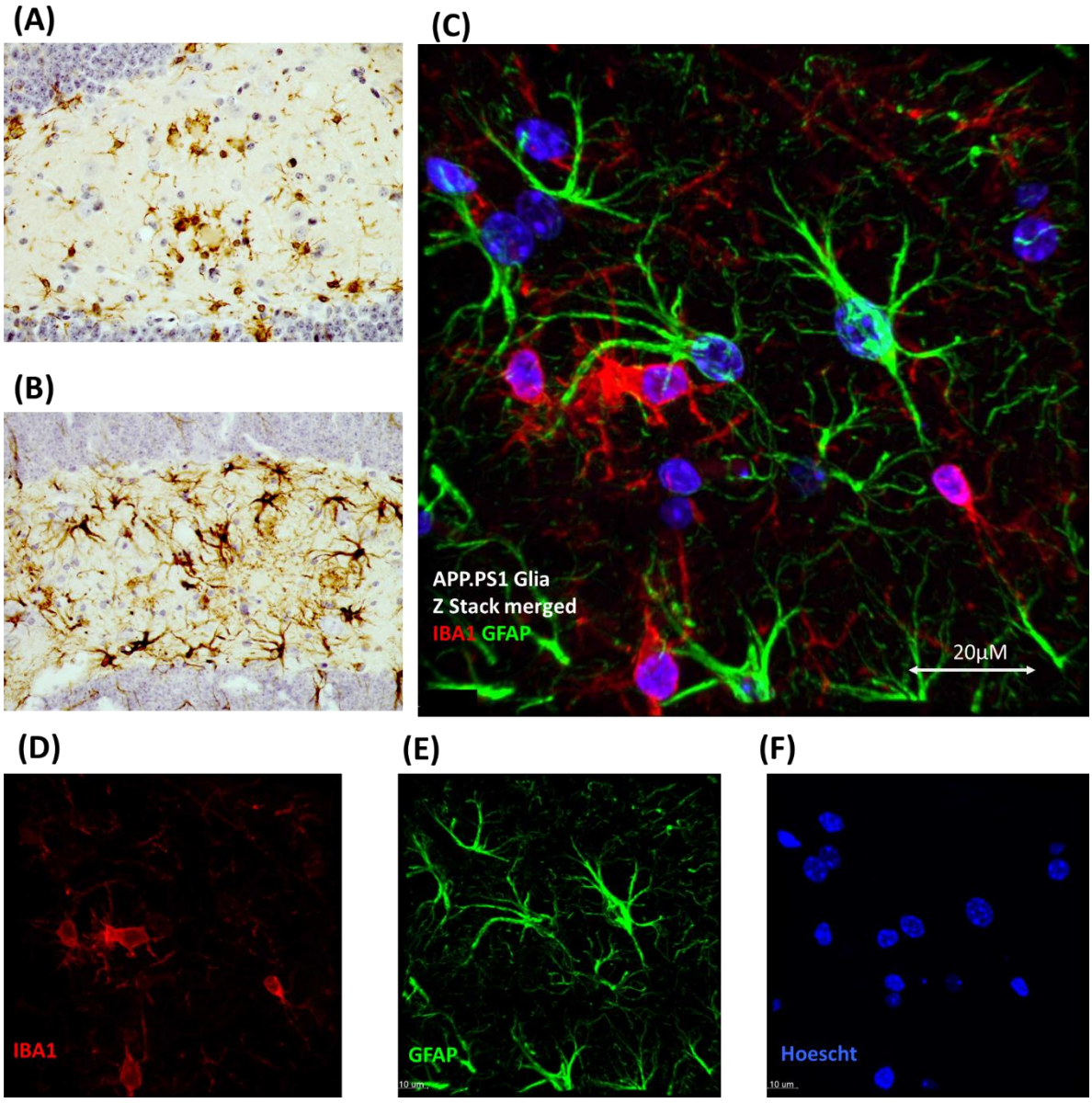

Figure 5.22 **Immunohistochemistry and immunofluorescent colocalisation of microglia and astrocytes: Hippocampus of 25-month-old WT male, 2 hours post I.C. challenge with saline. Immunohistochemical staining for (A) IBA1+ microglia and (B) GFAP+ astrocytes was assessed by light micrscopy. Demonstration of the close juxtaposition of these two glial cell types was performed by confocal microscopy (C-F) fluorescent labelling of IBA1 (red 633 nm), GFAP (green 488 nm) and DAPI nuclei (blue 450nm)**

5.2.2.1 Astrocytes are primed in APP/PS1 mice and produce exaggerated chemokine responses to intrahippocampal TNFα

Immmunohistochemical analysis of glial pathology in male APP/PS1 and C57 WT control animals challenged with saline or TNFα intrahippocampally at a dose of 300ng/µl revealed no statistically significant effect of TNFα upon amyloid pathology as assessed by 6E10 positive staining **(Figure 5.23 A – E),** upon $GFAP^+$ astrocytic **(Figure 5.23 F – J)** or $IBA1^+$ microglial pathology **(Figure 5.23 K – O).** Given the short time after TNFα challenge, this was expected. However, as demonstrated earlier in this chapter, astrocytes and microglia morphology and expression profile in the APP/PS1 glia suggest an activation and possible priming of these populations by the amyloid pathology. Lead by previous demonstrations of hypersensitivity of astrocytes to secondary challenge with IL-1b, in this model, assessment of the expression of macrophage chemoattractant protein CCL2 (MCP-1) was performed by immunohistochemistry. This revealed robust induction of CCL2 expression in the dentate gyrus of APP/PS1 animals challenged with 300ng/µl of TNFα, which was absent in saline-treated APP/PS1 animals and in WT animals challenged with saline or TNFα **(Figure 5.24 A-D)**. A similar pattern of induction of the inflammatory chemokine C-X-C motif chemokine ligand 10 (CXCL10) was also observed **(Figure 5.25 A-D).**

While only APP/PS1 animals challenged with TNFα showed clear CCL2 and CXCL10 labelling in the parenchyma of the dentate gyrus of the hippocampus, both WT and APP/PS1 mice challenged with TNFα exhibited labelling along the glia limitans and endothelium also **(Figure 5.24-3, F, H, J, L)**. The positive labelling within the parenchyma of the dentate gyrus, and throughout the hippocampi, of APP/PS1 animals challenged with TNFα showed a distinct expression pattern as a cloud of vesicle-like structures, proximal to the counterstained blue nuclei. This pattern of expression was suggestive of endoplasmic reticulum labelling, consistent with these proteins being located, at that time post-TNF, early the secretory pathway. Based on the morphology of the nuclei to which these vesicles were proximal, these chemokine-positive cells appeared to be astrocytes. Double immunofluorescence was used to confirm/refute this.

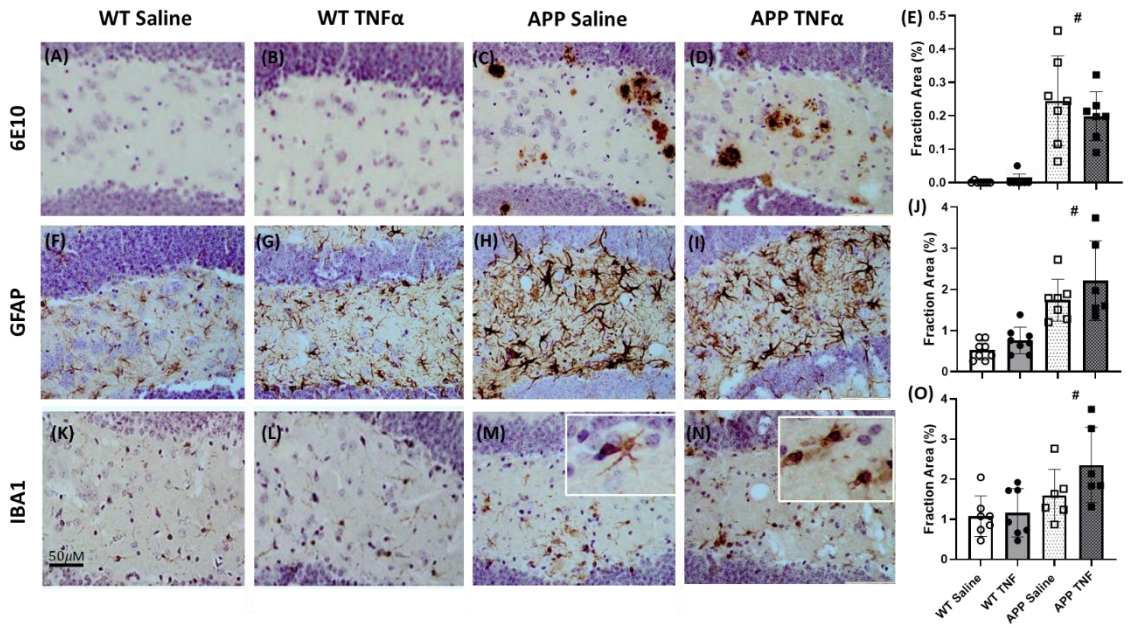

Figure 5.23 **Immunohistochemical analysis of hippocampal dentate gyrus amyloid and gliosis in APP/PS1 and WT male animals ± TNFα aged 23 ±3-month-old, 2 hours post I.C., saline or TNFα (300ng). (A-F) 6E10 (F-I) GFAP and (K-N) IBA1 (40x, scale = 50μm). Quantitative analysis of (E) 6E10 expression , (J) GFAP and (O) IBA1 by two-way ANOVA, data represented as mean ± SEM (WT sal n=7, WT TNF n=7, APP sal n=6, APP TNF n=6).**

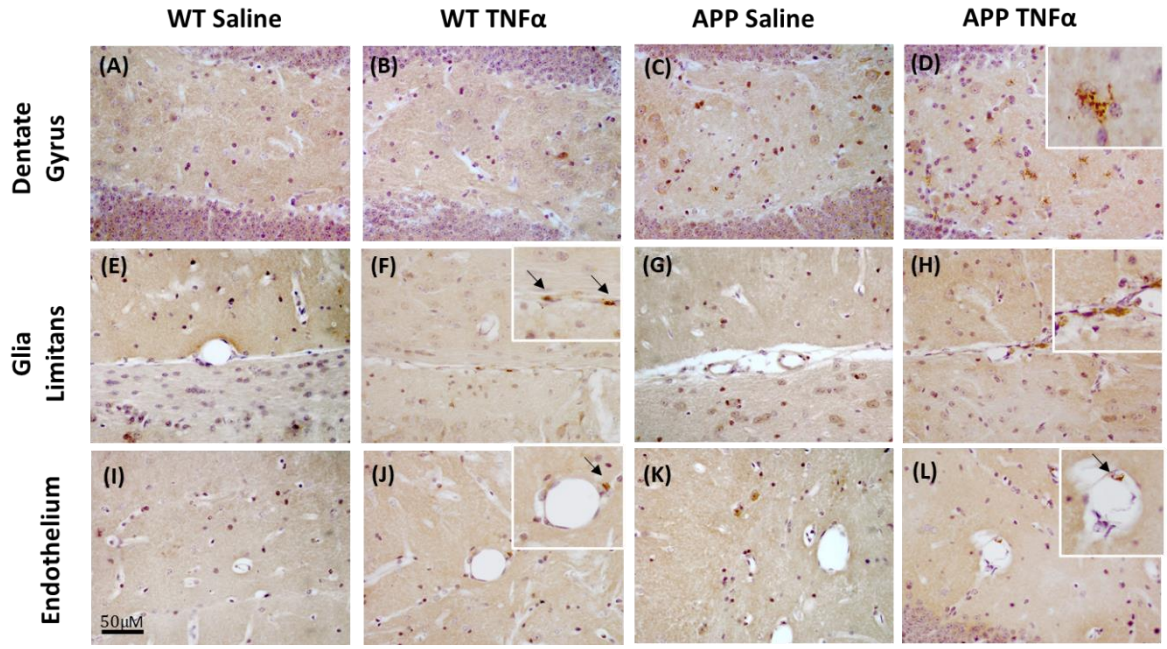

Figure 5.24 Immunohistochemical assessment of hippocampal CCL2 in APP/PS1 and WT animals ± TNFα – Assessment of wild type and APP/PS1 animals aged 23 ±3-month-old,, 2 hours post I.C., saline or TNFα (300ng). Macrophage chemoattractant protein CCL2 were immunolabelled in the (A-F) Dentate gyrus (E-H) glial limitans and (I-L) endothelial (40x, scale = 50µm).

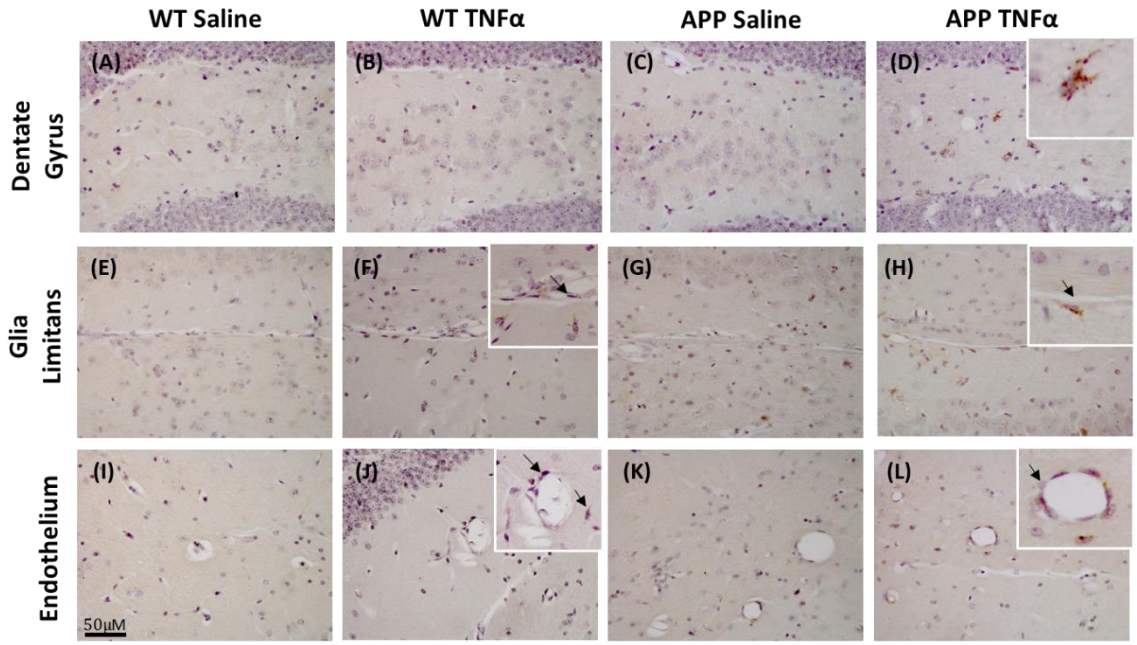

Figure 5.25 Immunohistochemical assessment of hippocampal CXCL10 in APP/PS1 and WT animals ± TNFα – Assessment of wild type and APP/PS1 animals aged 23 ±3-month-old,, 2 hours post I.C., saline or TNFα (300ng). Chemoattractant protein CXCL10 were immunolabelled in the (A-F) Dentate gyrus (E-H) glial limitans and (I-L) endothelial (40x, scale = 50µm).

Immunofluorescent double labelling for the examination of co-localisation of CCL2 with astrocytes and/or microglia was assessed in the dentate gyrus of 25-28-month-old APP/PS1 tissue **(Figure 5.26)**. Astrocytic GFAP (488nm – Green) and CCL2 (633nm – Red) were visualised with fluorescent antibodies and revealed clear colocalization of CCL2 with the astrocytic marker GFAP. Visualisation of microglial IBA1 (488nm – Green) and CCL2 (633nm – Red) in the same manner showed no clear co-localisation between the microglial cytoplasmic marker and the chemokine. While frequently visualised adjacent to the diffuse CCL2 clouds, the IBA1-positive microglia appeared distinct in most cases and this proximity appeared to be a result of the close contact between microglia and astrocytes, as seen in **Figure 5.21.** On the basis of the light and fluorescence images obtained here astrocytes appear to be predominantly responsible for the expression of CCL2 observed in the dentate gyrus of APP/PS1 animals challenged acutely with TNFα although the possibility that microglia do make some of these chemokines under the current conditions cannot be ruled out. What is clear is that astrocytes that are not making these chemokines at baseline in APP/PS1 mice begin to express them robustly upon TNFα challenge and this does not occur when WT animals are challenged with TNFα **(Figure 5.25 D)**.

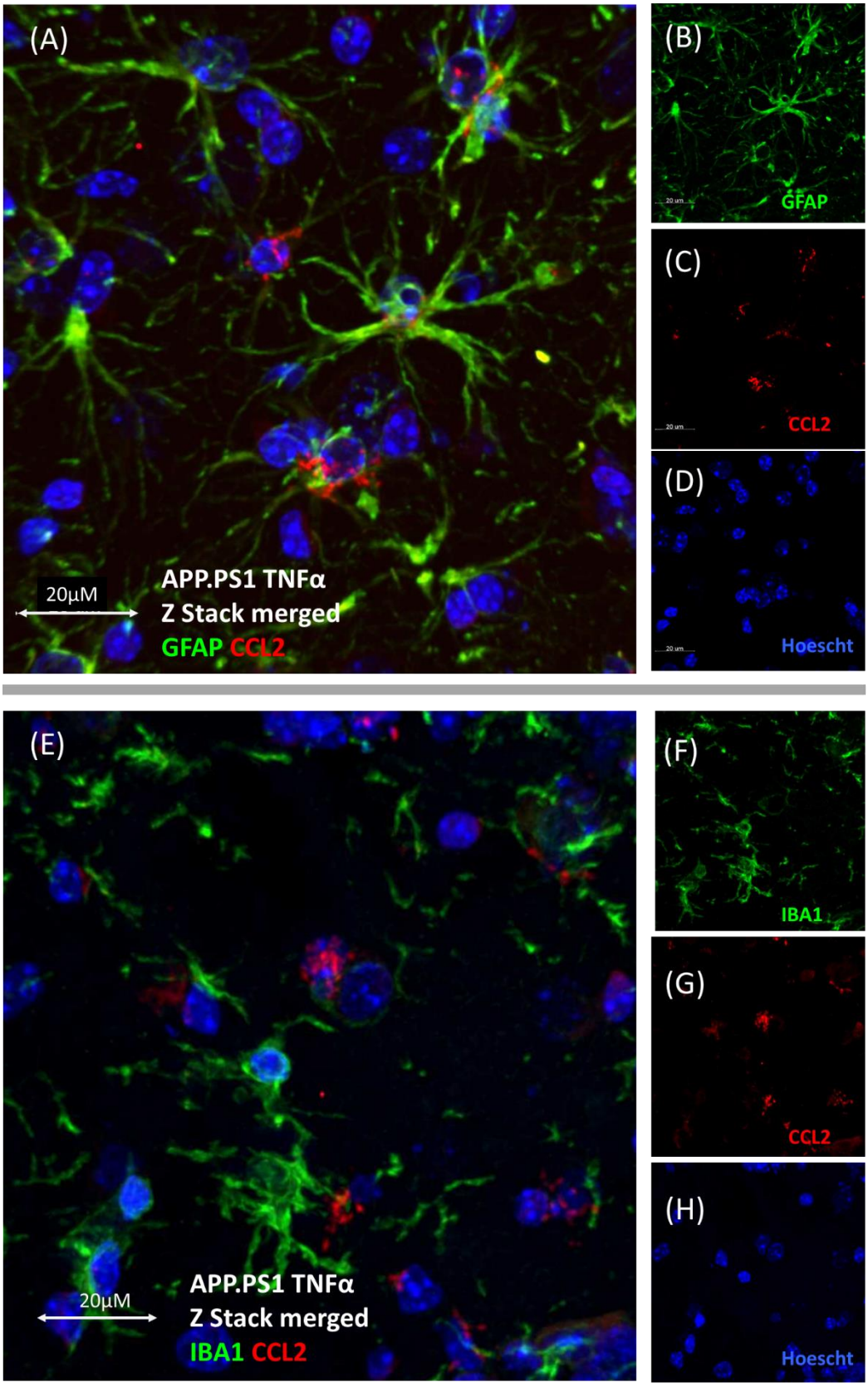

Figure 5.26 **Immunofluorescent colocalisation of glia and CCL2 – Hippocampal dentate gyrus of 28 month APP/PS1 animals, treated with TNFα (300ng) I.C., 2 hours post challenge. (A-D) fluorescent labelling of GFAP (488 nm) and CCL2 (633 nm) (E-H). Fluorescent labelling of IBA1 (488 nm) and CCL2 (633 nm).**

5.3 Discussion

Here APP/PS1 mice were shown to have significantly altered whole body metabolism, showing lower energy expenditure, body temperature and feeding. Acute challenge with TNFα brought about a shift in metabolism from predominantly carbohydrate usage to more fatty acid oxidation (FAO), with accompanying weight loss. Across 4 repeated TNFα challenges, this weight loss occurred in WT animals but APP/PS1 animals developed a tolerance to this weight loss. Sexual dimorphism became apparent in APP/PS1 mice with only females displaying cognitively impairment at 14 months and systemic challenge with TNFα lead to an exacerbation of MWM performance, only in females. Furthermore, the tolerization to TNFα-induced weight loss is only evident in female animals and was shown to be absent in APP/PS1 males. The X4 TNFα challenge regime also brought about many changes in astrocyte and microglial gene expression including upregulated cytokine and chemokine production. Finally, disease progression in APP/PS1 mice increased TNF receptor expression and left astrocytes 'primed' by prior amyloid pathology to produce exaggerated chemokine responses (CCL2 and CXCL10) to a direct intrahippocampal injection of TNFα.

5.3.1 Altered metabolism and frailty in the APP/PS1 genotype

As discussed in the previous chapters, frailty is an area of growing research in the fields of gerontology and is of particular interest in studying the occurrence and progression of age-associated morbidities such as dementia and neurodegeneration. Indeed, frailty has been shown to be positively associated with an increased risk of developing and worsening pathological conditions such as dementia (Searle et al. 2015). Here I have demonstrated using a novel 12-point cumulative deficit frailty index model that APP/PS1 animals exhibit a slightly, but significantly, higher degree of frailty compared to WT littermate controls. This is consistent with previous work in the 5XFAD mouse model of AD which has demonstrated that frailty is elevated and increases significantly with age in AD animals (Todorovic et al. 2020) as well as data from human studies showing that the prevalence of frailty within the Alzheimer's disease community was as high as 50% of the total population of five separate studies (Kojima et al. 2017). Furthermore, recent work by Reilly and colleagues in 5XFAD mice on a HFD, a known driver of frailty pathology as discussed earlier in this text, demonstrated a significantly exacerbated amyloid pathology, neuroinflammation and metabolic dysfunctions compared to WT/HFD control animals (Reilly et al. 2020). This is consistent with existing data from human studies highlighting that metabolic disorders such as diabetes conferred a 70% increased risk in the development of dementia of all types and a 60% increased likelihood of developing AD specifically (Gudala et al. 2013). As discussed previously, metabolic disruption is in turn one of the key drivers in ageing pathology and frailty.

Indeed, the disruption of homeostatic metabolic processes in the development and risk of Alzheimer's is a an area of growing research with recent meta-analyses highlighting the substantially increased risk of developing dementia associated with metabolic disorders such as diabetes mellitus (Gudala et al. 2013). In the APP/PS1 model of AD a hypermetabolic state was identified in the brains of APP/PS1 mice at 5-months of age and of these the hypothalamus was found to be the brain region most vulnerable to metabolic alterations (Zheng et al. 2018).

In keeping with these findings, I have demonstrated that APP/PS1 animals displayed higher adiposity of white adipose tissue as well as a more hypothermic core body temperatures compared to WT animals' indicative of altered metabolic homeostasis within the genotype. Further analysis of this using the Promethion metabolic cage system revealed that APP/PS1 animals showed robustly reduced activity and energy expenditure as well as lower food and water consumption during the dark cycle compared to WT control animals. Despite their increased frailty and altered metabolism, APP/PS1 animals showed equivalent acute sickness behaviour responses to WT animals during assessment of frailty status 24 hours after their first challenge with a 250μg/kg dose of TNFα or saline. Both APP and WT animals treated with TNFα displayed drastically reduced food and water consumption as well as lower activity levels and energy expenditure during their dark cycle. This anorexic reduction in food intake, in turn, correlated with commensurate reductions in RER, an indicator of fuel utilization, for both APP and WT animals challenged with TNFα; indicative of a TNFα-induced shift from carbohydrate metabolism toward fatty acid oxidation (FAO) to supply the bodies' energy. The ability to switch between carbohydrate and fat-metabolism is termed "metabolic flexibility" and is known to be impaired in type 2 diabetics and is believed to be one of the major risk factors in predisposing to insulin resistance (Ukropcova et al. 2007). Findings from recent human studies have shown that metabolic disorders like diabetes conferred increased risk of developing dementia (Gudala et al. 2013). Recent work in the APP/PS1 and 5XFAD AD models have demonstrated that high fat diet results in substantial increases in peripheral inflammation and alteration of metabolic processes in the 5XFAD model, cognitive impairment was exacerbated compared to animals on normal chow (Reilly et al. 2020; Fan et al. 2021). Consistent with the theory of AD being a CNS focussed variant of diabetes, a putative 'type 3 diabetes', several studies have reported impaired insulin resistance in several AD models (Macklin et al. 2017; Rodriguez-Rivera et al. 2011; Velazquez et al. 2017) and recent work in the APP/PS1 model demonstrated significantly elevated brain glucose levels, believed to be as a result of the development of amyloid pathology causing a reduction in glucose utilization and decreases in energy and NT metabolism (Zhou et al. 2018). Human studies have also demonstrated a reduction in glucose metabolism in AD patients which is positively correlated with the severity of the AD symptoms (Politis et al. 2012; Dukart et al. 2013). Recently it was shown that age-associated hyperinsulinemia in the serum is reflected in the

CSF and can result in neuronal insulin resistance, impairing glycolysis and inducing cell-cycle senescence (Chow et al. 2019). The putative neuroprotective drug S14g-humanin, a humanin (mitochondrial micropeptide) analogue generated by the replacement of Ser14 with glycine (Li et al. 2013), has been shown to alleviate the insulin resistance in the APP/PS1 model, improving learning ability and memory, through decreasing IRS- Ser636 phosphorylation and mTOR protein expression (Gao et al. 2017; Han et al. 2018). Recently, the AD anticholinesterase Donepzil has been shown to not only ameliorate spatial learning and memory deficits but also to enhance glucose metabolism in the hippocampus of APP/PS1 mice and alleviate mitochondrial dysfunction (Cao et al. 2017; Ye et al. 2015). Recent work at the synaptic level investigating mitochondrial function in APP/PS1 mice has highlighted that synaptic mitochondrial dysfunction is significantly associated with the degree of cognitive impairment in AD (Manczak et al. 2006; Dragicevic et al. 2010). Furthermore, inhibition of the mitochondrial respiratory chain complex 1 in APP/PS1 female specifically has been shown to result in neuroprotective outcomes on immune response, neurotransmission and cognition (Stojakovic et al. 2021). Consistent with the use of the anticholinesterase Donepzil as a palliative AD treatment, one of the strongest known AD risk factors, particularly in females is apolipoprotein E4 (APOE4) expression, a cholesterol carrying protein, responsible for participating in cholesterol homeostasis (Lambert et al. 2009; Harold et al. 2009; Corder et al. 1993). More recently it has been shown that ApoE4 is capable of impairing cerebral insulin signalling by trapping insulin receptor within endosomes, thereby reducing the number of insulin-insulin receptor interactions (Zhao et al. 2017). Previous studies have shown that a depletion of fats, primarily cholesterol, results in substantial impairment of synaptic vesicle exocytosis neuronal activity, neurotransmission and synapse degeneration (Linetti et al. 2010; Liu et al. 2010; Liu et al. 2007). Consistent with this, significant reductions in brain cholesterol levels have been shown in the APP/PS1 model (Fan et al. 2021) as well as in a recent metabolomic and transcriptomic study in AD patients (Varma et al. 2021). While this suggests that perhaps this depletion of brain cholesterol levels may be a causative factor for AD pathology it is also known that Aβ generation, aggregation and subsequent neurotoxicity are profoundly affected by cholesterol since it is the primary component of the lipid rafts in which APP, β-secretase and γ-secretase are found (Geifman et al. 2017). As such, statins, which are used to lower blood cholesterol levels, have been proposed as a potential prophylactic treatment for AD (Zissimopoulos et al. 2017; Poly et al. 2020). Recent meta-analysis studies has reported that the use of statins is significantly associated with an overall decreased risk of dementia (Poly et al. 2020) with the exception of individuals with pre-existing behavioural disorders (Cham et al. 2016; Wagstaff et al. 2003). Taken together these data highlight the substantial association between metabolic dysfunction and AD incidence as well as the risk factor it presents to pathology and cognitive dysfunction in turn.

Intriguingly, a growing body of research stresses the more advanced and severe pathology in female APP/PS1 animals (Jiao et al. 2016; C. Zhou et al. 2018; Li et al. 2016). Unfortunately the study was underpowered to assess the impact of sex in the APP/PS1 animal's frailty in any meaningful way here, but recent work in the 5X FAD model has reported significant sexual dimorphism in frailty prevalence and severity (Todorovic et al. 2020). Here, I have shown evidence of a resistance to acute weight loss in response to chronic systemic TNFα challenge which was not observed in WT and male APP/PS1 animals. Whether this is a tolerising effect conferred by their genotype or a delineation between TNF-induced anorexia/cachexia is unclear at this time. Anorexia might be defined as an eating disorder characterized by a restricted caloric intake resulting in severe weight loss and typically a result of a loss of appetite or an aversion to food (Kaye et al. 2009; Dobrescu et al. 2020). As discussed previously in this text sarcopenia is closely associated with age and related comorbidities (Cruz-Jentoft et al. 2010), while it shares many similar traits with cachexia, i.e. a loss of muscle tone often associated with inflammatory status and age, cachexia may be distinguished from sarcopenia, by the presence of an underlying chronic disease and anorexic-like behaviour (Muscaritoli et al. 2010). Indeed TNFα, also known as Cachexin, was originally discovered in 1985 and named for its role in cachexia (Beutler et al. 1985) and it has been extensively studied in this context. Previous studies using chronic TNFα (200μg/kg) treatment every four days five times in rats demonstrated a robust weight loss (Memon et al. 2002) while other rat studies demonstrated tachyphylaxis effect (i.e. a loss of tissue responsiveness to repeated or continuous administration of a drug (Lieb et al. 1984) with shorter times between each challenges tolerance developed and the anorectic effect diminished (4mg/kg daily (Kettelhut et al. 1988). At a lower the dose, with shorter recovery times, the recovery to normal food intake levels was more rapid (100μg/kg/twice daily (Fraker et al. 1988). Further work by Fraker and colleagues has demonstrated that this tolerance does not develop if TNFα administration is too regular as they demonstrated by continuous infusion (Fraker et al. 1990). Similarly, in nude mice implanted with Chinese hamster ovary cells transfected with the human TNF gene (Oliff et al. 1987) the resulting continuous production of TNFα induced a profound cachectic state from which the rodent never recovers. Together these data tell us that the timing and dosage of TNF used can elicit very different effects. Consistent with the pattern of weight loss observed in the WT animals in this study, work by Cope and colleagues, demonstrated that TNFα at 250μg/kg, every 48 hours for three weeks, showed consistent and persistent TNF-induced weight loss (Cope et al. 1997). At the regional level TNFα has been previously shown to affect the hypothalamus by causing an increase in leptin release and inducing lipolysis of adipose tissue (Kim et al. 2015) which should in turn result in a decrease in appetite, reduction in energy expenditure and over time, a loss of body weight. Here, all animals challenged with TNFα for the first time did indeed demonstrate a reduction in their cumulative food intake as well as a reduction in energy expenditure, switch to FAO and, in most cases, weight loss.

However, it was clearly observed that this weight loss effect gradually diminished in female APP/PS1 mice. Therefore, TNFα induced an initial anorexic response (decreased food intake), which may be indicative of TNF-induced lipolysis arising from effects of TNFα on the hypothalamus, but the APP/PS1 female mice show diminished responsiveness to subsequent challenges.

One potential implication for this may be that differential metabolic and sickness behavioural responses to acute inflammation, are adaptive and a failure to maintain them can prove detrimental. Wang et al. has demonstrated that anorexia is protective in the LPS bacterial sepsis model while nutritional supplementation, specifically glucose, is protective against mortality from the viral, Poly I:C, sepsis. This "feed a cold, starve a fever" duality observed in the two models of sepsis demonstrates there are highly specific metabolic requirements linked to the cellular stress adaptations critical to their tolerance of a specific inflammatory event (Wang et al. 2016). The current data suggest that while all animals show an equivalent initial TNFα-induced anorexic response (decreased food intake, loss of body weight) as well as a shift towards more fatty acid oxidation (demonstrated using the Promethion metabolic cage system), female APP/PS1 mice have lower body weights than WT controls initially and cannot maintain this weight loss change upon repeated challenges. This lower starting body weight may well be a result of lower adiposity of APP/PS1 females compared to WTs and in turn may contribute to the apparent limit of their ability to employ fatty acid oxidation for an extended period of time. Given the association between increased insulin resistance and reduced glucose metabolism and cognitive deficit in AD (Politis et al. 2012; Dukart et al. 2013; Q. Zhou et al. 2018), this further impairment of metabolism could in turn have detrimental effects on brain metabolism, inflammation and reactive oxygen species production (Wang et al. 2016).

However, APP/PS1 animals here exhibited greater adiposity in white fat deposits compared to WT controls. While the study was underpowered to assess differences in adiposity between sexes these 14±2-month old female animals should have experienced a post-menopausal alteration in muscle composition as lipoprotein lipase (LPL) function is impaired due to estrogen loss resulting in increased adiposity and reduced insulin sensitivity (Maltais et al. 2009). Therefore, an alternative explanation for the lower body weight of APP/PS1 female mice may not be a result of reduced adiposity but rather a result of a cachexic loss of lean muscle mass. Unintentional weight loss is known to be a key marker and predictor of AD and the degree of sarcopenic loss of lean muscle mass has been shown to correlate with the degree of cognitive impairment (Emmerzaal et al. 2015; Burfeind et al. 2016; Lin et al. 2019). APP/PS1 females have been shown to have significantly more advanced pathology, associated with greater proinflammatory cytokine levels (Jiao et al. 2016; Richetin et al. 2017; Wang et al. 2003) and I have demonstrated here female APP/PS1 mice are significantly lighter than WTs and APP/PS1 animals generally show reduced food intake compared

to WT controls. These conditions fit the criterion for cachexia, a loss of muscle tone associated with the presence of an underlying chronic disease (AD pathology) and anorexic-like behaviour (Muscaritoli et al. 2010). This suggests that APP/PS1 mice may be suffering a cachexic loss of muscle tone which is more progressed in the females due to the earlier manifestation of their disease. This may imply that subsequent TNFα challenges are eliciting weight loss are contributed to by cachexic responses (loss of muscle mass) which affect the male WT and APP/PS1 male mice equivalently due to the less advanced pathology of APP/PS1 males. It is unclear currently whether the wasting effect observed in AD is a prodromal symptom of dementia or whether it manifests during the intermediate stages of the disease with its associated elevated inflammation driving the normal age-associated sarcopenia to cachexia in the late stages of disease. However, these data would also suggest this apparent resistance to weight loss demonstrated by APP/PS1 animals is unlikely to be a tolerising, protective response conferred by the genotype.

To further assess this, serological expression of pro-inflammatory cytokines associated with cachexia, IL-6 and TNFα could be assessed to determine if APP/PS1 females are more at risk of cachexia compared to WT and male APP/PS1 animals at this more advanced age. Furthermore, metabolic changes in RER and food intake in response to the repeated second, third and fourth TNFα challenges should be assessed in an appropriately powered, sex balanced, population using the Promethion metabolic cage system. In theory if this is indeed a case of tachyphylaxis, tolerization to the repeated TNFα challenge, and not cachexia then APP/PS1 female food intake, energy expenditure and RER could also show diminishing deficits to TNFα challenge concurrent with those observed here for weight loss. Ultimately the most efficient assessment of this would be to assess the muscle tissue itself and to this end the Tibialis Anterior muscle was taken and flash frozen for OCT embedding at time of euthanisation for analysis by immunohistochemistry. Muscle tissue could be stained for cachexia-related factors such as IL-6, TNFα, proteolysis-inducing factor (PIF), zinc-α2-glycoprotein (ZAG) (Kamoshida et al. 2007) or assessed for its integrity looking at muscle cross-sectional area, fibre typing, localization of nuclei within the muscle fibre, the number of vessels, and fibre-associated stem cells could all be investigated to assess muscle physiology with markers such as Laminin, paired box protein (Pax7) or fibre types I -II A/B (Mayeuf-Louchart et al. 2018). APP/PS1 and WT animals could be assessed at baseline and after repeated TNFα challenge to ascertain whether female animals have suffered a cachexic loss of lean muscle due to their more advanced pathology and whether the recurrent systemic challenge drives cachexia further.

With the estimated populations of AD patients set to reach 1 152 million by the year 2050 (World Health Organization; 2020) there is a substantial need to better understand the complex etiologies driving its manifestation and progression. Taken together these data suggest that Alzheimer's disease pathology is associated with a significant perturbation of metabolic systems in the ageing-

vulnerable brain with significant cross talk between the cholesterol and glucose systems (Gamba et al. 2019) and potential therapeutic targets for both systems being investigated currently. The crosstalk between cholesterol dysmetabolism and insulin resistance has been shown to be bidirectional with dysfunction in either system capable of impairing the other (Suzuki et al. 2010), but the exact mechanism of interplay between the two in the context of AD remains to be elucidated and must be an area of focus going forward. Furthermore, there is a growing body of evidence highlighting the crucial role which sex plays in driving AD pathology, however the exact mechanisms by which this is achieved remain to be elucidated. New research should not only focus on the biological sex, but also focus on factors such as frailty, hormones, x linked mutations etc. which might contribute to the disparity observed in male and female populations. It is important to understand the interaction between sex and other risk factors of AD such as genetic and environmental factors.

5.3.2 Female APP/PS1 mice show increased vulnerability to impaired cognitive function and vulnerability to deficit following chronic TNFα administration

Increasing evidence emphasises differences in Alzheimer's disease pathology progression and severity between sexes for humans and in mouse models of AD, notably the APP/PS1 model. In humans, incidence and prevalence of AD are generally higher in women and although this is contested and argued to be a result of their longer life expectancy, longitudinal studies have shown that they do exhibit a faster cognitive decline, greater amyloid pathology and brain atrophy than men (Ferretti et al. 2018; Podcasy et al. 2016; Marongiu 2019; Wallace et al. 2019). This more aggressive pathology is also consistent with the higher prevalence and severity of frailty in women compared to males (Ott et al. 1998; Mitnitski et al. 2005; Song et al. 2010; Collard et al. 2012) and the significant risk factor this poses to the development and exacerbation of cognitive disorders (Borges et al. 2019; Kojima et al. 2017), especially Alzheimer's (Vest et al. 2013; Oveisgharan et al. 2018; Wallace et al. 2019). Indeed a comprehensive meta-analysis of 13 population studies has reported that two thirds of all AD cases are female (Laws et al. 2016). Consistent with this, the APP/PS1 mouse model showed significantly higher Aβ40 and Aβ42 in 12 and 17-month-old female mice compared to age matched litter mate males; this difference was absent in young 4-month-old male and females. Concurrently, amyloid plaque burden was substantially higher in females at 12 and 17 months compared to males of equivalent ages (Wang et al. 2003). This more advanced plaque pathology corresponds with increased cognitive impairments, reduced hippocampal neurogenesis (Jiao et al. 2016; Richetin et al. 2017) at 12 and 10 months of age respectively as well as reduced white matter integrity at 10 months old (C. Zhou et al. 2018) compared to male littermate controls. Contrary to this however, recent work in the 5XFAD model of AD has shown that female mice are less frail than male littermates (Todorovic et al. 2020).

Consistent with this pre-existing literature I have demonstrated that APP/PS1 female mice display worse cognitive performance across multiple measures of cognition. At baseline APP/PS1 female mice displayed a reduced ability to learn the shallow water visuospatial Y-maze task compared to male APP/PS1 animals. Furthermore, after repeated administration of saline/TNFα (250µg/kg), female APP/PS1 mice showed impaired freezing behaviour in response to contextual and auditory cued fear conditioning paradigms regardless of treatment. Although there were not significant differences in the ability of male and female APP/PS1 mice to learn the location of the hidden platform in the Morris water maze task female APP/PS1 mice showed an increased vulnerability to impaired learning when challenged sequentially with 4 x 250µg/kg TNFα. This finding resonates with studies showing that elevated baseline TNFα is associated with a reduction in hippocampal volume (Sudheimer D. et al. 2014), progression of mild cognitive impairment to AD (Tarkowski et al. 2003) and more rapid cognitive decline in AD patients (Holmes et al. 2009). Nonetheless the sex-dependent differences observed here suggest that cognitive impairments may have been more obvious had larger numbers of female animals been included. In this regard it is significant that performance on the probe trial revealed a difference in memory of the prior location of the platform in female APP animals only.

While our data has demonstrated no significant difference in cognitive function between saline challenged female APP/PS1 mice compared to male APP/PS1 performance in the MWM task, other studies have previously reported significant cognitive impairment in MWM performance at baseline between male and female APP/PS1 mice earlier in disease pathology at 6 and 9 months of age (Li et al. 2016). Another study assessing 9-month old APP/PS1 animals revealed a deficit in female APP/PS1 mice during the reversal phase of learning in the MWM which was associated with their accumulated Aβ levels, IL-1β expression and microglial activation (Gallagher et al. 2012). Mifflin and colleagues reported significantly worse performance in the MWM task in similarly aged, 12-month old female APP/PS1 animals assessed as latency to locating the platform, however, a closer look at their data revealed that male APP/PS1 animals performed better than WT animals as well as APP/PS1 females suggesting that female APP/PS1 cognition is not truly worse than WT animals for any pathological reason and this report is misleading (Mifflin et al. 2021).

It is hypothesised that the disparity between estrogen levels in the sexes and especially the dramatic change which follows menopause may account for some of these differences. Estrogen has been shown to be involved in cognitive functioning through a series of complex signalling pathways including estrogen-regulated synapse formation and turnover (Hara et al. 2015). Furthermore, in humans it has been shown that estrogen will promote neurotrophin synthesis (Milne et al. 2015), modulate the cholinergic and dopaminergic neurotransmitter systems (Mennenga et al. 2015; Sinclair et al. 2014) as well as protect the brain against stress and

inflammation (Luine 2016). Use of surgical menopause models by ovariectomy has been shown to confer an increased risk of cognitive impairment and dementia in mice (Rocca et al. 2007) as well as a 50% increase in mortality compared to sham-ovariectomy transgenic controls showed no significant change in Aβ40 and Aβ42 levels in APP/PS1 females (Levin-Allerhand et al. 2002). Studies of estrogen treatment have been shown to enhance learning and memory and while the impact of estrogen-containing hormone therapies have shown mixed outcomes in human studies they have also been shown to have generally positive outcomes (Galea et al. 2017; Luine 2014). Interestingly, treatment with 17α-estradiol in ovariectomised mice resulted in decreased levels of Aβ40 and Aβ42 but not plaque burden 6 weeks after surgery (Lominska et al. 2002). These data suggest that hormonal replacement therapy may be a viable prophylactic treatment to delay and slow AD disease onset.

5.3.3 Microglial and astrocyte transcriptional changes in the APP/PS1 brain

Numerous studies in recent years have shown that microglial and astrocyte populations are activated by neurodegenerative disease and have performed in-depth detailed phenotypic analysis of their transcript expression (Holtman et al. 2015; Liddelow et al. 2017; Keren-Shaul et al. 2017; Mrdjen et al. 2018). Although these changes are important in their own right, indeed many may be contributing to the progression of disease, but in the context of the current study it was important to assess how these glial profiles change under chronic repeated systemic inflammatory events, as AD patients are notoriously vulnerable to chronic urinary tract infections and pneumonia (Zonsius et al. 2020; Brown et al. 2011). As discussed earlier, the hippocampus has a major role in learning and memory and is known to be particularly vulnerable to damage in AD (Braak et al. 1993; Anand et al. 2012). As such, I utilised a repeated i.p. TNFα challenge to mimic a recurrent systemic infection to study how this affects glial activation and immune profiles in the hippocampus of APP/PS1 animals. Given the mounting body of evidence pointing to metabolic dysfunction's role in the AD phenotype and my own data investigating the contribution of metabolic deficits to frailty severity and the hypothalamus' role in this

TNFα is a member of the TNF super family which exerts pro-inflammatory actions via stimulation of nuclear factor kappa B (NF-κB) and activating protein-1 (AP-1) (Oeckinghaus et al. 2009; Leong et al. 2000). TNFα is a crucial proinflammatory cytokine in stimulating acute inflammatory responses contributing to resistance to infections and cancers (Vilcek et al. 1991). This can be mediated by activation of neutrophils and platelets, enhancement of macrophage/Natural killer cell potential and stimulation of the immune system (Fiers 1991). TNFα KO animals have been shown to fail to form germinal centres in their spleen (Goldfeld et al. 1996) and similarly, have an increased susceptibility to microbial infection and a suppressed inflammatory response to bacterial endotoxins (Acton et al. 1996; Steinshamn et al. 1996). However, while TNFα's transient presence

may be neuroprotective in dealing with acute inflammatory events, elevated baseline TNFα has been shown to be associated with a reduction in hippocampal volume (Sudheimer D. et al. 2014), a progression from mild cognitive impairment to AD (Tarkowski et al. 2003) and, whether in the presence or absence of acute inflammatory episodes, confers a greater rate of decline over 6 months in AD patients (Holmes et al. 2009). Etanercept, a TNFα blocking antibody, showed borderline effects on cognitive status in AD patients (Holmes et al. 2014); Butchart et al, 2015) and large medical insurance data sets and in-house Pfizer studies indicated that long-term use of etanercept very significantly reduced the risk of AD (Chou et al. 2016; Rowland 2019). Those data have been interpreted by many in the context of TNFα changes in the brain and access of these blocking antibodies to the brain. However, the data presented here show that repeated systemic TNFα challenge brings about significant changes in astrocyte and microglial phenotypes.

Consistent with this, I have demonstrated that isolated microglial cells from the hippocampus of APP/PS1 animals exhibited a significant upregulation of transcripts associated with their primed phenotype, *Cd11c, Il1b,* and microglial activation *, Trem2, C3, Stat3, Ctss,* and reduced neurogenic marker *Hes5*. Furthermore, in APP/PS1 animals challenged repeatedly with 250µg/kg of TNFα I have demonstrated an exaggerated *Tnfa* and *Ccl4* transcript expression which was absent in WT and saline controls. Interestingly this elevation of proinflammatory cytokines and chemokines has persisted 6 days after the fourth and final TNFα challenge suggesting a robust enduring pathological effect of the repeated TNFα i.p. challenge upon the microglial profile. In the clinical setting it is believed that underlying chronic morbidity, such as the AD pathology here, will prime the microglia and upon exposure to a new trauma, such as our TNFα, will result in an exaggerated, flooding release of pro-inflammatory cytokines and other microglial neurotoxic substances elicited under acute inflammatory conditions such as nitric oxide, oxygen radicals and proteolytic enzymes. These in turn will cause further damage to the vulnerable brain, exacerbating neuronal damage and the loss of neurons in vulnerable brains in multiple rodent models of neurodegenerative disorders such as MS, TBI, AD, and white matter injury (Perry et al. 2010; Norden et al. 2015) contributing to cognitive decline (Holmes et al. 2009). Indeed, in the ME7 model of prion disease our group has demonstrated that an acute systemic 250µg/kg dose of TNFα is sufficient to induce nuclear translocation of NF-κB in astrocytes, exaggerated chemokine and cell infiltration as well as deficits in cognition and exacerbated sickness behaviour and (Hennessy et al. 2017; Hennessy et al. 2015). Recent work by our group has demonstrated that in APP/PS1 mice neuronal and cognitive dysfunction are driven these hypersensitive inflammatory responses from both primed microglia and the newly described primed astrocytes (Lopez-Rodriguez et al. 2021).

In keeping with this I have shown that astrocytes isolated from APP/PS1 animals revealed a similar profile of activation with AD pathology as evidenced by robust upregulation of *Gfap, Irf7, Stat3* and

Tnfr along with downregulation of the neurogenic *Hes5*. Interestingly the robustly upregulated *Tnfr* on APP/PS1 astrocytic cells suggests there may be an increased astrocytic sensitivity to a TNFα challenge. Indeed, as was observed in microglial isolates, APP/PS1 astrocytes challenged repeatedly with i.p. TNFα 250μg/kg showed upregulated gene expression for markers of astrocytosis (Liddelow et al. 2017; Lopez-Rodriguez et al. 2021), including *Gbp2, Ptx3, Cst7* and *Tgm1* as well as elevated chemokine expression, *Ccl3* and *Ccl4*. As was observed with microglial isolates these changes were found to be persisting 6 days after the fourth and final TNFα challenge in APP/PS1 animals. Additionally, there was a significant elevation of astrocytic *Il1r* in APP/PS1 animals challenged with TNFα suggesting a resulting increased sensitivity to the elevated *Il1b* expressed in APP/PS1 microglial cells which our group has previously shown is sufficient to cause significant cognitive deficits (Lopez-Rodriguez et al. 2021).

In addition to these findings of exaggerated proinflammatory responses and priming phenotype in APP/PS1 animals subjected to chronic TNFα, I have also demonstrated evidence for this glial priming phenotype and morphology by immunohistochemistry in 21±3-month APP/PS1 male animals acutely challenged intrahippocampally with a 300ng dose of TNFα or saline. APP/PS1 animals display aggressive glial morphology indicative of gliosis for both astrocytes and microglia as assessed by immunohistochemical staining for GFAP and IBA1 labelling. This activated morphology was found to be unaffected by treatment with TNFα. Furthermore, assessment of chemokine production at the site of TNFα challenge in APP/PS1 animals revealed expression of CCL2 and CXCL10 that was absent in saline and WT animals challenged with TNFα, indicative of the exaggerated priming response. Immunofluorescent co-localisation of CCL2 with glial cells revealed a strong co-localisation of $CCL2^{+}$ labelling with astrocytic cells labelled for their intermediate filament protein, GFAP, indicative that astrocytes are the primary source of this CCL2 production in the TNFα challenged dentate gyrus of APP/PS1 animals. This is consistent with previous work which has demonstrated while astrocytosis was evident at all times in disease models it was only upon exposure to a secondary inflammatory challenge that NFκB was translocated to the nucleus (Hennessy et al. 2015; Lopez-Rodriguez et al. 2021), consistent with the reported A1 phenotype (Liddelow et al. 2017). Microglia have been shown to be the most rapid responders to acute injuries migrating toward them (Nimmerjahn et al. 2005) while astrocytes remain largely static, instead altering their morphology and proliferating in response (Burda et al. 2014). Work by Holm and colleagues has demonstrated that microglia are imperative to astrocytic responses to acute challenge, demonstrating that astrocytic response to TLR2-4 agonists is significantly less efficient in the absence of microglia (Holm et al. 2012). This in turn is consistent with data from our own group, demonstrating that a central challenge of LPS is capable of triggering rapid microglial production of IL-1β but that direct application IL-1β and TNFα will cause NFκB to be translocated to the nucleus

and a robust ensuing production of chemokines (Hennessy et al. 2015; Lopez-Rodriguez et al. 2021). In keeping with these findings, I have shown a strong co-localisation of CCL2 with activated astrocytic cells, with activated microglial cells also in close proximity, consistent with their rapid, motile response to stimuli and role in the activation of astrocytes. Hennessy et al. also demonstrated that this TNFα-induced exaggerated CCL2 facilitates significant monocyte infiltration into the degenerating ME7 model brain and may have significant deleterious consequences (Hennessy et al. 2015). In keeping with the theory that the exaggerated inflammatory response associated with the priming phenotype is ultimately harmful to an appropriate resolution of the immune response, i*n vitro* work using TNFα or HIV infection to prime astrocytes resulted in an enhanced interaction and infection rate between *Trypansomoa Cruzi* infection and astrocytic cells (Silva et al. 2017; Urquiza et al. 2020). Perhaps the best studied example of the detrimental consequences of robust chemokine expression inflammatory cell infiltration to the brain comes from the study of multiple sclerosis (MS). As with chronic inflammatory diseases microglia are primed in the CNS in MS (Ramaglia et al. 2012) and the condition is characterized by a resulting leukocyte infiltration into the CNS, resulting in axonal damage, demyelinating inflammation and the formation of sclerosing plaques within the brain (Cui et al. 2020; Zhang et al. 2018; Kurschus 2015). However, inflammation is not an inherently detrimental process and it is possible that neuroinflammation serves a beneficial purpose to some degree. Nude mice lacking T and B cells have previously been reported to exhibit impaired neurogenesis (Ziv et al. 2006). Similarly, the formation of adult hippocampal neurons from neural progenitor cells has been reported to occur through toll-like receptor (TLR)-2 signalling, conversely, TLR-4 signalling may retard neurogenesis (Rolls et al. 2007). Neuroinflammation has also been reported to facilitate axonal regeneration in spinal cord injury models injected with activated macrophages (Prewitt et al. 1997). In the EAE model of MS depletion of monocytes after injury or *Il-1-/- Tnfa-/-* mice have been shown to exhibit significantly reduced remyelination (Mason et al. 2001; Arnett et al. 2001; Kotter et al. 2001). Taken together these data suggest that during the early disease states elevated systemic TNFα may drive neuroinflammation in an attempt to resolve the infection or injury and promote CNS repair, however it is likely that chronic exposure to becomes detrimental and drives cognitive decline and neurodegeneration.

The neuroinflammatory hypothesis of Alzheimer's disease was originally proposed more than 30 years ago with the glial cells, microglia and astrocytes, heavily implicated in the pathogenesis of the disease. While microglia as the resident immune cell population have been shown to be both beneficial and adversely activated at various stages, the contribution of astrocytes remains to be fully elucidated. As discussed earlier in this text, the astrocytes have significant impact upon neuronal homeostasis and longevity due to their homeostatic role in the CNS offering trophic

support to neurons and so one theory proposes that the astrocytes contribution to the cortical atrophy associated with this disease may be a result of the loss of this supportive function. Initial forays into classification of astrocytes as neurotoxic/neuroprotective or A1/A2 (Liddelow et al. 2017) has been met with substantial debate and been argued to be overly simplistic and that more robust assessment of molecular and functional parameters to determine the impact of reactive astrocytes on pathology is required when studying astrocytosis in disease .

Alternatively, it has been suggested that astrocytes gain neurotoxic functions resulting from their activation in the chronic diseased brain and thus more directly impact neuronal health and cognition. In reality, a combination of the two is the most likely explanation as recent attempts to characterise reactive astrocytes in disease pathology have shown the loss of normal functions alongside the gain of new abnormal ones that may contribute to pathology (Verkhratsky et al. 2018). Indeed, characterisation of reactive astrocytes *in vitro* as the A1 activated phenotype induced by reactive microglia under pathological conditions is associated with a significant enrichment of proinflammatory-associated genes and secretion of a weak neurotoxin, that induces neuronal and oligodendrocyte death, as well as a suppression of homeostatic genes such as *Sparcl1 and Gpc6* (Liddelow et al. 2017). Consistent with this Hasel and colleagues has demonstrated that astrocytes in close proximity to neurons will express *Hes5* and *Hey2* but upon the loss of these neurons under chronic degeneration (Hasel et al. 2017), astrocytes will downregulate genes such as these which are associated with neuronal support, as I demonstrated in our astrocytic cell isolates also. Recently, our lab has demonstrated *in vivo* evidence that astrocytes proximal to A-plaques in the APP/PS1 model are primed to produce exaggerated chemokine responses as well as significant vulnerability to exaggerate changes in expression of astrocytosis-associated genes following a secondary central challenge (Lopez-Rodriguez et al. 2021). However, it has been also been shown that attenuation of astrocytic activation through deletion of *Gfap* and *Vimentin* fails to ameliorate the AD phenotype and rather sees a significant acceleration of plaque pathology in APP/PS1 animals (Kraft et al. 2013). Similar to microglial activation, this suggests that astrocytes may be beneficially or adversely activated at various stages of disease pathology and further work is needed to identify time points at which intervention may be helpful to managing pathology.

Furthermore, there is mounting evidence pointing to the role which sex-linked chromosomes have in the heterogeneity of AD prevalence. Many genes associated with the immune process are located on the x chromosome (Libert et al. 2010) and females have been shown to demonstrate a greater diversity in immune responses due to random or incomplete X chromosome inactivation (Spolarics et al. 2017). Additionally, premature centromere division, a genetic mechanism known to be closely associated with aneuploidy (the absence of or presence of extra chromosomes), is known to be substantially elevated in older women compared to younger (Russell et al. 2007), with a significantly

greater rate specifically in the neural cells of the hippocampus and cerebrum of AD patients compared to age-matched non-demented controls (Spremo-Potparević et al. 2008; Yurov et al. 2014). Consistent with this it has recently been shown that microglia exhibit distinct metabolic profiles in sexual dimorphism in AD. Female APP/PS1 microglia were found to be morphologically and functionally distinct from males with a more glycolytic, less phagocytic profile which preferentially upregulated markers of microglial activation compared to male APP/PS1 mice (Guillot-Sestier et al. 2021).

Here, microglia and astrocytes were isolated from the hippocampus and the overlying cortex for its role in learning and memory, rich plaque pathology and vulnerability to damage in AD (Braak et al. 1993; Anand et al. 2012). However, given this mounting body of evidence pointing to metabolic dysfunction's role in the AD phenotype and in APP animals specifically where a hypermetabolic state has been identified with the hypothalamus found to be particularly vulnerable to metabolic alterations (Zheng et al. 2018), as well as the data presented here investigating the contribution of metabolic deficits to frailty severity and the hypothalamus' role in this it would have been ideal to isolate and assess transcriptomic changes in the hypothalamic microglia. As discussed earlier, the microglia of the ageing brain show regionally heterogenous vulnerability to ageing associated transcriptomic changes (Grabert et al. 2016; Hart et al. 2012; Tan et al. 2020) and the hypothalamus has been reported to be particularly vulnerable to these ageing changes (Zheng et al. 2018; Suda et al. 2021; Yan et al. 2014). Unfortunately, successfully isolating sufficient glial numbers from a structure as small as the murine hypothalamus in order to do accurate qPCR analysis was not possible at the time and so the hippocampus and its overlying cortex were used for this study. Given the data and studies discussed above and the recent work by Guillot-Sestier demonstrating distinct metabolic profiles in microglia (Guillot-Sestier et al. 2021), future studies should undoubtedly assess the differences in APP/PS1 hypothalamic microglia's transcriptomic signatures compared to WT controls.

Taken together, these data indicate that Alzheimer's disease incidence confers an increased frailty burden upon individuals. Its progression may in turn be influenced by systemic inflammatory events which will accelerate or worsen the pathology acutely, but which can also have significant long-term negative effects, both centrally and peripherally, worsening the individual's long-term recovery and progression long after the systemic event has passed. Within this, it is clear sex plays an important role which must be considered and assessed as rigorously as possible to elucidate the molecular underpinnings behind these events both when using animal models and in human studies.

Chapter 6:

Discussion

6.1 Brief Summary of results

In the field of geriatric medicine it has become increasingly clear that ageing is not a uniform process with individuals with higher frailty due to poor biological ageing, being at increased risk of long-term negative outcomes (Shamliyan et al. 2013; Mitnitski et al. 2015; Song et al. 2010). As such there is a growing need for accurate frailty indices to capture the underlying mechanisms of ageing pathology and to elucidate the pathways by which it influences and may also be shaped by changes in the ageing brain. This body of work has significantly expanded this knowledge through the development of novel frailty indices with components designed to capture different aspects of the pathology of ageing. These features include metabolism, physiological condition and cognitive status and this work has assessed the degree with which they, as individual components, contribute to the frailty of an individual as well as how this cumulative frailty status informs on the brain's vulnerability to, and recovery from, an acute stressor. This has been characterised in ageing mice at physiological, cognitive and molecular levels, showing correlations with inflammation and metabolic indicators in the blood and in discrete brain regions. Following this characterisation of relationships between frailty and brain inflammation/integrity the work demonstrated the ability of repeated episodic systemic inflammation to exacerbate neuroinflammation and cognitive function in the APP/PS1 animal model of AD. A generally increased susceptibility of females was observed across many of the parameters measured here.

6.2 Features of biological aging contribute to frailty and cognitive vulnerability

An exaggerated sickness behaviour response to the acute systemic stressor LPS has been observed here in aged mice as has previously been demonstrated in mouse models of neurodegenerative disease (Cunningham et al. 2009) and in ageing (Godbout et al. 2005). This exacerbated sickness behaviour is proposed to be a maladaptive response by the organism, divergent from the normal adaptive nature of sickness behaviour in healthy resilient animals (Cunningham et al. 2013). As such, it carries with it the potential for adverse long-term consequences in vulnerable individuals, including an increased risk of cognitive dysfunction (Murray et al. 2012; Chen et al. 2008), acceleration of disease features (Torvell et al. 2019; Skelly et al. 2019; Sy et al. 2011) and both increased morbidity and mortality as the individual's physiological reserve is diminished (Shamliyan et al. 2013; Rockwood et al. 2017) .

With increasing age, mice challenged with an acute bacterial or viral stressor, LPS or Poly I:C respectively, exhibited exacerbated sickness behaviour compared to younger animals and cognitive testing revealed an increasing vulnerability to acute cognitive impairment in the hippocampal-dependent T-maze working memory task. However, consistent with the idea of frailty, there was

substantial variability within aged groups and neuropathological analysis showed that these cognitively vulnerable (or frail) animals exhibited more severe microgliosis in white matter tracts as well as more robust loss of myelin and $SY38^{+}$ synaptic terminals in key hippocampal regions compared to cognitively resilient individuals. This is consistent with numerous reports that microgliosis, reduced density of white matter and synaptic terminals are significant risk factors for the incidence of delirium and exacerbation of dementia (Wijdicks 2015; Nitchingham et al. 2018; MacLullich et al. 2009; Seo et al. 2021; Scheff et al. 2011); as such they are potential metrics of frailty in the brain.

Although frailty is becoming increasingly recognised as a significant predictor of long-term outcomes and both the response to and recovery from acute stressors, there is little account of demonstrable brain function/dysfunction in animal models of frailty. The novel cumulative deficit frailty indices developed here included metrics of cognition, metabolism and physiology, to better capture the biological ageing of animals. The strongest correlates of biological ageing appeared be linked to metabolism: excess body weight, hypothermia, hyperinsulinemia and low blood glucose levels, and these were in turn the greatest contributors to the calculated frailty score. These are all characteristics which are frequently observed in HFD, *Igf-/-* and *Gh-/-* models of frailty (List et al. 2021; Yakar et al. 2002; Morrison et al. 2010). Ageing is a cumulative, progressive and deleterious loss of function resulting in the life-long accumulation of molecular and cellular defects (Kirkwood 2005) and metabolism has been cited as one of the "seven pillars of ageing" proposed by Kennedy et al to describe the multisystem progression of morbidity with age (Kennedy et al. 2014). Ageing is associated with a decline in metabolic function, characterized by changes in fat distribution, obesity and insulin resistance (Gabriely et al. 2002). As discussed previously, one of the five criterion of the Fried Frailty phenotype is unexpected weight loss (Fried et al. 2001) which is frequently associated with sarcopenic and cachexic responses in ageing frail individuals leading to reduced lean muscle mass and rendering them at increased risk of falls, injury (Yeung et al. 2019) and negative long term outcomes (Seltzer et al. 1982). In contrast across numerous large scale human ageing studies it has been shown that obesity and its associated deficits such as insulin resistance and glucose intolerance and has been shown to be associated with hypothermia (Bastardot et al. 2019) contribute to many metabolic diseases which can exacerbate age-related decline and increase frailty (Eckel et al. 2011; Yokoyama et al. 2020; Munshi 2017; Villareal et al. 2005).Metabolic syndrome, a condition characterised by a combination of diabetes with hypertension and obesity, is highly prevalent in the ageing community and has been shown to correlate strongly with frailty score for each metabolic risk factor measured as well as a cumulative syndrome when measured in a recent nationwide study in Taiwan (Lee et al. 2020). Therefore, altered energy metabolism is a consistent feature of frailty, if defined by the accumulation of

deficits, but these changes may occur in either direction: towards significant weight loss or significant weight gain.

Consistent with this individual assessment of each of the frailty index component measures' contribution to the overall score revealed that measures associated with metabolism were all more strongly correlated with frailty than age at baseline across both frailty studies. Furthermore, frailty score was shown consistently to be the best descriptor not only of an animal's baseline metabolic status but also the best predictor of their vulnerability to acute deficits in the same measures, following a stressor of 250µg/kg dose of LPS administered i.p., Additionally, this frailty score was also stronger predictor of their recovery trajectory thereafter: the speed and degree to which an animal was able to recover to their baseline level over the week recovery period. For example, both the severity of weight loss after LPS challenge, how long it took them to begin recovering weight and the extent to which this returned to baseline levels. This is consistent with the core definition of frailty as a state of increased vulnerability to a stressor event stemming from multiple co-morbidities and resulting in an increased risk of adverse outcomes and failure to return to baseline homeostasis.

However, these animals have been raised in a deliberately homogenous environment in pathogen free cages with a uniform diet and space in which to live and be active. These mice were not given access to high fat, ketogenic and caloric restricting diets which have been shown to impact upon CNS ageing pathology (Krabbe et al., 2001). Nor were they genetically manipulated in any way as with the previously discussed Gh-/- mice who have also been shown to exhibit obesity and metabolic dysfunction (Ding et al., 2013). This begs the question as to what is driving this decline in metabolic dysfunction in ageing frail animals. Ageing is a multifactorial process which is determined by genetic and environmental factors. In the absence of environmental variation, these changes could be purely a product of varying degrees of gradual accumulated DNA damage and epigenetic changes in DNA structure that affect correct gene expression and lead to the altered cell function in individual animals. However, another potential contributor to the individual variation in frailty and metabolic dysfunction among cage and littermate animals of equivalent age might be offered by the microbiome-gut-brain axis.

The intestinal microbiome is a diverse community of microorganisms with 100 times more genes than the human genome (Bäckhed et al., 2015; Blekhman et al., 2015) and exists in and evolves with its human host in a symbiotic relationship, it is incredibly diverse and unique to each individual. The development of the microbiome as a finely tuned ecosystem depends on a number of factors which are notably common to those which contribute to biological ageing, including diet, eating habits, lifestyle, stress, genetics and age (David et al., 2014; Magnusson et al., 2015). Extensive work

in recent years has demonstrated that there is a bidirectional, functional communication network between microbes, the gut and the brain, this cross-talk has come to be known as the gut–microbiome–brain axis, (Bruce-Keller et al., 2015; Hsiao et al., 2013). The functional pathways through which this is achieved comprises of neuronal, neuroendocrine, and neuroimmune signalling pathways (Saji, et al., 2019). The enteric nervous system is composed of an autonomic mesh-like system of neurons surrounding the gastrointestinal tract, while enteroendocrine cells are dispersed through the intestinal epithelium. Together these systems are capable of secreting and responding to neurotransmitters and hormones produced by the gut and microbiota respectively (Clarke et al., 2014; Strandwitz, 2018).

However, as discussed previously one of the most significant and prevalent contributors to ageing pathology is inflammation. Dysbiosis, an imbalance between the organism and its natural microflora, has been known to cause increases in immune cell production of inflammatory markers, cytokines and metabolites, both locally and peripherally. These changes have in turn been linked to increased intestinal permeability and many diseases including inflammatory bowel disease, coeliac and allergies (Carding et al., 2015); this might subsequently heighten the inflammatory state and affect the BBB permeability (Tang et al., 2017) with the potential for substantial negative impact upon CNS function. Indeed, dysbiosis has been linked to anxiety and depression (Chen et al., 2018; Jiang et al., 2018; Stower, 2019) and stress has been shown to be capable of inducing dysbiosis (Kan, et al., 2013). Furthermore, fecal transplants from an animal subjected to stressful stimuli will elicit anxiety like behaviour in the recipient animal (Bercik et al., 2011). Microorganisms (specifically Bifidocaterium) can modulate this gut-microbiome-brain axis, under stress as it has been reported that sterile mouse corticosteroid levels and adrenal cortex hormones are much higher than those of conventional microbial mice, which could in turn be reversed by postnatal colonisation with bifidobacterium (Sudo et al., 2004). Conversely, hippocampal, cortical and amygdala BDNF mRNA and protein expression is significantly lower in sterile mice (Heijtz et al., 2011; Sudo et al., 2004) this is particularly interesting given my own demonstration of significantly reduced *Bdnf* across the ageing brain with frailty.

The negative impact of dysbiosis on cognitive function extends beyond stress and anxiety to memory function also as infection of animals with Citrobacter rodentium in combination with acute stress has resulted in memory failure in mice but was prevented by the prophylactic administration of probiotics prior to infection (Gareau et al., 2011; Liang et al., 2015). Indeed, several researchers have identified novel associations between the gut microbiome and dementia (Alkasir et al., 2017; Saji et al., 2019; Vogt et al., 2017). Data from geriatric care facilities has reported that a reduced gut microbiome diversity predicts poorer cognitive function in older adults (Canipe et al., 2021). These negative changes in intestine bacteria colonies, increased intestinal permeability and lower

blood brain barrier has been shown to be associated with malnutrition (H. Wang et al., 2016), obesity as a product of high fat and sugar diets (Noble et al., 2017) and with metabolic disorders such as diabetes (Gurung et al., 2020; Li et al., 2020). Interestingly, patients with MCI (but not a diagnosed dementia) have been shown to have divergent microflora profiles compared to cognitively resilient individuals and these same patients in turn have been shown to have a higher prevalence of white matter hyperintensities and high voxel-based specific regional analysis system for Alzheimer's Disease (VSRAD) scores, indicating greater cortical and hippocampal atrophy (Saji et al., 2019). This is consistent with our own observations between cognitive frailty and white matter integrity. Thus, it is conceivable that subtle differences in individual animal's gut-microbiome profiles has contributed to the extent of their "inflammaging" profile and rendering their immune cells more vulnerable to exaggerated responses to subsequent acute systemic challneges. Given the uniform lifestyle, diet and purified watersource which our mice have access to, coupled with the fact that as animals who are not only social groomers but also coprophages it is likely that there is relatively little variation in gut microbiotas within the population compared with what would be expected in the human population. As such the variation in frailty scores which I have observed within pathogen free cages of age-matched littermates is unlikely to be wholly explained by differences in microbiota but is a metric which should be accounted for when assessing frailty in the clinical setting given the significant impact which it can have upon metabolic, behavioural and neuronal functions.

Data from care home facilities has also demonstrated that metabolic dysfunction, obesity and its associated co-morbidities are associated with learning and memory impairment in early old age (Canipe et al., 2021, Singh-Manoux et al. 2012; Sabia et al. 2009). However, it is has been reported that differential metabolic and sickness behavioural responses to bacterial and virally-induced inflammation are adaptive and a failure to maintain these metabolic adaptations to acute inflammation is, itself, detrimental. Wang and colleagues demonstrated that glucose supplementation was detrimental to mortality outcomes following a bacterial stressor but improved them following a viral Poly I:C challenge (Wang et al. 2016). This "feed a cold, starve a fever" dichotomy has been shown to extend to cognitive dysfunction with acute LPS inflammation altering energy metabolism and impairing cognition which were mitigated or exacerbated by treatment with glucose or LPS respectively (Kealy et al. 2020; Del Rey et al. 2006). Consistent with these previous findings, which have cited metabolic dysfunction as a risk factor for cognitive dysfunction (Singh-Manoux et al. 2012; Sabia et al. 2009) and the data presented here showing that our frailty index is heavily influenced by metabolic dysfunction, I have demonstrated that learning of a visuospatial learning task (shallow-water hippocampal-dependent Y-maze task) is better predicted by frailty than by age and, under acute LPS challenge, frailty better described the animal's

ability to retain that memory. Although only weakly correlated, the baseline (pre-LPS) cognitive score was also the best predictor of the number of errors made when the location of the maze was shifted in the post-LPS period.

It should be noted that one distinct limitation of frailty testing in animals using behavioural components is the impact of habituation and handling upon the animals' engagement with the task. It is now widely accepted that picking mice up by the tail is an aversive experience. Tail handled animals have been shown to exhibit reduced exploratory activity, greater anxiety and worse performance in tasks such as the elevated plus maze compared to animals who were handled using the tunnelling technique (Clarkson et al., 2018; Gouveia et al., 2017; Hurst et al, 2010). Historically, pre-test handling has been shown to have some anxiolytic effects in rodents and to reduce the impact of scruffing and tail-handling on behavioural performance (File, 1978; Rebouças et al., 1997; Schmitt et al., 1998). To this end animals were familiarised with and handled by the experimenter by cupping of the animal in the open palm, scruffing and picking up by the tail in the weeks leading up to behavioural testing. All of these are inferior to tunnelling as a means of reducing anxiety from handling the animal (Clarkson et al., 2018; Gouveia et al., 2017; Hurst et al., 2010), however, it was not feasible to strictly handle animals by tunnelling in these experimental designs. Due to the nature of the testing I was conducting it was necessary at times to scruff the animal for i.p. challenge or rectal probe temperature readings, and to hold the animal by the tail for tail vein lancing and the Deacon weight lifting task for instance. Therefore, there is a risk that some behavioural tasks which mice were repeatedly exposed to such as the Deacon weight-lifting, Open Field and Treadmill running tests may have been affected by a depressive anxious state as a product of their repeated handling and exposure to the individual tasks as well as the cumulative effect of all the tasks on any given day. As such, on frailty testing days wherever possible, animals were always tested from the least invasive measurements to the most invasive last so as to minimise the negative impact of handling/injecting on behavioural readings as much as possible. However, the impact or extent of anxiety and depression's influence on behavioural outcomes as a result of repeated handling and habituation to tasks cannot be excluded at this time.

6.3 Regional heterogeneity of brain transcriptional signatures of frailty/age

Taken together the preceding data pose the question as to whether frailty is associated with differential molecular signals in regions of the brain that are influential in metabolic state or whether the brain's inflammatory and metabolic correlates of frailty/ageing are more global.

i) Ubiquity of primed microglial phenotype

Under chronic activation, such as that which is imposed under neurodegenerative conditions and ageing, microglia display an exaggerated IL-1β response to secondary, acute, inflammatory insults. This is known as priming and was first demonstrated in microglia using the ME7 prion model of neurodegeneration (Cunningham et al. 2005). While microglial priming in the ageing brain has also been established (Godbout 2005), I demonstrate for the first time the presence of the microglial priming signature *Clec7a* across multiple distinct brain regions (pre-frontal cortex, hippocampus, hypothalamus and cerebellum) in aged animals in addition to the expected associated exaggerated pro-inflammatory response to an acute stimulus as shown here by *Il1b, Il1a* and *Tnfa* transcript expression. Furthermore, I demonstrate for the first time a robust correlation between frailty and the microglial core hub signature genes *Clec7a* and *Cd11c* expression across the ageing brain. In the APP/PS1 model I have also shown isolated microglial cells from hippocampal and cortical tissue to be primed with significant up regulation of the *Cd11c* and *Il1b* transcripts in APP/PS1 animals compared to WT controls.

While endogenous ligands for the Dectin-1 receptor in the pathological CNS environment remain little investigated, the C-type lectin receptor is an attractive therapeutic target with early work demonstrating its detrimental pathogenic role in mouse models of spinal cord injury (Gensel et al. 2015) stroke (Ye et al. 2020) and Experimental Autoimmune uveoretinitis (Stoppelkamp et al. 2015). In intracerebral haemorrhage Dectin-1 inhibition alleviated neurological dysfunction and promoted an anti-inflammatory phenotype, encouraging hematoma clearance (Fu et al. 2021). Given the apparent Clec7a-associated facilitation of exaggerated IL-1β expression in our models of ageing and neurodegeneration, and the detrimental effects thereof (Skelly et al. 2019; Lopez-Rodriguez et al. 2021), there is a pressing need to better understand Dectin-1 signalling in the brain. While endogenous CNS ligands for Dectin-1 and resulting signalling pathways and outcome are a subject of ongoing investigation I present some evidence for a neuroprotective response at the transcriptional level within the hypothalamus. Hypothalamic mRNA transcripts for proinflammatory mediators *Nlrp3* and *Tnfa* showed a decline with age while the myeloid-cell product and neuroprotective cytokine *Osm* and its corresponding astrocytic receptor, *Osmr,* both show upregulated transcript expression suggesting a favouring of the Dectin-1 CARD9-independent signalling pathway reported by Deerhake and colleagues (Deerhake et al. 2021). Further analysis of protein expression of Dectin-1 and its downstream signalling molecules would be required to further assess the extent to which these transcript changes are contributing to ageing pathology. Furthermore, given the unique structure of the BBB at the hypothalamus and the age-associated increases in permeability (Haddad-Tóvolli et al. 2017; Montagne et al. 2015) it will be important to

validate these observations in isolated microglial cells so as to rule out peripheral infiltrated myeloid cells contribution to the transcriptional profiles I have described here.

Microglial immune transcriptional profiles have been shown to be divergent across the ageing brain (Grabert et al. 2016) and white matter regions have been previously shown to exhibit a particularly enhanced microglial response following activation (Hart et al. 2012). White matter degeneration is a common pathology to many neurodegenerative disorders including AD and PD and has been shown to be predictive of cognitive decline (Bendlin et al. 2010; Raj et al. 2017; Safaiyan et al. 2021; Klosinski et al. 2015; Ruckh et al. 2012). Consistent with these findings I have demonstrated a significantly greater microglial response in white matter regions of the hippocampus and cerebellum in aged cognitively frail animals. There was a similar reduction in white matter integrity observed in these animals as assessed by Luxol fast blue histochemical staining. Taken together this enhanced microgliosis coupled with reduced myelin density in cognitively vulnerable animals suggests a likely impairment of neuronal integrity. In keeping with this there was a significant reduction of pre-synaptic terminal density observed in the hippocampal layers of aged cognitively vulnerable animals. This is consistent with previous reports that reduced density of functional synapses is associated with cognitive impairment in several neurodegenerative disorders including AD and PD (Seo et al. 2021; Scheff et al. 2011; Sri et al. 2019; Perez-Cruz et al. 2011; Terry et al. 1991). Moreover, progressive synaptic loss in the ME7 model of chronic neurodegeneration progressively increased cognitive 'vulnerability' leading to progressively more severe and longer lasting acute cognitive dysfunction upon acute systemic inflammation induced by LPS (Davis et al. 2015).

In addition to these substantial differences in immune reactivity between grey and white matter structures of the ageing brain, significant differences between regional immune responses along the anterior-poster axis were observed. As discussed previously in this text, Grabert and colleagues have demonstrated by microarray analysis that the brain's primary immune cell population, the microglia, exhibit distinct regional profiles within the brain. Notably, Grabert demonstrated the cerebellum and hippocampus exhibit a transcriptional profile which favours immune function and energy metabolism in young animals, setting them distinctly apart from the cortex and striatum. However, as age advances it was found that the hippocampus was sensitive to the loss of this distinct transcriptional signature (Grabert et al. 2016). Here I have demonstrated that the cerebellum exhibits a more immune vigilant profile than the hippocampus within saline-treated animals as evident by distinct age dependent increases in gene transcriptional expression of markers of microglial activation, *Trem2, Tyrobp, Csf1r* and *CD68*, as well as pro-inflammatory cytokines*, Il1b, Il1a* and *Tnfa*, chemokine *Cxcl10* and type 1 IFN induced genes *Irf7* and *Oas1a* that were absent in hippocampal tissue **(Table 3.1).** However, the hippocampus did show robust

upregulation of microglial markers of activation once challenged with LPS. Here I have shown that the hypothalamus exhibits a similar state of heightened immune reactivity to that seen in the cerebellum while the hippocampus and cortex demonstrated a more intermediate profile of immune reactivity, only revealing an age-associated difference between adult and aged animals when challenged with the acute inflammatory LPS. That is, aged animals showed significantly greater increases in expression of pro-inflammatory cytokines, chemokines and type 1 IFN-induced genes compared to adult animals. Assessment of regional immune responses by biological age, i.e. frailty status, corroborated these findings with the cerebellum's transcript expression showing robust correlations between markers of immune response with frailty. Frailty score severity was shown to robustly correlate with elevated expression of markers of microglial activation, *Trem2, Tyrobp,* complement *C3,* pro-inflammatory cytokines *Tnfa*, chemokine *Cxcl10, Cxcl13 and Ccl2* and type 1 IFN induced genes *IRF7* as well as decreased expression of growth factors *Igf1, Bdnf* and *Tgfb.* The hippocampus showed a similar increase in gene transcriptional expression of microglial activation and chemokine responses and decrease in growth factors but failed to show any statistically significant changes in pro-inflammatory cytokines or type-1 IFN induced genes. These data are consistent with Grabert's suggestion of a transcriptional profile favouring immune function in the cerebellum and hippocampus, but advancing age causing a loss of the distinct transcriptional signature of the hippocampus over time (Grabert et al. 2016).

However, in the APP/PS1 animal model of Alzheimer's disease microglial cells isolated from the hippocampal and cortical tissue of APP/PS1 mice did not show this more reserved immune profile with robust upregulation of *Trem2, C3* and *Stat3* transcripts in saline-challenged APP/PS1 animals compared to WT controls. Taken together these are indicative of robust microgliosis in the Aβ rich APP/PS1 brain. As discussed above, the presence of the microglial priming signature gene *Cd11c* suggests microglia are primed as a result of the amyloid pathology and consistent with this a robust expression of the DAM signature gene *Ctss* and robust downregulation of the neurogenic *Hes5* was observed in APP/PS1 animals.

Overall, this data highlights the highly heterogenous immune responses across the brain in ageing and disease pathology. The cerebellum has been shown here to exhibit a more immune vigilant profile in aged animals with elevated expression of proinflammatory and microglial activation marker transcripts at baseline compared to young animals, which was absent in the hippocampus. However, the hippocampus was still capable of a robust immune response once stimulated as demonstrated by upregulation of these same transcripts in response to an acute inflammatory stimulus or AD disease pathology. Most interesting of these heterogenous immune responses across different regions of the ageing brain was the highly divergent nature of the hypothalamic response.

ii) Divergent hypothalamic response

The hypothalamus is of particular interest given the pivotal role which it plays in regulating food intake and energy expenditure of the organism, alongside integrating central and peripheral metabolic responses and the export of newly synthesised hormones from the pituitary (Gross 1992; Haddad-Tóvolli et al. 2017). As discussed earlier in this text frailty (adverse biological aging) is closely associated with a steady decline in the pituitary's Growth Hormone levels (Cummings et al. 2003) resulting in many of the phenotypic characteristics of frailty. $GH^{-/-}$ mice also display many features of biological ageing including decreased fertility, reduced muscle mass, increased adiposity, smaller body size, and glucose intolerance (Alba et al. 2004; List et al. 2021). Furthermore, obesity, a known driver of frailty which is prevalent in the ageing population (Crow et al. 2019), is known to result in an increase in hypothalamic TLR4 expression (Milanski et al. 2009) a known contributor to autoimmune disorders (Kerfoot et al. 2004) and AD (Ledo et al. 2016). In obese pathology, the abundant saturated fatty acids, arising from a high fat diet, can induce activation of microglia through TLR4/NFκB signalling (Wang et al. 2012) resulting in hypothalamic inflammation (Valdearcos et al. 2014) and glucose intolerance (Yan et al. 2014) that are observed in obese animals.

In chapter 3 of the current study the hypothalamus was found to exhibit a similar state of heightened immune reactivity as that of the cerebellum in young and aged animals challenged with saline with elevated markers of microglial activation transcripts for *Trem2, Tyrobp* and *Cd68,* as well as exaggerated expression of proinflammatory cytokines and chemokines *Cxcl10, Il1b, Tnfa* and *Il1a* in aged animals compared to young when challenged with LPS. However, assessment of inflammatory expression profiles in a larger population of animals by frailty, in chapter 4, revealed a significantly divergent response between the two regions with advancing age. The expression of growth factor transcripts, *Bdnf* and *Igf1,* were found to decline robustly with ageing and frailty while *Tgfb* showed a significant increase with age. This is consistent with previous data in $IGF^{-/-}$ animals who present with significant frailty-like pathology (Yakar et al. 2002) while TGF-β levels have been shown to be excessively elevated in the aging mouse brain, causing chronic hypothalamic inflammation and exacerbation of metabolic co-morbidities, which could be ameliorated through frailty management mechanisms such as diet management and aerobic exercise (Mendes et al. 2018; Yan et al. 2014; Bosch-Queralt et al. 2021; V. Silva et al. 2017). TGF-β has also been shown to be one of the primary components of the senescence-associated secretory phenotype secretome along with IL-6 and CCL2 (Coppé et al. 2010) all of which also showed significant transcript elevation with frailty. Consistent with this downregulation of growth factor transcripts and increase in the SASP secretome of *Tgfb, Ccl2, Il6,* there was a commensurate increase in transcriptional expression of ageing-associated senescent marker $p16^{INK4A}$ indicative of elevated senescence in the frail

hypothalamus. Recently it was shown that age-associated hyperinsulinemia in the serum, as was observed in highly frail animals, is reflected in the CSF and can result in neuronal insulin resistance, impairing glycolysis and inducing cell-cycle senescence (Chow et al. 2019). Since then Suda and colleagues have also demonstrated a robust increase in *p16*^{INK4A} in hypothalamic mRNA as well as a substantial age-associated accumulation of senescent microglia and astrocytes (Suda et al. 2021). Consistent with this report of increased hypothalamic microglial senescence I also demonstrated a unique decline in hypothalamic microglial transcripts *Tyrobp* and *Trem2* with age and to a lesser degree frailty. However, *p21,* a p53 target gene implicated in cell-cycle arrest and senescence (Cheung et al. 2012) and the SASP product *Pai1* (Coppé et al. 2010) failed to show any significant increase in transcript expression with age or frailty despite reports of their induction by TGF-β *in vitro* (Sawdey et al. 1989; Yoo et al. 1999). This could suggest that the robust increase in *Tgfb* transcript expression observed is not in turn translated to protein to induce their expression as has been reported or perhaps that its influence may be affecting alternative pathways to senescence despite these strong correlations. Further assessment of the senescent markers and SASP secretome products at the protein level would be required to determine this with any confidence.

Here I have demonstrated that highly frail individuals typically show a higher body weight, hypothermia, hyperinsulinemia and lower blood glucose levels; all characteristics frequently observed in HFD, *Igf-/-* and *Gh-/-* models of frailty (List et al. 2021; Yakar et al. 2002; Morrison et al. 2010) and modulated by the hypothalamus (Roh et al. 2016). Recent analysis of gene expression databases and longitudinal ageing studies for biomarkers of frailty have identified metabolic associated growth factors, BDNF, TGF-β and Insulin-like growth factor 1 (IGF1), and inflammatory mediators CCL2, CXCL13, IL-6 as potential biomarkers (Cardoso et al. 2018; Lu et al. 2016), all of which I have observed to show significantly altered transcript expression with frailty across the ageing brain and especially within the hypothalamus. This is consistent with numerous reports that ageing is associated with a chronic low-grade inflammation (Franceschi et al. 2014; Pawelec et al. 2014) which is exacerbated by obesity and will might alter blood brain barrier permeability and exacerbated microgliosis and inflammation within the CNS, particularly within the hypothalamus (Thaler et al. 2012; Haddad-Tóvolli et al. 2017; Gupta et al. 2012; Montagne et al. 2015). Villeda and colleagues demonstrated using heterochronic parabiosis that young animals exposed to an old systemic environment's blood-borne factors, including CCL2, showed decreased synaptic plasticity and impaired contextual fear conditioning and spatial learning and memory (Villeda et al. 2011). Kealy et al. has demonstrated that acute cognitive dysfunction under inflammatory LPS is a result of altered energy metabolism which was mitigated or exacerbated by treatment with glucose or LPS respectively (Kealy et al. 2020; Del Rey et al. 2006). Furthermore, hyperinsulinemia, such as that induced in obesity and which I have observed in highly frail individuals is not only associated with

the frailty biomarker IGF-1's serological levels (Friedrich et al. 2012) but has most recently been shown to be reflected in elevated CSF insulin levels, resulting in neuronal insulin resistance and impairing glycolysis (Chow et al. 2019). This is consistent with the growing sentiment in the field of Alzheimer's research which considers neuronal insulin resistance observed in AD to be a CNS focussed variant of diabetes, termed "type 3 diabetes" (Rorbach-Dolata et al. 2019; Nguyen et al. 2020; Velazquez et al. 2017) and results in systemic hyperglycaemia, which can lead to glutamate-induced excitotoxicity in neurons (Datusalia et al. 2018). Additionally, Chow et al. demonstrated that this age-associated hyper-insulinemia induced neuronal insulin resistance has been shown to in turn induce cell-cycle senescence (Chow et al. 2019). Consistent with this I have also demonstrated elevated senescence in the hypothalamus according to transcriptional expression of ageing-associated senescent marker *p16*^{INK4A} and the SASP secretome of *Tgfb, Ccl2, Il6.* Taken together these data suggest that the frailty phenotype observed here is a product of age associated obesity and the resulting exaggerated low-grade chronic inflammation and hyperinsulinemia disrupting the CNS metabolic and microglial homeostasis through increased BBB permeability and elevated insulin levels in the CSF, inducing insulin resistance in neurons. This insulin resistance in turn alters glycolysis, risks inducing glutamate-induced excitotoxicity, cellular senescence and downregulation of metabolic associated growth factors. Increased cellular excitotoxicity and senescence in turn renders the frail brain more vulnerable to cognitive dysfunction as has been demonstrated for multiple metabolic co-morbidities previously (Singh-Manoux et al. 2012; Sabia et al. 2009; Aleman et al. 1999).

These data suggest that hypothalamic function is a critical regulator of systemic ageing with significant implications for cognitive function. Going forward, further examination of the hypothalamic molecular signature of aging and functional changes will be critical in understanding systemic aging and its contribution to the severity of an individual's frailty and in time, the development of targeted potential therapeutic intervention to hypothalamic senescence, insulin signalling or inflammation could possibly increase both the quality and extent of an ageing individual's lifespan.

6.4 APP/PS1 animals show higher frailty and sexual dimorphism in cognitive vulnerability to chronic systemic challenge

As has been discussed in length throughout this text, frailty severity is a substantial risk factor for the development and exacerbation of cognitive disorders (Borges et al. 2019; Kojima et al. 2017), especially Alzheimer's (Vest et al. 2013; Oveisgharan et al. 2018; Wallace et al. 2019). Within frailty itself however sex has been shown to be a significant driving factor with both a higher prevalence

of and severity of frailty in women compared to males (Ott et al. 1998; Mitnitski et al. 2005; Song et al. 2010; Collard et al. 2012). This has, in turn, been shown to correspond with a higher incidence and prevalence of AD in women (Laws et al. 2016) as well as more severe pathology as evidenced by faster cognitive decline, greater amyloid pathology and brain atrophy than men (Ferretti et al. 2018; Podcasy et al. 2016; Marongiu 2019). Furthermore, both frailty and AD have been shown to have strong links to metabolic dysfunction with metabolic disorders such as diabetes conferring a 60% increased likelihood of developing AD (Gudala et al. 2013) and frailty (Bouillon et al. 2013).

Here I have demonstrated that APP/PS1 animals exhibit slightly higher frailty scores as well as reduced food and water intake, greater adiposity, lower energy expenditure and home cage activity compared to age matched C57 WT animals. This is consistent with previous reports across several AD models of higher frailty (Todorovic et al. 2020) and impaired insulin sensitivity (Macklin et al. 2017; Rodriguez-Rivera et al. 2011; Velazquez et al. 2017) with AD pathology. However, as discussed above sex is an important risk factor in driving pathology in AD and APP/PS1 female mice have been previously shown to exhibit higher amyloid burden (Wang et al. 2003) as well as increased cognitive impairments, reduced hippocampal neurogenesis (Jiao et al. 2016; Richetin et al. 2017) and reduced white matter integrity compared to age matched male APP/PS1 animals (C. Zhou et al. 2018). Menopausal reductions in estrogen levels are believed to be responsible for these differences in AD pathology progression observed between male and female animals as estrogen has also been shown to be involved in cognitive functioning (Hara et al. 2015), neurotrophin synthesis (Milne et al. 2015), modulation of the cholinergic and dopaminergic neurotransmitter systems (Mennenga et al. 2015; Sinclair et al. 2014) and has even been shown to protect the brain against stress and inflammation (Luine 2016) with hormone replacement therapies in human studies showing improved cognitive outcomes (Galea et al. 2017; Luine 2014). Here I have demonstrated that APP/PS1 female mice show greater cognitive deficits than male APP/PS1 animals. At baseline APP/PS1 female mice displayed a reduced ability to learn the shallow water visuospatial Y-maze task and females also showed impaired freezing behaviour in response to contextual and auditory cued fear conditioning paradigms. It has been reported that elevated baseline TNFα is associated with a reduction in hippocampal volume (Sudheimer D. et al. 2014) and progression of mild cognitive impairment to AD (Tarkowski et al. 2003). Here I have demonstrated that APP/PS1 female mice challenged repeatedly with TNFα (250µg/kg) showed impaired performance in the MWM task that was not evident in saline-challenged APP/PS1 females nor in TNFα-challenged WT or APP/PS1 males. Previously unpublished data from our group using the same treatment regime strictly in females also revealed significantly decreased $Ki67^{+}$ cell proliferation and reduced amyloid-β and APP^{+} deposition in the hippocampus as assessed by immunohistochemical labelling in APP/PS1 females challenged repeatedly with TNFα. Furthermore,

there was a slight increase in $CD3^+$ labelled T-cells in APP/PS1 females challenged with TNFα that was not present in WT animals similarly challenged, suggesting increased permeability of the BBB courtesy of the repeated TNFα challenges, as has previously been reported (Nawashiro et al. 1997; Yang et al. 1999; Chen et al. 2019), and peripheral T-cell infiltration in the APP/PS1 animal. Consistent with this, previous studies have shown that the choroid plexus is a reservoir for T cells, which can cross the Blood-CSF-Barrier from the choroid plexus into the parenchyma only when the choroid plexus has been primed by inflammation (Engelhardt et al. 2005; Engelhardt 2010). However, whether similar changes occur and to what extent in equivalently aged male animals following repeated TNFα also will require further investigation.

Interestingly, while female APP/PS1 animals were at an increased risk of exacerbated cognitive deficits in response to repeated systemic challenge they did not experience the same repeated weight loss in response to the sequential acute TNFα challenges that TNF-challenged WT animals showed and this 'tolerance' to TNF-induced weight loss was also not observed in male APP/PS1 animals. Given the higher frailty, more advanced AD pathology and increased vulnerability to cognitive deficit observed in APP/PS1 females this 'tolerance' is not intuitively explained by their more advanced pathology with respect to males. However, it is possible that this "tolerance" is not beneficial. Previous work by Wang et al. demonstrated that metabolic and sickness behavioural responses to bacterial and virally-induced inflammation, such as anorexia and anhedonia, are adaptive and a failure to maintain these metabolic adaptations to acute inflammation can be detrimental (Wang et al. 2016). The current data suggest that while all animals show an equivalent initial TNFα-induced anorexic response (decreased food intake, loss of body weight) as well as a shift towards more FAO (demonstrated using the Promethion metabolic cage system), female APP/PS1 mice cannot maintain this weight loss change upon repeated challenges and this failed metabolic response to acute inflammation may have detrimental effects on brain metabolism, inflammation and reactive oxygen species production (Wang et al. 2016).

Whether or not fatty acid oxidation (FAO) is deleterious or beneficial has been reported to be tissue dependent. In skeletal muscle, a tissue with a high metabolic rate and mitochondrial activity, inhibition of FAO in rodents and humans has been shown to increase insulin resistance (Barnett et al. 1992; Hubinger et al. 1992; Timmers et al. 2012; Keung et al. 2013) and is vulnerable to proinflammatory outcomes as a result of the elevated production of ROS (Seifert et al. 2010). In contrast however, i*n vitro* studies have demonstrated beneficial effects of enhancing FAO in reducing insulin resistance in hepatic cells (Orellana-Gavaldà et al. 2011; Sebastián et al. 2007) or in adipose tissue macrophages FAO enhancement is capable of ameliorating inflammation (Malandrino et al. 2015; Namgaladze et al. 2014). Thus, the FAO observed in response to repeated TNFα may well be a protective response of macrophages intended to attenuate inflammation and

restore homeostasis; a process which APP/PS1 females appear unable to maintain. This is particularly interesting as I have demonstrated here that female APP/PS1 mice show significantly lower body weights compared to age-matched WT control females at day 0, before treatment with TNFα begins. This suggests the AD pathology, which is more advanced, may have reduced the APP/PS1 females adiposity compared to WT controls and/or their ability to mount an efficient FAO metabolic response utilising these (potentially limited) lipids. Further assessment of metabolic changes in RER, adiposity, and food intake in response to repeated second, third and fourth TNFα challenges should be assessed in an appropriately powered, sex balanced, population using the Promethion metabolic cage system to determine if APP/PS1 females show altered RER favouring FAO commensurate to their reduced weight-loss responses to repeated TNFα challenge.

However, whether this lower body weight observed in APP/PS1 females compared to WT controls is a result of reduced lean muscle mass or adiposity in APP/PS1 females is difficult to say. However, in addition to the more advanced AD pathology these 14±2-month old female animals should have experienced a post-menopausal alteration in body composition with increased adiposity and reduced insulin sensitivity (Maltais et al. 2009). Consistent with this APP/PS1 animals showed greater adiposity of white fat deposits compared to WTs, unfortunately however the study was unfortunately underpowered to assess this specifically in females. Taken together however this does suggest that the difference in body mass between APP/PS1 and WT females may be a product of a cachexic loss of lean muscle rather than reduced adiposity. As discussed earlier in this text cachexia is defined as a loss of lean muscle under systemic inflammatory conditions as a result of the concomitant presence of an underlying chronic disease and anorexic-like behaviour (Muscaritoli et al. 2010). This definition of cachexia is consistent with the conditions here as previous reports have shown that APP/PS1 females have significantly more advanced pathology associated with greater proinflammatory cytokine expression (Jiao et al. 2016; Richetin et al. 2017; Wang et al. 2003) and our own demonstration of reduced food intake in APP/PS1 animals. Thus, female APP/PS1 animals, in theory, may as a result of their more aggressive pathology have experienced a more advanced cachexic loss of muscle tone compared to age matched male animals. It is possible then that the repeated systemic inflammatory challenges are eliciting cachexic responses (loss of muscle mass) which contribute to the WT and APP/PS1 male mice more to their weight loss to due to their less advanced pathology compared to APP/PS1 females. However further analysis of changes in RER, adiposity and muscle density using cachexic markers in the muscle and serum of APP/PS1 animals to repeated TNF challenge would be required in order to determine the exact cause and implications of this apparent tolerisation of APP/PS1 animals.

With current projections estimating the number of people suffering this condition expected to double over the next 25 years (Alzheimer Europe 2019) there is a growing need to understand the

underlying pathology and risk factors associated with dementia and Alzheimer's disease specifically in order to identify and prophylactically treat patients with preclinical AD and risk factors, such as frailty or metabolic co-morbidities, for cognitive decline. While the underlying mechanisms are still being investigated and remain widely debated, the contribution of metabolism to disease progression and the evident dichotomy in vulnerability between male and female individuals to ageing associated conditions such as frailty and subsequent susceptibility to co-morbidities and cognitive deficits is apparent. Further work systematically assessing metabolisms contribution both peripherally and central to AD pathology and cognitive decline over time in the APP/PS1 model, controlled for sex and genotype, would be required in order to outline the exact time course and trajectory of disease pathology and its impact upon the male and or female brain. Furthermore, the use insulin-targeted and estrogen-containing hormone therapies to modulate AD pathology is a promising avenue of prophylactic treatment whose underlying mechanistic pathways remains to be elucidated and the exact contribution of sex and metabolism to driving AD progression in APP/PS1 animals should be an area of focus in the coming years.

6.5 CNS inflammatory changes to acute insult

As discussed in chapter three of this thesis and has been well established in the literature an acute insult such as 100µg/kg of the bacterial mimetic LPS is sufficient to induce upregulated expression of proinflammatory cytokines, chemokines and type one interferon associated genes in both young and aged animals across several distinct brain regions. However as discussed earlier in this chapter the aged, frail and APP/PS1 CNS all exhibited a ubiquitous microglial priming signature, *Cd11c* and/or *Clec7a,* across every region assessed. Consistent with their primed phenotype aged animals exhibited exaggerated expression of the proinflammatory cytokines and chemokines in response to an acute LPS challenge, across all regions assessed. Within APP/PS1 animals' isolated microglial cells there was also significant upregulation of transcripts associated with the primed phenotype, *Cd11c, Il1b,* and microglial activation *, Trem2, C3, Ctss,* was found in all APP/PS1 animals regardless of challenge. However, in APP/PS1 animals challenged repeatedly with 250µg/kg of TNFα I demonstrated exaggerated *Tnfa* and *Ccl4* transcript expression compared to WT and saline controls. This is particularly noteworthy given that this elevation of proinflammatory cytokines and chemokines has persisted 6 days after the fourth and final TNFα challenge, suggesting the repeated systemic challenge has potentially altered blood brain barrier permeability and the resulting chemokine and TNFα infiltration likely stimulated microglial production of the cytokine and chemokines as has been previously reported (Deli et al. 1995; Aslam et al. 2012; Trickler et al. 2005;

Chen et al. 2019). Further analysis of the extent and duration of this permeability and the protein expression of these elevated cytokine and chemokine transcripts should be assessed in future work.

In addition to immunohistochemistry labelling of $IBA1^+$ microglia confirming this activated microglial morphology in the APP/PS1 brain associated with amyloid plaques, $GFAP^+$ labelling was found to also exhibit significant astrocytosis within the hippocampus. Furthermore, astrocytes isolated from APP/PS1 animals revealed a similar transcriptional profile of activation with AD pathology as evidenced by robust upregulation of *Gfap, Irf7, Stat3* and *Tnfr* along with downregulation of the neurogenic *Hes5*. The robustly upregulated *Tnfr* on APP/PS1 astrocytic cells was particularly interesting given the potential implications of this to astrocytic sensitivity and responsiveness to a TNFα challenge. Indeed, similar to microglia it was found that astrocytes from APP/PS1 animals challenged repeatedly with TNFα 250μg/kg show upregulated gene expression for markers of astrocytosis (Liddelow et al. 2017; Lopez-Rodriguez et al. 2021), including *Gbp2, Ptx3, Cst7* and *Tgm1* as well as elevated chemokine expression, *Ccl3* and *Ccl4*, persisting 6 days after the fourth and final TNFα challenge. Additionally, there was a significant elevation of astrocytic *Il1r* in APP/PS1 animals challenged with TNFα suggesting a resulting increased sensitivity to the elevated *Il1b* expressed in APP/PS1 microglial cells. This led us to investigate the impact of a central acute TNFα challenge on the hippocampus of APP/PS1 and WT animals. Chemokine expression by $CCL2^+$ and $CXCL10^+$ labelling revealed that TNFα treatment saw significant induction in the dentate gyrus of APP/PS1 animals which was absent in similarly challenged WT animals. Immunofluorescent labelling of glial cells with CCL2 labelling revealed a significant co-localisation of $CCl2^+$ labelling with astrocytic $GFAP^+$ cells. This in turn is consistent with data from our own group, demonstrating that a central challenge of IL-1β and TNFα will cause NFκB to be translocated to the nucleus and a robust ensuing production of chemokines (Hennessy et al. 2015; Lopez-Rodriguez et al. 2021). Consistent with these findings, I have shown a strong co-localisation of CCL2 with activated astrocytic cells, with activated microglial cells also in close proximity, consistent with their rapid, motile response to stimuli and role in the activation of astrocytes. Taken together this transcriptional profile and morphology of activated astrocytes coupled with exaggerated expression of proinflammatory mediators to systemic and central TNFα support our labs recent demonstration of the presence of an astrocytic priming phenotype proximal to Aβ plaques in the amyloid-rich dentate gyrus of APP/PS1 mice. These astrocytic cells were found to be primed to show exaggerated chemokine responses to acute IL-1β stimulation (Lopez-Rodriguez et al. 2021).

Recurrent and chronic infections such as urinary tract infections (Zonsius et al. 2020; Brown et al. 2011), are extremely prevalent in Alzheimer's disease and are often associated with bouts of delirium and cognitive dysfunction (Davis et al. 2015; Fong et al. 2015). Here I have utilised a repeated i.p. TNFα challenge to mimic a recurrent systemic infection and demonstrated the

presence of microglial priming alongside the newly described astrocytic priming phenotype in the APP/PS1 brain. Upon challenge with an acute central inflammatory stimulus, these primed glial cells are capable of a robust, exaggerated pro-inflammatory cytokine and chemokine response (Lopez-Rodriguez et al. 2021). Chronic systemic inflammatory episodes alteration of glial inflammatory profiles persisted up to six days after the fourth and final acute inflammatory event as shown here by elevated proinflammatory cytokine and chemokine and receptor transcript expression. These hypersensitive inflammatory responses have previously been shown in APP/PS1 mice to be sufficient to drive neuronal and cognitive dysfunction (Lopez-Rodriguez et al. 2021). As has been discussed extensively in this text, sex is a significant contributor to ageing pathology and associated co-morbidities, especially Alzheimer's disease (Pike 2017; Laws et al. 2016; Toro et al. 2019). Consistent with this it has recently been shown that microglia exhibit distinct metabolic profiles in sexual dimorphism in AD. Female APP/PS1 microglia were found to be morphologically and functionally distinct from males' with a more glycolytic, less phagocytic profile which preferentially upregulated markers of microglial activation compared to male APP/PS1 mice (Guillot-Sestier et al. 2021). Given the robust differences in cognitive and metabolic vulnerability to repeated TNFα observed in APP/PS1 animals and the significant influence which these have upon frailty severity it is imperative that future work investigating inflammatory and metabolic changes in AD and frailty models under homeostatic and inflammatory conditions be appropriately powered to assess the impact of sex on observed outcomes. Going forward the targeting of this interaction between underlying disease and secondary inflammation to limit the impact of acute and repeated secondary inflammatory events on the exacerbation of disease should become an area of interest in designing therapeutic interventions and elucidating the signalling mechanisms by which acute inflammation induces delirium-like episodes.

6.6 Conclusions and future directions

Remarkable advancements in science and medicine over the last century have led to a steady rise in lifespan (World Health Organization; 2011) and with it an increased prevalence of associated chronic diseases and an inevitable decline in functional capabilities (Niccoli et al. 2012; Hou et al. 2019). As a result, the field of gerontology has seen a paradigm shift in recent years, from extending lifespan toward maintaining and improving the quality of life for the elderly. Traditionally health-care systems are organised into speciality disciplines targeting single-system illnesses; however, ageing is at its core a chronic multi-system co-morbidity. In the age of precision medicine, the characterisation and study of the Frailty phenotype has been an integral methodology in directing treatment plans away from organ-specific illnesses towards a more holistic approach of targeted treatment plans tailored toward the elderly individual. Here I have demonstrated the extent to

which measures of metabolism influence an individual's frailty and the importance of incorporating and appropriately weighting measures of metabolism in any frailty assay for use in a clinical setting. Furthermore, frailty is a robust predictor of cognitive status and correlates strongly with molecular measures and immune reactivity across the ageing brain. The hypothalamus particularly showed intriguing and divergent molecular signatures of microglial reactivity compared to other regions and exhibited evidence of elevated senescence and decreased growth factor production. Within the APP/PS1 model of AD significant deficits in metabolism and activity were also evident in APP/PS1 animals at baseline and with repeated systemic inflammatory events they exhibited robust changes in metabolism, energy expenditure and central glial immune responses with evidence of both microglial and astrocytic priming. Taken together these data stress the crucial role of metabolism in ageing and neurodegenerative disorders, the impact of repeated or chronic systemic inflammation on the ageing/degenerating brain and suggests that the hypothalamus and associated metabolic systems are promising therapeutic targets for future work.

Bibliography

Acaz-Fonseca, E., Ortiz-Rodriguez, A., Azcoitia, I., Garcia-Segura, L.M., & Arevalo, M.A. 2019. Notch signaling in astrocytes mediates their morphological response to an inflammatory challenge. Cell Death Discovery 5(1).

Acosta, J.C. et al. 2013. A complex secretory program orchestrated by the inflammasome controls paracrine senescence. Nature Cell Biology 15(8).

Acosta-Rodríguez, Victoria A., Filipa Rijo-Ferreira, Carla B. Green, and Joseph S. Takahashi. 2021. "Importance of Circadian Timing for Aging and Longevity." Nature Communications 12(1).

Acton, R.D. et al. 1996. Differential sensitivity to Escherichia coli infection in mice lacking tumor necrosis factor p55 or interleukin-1 p80 receptors. In Archives of Surgery, 1216–1221.

Adams, P.D. 2009. Healing and Hurting: Molecular Mechanisms, Functions, and Pathologies of Cellular Senescence. Molecular Cell 36(1): p.2–14.

Agostini, A., Yuchun, D., Li, B., Kendall, D.A., & Pardon, M.C. 2020. Sex-specific hippocampal metabolic signatures at the onset of systemic inflammation with lipopolysaccharide in the APPswe/PS1dE9 mouse model of Alzheimer's disease. Brain, Behavior, and Immunity 83: p.87–111.

Aguirre, L.E., & Villareal, D.T. 2015. Physical Exercise as Therapy for Frailty. Nestle Nutrition Institute Workshop Series 83: p.83–92. Available at: https://www.karger.com/Article/FullText/382065 [Accessed August 28, 2021].

Ajami, B., Bennett, J.L., Krieger, C., Tetzlaff, W., & Rossi, F.M.V. 2007. Local self-renewal can sustain CNS microglia maintenance and function throughout adult life. Nature Neuroscience 10(12): p.1538–1543.

Ajuebor, M.N. et al. 1998. Endogenous monocyte chemoattractant protein-1 recruits monocytes in the zymosan peritonitis model. Journal of Leukocyte Biology 63(1): p.108–116.

Akash, M.S.H., Rehman, K., & Liaqat, A. 2018. Tumor Necrosis Factor-Alpha: Role in Development of Insulin Resistance and Pathogenesis of Type 2 Diabetes Mellitus. Journal of Cellular Biochemistry 119(1): p.105–110.

Akiguchi, I. et al. 2017. SAMP8 mice as a neuropathological model of accelerated brain aging and dementia: Toshio Takeda's legacy and future directions. Neuropathology 37(4): p.293–305.

Available at: http://doi.wiley.com/10.1111/neup.12373 [Accessed March 20, 2021].

Alawieh, A. et al. 2021. Complement drives synaptic degeneration and progressive cognitive decline in the chronic phase after traumatic brain injury. Journal of Neuroscience 41(8).

Alba, M., & Salvatori, R. 2004. A mouse with targeted ablation of the growth hormone-releasing hormone gene: A new model of isolated growth hormone deficiency. Endocrinology 145(9): p.4134–4143. Available at: https://pubmed.ncbi.nlm.nih.gov/15155578/ [Accessed August 27, 2021].

Aleman, A. et al. 1999. Insulin-like growth factor-I and cognitive function in healthy older men. Journal of Clinical Endocrinology and Metabolism 84(2): p.471–475.

Alkasir, R., Li, J., Li, X., Jin, M., & Zhu, B. (2017). Human gut microbiota: the links with dementia development. In Protein and Cell (Vol. 8, Issue 2, pp. 90–102). https://doi.org/10.1007/s13238-016-0338-6

Alzheimer'sAssociation. 2015. Alzhiemer's Disease Facts and Figures. Alzheimers Dement 11(3): p.332–384. Available at: https://www.alz.org/alzheimers-dementia/facts-figures.

Alzheimer Europe. 2019. Dementia in Europe Yearbook. Estimating the prevalence of dementia in Europe.

Amor, S. et al. 2014. Inflammation in neurodegenerative diseases - an update. Immunology 142(2): p.151–166.

Anand, K., & Dhikav, V. 2012. Hippocampus in health and disease: An overview. Annals of Indian Academy of Neurology 15(4): p.239–246.

Angulo, J., El Assar, M., Álvarez-Bustos, A., & Rodríguez-Mañas, L. 2020. Physical activity and exercise: Strategies to manage frailty. Redox Biology 35: p.101513.

Antoch, M.P. et al. 2017. Physiological frailty index (PFI): Quantitative in-life estimate of individual biological age in mice. Aging 9(3): p.615–626.

Antonelli, A. et al. 2006. Increase of CXC chemokine CXCL10 and CC chemokine CCL2 serum levels in normal ageing. Cytokine 34(1–2): p.32–38.

Arnett, H.A. et al. 2001. TNFα promotes proliferation of oligodendrocyte progenitors and remyelination. Nature Neuroscience 4(11): p.1116–1122. Available at: https://pubmed.ncbi.nlm.nih.gov/11600888/ [Accessed September 23, 2021].

Arrieta, H. et al. 2019. Effects of Multicomponent Exercise on Frailty in Long-Term Nursing Homes: A Randomized Controlled Trial. Journal of the American Geriatrics Society 67(6): p.1145–1151.

Ashraf, G.M. et al. 2019. The Possibility of an Infectious Etiology of Alzheimer Disease. Molecular Neurobiology 56(6): p.4479–4491.

Askew, K. et al. 2017. Coupled Proliferation and Apoptosis Maintain the Rapid Turnover of Microglia in the Adult Brain. Cell Reports 18(2): p.391–405.

Aslam, M., Ahmad, N., Srivastava, R., & Hemmer, B. 2012. TNF-alpha induced NFκB signaling and p65 (RelA) overexpression repress Cldn5 promoter in mouse brain endothelial cells. Cytokine 57(2): p.269–275.

Audrain, M. et al. 2021. Reactive or transgenic increase in microglial TYROBP reveals a TREM2-independent TYROBP–APOE link in wild-type and Alzheimer's-related mice. Alzheimer's and Dementia 17(2): p.149–163.

Aviello, G., Cristiano, C., Luckman, S.M., & D'Agostino, G. 2021. Brain control of appetite during sickness. British Journal of Pharmacology 178(10): p.2096–2110.

Babayan, B.M. et al. 2017. A hippocampo-cerebellar centred network for the learning and execution of sequence-based navigation. Scientific Reports 7(1).

Bachelerie, F. et al. 2014. International union of pharmacology. LXXXIX. Update on the extended family of chemokine receptors and introducing a new nomenclature for atypical chemokine receptors. Pharmacological Reviews 66(1): p.1–79.

Bachiller, S. et al. 2018. Microglia in neurological diseases: A road map to brain-disease dependent-inflammatory response. Frontiers in Cellular Neuroscience 12.

Baker, D. et al. 1994. Control of established experimental allergic encephalomyelitis by inhibition of tumor necrosis factor (TNF) activity within the central nervous system using monoclonal antibodies and TNF receptor ‐ immunoglobulin fusion proteins. European Journal of Immunology 24(9): p.2040–2048.

Baker, D. et al. 2008. Opposing roles for p16Ink4a and p19Arf in senescence and ageing caused by BubR1 insufficiency. Nature Cell Biology 10(7): p.825–836.

Baker, D., Weaver, R.L., & VanDeursen, J.M. 2013. P21 Both Attenuates and Drives Senescence and Aging in BubR1 Progeroid Mice. Cell Reports 3(4): p.1164–1174.

Baker, D.J. et al. 2004. BubR1 insufficiency causes early onset of aging-associated phenotypes and

infertility in mice. Nature Genetics 36(7): p.744–749.

Baker, D.J. et al. 2011. Clearance of p16 Ink4a-positive senescent cells delays ageing-associated disorders. Nature 479(7372): p.232–236.

Bäckhed, F., Roswall, J., Peng, Y., Feng, Q., Jia, H., Kovatcheva-Datchary, P., Li, Y., Xia, Y., Xie, H., Zhong, H., Khan, M. T., Zhang, J., Li, J., Xiao, L., Al-Aama, J., Zhang, D., Lee, Y. S., Kotowska, D., Colding, C., … Jun, W. (2015). Dynamics and stabilization of the human gut microbiome during the first year of life. Cell Host and Microbe, 17(5), 690–703. https://doi.org/10.1016/j.chom.2015.04.004

Ballak, S.B., Degens, H., de Haan, A., & Jaspers, R.T. 2014. Aging related changes in determinants of muscle force generating capacity: A comparison of muscle aging in men and male rodents. Ageing Research Reviews 14(1): p.43–55.

Banks, W.A. et al. 2015. Lipopolysaccharide-induced blood-brain barrier disruption: Roles of cyclooxygenase, oxidative stress, neuroinflammation, and elements of the neurovascular unit. Journal of Neuroinflammation 12(1).

Banks, W.A., Moinuddin, A., & Morley, J.E. 2001. Regional transport of TNF-α across the blood-brain barrier in young ICR and young and aged SAMP8 mice. Available at: www.elsevier.com/locate/neuaging.

Banks, W.A., & Robinson, S.M. 2010. Minimal penetration of lipopolysaccharide across the murine blood-brain barrier. Brain, Behavior, and Immunity 24(1): p.102–109.

Barna, B.P. et al. 1994. Regulation of monocyte chemoattractant protein-1 expression in adult human non-neoplastic astrocytes is sensitive to tumor necrosis factor (TNF) or antibody to the 55-kDa TNF receptor. Journal of Neuroimmunology 50(1): p.101–107.

Barnett, M., Collier, G.R., & O'Dea, K. 1992. The longitudinal effect of inhibiting fatty acid oxidation in diabetic rats fed a high fat diet. Hormone and Metabolic Research 24(8).

Barnett, M.L. et al. 2018. Exploring the multiple-hit hypothesis of preterm white matter damage using diffusion MRI. NeuroImage: Clinical 17: p.596–606.

Barreto, G., Huang, T.T., & Giffard, R.G. 2010. Age-related defects in sensorimotor activity, spatial learning, and memory in c57bl/6 mice. Journal of Neurosurgical Anesthesiology 22(3): p.214–219.

Bastardot, F., Marques-Vidal, P., & Vollenweider, P. 2019. Association of body temperature with

obesity. The CoLaus study. International Journal of Obesity 43(5): p.1026–1033.

Baxter, M.G., & Chiba, A.A. 1999. Cognitive functions of the basal forebrain. Current Opinion in Neurobiology 9(2): p.178–183.

Bayer, D. et al. 2021. Disruption of orbitofrontal-hypothalamic projections in a murine ALS model and in human patients. Translational Neurodegeneration 10(1): p.1–17. Available at: https://translationalneurodegeneration.biomedcentral.com/articles/10.1186/s40035-021-00241-6 [Accessed January 20, 2022].

Baylis, D., Bartlett, D.B., Patel, H.P., & Roberts, H.C. 2013. Understanding how we age: insights into inflammaging. Longevity & Healthspan 2(1).

Beck, J. et al. 1988. Increased production of interferon gamma and tumor necrosis factor precedes clinical manifestation in multiple sclerosis: Do cytokines trigger off exacerbations? Acta Neurologica Scandinavica 78(4).

Beck, C.H.M., & Fibiger, H.C. 1995. Conditioned fear-induced changes in behavior and in the expression of the immediate early gene c-fos: With and without diazepam pretreatment. Journal of Neuroscience 15(1 II): p.709–720.

Bélanger, M., Allaman, I., & Magistretti, P.J. 2011. Differential effects of pro- and anti-inflammatory cytokines alone or in combinations on the metabolic profile of astrocytes. Journal of Neurochemistry 116(4): p.564–576.

Belkina, A.C., & Denis, G. V. 2010. Obesity genes and insulin resistance. Current Opinion in Endocrinology, Diabetes and Obesity 17(5): p.472–477.

Bell, R. D., Winkler, E. A., Sagare, A. P., Singh, I., LaRue, B., Deane, R., & Zlokovic, B. v. (2010). Pericytes Control Key Neurovascular Functions and Neuronal Phenotype in the Adult Brain and during Brain Aging. Neuron, 68(3), 409–427. https://doi.org/10.1016/j.neuron.2010.09.043

Bellizzi, D. et al. 2012. Global DNA methylation in old subjects is correlated with frailty. Age 34(1): p.169–179.

Bendlin, B.B. et al. 2010. White matter in aging and cognition: A cross-sectional study of microstructure in adults aged eighteen to eighty-three. Developmental Neuropsychology 35(3).

Benzing, W.C. et al. 1999. Evidence for glial-mediated inflammation in aged APP(SW) transgenic

mice. Neurobiology of Aging 20(6): p.581–589.

Bercik, P., Denou, E., Collins, J., Jackson, W., Lu, J., Jury, J., Deng, Y., Blennerhassett, P., MacRi, J., McCoy, K. D., Verdu, E. F., & Collins, S. M. (2011). The intestinal microbiota affect central levels of brain-derived neurotropic factor and behavior in mice. Gastroenterology, 141(2). https://doi.org/10.1053/j.gastro.2011.04.052

Bergold, P.J. et al. 2011. Evaluation of clinically relevant rodent models of TBI. FASEB Journal 25. Available at: https://www.embase.com/search/results?subaction=viewrecord&id=L70750972&from=export%0Ahttp://www.fasebj.org/cgi/content/meeting_abstract/25/1_MeetingAbstracts/419.1?sid=a3ede77f-a9a9-4262-be9f-e33d624eed1e.

Bermejo, P., Martín-Aragón, S., Benedí, J., Susín, C., Felici, E., Gil, P., Ribera, J. M., & Villar, Á. M. (2008). Differences of peripheral inflammatory markers between mild cognitive impairment and Alzheimer's disease. Immunology Letters, 117(2), 198–202. https://doi.org/10.1016/j.imlet.2008.02.002

Bernard, J.A., Ballard, H.K., & Jackson, T.B. 2021. Cerebellar Dentate Connectivity across Adulthood: A Large-Scale Resting State Functional Connectivity Investigation. Cerebral Cortex Communications 2(3): p.1–13. Available at: https://academic.oup.com/cercorcomms/article/2/3/tgab050/6347252 [Accessed January 25, 2022].

Von Bernhardi, R., & Eugenín, J. 2004. Microglial reactivity to β-amyloid is modulated by astrocytes and proinflammatory factors. Brain Research 1025(1–2): p.186–193. Available at: https://pubmed.ncbi.nlm.nih.gov/15464759/ [Accessed August 30, 2021].

Beutler, B. et al. 1985. Identity of tumour necrosis factor and the macrophage-secreted factor cachectin. Nature 316(6028): p.552–554.

Bi, P. et al. 2016. Stage-specific effects of Notch activation during skeletal myogenesis. eLife 5.

Bittel, A.J. et al. 2020. A single bout of resistance exercise improves postprandial lipid metabolism in overweight/obese men with prediabetes. Diabetologia 63(3): p.611–623.

Blaylock, R., & Maroon, J. 2011. Immunoexcitotoxicity as a central mechanism in chronic traumatic encephalopathy-A unifying hypothesis. Surgical Neurology International 2(1): p.107.

Blekhman, R., Goodrich, J. K., Huang, K., Sun, Q., Bukowski, R., Bell, J. T., Spector, T. D., Keinan, A., Ley, R. E., Gevers, D., & Clark, A. G. (2015). Host genetic variation impacts microbiome

composition across human body sites. Genome Biology, 16(1). https://doi.org/10.1186/s13059-015-0759-1

Block, M.L., Zecca, L., & Hong, J.S. 2007. Microglia-mediated neurotoxicity: Uncovering the molecular mechanisms. Nature Reviews Neuroscience 8(1): p.57–69.

Block, R., Dorsey, E.R., Beck, C.A., Brenna, J.T., & Shoulson, I. 2010. Altered cholesterol and fatty acid metabolism in Huntington disease. Journal of Clinical Lipidology 4(1): p.17–23.

Bohland, M.A. et al. 2014. Activation of hindbrain neurons is mediated by portal-mesenteric vein glucosensors during slow-onset hypoglycemia. Diabetes 63(8).

Bocarsly, M.E. et al. 2015. Obesity diminishes synaptic markers, alters Microglial morphology, and impairs cognitive function. Proceedings of the National Academy of Sciences of the United States of America 112(51): p.15731–15736.

Boche, D., Perry, V.H., & Nicoll, J.A.R. 2013. Review: Activation patterns of microglia and their identification in the human brain. Neuropathology and Applied Neurobiology 39(1): p.3–18.

Bode, K. et al. 2019. Dectin-1 Binding to Annexins on Apoptotic Cells Induces Peripheral Immune Tolerance via NADPH Oxidase-2. Cell Reports 29(13): p.4435-4446.e9.

Bohne, P., Schwarz, M.K., Herlitze, S., & Mark, M.D. 2019. A New Projection From the Deep Cerebellar Nuclei to the Hippocampus via the Ventrolateral and Laterodorsal Thalamus in Mice. Frontiers in Neural Circuits 13: p.51

Bolton, S.J., Anthony, D.C., & Perry, V.H. 1998. Loss of the tight junction proteins occludin and zonula occludens-1 from cerebral vascular endothelium during neutrophil-induced blood-brain barrier breakdown in vivo. Neuroscience 86(4): p.1245–1257.

Bonilla, F.A., & Oettgen, H.C. 2010. Adaptive immunity. Journal of Allergy and Clinical Immunology 125(2 SUPPL. 2): p.S33–S40. Available at: http://www.jacionline.org/article/S0091674909014055/fulltext [Accessed March 17, 2021].

Borges, M.K., Canevelli, M., Cesari, M., & Aprahamian, I. 2019. Frailty as a predictor of cognitive disorders: A systematic review and meta-analysis. Frontiers in Medicine 6(FEB).

Borghesi, L., & Milcarek, C. 2006. From B cell to plasma cell: Regulation of V(D)J recombination and antibody secretion. Immunologic Research 36(1–3): p.27–32.

Bornemann, K.D. et al. 2001. Aβ-induced inflammatory processes in microglia cells of APP23 transgenic mice. American Journal of Pathology 158(1): p.63–73. Available at:

https://pubmed.ncbi.nlm.nih.gov/11141480/ [Accessed August 30, 2021].

Boros, B.D. et al. 2017. Dendritic spines provide cognitive resilience against Alzheimer's disease. Annals of Neurology 82(4): p.602–614. Available at: https://pubmed.ncbi.nlm.nih.gov/28921611/ [Accessed September 5, 2021].

Bosch-Queralt, M. et al. 2021. Diet-dependent regulation of TGFβ impairs reparative innate immune responses after demyelination. Nature Metabolism 3(2): p.211–227.

Bouillon, K. et al. 2013. Diabetes risk factors, diabetes risk algorithms, and the prediction of future frailty: The whitehall II prospective cohort study. Journal of the American Medical Directors Association 14(11): p.851.e1-851.e6.

Bouret, S.G., Draper, S.J., & Simerly, R.B. 2004. Formation of Projection Pathways from the Arcuate Nucleus of the Hypothalamus to Hypothalamic Regions Implicated in the Neural Control of Feeding Behavior in Mice. Journal of Neuroscience 24(11).

Braak, H., Braak, E., & Bohl, J. 1993. Staging of alzheimer-related cortical destruction. European Neurology 33(6): p.403–408.

Brayton, C.F., Treuting, P.M., & Ward, J.M. 2012. Pathobiology of aging mice and GEM: Background strains and experimental design. Veterinary Pathology 49(1): p.85–105.

Brown, G.D. 2006. Dectin-1 : A signalling non-TLR pattern-recognition receptor. Nature Reviews Immunology 6(1): p.33–43.

Brown, L.A. et al. 2021. Moderators of skeletal muscle maintenance are compromised in sarcopenic obese mice. Mechanisms of Ageing and Development 194: p.111404.

Brown, L.J.E. et al. 2011. Differential effects of delirium on fluid and crystallized cognitive abilities. Archives of Gerontology and Geriatrics 52(2): p.153–158.

Brown, M.S., & Goldstein, J.L. 2008. Selective versus Total Insulin Resistance: A Pathogenic Paradox. Cell Metabolism 7(2): p.95–96.

Brown, R.E., & Wong, A.A. 2007. The influence of visual ability on learning and memory performance in 13 strains of mice. Learning and Memory 14(3): p.134–144.

Bruce-Keller, A.J. et al. 2011. Cognitive impairment in humanized APP×PS1 mice is linked to Aβ 1-42 and NOX activation. Neurobiology of Disease 44(3): p.317–326.

Bruce-Keller, A. J., Salbaum, J. M., Luo, M., Blanchard, E., Taylor, C. M., Welsh, D. A., & Berthoud, H.

R. (2015). Obese-type gut microbiota induce neurobehavioral changes in the absence of obesity. Biological Psychiatry, 77(7), 607–615. https://doi.org/10.1016/j.biopsych.2014.07.012

Bruttger, J. et al. 2015. Genetic Cell Ablation Reveals Clusters of Local Self-Renewing Microglia in the Mammalian Central Nervous System. Immunity 43(1): p.92–106.

Bruunsgaard, H. 1999. A high plasma concentration of tnf-α is associated with dementia in centenarians. Journals of Gerontology - Series A Biological Sciences and Medical Sciences 54(7).

Buchhave, P. et al. 2010. Soluble TNF receptors are associated with Aβ metabolism and conversion to dementia in subjects with mild cognitive impairment. Neurobiology of Aging 31(11): p.1877–1884.

Buchman, A.S. et al. 2014. Brain pathology contributes to simultaneous change in physical frailty and cognition in old age. Journals of Gerontology - Series A Biological Sciences and Medical Sciences 69(12): p.1536–1544.

Buckman, L.B., Thompson, M.M., Moreno, H.N., & Ellacott, K.L.J. 2013. Regional astrogliosis in the mouse hypothalamus in response to obesity. Journal of Comparative Neurology 521(6): p.1322–1333.

Burd, C.E. et al. 2013. Monitoring tumorigenesis and senescence in vivo with a p16 INK4a-luciferase model. Cell 152(1–2): p.340–351.

Burda, J.E., & Sofroniew, M. V. 2014. Reactive gliosis and the multicellular response to CNS damage and disease. Neuron 81(2): p.229–248.

Burfeind, K.G., Michaelis, K.A., & Marks, D.L. 2016. The central role of hypothalamic inflammation in the acute illness response and cachexia. Seminars in Cell and Developmental Biology 54: p.42–52.

Burtner, C.R., & Kennedy, B.K. 2010. Progeria syndromes and ageing: What is the connection? Nature Reviews Molecular Cell Biology 11(8): p.567–578.

Bussian, T.J. et al. 2018. Clearance of senescent glial cells prevents tau-dependent pathology and cognitive decline. Nature 562(7728): p.578–582.

Butchart, J. et al. 2015. Etanercept in Alzheimer disease. Neurology 84(21): p.2161–2168.

Butovsky, O. et al. 2014. Identification of a unique TGF-β-dependent molecular and functional

signature in microglia. Nature Neuroscience 17(1): p.131–143.

Butterfield, D.A., & Poon, H.F. 2005. The senescence-accelerated prone mouse (SAMP8): A model of age-related cognitive decline with relevance to alterations of the gene expression and protein abnormalities in Alzheimer's disease. Experimental Gerontology 40(10): p.774–783.

Buttgereit, A. et al. 2016. Sall1 is a transcriptional regulator defining microglia identity and function. Nature Immunology 17(12): p.1397–1406.

Cadore, E.L., Rodríguez-Mañas, L., Sinclair, A., & Izquierdo, M. 2013. Effects of different exercise interventions on risk of falls, gait ability, and balance in physically frail older adults: A systematic review. Rejuvenation Research 16(2): p.105–114.

Cai, D. 2013. Neuroinflammation and neurodegeneration in overnutrition-induced diseases. Trends in Endocrinology and Metabolism 24(1): p.40–47. Available at: https://pubmed.ncbi.nlm.nih.gov/23265946/ [Accessed August 25, 2021].

Cai, H.Q. et al. 2020. Increased macrophages and changed brain endothelial cell gene expression in the frontal cortex of people with schizophrenia displaying inflammation. Molecular Psychiatry 25(4): p.761–775. Available at: https://www.nature.com/articles/s41380-018-0235-x [Accessed September 17, 2021].

Cao, B.B. et al. 2013. Cerebellar fastigial nuclear GABAergic projections to the hypothalamus modulate immune function. Brain, Behavior, and Immunity 27(1).

Canas, P.M., Duarte, J.M.N., Rodrigues, R.J., Köfalvi, A., & Cunha, R.A. 2009. Modification upon aging of the density of presynaptic modulation systems in the hippocampus. Neurobiology of Aging 30(11): p.1877–1884.

Canipe, L. G., Sioda, M., & Cheatham, C. L. (2021). Diversity of the gut-microbiome related to cognitive behavioral outcomes in healthy older adults. Archives of Gerontology and Geriatrics, 96, 104464. https://doi.org/10.1016/j.archger.2021.104464

Cantoni, C. et al. 2015. TREM2 regulates microglial cell activation in response to demyelination in vivo. Acta Neuropathologica 129(3): p.429–447.

Cao, J. et al. 2017. Behavioral changes and hippocampus glucose metabolism in APP/PS1 transgenic mice via electro-acupuncture at governor vessel acupoints. Frontiers in Aging Neuroscience 9(JAN). Available at: www.frontiersin.org.

Carcaillon, L. et al. 2012. Higher levels of endogenous estradiol are associated with frailty in

postmenopausal women from the toledo study for healthy aging. Journal of Clinical Endocrinology and Metabolism 97(8): p.2898–2906. Available at: https://pubmed.ncbi.nlm.nih.gov/22679065/ [Accessed March 17, 2021].

Carding, S., Verbeke, K., Vipond, D. T., Corfe, B. M., & Owen, L. J. (2015). Dysbiosis of the gut microbiota in disease. Microbial Ecology in Health & Disease, 26(0). https://doi.org/10.3402/mehd.v26.26191

Cardoso, A.L. et al. 2018. Towards frailty biomarkers: Candidates from genes and pathways regulated in aging and age-related diseases. Ageing Research Reviews 47: p.214–277.

Carson, M.J. et al. 2007. A Rose by Any Other Name? The Potential Consequences of Microglial Heterogeneity During CNS Health and Disease. Neurotherapeutics 4(4): p.571–579.

Carter-Dawson, L.D., LaVail, M.M., & Sidman, R.L. 1978. Differential effect of the rd mutation on rods and cones in the mouse retina. Investigative Ophthalmology and Visual Science 17(6): p.489–498.

Carter, S.F. et al. 2012. Evidence for astrocytosis in prodromal alzheimer disease provided by 11C-deuterium-L-deprenyl: A multitracer PET paradigm combining 11C-Pittsburgh compound B and 18F-FDG. Journal of Nuclear Medicine 53(1): p.37–46.

Castanon-Cervantes, O., Wu, M., Ehlen, J. C., Paul, K., Gamble, K. L., Johnson, R. L., Besing, R. C., Menaker, M., Gewirtz, A. T., & Davidson, A. J. (2010). Dysregulation of Inflammatory Responses by Chronic Circadian Disruption. The Journal of Immunology, 185(10), 5796–5805. https://doi.org/10.4049/jimmunol.1001026

Castoldi, A. et al. 2017. Dectin-1 Activation Exacerbates Obesity and Insulin Resistance in the Absence of MyD88. Cell Reports 19(11): p.2272–2288.

Cengiz, E., & Tamborlane, W. V. 2009. A tale of two compartments: Interstitial versus blood glucose monitoring. Diabetes Technology and Therapeutics 11(SUPPL.1): p.S-11. Available at: /pmc/articles/PMC2903977/ [Accessed August 21, 2021].

Chagas, E.F.B., Bonfim, M.R., Turi, B.C., Brondino, N.C.M., & Monteiro, H.L. 2017. Effect of moderate-intensity exercise on inflammatory markers among postmenopausal women. Journal of Physical Activity and Health 14(6): p.479–485.

Cham, S., Koslik, H.J., & Golomb, B.A. 2016. Mood, personality, and behavior changes during treatment with statins: A case series. Drug Safety - Case Reports 3(1).

Chang, B. et al. 2002. Retinal degeneration mutants in the mouse. Vision Research 42(4): p.517–525.

Chauhan, N.B., & Sandoval, J. 2007. Amelioration of early cognitive deficits by aged garlic extract in Alzheimer's transgenic mice. Phytotherapy Research 21(7): p.629–640.

Chen, A.Q. et al. 2019. Microglia-derived TNF-α mediates endothelial necroptosis aggravating blood brain–barrier disruption after ischemic stroke. Cell Death and Disease 10(7): p.1–18. Available at: https://www.nature.com/articles/s41419-019-1716-9 [Accessed September 19, 2021].

Chen, J. et al. 2008. Neuroinflammation and disruption in working memory in aged mice after acute stimulation of the peripheral innate immune system. Brain, Behavior, and Immunity 22(3): p.301–311.

Chen, P., Stanojcic, M., & Jeschke, M. G. (2014). Differences between murine and human sepsis. In Surgical Clinics of North America (Vol. 94, Issue 6, pp. 1135–1149). https://doi.org/10.1016/j.suc.2014.08.001

Chen, Z., Li, J., Gui, S., Zhou, C., Chen, J., Yang, C., Hu, Z., Wang, H., Zhong, X., Zeng, L., Chen, K., Li, P., & Xie, P. (2018). Comparative metaproteomics analysis shows altered fecal microbiota signatures in patients with major depressive disorder. NeuroReport, 29(5), 417–425. https://doi.org/10.1097/WNR.0000000000000985

Cherry, J.D., Olschowka, J.A., & O'Banion, M.K. 2014. Neuroinflammation and M2 microglia: The good, the bad, and the inflamed. Journal of Neuroinflammation 11(1): p.98. Available at: http://jneuroinflammation.biomedcentral.com/articles/10.1186/1742-2094-11-98 [Accessed March 20, 2021].

Chesky, J.A. 2007. THE BIOLOGY OF AGING: OBSERVATIONS & PRINCIPLES (3 rd Edition) By Robert Arking .

Cheung, T.H. et al. 2012. Maintenance of muscle stem-cell quiescence by microRNA-489. Nature 482(7386).

Chou, R.C., Kane, M., Ghimire, S., Gautam, S., & Gui, J. 2016. Treatment for Rheumatoid Arthritis and Risk of Alzheimer's Disease: A Nested Case-Control Analysis. CNS Drugs 30(11): p.1111–1120.

Choutko-Joaquim, S., Tacchini-Jacquier, N., Pralong D'alessio, G., & Verloo, H. 2019. Associations between Frailty and Delirium among Older Patients Admitted to an Emergency Department. Dementia and Geriatric Cognitive Disorders Extra 9(2): p.236–249. Available at:

http://www.karger.com/Services/OpenAccessLicense [Accessed September 2, 2021].

Chow, H.M. et al. 2019. Age-related hyperinsulinemia leads to insulin resistance in neurons and cell-cycle-induced senescence. Nature Neuroscience 22(11): p.1806–1819.

Chu, Z., Wu, Y., Dai, X., Zhang, C., & He, Q. 2021. The risk factors of postoperative delirium in general anesthesia patients with hip fracture: Attention needed. Medicine 100(22): p.e26156. Available at: https://journals.lww.com/md-journal/Fulltext/2021/06040/The_risk_factors_of_postoperative_delirium_in.56.aspx [Accessed September 22, 2021].

Chun, H., Marriott, I., Lee, C.J., & Cho, H. 2018. Elucidating the interactive roles of Glia in Alzheimer's disease using established and newly developed experimental models. Frontiers in Neurology 9(SEP): p.797. Available at: /pmc/articles/PMC6168676/ [Accessed August 30, 2021].

Clamp, L.D., Hume, D.J., Lambert, E. V., & Kroff, J. 2017. Enhanced insulin sensitivity in successful, long-term weight loss maintainers compared with matched controls with no weight loss history. Nutrition & diabetes 7(6).

Clarke, G., Stilling, R. M., Kennedy, P. J., Stanton, C., Cryan, J. F., & Dinan, T. G. (2014). Minireview: Gut microbiota: The neglected endocrine organ. Molecular Endocrinology, 28(8), 1221–1238. https://doi.org/10.1210/me.2014-1108

Clarkson, J. M., Dwyer, D. M., Flecknell, P. A., Leach, M. C., & Rowe, C. (2018). Handling method alters the hedonic value of reward in laboratory mice. Scientific Reports, 8(1). https://doi.org/10.1038/s41598-018-20716-3

Clegg, A., Young, J., Iliffe, S., Rikkert, M.O., & Rockwood, K. 2013. Frailty in elderly people. The Lancet 381(9868): p.752–762.

Coelho-Junior, H.J. et al. 2020. Protein intake and frailty: A matter of quantity, quality, and timing. Nutrients 12(10): p.1–20.

Collard, R.M., Boter, H., Schoevers, R.A., & Oude Voshaar, R.C. 2012. Prevalence of frailty in community-dwelling older persons: A systematic review. Journal of the American Geriatrics Society 60(8): p.1487–1492.

Collerton, J. et al. 2012. Frailty and the role of inflammation, immunosenescence and cellular ageing in the very old: Cross-sectional findings from the Newcastle 85+ Study. Mechanisms of Ageing and Development 133(6): p.456–466.

Collerton, J. et al. 2014. Acquisition of aberrant DNA methylation is associated with frailty in the very old: Findings from the Newcastle 85+ Study. Biogerontology 15(4): p.317–328.

Combrinck, M.I., Perry, V.H., & Cunningham, C. 2002. Peripheral infection evokes exaggerated sickness behaviour in pre-clinical murine prion disease. Neuroscience 112(1): p.7–11.

Connolly, S., Gillespie, P., O'Shea, E., Cahill, S., & Pierce, M. 2014. Estimating the economic and social costs of dementia in Ireland. Dementia 13(1): p.5–22.

Cope, A.P. et al. 1997. Chronic tumor necrosis factor alters T cell responses by attenuating T cell receptor signaling. Journal of Experimental Medicine 185(9): p.1573–1584.

Coppé, J.P. et al. 2008. Senescence-associated secretory phenotypes reveal cell-nonautonomous functions of oncogenic RAS and the p53 tumor suppressor. PLoS biology 6(12). Available at: www.plosbiology.org.

Coppé, J.P., Desprez, P.Y., Krtolica, A., & Campisi, J. 2010. The senescence-associated secretory phenotype: The dark side of tumor suppression. Annual Review of Pathology: Mechanisms of Disease 5: p.99–118.

Corder, E.H. et al. 1993. Gene dose of apolipoprotein E type 4 allele and the risk of Alzheimer's disease in late onset families. Science 261(5123): p.921–923.

Couturier, J. et al. 2016. Activation of phagocytic activity in astrocytes by reduced expression of the inflammasome component ASC and its implication in a mouse model of Alzheimer disease. Journal of Neuroinflammation 13(1): p.1–13. Available at: https://jneuroinflammation.biomedcentral.com/articles/10.1186/s12974-016-0477-y [Accessed September 24, 2021].

Crow, R.S. et al. 2019. Association of Obesity and Frailty in Older Adults: NHANES 1999–2004. Journal of Nutrition, Health and Aging 23(2): p.138–144.

Cruz-Jentoft, A.J. et al. 2010. Sarcopenia: European consensus on definition and diagnosis. Age and Ageing 39(4): p.412–423.

Cuervo, A.M. 2003. Autophagy and aging--when 'all you can eat' is yourself. Science of aging knowledge environment : SAGE KE 2003(36).

Cuervo, A.M., & Dice, J.F. 2000. When lysosomes get old. Experimental Gerontology 35(2): p.119–131.

Cui, L.Y., Chu, S.F., & Chen, N.H. 2020. The role of chemokines and chemokine receptors in multiple

sclerosis. International Immunopharmacology 83.

Cui, Z., Gerfen, C.R., & Young, W.S. 2013. Hypothalamic and other connections with dorsal CA2 area of the mouse hippocampus. Journal of Comparative Neurology 521(8): p.1844–1866.

Cummings, D., & Merriam, G. 1999. Age-related changes in growth hormone secretion: Should the somatopause be treated? Seminars in Reproductive Endocrinology 17(4): p.311–325.

Cummings, D., & Merriam, G. 2003. Growth Hormone Therapy in Adults. Annual Review of Medicine 54: p.513–533. Available at: https://www.annualreviews.org/doi/abs/10.1146/annurev.med.54.101601.152147 [Accessed August 28, 2021].

Cunningham, C. et al. 2009. Systemic Inflammation Induces Acute Behavioral and Cognitive Changes and Accelerates Neurodegenerative Disease. Biological Psychiatry 65(4): p.304–312.

Cunningham, C., Dunne, A., & Lopez-Rodriguez, A.B. 2019. Astrocytes: Heterogeneous and Dynamic Phenotypes in Neurodegeneration and Innate Immunity. Neuroscientist 25(5): p.455–474.

Cunningham, C., & MacLullich, A.M.J. 2013. At the extreme end of the psychoneuroimmunological spectrum: Delirium as a maladaptive sickness behaviour response. Brain, Behavior, and Immunity 28: p.1–13.

Cunningham, C., Wilcockson, D.C., Campion, S., Lunnon, K., & Perry, V.H. 2005. Central and systemic endotoxin challenges exacerbate the local inflammatory response and increase neuronal death during chronic neurodegeneration. Journal of Neuroscience 25(40): p.9275–9284.

Cushing, S.D. et al. 1990. Minimally modified low density lipoprotein induces monocyte chemotactic protein 1 in human endothelial cells and smooth muscle cells. Proceedings of the National Academy of Sciences of the United States of America 87(13): p.5134–5138.

Custódio, C. S., Mello, B. S. F., Cordeiro, R. C., de Araújo, F. Y. R., Chaves, J. H., Vasconcelos, S. M. M., Júnior, H. V. N., de Sousa, F. C. F., Vale, M. L., Carvalho, A. F., & Macêdo, D. S. (2013). Time course of the effects of lipopolysaccharide on prepulse inhibition and brain nitrite content in mice. European Journal of Pharmacology, 713(1–3), 31–38. https://doi.org/10.1016/j.ejphar.2013.04.040

D'Mello, C., Le, T., & Swain, M.G. 2009. Cerebral microglia recruit monocytes into the brain in response to tumor necrosis factora signaling during peripheral organ inflammation. Journal of Neuroscience 29(7): p.2089–2102.

D'Mello, C., & Swain, M.G. 2014. Liver-brain interactions in inflammatory liver diseases: Implications for fatigue and mood disorders. Brain, Behavior, and Immunity 35: p.9–20.

Daley, D. et al. 2017. Dectin 1 activation on macrophages by galectin 9 promotes pancreatic carcinoma and peritumoral immune tolerance. Nature Medicine 23(5): p.556–567. Available at: https://www.nature.com/articles/nm.4314 [Accessed July 5, 2021].

Dantzer, R. et al. 1998. Molecular basis of sickness behavior. In Annals of the New York Academy of Sciences, 132–138.

Dantzer, R., O'Connor, J.C., Freund, G.G., Johnson, R.W., & Kelley, K.W. 2008. From inflammation to sickness and depression: When the immune system subjugates the brain. Nature Reviews Neuroscience 9(1): p.46–56.

Datusalia, A.K., Agarwal, P., Singh, J.N., & Sharma, S.S. 2018. Hyper-insulinemia increases the glutamate-excitotoxicity in cortical neurons: A mechanistic study. European Journal of Pharmacology 833: p.524–530.

Davalos, D. et al. 2005. ATP mediates rapid microglial response to local brain injury in vivo. Nature Neuroscience 8(6): p.752–758.

David, L. A., Maurice, C. F., Carmody, R. N., Gootenberg, D. B., Button, J. E., Wolfe, B. E., Ling, A. v., Devlin, A. S., Varma, Y., Fischbach, M. A., Biddinger, S. B., Dutton, R. J., & Turnbaugh, P. J. (2014). Diet rapidly and reproducibly alters the human gut microbiome. Nature, 505(7484), 559–563. https://doi.org/10.1038/nature12820

Davidson, T. L., Monnot, A., Neal, A. U., Martin, A. A., Horton, J. J., & Zheng, W. (2012). The effects of a high-energy diet on hippocampal-dependent discrimination performance and blood-brain barrier integrity differ for diet-induced obese and diet-resistant rats. Physiology and Behavior, 107(1), 26–33. https://doi.org/10.1016/j.physbeh.2012.05.015

Davis, D.H.J. et al. 2012. Delirium is a strong risk factor for dementia in the oldest-old: A population-based cohort study. Brain 135(9): p.2809–2816.

Davis, D.H.J. et al. 2015. Worsening cognitive impairment and neurodegenerative pathology progressively increase risk for delirium. American Journal of Geriatric Psychiatry 23(4): p.403–415.

Davis, D.H.J. et al. 2017. Association of delirium with cognitive decline in late life: A neuropathologic study of 3 population-based cohort studies. JAMA Psychiatry 74(3): p.244–251.

Deacon, R.M.J. 2006. Burrowing in rodents: A sensitive method for detecting behavioral dysfunction. Nature Protocols 1(1): p.118–121.

Deacon, R.M.J. 2013. Measuring the strength of mice. Journal of visualized experiments : JoVE (76).

Deacon, R.M.J., & Rawlins, J.N.P. 2002. Learning impairments of hippocampal-lesioned mice in a paddling pool. Behavioral Neuroscience 116(3): p.472–478.

Deerhake, M.E. et al. 2021. Dectin-1 limits autoimmune neuroinflammation and promotes myeloid cell-astrocyte crosstalk via Card9-independent expression of Oncostatin M. Immunity 54(3): p.484-498.e8.

Deerhake, M.E., Biswas, D.D., Barclay, W.E., & Shinohara, M.L. 2019. Pattern Recognition Receptors in Multiple Sclerosis and Its Animal Models. Frontiers in Immunology 10.

Dejanovic, B. et al. 2018. Changes in the Synaptic Proteome in Tauopathy and Rescue of Tau-Induced Synapse Loss by C1q Antibodies. Neuron 100(6): p.1322-1336.e7. Available at: https://pubmed.ncbi.nlm.nih.gov/30392797/ [Accessed September 1, 2021].

Dekaban, A.S., & Sadowsky, D. 1978. Changes in brain weights during the span of human life: Relation of brain weights to body heights and body weights. Annals of Neurology 4(4): p.345–356.

Deli, M.A. et al. 1995. Exposure of tumor necrosis factor - α to luminal membrane of bovine brain capillary endothelial cells cocultured with astrocytes induces a delayed increase of permeability and cytoplasmic stress fiber formation of actin. Journal of Neuroscience Research 41(6): p.717–726. Available at: https://onlinelibrary.wiley.com/doi/full/10.1002/jnr.490410602 [Accessed September 18, 2021].

Dennehy, K.M., & Brown, G.D. 2007. The role of the β-glucan receptor Dectin-1 in control of fungal infection. Journal of Leukocyte Biology 82(2): p.253–258.

Dent, E. et al. 2019. Management of frailty: opportunities, challenges, and future directions. The Lancet 394(10206): p.1376–1386.

Dermietzel, R., Spray, D.C., & Nedergaard, M. 2007. Blood-Brain Barriers: From Ontogeny to Artificial Interfaces.

Deshmane, S.L., Kremlev, S., Amini, S., & Sawaya, B.E. 2009. Monocyte chemoattractant protein-1 (MCP-1): An overview. Journal of Interferon and Cytokine Research 29(6): p.313–325.

Desseille, C. et al. 2017. Specific physical exercise improves energetic metabolism in the skeletal muscle of amyotrophic-lateral- sclerosis mice. Frontiers in Molecular Neuroscience 10.

Van Deursen, J.M. 2014. The role of senescent cells in ageing. Nature 509(7501): p.439–446.

Dienel, G.A. 2019. Brain glucose metabolism: Integration of energetics with function. Physiological Reviews 99(1): p.949–1045.

Dietrichs, E., Haines, D. E., Roste, G. K., & Roste, L. S. (1994). Hypothalamocerebellar and cerebollohypothalamic projections - Circuits for regulating nonsomatic cerebellar activity? In Histology and Histopathology (Vol. 9, Issue 3, pp. 603–614).

van Dijk, G. et al. 2015. Integrative neurobiology of metabolic diseases, neuroinflammation, and neurodegeneration. Frontiers in Neuroscience 9(APR).

Dilger, R.N., & Johnson, R.W. 2008. Aging, microglial cell priming, and the discordant central inflammatory response to signals from the peripheral immune system. Journal of Leukocyte Biology 84(4): p.932–939.

Dinarello, C.A. 2005. Blocking IL-1 in systemic inflammation. Journal of Experimental Medicine 201(9): p.1355–1359.

Ding, J. et al. 2019. β-Glucan induces autophagy in dendritic cells and influences T-cell differentiation. Medical Microbiology and Immunology 208(1): p.39–48.

Ding, J., Sackmann-Sala, L., & Kopchick, J. J. (2013). Mouse models of growth hormone action and aging: A proteomic perspective. Proteomics, 13(3–4), 674–685. https://doi.org/10.1002/pmic.201200271

Ding, Q. et al. 2003. Characterization of chronic low-level proteasome inhibition on neural homeostasis. Journal of Neurochemistry 86(2): p.489–497.

Dobrescu, S.R. et al. 2020. Anorexia nervosa: 30-year outcome. British Journal of Psychiatry 216(2): p.97–104.

Dragicevic, N. et al. 2010. Mitochondrial amyloid-β levels are associated with the extent of mitochondrial dysfunction in different brain regions and the degree of cognitive impairment in Alzheimer's transgenic mice. Journal of Alzheimer's Disease 20(SUPPL.2).

Duarte, A.I., Moreira, P.I., & Oliveira, C.R. 2012. Insulin in central nervous system: More than just a peripheral hormone. Journal of Aging Research 2012.

Dubal, D.B., Broestl, L., & Worden, K. 2012. Sex and gonadal hormones in mouse models of Alzheimer's disease: What is relevant to the human condition? Biology of Sex Differences 3(1).

DuBois, R.N. et al. 1998. Cyclooxygenase in biology and disease. The FASEB Journal 12(12): p.1063–1073.

Dudvarski Stankovic, N., Teodorczyk, M., Ploen, R., Zipp, F., & Schmidt, M.H.H. 2016. Microglia–blood vessel interactions: a double-edged sword in brain pathologies. Acta Neuropathologica 131(3): p.347–363.

Dukart, J. et al. 2013. Relationship between imaging biomarkers, age, progression and symptom severity in Alzheimer's disease. NeuroImage: Clinical 3: p.84–94.

Dunkelberger, J.R., & Song, W.C. 2010. Complement and its role in innate and adaptive immune responses. Cell Research 20(1): p.34–50.

Eckel, R.H. et al. 2011. Obesity and type 2 diabetes: What Can be unified and what needs to be individualized? In Diabetes Care, 1424–1430.

Eeles, E.M.P., White, S. V., O'mahony, S.M., Bayer, A.J., & Hubbard, R.E. 2012. The impact of frailty and delirium on mortality in older inpatients. Age and Ageing 41(3): p.412–416.

Elder, M.J. et al. 2017. β-glucan size controls dectin-1-mediated immune responses in human dendritic cells by regulating IL-1β production. Frontiers in Immunology 8(JUL): p.791.

Elie, M., Cole, M.G., Primeau, F.J., & Bellavance, F. 1998. Delirium risk factors in elderly hospitalized patients. Journal of General Internal Medicine 13(3): p.204–212.

Elmore, M.R.P. et al. 2014. Colony-stimulating factor 1 receptor signaling is necessary for microglia viability, unmasking a microglia progenitor cell in the adult brain. Neuron 82(2): p.380–397.

Elmquist, J.K., Scammell, T.E., & Saper, C.B. 1997. Mechanisms of CNS response to systemic immune challenge: The febrile response. Trends in Neurosciences 20(12).

Ely, E.W. et al. 2004. Delirium as a Predictor of Mortality in Mechanically Ventilated Patients in the Intensive Care Unit. Journal of the American Medical Association 291(14): p.1753–1762.

Emmerzaal, T.L., Kiliaan, A.J., & Gustafson, D.R. 2015. 2003-2013: A decade of body mass index, Alzheimer's disease, and dementia. Journal of Alzheimer's Disease 43(3): p.739–755.

Engelhardt, B. 2010. T cell migration into the central nervous system during health and disease: Different molecular keys allow access to different central nervous system compartments.

Clinical and Experimental Neuroimmunology 1(2): p.79–93.

Engelhardt, B., & Ransohoff, R.M. 2005. The ins and outs of T-lymphocyte trafficking to the CNS: Anatomical sites and molecular mechanisms. Trends in Immunology 26(9).

Engelhardt, B., Vajkoczy, P., & Weller, R.O. 2017. The movers and shapers in immune privilege of the CNS. Nature Immunology 18(2): p.123–131.

Epelman, S., Lavine, K.J., & Randolph, G.J. 2014. Origin and Functions of Tissue Macrophages. Immunity 41(1): p.21–35. Available at: /pmc/articles/PMC4470379/ [Accessed January 12, 2022].

Eren, M., Boe, A.E., Klyachko, E.A., & Vaughan, D.E. 2014. Role of plasminogen activator inhibitor-1 in senescence and aging. Seminars in Thrombosis and Hemostasis 40(6): p.645–651. Available at: /pmc/articles/PMC6563930/ [Accessed August 26, 2021].

Eroglu, C. 2009. The role of astrocyte-secreted matricellular proteins in central nervous system development and function. Journal of Cell Communication and Signaling 3(3–4): p.167–176.

Ershler, W.B., & Keller, E.T. 2000. Age-associated increased interleukin-6 gene expression, late-life diseases, and frailty. Annual Review of Medicine 51: p.245–270.

Escartin, C. et al. 2021. Reactive astrocyte nomenclature, definitions, and future directions. Nature Neuroscience 24(3): p.312–325.

Esiri, M.M. 2007. Ageing and the brain. Journal of Pathology 211(2): p.181–187.

Eyüpoglu, I.Y., Bechmann, I., & Nitsch, R. 2003. Modification of microglia function protects from lesion-induced neuronal alterations and promotes sprouting in the hippocampus. The FASEB journal : official publication of the Federation of American Societies for Experimental Biology 17(9): p.1110–1111.

Fan, X. et al. 2021. High-Fat Diet Alleviates Neuroinflammation and Metabolic Disorders of APP/PS1 Mice and the Intervention With Chinese Medicine. Frontiers in Aging Neuroscience 13: p.277.

Farr, S.A. et al. 2003. The antioxidants α-lipoic acid and N-acetylcysteine reverse memory impairment and brain oxidative stress in aged SAMP8 mice. Journal of Neurochemistry 84(5): p.1173–1183. Available at: http://doi.wiley.com/10.1046/j.1471-4159.2003.01580.x [Accessed March 20, 2021].

Farrall, A.J., & Wardlaw, J.M. 2009. Blood-brain barrier: Ageing and microvascular disease - systematic review and meta-analysis. Neurobiology of Aging 30(3): p.337–352.

Farthing, M.J.G. 1995. Irritable bowel, irritable body or irritable brain? Biomedicine and Pharmacotherapy 49(6): p.312–313.

Feghali, C.A., & Wright, T.M. 1997. Cytokines in acute and chronic inflammation. Frontiers in bioscience : a journal and virtual library 2.

Feldman, E. 2018. Mediterranean diet and frailty risk. Integrative Medicine Alert 21(4): p.37–40.

Ferreira, L.S.S., Fernandes, C.S., Vieira, M.N.N., & De Felice, F.G. 2018. Insulin resistance in Alzheimer's disease. Frontiers in Neuroscience 12(NOV).

Ferrero-Miliani, L., Nielsen, O.H., Andersen, P.S., & Girardin, S.E. 2007. Chronic inflammation: Importance of NOD2 and NALP3 in interleukin-1β generation. Clinical and Experimental Immunology 147(2): p.227–235.

Ferretti, M.T. et al. 2018. Sex differences in Alzheimer disease — The gateway to precision medicine. Nature Reviews Neurology 14(8): p.457–469.

Field, R.H., Gossen, A., & Cunningham, C. 2012. Prior pathology in the basal forebrain cholinergic system predisposes to inflammation-induced working memory deficits: Reconciling inflammatory and cholinergic hypotheses of delirium. Journal of Neuroscience 32(18): p.6288–6294.

Fiers, W. 1991. Tumor necrosis factor Characterization at the molecular, cellular and in vivo level. FEBS Letters 285(2): p.199–212.

File, S. E. (1978). The ontogeny of exploration in the rat: Habituation and effects of handling. Developmental Psychobiology, 11(4), 321–328. https://doi.org/10.1002/dev.420110405

Fink, M. P. (2014). Animal models of sepsis. In Virulence (Vol. 5, Issue 1, pp. 143–153). https://doi.org/10.4161/viru.26083

Flanary, B.E., Sammons, N.W., Nguyen, C., Walker, D., & Streit, W.J. 2007. Evidence that aging and amyloid promote microglial cell senescence. Rejuvenation Research 10(1): p.61–74.

La Fleur, S.E., Kalsbeek, A., Wortel, J., & Buijs, R.M. 2000. Polysynaptic neural pathways between the hypothalamus, including the suprachiasmatic nucleus, and the liver. Brain Research 871(1).

Flood, J.F., Farr, 1. Susan A., Kaiser, F.E., & Morley, J.E. 1995. Age-related impairment in learning but not memory in SAMP8 female mice. Pharmacology, Biochemistry and Behavior 50(4): p.661–664.

Foley, A.M., Ammar, Z.M., Lee, R.H., & Mitchell, C.S. 2015. Systematic review of the relationship between amyloid-β levels and measures of transgenic mouse cognitive deficit in Alzheimer's disease. Journal of Alzheimer's Disease 44(3): p.787–795.

Fong, T.G. et al. 2009. Delirium accelerates cognitive decline in alzheimer disease. Neurology 72(18): p.1570–1575.

Fong, T.G., Davis, D., Growdon, M.E., Albuquerque, A., & Inouye, S.K. 2015. The interface between delirium and dementia in elderly adults. The Lancet Neurology 14(8): p.823–832.

Fortier, M.E. et al. 2004. The viral mimic, polyinosinic:polycytidylic acid, induces fever in rats via an interleukin-1-dependent mechanism. American Journal of Physiology - Regulatory Integrative and Comparative Physiology 287(4 56-4).

Fraker, D.L., Sheppard, B.C., & Norton, J.A. 1990. Impact of Tolerance on Antitumor Efficacy of Tumor Necrosis Factor in Mice. Cancer Research 50(8): p.2261–2267.

Fraker, D.L., Stovroff, M.C., Merino, M.J., & Norton, J.A. 1988. Tolerance to tumor necrosis factor in rats and the relationship to endotoxin tolerance and toxicity. Journal of Experimental Medicine 168(1): p.95–105.

Franceschi, C. et al. 2000. Inflamm-aging. An evolutionary perspective on immunosenescence. Annals of the New York Academy of Sciences 908: p.244–254.

Franceschi, C., Zaikin, A., et al. 2018. Inflammaging 2018: An update and a model. Seminars in Immunology 40: p.1–5.

Franceschi, C., & Campisi, J. 2014. Chronic inflammation (Inflammaging) and its potential contribution to age-associated diseases. Journals of Gerontology - Series A Biological Sciences and Medical Sciences 69: p.S4–S9.

Franceschi, C., Garagnani, P., Parini, P., Giuliani, C., & Santoro, A. 2018. Inflammaging: a new immune–metabolic viewpoint for age-related diseases. Nature Reviews Endocrinology 14(10): p.576–590.

Franceschi, C., Garagnani, P., Vitale, G., Capri, M., & Salvioli, S. 2017. Inflammaging and 'Garb-aging'. Trends in Endocrinology and Metabolism 28(3): p.199–212.

Franco, C. et al. 2005. Growth hormone treatment reduces abdominal visceral fat in postmenopausal women with abdominal obesity: A 12-month placebo-controlled trial. Journal of Clinical Endocrinology and Metabolism 90(3): p.1466–1474.

Freeman, L. R., & Granholm, A. C. E. (2012). Vascular changes in rat hippocampus following a high saturated fat and cholesterol diet. Journal of Cerebral Blood Flow and Metabolism, 32(4), 643–653. https://doi.org/10.1038/jcbfm.2011.168

Fried, L.P. et al. 2001. Frailty in older adults: Evidence for a phenotype. Journals of Gerontology - Series A Biological Sciences and Medical Sciences 56(3).

Friedrich, N. et al. 2012. The association between IGF-I and insulin resistance: A general population study in Danish adults. Diabetes Care 35(4): p.768–773.

Frison, E. et al. 2017. Plasma fatty acid biomarkers are associated with gait speed in community-dwelling older adults: The Three-City-Bordeaux study. Clinical Nutrition 36(2): p.416–422.

Fu, X. et al. 2021. Inhibition of Dectin-1 Ameliorates Neuroinflammation by Regulating Microglia/Macrophage Phenotype After Intracerebral Hemorrhage in Mice. Translational Stroke Research. Available at: https://pubmed.ncbi.nlm.nih.gov/33539006/ [Accessed July 5, 2021].

Fujita, T. et al. 2015. A high-fat diet delays age-related hearing loss progression in C57BL/6J mice. PLoS ONE 10(1).

Fuller, S., Münch, G., & Steele, M. 2009. Activated astrocytes: A therapeutic target in Alzheimer's disease? Expert Review of Neurotherapeutics 9(11): p.1585–1594.

Furman, J.L. et al. 2012. Targeting astrocytes Ameliorates neurologic changes in a mouse model of Alzheimer's disease. Journal of Neuroscience 32(46): p.16129–16140.

Gabay, C. 2006. Interleukin-6 and chronic inflammation. Arthritis Research and Therapy 8(SUPPL. 2): p.S3. Available at: /pmc/articles/PMC3226076/ [Accessed August 28, 2021].

Gabay, C., Smith, M.F., Eidlen, D., & Arend, W.P. 1997. Interleukin 1 receptor antagonist (IL-1Ra) is an acute-phase protein. Journal of Clinical Investigation 99(12): p.2930–2940.

Gabriely, I., Xiao Hui, M., Yang, X.M., Rossetti, L., & Barzilai, N. 2002. Leptin resistance during aging is independent of fat mass. Diabetes 51(4): p.1016–1021.

Gale, C.R., Baylis, D., Cooper, C., & Sayer, A.A. 2013. Inflammatory markers and incident frailty in men and women: The english longitudinal study of ageing. Age 35(6): p.2493–2501.

Gale, C.R., Marioni, R.E., Harris, S.E., Starr, J.M., & Deary, I.J. 2018. DNA methylation and the epigenetic clock in relation to physical frailty in older people: The Lothian Birth Cohort 1936. Clinical Epigenetics 10(1).

Galea, I., Bechmann, I., & Perry, V.H. 2007. What is immune privilege (not)? Trends in Immunology 28(1): p.12–18.

Galea, L.A.M., Frick, K.M., Hampson, E., Sohrabji, F., & Choleris, E. 2017. Why estrogens matter for behavior and brain health. Neuroscience and Biobehavioral Reviews 76: p.363–379.

Gallagher, J.J., Minogue, A.M., & Lynch, M.A. 2012. Impaired performance of female APP/PS1 mice in the morris water maze is coupled with increased Aβ accumulation and microglial activation. Neurodegenerative Diseases 11(1): p.33–41. Available at: https://pubmed.ncbi.nlm.nih.gov/22627185/ [Accessed September 7, 2021].

Gallo, R.L., & Nakatsuji, T. 2011. Microbial symbiosis with the innate immune defense system of the skin. Journal of Investigative Dermatology 131(10): p.1974–1980.

Gamba, P. et al. 2019. A crosstalk between brain cholesterol oxidation and glucose metabolism in Alzheimer's disease. Frontiers in Neuroscience 13(MAY): p.556.

Gao, G.S. et al. 2017. Humanin analogue, S14G-humanin, has neuroprotective effects against oxygen glucose deprivation/reoxygenation by reactivating Jak2/Stat3 signaling through the PI3K/AKT pathway. Experimental and Therapeutic Medicine 14(4): p.3926–3934.

Gareau, M. G., Wine, E., Rodrigues, D. M., Cho, J. H., Whary, M. T., Philpott, D. J., MacQueen, G., & Sherman, P. M. (2011). Bacterial infection causes stress-induced memory dysfunction in mice. Gut, 60(3), 307–317. https://doi.org/10.1136/gut.2009.202515

García-Esquinas, E. et al. 2016. Consumption of fruit and vegetables and risk of frailty: A dose-response analysis of 3 prospective cohorts of community-dwelling older adults. American Journal of Clinical Nutrition.

Gasparotto, J. et al. 2018. Receptor for advanced glycation end products mediates sepsis-triggered amyloid-β accumulation, Tau phosphorylation, and cognitive impairment. Journal of Biological Chemistry 293(1): p.226–244.

Gauldie, J., Richards, C., Harnish, D., Lansdorp, P., & Baumann, H. 1987. Interferon beta 2/B-cell stimulatory factor type 2 shares identity with monocyte-derived hepatocyte-stimulating factor and regulates the major acute phase protein response in liver cells. Proceedings of the National Academy of Sciences of the United States of America 84(20): p.7251–7255.

Gavard, J. 2014. Endothelial permeability and VE-cadherin: A wacky comradeship. Cell Adhesion and Migration 8(2): p.158–164.

Gavillet, M., Allaman, I., & Magistretti, P.J. 2008. Modulation of astrocytic metabolic phenotype by proinflammatory cytokines. Glia 56(9): p.975–989.

Gefen, T. et al. 2019. Activated microglia in cortical white matter across cognitive aging trajectories. Frontiers in Aging Neuroscience 11(MAY).

Geifman, N., Brinton, R.D., Kennedy, R.E., Schneider, L.S., & Butte, A.J. 2017. Evidence for benefit of statins to modify cognitive decline and risk in Alzheimer's disease. Alzheimer's Research and Therapy 9(1).

Gensel, J.C. et al. 2015. Toll-Like receptors and Dectin-1, a C-type lectin receptor, trigger divergent functions in CNS macrophages. Journal of Neuroscience 35(27): p.9966–9976.

George, J., Bleasdale, S., & Singleton, S.J. 1997. Causes and prognosis of deliriun in elderly patients admitted to a district general hospital. Age and Ageing 26(6): p.423–427.

Gerszten, R.E. et al. 1999. MCP-1 and IL-8 trigger firm adhesion of monocytes to vascular endothelium under flow conditions. Nature 398(6729): p.718–725.

Ghosh, C. et al. 2018. Modulation of glucocorticoid receptor in human epileptic endothelial cells impacts drug biotransformation in an in vitro blood–brain barrier model. Epilepsia 59(11): p.2049–2060. Available at: https://pubmed.ncbi.nlm.nih.gov/30264400/ [Accessed September 19, 2021].

Gill, T.M., Gahbauer, E.A., Han, L., & Allore, H.G. 2010. Trajectories of Disability in the Last Year of Life. New England Journal of Medicine 362(13): p.1173–1180.

Giné-Garriga, M., Roqué-Fíguls, M., Coll-Planas, L., Sitjà-Rabert, M., & Salvà, A. 2014. Physical exercise interventions for improving performance-based measures of physical function in community-dwelling, frail older adults: A systematic review and meta-analysis. Archives of Physical Medicine and Rehabilitation 95(4).

Ginhoux, F. et al. 2010. Fate mapping analysis reveals that adult microglia derive from primitive macrophages. Science 330(6005): p.841–845.

Giridharan, V. V., Masud, F., Petronilho, F., Dal-Pizzol, F., & Barichello, T. 2019. Infection-induced systemic inflammation is a potential driver of Alzheimer's disease progression. Frontiers in Aging Neuroscience 11(MAY).

Glass, C.K., Saijo, K., Winner, B., Marchetto, M.C., & Gage, F.H. 2010. Mechanisms Underlying Inflammation in Neurodegeneration. Cell 140(6): p.918–934.

Glenner, G.G., & Wong, C.W. 1984. Alzheimer's disease: Initial report of the purification and characterization of a novel cerebrovascular amyloid protein. Biochemical and Biophysical Research Communications 120(3): p.885–890.

Godbout, J.P. et al. 2005. Exaggerated neuroinflammation and sickness behavior in aged mice after activation of the peripheral innate immune system. The FASEB Journal 19(10): p.1329–1331.

Godbout, J.P. et al. 2008. Aging exacerbates depressive-like behavior in mice in response to activation of the peripheral innate immune system. Neuropsychopharmacology 33(10): p.2341–2351.

Godoy, M.C.P., Tarelli, R., Ferrari, C.C., Sarchi, M.I., & Pitossi, F.J. 2008. Central and systemic IL-1 exacerbates neurodegeneration and motor symptoms in a model of Parkinson's disease. Brain 131(7): p.1880–1894.

Golden, E. et al. 2010. Circulating brain-derived neurotrophic factor and indices of metabolic and cardiovascular health: Data from the baltimore longitudinal study of aging. PLoS ONE 5(4).

Goldfeld, A.E., & Tsai, E.Y. 1996. TNF-α and genetic susceptibility to parasitic disease. Experimental Parasitology 84(2): p.300–303.

Goldmann, T. et al. 2013. A new type of microglia gene targeting shows TAK1 to be pivotal in CNS autoimmune inflammation. Nature Neuroscience 16(11): p.1618–1626.

Golub, M.S. et al. 2008. Behavioral consequences of ovarian atrophy and estrogen replacement in the APPswe mouse. Neurobiology of Aging 29(10): p.1512–1523.

Gon, Y. et al. 1996. Lower serum concentrations of cytokines in elderly patients with pneumonia and the impaired production of cytokines by peripheral blood monocytes in the elderly. Clinical and experimental immunology 106(1): p.120–6. Available at: http://www.ncbi.nlm.nih.gov/pubmed/8870709.

Gonzalez-Meljem, J.M., Apps, J.R., Fraser, H.C., & Martinez-Barbera, J.P. 2018. Paracrine roles of cellular senescence in promoting tumourigenesis. British Journal of Cancer 118(10).

Gouveia, K., & Hurst, J. L. (2013). Reducing Mouse Anxiety during Handling: Effect of Experience with Handling Tunnels. PLoS ONE, 8(6). https://doi.org/10.1371/journal.pone.0066401

Gouveia, K., & Hurst, J. L. (2017). Optimising reliability of mouse performance in behavioural testing: The major role of non-aversive handling. Scientific Reports, 7(1), 1–12. https://doi.org/10.1038/srep44999

Gordon, S., & Plüddemann, A. 2017. Tissue macrophages: Heterogeneity and functions. BMC Biology 15(1).

Gorina, R., Lyck, R., Vestweber, D., & Engelhardt, B. 2014. β 2 Integrin–Mediated Crawling on Endothelial ICAM-1 and ICAM-2 Is a Prerequisite for Transcellular Neutrophil Diapedesis across the Inflamed Blood–Brain Barrier . The Journal of Immunology 192(1): p.324–337. Available at: http://www.jimmunol.org/content/192/1/324.

Goto, M. 2010. Immune system-driven human ageing:Inflammageing. International Journal of Cosmetic Science 32(2): p.163–163.

Grabert, K. et al. 2016. Microglial brain regionâ 'dependent diversity and selective regional sensitivities to aging. Nature Neuroscience 19(3): p.504–516.

De Groot, C.J.A., Huppes, W., Sminia, T., Kraal, G., & Dijkstra, C.D. 1992. Determination of the origin and nature of brain macrophages and microglial cells in mouse central nervous system, using non‐radioactive in situ hybridization and immunoperoxidase techniques. Glia 6(4): p.301–309.

Gross, P.M. 1992. Circumventricular organ capillaries. Progress in Brain Research 91(C): p.219–233.

Gudala, K., Bansal, D., Schifano, F., & Bhansali, A. 2013. Diabetes mellitus and risk of dementia: A meta-analysis of prospective observational studies. Journal of Diabetes Investigation 4(6): p.640–650.

Guerrero-Vargas, N. N., Guzmán-Ruiz, M., Fuentes, R., García, J., Salgado-Delgado, R., Basualdo, M. D. C., Escobar, C., Markus, R. P., & Buijs, R. M. (2015). Shift work in rats results in increased inflammatory response after lipopolysaccharide administration. Journal of Biological Rhythms, 30(4), 318–330. https://doi.org/10.1177/0748730415586482

Guerrero-Vargas, N. N., Salgado-Delgado, R., Basualdo, M. del C., García, J., Guzmán-Ruiz, M., Carrero, J. C., Escobar, C., & Buijs, R. M. (2014). Reciprocal interaction between the suprachiasmatic nucleus and the immune system tunes down the inflammatory response to lipopolysaccharide. Journal of Neuroimmunology, 273(1–2), 22–30. https://doi.org/10.1016/j.jneuroim.2014.05.012

Guillemot-Legris, O. et al. 2016. High-fat diet feeding differentially affects the development of inflammation in the central nervous system. Journal of Neuroinflammation 13(1).

Guillot-Sestier, M.V. et al. 2021. Microglial metabolism is a pivotal factor in sexual dimorphism in Alzheimer's disease. Communications Biology 4(1). Available at:

https://doi.org/10.1038/s42003-021-02259-y.

Gupta, Sunita, Knight, A.G., Gupta, Shruti, Keller, J.N., & Bruce-Keller, A.J. 2012. Saturated long-chain fatty acids activate inflammatory signaling in astrocytes. Journal of Neurochemistry 120(6): p.1060–1071.

Gurung, M., Li, Z., You, H., Rodrigues, R., Jump, D. B., Morgun, A., & Shulzhenko, N. (2020). Role of gut microbiota in type 2 diabetes pathophysiology. EBioMedicine, 51, 102590. https://doi.org/10.1016/j.ebiom.2019.11.051

Gutierrez, E.G., Banks, W.A., & Kastin, A.J. 1993. Murine tumor necrosis factor alpha is transported from blood to brain in the mouse. Journal of Neuroimmunology 47(2): p.169–176.

Guzmán-Ruiz, M.A. et al. 2015. Role of the suprachiasmatic and arcuate nuclei in diurnal temperature regulation in the rat. Journal of Neuroscience 35(46).

Haapanen, M.J. et al. 2018. Telomere Length and Frailty: The Helsinki Birth Cohort Study. Journal of the American Medical Directors Association 19(8): p.658–662.

Haber, M. et al. 2018. Minocycline plus N-acteylcysteine induces remyelination, synergistically protects oligodendrocytes and modifies neuroinflammation in a rat model of mild traumatic brain injury. Journal of Cerebral Blood Flow and Metabolism 38(8): p.1312–1326.

Haddad-Tóvolli, R., Dragano, N.R.V., Ramalho, A.F.S., & Velloso, L.A. 2017. Development and function of the blood-brain barrier in the context of metabolic control. Frontiers in Neuroscience 11(APR).

Haim, L. Ben, Carrillo-de Sauvage, M.A., Ceyzériat, K., & Escartin, C. 2015. Elusive roles for reactive astrocytes in neurodegenerative diseases. Frontiers in Cellular Neuroscience 9(AUGUST).

Haines, D. E., Dietrichs, E., Mihailoff, G. A., & McDonald, E. F. (1997). The cerebellar-hypothalamic axis: basic circuits and clinical observations. International Review of Neurobiology, 41, 83–107. https://doi.org/10.1016/s0074-7742(08)60348-7

Hamilton, G., Colbert, J.D., Schuettelkopf, A.W., & Watts, C. 2008. Cystatin F is a cathepsin C-directed protease inhibitor regulated by proteolysis. EMBO Journal 27(3): p.499–508.

Hamilton, J.A. 2008. Colony-stimulating factors in inflammation and autoimmunity. Nature Reviews Immunology 8(7): p.533–544.

Hammond, J.W. et al. 2020. Complement-dependent synapse loss and microgliosis in a mouse model of multiple sclerosis. Brain, Behavior, and Immunity 87.

Han, J., Harris, R.A., & Zhang, X.M. 2017. An updated assessment of microglia depletion: Current concepts and future directions. Molecular Brain 10(1).

Han, J., Zhu, K., Zhang, X.M., & Harris, R.A. 2019. Enforced microglial depletion and repopulation as a promising strategy for the treatment of neurological disorders. GLIA 67(2).

Han, K., Jia, N., Zhong, Y., & Shang, X. 2018. S14G-humanin alleviates insulin resistance and increases autophagy in neurons of APP/PS1 transgenic mouse. Journal of Cellular Biochemistry 119(4): p.3111–3117.

Handforth, C. et al. 2015. The prevalence and outcomes of frailty in older cancer patients: A systematic review. Annals of Oncology 26(6): p.1091–1101.

Hara, Y., Waters, E.M., McEwen, B.S., & Morrison, J.H. 2015. Estrogen effects on cognitive and synaptic health over the lifecourse. Physiological Reviews 95(3): p.785–807.

Harold, D. et al. 2009. Genome-wide association study identifies variants at CLU and PICALM associated with Alzheimer's disease. Nature Genetics 41(10): p.1088–1093.

Harrington, J.R. 2000. The Role of MCP-1 in Atherosclerosis. Stem Cells 18(1): p.65–66.

Hart, A.D., Wyttenbach, A., Hugh Perry, V., & Teeling, J.L. 2012. Age related changes in microglial phenotype vary between CNS regions: Grey versus white matter differences. Brain, Behavior, and Immunity 26(5): p.754–765.

Hasel, P. et al. 2017. Neurons and neuronal activity control gene expression in astrocytes to regulate their development and metabolism. Nature Communications 8.

Haseloff, R.F., Dithmer, S., Winkler, L., Wolburg, H., & Blasig, I.E. 2015. Transmembrane proteins of the tight junctions at the blood-brain barrier: Structural and functional aspects. Seminars in Cell and Developmental Biology 38: p.16–25.

Haure-Mirande, J.V. et al. 2017. Deficiency of TYROBP, an adapter protein for TREM2 and CR3 receptors, is neuroprotective in a mouse model of early Alzheimer's pathology. Acta Neuropathologica 134(5): p.769–788. Available at: /pmc/articles/PMC5645450/ [Accessed August 15, 2021].

Hayflick, L. 1965. The limited in vitro lifetime of human diploid cell strains. Experimental Cell Research 37(3): p.614–636.

Hayflick, L., & Moorhead, P.S. 1961. The serial cultivation of human diploid cell strains. Experimental Cell Research 25(3): p.585–621.

Hebert, L.E., Scherr, P.A., McCann, J.J., Beckett, L.A., & Evans, D.A. 2001. Is the risk of developing Alzheimer's disease greater for women than for men? American Journal of Epidemiology 153(2): p.132–136.

Hedden, T., & Gabrieli, J.D.E. 2004. Insights into the ageing mind: A view from cognitive neuroscience. Nature Reviews Neuroscience 5(2): p.87–96.

Heinemann, U., Kaufer, D., & Friedman, A. 2012. Blood-brain barrier dysfunction, TGFβ signaling, and astrocyte dysfunction in epilepsy. Glia 60(8): p.1251–1257. Available at: /pmc/articles/PMC3615248/ [Accessed September 20, 2021].

Heijtz, R. D., Wang, S., Anuar, F., Qian, Y., Björkholm, B., Samuelsson, A., Hibberd, M. L., Forssberg, H., & Pettersson, S. (2011). Normal gut microbiota modulates brain development and behavior. Proceedings of the National Academy of Sciences of the United States of America, 108(7), 3047–3052. https://doi.org/10.1073/pnas.1010529108

Held, N.M. et al. 2021. Aging selectively dampens oscillation of lipid abundance in white and brown adipose tissue. Scientific Reports 11(1): p.1–13. Available at: https://www.nature.com/articles/s41598-021-85455-4 [Accessed August 14, 2021].

Henderson, Y.O. et al. 2021. Late-life intermittent fasting decreases aging-related frailty and increases renal hydrogen sulfide production in a sexually dimorphic manner. GeroScience: p.1–28. Available at: https://link.springer.com/article/10.1007/s11357-021-00330-4 [Accessed August 29, 2021].

Heng, Y. et al. 2021. Systemic administration of β-glucan induces immune training in microglia. Journal of Neuroinflammation 2021 18:1 18(1): p.1–15. Available at: https://jneuroinflammation.biomedcentral.com/articles/10.1186/s12974-021-02103-4 [Accessed July 25, 2021].

Hennessy, E. et al. 2017. Systemic TNF-α produces acute cognitive dysfunction and exaggerated sickness behavior when superimposed upon progressive neurodegeneration. Brain, Behavior, and Immunity 59: p.233–244.

Hennessy, E., Griffin, E.W., & Cunningham, C. 2015. Astrocytes are primed by chronic neurodegeneration to produce exaggerated chemokine and cell infiltration responses to acute stimulation with the cytokines IL-1β and TNF-α. Journal of Neuroscience 35(22): p.8411–8422.

Henry, C.J., Huang, Y., Wynne, A.M., & Godbout, J.P. 2009. Peripheral lipopolysaccharide (LPS) challenge promotes microglial hyperactivity in aged mice that is associated with exaggerated

induction of both pro-inflammatory IL-1β and anti-inflammatory IL-10 cytokines. Brain, Behavior, and Immunity 23(3): p.309–317.

Henry, L. et al. 2019. Frailty in the Cardiac Surgical Patient: Comparison of Frailty Tools and Associated Outcomes. Annals of Thoracic Surgery 108(1): p.16–22.

Heuer, E., F. Rosen, R., Cintron, A., & C. Walker, L. 2012. Nonhuman Primate Models of Alzheimer-Like Cerebral Proteopathy. Current Pharmaceutical Design 18(8): p.1159–1169.

Hickman, S.E. et al. 2013. The microglial sensome revealed by direct RNA sequencing. Nature Neuroscience 16(12): p.1896–1905.

van Himbergen, T. M., Beiser, A. S., Ai, M., Seshadri, S., Otokozawa, S., Au, R., Thongtang, N., Wolf, P. A., & Schaefer, E. J. (2012). Biomarkers for insulin resistance and inflammation and the risk for all-cause dementia and Alzheimer disease: Results from the Framingham Heart Study. Archives of Neurology, 69(5), 594–600. https://doi.org/10.1001/archneurol.2011.670

Hirani, V. et al. 2017. Longitudinal associations between body composition, sarcopenic obesity and outcomes of frailty, disability, institutionalisation and mortality in community-dwelling older men: The Concord Health and Ageing in men project. Age and Ageing.

Holloway, L., Butterfield, G., Hintz, R.L., Gesundheit, N., & Marcus, R. 1994. Effects of recombinant human growth hormone on metabolic indices, body composition, and bone turnover in healthy elderly women. Journal of Clinical Endocrinology and Metabolism 79(2): p.470–479.

Holm, T.H., Draeby, D., & Owens, T. 2012. Microglia are required for astroglial toll-like receptor 4 response and for optimal TLR2 and TLR3 response. Glia 60(4): p.630–638.

Holmes, C. et al. 2003. Systemic infection, interleukin 1β, and cognitive decline in Alzheimer's disease. Journal of Neurology Neurosurgery and Psychiatry 74(6): p.788–789.

Holmes, C. et al. 2009. Systemic inflammation and disease progression in alzheimer disease. Neurology 73(10): p.768–774.

Holmes, C. et al. 2014. O4‐11‐02: the Safety and Tolerability of Etanercept in Alzheimer'S Disease (Steadi‐09): a Phase Ii Double Blind Randomised Placebo Controlled Trial. Alzheimer's & Dementia 10(4S_Part_5).

Holmes, C., Cunningham, C., Zotova, E., Culliford, D., & Perry, V.H. 2011. Proinflammatory cytokines, sickness behavior, and Alzheimer disease. Neurology 77(3): p.212–218.

Holtman, I.R. et al. 2015. Induction of a common microglia gene expression signature by aging and

neurodegenerative conditions: a co-expression meta-analysis. Acta neuropathologica communications 3: p.31.

Holzenberger, M. 2004. The GH/IGF-I axis and longevity. European Journal of Endocrinology 151(SUPPL. 1).

Hong, S. et al. 2016. Complement and microglia mediate early synapse loss in Alzheimer mouse models. Science 352(6286): p.712–716.

Hou, Y. et al. 2019. Ageing as a risk factor for neurodegenerative disease. Nature Reviews Neurology 15(10): p.565–581.

Howell, T.H. 1948. Normal Temperatures in Old Age. The Lancet 251(6501): p.517–519.

Hsiao, K. et al. 1996. Correlative memory deficits, Aβ elevation, and amyloid plaques in transgenic mice. Science 274(5284): p.99–102.

Hsiao, E. Y., McBride, S. W., Hsien, S., Sharon, G., Hyde, E. R., McCue, T., Codelli, J. A., Chow, J., Reisman, S. E., Petrosino, J. F., Patterson, P. H., & Mazmanian, S. K. (2013). Microbiota modulate behavioral and physiological abnormalities associated with neurodevelopmental disorders. Cell, 155(7), 1451–1463. https://doi.org/10.1016/j.cell.2013.11.024

Huang, B. et al. 2007. CCL2/CCR2 pathway mediates recruitment of myeloid suppressor cells to cancers. Cancer Letters 252(1): p.86–92.

Huang, E.J., & Reichardt, L.F. 2001. Neurotrophins: Roles in neuronal development and function. Annual Review of Neuroscience 24: p.677–736.

Huang, J. et al. 2009. Activation of antibacterial autophagy by NADPH oxidases. Proceedings of the National Academy of Sciences of the United States of America 106(15): p.6226–6231.

Huang, S. et al. 2012. Saturated fatty acids activate TLR-mediated proinflammatory signaling pathways. Journal of Lipid Research 53(9): p.2002–2013.

Hubbard-Turner, T., Guderian, S., & Turner, M.J. 2015. Lifelong physical activity and knee osteoarthritis development in mice. International Journal of Rheumatic Diseases 18(1): p.33–39.

Hubbard, R.E., & Woodhouse, K.W. 2010. Frailty, inflammation and the elderly. Biogerontology 11(5): p.635–641.

Hubinger, A., Weikert, G., Wolf, H.P.O., & Gries, F.A. 1992. The effect of Etomoxir on insulin

sensitivity in type 2 diabetic patients. Hormone and Metabolic Research 24(3).

Hume, D.A., & MacDonald, K.P.A. 2012. Therapeutic applications of macrophage colony-stimulating factor-1 (CSF-1) and antagonists of CSF-1 receptor (CSF-1R) signaling. Blood 119(8): p.1810–1820.

Hurst, J. L., & West, R. S. (2010). Taming anxiety in laboratory mice. Nature Methods, 7(10), 825–826. https://doi.org/10.1038/nmeth.1500

Hutchins-Wiese, H.L. et al. 2013. The impact of supplemental N-3 long chain polyunsaturated fatty acids and dietary antioxidants on physical performance in postmenopausal women. Journal of Nutrition, Health and Aging.

Ifrim, D. C., Quintin, J., Joosten, L. A. B., Jacobs, C., Jansen, T., Jacobs, L., Gow, N. A. R., Williams, D. L., van der Meer, J. W. M., & Netea, M. G. (2014). Trained immunity or tolerance: Opposing functional programs induced in human monocytes after engagement of various pattern recognition receptors. Clinical and Vaccine Immunology, 21(4), 534–545. https://doi.org/10.1128/CVI.00688-13

Iglói, K. et al. 2015. Interaction between hippocampus and cerebellum crus i in sequence-based but not place-based navigation. Cerebral Cortex 25(11): p.4146–4154.

Iqbal, G., & Ahmed, T. 2019. Co-exposure of metals and high fat diet causes aging like neuropathological changes in non-aged mice brain. Brain Research Bulletin 147: p.148–158.

Ishihara, K., & Hirano, T. 2002. IL-6 in autoimmune disease and chronic inflammatory proliferative disease. Cytokine and Growth Factor Reviews 13(4–5): p.357–368.

Itoh, N. et al. 2017. Cell-specific and region-specific transcriptomics in the multiple sclerosis model: Focus on astrocytes. Proceedings of the National Academy of Sciences of the United States of America 115(2): p.E302–E309.

Ito, M., Shirao, T., Doya, K., & Sekino, Y. 2009. Three-dimensional distribution of Fos-positive neurons in the supramammillary nucleus of the rat exposed to novel environment. Neuroscience Research 64(4): p.397–402.

Iwasaki, A., & Medzhitov, R. 2004. Toll-like receptor control of the adaptive immune responses. Nature Immunology 5(10): p.987–995.

Janeway, C.A., & Medzhitov, R. 2002. Innate immune recognition. Annual Review of Immunology 20: p.197–216.

Jefferson, A.L. et al. 2007. Inflammatory biomarkers are associated with total brain volume: The Framingham Heart Study. Neurology 68(13): p.1032–1038.

Jeljeli, M., Riccio, L. G. C., Doridot, L., Chêne, C., Nicco, C., Chouzenoux, S., Deletang, Q., Allanore, Y., Kavian, N., & Batteux, F. (2019). Trained immunity modulates inflammation-induced fibrosis. Nature Communications, 10(1), 1–15. https://doi.org/10.1038/s41467-019-13636-x

Jergović, M. et al. 2021. IL-6 can singlehandedly drive many features of frailty in mice. GeroScience 43(2): p.539–549. Available at: https://pubmed.ncbi.nlm.nih.gov/33629207/ [Accessed April 25, 2021].

Jiang, H. yin, Zhang, X., Yu, Z. he, Zhang, Z., Deng, M., Zhao, J. hua, & Ruan, B. (2018). Altered gut microbiota profile in patients with generalized anxiety disorder. Journal of Psychiatric Research, 104, 130–136. https://doi.org/10.1016/j.jpsychires.2018.07.007

Jiao, S.S. et al. 2016. Sex Dimorphism Profile of Alzheimer's Disease-Type Pathologies in an APP/PS1 Mouse Model. Neurotoxicity Research 29(2): p.256–266.

Jimenez, J.C. et al. 2018. Anxiety Cells in a Hippocampal-Hypothalamic Circuit. Neuron 97(3): p.670-683.e6.

Joaquin, A.M., & Gollapudi, S. 2001. Functional decline in aging and disease: A role for apoptosis. Journal of the American Geriatrics Society 49(9): p.1234–1240.

Johannsson, G. et al. 1997. Growth Hormone Treatment of Abdominally Obese Men Reduces Abdominal Fat Mass, Improves Glucose and Lipoprotein Metabolism, and Reduces Diastolic Blood Pressure 1 . The Journal of Clinical Endocrinology & Metabolism 82(3): p.727–734.

Johanson, C. 2018. Choroid Plexus Blood-CSF Barrier: Major Player in Brain Disease Modeling and Neuromedicine. Journal of Neurology & Neuromedicine 3(4): p.39–58. Available at: www.jneurology.comNeuromedicine [Accessed September 19, 2021].

Joosten, E., Demuynck, M., Detroyer, E., & Milisen, K. 2014. Prevalence of frailty and its ability to predict in hospital delirium, falls, and 6-month mortality in hospitalized older patients. BMC Geriatrics 14(1).

Jorge, Y.C. et al. 2013. Expression of annexin-A1 and galectin-1 anti-inflammatory proteins and mRNA in chronic gastritis and gastric cancer. Mediators of Inflammation 2013: p.11. Available at: http://dx.

Jun, G. et al. 2010. Meta-analysis confirms CR1, CLU, and PICALM as Alzheimer disease risk loci and

reveals interactions with APOE genotypes. Archives of Neurology 67(12): p.1473–1484.

Kalia, N., Singh, J., & Kaur, M. 2021. The role of dectin-1 in health and disease. Immunobiology 226(2): p.152071.

Kälin, S. et al. 2015. Hypothalamic innate immune reaction in obesity. Nature Reviews Endocrinology 11(6): p.339–351.

Kalsbeek, A. et al. 2012. Differential involvement of the suprachiasmatic nucleus in lipopolysaccharide-induced plasma glucose and corticosterone responses. Chronobiology International 29(7).

Kamoshida, S. et al. 2007. Expression of cancer cachexia-related factors in human cancer xenografts: An immunohistochemical analysis. Biomedical Research 27(6): p.275–281.

Karch, C.M., & Goate, A.M. 2015. Alzheimer's disease risk genes and mechanisms of disease pathogenesis. Biological Psychiatry 77(1): p.43–51.

Katakura, Y., Nakata, E., Miura, T., & Shirahata, S. 1999. Transforming growth factor β triggers two independent-senescence programs in cancer cells. Biochemical and Biophysical Research Communications 255(1): p.110–115. Available at: https://pubmed.ncbi.nlm.nih.gov/10082664/ [Accessed August 25, 2021].

Katsanos, C.S., Kobayashi, H., Sheffield-Moore, M., Aarsland, A., & Wolfe, R.R. 2005. Aging is associated with diminished accretion of muscle proteins after the ingestion of a small bolus of essential amino acids. American Journal of Clinical Nutrition 82(5): p.1065–1073.

Katsanos, C.S., Kobayashi, H., Sheffield-Moore, M., Aarsland, A., & Wolfe, R.R. 2006. A high proportion of leucine is required for optimal stimulation of the rate of muscle protein synthesis by essential amino acids in the elderly. American Journal of Physiology - Endocrinology and Metabolism 291(2).

Kawarabayashi, T. et al. 2001. Age-dependent changes in brain, CSF, and plasma amyloid β protein in the Tg2576 transgenic mouse model of Alzheimer's disease. Journal of Neuroscience 21(2): p.372–381.

Kaye, W.H., Fudge, J.L., & Paulus, M. 2009. New insights into symptoms and neurocircuit function of anorexia nervosa. Nature Reviews Neuroscience 10(8): p.573–584.

Kealy, J. et al. 2020. Acute inflammation alters brain energy metabolism in mice and humans: Role in suppressed spontaneous activity, impaired cognition, and delirium. Journal of Neuroscience

40(29): p.5681–5696.

Kelley, K.W. et al. 2003. Cytokine-induced sickness behavior. In Brain, Behavior, and Immunity, 112–118.

Kelley, K.W. 2004. From hormones to immunity: The physiology of immunology. Brain, Behavior, and Immunity 18(2): p.95–113.

Kennedy, B.K. et al. 2014. Geroscience: Linking aging to chronic disease. Cell 159(4): p.709–713.

Kent, S., Bluthé, R.M., Kelley, K.W., & Dantzer, R. 1992. Sickness behavior as a new target for drug development. Trends in Pharmacological Sciences 13(C): p.24–28.

Keren-Shaul, H. et al. 2017. A Unique Microglia Type Associated with Restricting Development of Alzheimer's Disease. Cell 169(7): p.1276-1290.e17.

Kerfoot, S.M. et al. 2004. TLR4 Contributes to Disease-Inducing Mechanisms Resulting in Central Nervous System Autoimmune Disease. The Journal of Immunology 173(11): p.7070–7077.

Kettelhut, I.C., & Goldberg, A.L. 1988. Tumor necrosis factor can induce fever in rats without activating protein breakdown in muscle or lipolysis in adipose tissue. Journal of Clinical Investigation 81(5): p.1384–1389.

Keung, W. et al. 2013. Inhibition of carnitine palmitoyltransferase-1 activity alleviates insulin resistance in diet-induced obese mice. Diabetes 62(3).

Kierdorf, K. et al. 2013. Microglia emerge from erythromyeloid precursors via Pu.1-and Irf8-dependent pathways. Nature Neuroscience 16(3): p.273–280.

Kim, M.S. et al. 2015. Rapid linkage of innate immunological signals to adaptive immunity by the brain-fat axis. Nature Immunology 16(5): p.525–533.

Kim, Y., Park, J., & Choi, Y.K. 2019. The role of astrocytes in the central nervous system focused on BK channel and heme oxygenase metabolites: A review. Antioxidants 8(5). Available at: /pmc/articles/PMC6562853/ [Accessed August 30, 2021].

Kinney, J.W. et al. 2018. Inflammation as a central mechanism in Alzheimer's disease. Alzheimer's and Dementia: Translational Research and Clinical Interventions 4.

Kirkland, J.L., Stout, M.B., & Sierra, F. 2016. Resilience in Aging Mice. In Journals of Gerontology - Series A Biological Sciences and Medical Sciences, 1407–1414.

Kirkwood, T.B.L. 2005. Understanding the odd science of aging. Cell.

Kirkwood, T.B.L. 2015. Deciphering death: A commentary on Gompertz (1825) 'On the nature of the function expressive of the law of human mortality, and on a new mode of determining the value of life contingencies'. Philosophical Transactions of the Royal Society B: Biological Sciences 370(1666).

Klosinski, L.P. et al. 2015. White Matter Lipids as a Ketogenic Fuel Supply in Aging Female Brain: Implications for Alzheimer's Disease. EBioMedicine 2(12): p.1888–1904.

Kluger, M.J., & Rothenburg, B.A. 1979. Fever and reduced iron: Their interaction as a host defense response to bacterial infection. Science 203(4378): p.374–376.

Ko, F. et al. 2012. Inflammation and mortality in a frail mouse model. Age 34(3): p.705–715.

Ko, F.C. 2019. Preoperative Frailty Evaluation: A Promising Risk-stratification Tool in Older Adults Undergoing General Surgery. Clinical Therapeutics 41(3): p.387–399.

Koesters, R. et al. 2010. Tubular overexpression of transforming growth factor-β1 induces autophagy and fibrosis but not mesenchymal transition of renal epithelial cells. American Journal of Pathology 177(2): p.632–643.

Koivisto, K. et al. 1995. Prevalence of age-associated memory impairment in a randomly selected population from eastern Finland. Neurology 45(4): p.741–747.

Kojima, G., Liljas, A., Iliffe, S., & Walters, K. 2017. Prevalence of Frailty in Mild to Moderate Alzheimer's Disease: A Systematic Review and Meta-analysis. Current Alzheimer Research 14(12).

Kojima, G., Taniguchi, Y., Iliffe, S., & Walters, K. 2016. Frailty as a Predictor of Alzheimer Disease, Vascular Dementia, and All Dementia Among Community-Dwelling Older People: A Systematic Review and Meta-Analysis. Journal of the American Medical Directors Association 17(10): p.881–888.

Konsman, J.P., Parnet, P., & Dantzer, R. 2002. Cytokine-induced sickness behaviour: Mechanisms and implications. Trends in Neurosciences 25(3): p.154–159.

Kotfis, K. et al. 2019. Diabetes and elevated preoperative hba1c level as risk factors for postoperative delirium after cardiac surgery: An observational cohort study. Neuropsychiatric Disease and Treatment 15: p.511–521.

Kotter, M.R., Li, W.W., Zhao, C., & Franklin, R.J.M. 2006. Myelin impairs CNS remyelination by inhibiting oligodendrocyte precursor cell differentiation. Journal of Neuroscience 26(1):

p.328–332.

Kotter, M.R., Setzu, A., Sim, F.J., Van Rooijen, N., & Franklin, R.J.M. 2001. Macrophage depletion impairs oligodendrocyte remyelination following lysolecithin-induced demyelination. Glia 35(3): p.204–212.

Koychev, I. et al. 2018. Erratum: PET Tau and Amyloid-β Burden in Mild Alzheimer's Disease: Divergent Relationship with Age, Cognition, and Cerebrospinal Fluid Biomarkers (Journal of Alzheimer's disease : JAD (2017) 60 1 (283-293)). Journal of Alzheimer's disease : JAD 63(1): p.407.

Krabbe, K.S. et al. 2001. Ageing is associated with a prolonged fever response in human endotoxemia. Clinical and Diagnostic Laboratory Immunology 8(2): p.333–338.

Kraft, A.W. et al. 2013. Attenuating astrocyte activation accelerates plaque pathogenesis in APP/PS1 mice. FASEB Journal 27(1): p.187–198.

Kramer, J.M., Klimatcheva, E., & Rothstein, T.L. 2013. CXCL13 is elevated in Sjögren's syndrome in mice and humans and is implicated in disease pathogenesis. Journal of Leukocyte Biology 94(5): p.1079–1089. Available at: www.jleukbio.org.

Krasemann, S. et al. 2017. The TREM2-APOE Pathway Drives the Transcriptional Phenotype of Dysfunctional Microglia in Neurodegenerative Diseases. Immunity 47(3): p.566-581.e9.

Krizanac-Bengez, L. et al. 2006. Loss of shear stress induces leukocyte-mediated cytokine release and blood-brain barrier failure in dynamic in vitro blood-brain barrier model. Journal of Cellular Physiology 206(1): p.68–77.

Krizhanovsky, V. et al. 2008. Senescence of Activated Stellate Cells Limits Liver Fibrosis. Cell 134(4): p.657–667.

Kuchipudi, S. V. et al. 2012. 18S rRNA is a reliable normalisation gene for real time PCR based on influenza virus infected cells. Virology Journal 9.

Kulkarni, A.B. et al. 1993. Transforming growth factor β1 null mutation in mice causes excessive inflammatory response and early death. Proceedings of the National Academy of Sciences of the United States of America 90(2): p.770–774.

Kullmann, S. et al. 2016. Brain insulin resistance at the crossroads of metabolic and cognitive disorders in humans. Physiological Reviews 96(4): p.1169–1209.

Kurschus, F.C. 2015. T cell mediated pathogenesis in EAE: Molecular mechanisms. Biomedical

Journal 38(3): p.183–193.

Kwak, D., Baumann, C.W., & Thompson, L.D. V. 2020. Identifying characteristics of frailty in female mice using a phenotype assessment tool. Journals of Gerontology - Series A Biological Sciences and Medical Sciences 75(4): p.640–646.

Kyung-Ah Kim, Wan Gu, In-Ah Lee, Eun-Ha Joh, and Dong-Hyun Kim. (2012). High Fat Diet-Induced Gut Microbiota Exacerbates Inflammation and Obesity in Mice via the TLR4 Signaling Pathway. PLosOne, 7(10). doi: 10.1371/journal.pone.0047713

De Labra, C., Guimaraes-Pinheiro, C., Maseda, A., Lorenzo, T., & Millán-Calenti, J.C. 2015. Effects of physical exercise interventions in frail older adults: A systematic review of randomized controlled trials Physical functioning, physical health and activity. BMC Geriatrics 15(1).

Łabuzek, K., Skrudlik, E., Gabryel, B., & Okopień, B. 2015. Anti-inflammatory microglial cell function in the light of the latest scientific research. Annales Academiae Medicae Silesiensis 69: p.99–110.

Lai, J.C. et al. 2019. Frailty in liver transplantation: An expert opinion statement from the American Society of Transplantation Liver and Intestinal Community of Practice. In American Journal of Transplantation, 1896–1906.

Lajqi, T. et al. 2019. Memory-Like Inflammatory Responses of Microglia to Rising Doses of LPS: Key Role of PI3Kγ. Frontiers in Immunology 10.

Lambert, J.C. et al. 2009. Genome-wide association study identifies variants at CLU and CR1 associated with Alzheimer's disease. Nature Genetics 41(10): p.1094–1099.

Lane, J.M., Serota, A.C., & Raphael, B. 2006. Osteoporosis: Differences and Similarities in Male and Female Patients. Orthopedic Clinics of North America 37(4): p.601–609.

Lange, K.H.W. et al. 2002. GH administration changes myosin heavy chain isoforms in skeletal muscle but does not augment muscle strength or hypertrophy, either alone or combined with resistance exercise training in healthy elderly men. Journal of Clinical Endocrinology and Metabolism 87(2): p.513–523.

Lauer, M.S. 2009. Comparative Effectiveness Research: The View From the NHLBI. Journal of the American College of Cardiology 53(12): p.1084–1086.

Laws, K.R., Irvine, K., & Gale, T.M. 2016. Sex differences in cognitive impairment in Alzheimer's disease. World Journal of Psychiatry 6(1): p.54.

Lawson, L.J., Perry, V.H., Dri, P., & Gordon, S. 1990. Heterogeneity in the distribution and morphology of microglia in the normal adult mouse brain. Neuroscience 39(1): p.151–170.

Lawson, L.J., Perry, V.H., & Gordon, S. 1992. Turnover of resident microglia in the normal adult mouse brain. Neuroscience 48(2): p.405–415.

Ledo, J.H. et al. 2016. Cross talk between brain innate immunity and serotonin signaling underlies depressive-like behavior induced by Alzheimer's amyloid-β oligomers in mice. Journal of Neuroscience 36(48): p.12106–12116.

Lee, C.Y., Dallérac, G., Ezan, P., Anderova, M., & Rouach, N. 2016. Glucose tightly controls morphological and functional properties of astrocytes. Frontiers in Aging Neuroscience.

Lee, J.Y. et al. 2004. Saturated Fatty Acid Activates but Polyunsaturated Fatty Acid Inhibits Toll-like Receptor 2 Dimerized with Toll-like Receptor 6 or 1. Journal of Biological Chemistry 279(17): p.16971–16979.

Lee, S.C., Liu, W., Dickson, D.W., Brosnan, C.F., & Berman, J.W. 1993. Cytokine production by human fetal microglia and astrocytes. Differential induction by lipopolysaccharide and IL-1 beta. Journal of immunology (Baltimore, Md. : 1950) 150(7): p.2659–67. Available at: http://www.ncbi.nlm.nih.gov/pubmed/8454848.

Lee, S.Y., Wang, J., Chao, C. Ter, Chien, K.L., & Huang, J.W. 2021. Frailty is associated with a higher risk of developing delirium and cognitive impairment among patients with diabetic kidney disease: A longitudinal population-based cohort study. Diabetic Medicine 38(7).

Lee, W.J., Peng, L.N., & Chen, L.K. 2020. Metabolic syndrome and its components are associated with frailty: A nationwide population-based study in Taiwan. Aging Medicine and Healthcare 11(2): p.47–52.

LeibundGut-Landmann, S. et al. 2007. Syk- and CARD9-dependent coupling of innate immunity to the induction of T helper cells that produce interleukin 17. Nature Immunology 8(6): p.630–638.

Leng, S.X. et al. 2004. Serum levels of insulin-like growth factor-I (IGF-I) and dehydroepiandrosterone sulfate (DHEA-S), and their relationships with serum interleukin-6, in the geriatric syndrome of frailty. Aging Clinical and Experimental Research 16(2): p.153–157.

León-Muñoz, L.M., García-Esquinas, E., López-García, E., Banegas, J.R., & Rodríguez-Artalejo, F. 2015. Major dietary patterns and risk of frailty in older adults: A prospective cohort study.

BMC Medicine 13(1).

Leong, K.G., & Karsan, A. 2000. Signaling pathways mediated by tumor necrosis factor α. Histology and Histopathology 15(4): p.1303–1325.

Leung, R. et al. 2013. Inflammatory Proteins in Plasma Are Associated with Severity of Alzheimer's Disease. PLoS ONE 8(6).

Lévesque, S.A. et al. 2016. Myeloid cell transmigration across the CNS vasculature triggers IL-1ß-driven neuroinflammation during autoimmune encephalomyelitis in mice. Journal of Experimental Medicine 213(6): p.929–949.

Levick, J.R., & Michel, C.C. 2010. Microvascular fluid exchange and the revised Starling principle. Cardiovascular Research 87(2): p.198–210.

Levin-Allerhand, J.A., & Smith, J.D. 2002. Ovariectomy of young mutant amyloid precursor protein transgenic mice leads to increased mortality. Journal of Molecular Neuroscience 19(1–2): p.163–166.

Li, H.C. et al. 2021. Surviving and Thriving 1 Year After Cardiac Surgery: Frailty and Delirium Matter. Annals of Thoracic Surgery 111(5): p.1578–1584.

Li, L., & Hölscher, C. 2007. Common pathological processes in Alzheimer disease and type 2 diabetes: A review. Brain Research Reviews 56(2): p.384–402.

Li, Q., & Verma, I.M. 2002. NF-κB regulation in the immune system. Nature Reviews Immunology 2(10): p.725–734.

Li, X. et al. 2016. Sex differences between APPswePS1dE9 mice in a-beta accumulation and pancreatic islet function during the development of Alzheimer's disease. Laboratory Animals 50(4): p.275–285. Available at: https://journals.sagepub.com/doi/10.1177/0023677215615269 [Accessed September 7, 2021].

Li, X., Zhao, W.C., Yang, H.Q., Zhang, J.H., & Ma, J.J. 2013. S14G-humanin restored cellular homeostasis disturbed by amyloid-beta protein. Neural Regeneration Research 8(27): p.2573–2580.

Li, X., Kan, E. M., Lu, J., Cao, Y., Wong, R. K., Keshavarzian, A., & Wilder-Smith, C. H. (2013). Combat-training increases intestinal permeability, immune activation and gastrointestinal symptoms in soldiers. Alimentary Pharmacology and Therapeutics, 37(8), 799–809.

Li, W.-Z., Stirling, K., Yang, J.-J., & Zhang, L. (2020). Gut microbiota and diabetes: From correlation to causality and mechanism. World Journal of Diabetes, 11(7), 293–308.

Lian, H. et al. 2016. Astrocyte-microglia cross talk through complement activation modulates amyloid pathology in mouse models of alzheimer's disease. Journal of Neuroscience 36(2): p.577–589.

Liang, S., Wang, T., Hu, X., Luo, J., Li, W., Wu, X., Duan, Y., & Jin, F. (2015). Administration of Lactobacillus helveticus NS8 improves behavioral, cognitive, and biochemical aberrations caused by chronic restraint stress. Neuroscience, 310, 561–577. https://doi.org/10.1016/j.neuroscience.2015.09.033

Liao, C. De, Chen, H.C., Huang, S.W., & Liou, T.H. 2019. The role of muscle mass gain following protein supplementation plus exercise therapy in older adults with sarcopenia and frailty risks: A systematic review and meta-regression analysis of randomized trials. Nutrients 11(8).

Libert, C., Dejager, L., & Pinheiro, I. 2010. The X chromosome in immune functions: When a chromosome makes the difference. Nature Reviews Immunology 10(8): p.594–604.

Liddelow, S.A. et al. 2017. Neurotoxic reactive astrocytes are induced by activated microglia. Nature 541(7638): p.481–487. Available at: https://www.nature.com/articles/nature21029 [Accessed August 19, 2021].

Lieb, J., & Balter, A. 1984. Antidepressant tachyphylaxis. Medical Hypotheses 15(3): p.279–291.

Lima, J.B.M., Veloso, C.C., Vilela, F.C., & Giusti-Paiva, A. 2017. Prostaglandins mediate zymosan-induced sickness behavior in mice. Journal of Physiological Sciences 67(6): p.673–679. Available at: https://jps.biomedcentral.com/articles/10.1007/s12576-016-0494-8 [Accessed September 17, 2021].

Lin, H. et al. 2008. Discovery of a cytokine and its receptor by functional screening of the extracellular proteome. Science 320(5877): p.807–811.

Lin, Y.S., Lin, F.Y., & Hsiao, Y.H. 2019. Myostatin Is Associated With Cognitive Decline in an Animal Model of Alzheimer's Disease. Molecular Neurobiology 56(3): p.1984–1991.

Linetti, A. et al. 2010. Cholesterol reduction impairs exocytosis of synaptic vesicles. Journal of Cell Science 123(4): p.595–605.

Lisignoli, G. et al. 2003. Age-associated changes in functional response to CXCR3 and CXCR5 chemokine receptors in human osteoblasts. Biogerontology 4(5): p.309–317.

List, E.O., Basu, R., Duran-Ortiz, S., Krejsa, J., & Jensen, E.A. 2021. Mouse models of growth hormone deficiency. Reviews in Endocrine and Metabolic Disorders 22(1): p.3–16. Available at: https://pubmed.ncbi.nlm.nih.gov/33033978/ [Accessed April 25, 2021].

Liu, K. et al. 2009. In vivo analysis of dendritic cell development and homeostasis. Science 324(5925): p.392–397.

Liu, L.R., Liu, J.C., Bao, J.S., Bai, Q.Q., & Wang, G.Q. 2020. Interaction of Microglia and Astrocytes in the Neurovascular Unit. Frontiers in Immunology 11.

Liu, Q. et al. 2007. Amyloid Precursor Protein Regulates Brain Apolipoprotein E and Cholesterol Metabolism through Lipoprotein Receptor LRP1. Neuron 56(1): p.66–78.

Liu, Q. et al. 2010. Neuronal LRP1 knockout in adult mice leads to impaired brain lipid metabolism and progressive, age-dependent synapse loss and neurodegeneration. Journal of Neuroscience 30(50): p.17068–17078.

Lo, L. et al. 2019. Connectional architecture of a mouse hypothalamic circuit node controlling social behavior. Proceedings of the National Academy of Sciences of the United States of America 116(15): p.7503–7512. Available at: https://www.pnas.org/content/116/15/7503 [Accessed January 20, 2022].

Lominska, C.E., Levin-Allerhand, J.A., Wang, J., & Smith, J.D. 2002. 17α-estradiol and 17β-estradiol treatments are effective in lowering cerebral amyloid-β levels in AβPPSWE transgenic mice. Journal of Alzheimer's Disease 4(6): p.449–457.

Lopez-Garcia, E., Hagan, K.A., Fung, T.T., Hu, F.B., & Rodríguez-Artalejo, F. 2018. Mediterranean diet and risk of frailty syndrome among women with type 2 diabetes. American Journal of Clinical Nutrition.

López-Otín, C., Blasco, M.A., Partridge, L., Serrano, M., & Kroemer, G. 2013. The hallmarks of aging. Cell 153(6): p.1194.

López-Ramos, J.C., Jurado-Parras, M.T., Sanfeliu, C., Acuña-Castroviejo, D., & Delgado-García, J.M. 2012. Learning capabilities and CA1-prefrontal synaptic plasticity in a mice model of accelerated senescence. Neurobiology of Aging 33(3): p.627.e13-627.e26.

Lopez-Rodriguez, A.B. et al. 2018. Microglial and Astrocyte priming in the APP/PS1 model of Alzheimer's Disease: Increased vulnerability to acute inflammation and cognitive deficits. bioRxiv: p.344218. Available at: https://www.biorxiv.org/content/10.1101/344218v1 [Accessed August 19, 2021].

Lopez-Rodriguez, A.B. et al. 2021. Acute systemic inflammation exacerbates neuroinflammation in Alzheimer's disease: IL-1β drives amplified responses in primed astrocytes and neuronal network dysfunction. Alzheimer's and Dementia.

Louveau, A., Harris, T.H., & Kipnis, J. 2015. Revisiting the Mechanisms of CNS Immune Privilege. Trends in Immunology 36(10): p.569–577.

Lu, Y. et al. 2016. Inflammatory and immune markers associated with physical frailty syndrome: Findings from Singapore longitudinal aging studies. Oncotarget 7(20): p.28783–28795.

Lui, H. et al. 2016. Progranulin Deficiency Promotes Circuit-Specific Synaptic Pruning by Microglia via Complement Activation. Cell 165(4): p.921–935. Available at: https://pubmed.ncbi.nlm.nih.gov/27114033/ [Accessed September 1, 2021].

Luine, V. 2016. Estradiol: Mediator of memories, spine density and cognitive resilience to stress in female rodents. Journal of Steroid Biochemistry and Molecular Biology 160: p.189–195.

Luine, V.N. 2014. Estradiol and cognitive function: Past, present and future. Hormones and Behavior 66(4): p.602–618.

Lull, M.E., & Block, M.L. 2010. Microglial Activation and Chronic Neurodegeneration. Neurotherapeutics 7(4): p.354–365.

Lundman, P. et al. 2007. A high-fat meal is accompanied by increased plasma interleukin-6 concentrations. Nutrition, Metabolism and Cardiovascular Diseases 17(3): p.195–202. Available at: http://www.nmcd-journal.com/article/S0939475305002528/fulltext [Accessed August 28, 2021].

Ma, J., Becker, C., Lowell, C.A., & Underhill, D.M. 2012. Dectin-1-triggered recruitment of light chain 3 protein to phagosomes facilitates major histocompatibility complex class II presentation of fungal-derived antigens. Journal of Biological Chemistry 287(41): p.34149–34156.

Ma, L. et al. 2021. Targeted deletion of interleukin-6 in a mouse model of chronic inflammation demonstrates opposing roles in aging: Benefit and harm. Journals of Gerontology - Series A Biological Sciences and Medical Sciences 76(2): p.211–215. Available at: https://academic.oup.com/biomedgerontology/article/76/2/211/5862779 [Accessed August 28, 2021].

Macklin, L. et al. 2017. Glucose tolerance and insulin sensitivity are impaired in APP/PS1 transgenic mice prior to amyloid plaque pathogenesis and cognitive decline. Experimental Gerontology 88: p.9–18.

MacLullich, A.M.J., Beaglehole, A., Hall, R.J., & Meagher, D.J. 2009. Delirium and long-term cognitive impairment. International Review of Psychiatry 21(1): p.30–42.

Maes, M. et al. 2012. Depression and sickness behavior are Janus-faced responses to shared inflammatory pathways. BMC Medicine 10.

Magnusson, K. R., Hauck, L., Jeffrey, B. M., Elias, V., Humphrey, A., Nath, R., Perrone, A., & Bermudez, L. E. (2015). Relationships between diet-related changes in the gut microbiome and cognitive flexibility. Neuroscience, 300, 128–140. https://doi.org/10.1016/j.neuroscience.2015.05.016

Mahad, D.J., & Ransohoff, R.M. 2003. The role of MCP-1 (CCL2) and CCR2 in multiple sclerosis and experimental autoimmune encephalomyelitis (EAE). Seminars in Immunology 15(1): p.23–32.

Mahanna-Gabrielli, E. et al. 2020. Frailty Is Associated with Postoperative Delirium but Not with Postoperative Cognitive Decline in Older Noncardiac Surgery Patients. Anesthesia and Analgesia: p.1516–1523.

Mailliez, A., Guilbaud, A., Puisieux, F., Dauchet, L., & Boulanger, É. 2020. Circulating biomarkers characterizing physical frailty: CRP, hemoglobin, albumin, 25OHD and free testosterone as best biomarkers. Results of a meta-analysis. Experimental Gerontology 139: p.111014.

Malandrino, M.I. et al. 2015. Enhanced fatty acid oxidation in adipocytes and macrophages reduces lipid-induced triglyceride accumulation and inflammation. American Journal of Physiology - Endocrinology and Metabolism 308(9).

Malik, M. et al. 2015. Genetics ignite focus on microglial inflammation in Alzheimer's disease. Molecular Neurodegeneration 10(1).

Maltais, M.L., Desroches, J., & Dionne, I.J. 2009. Changes in muscle mass and strength after menopause. Journal of Musculoskeletal Neuronal Interactions 9(4): p.186–197.

Man, S., Ubogu, E. E., & Ransohoff, R. M. (2007). Inflammatory cell migration into the central nervous system: A few new twists on an old tale. Brain Pathology, 17(2), 243–250. https://doi.org/10.1111/j.1750-3639.2007.00067.

Manczak, M. et al. 2006. Mitochondria are a direct site of Aβ accumulation in Alzheimer's disease neurons: Implications for free radical generation and oxidative damage in disease progression. Human Molecular Genetics 15(9): p.1437–1449.

Mangano, E.N., & Hayley, S. 2009. Inflammatory priming of the substantia nigra influences the

impact of later paraquat exposure: Neuroimmune sensitization of neurodegeneration. Neurobiology of Aging 30(9): p.1361–1378.

Marongiu, R. 2019. Accelerated Ovarian Failure as a Unique Model to Study Peri-Menopause Influence on Alzheimer's Disease. Frontiers in Aging Neuroscience 11.

Martinez, J. et al. 2011. Microtubule-associated protein 1 light chain 3 alpha (LC3)-associated phagocytosis is required for the efficient clearance of dead cells. Proceedings of the National Academy of Sciences of the United States of America 108(42): p.17396–17401.

Maschke, M. et al. 2004. Age-related changes of the dentate nuclei in normal adults as revealed by 3D fast low angle shot (FLASH) echo sequence magnetic resonance imaging. Journal of Neurology 251(6): p.740–746. Available at: https://pubmed.ncbi.nlm.nih.gov/15311352/ [Accessed January 25, 2022].

Mason, J.L., Suzuki, K., Chaplin, D.D., & Matsushima, G.K. 2001. Interleukin-1β promotes repair of the CNS. Journal of Neuroscience 21(18): p.7046–7052.

Mattay, V.S. et al. 2002. Neurophysiological correlates of age-related changes in human motor function. Neurology 58(4): p.630–635.

Mayeuf-Louchart, A. et al. 2018. MuscleJ: A high-content analysis method to study skeletal muscle with a new Fiji tool. Skeletal Muscle 8(1): p.1–11. Available at: https://link.springer.com/articles/10.1186/s13395-018-0171-0 [Accessed September 23, 2021].

McAlpine, F.E. et al. 2009. Inhibition of soluble TNF signaling in a mouse model of Alzheimer's disease prevents pre-plaque amyloid-associated neuropathology. Neurobiology of Disease 34(1): p.163–177.

McKhann, G.M. et al. 2011. The diagnosis of dementia due to Alzheimer's disease: Recommendations from the National Institute on Aging-Alzheimer's Association workgroups on diagnostic guidelines for Alzheimer's disease. Alzheimer's and Dementia 7(3): p.263–269.

McMillin, M.A. et al. 2015. TGFβ1 exacerbates blood-brain barrier permeability in a mouse model of hepatic encephalopathy via upregulation of MMP9 and downregulation of claudin-5. Laboratory Investigation 95(8): p.903–913. Available at: /pmc/articles/PMC5040071/ [Accessed September 20, 2021].

Van der Meer, J.W.M., Joosten, L.A.B., Riksen, N., & Netea, M.G. 2015. Trained immunity: A smart way to enhance innate immune defence. Molecular Immunology 68(1): p.40–44.

Melchior, B., Puntambekar, S.S., & Carson, M.J. 2006. Microglia and the control of autoreactive T cell responses. Neurochemistry International 49(2): p.145–153.

Melief, J. et al. 2016. Characterizing primary human microglia: A comparative study with myeloid subsets and culture models. Glia 64(11): p.1857–1868.

Memon, A., Darif, M., Al-Saleh, K., & Suresh, A. 2002. Pegylated liposomal tumor necrosis factor-α results in reduced toxicity and synergistic antitumor activity after systemic administration in combination with liposomal doxorubicin (Doxil®) in soft tissue sarcoma-bearing rats. International Journal of Cancer 97(1): p.115–120. Available at: https://pubmed.ncbi.nlm.nih.gov/11774252/ [Accessed September 6, 2021].

Mendes, N.F. et al. 2018. TGF-β1 down-regulation in the mediobasal hypothalamus attenuates hypothalamic inflammation and protects against diet-induced obesity. Metabolism: Clinical and Experimental 85: p.171–182. Available at: https://pubmed.ncbi.nlm.nih.gov/29660453/ [Accessed September 12, 2021].

Mennenga, S.E. et al. 2015. Understanding the cognitive impact of the contraceptive estrogen Ethinyl Estradiol: Tonic and cyclic administration impairs memory, and performance correlates with basal forebrain cholinergic system integrity. Psychoneuroendocrinology 54: p.1–13.

Michael-Titus, A., Revest, P., & Shortland, P. 2010. HEARING AND BALANCE: THE AUDITORY AND VESTIBULAR SYSTEMS. The Nervous System: p.141–158.

Mifflin, M.A. et al. 2021. Sex differences in the IntelliCage and the Morris water maze in the APP/PS1 mouse model of amyloidosis. Neurobiology of Aging 101: p.130–140.

Milanski, M. et al. 2009. Saturated fatty acids produce an inflammatory response predominantly through the activation of TLR4 signaling in hypothalamus: Implications for the pathogenesis of obesity. Journal of Neuroscience 29(2): p.359–370.

Milne, M.R., Haug, C.A., Ábrahám, I.M., & Kwakowsky, A. 2015. Estradiol modulation of neurotrophin receptor expression in female mouse basal forebrain cholinergic neurons in vivo. Endocrinology 156(2): p.613–626.

Mitnitski, A. et al. 2005. Relative fitness and frailty of elderly men and women in developed countries and their relationship with mortality. Journal of the American Geriatrics Society 53(12): p.2184–2189.

Mitnitski, A. et al. 2015. Age-related frailty and its association with biological markers of ageing. BMC Medicine 13(1): p.1–10.

Mitnitski, A.B., Mogilner, A.J., MacKnight, C., & Rockwood, K. 2002. The mortality rate as a function of accumulated deficits in a frailty index. Mechanisms of Ageing and Development 123(11): p.1457–1460.

Mittelbronn, M., Dietz, K., Schluesener, H.J., & Meyermann, R. 2001. Local distribution of microglia in the normal adult human central nervous system differs by up to one order of magnitude. Acta Neuropathologica 101(3): p.249–255.

Miyamoto, M. et al. 1986. Age-related changes in learning and memory in the senescence-accelerated mouse (SAM). Physiology and Behavior 38(3): p.399–406.

Miyazaki, Y., Pipek, R., Mandarino, L.J., & DeFronzo, R.A. 2003. Tumor necrosis factor α and insulin resistance in obese type 2 diabetic patients. International Journal of Obesity 27(1): p.88–94.

Mizushima, N., Levine, B., Cuervo, A.M., & Klionsky, D.J. 2008. Autophagy fights disease through cellular self-digestion. Nature 451(7182): p.1069–1075.

Moffat, J.G., Edens, A., & Talamantes, F. 1999. Structure and expression of the mouse growth hormone receptor/growth hormone binding protein gene. Journal of Molecular Endocrinology 23(1): p.33–44.

Mogensen, T.H. 2009. Pathogen recognition and inflammatory signaling in innate immune defenses. Clinical Microbiology Reviews 22(2): p.240–273.

Mogi, M. et al. 1994. Tumor necrosis factor-α (TNF-α) increases both in the brain and in the cerebrospinal fluid from parkinsonian patients. Neuroscience Letters 165(1–2): p.208–210.

Mohler, M.J., Fain, M.J., Wertheimer, A.M., Najafi, B., & Nikolich-Žugich, J. 2014. The Frailty Syndrome: Clinical measurements and basic underpinnings in humans and animals. Experimental Gerontology 54: p.6–13.

Molina, H. et al. 1996. Markedly impaired humoral immune response in mice deficient in complement receptors 1 and 2. Proceedings of the National Academy of Sciences of the United States of America 93(8): p.3357–3361.

Montagne, A. et al. 2015. Blood-Brain barrier breakdown in the aging human hippocampus. Neuron 85(2): p.296–302. Available at: /pmc/articles/PMC4350773/ [Accessed September 13, 2021].

Monteil, D., Walrand, S., Vannier-Nitenberg, C., Van Oost, B., & Bonnefoy, M. 2020. The Relationship Between Frailty, Obesity and Social Deprivation in Non-Institutionalized Elderly People. Journal of Nutrition, Health and Aging 24(8): p.821–826.

Mooradian, A.D., Reed, R.L., Osterweil, D., & Scuderi, P. 1991. Detectable Serum Levels of Tumor Necrosis Factor Alpha May Predict Early Mortality in Elderly Institutionalized Patients. Journal of the American Geriatrics Society 39(9): p.891–894.

Moore, D.R. et al. 2015. Protein ingestion to stimulate myofibrillar protein synthesis requires greater relative protein intakes in healthy older versus younger men. Journals of Gerontology - Series A Biological Sciences and Medical Sciences 70(1): p.57–62.

Mor-Vaknin, N., Punturieri, A., Sitwala, K., & Markovitz, D.M. 2003. Vimentin is secreted by activated macrophages. Nature Cell Biology 5(1): p.59–63.

Moraes, J.C. et al. 2009. High-fat diet induces apoptosis of hypothalamic neurons. PLoS ONE 4(4).

Morales, H., & Tomsick, T. 2015. Middle cerebellar peduncles: Magnetic resonance imaging and pathophysiologic correlate. World Journal of Radiology 7(12): p.438.

Morley, J.E. et al. 1997. Potentially predictive and manipulable blood serum correlates of aging in the healthy human male: Progressive decreases in bioavailable testosterone, dehydroepiandrosterone sulfate, and the ratio of insulin-like growth factor 1 to growth hormone. Proceedings of the National Academy of Sciences of the United States of America 94(14): p.7537–7542.

Morley, J.E. et al. 2000. β-Amyloid precursor polypeptide in SAMP8 mice affects learning and memory. Peptides 21(12): p.1761–1767.

Morley, J.E., & Malmstrom, T.K. 2013. Frailty, Sarcopenia, and Hormones. Endocrinology and Metabolism Clinics of North America 42(2): p.391–405.

Morley, J.E., & Silver, A.J. 1988. Anorexia in the elderly. Neurobiology of Aging 9(C): p.9–16.

Morris, R.G.M., Garrud, P., Rawlins, J.N.P., & O'Keefe, J. 1982. Place navigation impaired in rats with hippocampal lesions. Nature 297(5868): p.681–683.

Morrison, C.D. et al. 2010. High fat diet increases hippocampal oxidative stress and cognitive impairment in aged mice: Implications for decreased Nrf2 signaling. Journal of Neurochemistry 114(6): p.1581–1589.

Morrison, J.H., & Baxter, M.G. 2012. The ageing cortical synapse: Hallmarks and implications for cognitive decline. Nature Reviews Neuroscience 13(4).

Mrdjen, D. et al. 2018. High-Dimensional Single-Cell Mapping of Central Nervous System Immune Cells Reveals Distinct Myeloid Subsets in Health, Aging, and Disease. Immunity 48(2): p.380-

395.e6. Available at: https://pubmed.ncbi.nlm.nih.gov/29426702/ [Accessed August 20, 2021].

Mughal, M.R. et al. 2011. Electroconvulsive shock ameliorates disease processes and extends survival in huntingtin mutant mice. Human Molecular Genetics 20(4): p.659–669.

Muñoz-Castañeda, R. et al. 2021. Cellular anatomy of the mouse primary motor cortex. Nature 598(7879): p.159–166. Available at: https://www.nature.com/articles/s41586-021-03970-w [Accessed January 20, 2022].

Munshi, M.N. 2017. Cognitive dysfunction in older adults with diabetes: What a clinician needs to know. Diabetes Care 40(4): p.461–467. Available at: https://care.diabetesjournals.org/content/40/4/461 [Accessed August 26, 2021].

Murayi, R., & Chittiboina, P. 2016. Glucocorticoids in the management of peritumoral brain edema: a review of molecular mechanisms. Child's Nervous System 32(12): p.2293–2302.

Murray, C. et al. 2012. Systemic inflammation induces acute working memory deficits in the primed brain: Relevance for delirium. Neurobiology of Aging 33(3): p.603-616.e3.

Muscaritoli, M. et al. 2010. Consensus definition of sarcopenia, cachexia and pre-cachexia: Joint document elaborated by Special Interest Groups (SIG) ' cachexia-anorexia in chronic wasting diseases' and ' nutrition in geriatrics'. Clinical Nutrition 29(2): p.154–159.

Nachun, D.C. 2019. Peripheral inflammation in neurodegenerative diseases. Dissertation Abstracts International: Section B: The Sciences and Engineering 80(2-B(E)): p.No-Specified. Available at: http://ovidsp.ovid.com/ovidweb.cgi?T=JS&PAGE=reference&D=psyc16&NEWS=N&AN=2018-58621-209.

Nahrendorf, M. et al. 2007. The healing myocardium sequentially mobilizes two monocyte subsets with divergent and complementary functions. Journal of Experimental Medicine 204(12): p.3037–3047.

Nakagawa, T. et al. 2003. Antiobesity and antidiabetic effects of brain-derived neurotrophic factor in rodent models of leptin resistance. International Journal of Obesity 27(5): p.557–565.

Namgaladze, D. et al. 2014. Inhibition of macrophage fatty acid β-oxidation exacerbates palmitate-induced inflammatory and endoplasmic reticulum stress responses. Diabetologia 57(5): p.1067–1077.

Nawashiro, H., Martin, D., & Hallenbeck, J.M. 1997. Inhibition of tumor necrosis factor and amelioration of brain infarction in mice. Journal of Cerebral Blood Flow and Metabolism 17(2): p.229–232.

Nazmi, A. et al. 2021. Cholinergic signalling in the forebrain controls microglial phenotype and responses to systemic inflammation. bioRxiv: p.2021.01.18.427123. Available at: https://app.dimensions.ai/details/publication/pub.1134716509%0Ahttps://www.biorxiv.org/content/biorxiv/early/2021/01/19/2021.01.18.427123.full.pdf.

Naznin, F. et al. 2015. Diet-induced obesity causes peripheral and central ghrelin resistance by promoting inflammation. Journal of Endocrinology 226(1): p.81–92.

Neher, J.J., & Cunningham, C. 2019. Priming Microglia for Innate Immune Memory in the Brain. Trends in Immunology 40(4): p.358–374.

Neumann, H., & Daly, M.J. 2013. Variant TREM2 as Risk Factor for Alzheimer's Disease . New England Journal of Medicine 368(2): p.182–184.

Newman, J.C. et al. 2017. Ketogenic Diet Reduces Midlife Mortality and Improves Memory in Aging Mice. Cell Metabolism 26(3): p.547-557.e8. Available at: /pmc/articles/PMC5605815/ [Accessed March 14, 2021].

Ng, T.K.S., Ho, C.S.H., Tam, W.W.S., Kua, E.H., & Ho, R.C.M. 2019. Decreased serum brain-derived neurotrophic factor (BDNF) levels in patients with Alzheimer's disease (AD): A systematic review and meta-analysis. International Journal of Molecular Sciences 20(2).

Ng, T.P. et al. 2015. Markers of T-cell senescence and physical frailty: Insights from Singapore longitudinal ageing studies. npj Aging and Mechanisms of Disease 1(1): p.15005.

Nguyen, T.T., Ta, Q.T.H., Nguyen, T.K.O., Nguyen, T.T.D., & Giau, V. Van. 2020. Type 3 diabetes and its role implications in alzheimer's disease. International Journal of Molecular Sciences 21(9).

Niccoli, T., & Partridge, L. 2012. Ageing as a risk factor for disease. Current Biology 22(17).

Nikodemova, M. et al. 2015. Microglial numbers attain adult levels after undergoing a rapid decrease in cell number in the third postnatal week. Journal of Neuroimmunology 278: p.280–288.

Nikolich-Žugich, J. 2008. Ageing and life-long maintenance of T-cell subsets in the face of latent persistent infections. Nature Reviews Immunology 8(7): p.512–522.

Nimmerjahn, A., Kirchhoff, F., & Helmchen, F. 2005. Neuroscience: Resting microglial cells are highly

dynamic surveillants of brain parenchyma in vivo. Science 308(5726): p.1314–1318.

Nitchingham, A., Kumar, V., Shenkin, S., Ferguson, K.J., & Caplan, G.A. 2018. A systematic review of neuroimaging in delirium: predictors, correlates and consequences. In International Journal of Geriatric Psychiatry, 1458–1478.

Nixon, R.A., Cataldo, A.M., & Mathews, P.M. 2000. The Endosomal-Lysosomal System of Neurons in Alzheimer's Disease Pathogenesis: A Review. Neurochemical Research 25(9–10): p.1161–1172.

Noble, E. E., Hsu, T. M., & Kanoski, S. E. (2017). Gut to brain dysbiosis: Mechanisms linking western diet consumption, the microbiome, and cognitive impairment. Frontiers in Behavioral Neuroscience, 11. https://doi.org/10.3389/fnbeh.2017.00009

Noguerón García, A. et al. 2020. Gait plasticity impairment as an early frailty biomarker. Experimental Gerontology 142: p.111137.

Nolan, C.R., Wyeth, G., Milford, M., & Wiles, J. 2011. The race to learn: Spike timing and STDP can coordinate learning and recall in CA3. Hippocampus 21(6): p.647–660.

Norden, D.M., Fenn, A.M., Dugan, A., & Godbout, J.P. 2014. TGFβ produced by IL-10 redirected astrocytes attenuates microglial activation. Glia 62(6): p.881–895.

Norden, D.M., Muccigrosso, M.M., & Godbout, J.P. 2015. Microglial priming and enhanced reactivity to secondary insult in aging, and traumatic CNS injury, and neurodegenerative disease. Neuropharmacology 96(PA): p.29–41.

Nordgreen, J., Munsterhjelm, C., Aae, F., Popova, A., Boysen, P., Ranheim, B., Heinonen, M., Raszplewicz, J., Piepponen, P., Lervik, A., Valros, A., & Janczak, A. M. (2018). The effect of lipopolysaccharide (LPS) on inflammatory markers in blood and brain and on behavior in individually-housed pigs. Physiology and Behavior, 195, 98–111. https://doi.org/10.1016/j.physbeh.2018.07.013

Oakley, H. et al. 2006. Intraneuronal β-amyloid aggregates, neurodegeneration, and neuron loss in transgenic mice. J Neurosci 26(40): p.10129–10140. Available at: http://eutils.ncbi.nlm.nih.gov/entrez/eutils/elink.fcgi?dbfrom=pubmed&id=17021169&retmode=ref&cmd=prlinks.

Oeckinghaus, A., & Ghosh, S. 2009. The NF-kappaB family of transcription factors and its regulation. Cold Spring Harbor perspectives in biology 1(4).

Öhman, T. et al. 2014. Dectin-1 Pathway Activates Robust Autophagy-Dependent Unconventional Protein Secretion in Human Macrophages. The Journal of Immunology 192(12): p.5952–5962.

Olesen, M.A., Torres, A.K., Jara, C., Murphy, M.P., & Tapia-Rojas, C. 2020. Premature synaptic mitochondrial dysfunction in the hippocampus during aging contributes to memory loss. Redox Biology 34: p.101558.

Oliff, A. et al. 1987. Tumors secreting human TNF/cachectin induce cachexia in mice. Cell 50(4): p.555–563.

Ono, M. et al. 2000. Intermittent administration of brain-derived neurotrophic factor ameliorates glucose metabolism in obese diabetic mice. Metabolism: Clinical and Experimental 49(1): p.129–133.

Opal, S. M., Scannon, P. J., Vincent, J. L., White, M., Carroll, S. F., Palardy, J. E., Parejo, N. A., Pribble, J. P., & Lemke, J. H. (1999). Relationship between plasma levels of lipopolysaccharide (LPS) and LPS- binding protein in patients with severe sepsis and septic shock. Journal of Infectious Diseases, 180(5), 1584–1589. https://doi.org/10.1086/315093

Orellana-Gavaldà, J.M. et al. 2011. Molecular therapy for obesity and diabetes based on a long-term increase in hepatic fatty-acid oxidation. Hepatology 53(3): p.821–832.

Orihuela, R., McPherson, C.A., & Harry, G.J. 2016. Microglial M1/M2 polarization and metabolic states. British Journal of Pharmacology 173(4): p.649–665.

Ormazabal, V. et al. 2018. Association between insulin resistance and the development of cardiovascular disease. Cardiovascular Diabetology 17(1).

Osburg, B. et al. 2002. Effect of endotoxin on expression of TNF receptors and transport of TNF-α at the blood-brain barrier of the rat. American Journal of Physiology - Endocrinology and Metabolism 283(5 46-5). Available at: https://pubmed.ncbi.nlm.nih.gov/12376316/ [Accessed September 19, 2021].

Ota, K. et al. 2011. Identification of senescence-associated genes and their networks under oxidative stress by the analysis of bach1. Antioxidants and Redox Signaling 14(12): p.2441–2451.

Ott, A., Breteler, M.M.B., Van Harskamp, F., Stijnen, T., & Hofman, A. 1998. Incidence and risk of dementia: The Rotterdam Study. American Journal of Epidemiology 147(6): p.574–580.

Oveisgharan, S. et al. 2018. Sex differences in Alzheimer's disease and common neuropathologies

of aging. Acta Neuropathologica 136(6): p.887–900.

Pace, J.L., Russell, S.W., Torres, B.A., Johnson, H.M., & Gray, P.W. 1983. Recombinant mouse gamma interferon induces the priming step in macrophage activation for tumor cell killing. Journal of immunology (Baltimore, Md. : 1950) 130(5): p.2011–3. Available at: http://www.ncbi.nlm.nih.gov/pubmed/6403616.

Paganelli, R. et al. 2002. Proinflammatory cytokines in sera of elderly patients with dementia: Levels in vascular injury are higher than those of mild-moderate Alzheimer's disease patients. Experimental Gerontology 37(2–3): p.257–263.

Palin, K. et al. 2009. The type 1 TNF receptor and its associated adapter protein, FAN, are required for TNFα-induced sickness behavior. Psychopharmacology 201(4): p.549–556.

Palin, K., Cunningham, C., Forse, P., Perry, V.H., & Platt, N. 2008. Systemic inflammation switches the inflammatory cytokine profile in CNS Wallerian degeneration. Neurobiology of Disease 30(1): p.19–29.

Pan, W., Banks, W.A., & Kastin, A.J. 1997. Permeability of the blood-brain and blood-spinal cord barriers to interferons. Journal of Neuroimmunology 76(1–2): p.105–111.

Pan, W., & Kastin, A.J. 2002. TNFα transport across the blood-brain barrier is abolished in receptor knockout mice. Experimental Neurology 174(2): p.193–200. Available at: http://www.idealibrary.com [Accessed September 19, 2021].

Pan, W., Zhang, L., Liao, J., Csernus, B., & Kastin, A.J. 2003. Selective increase in TNFα permeation across the blood-spinal cord barrier after SCI. Available at: www.elsevier.com/locate/jneuroim.

Pandharipande, P.P. et al. 2013. Long-Term Cognitive Impairment after Critical Illness. New England Journal of Medicine 369(14): p.1306–1316.

Panee, J. 2012. Monocyte Chemoattractant Protein 1 (MCP-1) in obesity and diabetes. Cytokine 60(1): p.1–12.

Di Paolo, G., & Kim, T.W. 2011. Linking lipids to Alzheimer's disease: Cholesterol and beyond. Nature Reviews Neuroscience 12(5): p.284–296.

Papadakis, M.A. et al. 1996. Growth hormone replacement in healthy older men improves body composition but not functional ability. Annals of Internal Medicine 124(8): p.708–716.

Paré, A. et al. 2018. IL-1β enables CNS access to CCR2hi monocytes and the generation of

pathogenic cells through GM-CSF released by CNS endothelial cells. Proceedings of the National Academy of Sciences of the United States of America 115(6): p.E1194–E1203.

Park, Y., Choi, J.E., & Hwang, H.S. 2018. Protein supplementation improves muscle mass and physical performance in undernourished prefrail and frail elderly subjects: A randomized, double-blind, placebo-controlled trial. American Journal of Clinical Nutrition 108(5).

Parks, R.J. et al. 2012. A procedure for creating a frailty index based on deficit accumulation in aging mice. Journals of Gerontology - Series A Biological Sciences and Medical Sciences 67 A(3): p.217–227.

Parpura, V., & Zorec, R. 2010. Gliotransmission: Exocytotic release from astrocytes. Brain Research Reviews 63(1–2): p.83–92.

Pasparakis, M., & Vandenabeele, P. 2015. Necroptosis and its role in inflammation. Nature 517(7534): p.311–320.

Paul, S., Jeon, W.K., Bizon, J.L., & Han, J.S. 2015. Interaction of basal forebrain cholinergic neurons with the glucocorticoid system in stress regulation and cognitive impairment. Frontiers in Aging Neuroscience 7(MAR).

Paul Stroemer, R., & Rothwell, N.J. 1998. Exacerbation of ischemic brain damage by localized striatal injection of interleukin-1β in the rat. Journal of Cerebral Blood Flow and Metabolism 18(8).

Pawelec, G., Goldeck, D., & Derhovanessian, E. 2014. Inflammation, ageing and chronic disease. Current Opinion in Immunology 29(1): p.23–28.

Pelleymounter, M.A., Cullen, M.J., & Wellman, C.L. 1995. Characteristics of BDNF-induced weight loss. Experimental Neurology 131(2): p.229–238.

Perez-Cruz, C. et al. 2011. Reduced spine density in specific regions of CA1 pyramidal neurons in two transgenic mouse models of Alzheimer's disease. Journal of Neuroscience 31(10): p.3926–3934. Available at: https://www.jneurosci.org/content/31/10/3926 [Accessed September 5, 2021].

Perry, C.D. et al. 2008. Centrally located body fat is related to inflammatory markers in healthy postmenopausal women. Menopause 15(4): p.619–627.

Perry, V.H., Cunningham, C., & Holmes, C. 2007. Systemic infections and inflammation affect chronic neurodegeneration. Nature Reviews Immunology 7(2): p.161–167.

Perry, V.H., Nicoll, J.A.R., & Holmes, C. 2010. Microglia in neurodegenerative disease. Nature

Reviews Neurology 6(4): p.193–201.

Persico, I. et al. 2018. Frailty and Delirium in Older Adults: A Systematic Review and Meta-Analysis of the Literature. Journal of the American Geriatrics Society 66(10): p.2022–2030. Available at: https://agsjournals.onlinelibrary.wiley.com/doi/full/10.1111/jgs.15503 [Accessed September 2, 2021].

Petrosini, L., Leggio, M.G., & Molinari, M. 1998. The cerebellum in the spatial problem solving: A co-star or a guest star? Progress in Neurobiology 56(2): p.191–210.

Phillips, M.L., Robinson, H.A., & Pozzo-Miller, L. 2019. Ventral hippocampal projections to the medial prefrontal cortex regulate social memory. eLife 8.

Pierse, T., O'Shea, E., & Carney, P. 2019. Estimates of the prevalence, incidence and severity of dementia in Ireland. Irish Journal of Psychological Medicine 36(2): p.129–137.

Pike, C.J. 2017. Sex and the development of Alzheimer's disease. Journal of Neuroscience Research 95(1–2): p.671–680.

Pistell, P.J. et al. 2010. Cognitive impairment following high fat diet consumption is associated with brain inflammation. Journal of Neuroimmunology 219(1–2): p.25–32.

Plemel, J.R., Manesh, S.B., Sparling, J.S., & Tetzlaff, W. 2013. Myelin inhibits oligodendroglial maturation and regulates oligodendrocytic transcription factor expression. Glia 61(9): p.1471–1487.

Plum, L., Schubert, M., & Brüning, J.C. 2005. The role of insulin receptor signaling in the brain. Trends in Endocrinology and Metabolism 16(2): p.59–65.

Podcasy, J.L., & Epperson, C.N. 2016. Considering sex and gender in Alzheimer disease and other dementias. Dialogues in Clinical Neuroscience 18(4): p.437–446.

Politis, M., Su, P., & Piccini, P. 2012. Imaging of microglia in patients with neurodegenerative disorders. Frontiers in Pharmacology 3 MAY.

Poli-de-Figueiredo, L. F., Garrido, A. G., Nakagawa, N., & Sannomiya, P. (2008). Experimental models of sepsis and their clinical relevance. Shock, 30(SUPPL. 1), 53–59. https://doi.org/10.1097/SHK.0b013e318181a343

Pollack, M., & Leeuwenburgh, C. 2001. Apoptosis and aging: Role of the mitochondria. Journals of Gerontology - Series A Biological Sciences and Medical Sciences 56(11).

Poly, T.N. et al. 2020. Association between Use of Statin and Risk of Dementia: A Meta-Analysis of Observational Studies. Neuroepidemiology 54(3): p.214–226.

Presumey, J., Bialas, A.R., & Carroll, M.C. 2017. Complement System in Neural Synapse Elimination in Development and Disease. Advances in Immunology 135: p.53–79.

Prewitt, C.M.F., Niesman, I.R., Kane, C.J.M., & Houlé, J.D. 1997. Activated macrophage/microglial cells can promote the regeneration of sensory axons into the injured spinal cord. Experimental Neurology 148(2): p.433–443.

Preziosa, P. et al. 2020. Effects of Natalizumab and Fingolimod on Clinical, Cognitive, and Magnetic Resonance Imaging Measures in Multiple Sclerosis. Neurotherapeutics 17(1): p.208–217. Available at: https://link.springer.com/article/10.1007/s13311-019-00781-w [Accessed September 5, 2021].

Qian, B.Z. et al. 2011. CCL2 recruits inflammatory monocytes to facilitate breast-tumour metastasis. Nature 475(7355): p.222–225.

Qin, Q. et al. 2021. TREM2, microglia, and Alzheimer's disease. Mechanisms of Ageing and Development 195: p.111438.

Qin, Y. et al. 2020. Estradiol Replacement at the Critical Period Protects Hippocampal Neural Stem Cells to Improve Cognition in APP/PS1 Mice. Frontiers in Aging Neuroscience 12.

Qu, W., & Li, L. 2020. Loss of TREM2 confers resilience to synaptic and cognitive impairment in aged mice. Journal of Neuroscience 40(50): p.9552–9563.

Radde, R. et al. 2006. Aβ42-driven cerebral amyloidosis in transgenic mice reveals early and robust pathology. EMBO Reports 7(9): p.940–946.

Radloff, L.S. 1977. The CES-D Scale: A Self-Report Depression Scale for Research in the General Population. Applied Psychological Measurement 1(3): p.385–401.

Rahtes, A., & Li, L. (2020). Polarization of Low-Grade Inflammatory Monocytes Through TRAM-Mediated Up-Regulation of Keap1 by Super-Low Dose Endotoxin. Frontiers in Immunology, 11. https://doi.org/10.3389/fimmu.2020.01478

Raj, D. et al. 2017. Increased white matter inflammation in aging- and alzheimer's disease brain. Frontiers in Molecular Neuroscience 10.

Ramaglia, V. et al. 2012. C3-dependent mechanism of microglial priming relevant to multiple sclerosis. Proceedings of the National Academy of Sciences of the United States of America

109(3): p.965–970. Available at: https://pubmed.ncbi.nlm.nih.gov/22219359/ [Accessed September 23, 2021].

Rawji, K.S. et al. 2018. Deficient surveillance and phagocytic activity of myeloid cells within demyelinated lesions in aging mice visualized by ex vivo live multiphoton imaging. Journal of Neuroscience 38(8): p.1973–1988.

Rea, I.M. et al. 2018. Age and age-related diseases: Role of inflammation triggers and cytokines. Frontiers in Immunology 9(APR).

Rebouças, R. C. R., & Schmidek, W. R. (1997). Handling and isolation in three strains of rats affect open field, exploration, hoarding and predation. Physiology and Behavior, 62(5), 1159–1164. https://doi.org/10.1016/S0031-9384(97)00312-0

Record, S.C., Employers, N.H.S., England, N.H.S., & England, N.H.S. 2017. GMS Contract requirements for the identification and management of people with frailty - guidance on Batch-coding. : p.1–2.

Reilly, A.M. et al. 2020. Metabolic defects caused by high-fat diet modify disease risk through inflammatory and amyloidogenic pathways in a mouse model of Alzheimer's disease. Nutrients 12(10): p.1–18.

Reisel, D. et al. 2002. Spatial memory dissociations in mice lacking GluR1. Nature Neuroscience 5(9): p.868–873.

Remick, D. G., & Ward, P. A. (2005). Evaluation of endotoxin models for the study of sepsis. In Shock (Vol. 24, Issue SUPPL. 1, pp. 7–11). https://doi.org/10.1097/01.shk.0000191384.34066.85

Rennick, D., Davidson, N., & Berg, D. 1995. Interleukin-10 gene knock-out mice: a model of chronic inflammation. Clinical Immunology and Immunopathology 76(3 PART 2).

Réu, P. et al. 2017. The Lifespan and Turnover of Microglia in the Human Brain. Cell Reports 20(4): p.779–784.

Del Rey, A. et al. 2006. IL-1 resets glucose homeostasis at central levels. Proceedings of the National Academy of Sciences of the United States of America 103(43): p.16039–16044. Available at: /pmc/articles/PMC1635123/ [Accessed August 15, 2021].

Richardson, N.E. et al. 2021. Lifelong restriction of dietary branched-chain amino acids has sex-specific benefits for frailty and life span in mice. Nature Aging 1(1): p.73–86. Available at: https://www.nature.com/articles/s43587-020-00006-2 [Accessed August 29, 2021].

Richetin, K., Petsophonsakul, P., Roybon, L., Guiard, B.P., & Rampon, C. 2017. Differential alteration of hippocampal function and plasticity in females and males of the APPxPS1 mouse model of Alzheimer's disease. Neurobiology of Aging 57: p.220–231.

Richwine, A.F., Sparkman, N.L., Dilger, R.N., Buchanan, J.B., & Johnson, R.W. 2009. Cognitive deficits in interleukin-10-deficient mice after peripheral injection of lipopolysaccharide. Brain, Behavior, and Immunity 23(6): p.794–802. Available at: https://pubmed.ncbi.nlm.nih.gov/19272439/ [Accessed September 1, 2021].

Ricquier, D. 1999. Genetic and molecular aspects of obesity: Recent data. Pathologie-biologie 47(10): p.1080–104.

Rivest, S. 2015. TREM2 enables amyloid β clearance by microglia. Cell Research 25(5): p.535–536.

Robert, V. et al. 2021. Local circuit allowing hypothalamic control of hippocampal area CA2 activity and consequences for CA1. eLife 10.

Robertson, D.A., Savva, G.M., & Kenny, R.A. 2013. Frailty and cognitive impairment-A review of the evidence and causal mechanisms. Ageing Research Reviews 12(4): p.840–851.

Rocca, W.A. et al. 2007. Increased risk of cognitive impairment or dementia in women who underwent oophorectomy before menopause. Neurology 69(11): p.1074–1083.

Rockwood, K. et al. 1999. The risk of dementia and death after delirium. Age and Ageing 28(6): p.551–556.

Rockwood, K. et al. 2005. A global clinical measure of fitness and frailty in elderly people. Cmaj 173(5): p.489–495.

Rockwood, K. et al. 2017. A Frailty Index Based on Deficit Accumulation Quantifies Mortality Risk in Humans and in Mice. Scientific Reports 7.

Rodriguez-Rivera, J., Denner, L., & Dineley, K.T. 2011. Rosiglitazone reversal of Tg2576 cognitive deficits is independent of peripheral gluco-regulatory status. Behavioural Brain Research 216(1): p.255–261.

Rogers, J.L., & Kesner, R.P. 2004. Cholinergic Modulation of the Hippocampus during Encoding and Retrieval of Tone/Shock-Induced Fear Conditioning. Learning and Memory 11(1): p.102–107.

Roghmann, M.C., Warner, J., & Mackowiak, P.A. 2001. The relationship between age and fever magnitude. American Journal of the Medical Sciences 322(2): p.68–70. Available at: https://pubmed.ncbi.nlm.nih.gov/11523629/ [Accessed August 3, 2021].

Roh, E., Song, D.K., & Kim, M.S. 2016. Emerging role of the brain in the homeostatic regulation of energy and glucose metabolism. Experimental and Molecular Medicine 48(3).

Rolls, A. et al. 2007. Toll-like receptors modulate adult hippocampal neurogenesis. Nature Cell Biology 9(9): p.1081–1088.

Romano, M. et al. 1997. Role of IL-6 and its soluble receptor in induction of chemokines and leukocyte recruitment. Immunity 6(3): p.315–325.

Rorbach-Dolata, A., & Piwowar, A. 2019. Neurometabolic Evidence Supporting the Hypothesis of Increased Incidence of Type 3 Diabetes Mellitus in the 21st Century. BioMed Research International 2019.

Rothman, M.D., Leo-Summers, L., & Gill, T.M. 2008. Prognostic significance of potential frailty criteria. Journal of the American Geriatrics Society 56(12): p.2211–2216.

Rouault, C. et al. 2021. Senescence-associated β-galactosidase in subcutaneous adipose tissue associates with altered glycaemic status and truncal fat in severe obesity. Diabetologia 64(1): p.240–254.

Rowland, C. 2019. Why Pfizer didn't report that its rheumatoid arthritis medication might prevent Alzheimer's - The Washington Post. The Washington Post. Available at: https://www.washingtonpost.com/business/economy/pfizer-had-clues-its-blockbuster-drug-could-prevent-alzheimers-why-didnt-it-tell-the-world/2019/06/04/9092e08a-7a61-11e9-8bb7-0fc796cf2ec0_story.html?arc404=true [Accessed September 23, 2021].

Ruckh, J.M. et al. 2012. Rejuvenation of regeneration in the aging central nervous system. Cell Stem Cell 10(1): p.96–103.

Rudman, D. et al. 1990. Effects of Human Growth Hormone in Men over 60 Years Old. New England Journal of Medicine 323(1): p.1–6.

Ruiz, J. et al. 2019. Frailty assessment predicts toxicity during first cycle chemotherapy for advanced lung cancer regardless of chronologic age. Journal of Geriatric Oncology 10(1): p.48–54.

Russell, L.M., Strike, P., Browne, C.E., & Jacobs, P.A. 2007. X chromosome loss and ageing. Cytogenetic and Genome Research 116(3): p.181–185.

Sabia, S., Kivimaki, M., Shipley, M.J., Marmot, M.G., & Singh-Manoux, A. 2009. Body mass index over the adult life course and cognition in late midlife: The Whitehall II Cohort Study. American Journal of Clinical Nutrition 89(2): p.601–607.

Safaiyan, S. et al. 2021. White matter aging drives microglial diversity. Neuron 109(7): p.1100-1117.e10.

Saji, N., Murotani, K., Hisada, T., Tsuduki, T., Sugimoto, T., Kimura, A., Niida, S., Toba, K., & Sakurai, T. (2019). The relationship between the gut microbiome and mild cognitive impairment in patients without dementia: a cross-sectional study conducted in Japan. Scientific Reports, 9(1). https://doi.org/10.1038/s41598-019-55851-y

Salameh, T.S., Mortell, W.G., Logsdon, A.F., Butterfield, D.A., & Banks, W.A. 2019. Disruption of the hippocampal and hypothalamic blood-brain barrier in a diet-induced obese model of type II diabetes: Prevention and treatment by the mitochondrial carbonic anhydrase inhibitor, topiramate. Fluids and Barriers of the CNS 16(1): p.1–17. Available at: https://fluidsbarrierscns.biomedcentral.com/articles/10.1186/s12987-018-0121-6 [Accessed September 1, 2021].

Sallusto, F., & Baggiolini, M. 2008. Chemokines and leukocyte traffic. Nature Immunology 9(9): p.949–952.

Salminen, A.T. et al. 2020. In vitro Studies of Transendothelial Migration for Biological and Drug Discovery. Frontiers in Medical Technology 2: p.600616. Available at: www.frontiersin.org.

Salpeter, S.J. et al. 2013. Systemic regulation of the age-Related decline of pancreatic β-Cell replication. Diabetes 62(8): p.2843–2848.

Salvosa, C.B., Payne, P.R., & Wheeler, E.F. 1971. Environmental conditions and body temperatures of elderly women living alone or in local authority home. British Medical Journal 4(5788): p.656–659.

Sanchez, D. et al. 2020. Frailty, delirium and hospital mortality of older adults admitted to intensive care: the Delirium (Deli) in ICU study. Critical Care 24(1): p.1–8. Available at: https://link.springer.com/articles/10.1186/s13054-020-03318-2 [Accessed September 2, 2021].

Sanjuan, M.A. et al. 2007. Toll-like receptor signalling in macrophages links the autophagy pathway to phagocytosis. Nature 450(7173): p.1253–1257.

Santin, Y. et al. 2021. Towards a Large-Scale Assessment of the Relationship between Biological and Chronological Aging: The INSPIRE Mouse Cohort. The Journal of frailty & aging 10(2): p.121–131. Available at: https://link.springer.com/article/10.14283/jfa.2020.43 [Accessed August 29, 2021].

Sawdey, M., Podor, T.J., & Loskutoff, D.J. 1989. Regulation of type 1 plasminogen activator inhibitor gene expression in cultured bovine aortic endothelial cells. Induction by transforming growth factor-β, lipopolysaccharide, and tumor necrosis factor-α. Journal of Biological Chemistry 264(18): p.10396–10401.

Scalzo, P., Kümmer, A., Bretas, T.L., Cardoso, F., & Teixeira, A.L. 2010. Serum levels of brain-derived neurotrophic factor correlate with motor impairment in Parkinson's disease. Journal of Neurology 257(4): p.540–545.

Scheff, S.W., Price, D.A., Schmitt, F.A., Scheff, M.A., & Mufson, E.J. 2011. Synaptic loss in the inferior temporal gyrus in mild cognitive impairment and Alzheimer's disease. Journal of Alzheimer's Disease 24(3): p.547–557. Available at: https://pubmed.ncbi.nlm.nih.gov/21297265/ [Accessed September 5, 2021].

Schmid, S. et al. 2019. Cognitive decline in Tg2576 mice shows sex-specific differences and correlates with cerebral amyloid-beta. Behavioural Brain Research 359: p.408–417.

Schmitt, U., & Hiemke, C. (1998). Strain differences in open-field and elevated plus-maze behavior of rats without and with pretest handling. Pharmacology Biochemistry and Behavior, 59(4), 807–811. https://doi.org/10.1016/S0091-3057(97)00502-9

Schnell, L. 1999. Acute inflammatory responses to mechanical lesions in the CNS: Differences between brain and spinal cord. European Journal of Neuroscience 11(10): p.3648–3658.

Schorr, A., Carter, C., & Ladiges, W. 2018. The potential use of physical resilience to predict healthy aging. Pathobiology of Aging & Age-related Diseases 8(1): p.1403844.

Schultz, M.B. et al. 2020. Age and life expectancy clocks based on machine learning analysis of mouse frailty. Nature Communications 11(1): p.1–12. Available at: https://www.nature.com/articles/s41467-020-18446-0 [Accessed August 27, 2021].

Schuster, N., Dünker, N., & Krieglstein, K. 2002. Transforming growth factor-β induced cell death in the developing chick retina is mediated via activation of c-jun N-terminal kinase and downregulation of the anti-apoptotic protein Bcl-XL. Neuroscience Letters 330(3): p.239–242.

Searle, S.D., & Rockwood, K. 2015. Frailty and the risk of cognitive impairment. Alzheimer's Research and Therapy 7(1): p.54. Available at: http://alzres.com/content/7/1/54.

Sebastián, D., Herrero, L., Serra, D., Asins, G., & Hegardt, F.G. 2007. CPT I overexpression protects L6E9 muscle cells from fatty acid-induced insulin resistance. American Journal of Physiology - Endocrinology and Metabolism 292(3).

Sedelnikova, O.A. et al. 2004. Senescing human cells and ageing mice accumulate DNA lesions with unrepairable double-strand breaks. Nature Cell Biology 6(2): p.168–170.

Seeley, J. J., & Ghosh, S. (2017). Molecular mechanisms of innate memory and tolerance to LPS. Journal of Leukocyte Biology, 101(1), 107–119. https://doi.org/10.1189/jlb.3mr0316-118rr

Seifert, E.L., Estey, C., Xuan, J.Y., & Harper, M.E. 2010. Electron transport chain-dependent and -independent mechanisms of mitochondrial H2O2 emission during long-chain fatty acid oxidation. Journal of Biological Chemistry 285(8): p.5748–5758.

Seldeen, K.L., Pang, M., & Troen, B.R. 2015. Mouse Models of Frailty: an Emerging Field. Current Osteoporosis Reports 13(5): p.280–286.

Selkoe, D.J., & Hardy, J. 2016. The amyloid hypothesis of Alzheimer's disease at 25 years. EMBO Molecular Medicine 8(6): p.595–608.

Seltzer, M.H., Slocum, B.A., Cataldi-Betcher, E.L., Fileti, C., & Gerson, N. 1982. Instant nutritional assessment: absolute weight loss and surgical mortality. JPEN. Journal of parenteral and enteral nutrition 6(3): p.218–221.

Semmler, A. et al. 2013. Persistent cognitive impairment, hippocampal atrophy and EEG changes in sepsis survivors. Journal of Neurology, Neurosurgery and Psychiatry 84(1): p.62–70

Semra, Y.K., Smith, N.C.E., & Lincoln, J. 2004. Comparative effects of high glucose on different adult sympathetic neurons in culture. NeuroReport 15(15): p.2321–2325.

Sengillo, J. D., Winkler, E. A., Walker, C. T., Sullivan, J. S., Johnson, M., & Zlokovic, B. v. (2013). Deficiency in mural vascular cells coincides with blood-brain barrier disruption in alzheimer's disease. Brain Pathology, 23(3), 303–310. https://doi.org/10.1111/bpa.12004

Seo, N.Y. et al. 2021. Selective Regional Loss of Cortical Synapses Lacking Presynaptic Mitochondria in the 5xFAD Mouse Model. Frontiers in Neuroanatomy 15: p.46.

Serbina, N. V., Jia, T., Hohl, T.M., & Pamer, E.G. 2008. Monocyte-mediated defense against microbial pathogens. Annual Review of Immunology 26: p.421–452.

Serhan, C.N., Chiang, N., & Van Dyke, T.E. 2008. Resolving inflammation: Dual anti-inflammatory and pro-resolution lipid mediators. Nature Reviews Immunology 8(5): p.349–361.

Shah, V.B. et al. 2008. β-Glucan Activates Microglia without Inducing Cytokine Production in Dectin-1-Dependent Manner. The Journal of Immunology 180(5): p.2777–2785.

Shah, V.B., Ozment-Skelton, T.R., Williams, D.L., & Keshvara, L. 2009. Vav1 and PI3K are required for phagocytosis of β-glucan and subsequent superoxide generation by microglia. Molecular Immunology 46(8–9): p.1845–1853.

Shah, V.B., Williams, D.L., & Keshvara, L. 2009. β-Glucan attenuates TLR2- and TLR4-mediated cytokine production by microglia. Neuroscience Letters 458(3): p.111–115.

Shahidehpour, R.K. et al. 2021. Dystrophic microglia are associated with neurodegenerative disease and not healthy aging in the human brain. Neurobiology of aging 99: p.19–27.

Shamliyan, T., Talley, K.M.C., Ramakrishnan, R., & Kane, R.L. 2013. Association of frailty with survival: A systematic literature review. Ageing Research Reviews 12(2): p.719–736.

Shi, Q. et al. 2015. Complement C3-deficient mice fail to display age-related hippocampal decline. Journal of Neuroscience 35(38).

Shi, Q. et al. 2017. Complement C3 deficiency protects against neurodegeneration in aged plaque-rich APP/PS1 mice. Science Translational Medicine 9(392): p.eaaf6295.

Shi, W. et al. 2021. Progesterone Suppresses Cholesterol Esterification in APP/PS1 mice and a cell model of Alzheimer's Disease. Brain Research Bulletin 173: p.162–173. Available at: https://linkinghub.elsevier.com/retrieve/pii/S0361923021001519 [Accessed June 1, 2021].

Shibata, M. et al. 2006. Regulation of intracellular accumulation of mutant huntingtin by beclin 1. Journal of Biological Chemistry 281(20): p.14474–14485.

Shimizu, N., Oomura, Y., Plata-Salamán, C.R., & Morimoto, M. 1987. Hyperphagia and obesity in rats with bilateral ibotenic acid-induced lesions of the ventromedial hypothalamic nucleus. Brain Research 416(1).

Shoji, H., Takao, K., Hattori, S., & Miyakawa, T. 2014. Contextual and cued fear conditioning test using a video analyzing system in mice. Journal of Visualized Experiments (85).

Shull, M.M. et al. 1992. Targeted disruption of the mouse transforming growth factor-β1 gene results in multifocal inflammatory disease [14]. Nature 359(6397): p.693–699. Available at: https://pubmed.ncbi.nlm.nih.gov/1436033/ [Accessed August 26, 2021].

Silva, A.A. et al. 2017. Priming astrocytes with TNF enhances their susceptibility to Trypanosoma cruzi infection and creates a self-sustaining inflammatory milieu. Journal of Neuroinflammation 14(1).

Silva, V. et al. 2017. Chronic exercise reduces hypothalamic transforming growth factor-β1 in

middle-aged obese mice. Aging 9(8). Available at: https://pubmed.ncbi.nlm.nih.gov/28854149/ [Accessed September 12, 2021].

Sinclair, D., Purves-Tyson, T.D., Allen, K.M., & Weickert, C.S. 2014. Impacts of stress and sex hormones on dopamine neurotransmission in the adolescent brain. Psychopharmacology 231(8): p.1581–1599.

Singh-Manoux, A. et al. 2012. Obesity phenotypes in midlife and cognition in early old age: The Whitehall II cohort study. Neurology 79(8): p.755–762.

Singh, A.K., & Jiang, Y. 2004. How does peripheral lipopolysaccharide induce gene expression in the brain of rats? Toxicology 201(1–3): p.197–207.

Sipilä, S., & Poutamo, J. 2003. Muscle performance, sex hormones and training in peri-menopausal and post-menopausal women. Scandinavian Journal of Medicine and Science in Sports 13(1): p.19–25. Available at: http://doi.wiley.com/10.1034/j.1600-0838.2003.20210.x [Accessed March 17, 2021].

Sipilä, P.N. et al. 2021. Hospital-treated infectious diseases and the risk of dementia: a large, multicohort, observational study with a replication cohort. The Lancet Infectious Diseases 21(11).

Skelly, D.T. et al. 2019. Acute transient cognitive dysfunction and acute brain injury induced by systemic inflammation occur by dissociable IL-1-dependent mechanisms. Molecular Psychiatry 24(10): p.1533–1548.

Skelly, D.T., Hennessy, E., Dansereau, M.A., & Cunningham, C. 2013. A Systematic Analysis of the Peripheral and CNS Effects of Systemic LPS, IL-1B, TNF-α and IL-6 Challenges in C57BL/6 Mice. PLoS ONE 8(7).

Sliogeryte, K., & Gavara, N. 2019. Vimentin Plays a Crucial Role in Fibroblast Ageing by Regulating Biophysical Properties and Cell Migration. Cells 8(10). Available at: /pmc/articles/PMC6848922/ [Accessed September 12, 2021].

Sloane, J.A., Hollander, W., Moss, M.B., Rosene, D.L., & Abraham, C.R. 1999. Increased microglial activation and protein nitration in white matter of the aging monkey. Neurobiology of Aging 20(4).

Sly, L.M. et al. 2001. Endogenous brain cytokine mRNA and inflammatory responses to lipopolysaccharide are elevated in the Tg2576 transgenic mouse model of Alzheimer's disease. Brain Research Bulletin 56(6): p.581–588.

Smith, M.A., Makino, S., Kim, S.Y., & Kvetnansky, R. 1995. Stress increases brain-derived neurotropic factor messenger ribonucleic acid in the hypothalamus and pituitary. Endocrinology 136(9): p.3743–3750.

Smyth, E.M., Grosser, T., Wang, M., Yu, Y., & FitzGerald, G.A. 2009. Prostanoids in health and disease. Journal of Lipid Research 50(SUPPL.).

Sochocka, M., Zwolińska, K., & Leszek, J. 2017. The Infectious Etiology of Alzheimer's Disease. Current Neuropharmacology 15(7).

Sohrabji, F., & Lewis, D.K. 2006. Estrogen-BDNF interactions: Implications for neurodegenerative diseases. Frontiers in Neuroendocrinology 27(4): p.404–414.

Song, X., Mitnitski, A., & Rockwood, K. 2010. Prevalence and 10-Year outcomes of frailty in older adults in relation to deficit accumulation. Journal of the American Geriatrics Society 58(4): p.681–687.

Song, X., Mitnitski, A., & Rockwood, K. 2011. Nontraditional risk factors combine to predict Alzheimer disease and dementia. Neurology 77(3): p.227–234.

Song, X., Mitnitski, A., & Rockwood, K. 2014. Age-related deficit accumulation and the risk of late-life dementia. Alzheimer's Research and Therapy 6(5–8).

Sosa, R.A., Murphey, C., Ji, N., Cardona, A.E., & Forsthuber, T.G. 2013. The Kinetics of Myelin Antigen Uptake by Myeloid Cells in the Central Nervous System during Experimental Autoimmune Encephalomyelitis. The Journal of Immunology 191(12): p.5848–5857.

Spittau, B. 2017. Aging microglia-phenotypes, functions and implications for age-related neurodegenerative diseases. Frontiers in Aging Neuroscience 9(JUN): p.194.

Spolarics, Z., Peña, G., Qin, Y., Donnelly, R.J., & Livingston, D.H. 2017. Inherent X-linked genetic variability and cellular mosaicism unique to females contribute to sex-related differences in the innate immune response. Frontiers in Immunology 8(NOV).

Spremo-Potparević, B. et al. 2008. Premature centromere division of the X chromosome in neurons in Alzheimer's disease. Journal of Neurochemistry 106(5): p.2218–2223.

Sri, S. et al. 2019. Emergence of synaptic and cognitive impairment in a mature-onset APP mouse model of Alzheimer's disease. Acta neuropathologica communications 7(1): p.25. Available at: https://actaneurocomms.biomedcentral.com/articles/10.1186/s40478-019-0670-1 [Accessed September 5, 2021].

Stankovic, A. et al. 2009. Serum and synovial fluid concentrations of CCL2 (MCP-1) chemokine in patients suffering rheumatoid arthritis and osteoarthritis reflect disease activity. Bratislava Medical Journal 110(10): p.641–646.

Steeland, S. et al. 2017. TNFR1 inhibition with a Nanobody protects against EAE development in mice. Scientific Reports 7(1).

Steelman, A.J., & Li, J. 2014. Astrocyte galectin-9 potentiates microglial TNF secretion. Journal of Neuroinflammation 11(1).

Stefanis, L., Larsen, K.E., Rideout, H.J., Sulzer, D., & Greene, L.A. 2001. Expression of A53T mutant but not wild-type α-synuclein in PC12 cells induces alterations of the ubiquitin-dependent degradation system, loss of dopamine release, and autophagic cell death. Journal of Neuroscience 21(24): p.9549–9560.

Steinman, L. 2004. Elaborate interactions between the immune and nervous systems. Nature Immunology 5(6): p.575–581.

Steinshamn, S. et al. 1996. TNF Receptors in Murine Candida albicans Infection: Evidence for an Important Role of TNF Receptor p55 in Antifungal Defense. The Journal of Immunology 157(5): p.2155–2159.

Stephan, A.H. et al. 2013. A dramatic increase of C1q protein in the CNS during normal aging. Journal of Neuroscience 33(33).

Stewart, W.F., Kawas, C., Corrada, M., & Metter, E.J. 1997. Risk of Alzheimer's disease and duration of NSAID use. Neurology 48(3): p.626–632.

Stiel, J.N. 1968. Physiology of growth hormone. Journal of the Tennessee Medical Association 61(12): p.1196–1199. Available at: https://www.uptodate.com/contents/physiology-of-growth-hormone [Accessed August 28, 2021].

Stojakovic, A. et al. 2021. Partial inhibition of mitochondrial complex I ameliorates Alzheimer's disease pathology and cognition in APP/PS1 female mice. Communications Biology 4(1): p.1–20. Available at: https://www.nature.com/articles/s42003-020-01584-y [Accessed September 6, 2021].

Stoodley, C.J. et al. 2017. Altered cerebellar connectivity in autism and cerebellar-mediated rescue of autism-related behaviors in mice. Nature Neuroscience 20(12): p.1744–1751.

Stoppelkamp, S. et al. 2015. Murine pattern recognition receptor dectin-1 is essential in the

development of experimental autoimmune uveoretinitis. Molecular Immunology 67(2): p.398–406.

Stower, H. (2019). Depression linked to the microbiome. In Nature Medicine (Vol. 25, Issue 3, p. 358). https://doi.org/10.1038/s41591-019-0396-4

Strandwitz, P. (2018). Neurotransmitter modulation by the gut microbiota. Brain Research, 1693(Pt B), 128–133. https://doi.org/10.1016/j.brainres.2018.03.015

Streit, W.J. 2006. Microglial senescence: does the brain's immune system have an expiration date? Trends in Neurosciences 29(9).

Streit, W.J., Braak, H., Xue, Q.S., & Bechmann, I. 2009. Dystrophic (senescent) rather than activated microglial cells are associated with tau pathology and likely precede neurodegeneration in Alzheimer's disease. Acta Neuropathologica 118(4): p.475–485.

Streit, W.J., Sammons, N.W., Kuhns, A.J., & Sparks, D.L. 2004. Dystrophic Microglia in the Aging Human Brain. Glia 45(2): p.208–212.

Sturchler-Pierrat, C. et al. 1997. Two amyloid precursor protein transgenic mouse models with Alzheimer disease-like pathology. Proceedings of the National Academy of Sciences of the United States of America 94(24): p.13287–13292.

Suda, Y. et al. 2021. Normal aging induces PD-1-enriched exhausted microglia and A1-like reactive astrocytes in the hypothalamus. Biochemical and Biophysical Research Communications 541: p.22–29.

Sudheimer D., K.D. et al. 2014. Cortisol, cytokines, and hippocampal volume interactions in the elderly. Frontiers in Aging Neuroscience 6(JUL).

Sudo, N., Chida, Y., Aiba, Y., Sonoda, J., Oyama, N., Yu, X. N., Kubo, C., & Koga, Y. (2004). Postnatal microbial colonization programs the hypothalamic-pituitary-adrenal system for stress response in mice. Journal of Physiology, 558(1), 263–275. https://doi.org/10.1113/jphysiol.2004.063388

Suh, S.W. et al. 2003. Hypoglycemic Neuronal Death and Cognitive Impairment are Prevented by Poly(ADP-Ribose) Polymerase Inhibitors Administered after Hypoglycemia. Journal of Neuroscience 23(33): p.10681–10690.

Sumagin, R., Prizant, H., Lomakina, E., Waugh, R.E., & Sarelius, I.H. 2010. LFA-1 and Mac-1 Define Characteristically Different Intralumenal Crawling and Emigration Patterns for Monocytes and

Neutrophils In Situ. The Journal of Immunology 185(11): p.7057–7066. Available at: http://www.jimmunol.org/content/185/11/7057http://www.jimmunol.org/content/185/11/7057.full#ref-list-1.

Suzuki, R. et al. 2010. Diabetes and insulin in regulation of brain cholesterol metabolism. Cell Metabolism 12(6): p.567–579.

Suzumura, A., Sawada, M., Yamamoto, H., & Marunouchi, T. 1993. Transforming growth factor-beta suppresses activation and proliferation of microglia in vitro. Journal of immunology (Baltimore, Md. : 1950) 151(4): p.2150–8. Available at: http://www.ncbi.nlm.nih.gov/pubmed/8345199.

Swardfager, W., Lanctt, K., Rothenburg, L., Wong, A., Cappell, J., & Herrmann, N. (2010). A meta-analysis of cytokines in Alzheimer's disease. Biological Psychiatry, 68(10), 930–941. https://doi.org/10.1016/j.biopsych.2010.06.012

Sy, M. et al. 2011. Inflammation induced by infection potentiates tau pathological features in transgenic mice. American Journal of Pathology 178(6): p.2811–2822.

Syed, Y.A. et al. 2008. Inhibition of oligodendrocyte precursor cell differentiation by myelin-associated proteins. Neurosurgical Focus 24(3–4).

Takeda, S. et al. 2013. Increased blood-brain barrier vulnerability to systemic inflammation in an Alzheimer disease mouse model. Neurobiology of Aging 34(8): p.2064–2070.

Takeda, T. et al. 1981. A new murine model of accelerated senescence. Mechanisms of Ageing and Development 17(2): p.183–194.

Takeda, T. et al. 1997. Pathobiology of the Senescence-Accelerated Mouse (SAM). In Experimental Gerontology, 117–127.

Talar, K. et al. 2021. Benefits of Resistance Training in Early and Late Stages of Frailty and Sarcopenia: A Systematic Review and Meta-Analysis of Randomized Controlled Studies. Journal of Clinical Medicine 10(8): p.1630. Available at: https://pubmed.ncbi.nlm.nih.gov/33921356/ [Accessed May 8, 2021].

Tam, J.M. et al. 2014. Dectin-1-dependent LC3 recruitment to phagosomes enhances fungicidal activity in macrophages. Journal of Infectious Diseases 210(11): p.1844–1854.

Tan, Y.L., Yuan, Y., & Tian, L. 2020. Microglial regional heterogeneity and its role in the brain. Molecular Psychiatry 25(2): p.351–367.

Tang, J., Lin, G., Langdon, W.Y., Tao, L., & Zhang, J. 2018. Regulation of C-type lectin receptor-mediated antifungal immunity. Frontiers in Immunology 9(FEB): p.123.

Tang, W. H. W., Kitai, T., & Hazen, S. L. (2017). Gut microbiota in cardiovascular health and disease. In Circulation Research (Vol. 120, Issue 7, pp. 1183–1196). https://doi.org/10.1161/CIRCRESAHA.117.309715

Tarkowski, E., Andreasen, N., Tarkowski, A., & Blennow, K. 2003. Intrathecal inflammation precedes development of Alzheimer's disease. Journal of Neurology, Neurosurgery and Psychiatry 74(9): p.1200–1205.

Tateda, K., Matsumoto, T., Miyazaki, S., & Yamaguchi, K. (1996). Lipopolysaccharide-induced lethality and cytokine production in aged mice. Infection and Immunity, 64(3), 769–774. https://doi.org/10.1128/iai.64.3.769-774.1996

Teles-Grilo Ruivo, L.M., & Mellor, J.R. 2013. Cholinergic modulation of hippocampal network function. Frontiers in Synaptic Neuroscience 5(JUL).

Terry, R.D. et al. 1991. Physical basis of cognitive alterations in alzheimer's disease: Synapse loss is the major correlate of cognitive impairment. Annals of Neurology 30(4): p.572–580.

Thaler, J.P. et al. 2012. Obesity is associated with hypothalamic injury in rodents and humans. Journal of Clinical Investigation 122(1): p.153–162.

Thaler, J.P., Guyenet, S.J., Dorfman, M.D., Wisse, B.E., & Schwartz, M.W. 2013. Hypothalamic inflammation: Marker or mechanism of obesity pathogenesis? Diabetes 62(8): p.2629–2634.

Thiagarajan, P.S. et al. 2013. Vimentin is an endogenous ligand for the pattern recognition receptor Dectin-1. Cardiovascular Research 99(3): p.494–504.

Timmers, S. et al. 2012. Augmenting muscle diacylglycerol and triacylglycerol content by blocking fatty acid oxidation does not impede insulin sensitivity. Proceedings of the National Academy of Sciences of the United States of America 109(29).

Todorovic, S. et al. 2020. Frailty index and phenotype frailty score: Sex- and age-related differences in 5XFAD transgenic mouse model of Alzheimer's disease. Mechanisms of Ageing and Development 185: p.111195.

Tomiyama, T. et al. 2010. A mouse model of amyloid β oligomers: Their contribution to synaptic alteration, abnormal tau phosphorylation, glial activation, and neuronal loss in vivo. Journal of Neuroscience 30(14): p.4845–4856.

Toro, C.A., Zhang, L., Cao, J., & Cai, D. 2019. Sex differences in Alzheimer's disease: Understanding the molecular impact. Brain Research 1719: p.194–207.

Torres, J.M., Cardenas, O., Vasquez, A., & Schlossberg, D. 1998. Streptococcus pneumoniae bacteremia in a community hospital. Chest 113(2): p.387–390.

Torvell, M. et al. 2019. A single systemic inflammatory insult causes acute motor deficits and accelerates disease progression in a mouse model of human tauopathy. Alzheimer's and Dementia: Translational Research and Clinical Interventions 5.

Travison, T.G. et al. 2011. Changes in reproductive hormone concentrations predict the prevalence and progression of the frailty syndrome in older men: The Concord Health and Ageing in Men Project. Journal of Clinical Endocrinology and Metabolism 96(8): p.2464–2474.

Trickler, W.J., Mayhan, W.G., & Miller, D.W. 2005. Brain microvessel endothelial cell responses to tumor necrosis factor-alpha involve a nuclear factor kappa B (NF-κB) signal transduction pathway. Brain Research 1048(1–2): p.24–31. Available at: www.elsevier.com/locate/brainres.

Tucsek, Z., Toth, P., Sosnowska, D., Gautam, T., Mitschelen, M., Koller, A., Szalai, G., Sonntag, W. E., Ungvari, Z., & Csiszar, A. (2014). Obesity in aging exacerbates blood-brain barrier disruption, neuroinflammation, and oxidative stress in the mouse hippocampus: Effects on expression of genes involved in beta-amyloid generation and Alzheimer's disease. Journals of Gerontology - Series A Biological Sciences and Medical Sciences, 69(10), 1212–1226. https://doi.org/10.1093/gerona/glt177

Turk, V. et al. 2012. Cysteine cathepsins: From structure, function and regulation to new frontiers. Biochimica et Biophysica Acta - Proteins and Proteomics 1824(1): p.68–88.

Turner, M.D., Nedjai, B., Hurst, T., & Pennington, D.J. 2014. Cytokines and chemokines: At the crossroads of cell signalling and inflammatory disease. Biochimica et Biophysica Acta - Molecular Cell Research 1843(11): p.2563–2582. Available at: http://dx.doi.org/10.1016/j.bbamcr.2014.05.014 [Accessed March 13, 2021].

Tzourio-Mazoyer, N. 2016. Intra- and inter-hemispheric connectivity supporting hemispheric specialization. In Research and Perspectives in Neurosciences, 129–146.

Ukropcova, B. et al. 2007. Family history of diabetes links impaired substrate switching and reduced mitochondrial content in skeletal muscle. Diabetes 56(3): p.720–727.

Ulland, T.K. et al. 2017. TREM2 Maintains Microglial Metabolic Fitness in Alzheimer's Disease. Cell

170(4): p.649-663.e13.

Urquiza, J., Cevallos, C., Elizalde, M.M., Delpino, M.V., & Quarleri, J. 2020. Priming Astrocytes With HIV-Induced Reactive Oxygen Species Enhances Their Trypanosoma cruzi Infection. Frontiers in Microbiology 11.

Valdearcos, M. et al. 2014. Microglia Dictate the Impact of Saturated Fat Consumption on Hypothalamic Inflammation and Neuronal Function. Cell Reports 9(6): p.2124–2138.

Valentin-Torres, A. et al. 2016. Sustained TNF production by central nervous system infiltrating macrophages promotes progressive autoimmune encephalomyelitis. Journal of Neuroinflammation 13(1): p.1–14. Available at: https://link.springer.com/articles/10.1186/s12974-016-0513-y [Accessed September 19, 2021].

Varma, V.R. et al. 2021. Abnormal brain cholesterol homeostasis in Alzheimer's disease—a targeted metabolomic and transcriptomic study. npj Aging and Mechanisms of Disease 7(1): p.1–14. Available at: https://www.nature.com/articles/s41514-021-00064-9 [Accessed September 6, 2021].

Vasconcellos Romanini, C. et al. 2020. Prediction of Death with the Frail-NH in Institutionalized Older Adults: A Longitudinal Study from a Middle-Income Country. Journal of Nutrition, Health and Aging 24(8): p.817–820.

Vehmas, A.K., Kawas, C.H., Stewart, W.F., & Troncoso, J.C. 2003. Immune reactive cells in senile plaques and cognitive decline in Alzheimer's disease. Neurobiology of Aging 24(2): p.321–331.

Velazquez, R. et al. 2017. Central insulin dysregulation and energy dyshomeostasis in two mouse models of Alzheimer's disease. Neurobiology of Aging 58: p.1–13.

Verkhratsky, A., & Nedergaard, M. 2018. Physiology of astroglia. Physiological Reviews 98(1): p.239–389.

Verschoor, C.P., & Tamim, H. 2019. Frailty is inversely related to age at menopause and elevated in women who have had a hysterectomy: An analysis of the Canadian longitudinal study on aging. Journals of Gerontology - Series A Biological Sciences and Medical Sciences 74(5): p.675–682.

Vest, R.S., & Pike, C.J. 2013. Gender, sex steroid hormones, and Alzheimer's disease. Hormones and Behavior 63(2): p.301–307.

Vilcek, J., & Lee, T.H. 1991. Tumor necrosis factor: New insights into the molecular mechanisms of its multiple actions. Journal of Biological Chemistry 266(12): p.7313–7316.

Villareal, D.T. et al. 2001. Bone mineral density response to estrogen replacement in frail elderly women; A randomized controlled trial. Journal of the American Medical Association 286(7): p.815–820. Available at: https://jamanetwork.com/ [Accessed March 17, 2021].

Villareal, D.T., Apovian, C.M., Kushner, R.F., & Klein, S. 2005. Obesity in older adults: Technical review and position statement of the American Society for Nutrition and NAASO, the Obesity Society. Obesity Research 13(11): p.1849–1863.

Villeda, S.A. et al. 2011. The ageing systemic milieu negatively regulates neurogenesis and cognitive function. Nature 477(7362): p.90–96.

Voelker, R. 2018. The Mediterranean Diet's fight against frailty. JAMA - Journal of the American Medical Association 319(19): p.1971–1972.

Volpi, E., Mittendorfer, B., Rasmussen, B.B., & Wolfe, R.R. 2000. The response of muscle protein anabolism to combined hyperaminoacidemia and glucose-induced hyperinsulinemia is impaired in the elderly. Journal of Clinical Endocrinology and Metabolism 85(12): p.4481–4490.

Vorhees, C. V., & Williams, M.T. 2006. Morris water maze: Procedures for assessing spatial and related forms of learning and memory. Nature Protocols 1(2): p.848–858.

Voß, E.V. et al. 2012. Characterisation of microglia during de- and remyelination: Can they create a repair promoting environment? Neurobiology of Disease 45(1): p.519–528.

Vrachnis, N. et al. 2014. Probing the impact of sex steroids and menopause-related sex steroid deprivation on modulation of immune senescence. Maturitas 78(3): p.174–178.

Vrillon, A. et al. 2020. COVID-19 in Older Adults: A Series of 76 Patients Aged 85 Years and Older with COVID-19. Journal of the American Geriatrics Society 68(12): p.2735–2743.

Vukojicic, A. et al. 2019. The Classical Complement Pathway Mediates Microglia-Dependent Remodeling of Spinal Motor Circuits during Development and in SMA. Cell Reports 29(10).

Wagener, M., Hoving, J.C., Ndlovu, H., & Marakalala, M.J. 2018. Dectin-1-Syk-CARD9 signaling pathway in TB immunity. Frontiers in Immunology 9(FEB): p.225.

Wagner, E., & Frank, M.M. 2010. Therapeutic potential of complement modulation. Nature Reviews Drug Discovery 9(1): p.43–56.

Wagstaff, L.R., Mitton, M.W., Arvik, B.M.L., & Doraiswamy, P.M. 2003. Statin-associated memory loss: Analysis of 60 case reports and review of the literature. Pharmacotherapy 23(7): p.871–880.

Wall, B.T. et al. 2015. Aging is accompanied by a blunted muscle protein synthetic response to protein ingestion. PLoS ONE 10(11).

Wallace, L.M.K. et al. 2019. Investigation of frailty as a moderator of the relationship between neuropathology and dementia in Alzheimer's disease: a cross-sectional analysis of data from the Rush Memory and Aging Project. The Lancet Neurology 18(2): p.177–184.

Walston, J. et al. 2008. The physical and biological characterization of a frail mouse model. Journals of Gerontology - Series A Biological Sciences and Medical Sciences 63(4): p.391–398.

Wang, A. et al. 2016. Opposing Effects of Fasting Metabolism on Tissue Tolerance in Bacterial and Viral Inflammation. Cell 166(6): p.1512-1525.e12.

Wang, J., Tanila, H., Puoliväli, J., Kadish, I., & Van Groen, T. 2003. Gender differences in the amount and deposition of amyloidβ in APPswe and PS1 double transgenic mice. Neurobiology of Disease 14(3): p.318–327.

Wang, Q. et al. 2011. Statins: Multiple neuroprotective mechanisms in neurodegenerative diseases. Experimental Neurology 230(1): p.27–34.

Wang, S. et al. 2006. Venular basement membranes contain specific matrix protein low expression regions that act as exit points for emigrating neutrophils. Journal of Experimental Medicine 203(6): p.1519–1532.

Wang, Y. et al. 2015. TREM2 lipid sensing sustains the microglial response in an Alzheimer's disease model. Cell 160(6): p.1061–1071.

Wang, Z. et al. 2012. Saturated fatty acids activate microglia via Toll-like receptor 4/NF-κB signalling. British Journal of Nutrition 107(2): p.229–241.

Watson, T.C. et al. 2018. Anatomical and physiological foundations of cerebello-hippocampal interactions. bioRxiv: p.403394. Available at: https://www.biorxiv.org/content/10.1101/403394v1 [Accessed January 20, 2022].

Weaving, G., Batstone, G.F., & Jones, R.G. 2016. Age and sex variation in serum albumin concentration: an observational study. Annals of Clinical Biochemistry 53(1): p.106–111.

Weksler, M.E., Pawelec, G., & Franceschi, C. 2009. Immune therapy for age-related diseases. Trends

in Immunology 30(7): p.344–350.

Werneburg, S. et al. 2020. Targeted Complement Inhibition at Synapses Prevents Microglial Synaptic Engulfment and Synapse Loss in Demyelinating Disease. Immunity 52(1).

Westerman, M.A. et al. 2002. The relationship between Aβ and memory in the Tg2576 mouse model of Alzheimer's disease. Journal of Neuroscience 22(5): p.1858–1867.

Wharton, S.B. et al. 2011. Epidemiological neuropathology: The MRC cognitive function and aging study experience. Journal of Alzheimer's Disease 25(2): p.359–372.

Whitehead, J.C. et al. 2014. A clinical frailty index in aging mice: Comparisons with frailty index data in humans. Journals of Gerontology - Series A Biological Sciences and Medical Sciences 69(6): p.621–632.

Widmann, C.N., & Heneka, M.T. 2014. Long-term cerebral consequences of sepsis. The Lancet Neurology 13(6): p.630–636.

Wijdicks, E.F.M. 2015. Brain Disorders in Critical Illness. Cognitive and Behavioral Neurology 28(1): p.41.

Williams, J.G., Jurkovich, G.J., Hahnel, G.B., & Maier, R. V. 1992. Macrophage priming by interferon gamma: A selective process with potentially harmful effects. Journal of Leukocyte Biology 52(6): p.579–584.

Wlodarczyk, A. et al. 2017. A novel microglial subset plays a key role in myelinogenesis in developing brain. The EMBO Journal 36(22): p.3292–3308.

Wlodarczyk, A., Løbner, M., Cédile, O., & Owens, T. 2014. Comparison of microglia and infiltrating CD11c+ cells as antigen presenting cells for T cell proliferation and cytokine response. Journal of Neuroinflammation 11.

World Health Organization; 2011. Global Health And Aging [Internet]. Available at: http://www.who.int/Ageing/Publications/Global_Health.Pdf.

World Health Organization; 2020. Dementia. Available at: https://www.who.int/news-room/fact-sheets/detail/dementia [Accessed March 14, 2021].

Wynn, T.A., & Vannella, K.M. 2016. Macrophages in Tissue Repair, Regeneration, and Fibrosis. Immunity 44(3): p.450–462.

Xin, D.L. et al. 2011. Aging enhances serum cytokine response but not task-induced grip strength

declines in a rat model of work-related musculoskeletal disorders. BMC Musculoskeletal Disorders 12.

Yakar, S. et al. 2002. Circulating levels of IGF-1 directly regulate bone growth and density. Journal of Clinical Investigation 110(6): p.771–781. Available at: /pmc/articles/PMC151128/ [Accessed August 28, 2021].

Yamamoto, K., Shishido, T., Masaoka, T., & Imakiire, A. 2005. Morphological studies on the ageing and osteoarthritis of the articular cartilage in C57 black mice. Journal of orthopaedic surgery (Hong Kong) 13(1): p.8–18.

Yamamoto, Koji, Takeshita, K., Kojima, T., Takamatsu, J., & Saito, H. 2005. Aging and plasminogen activator inhibitor-1 (PAI-1) regulation: Implication in the pathogenesis of thrombotic disorders in the elderly. Cardiovascular Research 66(2): p.276–285. Available at: https://pubmed.ncbi.nlm.nih.gov/15820196/ [Accessed August 26, 2021].

Yamasaki, R. 2014. Microglia in vivo and in vitro. Clinical and Experimental Neuroimmunology 5(2): p.114–116. Available at: https://onlinelibrary.wiley.com/doi/full/10.1111/cen3.12120 [Accessed August 25, 2021].

Yan, J. et al. 2014. Obesity-and aging-induced excess of central transforming growth factor-β 2 potentiates diabetic development via an RNA stress response. Nature Medicine 20(9): p.1001–1008. Available at: https://www.nature.com/articles/nm.3616 [Accessed September 12, 2021].

Yang, G.Y., Gong, C., Qin, Z., Liu, X.H., & Lorris Betz, A. 1999. Tumor necrosis factor alpha expression produces increased blood-brain barrier permeability following temporary focal cerebral ischemia in mice. Molecular Brain Research 69(1): p.135–143.

Yassine, N. et al. 2013. Detecting spatial memory deficits beyond blindness in tg2576 Alzheimer mice. Neurobiology of Aging 34(3): p.716–730.

Ye, C.Y., Lei, Y., Tang, X.C., & Zhang, H.Y. 2015. Donepezil attenuates Aβ-associated mitochondrial dysfunction and reduces mitochondrial Aβ accumulation in vivo and in vitro. Neuropharmacology 95: p.29–36.

Ye, X.C. et al. 2020. Dectin-1/Syk signaling triggers neuroinflammation after ischemic stroke in mice. Journal of Neuroinflammation 17(1).

Yeh, S.H.H. et al. 2020. A high-sucrose diet aggravates Alzheimer's disease pathology, attenuates hypothalamic leptin signaling, and impairs food-anticipatory activity in APPswe/PS1dE9 mice.

Neurobiology of Aging 90: p.60–74.

Yeoman, M., Scutt, G., & Faragher, R. 2012. Insights into CNS ageing from animal models of senescence. Nature Reviews Neuroscience 13(6): p.435–445. Available at: http://dx.doi.org/10.1038/nrn3230.

Yeung, S.S.Y. et al. 2019. Sarcopenia and its association with falls and fractures in older adults: A systematic review and meta-analysis. Journal of Cachexia, Sarcopenia and Muscle 10(3): p.485–500.

Yin, Z. et al. 2018. Low-fat diet with caloric restriction reduces white matter microglia activation during aging. Frontiers in Molecular Neuroscience 11(March). Available at: http://journal.frontiersin.org/article/10.3389/fnmol.2018.00065/full.

Yokoyama, H. et al. 2020. Applications of physical performance measures to routine diabetes care for frailty prevention concept: Fundamental data with grip strength, gait speed, timed chair stand speed, standing balance, and knee extension strength. BMJ Open Diabetes Research and Care 8(1).

Yokoyama, J.S. et al. 2016. Association between genetic traits for immune-mediated diseases and Alzheimer disease. JAMA Neurology 73(6): p.691–697.

Yoo, D., Paracatu, L.C., Xu, E., Lin, X., & Dinauer, M.C. 2021. NADPH Oxidase Limits Collaborative Pattern-Recognition Receptor Signaling to Regulate Neutrophil Cytokine Production in Response to Fungal Pathogen-Associated Molecular Patterns. The Journal of Immunology 207(3): p.923–937. Available at: https://pubmed.ncbi.nlm.nih.gov/34301842/ [Accessed July 25, 2021].

Yoo, Y.D. et al. 1999. TGF-β-induced cell-cycle arrest through the p21(WAF1/CIP1)-G1 cyclin/CDKS-p130 pathway in gastric-carcinoma cells. International Journal of Cancer 83(4).

Youm, Y.H. et al. 2013. Canonical Nlrp3 inflammasome links systemic low-grade inflammation to functional decline in aging. Cell Metabolism 18(4): p.519–532.

Yu, B.P. 1996. Aging and oxidative stress: Modulation by dietary restriction. Free Radical Biology and Medicine 21(5): p.651–668.

Yu, W., & Krook-Magnuson, E. 2015. Cognitive collaborations: Bidirectional functional connectivity between the cerebellum and the hippocampus. Frontiers in Systems Neuroscience 9(DEC).

Yue, F. et al. 2016. Conditional Loss of Pten in Myogenic Progenitors Leads to Postnatal Skeletal

Muscle Hypertrophy but Age-Dependent Exhaustion of Satellite Cells. Cell Reports 17(9): p.2340–2353.

Yurov, Y.B., Vorsanova, S.G., Liehr, T., Kolotii, A.D., & Iourov, I.Y. 2014. X chromosome aneuploidy in the Alzheimer's disease brain. Molecular Cytogenetics 7(1).

Zamanian, J.L. et al. 2012. Genomic analysis of reactive astrogliosis. Journal of Neuroscience 32(18): p.6391–6410.

Zeng, B., Zhao, G., & Liu, H.L. 2020. The Differential Effect of Treadmill Exercise Intensity on Hippocampal Soluble Aβ and Lipid Metabolism in APP/PS1 Mice. Neuroscience 430: p.73–81.

Vogt, N. M., Kerby, R. L., Dill-McFarland, K. A., Harding, S. J., Merluzzi, A. P., Johnson, S. C., Carlsson, C. M., Asthana, S., Zetterberg, H., Blennow, K., Bendlin, B. B., & Rey, F. E. (2017). Gut microbiome alterations in Alzheimer's disease. Scientific Reports, 7(1). https://doi.org/10.1038/s41598-017-13601-y

Von Zglinicki, T. 2002. Oxidative stress shortens telomeres. Trends in Biochemical Sciences 27(7): p.339–344.

Zhang, J., Xiao, B., Li, C.X., & Wang, Y. 2020. Fingolimod (FTY720) improves postoperative cognitive dysfunction in mice subjected to D-galactose-induced aging. Neural Regeneration Research 15(7): p.1308–1315. Available at: /pmc/articles/PMC7047799/ [Accessed September 5, 2021].

Zhang, X. et al. 2008. Hypothalamic IKKβ/NF-κB and ER Stress Link Overnutrition to Energy Imbalance and Obesity. Cell 135(1): p.61–73. Available at: https://pubmed.ncbi.nlm.nih.gov/18854155/ [Accessed July 24, 2021].

Zhang, Y. et al. 2018. miR-23b Suppresses Leukocyte Migration and Pathogenesis of Experimental Autoimmune Encephalomyelitis by Targeting CCL7. Molecular Therapy 26(2): p.582–592.

Zhao, N. et al. 2017. Apolipoprotein E4 Impairs Neuronal Insulin Signaling by Trapping Insulin Receptor in the Endosomes. Neuron 96(1): p.115-129.e5.

Zhao, N., Liu, C. C., van Ingelgom, A. J., Martens, Y. A., Linares, C., Knight, J. A., Painter, M. M., Sullivan, P. M., & Bu, G. (2017). Apolipoprotein E4 Impairs Neuronal Insulin Signaling by Trapping Insulin Receptor in the Endosomes. Neuron, 96(1), 115-129.e5. https://doi.org/10.1016/j.neuron.2017.09.003

Zheng, H. et al. 2018. The hypothalamus as the primary brain region of metabolic abnormalities in APP/PS1 transgenic mouse model of Alzheimer's disease. Biochimica et Biophysica Acta -

Molecular Basis of Disease 1864(1): p.263–273.

Zhou, C. et al. 2018. Sex differences in the white matter and myelinated fibers of APP/PS1 mice and the effects of running exercise on the sex differences of AD mice. Frontiers in Aging Neuroscience 10(AUG).

Zhou, Q. et al. 2018. Metabolic fate of glucose in the brain of APP/PS1 transgenic mice at 10 months of age: a 13 C NMR metabolomic study. Metabolic Brain Disease 33(5): p.1661–1668.

Zhu, J.N., Yung, W.H., Kwok-Chong Chow, B., Chan, Y.S., & Wang, J.J. 2006. The cerebellar-hypothalamic circuits: Potential pathways underlying cerebellar involvement in somatic-visceral integration. Brain Research Reviews 52(1): p.93–106.

Zhu, S. et al. 2017. The role of neuroinflammation and amyloid in cognitive impairment in an APP/PS1 transgenic mouse model of Alzheimer's disease. CNS Neuroscience and Therapeutics 23(4): p.310–320.

Zindler, E., & Zipp, F. 2010. Neuronal injury in chronic CNS inflammation. Best Practice and Research: Clinical Anaesthesiology 24(4): p.551–562. Available at: https://pubmed.ncbi.nlm.nih.gov/21619866/ [Accessed September 4, 2021].

Zissimopoulos, J.M., Barthold, D., Brinton, R.D., & Joyce, G. 2017. Sex and race differences in the association between statin use and the incidence of Alzheimer disease. JAMA Neurology 74(2): p.225–232.

Ziv, Y. et al. 2006. Immune cells contribute to the maintenance of neurogenesis and spatial learning abilities in adulthood. Nature Neuroscience 9(2): p.268–275.

Zonsius, M.C., Cothran, F.A., & Miller, J.M. 2020. Acute Care for Patients with Dementia: A review of best practices for integrating person-centered care throughout the hospital stay. AJN American Journal of Nursing 124(4): p.34–43. Available at: http://search.ebscohost.com/login.aspx?direct=true&db=c8h&AN=144210345&authtype=shib&site=ehost-live&custid=s7108731&authtype=ip,shib.